DET KGL. DANSKE VIDENSKABERNES SELSKAB
MATEMATISK-FYSISKE MEDDELELSER, BIND XXI, Nr. 1

UNTERSUCHUNGEN ÜBER DIE RADIOMETERFUNKTION UND DIE KNUDSEN'SCHE RADIOMETERKRAFT

VON

SOPHUS WEBER

KØBENHAVN
I KOMMISSION HOS EJNAR MUNKSGAARD
1944

Printed in Denmark
Bianco Lunos Bogtrykkeri A/S

1. In einer früheren Arbeit[1] habe ich eine formale Einteilung von den bekannten Radiometererscheinungen gegeben und das absolute Manometer von MARTIN KNUDSEN, wie auch das Einplattenradiometer im Wärmestrom, näher untersucht; über das letzte sind neuerdings einige neue experimentelle Untersuchungen von E. FREDLUND[2] veröffentlicht worden. Ich hoffe in einer späteren Arbeit hierauf zurückzukommen.

Anschliessend an meine obengenannte Untersuchung ist es nicht ohne Interesse, die Radiometerkraft auf einer Kugel im Wärmestrom näher zu betrachten, auch weil die Erklärung von der von F. EHRENHAFT[3] entdeckten Erscheinung der Bewegung kleiner Materieteilchen im Lichte — die Photophorese — in der Radiometerkraft zu suchen ist.

Nach den grundlegenden theoretischen Arbeiten von A. RUBINOWICZ[4], G. HETTNER[5] und P. EPSTEIN[6] und nach den experimentellen Arbeiten von J. MATTAUCH[7] und den Schülern EHRENHAFT's besteht hierüber wohl kein Zweifel mehr, dass sowohl die positive als auch die negative Photophorese als Radiometereffekt zu deuten ist; auch die aufschlussreichen Experimente und Untersuchungen von MARTIN KNUDSEN[8] über die negative Radiometerkraft haben diese Auffassung bestätigt.

Es ist aber in dieser Verbindung von Bedeutung, zu untersuchen, wie die Radiometerkraft auf einer Kugel im Wärme-

[1] SOPHUS WEBER: D. Kgl. Danske Vidensk. Selskab, Math.-fys. Medd. XIV, 13, 1937.

[2] ERNST FREDLUND: Phil. Mag. 7. XXVI, 1938, S. 987. Arkiv f. Mat. Astr. Fys. 27 A, No. 12, 1940.

[3] F. EHRENHAFT: Ann. d. Ph. 56, 1918, S. 81.

[4] A. RUBINOWICZ: Ann. d. Ph. 62, 1920, S. 691.

[5] G. HETTNER: Z. S. Ph. 37, 1926, S. 179.

[6] P. EPSTEIN: Z. S. Ph. 54, 1929, S. 537.

[7] J. MATTAUCH: Ann. d. Ph. 85, 1938, S. 967.

[8] MARTIN KNUDSEN: D. Kgl. Danske Vidensk. Selskab, Math.-fys. Medd. XI, 1, 1930.

strom oder Strahlungsfeld in dem gesamten Druckgebiet von dem Radius der Kugel, r_0, und von der Natur des Gases abhängt.

Nach der theoretischen Arbeit von RUBINOWICZ für den Grenzfall $r_0 \ll \lambda$, wo λ die mittlere freie Weglänge des Gases bezeichnet, und nach den Arbeiten von G. HETTNER und insbesondere von P. EPSTEIN für den Fall $r_0 \gg \lambda$, sind die Werte der Radiometerkraft, K, für die zwei Grenzfälle, bezw. $K_\infty = \frac{A'}{p}$ und $K_0 = B' \cdot p$, bekannt.

Um eine Übersicht über den Verlauf der Radiometerkraft im gesamten Druckgebiet zu erhalten, hat HETTNER diese zwei Grenzformeln durch eine einfache Interpolationsformel:

$$\frac{1}{K} = \frac{1}{K_0} + \frac{1}{K_\infty}, \tag{1}$$

verbunden, worin K die Radiometerkraft bei dem Druck p bezeichnet; es ist aber möglich, durch Einführung der erweiterten MAXWELL'schen Grenzbedingung[9] in der Berechnung theoretisch abzuleiten, — jedenfalls annäherungsweise —, wie der Verlauf von der Radiometerkraft, K, im ganzen Druckgebiet $0 \leqq \frac{r_0}{\lambda} \leqq \infty$ wird, oder, mit andern Worten, die von W. WESTPHAL[10] eingeführte Radiometerfunktion: $K = f(\log p)$, zu bestimmen.

2. Bei der Berechnung können wir am einfachsten der von EPSTEIN[11] gegebenen Ableitung für $r_0 \gg \lambda$ folgen und seine Terminologie verwenden. Wir müssen also das Wärmeleitungsproblem und das Strömungsproblem lösen, für den Fall, dass sich eine Kugel in einem Gasraum befindet, in welchem in grosser Entfernung von der Kugel ein homogenes Temperaturfeld mit dem Temperaturgradienten, $G = \frac{dT}{dx}$, herrscht; an der Oberfläche der Kugel gilt aber nun die erweiterte MAXWELL'sche Grenzbedingung:

$$u_s - k_2 \cdot \gamma \cdot \frac{du_s}{dr} = k_1 \cdot \frac{3}{4} \cdot \frac{\eta}{\varrho T} \cdot \frac{dT}{ds} \cdot \frac{1}{1 + \psi_1\left(\frac{\lambda}{r_0}\right)}, \tag{2}$$

[9] SOPHUS WEBER: Comm. Kamerlingh Onnes Lab. Leiden No. 246[b], 1937.
[10] W. WESTPHAL: Z. S. Ph. 4, 1921, S. 221.
[11] P. EPSTEIN: loc. cit. S. 540.

wo u_s die tangentielle Gleitgeschwindigkeit des Gases an der Oberfläche der Kugel und T die Temperatur der an die Oberfläche grenzenden Gasschicht bezeichnen, während γ, η und ϱ der Gleitungskoeffizient, die innere Reibung und die Dichte des Gases sind. $\psi_1\left(\frac{\lambda}{r_0}\right)$ ist eine Funktion von $\frac{\lambda}{r_0}$, die in erster Annäherung gleich $m \cdot \frac{\lambda}{r_0}$ gesetzt werden kann; ausserdem ist $k_1 = k_2 = \frac{4}{3}$. Die Richtung der Gleitströme an der Oberfläche ist von Stellen niedrieger Temperatur nach Stellen höherer Temperatur; die Kugel wird sich also in die entgegengesetzte Richtung bewegen.

Da das Gas im Unendlichen ruht, wird die Lösung des hydrodynamischen Problems nach LAMB[12]:

$$u_r = \left(\frac{A}{\eta r} - \frac{2B}{r^3}\right) \cos\theta, \tag{3}$$

$$u_\theta = -\left(\frac{A}{2\eta r} + \frac{B}{r^3}\right) \sin\theta, \tag{4}$$

$$u_\varphi = 0, \tag{5}$$

wenn Polarkoordinaten, r, θ und φ verwendet werden, und die Richtung der polaren Achse als x-Richtung angenommen wird, so dass $x = r\cos\theta$. Die Schubspannung $p_{x,r}$ wird:

$$p_{x,r} = -\frac{x}{r} p_0 + \left(Ar - \frac{6\eta}{r} B\right) \frac{\partial}{\partial x} \frac{x}{r^3} - \frac{A}{r^2}, \tag{6}$$

woraus, der Symmetrie wegen, die totale Radiometerkraft auf der Kugel, bezw. der totale Impulstransport durch die Kugeloberfläche, folgendermassen wird:

$$K = \int p_{x,r_0} \cdot dS = 2\pi r_0^2 \int_0^\pi p_{x,r_0} \sin\theta \, d\theta. \tag{7}$$

Aus der Bedingung, $u_r = 0$ für $r = r_0$, folgt:

$$2B = \frac{A}{\eta} \cdot r_0^2, \tag{8}$$

und also:

[12] H. LAMB: Hydrodynamics, 4th Edition, Cambridge 1924, S. 565.

$$u_r = \frac{A}{\eta}\left(\frac{1}{r} - \frac{r_0^2}{r^3}\right)\cos\theta, \tag{9}$$

$$u_\theta = -\frac{A}{2\eta}\left(\frac{r_0^2}{r^3} + \frac{1}{r}\right)\sin\theta \tag{10}$$

und

$$\frac{\partial u_\theta}{\partial r} = \frac{A}{2\eta}\left[3\frac{r_0^2}{r^4} + \frac{1}{r^2}\right]\sin\theta. \tag{11}$$

Um den Wert von A zu finden, müssen wir das Wärmeleitungsproblem lösen. Nach EPSTEIN ist:

$$T_a - T_0 = G \cdot r\cos\theta + P \cdot \frac{\cos\theta}{r^2} \tag{12}$$

und

$$T_i - T_0 = Q \cdot r\cos\theta, \tag{13}$$

mit den Bedingungen an der Oberfläche der Kugel:

$$T_a = T_i \quad \text{und} \quad \varkappa_i \frac{dT_i}{dr} = \varkappa_a \frac{dT_a}{dr}, \tag{14}$$

wo $\varkappa_i$ und $\varkappa_a$ die Wärmeleitfähigkeiten der Kugel und des umgebenden Gasmediums bedeuten.

Hieraus erhält man:

Ausserhalb der Kugel:

$$T_a = T_0 + \left(r + \frac{\varkappa_a - \varkappa_i}{\varkappa_i + 2\varkappa_a} \cdot \frac{r_0^3}{r^2}\right) G\cos\theta \tag{15}$$

und innerhalb der Kugel:

$$T_i = T_0 + \frac{3\varkappa_a}{\varkappa_i + 2\varkappa_a} \cdot rG\cos\theta. \tag{16}$$

T_0 ist die Temperatur in dem Plan $x = 0$ und kann annäherungsweise, wenn der Temperaturunterschied in der Kugel klein ist, mit der Temperatur des Gases in dem Plan $x = 0$ gleich gesetzt werden.

Die Temperaturverteilung auf der Kugeloberfläche wird also:

$$T = T_0 + 3 \cdot \frac{\varkappa_a}{\varkappa_i + 2\varkappa_a} \cdot r_0 G\cos\theta, \tag{17}$$

oder:

$$T = T_0 + \frac{1}{2} \Delta T \cdot \cos\theta, \tag{18}$$

wo:

$$\Delta T = 6 \cdot \frac{\varkappa_a}{\varkappa_i + 2\,\varkappa_a} \cdot r_0 G,$$

die Temperaturdifferenz zwischen den Polen der Kugel, bezw. $y = 0$ und $x = \pm r_0$, bezeichnet.

Wir sehen hieraus, dass der Temperaturunterschied zwischen den Polen, ΔT, innerhalb eines sehr grossen Druckgebiets konstant bleibt, weil $\varkappa_a$ unabhängig von dem Gasdruck p ist, solange das Gas in dem MAXWELL'schen Gaszustand bleibt.

Die Druckunabhängigkeit von ΔT wird noch grösser, wenn die Temperaturdifferenz zwischen den Polen durch eine einseitige Bestrahlung, parallel zur x-Achse, erzeugt wird. Wird die Strahlung in der Oberflächenschicht der Kugel vollständig absorbiert, und ist die Intensität der Strahlung per cm^2, I, erhält man die folgenden Grenzbedingungen:

$$T_a = T_i \quad \text{und} \quad \varkappa_i \cdot \frac{dT_i}{dr} = \varkappa_a \cdot \frac{dT_a}{dr} + I \cos\theta, \tag{19}$$

woraus:

$$\Delta T_1 = \frac{2\,I}{\varkappa_i + 2\,\varkappa_a} r_0 \,^{13)}. \tag{20}$$

Ist $\varkappa_i$ gegenüber $\varkappa_a$ gross, wird ΔT_1 praktisch gesprochen unabhängig von dem Gasdruck p.

Aus der erweiterten MAXWELL'schen Grenzbedingung erhält man nun, weil:

$$\left.\begin{aligned} \frac{dT}{ds} = \left(\frac{1}{r} \cdot \frac{dT}{d\theta}\right)_{r = r_0} &= -\frac{3\,\varkappa_a}{\varkappa_i + 2\,\varkappa_a} \cdot G \sin\theta, \\ u_s = (u_\theta)_{r = r_0} \quad \text{und} \quad \frac{du_s}{dr} &= \left(\frac{du_\theta}{dr}\right)_{r = r_0} \end{aligned}\right\} \tag{21}$$

nach Einsetzung in (2):

[13] In diesem Wert von ΔT_1 ist der Einfluss von dem Temperatursprung an der Oberfläche der Kugel vernachlässigt. Wird auch hiermit gerechnet, muss die Bedingung:

$$T_a = T_i \text{ durch } T_i = T_a - \gamma_1 \cdot \left(\frac{dT_a}{dr}\right)_{r = r_0}$$

ersetzt werden.

Sind aber die Temperaturerhöhungen an den Polen der Kugel dem umgebenden Gase gegenüber klein, kann diese Korrektion vernachlässigt werden.

$$A = \frac{9}{4} k_1 \cdot \frac{\eta^2}{\varrho_0 T_0} \cdot \frac{\varkappa_a}{\varkappa_i + 2\varkappa_a} \cdot Gr_0 \cdot \frac{1}{\left(1 + 2k_2 \frac{\gamma}{r_0}\right)\left(1 + m \frac{\lambda}{r_0}\right)} \tag{22}$$

oder:

$$A = \frac{3}{8} k_1 \cdot \frac{\eta^2}{\varrho_0 T_0} \cdot \frac{1}{\left(1 + 2k_2 \frac{\lambda}{r_0}\right)\left(1 + m \frac{\lambda}{r_0}\right)} \cdot \Delta T \tag{23}$$

weil:

$$p\lambda = \sqrt{\frac{\pi}{2}} \cdot \frac{\eta}{\sqrt{{}_1\varrho}} = {}_1\lambda_0 \left(\frac{T}{T_0}\right)^{1+n} \quad \text{und} \quad \gamma = \sqrt{\frac{\pi}{2}} \cdot \frac{\eta}{p\sqrt{{}_1\varrho}} = \lambda.$$

Wir finden nun aus (7), da $2B = \frac{A}{\eta} \cdot r_0^2$:

$$K = 2\pi r_0^2 \int_0^{\pi} p_{x, r_0} \sin\theta \, d\theta = 6\pi A \int_0^{\pi} (2\cos^2\theta - 1) \sin\theta \, d\theta = -4\pi A,$$

oder:

$$K = -\frac{3\pi}{2} k_1 \cdot \frac{\eta^2}{\varrho_0 T_0} \Delta T \cdot \frac{1}{\left(1 + 2k_2 \frac{\lambda}{r_0}\right)\left(1 + m \frac{\lambda}{r_0}\right)}. \tag{24}$$

Für $\frac{\lambda}{r_0} \rightarrow 0$, findet man hieraus:

$$K_{1,\infty} = \frac{K_\infty}{\Delta T} = -\frac{3\pi}{2} k_1 \frac{\eta^2}{\varrho_0 T_0}, \tag{25}$$

oder den von HETTNER und EPSTEIN abgeleiteten Ausdruck, multipliciert mit dem Faktor $k_1 = \frac{4}{3}$.

Für $\frac{\lambda}{r_0} \rightarrow \infty$ erhält man:

$$K_{1,0} = \frac{K_0}{\Delta T} = -\frac{3\pi}{2} k_1 \frac{\eta^2}{\varrho_0 T_0} \cdot \frac{1}{2k_2 \left(\frac{\lambda}{r_0}\right)^2 m}, \tag{26}$$

oder, weil:

$$\frac{\pi}{2} \cdot \frac{\eta^2}{\varrho_0 T_0} = \lambda^2 \cdot \frac{p}{T_0},$$

$$K_{1,0} = -\frac{3}{2} \cdot \frac{p}{T_0} r_0^2 \cdot \frac{1}{m}, \tag{27}$$

worin der Wert von m noch unbekannt ist. —

Den Wert von $K_{1,0}$ können wir aber auch auf direkte Weise

ableiten; für $\frac{r_0}{\lambda} = 0$ hat man nach KNUDSEN für die Radiometerkraft dK_ν auf dem Oberflächenelement dS:

$$dK_\nu = -\frac{1}{4} a \cdot p \frac{T - T_0}{T} \cdot dS. \tag{28}$$

dK_ν ist die Radiometerkraft in der Richtung der Normale; T ist die Temperatur des Elementes dS, und p und T_0 der Druck und die Temperatur des Gases; a ist der Akkommodationskoefficient des Gases gegenüber der Oberfläche S.

Ist die Temperaturverteilung auf der Oberfläche der Kugel gegeben durch:

$$T - T_0 = \frac{1}{2} \Delta T \cos\theta,$$

erhält man, der Symmetrie wegen, die totale Radiometerkraft K_0 auf der Kugel mit Radius r_0:

$$\left.\begin{aligned} K_{1,0} = \frac{K_0}{\Delta T} = \frac{1}{\Delta T}\int dK_{\nu,x} = -\int \frac{1}{4}\frac{ap}{T_0} \cdot \frac{1}{2} \cos^2\theta \, dS \\ = -\frac{1}{8}\frac{ap}{T_0}\int_0^\pi \cos^2\theta \cdot 2\pi r_0 \sin\theta \cdot r_0 \, d\theta = -\frac{\pi}{6}\frac{a r_0^2}{T_0} \cdot p, \end{aligned}\right\} \tag{29}$$

in Übereinstimmung mit der von RUBINOWICZ abgeleiteten Formel.

Aus (27) und (29) folgt:

$$m = \frac{9}{\pi a} \quad \text{für} \quad \frac{r_0}{\lambda} = 0.$$

Inwieweit m in dem ganzen Gebiet $0 \leqq \frac{r_0}{\lambda} \leqq \infty$ diesen konstanten Wert hat, kann man a priori nicht mit Sicherheit sagen; erst wenn hinreichendes experimentelles Material vorliegt, kann dies festgestellt werden. Messungen in dem Gebiet $0 \leqq \frac{r_0}{\lambda} \leqq$ ca. 5 wären hierfür wünschenswert.

Mit diesem Wert von m erhält man für die Radiometerkraft in dem ganzen Gebiet: $0 \leqq \frac{r_0}{\lambda} \leqq \infty$, den Ausdruck:

$$K_1 = \frac{K}{\Delta T} = -\frac{3\pi}{2} k_1 \frac{\eta^2}{\varrho_0 T_0} \cdot \frac{1}{1 + \left(2k_2 + \frac{9}{\pi a}\right)\frac{\lambda}{r_0} + 2k_2 \cdot \frac{9}{\pi a} \cdot \left(\frac{\lambda}{r_0}\right)^2} \tag{30}$$

oder:
$$K_1 = \frac{K}{\Delta T} = -\frac{\pi}{6} a \frac{r_0^2}{T_0} \cdot \frac{p}{1 + \beta\left(\frac{r_0}{\lambda}\right) p + \alpha\left(\frac{r_0}{\lambda}\right)^2 \cdot p^2}, \tag{31}$$

worin:
$$\alpha = \frac{\pi}{24} a \quad \text{und} \quad \beta = \frac{3}{8} + \frac{\pi}{9} a, \quad \text{weil} \quad k_1 = k_2 = \frac{4}{3}^{14)}.$$

Aus dem Ausdruck für K_1 sehen wir, dass die Radiometerkraft bei dem Druck $p_{\max}$ ein Maximum, $K_{1,\max}$, hat, wo:
$$p_{\max} = \frac{{}_1\lambda}{r_0} \sqrt{\frac{1}{\alpha}} = \frac{{}_1\lambda}{r_0} \sqrt{\frac{24}{\pi a}}, \tag{32}$$

oder:
$$r_0 = \sqrt{\frac{24}{\pi}} \cdot \frac{\lambda_{\max}}{\sqrt{a}} = \frac{2{,}763}{\sqrt{a}} \cdot \lambda_{\max}.$$

Der Wert von $p_{\max}$ ist also unabhängig von der Temperaturdifferenz ΔT, wenn diese als unabhängig von p angesehen werden kann.

Der maximale Wert von K_1 wird in diesem Falle:
$$K_{1,\max} = \frac{K_{\max}}{\Delta T} = -\frac{\pi}{6} a \cdot \frac{{}_1\lambda}{T_0} \cdot \frac{1}{2\sqrt{\alpha} + \beta},$$

oder:
$$K_{1,\max} = -\frac{\pi}{6} \cdot \frac{r_0}{T_0} \cdot \frac{{}_1\lambda \cdot \sqrt{a}}{\sqrt{\frac{\pi}{6}} + \frac{\pi}{9}\sqrt{a} + \frac{3}{8} \cdot \frac{1}{\sqrt{a}}}. \tag{33}$$

Werden $K_{\max}$ und $p_{\max}$ als Einheiten für K und p verwendet, erhält man die »reducierte« Radiometerkurve:
$$\frac{K}{K_{\max}} = \frac{K_1}{K_{1,\max}} = \frac{2 + \delta}{\frac{p}{p_{\max}} + \frac{p_{\max}}{p} + \delta}, \quad \text{wo} \quad \delta = \frac{\beta}{\sqrt{\alpha}}, \tag{34}$$

14) Obwohl die Formel (31) den richtigen Grenzwert für $\frac{r_0}{\lambda} = 0$ gibt, ist nicht anzunehmen, dass der Wert $\beta = \frac{3}{8} + \frac{\pi}{9} a$ für das Gebiet $\frac{r_0}{\lambda} \to 0$ der Form nach richtig ist. Ausgehend von der Formel (29) für $\frac{r_0}{\lambda} = 0$, wird es möglich sein, den Einfluss von einsetzenden gegenseitigen Molekülstössen auf die Formel (29) zu berechnen, und hierdurch für das Gebiet $\frac{r_0}{\lambda} \to 0$ einen der Form nach besseren Wert für β zu berechnen.

oder:

$$\delta = \sqrt{\frac{24}{\pi}}\left(\frac{3}{8}\frac{1}{\sqrt{a}} + \frac{\pi}{9}\sqrt{a}\right).$$

Für $a = 1$ wird $\delta = 2{,}00$, für $a = 0{,}81$ $\delta = 2{,}02$ und für $a = 0{,}36$ $\delta = 2{,}30$, woraus erhellt, dass der Wert von a keinen grossen Einfluss auf den Wert von δ hat.

Durch die »reducierte« Radiometerkurve ist die von W. Westphal eingeführte Radiometerfunktion:

$$\frac{K}{K_{\max}} = f\left(\log \frac{p}{p_{\max}}\right) = f(x)$$

eindeutig bestimmt; wir finden aus der »reducierten« Radiometerkurve hierfür:

$$f(x) = \frac{2+\delta}{e^{x} + e^{-x} + \delta}, \quad \text{wo} \quad x = \log_e \frac{p}{p_{\max}}.$$

Wenn ΔT als konstant angesehen werden kann, kann die »reducierte« Radiometerkurve mit Vorteil verwendet werden, weil diese unabhängig ist von ΔT, die im Allgemeinen unbekannt ist.

Aus dem Ausdruck für K_1 sehen wir, dass die Radiometerkraft für $\frac{r_0}{\lambda} \gtrsim 0$ mit πr_0^2 proportional ist, also ein Oberflächeneffekt; für $\frac{r_0}{\lambda} \to \infty$ wird K_1, die Radiometerkraft für einen Temperaturunterschied von einem Grad zwischen den Polen, unabhängig von dem Radius der Kugel, während der Maximalwert, $K_{1,\max}$, proportional mit dem Radius ist.

Da aber die Temperaturdifferenz, ΔT, mit dem Radius der Kugel proportional ist, jedenfalls wenn die einfallende Strahlung vollständig in der Oberflächenschicht der Kugel absorbiert wird, sieht es aus, als ob die totale Radiometerkraft K für $\frac{r_0}{\lambda} \to \infty$ ein Randeffekt wäre.

Aus den zwei Formeln (32) und (33) kann man r_0 eliminieren und findet hieraus zur Bestimmung von ΔT:

$$K_{\max} \cdot p_{\max} = -\sqrt{\frac{2\pi}{3}} \cdot \frac{1}{T_0}\lambda^2 \cdot \frac{\Delta T}{\sqrt{\frac{\pi}{6}} + \frac{\pi}{9}\sqrt{a} + \frac{3}{8}\cdot\frac{1}{\sqrt{a}}}. \qquad (35)$$

3. Aus den in Par. 2 abgeleiteten Formeln erhellt die vollständige Analogie mit anderen bekannten Radiometererscheinungen, z. B. mit dem absoluten Manometer von MARTIN KNUDSEN, und mit der thermomolekularen Druckdifferenz. So finden wir auch für die Kugel, dass das Verhältnis zwischen der massgebenden Abmessung, r_0, und λ_{max} eine reine Zahl ist, weil:

$$\frac{r_0}{\lambda_{max}} = \frac{2{,}763}{\sqrt{a}}.$$

Wird der Wert von p_{max} gemessen, kann man aus dieser Formel r_0 bestimmen, weil der Einfluss von dem im Allgemeinen nicht so genau bekannten Akkommodationskoefficienten nicht sehr bedeutend ist; wird keine grosse Genauigkeit für r_0 verlangt, ist ein Annäherungswert für a hinreichend.

Da es bisher für mikroskopische Partikeln nur möglich war, mit Hilfe der Fallgeschwindigkeit und des Gesetzes von STOKES einen zuverlässigen Wert von r_0 zu erhalten, wäre es in dieser Verbindung von Interesse, durch Präcisionsmessungen die Formel für r_0 experimentell zu prüfen.

Aus den vorliegenden Messungen von J. MATTAUCH über die photophoretische Kraft auf mikroskopischen Tellurkugeln mit Radien von 3 bis $4 \cdot 10^{-5}$ cm ergibt sich, das p_{max} ca. 400 mm Hg ist; das benutzte Gas war Stickstoff, und wir können also annäherungsweise $a = 0{,}81$ setzen.

Aus der Formel erhält man somit:

$$\left(\frac{r_0}{\lambda_{max}}\right)_{ber.} = \frac{2{,}763}{\sqrt{a}} = 3{,}07,$$

während man mit $r_0 = 3{,}5 \cdot 10^{-5}$ cm und $p_{max} = 400$ mm Hg $= 400 \cdot 1330$ Bar findet:

$$\left(\frac{r_0}{\lambda_{max}}\right)_{obs.} = \frac{3.5 \cdot 10^{-4}}{6{,}42} \cdot 400 \cdot 1330 = 2{,}91,$$

weil für Stickstoff $(p\lambda)_{20°} = 6{,}42$.

Wenn die Unsicherheit der experimentellen Grössen in Betracht gezogen wird, muss die Übereinstimmung als befriedigend angesehen werden.

Später hat MATTAUCH eine experimentelle, sehr ausgebreitete Untersuchung mit sechs Probekörpern aus Selen durchgeführt; die Radien von diesen Probekörpern lagen nach seiner Angabe zwischen 2 und $3 \cdot 10^{-5}$ cm. —

MATTAUCH[15] hat in dieser Untersuchung mit einem verbesserten EHRENHAFT'schen Kondensator die Radiometerkraft oder die photophoretische Kraft auf diesen sechs Probekörpern in atm. Luft in einem grossen Druckgebiet untersucht und den Wert von $\frac{K}{e}$ (e = electr. Elementarquantum = $4{,}77 \cdot 10^{-10}$ e.st.E.) bei verschiedenen Drucken, p, gemessen, so dass die Werte von K_{max} und p_{max} bestimmt werden konnten, da die Probekörper nur eine Elementarladung hatten.

In der Tabelle I, Kolonne 2 und 3, sind die gemessenen Werte von p_{max} und $\left(\frac{K}{e}\right)_{max}$ angegeben, und in Kolonne 4 die Werte von K_{max}; diese sind von der Grössenordnung 5 bis $10 \cdot 10^{-10}$ Dyn. In Kolonne 5 stehen die aus den Werten für p_{max} berech-

Tabelle I.

No. des Pk.	p_{max} mm Hg	$\frac{K_{max}}{e}$	K_{max}	r_0, ber. (a = 0,81)	$p_{max} \cdot K_{max}$ (p in Bar.)	ΔT
36	282	1,44	$6{,}86 \cdot 10^{-10}$	$5{,}35 \cdot 10^{-5}$	$2{,}57 \cdot 10^{-4}$	$1{,}77 \cdot 10^{-3}$
37	399	0,94	4,48 »	3,79 »	2,38 »	1,63 »
59	620	1,08	5,15 »	2,44 »	4,25 »	2,92 »
69	473	1,17	5,58 »	3,20 »	3,51 »	2,41 »
74	452	2,37	11,30 »	3,35 »	6,79 »	4,67 »
76	570	1,41	6,72 »	2,66 »	5,09 »	3,50 »

neten Radien der Probekörper; bei der Berechnung ist $a = 0{,}81$ und $(p\lambda)_{20} = {}_1\lambda_{20} = 6{,}65$ verwendet. In Kolonne 6 sind die Werte von $K_{max} \cdot p_{max}$ angegeben, und in Kolonne 7 die hieraus nach Formel (35) berechneten Werte für ΔT.

Die Werte von K_{max} in Kolonne 4 sind nicht für den überlagerten Lichtdruck korrigiert, weil MATTAUCH mitteilt, dass der Lichtdruck jedenfalls um mehr als eine Grössenordnung kleiner ist als die photophoretischen Kräfte.

[15] J. MATTAUCH: loc. cit. S. 978.

MATTAUCH hat selber das ganze Beobachtungsmaterial für die sechs Probekörper bei den verschiedenen Drucken durch die reducierte Kurve $\left(\frac{K}{K_{max}}, \log_{10}\frac{p}{p_{max}}\right)$ wiedergegeben, und in Fig. 1 ist seine graphische Darstellung von dem Beobachtungsmaterial

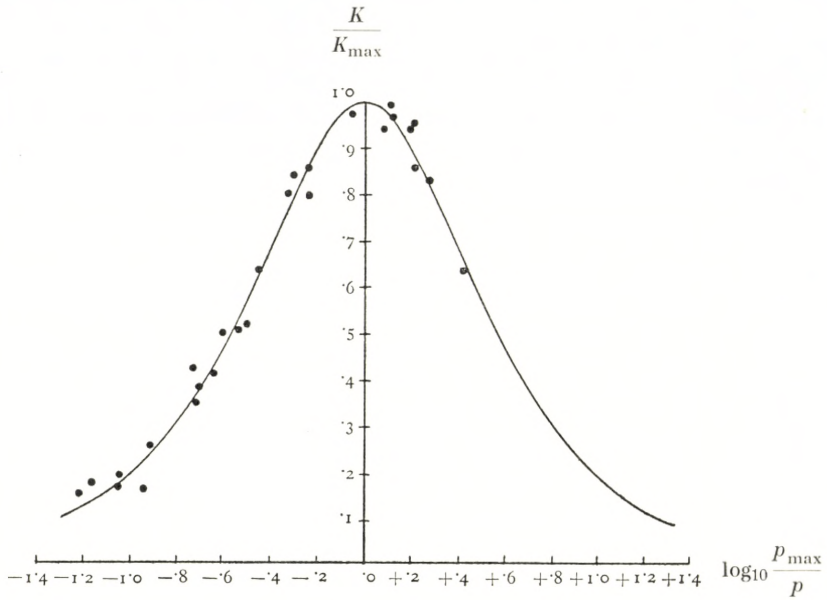

Fig. 1.

reproduciert. Diese Kurve muss also mit der theoretischen »reducierten« Formel:

$$\frac{K}{K_{max}} = \frac{2+\delta}{\frac{p}{p_{max}} + \frac{p_{max}}{p} + \delta}, \quad \text{wo} \quad \delta = \frac{\beta}{\sqrt{\alpha}},$$

übereinstimmen; nach der Berechnung muss für $a = 0{,}81$ $\delta =$ ca. 2,00 sein. In der Tabelle II sind in Kolonne 6 die Werte für $\frac{K}{K_{max}}$, genommen aus der graphischen Darstellung von MATTAUCH, angegeben und zur Vergleichung in den Kolonnen 3, 4 und 5 die theoretischen Werte, berechnet mit $\delta = 0$, $\delta = 1$ und $\delta = 2$. Der Wert $\delta = 0$ ist natürlich nicht theoretisch möglich,

ist aber hier mitgenommen, weil $\delta = 0$ der HETTNER'schen Interpolationsformel:

$$\frac{1}{K} = \frac{1}{K_0} + \frac{1}{K_\infty},$$

entspricht.

Aus der Tabelle II sieht man, dass die Übereinstimmung zwischen den berechneten und beobachteten Werten besser ist mit $\delta = 1$ als mit dem theoretischen Wert $\delta = 2$; ob die Genauigkeit dieser schwierigen Messungen so gross ist, dass dies eine Realität ist, dürfte aber ausserordentlich zweifelhaft sein. In grossen Zügen ist aber die Übereinstimmung befriedigend, und erst neue experimentelle Untersuchungen können über den genauen Wert von δ Auskunft geben.

Tabelle II.

$\log_{10}\frac{p}{p_{max}}$	$\frac{p}{p_{max}} + \frac{p_{max}}{p}$	$\frac{K}{K_{max}}$, teor.			$\frac{K}{K_{max}}$, beob.
		$\delta = 2$	$\delta = 1$	$\delta = 0$	
0,0	2,000	1,000	1,000	1,000	1,00
0,1	2,054	0,985	0,980	0,975	0,98
0,2	2,217	0,950	0,935	0,905	0,93
0,3	2,496	0,890	0,855	0,800	0,82
0,4	2,911	0,815	0,770	0,690	0,70
0,6	4,232	0,643	0,575	0,473	0,48
0,8	6,469	0,473	0,402	0,308	0,33
1,0	10,10	0,330	0,270	0,198	0,21
1,2	16,40	0,218	0,172	0,122	0,15
1,4	25,15	—	—	—	—

MATTAUCH hat auch versucht, den Einfluss des Gases zu bestimmen, wobei er mit zwei metallischen Probekörpern in Stickstoff, Wasserstoff und Kohlensäure gemessen hat.

Diese Versuche sind aber, der grossen experimentellen Schwierigkeiten wegen, nicht hinreichend gelungen, und es ist nicht möglich, hieraus einen Einfluss des Gases experimentell festzustellen; dies war aber auch theoretisch nicht zu erwarten, weil nach Formel (33) die Radiometerkraft praktisch gesprochen proportional mit ${}_1\lambda\sqrt{a}$ ist. Aus der Tabelle III, worin die Werte

Tabelle III.

Gas	$(p\lambda)_{273,1} = {}_1\lambda_0$	Akkommodations-koefficient a	${}_1\lambda_0 \sqrt{a}$
Argon	6,23	0,85	5,75
H_2	11,32	0,28	6,00
O_2	6,36	0,81	5,73
N_2	5,91	0,81	5,32
Atm. Luft	6,20	0,81	5,58
Neon	11,75	0,65	9,55
Helium	17,85	0,34	10,40
CO_2	4,00	0,81	3,60

von ${}_1\lambda \sqrt{a}$ für die verschiedenen Gase angegeben sind, erhellt, dass für metallische Probekörper in atm. Luft, Stickstoff und Wasserstoff kein grosser Unterschied zu erwarten ist. Nur wenn Neon oder Helium verwendet wird, kann man einen grösseren Unterschied erwarten.

4. Es liegt nahe, zu versuchen, die für die Kugel gebrauchte Ableitung auch für einen zirkularen Zylinder zu verwenden, um die Radiometerkraft in einem WESTPHAL'schen Quarzfadenradiometer und verwandten Radiometersystemen zu bestimmen.

Es ist der Verdienst von G. FANSELAU[16], dass er für diesen Fall eine brauchbare Lösung des Strömungsproblemes abgeleitet und anschliessend hieran die Radiometerkraft auf einem runden Faden berechnet hat, und zwar für den Fall, dass $\frac{r_0}{\lambda} \rightarrow \infty$.

Zu diesem Zweck untersuchte er den Strömungszustand für eine zähe Flüssigkeit und eine sehr langsame Strömung um einen zirkularen Zylinder mit Radius r_0, umgeben von einem coaxialen Zylinder mit Radius R; die Strömung findet in Ebenen senkrecht zur Achse der coaxialen Zylinder statt. Mit der Zylinderachse als z-Achse erhielt FANSELAU für die Stromfunktion:

$$\psi_5 = y f_3(r) = y \left[c_1 r^2 + c_2 \ln r + \frac{c_3}{r^2} + c_4 \right]. \qquad (36)$$

[16] G. FANSELAU: Dissertation, Berlin, 1927, S. 8.

Auf bekannte Weise wird hieraus der Drucktensor p berechnet und hiernach der Impulstransport, bzw. die Radiometerkraft per Längeneinheit des Zylinders:

$$K = \int (p_{x,r})_{r=r_0} \cdot r_0 d\theta .$$

FANSELAU findet nach Ausführung der Integration hierfür:

$$K = -4\pi\eta \cdot c_2 . \tag{37}$$

Wir werden nun untersuchen, ob es möglich ist, die Konstante c_2 durch die bekannten Grenzbedingungen zu bestimmen.

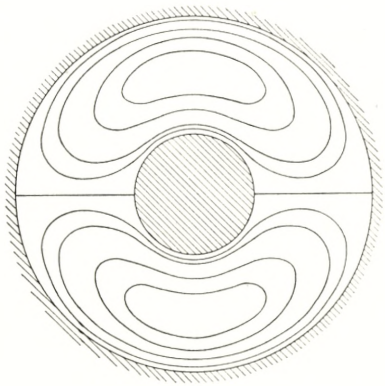

Fig. 2.

Die Stromlinien in den Ebenen, z = konst. (Fig. 2), sind gegeben durch:

$$\psi_5 = y \left[c_1 r^2 + c_2 \ln r + \frac{c_3}{r^2} + c_4 \right] = \text{const.} \tag{38}$$

und die Strömungsgeschwindigkeiten u und v in der x- und y-Richtung durch:

$$u = \frac{d\psi_5}{dy} = f_3(r) + \frac{y^2}{r} f_3'(r)$$

und

$$v = -\frac{d\psi_5}{dx} = -\frac{xy}{r} f_3'(r) .$$

Für die tangentiale Geschwindigkeit, u_s, und für die normale Geschwindigkeit, u_r, erhält man:

$$\left.\begin{aligned} u_s &= u\frac{y}{r} - v\frac{x}{r} = \frac{y}{r}\left[f_3(r) + rf_3'(r)\right] \\ \text{und} \qquad u_r &= u\frac{x}{r} + v\frac{y}{r} = \frac{x}{r}f_3(r). \end{aligned}\right\} \tag{39}$$

Für $r = r_0$ und $r = R$ muss für alle Werte von x, $u_{r_0} = u_R = 0$ sein, woraus:

$$f_3(r) = 0 \quad \text{für} \quad r = r_0 \quad \text{und} \quad r = R.$$

Für $r = r_0$ ist die Tangentialgeschwindigkeit u_s durch die erweiterte MAXWELL'sche Grenzbedingung bestimmt, während wir, jedenfalls wenn $r \ll R$, die Tangentialgeschwindigkeit u_s an der Oberfläche des äusseren Zylinders gleich Null setzen können; da für $r = R$, $f_3(r) = 0$, erhält man hierdurch aus (39):

$$f_3'(r) = 0 \quad \text{für} \quad r = R,$$

wozu also die erweiterte MAXWELL'sche Grenzbedingung für $r = r_0$ kommt:

$$u_s - k_2\gamma \cdot \frac{du_s}{dr} = \frac{3}{4}k_1\frac{\eta}{\varrho T} \cdot \frac{1}{1+\varphi\left(\frac{\lambda}{r_0}\right)} \cdot \frac{dT}{ds}, \tag{40}$$

worin:

$$\frac{dT}{ds} = \frac{1}{r_0} \cdot \frac{dT}{d\theta},$$

und in erster Annäherung:

$$\varphi\left(\frac{\lambda}{r_0}\right) = m\frac{\lambda}{r_0}.$$

Aus den drei ersten Bedingungen wird erhalten:

$$c_1 = \alpha'\frac{1}{R^2 - r_0^2}C', \quad c_2 = \frac{\alpha'}{ln\frac{R}{r_0}}, \quad c_3 = \alpha'\frac{R^2 \cdot r_0^2}{R^2 - r_0^2}[1 + C']$$

und:

$$c_4 = -c_1 r_0^2 - c_2 \ln r_0 - \frac{c_3}{r_0^2}, \quad \text{wo} \quad C' = \frac{r_0^2 - R^2 + 2 r_0^2 \ln \frac{R}{r_0}}{(R^2 - r_0^2)\, 2 \ln \frac{R}{r_0}}.$$

α' ist eine willkürliche Konstante, die durch die erweiterte MAXWELL'sche Grenzbedingung bestimmt werden muss.

Wir finden für $r = r_0$:

$$u_s = \left(u \frac{y}{r} - v \frac{x}{r}\right)_{r=r_0} = \frac{y}{r} \left[f_3(r) + r f_3'(r)\right]_{r=r_0} = \left[f_3(r_0) + r_0 f_3'(r_0)\right] \sin\theta,$$

oder, da $f_3(r_0) = 0$:

$$(u_s)_{r=r_0} = r_0 f_3'(r_0) \sin\theta = \alpha' C'' \sin\theta,$$

wo:

$$C'' = \frac{1}{R^2 - r_0^2}\left[r_0^2 - R^2 (1 + C')\right] + \frac{1}{\ln \frac{R}{r_0}},$$

oder, wenn $r_0 \ll R$:

$$C_\infty'' = \underset{\lim \frac{r_0}{R} \to 0}{C''} = -2 \cdot \frac{\ln \frac{R}{r_0} - 1}{\ln \frac{R}{r_0}}. \tag{41}$$

Für $r = r_0$ und $r_0 \ll R$ wird:

$$\frac{du_s}{dr} = \left[2 f_3'(r) + r f_3''(r)\right]_{r=r_0} \cdot \sin\theta = 2 f_3'(r) \cdot \sin\theta \left[1 + \frac{r}{2} \cdot \frac{f_3''(r)}{f_3'(r)}\right]_{r=r_0},$$

oder:

$$\frac{du_s}{dr} = 2 \cdot \frac{u_s}{r_0}\left[1 + \frac{r_0}{2} \cdot \frac{f_3''(r_0)}{f_3'(r_0)}\right] = \frac{u_s}{r_0} \cdot \frac{\ln \frac{R}{r_0}}{1 - \ln \frac{R}{r_0}}.$$

Nach Einsetzung in (40) bekommt man:

$$(u_s)_{r=r_0} = \frac{3}{4} k_1 \cdot \frac{\eta}{\varrho T} \cdot \frac{1}{r_0 \left[1 + k_2 \frac{\gamma}{r_0} \cdot \frac{\ln \frac{R}{r_0}}{\ln \frac{R}{r_0} - 1}\right]\left[1 + m \frac{\lambda}{r_0}\right]} \cdot \frac{dT}{d\theta} = q \cdot \frac{dT}{d\theta}.$$

Aus den zwei Ausdrücken für $(u_s)_{r=r_0}$ erhält man:

$$(u_s)_{r=r_0} = q \cdot \frac{dT}{d\theta} = \alpha' C'' \sin\theta . \tag{42}$$

Diese Gleichung kann nur erfüllt werden, wenn:

$$T = M\cos\theta + \text{const.}$$

oder:

$$T = T_0 + \frac{1}{2}\Delta T \cdot \cos\theta ,$$

wo ΔT den Temperaturunterschied zwischen den Punkten, $y = 0$ und $x = \pm r_0$, bezeichnet.

Diese Temperaturverteilung auf der Zylinderoberfläche ist in Übereinstimmung mit der Lösung des Wärmeleitungsproblemes, wenn die Temperatur innerhalb des Zylinders, T_i, und die Temperatur ausserhalb des Zylinders, T_a, wie folgt angesetzt werden:

$$T_i - T_0 = P\cos\theta \quad \text{und} \quad T_a - T_0 = Q + S \cdot \frac{\cos\theta}{r} .$$

Nach Einsetzung von C'' und $\frac{dT}{d\theta}$ in (42) wird erhalten:

$$\alpha' = -\frac{1}{2}\Delta T \frac{q}{C''} =$$

$$= -\frac{1}{2}\Delta T \cdot \frac{3}{4} k_1 \frac{\eta}{\varrho T} \cdot \frac{1}{C''} \cdot \frac{1}{r_0\left[1 + k_2 \frac{\gamma}{r_0} \cdot \frac{\ln\frac{R}{r_0}}{\ln\frac{R}{r_0} - 1}\right]\left[1 + m\frac{\lambda}{r_0}\right]} \tag{43}$$

woraus nach (37) für $r_0 \ll R$, da $\gamma = \lambda$:

$$K = -4\pi\eta c_2 = -4\pi\eta \frac{\alpha'}{\ln\frac{R}{r_0}} =$$

$$= -\frac{3\pi}{2} k_1 \cdot \frac{\eta^2}{\varrho T} \cdot \Delta T \cdot \frac{1}{2 r_0\left(\ln\frac{R}{r_0} - 1\right)} \cdot \frac{1}{\left\langle 1 + k_2 \frac{\lambda}{r_0} \frac{\ln\frac{R}{r_0}}{\ln\frac{R}{r_0} - 1} \right\rangle \left(1 + m\frac{\lambda}{r_0}\right)} \tag{44}$$

Da $k_1 = k_2 = \frac{4}{3}$ und $\frac{\pi}{2} \cdot \frac{\eta^2}{\varrho T} = p \frac{\lambda^2}{T}$, wird für $\frac{\lambda}{r_0} \rightarrow \infty$ erhalten:

$$K_{1,0} = \frac{K_0}{\Delta T} = -3 k_1 \frac{p}{T_0} \cdot \lambda^2 \cdot \frac{r_0}{2 m k_2 \cdot \lambda^2 \ln \frac{R}{r_0}} = -\frac{3}{2} \frac{p}{T_0} \cdot \frac{r_0}{\ln \frac{R}{r_0}} \cdot \frac{1}{m}. \quad (45)$$

Für $\frac{\lambda}{r_0} \rightarrow \infty$ finden wir durch direkte Berechnung, wenn die Temperaturverteilung auf der Oberfläche des Zylinders ist:

$$T = T_0 + \frac{1}{2} \Delta T \cdot \cos \theta,$$

$$K_0 = -2 \int_0^{\pi} \frac{1}{4} a \frac{p}{T} \cdot \frac{1}{2} \Delta T \cdot \cos^2 \theta \cdot r_0 \, d\theta$$

oder:

$$K_{1,0} = \frac{K_0}{\Delta T} = -\frac{\pi}{8} a \frac{p}{T} \cdot r_0 .$$

Aus den zwei Ausdrücken für $K_{1,0}$ erhält man:

$$m = \frac{12}{\pi} \cdot \frac{1}{a} \cdot \frac{1}{\ln \frac{R}{r_0}},$$

wo a der Akkommodationskoefficient des Gases gegenüber der Zylinderoberfläche ist. Mit diesem Wert für m findet man leicht aus (44):

$$K_1 = -\frac{\pi}{8} a \frac{r_0}{T_0} \cdot \frac{p}{1 + \beta \left(\frac{r_0}{\lambda}\right) p + \alpha \left(\frac{r_0}{\lambda}\right)^2 \cdot p^2}, \quad (47)$$

worin:

$$\alpha = \frac{\pi}{16} a \left[\ln \frac{R}{r_0} - 1 \right] \quad \text{und} \quad \beta = \frac{\pi}{12} a \ln \frac{R}{r_0} + \frac{3}{4} \cdot \frac{\ln \frac{R}{r_0} - 1}{\ln \frac{R}{r_0}}.$$

Aus der Formel für K_1 wird, wenn ΔT unabhängig von p ist, auf bekannte Weise gefunden:

$$p_{\max} = \frac{{}_1\lambda}{r_0}\sqrt{\frac{1}{\alpha}}, \quad \text{oder} \quad \lambda_{\max} = r_0\sqrt{\alpha}$$

und:

$$K_{1,\max} = -\frac{\pi}{8}\,a \cdot \frac{{}_1\lambda}{T_0} \cdot \frac{1}{\beta + 2\sqrt{\alpha}}. \qquad (48)$$

Hieraus erhellt, dass in diesem Falle $p_{\max}$ proportional mit ${}_1\lambda$ und unabhängig von ΔT wird.

$K_{1,\max} = \frac{K_{\max}}{\Delta T}$ wird praktisch gesprochen unabhängig von r_0, weil $\beta + 2\sqrt{\alpha}$ nur von $ln\,\frac{R}{r_0}$ abhängig ist und sich also nur langsam mit r_0 ändert, während die Radiometerkraft, K, für $\frac{\lambda}{r_0} \to 0$ praktisch gesprochen umgekehrt proportional mit dem Diameter, $2r_0$, des Fadens ist. Bei Bestrahlung wird die erzeugte Temperaturdifferenz, ΔT, proportional mit dem Radius, r_0, sodass die totale Radiometerkraft, K, auf dem Faden für $\frac{\lambda}{r_0} \to 0$ praktisch gesprochen unabhängig von der Dicke des Fadens wird.

Der Verlauf von der Radiometerkraft K in dem ganzen Gebiet $0 \leqq \frac{\lambda}{r} \leqq \infty$ wird auch, wenn ΔT konstant ist, gegeben durch:

$$\frac{K_1}{K_{1,\max}} = \frac{K}{K_{\max}} = \frac{2+\delta}{\frac{p}{p_{\max}} + \frac{p_{\max}}{p} + \delta}, \quad \text{mit} \quad \delta = \frac{\beta}{\sqrt{\alpha}},$$

also durch die bekannte »reducierte« Radiometerfunktion; δ ändert sich also in diesem Falle mit dem Wert von $ln\,\frac{R}{r_0}$; wird $ln\,\frac{R}{r_0} \gg 1$, erhält man:

$$\delta = \frac{\sqrt{\pi}}{3}\sqrt{a\,ln\,\frac{R}{r_0}} + \frac{1}{\frac{\sqrt{\pi}}{3}\sqrt{a\,ln\,\frac{R}{r_0}}},$$

woraus hervorgeht, dass der Wert von δ sich nur langsam mit $a\,ln\,\frac{R}{r_0}$ ändert, wenn der Wert von $\frac{\sqrt{\pi}}{3}\sqrt{a\,ln\,\frac{R}{r_0}}$ in der Nähe von 1 ist.

5. In dem WESTPHAL'schen Quarzfadenradiometer besteht der Radiometerkörper aus einem vertikalen berussten Quarzfaden mit Radius r_0, der in der Achse eines coaxialen Glaszylinders mit dem Radius R aufgehängt worden ist. Wird der berusste Quarzfaden durch eine einseitige Strahlung mit der Intensität I per cm^2 senkrecht zur Röhre bestrahlt, entsteht zwischen den Punkten, $y = 0$, $x = \pm r_0$, in dem berussten Quarzdraht eine Temperaturdifferenz, ΔT, und eine Radiometerkraft in der Richtung der Strahlung. Wird die ganze Strahlung in der Oberfläche des Fadens absorbiert, erhält man für ΔT:

$$\Delta T = \frac{2\,I}{\varkappa_i + \varkappa_a} r_0 . \tag{49}$$

Für geschmolzenes Quarz ist $\varkappa_i = 33 \cdot 10^{-4}$ cal/cm Gr. Sek., während für Wasserstoff $\varkappa_a = 4{,}2 \cdot 10^{-4}$ cal/cm Gr. Sek. ist, woraus erhellt, dass ΔT sich nur wenig ändert, selbst wenn der Gasdruck sehr niedrig wird. — Für das WESTPHAL'sche Radiometer ist die in Par. 4 entwickelte Theorie brauchbar, wenn $\frac{r_0}{R} \ll 1$, und wenn die Strömung in Ebenen senkrecht zu dem Quarzfaden, bzw. zur Röhrenachse, verläuft.

WILHELM WESTPHAL hat auch sein Instrument experimentell untersucht und hat sowohl die Abmessungen des berussten Quarzfadens und der Röhre, als auch das benutzte Gas variiert; für die verwendeten Apparate war $\frac{r_0}{R}$ = ca. 2 à $3 \cdot 10^{-3}$, sodass die erste Bedingung für seine Messungen erfüllt gewesen ist.

Für die reducierte Radiometerfunktion:

$$\frac{K}{K_{\max}} = f\left(\log \frac{p}{p_{\max}}\right),$$

hat WESTPHAL die richtige symmetrische Form gefunden; es stellt sich aber heraus, dass die beobachteten Werte für $p_{\max}$ nicht mit den aus der Formel (48):

$$p_{\max} = \frac{1}{r_0}\frac{\lambda}{\sqrt{\alpha}} \quad \text{oder} \quad \lambda_{\max} = r_0 \sqrt{\alpha},$$

wo:

$$\alpha = \frac{\pi}{16} a \left(ln \frac{R}{r_0} - 1 \right),$$

berechneten Werten übereinstimmen.

Ausserdem fand WESTPHAL für atm. Luft, dass:

$$\lambda_{max} = 8{,}0 \cdot r_0 \cdot d,$$

wo d der Abstand des Fadens von der Glaswand ist.

Für die untersuchten Gase, H_2, CO_2 und atm. Luft stellte es sich auch heraus, dass p_{max} nicht proportional mit ${}_1\lambda$ war.

In der Tabelle IV sind zur Erläuterung der Abweichungen die berechneten und beobachteten Werte für p_{max} angegeben:

Tabelle IV.

Quarzfadenradiometer $\begin{cases} 2\,r_0 \text{ (berusst)} = 0{,}0025 \text{ cm.} \\ 2\,R = 0{,}80 \text{ cm.} \end{cases}$

Gas	Akkommodations-koefficient α	$p_{max,ber.}$	$p_{max,obs.}$
H_2	0,72	4,3 mm Hg	0,98 mm Hg
Atm. Luft	0,96	2,0 — —	0,93 — —
CO_2	0,96	1,3 — —	0,73 — —

Hieraus erhellt, dass die Abweichungen so gross sind, dass nicht angenommen werden kann, dass die zweite principielle Voraussetzung für die Ableitung der Formel (47), nämlich, dass die Strömung nur in Ebenen senkrecht zu dem Quarzfaden stattfindet, erfüllt gewesen ist.

Bei den WESTPHAL'schen Experimenten, worin die Strahlung von der Nernstlampe wahrscheinlich nicht hinreichend abgeblendet oder auf dem Faden fokussiert war, muss man erwarten, dass bei den verhältnissmässig hohen Drucken, bei welchen K_{max} eintritt, vertikale Konvektionsströme einsetzen und den Verlauf der Radiometerkraft ändern, so dass die Werte von K_{max} und p_{max} bedeutend geändert und erniedrigt werden. Die in atm. Luft gefundene Relation, $\lambda_{max} = \text{const.}\ r_0 \cdot d$, deutet auch darauf hin.

Da das WESTPHAL'sche Radiometer durch seine einfache Konstruktion, momentane Einstellung und grosse Erschütterungs-

freiheit grosse experimentelle Vorteile bietet, wäre es von grosser Bedeutung, zu versuchen hierfür eine rationelle Konstruktion, z. B. durch zweckmässige Erzeugung von dem Temperaturgefälle in der Oberfläche des Fadens, zu finden. Durch passende Wahl der Form und Abmessungen, kombiniert mit Abschirmvorrichtungen, wäre es wahrscheinlich möglich, den Einfluss von eventuellen Konvektionsströmen zu beseitigen[17].

6. Aus dem vorigen Abschnitt erhellt, dass es nicht möglich ist, mit dem vorliegenden experimentellen Material für das WESTPHAL'sche Fadenradiometer die abgeleiteten Formeln zu prüfen; dies kann aber annäherungsweise gemacht werden durch die von MARTIN KNUDSEN[18] und von R. E. H. RASMUSSEN[19] ausgeführten Messungen über die KNUDSEN'sche Radiometerkraft, welche in verschiedenen Akkommodationskoefficienten der beiden Seiten eines geheizten Radiometerkörpers ihre Ursache hat.

Diese Untersuchungen können sowohl mit einem runden Draht, als auch mit einem flachen Band ausgeführt werden, wenn nur die zwei Hälften des Drahtes oder die zwei Seiten des Bandes dem Gase gegenüber verschiedene Akkommodationskoefficienten haben. Ein dünnes, flaches Band hat grosse experimentelle Vorteile, verursacht aber bei der theoretischen Berechnung grosse Schwierigkeiten, insbesondere bei hohen Drucken.

MARTIN KNUDSEN wie auch R. E. H. RASMUSSEN arbeiteten in ihren Untersuchungen mit einem oben und unten festmontierten flachen Platinband; dies wurde durch elektrische Heizung auf der konstanten Temperatur, T_1, gehalten. Die zwei Seiten des Bandes hatten verschiedene Akkommodationskoefficienten, a_2 und a_1 ($a_2 > a_1$), weil die eine Seite mit Platinschwarz rauh gemacht war, während die andere Seite blank war.

Der Temperaturunterschied zwischen den zwei Seiten, d. h. die Temperaturdifferenz der an das Band grenzenden Gasschich-

[17] Eine Konstruktion von dem WESTPHAL'schen Quarzfaden-radiometer in Analogie mit dem Quarzfaden-electrometer von PERUCCA und LEISS (Z. f. Ph. 49, 1928 S. 604) wäre z. B. eine Möglichkeit; wird der Quarzfaden vor der Berussung nur an einer Seite vergoldet, kann eine angemessene Temperaturdifferenz in der Oberfläche des Fadens durch elektrische Heizung erzeugt werden. —

[18] MARTIN KNUDSEN: loc. cit.

[19] R. E. H. RASMUSSEN: D. Kgl. Danske Vidensk. Selskab, Mat.-fys. Medd. XI, 9, 1932. D. Kgl. Danske Vidensk. Selskab, Mat.-fys. Medd. XIII, 9, 1935.

ten, ΔT, wird durch den Unterschied des Temperatursprunges an beiden Seiten des Bandes bestimmt.

Bei der Messung der Radiometerkraft muss im Allgemeinen die Aufmerksamkeit darauf gelenkt sein, dass sich in den meisten Apparaten die Radiometerkraft mit der Bewegung des Radiometerkörpers ändert, sodass es in den meisten Fällen notwendig ist, eine Kompensationsmethode zu verwenden.

In der einen von KNUDSEN und RASMUSSEN gebrauchten Aufstellung, worin das Band mit Breite B in der Achse eines zylindrischen Glasrohres mit dem Diameter $2R$ und der Temperatur T_0 ausgespannt war, wurde eine hübsche magnetische Kompensation von dem Ausschlage des Bandes verwendet. In dem anderen Messapparat waren zwei gleiche Bänder symmetrisch in einer Drehwaage montiert, deren Achse mit der Achse des umgebenden Glaszylinders zusammenfiel. In dieser Aufstellung hat die Drehung des Radiometerkörpers keinen Einfluss auf die ausgeübte Radiometerkraft. Diese letzte Methode ist sehr empfindlich, hat aber den Nachteil, dass die Messbänder ausserhalb der Achse des umgebenden Zylinders stehen, so dass hierfür eine Korrektion in die Formeln eingeführt werden muss. Die Beobachtungen nach den zwei Methoden stimmen aber befriedigend überein, wenn die Messgenauigkeit in Betracht gezogen wird.

Die Ableitung der hydrodynamischen Strömung und der Radiometerformel für ein flaches Band konnte man, wenn $\frac{B}{\lambda} \to \infty$, wahrscheinlich durch einen Grenzübergang aus der Strömung und der Radiometerformel für einen elliptischen Zylinder ableiten; hierdurch konnte man einerseits die bereits abgeleitete Formel für den zirkularen Zylinder und andererseits die Formel für ein flaches Band erhalten. In dem analogen Fall »Kugel-zirkulare Planscheibe« ist diese Berechnung bereits von TH. SEXL[20] und P. EPSTEIN[21] durchgeführt, nachdem sie laut unabhängigen Methoden die hydrodynamische Strömung und die Radiometerkraft für ein Rotationsellipsoid berechnet haben.

Für den Zustand, karakterisiert durch $\frac{r_0}{\lambda} \to \infty$, haben beide

[20] TH. SEXL: Z. S. Ph. 52, 1928, S. 249.
[21] P. EPSTEIN: loc. cit.

dasselbe Resultat erhalten und für eine Kugel und eine zirkulare Planscheibe mit demselben Radius gefunden:

$$\frac{K'_{1,\infty}\,(\text{Scheibe})}{K'_{1,\infty}\,(\text{Kugel})} = \sigma = 2. \tag{50}$$

In Analogie hiermit wollen wir, ausgehend von der abgeleiteten Formel für den zirkularen Zylinder mit Diameter, $2\,r_0$:

$$K_1 = \frac{K}{\Delta T} =$$

$$= -\frac{3\,\pi}{2}\,k_1 \cdot \frac{\eta^2}{\varrho\,T} \cdot \frac{1}{2\,r_0\left[ln\,\frac{R}{r_0} - 1\right]\left[1 + k_2\,\frac{ln\,\frac{R}{r_0}}{ln\,\frac{R}{r_0} - 1}\,\frac{\lambda}{r_0}\right]\left[1 + m\,\frac{\lambda}{r_0}\right]}$$

für das flache Band mit Breite B schreiben:

$$K'_1 = \frac{K'}{\Delta T} =$$

$$= -\sigma \cdot \frac{3\,\pi}{2}\,k_1 \cdot \frac{\eta^2}{\varrho\,T} \cdot \frac{1}{\frac{2\,B}{\pi}\,(f-1)\left(1 + k_2\,\frac{f}{f-1} \cdot \pi\,\frac{\lambda}{B}\right)\left(1 + m_1\,\frac{\lambda}{B}\right)}, \tag{51}$$

indem wir in Analogie mit der Wärmeleitung setzen:

$$2\,\pi\,r_0 = 2\,B \quad \text{und} \quad ln\,\frac{R}{r_0} = ln\,\frac{2\,\pi R}{2\,B} = f.$$

Hieraus folgt für $\frac{\lambda}{r_0}$, bzw. $\frac{\lambda}{B} \rightarrow 0$, dass:

$$\frac{K_{1,\infty}\,(\text{Band})}{K'_{1,\infty}\,(\text{Zylinder})} = \frac{\pi}{2} \cdot \sigma \cdot \frac{2\,r_0}{B} \cdot \frac{ln\,\frac{2\,\pi R}{2\,\pi\,r_0} - 1}{ln\,\frac{2\,\pi R}{2\,B} - 1}. \tag{52}$$

Betrachten wir nun den Fall: $\frac{r_0}{\lambda}$ bzw. $\frac{B}{\lambda} = 0$, erhalten wir leicht durch direkte Berechnung für den zirkularen Zylinder mit

Radius r_0, wenn die zwei Hälften des Zylinders verschiedene Akkommodationskoefficienten, a_2 und a_1, haben:

$$K_0 = -\frac{1}{4}(a_2 - a_1) \cdot p \cdot \frac{T_1 - T_0}{T_0} \int_{-\frac{\pi}{2}}^{+\frac{\pi}{2}} r_0 \cos\theta \, d\theta$$

oder:

$$K_0 = -\frac{1}{4}(a_2 - a_1) \cdot p \cdot \frac{T_1 - T_0}{T_0} \cdot 2 r_0 .$$

Bemerken wir, dass der Temperaturunterschied $\Delta T_{p=0} = \Delta T_0$ laut der Definition des Akkommodationskoefficienten ist:

$$\Delta T_0 = \frac{1}{2}(a_2 - a_1)(T_1 - T_0),$$

erhalten wir für $\frac{r_0}{\lambda} = 0$:

$$K_0 = -\frac{1}{2} \cdot \frac{p}{T_0} \cdot 2 r_0 \cdot \Delta T_0 . \tag{53}$$

Für das Band mit Breite B erhalten wir in derselben Weise für $\frac{B}{\lambda} = 0$:

$$K_0' = -\frac{1}{4}(a_2 - a_1) \cdot p \cdot \frac{T_1 - T_0}{T_0} \cdot B = -\frac{1}{2} \cdot \frac{p}{T_0} \cdot B \cdot \Delta T_0 \tag{54}$$

und hieraus:

$$\frac{K_0'}{K_0} = \frac{K_{1,0}'}{K_{1,0}} = \frac{B}{2 r_0} .$$

Der Faktor σ wird also in dem ganzen Bereich $0 \leqq \frac{B}{\lambda} \leqq \infty$ keine Konstante sein, sondern sich mit dem Wert von $\frac{B}{\lambda}$ ändern.

Wir können nun den Wert von m_1 bestimmen, so dass der Grenzwert von Formel (51) für $\frac{B}{\lambda} = 0$ mit dem direkt abgeleiteten Wert:

$$K_0' = -\frac{1}{2} \cdot \frac{p}{T_0} \cdot B \cdot \Delta T_0$$

übereinstimmt. Hieraus erhält man $m_1 = 3 \cdot \frac{\sigma}{f}$, wodurch die Formel (51) geschrieben werden kann:

$$K' = -\frac{1}{2}\frac{p}{T_0} \cdot B \cdot \frac{\Delta T}{1 + \left[\frac{1}{3} \cdot \frac{f}{\sigma} + \frac{3}{4\pi} \cdot \frac{f-1}{f}\right]\left(\frac{B}{{}_1\lambda}\right)p + \frac{f-1}{4\pi\sigma}\left(\frac{B}{{}_1\lambda}\right)^2 \cdot p^2}$$

oder:

$$K' = -\frac{1}{2}\frac{p}{T_0} \cdot B \cdot \frac{\Delta T}{1 + \beta\left(\frac{B}{{}_1\lambda}\right)p + \alpha\left(\frac{B}{{}_1\lambda}\right)^2 \cdot p^2}, \qquad (55)$$

wo:

$$\beta = \frac{1}{3} \cdot \frac{f}{\sigma} + \frac{3}{4\pi} \cdot \frac{f-1}{f} \quad \text{und} \quad \alpha = \frac{1}{4\pi\sigma}(f-1),$$

während $f = ln\frac{2\pi R}{2B}$.

7. Bevor wir den abgeleiteten Ausdruck für K' näher prüfen und mit den Beobachtungen vergleichen, werden wir versuchen, den Wert von ΔT, der Temperaturdifferenz zwischen den an die zwei Seiten des Bandes grenzenden Gasschichten, abzuleiten.

Ist ein Band mit der Temperatur T_1 und Breite B in der Achse eines Zylinders mit der Temperatur T_2 und dem inneren Diameter $2R$ aufgehängt, können wir für den Wärmeverlust des Bandes per cm², Sek., Grad., q_p, schreiben:

$$q_p(T_1 - T_2) = a \cdot \varepsilon \cdot p(T_1 - t_1).$$

a ist der Akkommodationskoefficient der Oberfläche und t_1 die mittlere Temperatur der auf dem Bande auffallenden Moleküle; p ist der Druck und ε das molekulare Wärmeleitungsvermögen des Gases.

Die Temperatur der an das Band grenzenden Gasschicht wird:

$$T_s = \frac{1}{2}(t_1 + t_2),$$

wo t_2 die mittlere Temperatur der von der Oberfläche zurückgeworfenen Molekülen bezeichnet.

Laut der Definition des Akkommodationskoefficienten, a, ist:

$$t_2 = t_1 + a(T_1 - t_1),$$

und also:

$$T_s = \frac{1}{2}(t_1 + t_2) = t_1 + \frac{a}{2}(T_1 - t_1).$$

Haben die zwei Seiten des Bandes verschiedene Akkommodationskoefficienten a_2 und a_1, erhalten wir:

$$\Delta T = T_s'' - T_s' = t'' + \frac{a_2}{2}(T_1 - t'') - \left[t' + \frac{a_1}{2}(T_1 - t')\right]$$

oder

$$\Delta T = T_s'' - T_s' = \left(1 - \frac{a_1}{2}\right)(T_1 - t') - \left(1 - \frac{a_2}{2}\right)(T_1 - t'').$$

Vernachlässigen wir den Einfluss der eventuellen Strömungen auf die Wärmeabgabe, erhalten wir für den Wärmeverlust der zwei Seiten des Bandes:

$$q_p''(T_1 - T_2) = a_2 \cdot \varepsilon p (T_1 - t'')$$

und

$$q_p'(T_1 - T_2) = a_1 \cdot \varepsilon p (T_1 - t'),$$

und also:

$$\Delta T = (T_1 - T_2)\left[\left(1 - \frac{a_1}{2}\right)\frac{q_p'}{a_1 \varepsilon p} - \left(1 - \frac{a_2}{2}\right)\frac{q_p''}{a_2 \varepsilon p}\right]. \qquad (56)$$

In einer früheren Arbeit[22] habe ich nachgewiesen, dass man auch annäherungsweise für die Wärmeabgabe eines flachen Bandes in einem zirkularen Zylinder die Formel:

$$\frac{1}{q_p} = \frac{1}{a \varepsilon p} + \frac{1}{q_\alpha}, \quad \text{wo} \quad q_\alpha = \frac{2\pi\varkappa}{2\pi r_0} \cdot \frac{1}{ln \dfrac{R + \frac{1}{2}k\lambda}{r_0 + \frac{1}{2}k\lambda}},$$

verwenden darf, wenn $B = \pi r_0$ gesetzt wird. Hieraus erhält man nach Einsetzung in die Formel (56):

$$\Delta T = \frac{1}{2}(a_2 - a_1)(T_1 - T_2) \cdot \frac{1 + 2\left(\frac{\varepsilon}{q_\alpha}\right)p}{1 + (a_2 + a_1)\left(\frac{\varepsilon}{q_\alpha}\right)p + a_2 a_1 \left(\frac{\varepsilon}{q_\alpha}\right)^2 \cdot p^2}. \qquad (57)$$

Für $p \geqq 0$ wird: $\Delta T = \Delta T_0 = \frac{1}{2}(a_2 - a_1)(T_1 - T_2)$.

[22] Sophus Weber: D. Kgl. Danske Vidensk. Selskab, Mat.-fys. Medd. XIX, 11, 1942.

Da $\varkappa = k\varepsilon p\lambda$, wird:

$$\Delta T_\infty = (a_2 - a_1)(T_1 - T_2)\frac{1}{a_1 a_2\left(\frac{\varepsilon}{q_\alpha}\right)p} = \frac{a_2 - a_1}{a_1 a_2} k \frac{\lambda}{r_0} \frac{T_1 - T_2}{ln \frac{R + \frac{1}{2}k\lambda}{r_0 + \frac{1}{2}k\lambda}}.$$

Aus Formel (57) sehen wir leicht, dass ΔT ein Maximum erreicht, wenn:

$$1 + 2\left(\frac{\varepsilon}{q_\alpha}\right)p_{max} = \sqrt{n} = \sqrt{\frac{(2 - a_2)(2 - a_1)}{a_1 a_2}}, \qquad (58)$$

während der Wert von ΔT_{max} wird:

$$\Delta T_{max} = \Delta T_0 \frac{1}{\frac{1}{2}(a_2 + a_1 - a_1 a_2) + \sqrt{\frac{a_1 a_2}{(2 - a_2)(2 - a_1)}}\left[2 - (a_2 + a_1) + \frac{1}{2}a_2 a_1\right]},$$

mit:

$$\Delta T_0 = \frac{1}{2}(a_2 - a_1)(T_1 - T_2).$$

Wir finden hieraus für Wasserstoff und $a_2 = 0{,}715$, $a_1 = 0{,}315$:

$$2\left(\frac{\varepsilon}{q_\alpha}\right)p_{max} = \sqrt{n} - 1 = 2{,}1005$$

und:

$$\Delta T_{max} = 1{,}3303 \cdot \Delta T_0.$$

Für Helium und $a_2 = 0{,}909$, $a_1 = 0{,}411$:

$$2\left(\frac{\varepsilon}{q_\alpha}\right)p_{max} = \sqrt{n} - 1 = 1{,}1540$$

und:

$$\Delta T_{max} = 1{,}1420 \cdot \Delta T_0.$$

Für atm. Luft und $a_2 = 0{,}980$, $a_1 = 0{,}835$:

$$2\left(\frac{\varepsilon}{q_\alpha}\right)p_{max} = \sqrt{n} - 1 = 0{,}2062$$

und:

$$\Delta T_{max} = 1{,}009 \cdot \Delta T_0.$$

Das Maximum von ΔT ist ein ziemlich flaches Maximum, wie aus den folgenden Werten für Wasserstoff und $a_2 = 0{,}715$, $a_1 = 0{,}315$ hervorgeht:

$$p = \frac{9}{10} p_{\max} : \Delta T = 1{,}3291 \cdot \Delta T_0,$$

$$p = \quad p_{\max} : \Delta T = 1{,}3303 \cdot \Delta T_0,$$

$$p = \frac{11}{10} p_{\max} : \Delta T = 1{,}3292 \cdot \Delta T_0.$$

8. Aus dem Vorhergehenden erhellt, dass der vollständige Ausdruck für K', die KNUDSEN'sche Radiometerkraft per cm Länge des Bandes, für $\frac{B}{R} \ll 1$, geschrieben werden kann:

$$K' = -\frac{1}{2} \cdot \frac{p}{T} \cdot B \frac{1}{1 + \beta \left(\frac{B}{{}_1\lambda}\right) p + \alpha \left(\frac{B}{{}_1\lambda}\right)^2 \cdot p^2} \Delta T_0 \frac{1 + 2\left(\frac{\varepsilon}{q_\alpha}\right) \cdot p}{1 + (a_2 + a_1)\left(\frac{\varepsilon}{q_\alpha}\right) p + a_2 a_1 \left(\frac{\varepsilon}{q_\alpha}\right)^2 \cdot p^2} \quad (60$$

oder:

$$K' = F(p) \cdot \Delta T_0 \cdot f(p),$$

wo $F(p)$ die gewöhnliche Radiometerfunktion ist.

In diesem Ausdruck sind alle Konstanten mit Ausnahme von σ bekannt; der Wert von σ wird wahrscheinlich zwischen 1 und 2 liegen.

Wäre die Temperaturdifferenz, ΔT, konstant oder beinahe unabhängig von dem Druck, p, würde man das Maximum von K' erhalten, wenn $F(p)$ sein Maximum erreicht; dies geschieht, wenn:

$$p = p_{\max} = \frac{{}_1\lambda}{B} \sqrt{\frac{1}{\alpha}} = \frac{{}_1\lambda}{B} \sqrt{\frac{4\pi\sigma}{f-1}}, \quad \text{oder} \quad \lambda_{\max} = B \sqrt{\alpha}. \qquad (61)$$

In diesem Falle wird der Maximumswert von K':

$$K'_{\max} = -\frac{1}{2} \cdot \frac{{}_1\lambda}{T} \cdot \frac{\Delta T}{\beta + 2\sqrt{\alpha}} = -\frac{1}{2} \cdot {}_1\lambda \cdot \frac{\Delta T}{T} \cdot \frac{1}{\frac{1}{3} \cdot \frac{f}{\sigma} + \frac{3}{4\pi} \frac{f-1}{f} + \frac{1}{\sqrt{\pi}} \sqrt{\frac{f-1}{\sigma}}}. \qquad (62)$$

Hieraus geht hervor, dass p_{max} in diesem Falle umgekehrt proportional mit der Breite des Bandes B ist, und das K'_{max} sich nur wenig mit dem Wert von B ändert, weil K'_{max} nur von $ln\frac{\pi R}{B}$ abhängt.

Fallen die Maxima von $F(p)$ und ΔT praktisch gesprochen zusammen, wird die Bestimmung von der Grösse und Lage des Maximumwertes von K' sehr einfach, weil das Maximum von ΔT sehr flach ist. Im Allgemeinen kann aber kein Zusammenfallen der Maxima erwartet werden, und es wird darum etwas umständlicher, die Grösse und die Lage des Maximums zu bestimmen. Bei der folgenden Vergleichung zwischen der hier entwickelten Theorie und dem RASMUSSEN'schen Beobachtungsmaterial werde ich hierauf zurückkommen.

Für $p \geqq 0$ gibt die Formel für K' den Wert:

$$K'_0 = -\frac{1}{2}\cdot\frac{p}{T}\cdot B\Delta T_0 = -\frac{1}{4}(a_2 - a_1)(T_1 - T_2)\frac{p}{T}\cdot B,$$

eine Formel, die bereits von MARTIN KNUDSEN abgeleitet ist.

Für sehr grosse Werte von p erhält man, wenn die Variation von $ln\frac{\pi R}{B}$ mit B vernachlässigt wird:

$$K'_\infty \sim (T_1 - T_2)\cdot\frac{a_2 - a_1}{a_1 a_2}\cdot\frac{{}_1\lambda^3}{B^2\cdot p^2},$$

weil:

$$\frac{q_\alpha}{\varepsilon} = \frac{\pi}{\varepsilon}\cdot\frac{\varkappa}{B}\cdot\frac{1}{ln\frac{\pi R}{B}} = \frac{\pi}{\varepsilon}\cdot\frac{k\varepsilon p\lambda}{B}\cdot\frac{1}{ln\frac{\pi R}{B}} = \pi k\frac{{}_1\lambda}{B\,ln\frac{\pi R}{B}}.$$

Auf diese Abhängigkeit hat bereits R. E. H. RASMUSSEN in Verbindung mit seiner empirischen Formel für $K'_{obs.}$, vgl. S. 35, hingewiesen.

Wir sehen also, dass die KNUDSEN'sche Radiometerkraft bei grossen Werten von p umgekehrt proportional mit $(B\cdot p)^2$ wird, weil $\Delta T_\infty \sim \frac{1}{B\cdot p}$ ist.

In dem Folgenden werde ich nun die Formel für K' mit den Messungen von R. E. H. RASMUSSEN vergleichen.

9. Über die KNUDSEN'sche Radiometerkraft liegen drei Untersuchungen vor; die erste Abhandlung ist die Pionierarbeit von MARTIN KNUDSEN[23]; diese Arbeit ist insbesondere auf grosse Genauigkeit bei den niedrigsten Drucken eingestellt.

Ausserdem hat R. E. H. RASMUSSEN[24] zwei Arbeiten veröffentlicht. In seiner ersten Arbeit wird für dasselbe Band, $B = 0{,}2540$ cm, nach der magnetischen Kompensationsmethode der Einfluss von dem äusseren Diameter, $2R$, untersucht. In der zweiten Arbeit von RASMUSSEN ist ein grosses und wertvolles Beobachtungsmaterial über die KNUDSEN'sche Radiometerkraft geschaffen, und man kann, da die Messungen nach der Torsionsmethode durchgeführt sind, annehmen, dass die Genauigkeit befriedigend ist. In dieser Untersuchung wurde in einem grossen Behälter mit dem Diameter, $2R_0 =$ ca. 23 cm, die Radiometerkraft auf drei verschiedenen Bändern, $B_1 = 0{,}253$ cm, $B_2 = 0{,}502$ cm und $B_3 = 1{,}001$ cm, in dem ganzen Druckbereich gemessen. Für alle drei Bänder ist praktisch gesprochen, auch wenn in Betracht genommen wird, dass die Bänder ca. 5 cm ausserhalb der Achse des Behälters stehen, die Bedingung $\frac{B}{2R} \ll 1$ erfüllt. Die eine Seite von den Bändern war glatt und blank, während die andere Seite, und zwar bei allen drei Bänder in derselben Weise, durch Platinierung schwarz und rauh gemacht war. Die Radiometerkraft und die Wärmeabgabe der Bänder wurden gleichzeitig gemessen; die Messungen von der Radiometerkraft bei den verschiedenen Werten von $T_1 - T_2$ in Wasserstoff und atm. Luft sind in der Abhandlung[25] veröffentlicht. Die folgenden Messungen von der Wärmeabgabe in Wasserstoff hat Dr. R. E. H. RASMUSSEN zu meiner Verfügung gestellt, wofür ich ihm auch hier meinen besten Dank aussprechen möchte.

Das ganze Beobachtungsmaterial über die Radiometerkraft hat RASMUSSEN auf $T_1 - T_2 = 40°$ C., $T_2 = 20°$ C. umgerechnet und graphisch dargestellt. Es stellte sich heraus, dass das ganze Versuchsmaterial für alle drei Bänder befriedigend durch die empirische Formel:

[23] MARTIN KNUDSEN: loc. cit.
[24] R. E. H. RASMUSSEN: loc. cit.
[25] In derselben Arbeit ist auch ein Spezialfall von der KNUDSEN'schen Radiometerkraft untersucht. Dieser Fall, $B = 1{,}00$ cm und $2R_0 =$ ca. 1,2 cm, wurde früher von mir theoretisch behandelt (D. Kgl. Danske Vidensk. Selskab, Mat.-fys. Medd. XIX, 11, 1942). Vgl. Zusammenfassung, Punkt 2.

$$K'_{\text{obs.}} = \frac{1}{4}(a''_2 - a''_1)\frac{B}{T_0} \cdot \frac{p(T_1 - T_2)}{1 + c\left(\frac{B}{{}_1\lambda}\right)p + c^2\left(\frac{B}{{}_1\lambda}\right)^2 \cdot p^2 + \frac{c^3}{27}\left(\frac{B}{{}_1\lambda}\right)^3 \cdot p^3}$$

dargestellt werden kann, woraus sofort erhellt, dass die Übereinstimmung mit der theoretischen Formel (60), der Form nach sowohl für $p \to 0$ als auch für grosse Werte von p, befriedigend ist.

Aus den Kurven hat RASMUSSEN folgende Werte von $p_{\max}$ und $K'_{\max}$ gefunden:

Tabelle V.

	No.	B, cm	$10^5 \cdot \left(\frac{K'_{\max}}{T_1 - T_2}\right)_{\text{obs.}}$	$p_{\max, \text{obs.}}$ (Bar.)
Wasserstoff:				
$T_2 = 20°$ C...	1	0,253	247	107
$T_1 - T_2 = 40°$ C...	2	0,502	272	59
	3	1,001	304	33
Atm. Luft:				
$T_2 = 20°$ C...	1	0,253	29,2	51
$T_1 - T_2 = 40°$ C...	2	0,502	25,8	22,4
	3	1.001	21,9	11,5

Wir sehen hieraus, das $K'_{\max}$ ziemlich unabhängig von B ist, und dass annäherungsweise $p_{\max} \infty \frac{1}{B}$; auffallend ist aber, dass die Maximalkraft in atm. Luft zehnmal kleiner ist als in Wasserstoff.

Wir werden nun erst aus den Wärmeabgabemessungen die Werte von $a_2 - a_1$, ΔT, und R bestimmen. Da die Bänder ausserhalb der Achse des Behälters stehen, muss der mittlere Wert von R auch durch die Wärmeabgabe abgeleitet werden.

10. Nach den Messungen von MARTIN KNUDSEN können wir für die blanke Seite der Messbänder in Wasserstoff $a_1 = 0{,}315$ setzen. Durch die Messungen der Wärmeabgabe bei sehr niedrigem Druck lässt sich der Wert von $(a_1 + a_2)$ bestimmen. In den folgenden Tabellen VI, VII und VIII sind für jedes Messband, bestehend aus 2 identischen Längen L, zwei Messreihen von q'_p, der Wärmeabgabe des Bandes per cm Länge und für eine Temperaturdifferenz von einem Grad, bei dem Druck p angegeben.

Tabelle VI.

$B_1 = 0{,}253$ cm, $T_1 - T_2 = 40°$ C., $T_2 = 20°$ C.

q'_p ist für die Strahlung und die Ableitung durch die Enden des Bandes korrigiert.

p (Bar.)	Δp	$q'_p \cdot 10^3$	$\Delta q'_p \cdot 10^3$	$\frac{\Delta q'_p}{\Delta p} \cdot 10^3$
0		0		
	3,08		0,033	0,0107
3,08		0,033		
	3,01		0,032	0,0106
6,09		0,065		
	2,98		0,031	0,0104
9,07		0,096		
	5,89		0,058	0,0099
14,96		0,154		
	5,78		0,057	0,0099
20,84		0,211		
	5,76		0,052	0,0091
26,60		0,263		
	5,80		0,048	0,0083
32,4		0,311		
	8,60		0,069	0,0080
41,0		0,380		
	8,60		0,064	0,0075
49,6		0,444		

$$\lim \left(\frac{\Delta q'_p}{\Delta p}\right)_{p=0} = 0{,}0110 \cdot 10^{-3}; \left(\frac{\Delta q_p}{\Delta p}\right)_0 = 218 \text{ Erg/cm}^2 \text{ Sek. Gr.}$$

0		0		
	5,24		0,061	0,0117
5,24		0,061		
	5,22		0,045	0,0087
10,46		0,106		
	5,18		0,046	0,0089
15,64		0,151		
	5,17		0,050	0,0097
20,81		0,201		

$$\lim \left(\frac{\Delta q'_p}{\Delta p}\right)_{p=0} = 0{,}0114 \cdot 10^{-3}; \left(\frac{\Delta q}{\Delta p}\right)_0 = 225 \text{ Erg/cm}^2 \text{ Sek. Gr.}$$

Mittelwert von $\left(\frac{\Delta q_p}{\Delta p}\right)_0 = 222$ Erg/cm^2 Sek. Gr.

Tabelle VII.

$B_2 = 0{,}502$ cm, $T_1 - T_2 = 40°$ C., $T_2 = 20°$ C.

q'_p ist für die Strahlung und die Ableitung durch die Enden des Bandes korrigiert.

p (Bar.)	Δp	$q'_p \cdot 10^3$	$\Delta q'_p \cdot 10^3$	$\frac{\Delta q'_p}{\Delta p} \cdot 10^3$
0		0		
	2,39		0,054	0,0226
2,39		0,054		
	2,33		0,051	0,0218
4,72		0,105		
	2,32		0,048	0,0207
7,04		0,153		
	2,31		0,050	0,0216
9,35		0,203		
	2,28		0,040	0,0175
11,63		0,243		
0		0		
	7,49		0,168	0,0224
7,49		0,168		
	7,40		0,148	0,0200
14,89		0,316		
	7,39		0,131	0,0177
22,28		0,447		
	7,32		0,118	0,0161
29,60		0,565		

$$\lim \left(\frac{\Delta q'_p}{\Delta p}\right)_{p=0} = 0{,}0233 \cdot 10^{-3} \text{ (Mittelwert)}$$

$$\left(\frac{\Delta q_p}{\Delta p}\right)_0 = 232 \text{ Erg/cm}^2 \text{ Sek. Gr.}$$

Tabelle VIII.

$B_3 = 1{,}001$ cm, $T_1 - T_2 = 40°$ C., $T_2 = 20°$ C.

q'_p ist für die Strahlung und die Ableitung durch die Enden des Bandes korrigiert.

p (Bar.)	Δp	$q'_p \cdot 10^3$	$\Delta q'_p \cdot 10^3$	$\frac{\Delta q'_p}{\Delta p} \cdot 10^3$
0		0		
	0,98		0.044	0,0450
0,98		0,044		
	0,93		0,042	0,0450
1,91		0,086		
	0,93		0,043	0,0463
2,84		0,129		
	0,92		0,042	0,0456
3,76		0,171		
	0,91		0,040	0,0440
4,67		0,211		
	0,92		0,040	0,0435
5,59		0,251		
	0,90		0,039	0,0432
6,49		0,290		
	0,91		0,039	0,0430
7,40		0,329		
	0,90		0,035	0,0390
8,30		0,364		
0		0		
	5,46		0,236	0,0433
5,46		0,236		
	5,36		0,214	0,0400
10,82		0,450		
	5,34		0,188	0,0353
16,16		0,638		
	5,31		0,151	0,0284
21,47		0,789		

$$\lim \left(\frac{\Delta q'_p}{\Delta p}\right)_{p=0} = 0{,}0462 \cdot 10^{-3} \text{ (Mittelwert)}$$

$$\left(\frac{\Delta q_p}{\Delta p}\right)_0 = 231 \text{ Erg/cm}^2 \text{ Sek. Gr.}$$

Aus den elektrischen Messungen bekommt man:

$$q_p' = \frac{w \cdot i^2}{2L(T_1 - T_2)} \text{ Watt/Sek. Gr.} = 2B \cdot q_p.$$

i ist die Stromstärke in Amp. und w der elektrische Widerstand des Bandes in Ohm bei der Temperatur T_1; q_p wird also die Wärmeabgabe per cm^2. Aus den Messreihen wird $\frac{\Delta q_p'}{\Delta p}$ berechnet und hieraus der Grenzwert $\left(\frac{\Delta q_p'}{\Delta p}\right)_0$ für $p = 0$ graphisch bestimmt.

Wenn ε_{20} das molekulare Wärmeleitungsvermögen in Wasserstoff bei $T_2 = 20°$ C. bezeichnet, wird:

$$\left(\frac{\Delta q_p}{\Delta p}\right)_0 = \left(\frac{\Delta q_p'}{\Delta p}\right)_{p=0} \cdot \frac{1}{2B} \cdot 10^7 \text{ Erg/cm}^2 \text{ Sek. Gr.} = \frac{1}{2}(a_2 + a_1) \cdot \varepsilon_{20}.$$

Für H_2 ist $\varepsilon_{T_2} = \varepsilon_{20} = 441{,}4$ Erg/cm^2 Sek. Gr., sodass hieraus $(a_1 + a_2)$ bestimmt werden kann.

Wir sehen aus den Tabellen, dass die experimentellen Werte von $\left(\frac{\Delta q_p}{\Delta p}\right)_0$ für die drei Bänder nur wenig von einander abweichen, so dass wir denselben Wert von $(a_1 + a_2)$ für alle drei Bänder verwenden können. Wir finden im Mittel für die drei Bänder:

$$\left(\frac{\Delta q_p}{\Delta p}\right)_0 = 228 = \frac{1}{2}(a_2 + a_1)\,\varepsilon_{20} = \frac{1}{2}(a_2 + a_1) \cdot 441{,}4$$

und also:

$$a_2 + a_1 = 1{,}030,$$

oder:

$$a_2 = 0{,}715, \quad \text{da} \quad a_1 = 0{,}315.$$

Nachdem a_2 auf diese Weise bestimmt ist, werden wir die Temperaturdifferenz, ΔT, zwischen den zwei Seiten des Bandes näher betrachten. Die Temperaturdifferenz ΔT wird durch Formel (58):

$$\Delta T = \frac{1}{2}(a_2 - a_1)(T_1 - T_2) \frac{1 + 2\left(\frac{\varepsilon}{q_\alpha}\right) \cdot p}{1 + (a_2 + a_1)\left(\frac{\varepsilon}{q_\alpha}\right) p + a_2 a_1 \left(\frac{\varepsilon}{q_\alpha}\right)^2 \cdot p^2},$$

berechnet, nachdem die Werte von $\left(\frac{\varepsilon}{q_\alpha}\right)$ in Wasserstoff für die drei Bänder B_1, B_2 und B_3 aus den RASMUSSEN'schen Messungen bei höheren Drucken bestimmt sind.

Mit Hilfe der Formel:

$$\frac{1}{q_p} = \frac{1}{q_0} + \frac{1}{q_\alpha}, \quad \text{wo} \quad q_0 = \frac{1}{2}(a_2 + a_1)\,\varepsilon_T \cdot p,$$

können wir aus den RASMUSSEN'schen Messungen von der Wärmeabgabe in Wasserstoff die Werte von $\left(\frac{\varepsilon_T}{q_\alpha}\right)$ für die drei Bänder bestimmen; hierdurch ist laut der obenstehenden Formel der Wert von ΔT in dem ganzen Druckbereich bestimmt.

Wir erhalten auf diese Weise die in Kolonne 4 der Tabellen IX, X und XI angegebenen Werte von $\frac{\varepsilon_T}{q_\alpha}$ für die drei Bänder, B_1, B_2 und B_3, in Wasserstoff:

a) $B_1 = 0{,}253$ cm; $T_1 - T_2 = 40°$ C.; $T_2 = 20°$ C.

und

$$\varepsilon_{40} = \frac{7555}{\sqrt{\frac{1}{2}(T_1 + T_2)}} = 427{,}1 \text{ Erg/cm}^2 \text{ Sek. Gr.}$$

Tabelle IX.

p (Bar.)	$q'_{p,\,\text{obs.}}$ (cm Länge) Erg/Sek. Gr.	$q_{p,\,\text{obs.}}$ (per cm²)	$\frac{\varepsilon}{q_\alpha}$
0,0	0	0	—
64,6	$0{,}561 \cdot 10^4$	$1{,}109 \cdot 10^4$	$84{,}7 \cdot 10^{-4}$
125,9	0,886 —	1,751 —	89,7 —
183,8	1,112 —	2,198 —	88,7 —
347,0	1,502 —	2,968 —	87,9 —
499,0	1,708 —	3,376 —	87,6 —
814,0	1,930 —	3,814 —	88,1 —
1408,0	2,150 —	4,249 —	86,8 —

woraus im Mittel: $\frac{\varepsilon}{q_\alpha} = 87{,}5 \cdot 10^{-4}$ für B_1.

Aus der Formel (58):

$$1 + 2\left(\frac{\varepsilon}{q_\alpha}\right) p''_{\max} = 3{,}1005,$$

erhalten wir, dass ΔT sein Maximum für $B_1 = 0{,}253$ und für Wasserstoff erreicht bei dem Druck:

$$p''_{\max} = \frac{2{,}1005}{2 \cdot 87{,}5 \cdot 10^{-4}} = 120 \text{ Bar.}$$

---

b) $B_2 = 0{,}502$ cm; $T_1 - T_2 = 43°$ C.; $T_2 = 20°$ C.

Tabelle X.

p (Bar.)	$q'_{p,\,\text{obs.}}$ (cm Länge) Erg/Sek. Gr.	$q_{p,\,\text{obs.}}$ (per cm^2)	$\frac{\varepsilon}{q_\alpha}$
0	0	0	—
33,1	$0{,}592 \cdot 10^4$	$0{,}590 \cdot 10^4$	$137{,}2 \cdot 10^{-4}$
64,5	0,957 —	0,953 —	147,1 —
94,2	1,207 —	1,202 —	149,2 —
122,4	1,388 —	1,382 —	150,4 —

woraus im Mittel: $\frac{\varepsilon}{q_\alpha} = 146{,}0 \cdot 10^{-4}$ für B_2.

Aus der Formel (58):

$$1 + 2\left(\frac{\varepsilon}{q_\alpha}\right) p''_{\max} = 3{,}1005,$$

erhalten wir für B_2:

$$p''_{\max} = 72{,}0 \text{ Bar.}$$

---

c) $B_3 = 1{,}001$ cm; $T_1 - T_2 = 42°$ C.; $T_2 = 20°$ C.

Tabelle XI.

p (Bar.)	$q'_{p,\,\text{obs.}}$ (cm Länge) Erg/Sek. Gr.	$q_{p,\,\text{obs.}}$ (per cm^2)	$\frac{\varepsilon}{q_\alpha}$
0	0	0	—
17,9	$0{,}638 \cdot 10^4$	$0{,}319 \cdot 10^4$	$255{,}4 \cdot 10^{-4}$
29,2	0,937 —	0,468 —	247,6 —
39,8	1,164 —	0,581 —	245,7 —
49,9	1,340 —	0,669 —	248,7 —
59,5	1,499 —	0,749 —	244,0 —

woraus im Mittel: $\frac{\varepsilon}{q_\alpha} = 248{,}0 \cdot 10^{-4}$ für B_3.

Hieraus erhalten wir für B_3:

$$1 + 2\left(\frac{\varepsilon}{q_\alpha}\right) p''_{\max} = 3{,}1005 \quad \text{oder} \quad p''_{\max} = 42{,}3 \text{ Bar.}$$

Die Wärmeabgabe der Bänder ist gleichzeitig mit der Radiometerkraft gemessen. Bei den Messungen waren, wie früher erwähnt, zwei identische Bänder, symmetrisch zur Achse und ungefähr 5 cm ausserhalb dieser, in der KNUDSEN'schen Drehwaage ausgespannt; diese war wieder coaxial in einem zirkularen Zylinder mit Diameter $2R_0 =$ ca. 23 cm aufgehängt. Bei niedrigen Drucken ist es ohne Bedeutung, dass die Bänder ausserhalb der Achse stehen; bei höheren Drucken ist es aber notwendig, dieser Abweichung Rechnung zu tragen, weil der Wert von $R_0 =$ ca. 11,5 cm in diesem Falle nicht in dem Ausdruck $ln \frac{R}{r_0}$ verwendet werden kann. Der wahre Wert von R wird in diesem Falle kleiner als ca. 11,5 cm sein und kann am besten durch die gemessene Wärmeabgabe bei höheren Drucken bestimmt werden.

Aus den RASMUSSEN'schen Bestimmungen findet man hierfür,

nach Bildung von Mittelwerten und Auswertung der verschiedenen Messungen, aus den Beobachtungen für $B_1 = 0{,}253$ cm:

$$p = 9210 \text{ Bar.}; \; q'_p \text{ (cm Länge)} = 2{,}330 \cdot 10^{-3} \text{ Watt/Sek. Gr.}$$
$$= 2{,}330 \cdot 10^4 \text{ Erg/Sek. Gr.},$$

wenn:

$$(T_1 - T_2) \to 0 \quad \text{und} \quad T_2 = 20^\circ \text{ C.}$$

Hieraus erhält man:

$$q_p \text{ (cm}^2\text{)} = \frac{q'_p}{2 B_1} = 4{,}605 \cdot 10^4 \text{ Erg/cm}^2 \text{ Sek. Gr.}$$

Mit Hilfe der Formeln:

$$\frac{1}{q_p} = \frac{1}{q_0} + \frac{1}{q_\alpha} \quad \text{und} \quad q_0 = \frac{1}{2}(a_2 + a_1)\, \varepsilon_{20} \cdot p,$$

erhält man hieraus:

$$\frac{\varepsilon_{20}}{q_\alpha} = 93{,}8 \cdot 10^{-4}$$

oder:

$$q_\alpha = 4{,}705 \cdot 10^4 \text{ Erg},$$

weil $\frac{1}{2}(a_1 + a_2) = 0{,}515$ und

$$\varepsilon_{20} = \frac{7555}{\sqrt{293 \cdot 1}} = 441{,}4 \text{ Erg/cm}^2 \text{ Sek. Gr.}$$

Für Wasserstoff ist $(p\lambda)_{20} = 12{,}32$ und

$$k = 3{,}34, \text{ sodass } \frac{1}{2} k\lambda = 0{,}0022 \text{ für } p = 9210 \text{ Bar.}$$

Aus der Formel:

$$q_\alpha = \frac{\varkappa_{20}}{r_0} \cdot \frac{1}{ln \dfrac{R + \frac{1}{2} k\lambda}{r_0 + \frac{1}{2} k\lambda}},$$

erhalten wir mit $r_0 = \frac{B_1}{\pi} = 0{,}08053$ cm und

$$\varkappa_{20} = 4130 \cdot 10^{-7} \cdot 4{,}19 \cdot 10^{7} \left(\frac{293{,}1}{273{,}1}\right)^{0{,}70} = 18188 \text{ Erg/cm}^2 \text{ Sek. Gr.}$$

$$R = 9{,}96 \text{ cm},$$

wodurch die Werte f_1, f_2 und f_3 von $f = ln \frac{R}{r_0} = ln \frac{\pi R}{B}$ für die drei Bänder berechnet werden können.

11. Wir können nun dazu übergehen, die abgeleitete theoretische Formel (60) für die KNUDSEN'sche Radiometerkraft:

$$K' = F(p)\,\Delta T = \frac{1}{2} \cdot \frac{p}{T} \cdot B \cdot \frac{\Delta T}{1 + \left[\frac{1}{3} \cdot \frac{f}{\sigma} + \frac{3}{4\pi} \frac{f-1}{f}\right] \left(\frac{B}{{}_1\lambda}\right) p + \frac{f-1}{4\pi\sigma} \left(\frac{B}{{}_1\lambda}\right)^2 \cdot p^2}$$

$$= \frac{1}{2} \cdot \frac{p}{T} \cdot B \cdot \frac{\sigma}{\sigma + \left[\frac{f}{3} + \frac{3}{4\pi} \cdot \frac{f-1}{f} \cdot \sigma\right] \left(\frac{B}{{}_1\lambda}\right) p + \frac{f-1}{4\pi} \left(\frac{B}{{}_1\lambda}\right)^2 \cdot p^2} \cdot \Delta T,$$

wo:

$$\Delta T = \frac{1}{4} (a_2 - a_1)(T_1 - T_2) \cdot \frac{1 + 2 \cdot \frac{\varepsilon}{q_\alpha} \cdot p}{1 + (a_2 + a_1) \left(\frac{\varepsilon}{q_\alpha}\right) p + a_2 a_1 \left(\frac{\varepsilon}{q_\alpha}\right)^2 \cdot p^2}$$

mit den Beobachtungen von R. E. H. RASMUSSEN zu vergleichen. Wir werden hierfür erst die von ihm bestimmten Maximalwerte: $K'_{1,\max} = \left(\frac{K'}{T_1 - T_2}\right)_{\max}$ und dessen Lage $p_{\max}$, gebrauchen.

1° Wasserstoff. Für Wasserstoff stellt sich heraus, dass die Lagen der Maxima für die Radiometerfunktion $F(p)$, und die Temperaturdifferenz, ΔT, bezw. $p'_{\max}$ und $p''_{\max}$ praktisch gesprochen zusammenfallen. Wir finden aus der Formel für ΔT:

Tabelle XII.

$B_1 = 0{,}253$ cm	$\frac{\varepsilon}{q_\alpha} = 87{,}5 \cdot 10^{-4}$	$p''_{\max} = 120$ Bar.	$\Delta T_{\max} = 1{,}3303 \cdot \Delta T_0$
$B_2 = 0{,}502$ –	– = 146,0 –	– = 72 –	– = – –
$B_3 = 1{,}001$ –	– = 248,0 –	– = 42,3 –	– = – –

und aus der Formel für $F(p)$, die Radiometerfunktion, mit $\sigma = 1{,}33$ und $f_1 = ln\frac{\pi R}{B} = 4{,}818$, $f_2 = 4{,}133$, $f_3 = 3{,}443$, ${}_1\lambda_{40°} = 13{,}35$:

Tabelle XIII.

$B_1 = 0{,}253$ cm	$p'_{max} = 110$	$F(p)_{max} \cdot \frac{\Delta T_{max}}{T_1 - T_2} = 239{,}6 \cdot 10^{-5}$
$B_2 = 0{,}502$ –	– = 61,2	– – = 270,3 –
$B_3 = 1{,}001$ –	– = 34,8	– – = 313,7 –

Wir sehen hieraus, dass die Werte von p'_{max} und p''_{max} für Wasserstoff nicht sehr verschieden sind, so dass die Maxima von $F(p)$ und ΔT einander verstärken.

Berechnet man aus Formel (60) die Werte von K'_1 für verschiedene Werte von p in der Nähe von den Maximalwerten p'_{max} und p''_{max}, kann man eine graphische Darstellung von dem Verlauf von K'_1 in diesem Druckbereich aufzeichnen und hieraus die zusammengehörigen Werte von $K'_{1,max}$ und p_{max} bestimmen. Auf diese Weise erhält man mit $\sigma = 1{,}33$ die folgende Werte:

Tabelle XIV.

B	$\left(\frac{K'}{T_1 - T_2}\right)_{max,ber.}$	$p_{max,ber.}$	$\left(\frac{K'}{T_1 - T_2}\right)_{max,obs.}$	$p_{max,obs.}$
0,253	$239{,}7 \cdot 10^{-5}$	113,0	$247 \cdot 10^{-5}$	107
0,502	270,5 –	64,5	272 –	59
1,001	313,8 –	36,8	304 –	33

Durch Vergleichung mit den beobachteten Werten, die in Kolonne 4 und 5 der Tabelle XIV angegeben sind, erhellt, dass die Übereinstimmung sowohl für $K'_{1,max}$ als auch für p_{max} befriedigend ist, wenn $\sigma = 1{,}33$.

Um den Verlauf von σ in dem ganzen Druckbereich zu untersuchen, wurden alle Beobachtungen von K' für $B_1 = 0{,}253$ cm von neuem auf $T_1 - T_2 = 40°$ C. und $T_2 = 20°$ C. umgerechnet; dieses Observationsmaterial wurde dann in einem Diagramm (K'_1, log p) dargestellt und graphisch ausgewertet; im Allgemeinen liegen die Punkte befriedigend auf der Kurve; bei der Neubestimmung des Maximums wurde gefunden:

$$B_1 = 0{,}253 \text{ cm}, \left(\frac{K'}{T_1 - T_2}\right)_{\max} = 243 \cdot 10^{-5}, \; p_{\max} = 110 \text{ Bar.},$$

wodurch die Übereinstimmung mit den berechneten Werten noch besser wird.

In der folgenden Tabelle XV sind die zusammengehörigen Werte von $K'_{1,40}$ und p aus dieser Kurve angegeben; in Kolonne 4 stehen die aus der Formel (60) berechneten Werte, und in Kolonne 3 sind die bei der Berechnung benutzten Werte von σ angegeben. Aus der Tabelle erhellt, dass sich der Wert von σ von 1 für $\frac{B_1}{\lambda} \rightarrow 0$ auf ca. 2,50 für $\frac{B_1}{\lambda} \rightarrow \infty$ ändert und also der Grössenordnung nach mit dem Resultat in dem analogen Fall »Kugel-zirkulare Planscheibe« in Übereinstimmung ist, worin sich σ in dem ganzen Druckgebiet von 1 auf 2 ändert.

Tabelle XV.

p (Bar.)	$\frac{K'_{40}}{T_1 - T_2} \cdot 10^5$ obs.	σ	$\frac{K'_{40}}{T_1 - T_2} \cdot 10^5$ ber.	$\frac{B}{\lambda}$
0	0	—	0	0
3,16	23,5	1,00	23,6	0,06
6,31	44,0	1,01	44,0	0,12
10,00	66,0	1,04	66,2	0,19
17,78	105,0	1,19	105,1	0,34
31,62	155,0	1,25	155,2	0,60
56,2	210,0	1,31	209,2	1,00
100,0	241,0	1,32	241,1	1,9
112,0	243,0	1,33	240,0	2,1
177,8	226,0	1,35	227,1	3,4
316,2	175,0	1,37	174,9	6,0
562	110,0	1,42	110,4	10,6
1000	59,0	1,59	59,0	19,0
1778	30,0	1,92	30,0	34,0
3162	15,0	2,50	14,7	60,0
5623	5,5	2,50	5,6	106
10000	2	2,50	1,8	190
14130	< 1	2,50	0,9	270

Eine weitere Diskussion von dem Wert von σ hat aber erst Zweck, wenn eine einwandfreie mathematische Berechnung der Radiometerkraft für ein flaches Band in dem Falle, $\frac{B}{\lambda} \rightarrow \infty$,

vorliegt, und wenn neue Beobachtungen, insbesondere in dem Gebiet, $\frac{B}{\lambda} \to \infty$, durchgeführt sind.

Annäherungsweise kann σ durch die Formel:

$$\sigma = \frac{1 + 0{,}333 \frac{B}{\lambda}}{1 + 0{,}133 \frac{B}{\lambda}},$$

dargestellt werden.

2° Atm. Luft. RASMUSSEN hat auch mit demselben Apparat Messungen für die drei Bänder in atmosphärischer Luft ausgeführt. Es stellte sich heraus, dass die maximale Radiometerkraft in atm. Luft ca. 10 Mal kleiner ist als in Wasserstoff; die Genauigkeit der Messreihen in atm. Luft ist aber bedeutend geringer als in Wasserstoff, weil der Einfluss von den nötigen Korrektionen in atm. Luft verhältnismässig viel grösser wird.

In atm. Luft können wir für die drei Bänder, B_1, B_2 und B_3, $a_1 = 0.835$ und $a_2 = 0{,}98$ setzen. Dadurch wird:

$$a_2 - a_1 = 0{,}145, \quad a_1 + a_2 = 1{,}815 \quad \text{und} \quad a_1 \cdot a_2 = 0{,}8183.$$

Mit diesen Werten wird:

$$1 + 2\left(\frac{\varepsilon}{q_\alpha}\right)' p''_{\max} = \sqrt{\frac{(2 - a_2)(2 - a_1)}{a_2 a_1}} = 1{,}2062,$$

und:

$$\Delta T_{\max} = 1{,}0090\ \Delta T_0.$$

Die Werte von $\left(\frac{\varepsilon}{q_\alpha}\right)'$ in atm. Luft für die drei Bänder können wir am einfachsten durch Umrechnung der beobachteten Werte von $\left(\frac{\varepsilon}{q_\alpha}\right)$ in Wasserstoff finden. Mit Hilfe der Formel für die Wärmeleitungsfähigkeit: $\varkappa = k \varepsilon p \lambda$, wo $k = 3{,}34$ für Wasserstoff und $k = 3{,}20$ für atm. Luft, erhalten wir leicht, für atm. Luft:

$$\begin{aligned} B_1 &= 0{,}253 \text{ cm}, & \left(\frac{\varepsilon}{q_\alpha}\right)' &= 171{,}0 \cdot 10^{-4}, \\ B_2 &= 0{,}502 \text{ — }, & \text{» } &= 285{,}3 \text{ — }, \\ B_3 &= 1{,}001 \text{ — }, & \text{» } &= 485{,}0 \text{ — }. \end{aligned}$$

In atm. Luft liegen die Maxima von ΔT und $F(p)$ weit auseinander, wie aus der folgenden Tabelle XVI zu ersehen ist. In

Kolonne 4 sind die Werte von p''_{max}, bezw. die Lagen der Maxima von ΔT, und in Kolonne 5 die Werte von p'_{max}, bezw. die Lagen der Maxima von $F(p)$, angegeben; die Werte von p'_{max} sind wie für Wasserstoff mit $\sigma = 1{,}33$, $f_1 = 4{,}818$, $f_2 = 4{,}133$ und $f_3 = 3{,}443$ berechnet; ${}_1\lambda_{40} = 7{,}21$ für atm. Luft.

Tabelle XVI.
Atm. Luft.

B in cm	$\left(\frac{\varepsilon}{q_\alpha}\right)'$	ΔT_{max}	p''_{max} (Lage ΔT_{max})	p'_{max} (Lage $F(p)_{max}$)
0,253	$171{,}0 \cdot 10^{-4}$	$1{,}009 \cdot \Delta T_0$	6,05 Bar.	59,4 Bar.
0,502	285,3 —	— —	3,62 —	33,0 —
1,001	485,0 —	— —	2,14 —	18,8 —

Berechnet man nach Formel (60) und mit $\sigma = 1{,}33$ die Werte von $K'_1 = \frac{K'}{T_1 - T_2}$ in atm. Luft für verschiedene Werte von p in der Nähe von den observierten Maximalwerten von K'_1, dann erhält man in derselben Weise wie für Wasserstoff die berechneten Maximalwerte von K'_{max} und die dazu gehörigen Werte von p_{max}, welche in Kolonne 2 und 3 der folgende Tabelle XVII angegeben sind, während die von R. E. H. Rasmussen experimentell gefundenen Maximalwerte in Kolonne 4 und 5 angegeben sind.

Tabelle XVII.
Atm. Luft.

B in cm	$\left(\frac{K'}{T_1 - T_2}\right)_{max,ber.}$	$p_{max,ber.}$	$\left(\frac{K'}{T_1 - T_2}\right)_{max,obs.}$	$p_{max,obs.}$
0,253	$28{,}7 \cdot 10^{-5}$	53,0	$29{,}2 \cdot 10^{-5}$	51
0,502	34,2 —	22,0	25,8 —	22,4
1.001	39,8 —	12,5	21,9 —	11,5

Aus dieser Tabelle ersehen wir, dass die Übereinstimmung in atm. Luft, sowohl für $K'_{1,max}$ als für p_{max} für das Band $B_1 = 0{,}253$, befriedigend ist, wenn $\sigma = 1{,}33$; für die Bänder B_2 und B_3 ist die Übereinstimmung, was p_{max} betrifft, auch befriedigend. Die theoretischen Werte von $K'_{1,max}$ stimmen aber für diese zwei Bänder mit den beobachteten Werten nicht überein;

die theoretischen Werte wachsen nämlich wie in Wasserstoff mit wachsendem Wert von B, während die beobachteten Werte für K_1 mit wachsendem B, im Gegensatz zu den Observationen in Wasserstoff, abnehmen.

Es wäre von Bedeutung, durch neue Experimente, auch mit anderen Gasen, zu untersuchen, ob dieser Verlauf eine Realität ist, oder ob unbekannte Fehlerquellen, z. B. Undichtigkeiten im Apparat oder Konvektionströmungen, bei den Messungen in atm. Luft für B_2 und B_3 eine Rolle gespielt haben.

Ausser den obenerwähnten Untersuchungen in Wasserstoff und atm. Luft von R. E. H. Rasmussen hat Martin Knudsen in seiner Pionierarbeit Messungen in Helium und Wasserstoff ausgeführt. Er verwendete hierfür hauptsächlich die Aufstellung mit der magnetischen Kompensationseinrichtung; die Breite des Bandes war 0,2428 cm und der innere Diameter des Glaszylinders ca. 6,5 cm.

Werden die Knudsen'schen Messungen mit der Formel (60) verglichen, dann stellt sich heraus, dass die Formel (60) mit $\sigma = 1{,}33$ auch die experimentellen Maximalwerte $K'_{1,\max}$ und $p_{\max}$ befriedigend wiedergibt, und zwar sowohl für Helium als auch für Wasserstoff, wenn die experimentelle Genauigkeit in Betracht gezogen wird.

R. E. H. Rasmussen hat auch nach derselben Methode eine Untersuchung in Wasserstoff durchgeführt. In dieser verwendete er ein Band, $B = 0{,}2540$ cm, umgeben von verschiedenen Zylindern, deren Diameter $2R = 4{,}11$ cm, 3,21 cm, 2,24 cm und 1,27 cm waren. Die Formel (60) gibt auch diese Messreihen befriedigend wieder; für die Maximalwerte von K'_1 und p gilt wieder $\sigma =$ ca. 1,30.

Für die kleinsten Zylinder sind aber die berechneten Werte von $K'_{1,\max}$ etwas zu klein, ca. 10 bis 15 %. Die Ursache hierzu wird sein, dass die Bedingung für Formel (60), $\frac{B}{R} \ll 1$, in diesem Falle nicht erfüllt ist, und dass es ausserdem, wenn die Bedingung $\frac{B}{R} \ll 1$ nicht erfüllt ist, unzulässig wird, in der Berechnung

das flache Band mit Breite B durch einen runden Faden mit Radius $r_0 = \frac{B}{\pi}$ zu ersetzen. Diese Ersetzung wird nämlich nur dann eine brauchbare Annäherung sein, wenn $\frac{B}{2R} \to 0$. Ist diese Bedingung nicht erfüllt, werden die Widerstandsverhältnisse für die Zurückströmung des Gases der Aussenwand entlang sich ändern, so dass der experimentelle Wert von K_1' für ein flaches Band mit Breite B grösser wird als für einen runden Draht mit Radius $\frac{B}{\pi}$ [26].

Zusammenfassung.

1° Nach den grundlegenden Untersuchungen von Martin Knudsen über den molekularen Zustand der Gase, d. h. den Zustand, in welchem die mittlere freie Weglänge, λ, im Vergleich mit der massgebenden Abmessung des Apparates, μ, sehr gross ist, ist auch die Theorie der Radiometerkraft auf einer Fläche, bezw. des totalen Impulstransportes durch die Fläche, in diesem Gebiet, wo $\frac{\mu}{\lambda} \gtrsim 0$, geklärt.

Für den Zustand $\frac{\mu}{\lambda} \to \infty$ wird die Theorie der Radiometererscheinungen etwas komplizierter, weil die in der Oberfläche des Radiometerkörpers anwesenden Temperaturunterschiede an der Oberfläche des Radiometerkörpers Gleitströme hervorrufen; diese Gleitströme veranlassen, wegen der inneren Reibung des Gases, eine hydrodynamische Strömung im Gase. Die Richtung der Gleitströme ist von Stellen niedriger Temperatur nach Stellen höherer Temperatur, und somit wird die Richtung der auf dem Radiometerkörper ausgeübten Kraft die entgegengesetzte. Die Theorie der Radiometerkraft wird in diesem Gebiet, wo $\frac{\mu}{\lambda} \to \infty$, ganz analog mit der abgeleiteten Theorie für die thermischen Molekulardrucke.

Um den totalen Impulstransport durch die Oberfläche des Radiometerkörpers, bezw. die Radiometerkraft auf dem Radiometerkörper, herrührend von der hydrodynamischen Strömung

[26] Vgl. den unter [25]) erwähnten Spezialfall.

in dem Radiometersystem, berechnen zu können, muss erst das Strömungsproblem im Zusammenhang mit dem Wärmeleitungsproblem im Radiometersystem gelöst werden. Da es sich bei kleinen Temperaturdifferenzen nur um langsame Reibungsströmungen handelt, kann die hydrodynamische Strömung als laminar angesehen werden, und es wird darum im Allgemeinen möglich, auch weil keine äusseren Kräfte vorhanden sind, eine befriedigende Lösung des Strömungsproblemes zu finden, wenn das Radiometersystem eine geometrisch einfache Form hat.

Wird die Gleitung, γ, und die erweiterte MAXWELL'sche Grenzbedingung, wie diese aus den Untersuchungen von den thermischen Molekulardrucken hervorgegangen ist:

$$u_s - k_2 \cdot \gamma \cdot \frac{du_s}{dr} = k_1 \cdot \frac{3}{4} \cdot \frac{\eta}{\varrho T} \cdot \frac{dT}{ds} \cdot \frac{1}{1 + m \cdot \frac{\lambda}{\mu}},$$

in den Randbedingungen des Strömungsproblemes eingeführt, und wird die unbekannte Konstante, m, in der obengenannten MAXWELL'schen Grenzbedingung so bestimmt, dass der abgeleitete Ausdruck für die Radiometerkraft, K, für $p \to 0$ mit dem für $\frac{\mu}{\lambda} = 0$ direkt abgeleiteten Ausdruck für K_0 übereinstimmt, erhält man einen Ausdruck für die Radiometerkraft, K, in dem ganzen Gebiet $0 \leqq \frac{\mu}{\lambda} \leqq \infty$.

Es stellt sich heraus, dass die Radiometerkraft, K, in den untersuchten Fällen für das ganze Gebiet, $0 \leqq \frac{\mu}{\lambda} \leqq \infty$, wie folgt geschrieben werden kann:

$$K = F(p) \cdot \Delta T.$$

$F(p)$ ist die Radiometerfunktion, während ΔT die massgebende oder wirksame Temperaturdifferenz an der Oberfläche des Radiometerkörpers ist. ΔT wird durch die Lösung des Wärmeleitungsproblemes gefunden und ist im Allgemeinen nicht nur von der Form und den Abmessungen des Radiometersystemes, sondern auch von dem Druck und den Eigenschaften des Gases abhängig. Der Wert von ΔT, der für die entstehenden Gleitströme massgebend ist, kann den Verlauf von K in dem ganzen Druckgebiet sehr stark beeinflussen.

Die Radiometerfunktion, $F(p)$, hat in den untersuchten Fällen, z. B. Kugel, planzirkulare Scheibe, runder Faden, flaches Band u. s. w., die folgende Form:

$$F(p) = A_1 \cdot \frac{p}{1 + \beta\left(\frac{\mu}{{}_1\lambda}\right) p + \alpha\left(\frac{\mu}{{}_1\lambda}\right)^2 \cdot p^2},$$

wo A_1 u. A. von den Abmessungen und dem Akkommodationskoefficienten des Radiometerkörpers abhängt; p ist der Druck des Gases und ${}_1\lambda$ die mittlere freie Weglänge des benutzten Gases bei dem Druck 1 Bar.; α und β sind Konstanten, die im Allgemeinen von den Abmessungen des Radiometersystemes abhängen.

Die Radiometerkraft, $K_1 = \frac{K}{\Delta T} = F(p)$, hat bei dem Druck p_{max} ein Maximum, K_{max}. Werden diese Maximalwerte als Einheiten für K und p gewählt, kann, wenn ΔT konstant ist, die WESTPHAL'sche »reducierte« Radiometerfunktion geschrieben werden:

$$\frac{K_1}{K_{1,\,max}} = \frac{2 + \delta_1}{e^x + e^{-x} + \delta_1},$$

wo:

$$x = ln\frac{p}{p_{max}} \quad \text{und} \quad \delta_1 = \frac{\beta}{\sqrt{\alpha}},$$

2° Der Einfluss der geometrischen Form des Radiometersystemes und der hiermit zusammenhängenden Strömungen bei grösserer Dichte auf die Radiometerkraft geht sehr klar aus zwei Versuchen mit identischem Radiometerkörper von Dr. R. E. H. RASMUSSEN hervor. Er arbeitete mit einem flachen Platinband, $B = 1{,}000$ cm, in Wasserstoff und untersuchte die KNUDSEN'sche Radiometerkraft, welche in verschiedenen Werten des Akkommodationskoefficienten an beiden Seiten des Radiometerkörpers ihre Ursache hat. Für das von RASMUSSEN benutzte Band war im Wasserstoff für die schwarze Seite $a_2 =$ ca. 0,72 und für die blanke Seite $a_1 = 0{,}315$.

Mit diesem Band als Radiometerkörper wurden in den Experimenten folgende Resultate erhalten:

a) In einem Radiometersystem, in dem die entstehenden Strömungen an den beiden Seiten des Bandes praktisch gesprochen

von einander unabhängig waren, so dass auch kein Druckausgleich zwischen den zwei Seiten des Bandes stattfinden konnte, wurde von RASMUSSEN gefunden:

$$\frac{K_{max}}{T_1 - T_0} = 147 \cdot 10^{-4} \text{ Dyn/cm. Grad und } p_{max} = 166 \text{ Bar.}$$

$T_1 - T_0$ ist die Temperaturdifferenz zwischen dem Band und dem umgebenden Zylinder, und in diesem Radiometersystem ist die massgebende Temperaturdifferenz, ΔT, praktisch gesprochen gleich $T_1 - T_0$ (vgl. SOPHUS WEBER: D. Kgl. Danske Vidensk. Selskab, Mat.-fys. Medd. XIX, 11, 1942, S. 28).

b) In einem Radiometersystem, worin das Band vollständig frei in einem grossen Behälter aufgehängt war, sodass sich die Strömungen frei um das Band entwickeln konnten und der sich bildende Druckunterschied zwischen den beiden Seiten des Bandes sich teilweise durch Rückströmung der Aussenwand entlang ausgleichen konnte, wurde gefunden:

$$\frac{K_{max}}{T_1 - T_0} = 30{,}4 \cdot 10^{-4} \text{ Dyn/cm. Grad und } p_{max} = 33 \text{ Bar.}$$

$T_1 - T_0$ ist wieder die Temperaturdifferenz zwischen dem Radiometerkörper und der Umgebung, aber in diesem Radiometersystem ist die massgebende oder wirksame Temperaturdifferenz hauptsächlich bestimmt durch den Unterschied im Temperatursprung an der schwarzen und blanken Seite des Bandes B.

c) In dem molekularen Zustande, $\frac{B}{\lambda} \rightarrow 0$, sind in beiden Radiometersystemen die Werte von K_0 einander gleich, wenn die Umgebung denselben Akkommodationskoefficienten, z. B. $a = 1$, hat, da in diesem Zustand keine Gleitströme vorhanden sind.

3° Besteht der Radiometerkörper aus einer Kugel mit Radius r_0 und herrscht zwischen den zwei Polen, $y = 0$, $x = \pm r_0$, in den die Kugeloberfläche angrenzenden Gasschichten eine Temperaturdifferenz ΔT, wird der abgeleitete Ausdruck für K:

$$K = -\frac{\pi}{6} a \cdot \frac{r_0^2}{T} \cdot \frac{p}{1 + \beta \left(\frac{r_0}{\lambda}\right) p + \alpha \left(\frac{r_0}{\lambda}\right)^2 \cdot p^2} \cdot \Delta T.$$

a ist der Akkommodationskoefficient der Kugeloberfläche; $\alpha = \frac{\pi}{24} a$ und $\beta = \frac{3}{8} + \frac{\pi}{9} a$.

Hieraus folgt:

$$r_0 = \frac{2{,}763}{\sqrt{a}} \cdot \lambda_{max}.$$

Wird die Temperaturdifferenz ΔT durch eine einseitige Bestrahlung von der Intensität, I, erzeugt, erhält man, wenn der Temperatursprung an der Oberfläche der Kugel vernachlässigt wird:

$$\Delta T = \frac{2\,I}{\varkappa_i + 2\,\varkappa_a} r_0.$$

Befindet sich die Kugel in einem Raum mit dem konstanten Temperaturgradienten, $G = \frac{dT}{dx}$, in grosser Entfernung von der Kugel, erhält man:

$$\Delta T = 6 \frac{\varkappa_a}{\varkappa_i + 2\,\varkappa_a} r_0 G.$$

Die Übereinstimmung mit dem vorliegenden Beobachtungsmaterial für K ist befriedigend. Eine ähnliche Formel kann für eine planzirkulare Scheibe und für ein Ellipsoid abgeleitet werden.

4° Ist der Radiometerkörper ein zirkularer Zylinder oder runder Faden mit Radius r_0, und ist dieser in der Achse eines umgebenden Zylinders mit Radius R aufgehängt, erhält man, wenn $r_0 \ll R$:

$$K = -\frac{3\pi}{2} \cdot k_1 \cdot \frac{\eta^2}{\varrho T} \cdot \frac{1}{2 r_0 \left[ln \frac{R}{r_0} - 1 \right] \left[1 + k_2 \frac{ln \frac{R}{r_0}}{ln \frac{R}{r_0} - 1} \cdot \frac{\lambda}{r_0} \right] \left[1 + m \frac{\lambda}{r_0} \right]} \cdot \Delta T,$$

oder nach Anschliessen an den direkt berechneten Wert,

$$K_0 = -\frac{\pi}{8} a r_0 \cdot \frac{p}{T} \cdot \Delta T_0, \text{ für } \frac{r_0}{\lambda} = 0:$$

$$K = -\frac{\pi}{8} a r_0 \cdot \frac{p}{T} \cdot \frac{1}{1 + \beta \left(\frac{r_0}{{}_1\lambda}\right) p + \alpha \left(\frac{r_0}{{}_1\lambda}\right)^2 \cdot p^2} \cdot \Delta T,$$

worin:

$$\alpha = \frac{\pi}{16} a \left(ln \frac{R}{r_0} - 1 \right) \quad \text{und} \quad \beta = \frac{\pi}{12} a \; ln \frac{R}{r_0} + \frac{3}{4} \cdot \frac{ln \frac{R}{r_0} - 1}{ln \frac{R}{r_0}}.$$

Der Wert von ΔT wird für einseitige Bestrahlung mit der Intensität, I:

$$\Delta T = \frac{2 I}{\varkappa_i + \varkappa_a} r_0.$$

Die quantitative Übereinstimmung mit den Messungen von Westphal für das Quarzfadenradiometer ist nicht befriedigend. Die Ursache hierzu wird in den Messungen gesucht, weil diese wahrscheinlich durch vertikale Konvektionsströmungen beeinflusst sind.

5° Bei der Knudsen'schen Radiometerkraft hat der Radiometerkörper eine konstante Temperatur, T_1, höher als die Temperatur der Umgebung, T_2. Die zwei Seiten des Radiometerkörpers haben aber verschiedene Akkommodationskoefficienten, a_2 und a_1, $(a_2 > a_1)$, dem Gase gegenüber. Hierdurch wird der Temperatursprung an den zwei Seiten des Radiometerkörpers verschieden, wodurch eine Temperaturdifferenz, ΔT, in den die Oberfläche angrenzenden Gasschichten entsteht. ΔT kann aus dem Ausdruck für den Temperatursprung, bezw. aus dem Ausdruck für den Wärmeverlust des Fadens, bestimmt werden.

Für einen runden Faden, wovon die zwei Hälften verschiedene Akkommodationskoefficienten haben, kann man die unter 4° abgeleitete Formel, wenn der richtige Wert von ΔT eingesetzt wird, verwenden.

Für ein flaches Band mit Breite B und mit den verschiedenen Akkommodationskoefficienten a_2 und a_1 kann, wenn das Band in der Achse eines umgebenden Zylinders mit Radius R aufgehängt ist, die Radiometerkraft in Analogie mit dem Ausdruck für einen zirkularen Faden annäherungsweise, für den Fall $B \ll R$, geschrieben werden:

$$K = -\sigma \cdot \frac{3\pi}{2} \cdot k_1 \cdot \frac{\eta^2}{\varrho T} \cdot \frac{\Delta T}{\frac{2B}{\pi}(f-1)\left[1+\pi \cdot k_2 \cdot \frac{f}{f-1} \cdot \frac{\lambda}{B}\right]\left[1+m_1 \cdot \frac{\lambda}{B}\right]}.$$

Diese Formel entsteht aus der Formel für den runden Faden, wenn $2\pi r_0 = 2B$ und $f = ln\frac{2\pi R}{2B}$ gesetzt werden; σ ist ein Zahlenfaktor.

Nach Anschliessen an den molekularen Zustand, $\frac{B}{\lambda} = 0$, für welchen:

$$K_0 = -\frac{1}{2} B \cdot \frac{p}{T} \cdot \Delta T_0,$$

erhält man:

$$K = -\frac{1}{2} B \cdot \frac{p}{T} \cdot \frac{1}{1+\beta\left(\frac{B}{\lambda}\right)p + \alpha\left(\frac{B}{\lambda}\right)^2 \cdot p^2} \cdot \Delta T,$$

mit

$$\beta = \frac{1}{3} \cdot \frac{f}{\sigma} + \frac{3}{4\pi} \cdot \frac{f-1}{f} \quad \text{und} \quad \alpha = \frac{1}{4\pi} \cdot \frac{f-1}{\sigma}.$$

Für ΔT wird aus der Wärmeabgabe des Bandes gefunden:

$$\Delta T = \frac{1}{2}(a_2 - a_1)(T_1 - T_2) \cdot \frac{1+2\left(\frac{\varepsilon}{q_\alpha}\right) \cdot p}{1+(a_2+a_1)\left(\frac{\varepsilon}{q_\alpha}\right)p + a_2 a_1 \left(\frac{\varepsilon}{q_\alpha}\right)^2 \cdot p^2},$$

wo ε das molekulare Wärmeleitungsvermögen ist, und

$$q_\alpha = \frac{2\pi\varkappa}{2B} \cdot \frac{T_1 - T_2}{ln\frac{R+\frac{1}{2}k\lambda}{\frac{B}{\pi}+\frac{1}{2}k\lambda}}.$$

Aus dem Ausdruck für ΔT erhellt, dass ΔT bei dem Druck p''_{max} auch ein Maximum, ΔT_{max}, hat; für den Wert von p''_{max} wird leicht erhalten:

$$1+2\left(\frac{\varepsilon}{q_\alpha}\right)p''_{max} = \sqrt{\frac{(2-a_2)(2-a_1)}{a_2 a_1}}$$

und hieraus:

$$\Delta T_{\max} = \Delta T_0 \cdot \frac{1}{\frac{1}{2}(a_2 + a_1 - a_2 a_1) + \sqrt{\frac{a_2 a_1}{(2-a_2)(2-a_1)}}\left(2 - [a_2 + a_1] + \frac{1}{2} a_2 a_1\right)},$$

wo:

$$\Delta T_0 = \frac{1}{2}(a_2 - a_1)(T_1 - T_2).$$

Diese Formeln werden mit dem ganzen vorliegenden Beobachtungsmaterial für die KNUDSEN'sche Radiometerkraft und insbesondere mit dem grossen Beobachtungsmaterial von Dr. R.E.H. RASMUSSEN, der mit Wasserstoff und atm. Luft arbeitete, verglichen.

In Wasserstoff ist die Vergleichung, dem Verlauf und der Grössenordnung nach, sehr befriedigend; σ ist aber, wie auch erwartet werden musste, keine Konstante und ändert sich in dem ganzen Gebiet, $0 \leqq \frac{B}{\lambda} \leqq \infty$, von 1 auf ca. 2,50.

6° Die angegebenen Formeln sind, obwohl bei der Ableitung einige Vernachlässigungen und Annäherungen, insbesondere in dem Gebiet $\frac{B}{\lambda} \to 0$, gebraucht sind, genügend, um den Verlauf und die Grösse der Radiometerkraft in dem ganzen Druckgebiet wiederzugeben; sie können auch für zukünftige experimentelle Untersuchungen über die Radiometerkräfte von Bedeutung sein, wenn einmal diese Untersuchungen in systematischer Weise vorgenommen werden.

Auch bei dieser Gelegenheit möchte ich der Direktion des Dänischen Carlsbergfonds meinen aufrichtigen Dank für die mir gewährte Unterstützung aussprechen.

Indleveret til Selskabet den 17. Maj 1943.
Færdig fra Trykkeriet den 1. September 1944.

DET KGL. DANSKE VIDENSKABERNES SELSKAB
MATEMATISK-FYSISKE MEDDELELSER, BIND XXI, Nr. 2

SURFACE TRANSFORMATION CLASSES OF ALGEBRAICALLY FINITE TYPE

BY

JAKOB NIELSEN

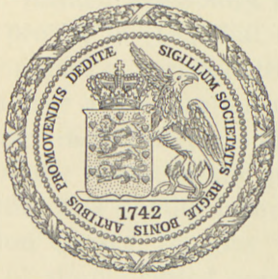

KØBENHAVN
I KOMMISSION HOS EJNAR MUNKSGAARD
1944

TABLE OF CONTENTS

Part I: Foundations.

Part II: Transformation classes of algebraically finite type.

Part III: Homology theory.

Printed in Denmark.
Bianco Lunos Bogtrykkeri A/S

INTRODUCTION

The theory of surface transformations has received a great deal of attention from many authors during the last 60 years. This is, of course, partly due to the rôle they play in the theory of analytic functions. But from the very beginning, even in the fundamental work of HENRI POINCARÉ, the theory of surfaces has had an interest of its own from a purely topological point of view. In recent developments of topology it is chiefly in the theory of surfaces that it has been possible to penetrate beyond the general line characterized by an extensive use of homology theory.

So far as surface transformations are concerned, many investigations have, for good reasons, been focussed upon periodic transformations. This may be seen from the list of works given at the end of this paper, a list to which we refer by numbers in square brackets and which does not pretend to cover all investigations on that topic. In view of generalizations transformation classes of finite order naturally present themselves. They do not, however, furnish essentially new features. This is explained by the fact, proved in [15], that every transformation class of finite order contains a periodic transformation. Hence it seemed to me that a true generalization might start from the fact that in the homology theory of periodic transformations all multipliers, i. e. roots of the characteristic polynomial, are roots of unity. It turns out that this quality belongs to a far-reaching totality of transformation classes. Imagine some part of a surface bounded by a set of simple closed curves and this set carried into a homotopic set by the members of some transformation class. One may then choose a transformation of the class such that this set is carried into itself and then look on the transformation class as carrying that part of the surface into itself.

The class may then be of finite order for that part of the surface, even if it is not so for the surface as a whole. Moreover, the entire surface may be decomposed into such parts. This is, roughly speaking, the idea of the present investigation. To carry it out requires a thorough application of the general properties of surface transformations, especially the methods of the universal covering surface and its limit points. In order not to refer the reader to investigations scattered in many different papers, I outline in part I the general foundations without proof. Part II then deals with a full investigation of the transformation classes concerned and part III with their homology theory.

In the homology theory of transformations the so-called trace formula has hitherto been one of the chief means. The trace is the sum of the roots of the characteristic polynomial. In this matter I want to show that to get full results one should not confine oneself to the trace but deal with the polynomial itself. It contains a good deal of information concerning the transformation class in question (section 22). In section 16 the general form of this polynomial is to be found. All its roots are roots of unity. Although it is actually not proved that all transformation classes with this quality are embraced,—which may well be the case for reasons which I do not intend to discuss here—I propose for the transformation classes investigated the term "classes of algebraically finite type".

The chief means of our investigation is the transformation group induced in the set of limit points of the universal covering surface by a prescribed transformation class. This group is an invariant of the transformation class, thus properties common to all transformations of the class, which concern their behaviour in a twodimensional field, are reflected by a topological transformation in a onedimensional set. It is evident that this means must be of great efficiency. If a generalization of this comprehensive invariant to manifolds of higher dimensions were discovered, a new development of the theory of their transformations might well be expected.

I am indebted to my friends S. Lauritzen and S. Bundgaard for reading the proof and suggesting many valuable improvements.

Part I.

Foundations.

1. Group F as starting point. The subject of the investigations to follow is the orientable, closed or bounded, surface of finite connectivity. Let p denote the genus and r the number of boundary curves of the surface S. These numbers are only submitted to the restriction $2p+r \geq 3$, thus excluding the cases $p = r = 0$ (sphere), $p = 0$, $r = 1$ (circular disc), $p = 0$, $r = 2$ (circular ring) and $p = 1$, $r = 0$ (torus), that is to say all cases in which the natural metric of the surface is spherical or euclidean. Since in the case $2p+r \geq 3$ the natural metric of S is hyperbolic, the universal covering surface of S may be mapped into the unit circular disc X of the plane of a complex variable x in such a way that the elements of the Poincaré group F of S correspond to linear hyperbolic transformations of x carrying X into itself and leaving two points of the bounding unit circle E of X invariant.

For the sake of clearness and generality, we may put the starting point in the following way: Let an arbitrary group F of (fractional) linear transformations of x be given, which is not abelian and the elements of which carry X into itself and —apart from unity—are all hyperbolic. I have shown in [13], § 4, that under the assigned conditions F is properly discontinuous in X, i. e. that each point x of X is imbedded in a neighbourhood containing no image point ($\neq x$) of x under the transformations of F. Let f be any element of F different from unity; the points U_f and V_f of E left invariant by f will be termed the *fundamental points* of f, the arc of circle joining them in X at right angles to E the *axis* of f. In terms of hyperbolic geometry based on E the axis is a straight line, and f is a translation of the hyperbolic plane along the axis in the direction

from U_f towards V_f, from the *negative* towards the *positive* fundamental point of f. Two different axes have no fundamental point in common, otherwise F would contain a parabolic transformation.

The set of fundamental points of all elements of F is called the *set of fundamental points of* F and denoted by G_F. Under the assigned conditions for F the elements of F are enumerable in consequence of the discontinuity of F in X, so G_F is an enumerable set of points of E. The closure $\overline{G}_F$ of G_F containing G_F and derived from G_F by adding all limit points of G_F is called the *set of limit points of* F. The set $\overline{G}_F$ is perfect (no point of $\overline{G}_F$ is isolated). Two cases may present themselves:

a) G_F is not dense on E. In this case $E - \overline{G}_F$ is made up of intervals, which are dense on E and which will be termed *intervals of regularity*,

b) G_F is dense on E. In this case $\overline{G}_F$ coincides with the entire circumference E.

The smallest subset of $X+E$ containing $\overline{G}_F$ and convex in a non-euclidean sense is denoted by $\overline{K}_F$. In case a) $\overline{K}_F$ is obtained by removing from $X+E$ each interval of regularity together with the non-euclidean half-plane bounded by it. Inside X therefore $\overline{K}_F$ is bounded by arcs of circle at right angles to E joining the end points of some interval of regularity. In case b) $\overline{K}_F$ coincides with $X+E$. In both cases the set of points common to $\overline{K}_F$ and X is termed *convex region* of F and denoted by K_F. The set $\overline{K}_F$ is obtained from K_F by adding G_F, which is precisely the set of limit points of K_F on E. In case b) the convex region of F coincides with X.

Now the group F evidently transforms G_F into itself, the fundamental points of f being transformed into the fundamental points of gfg^{-1} by an element g of F. Therefore by continuity F transforms $\overline{G}_F$ into itself and, being a group of non-euclidean displacements, transforms $\overline{K}_F$ and X and thus their common part K_F into itself. Speaking of F as a group of transformations of K_F we may in abstracto consider the whole set Fx of images of x under the transformations of F as one point $\{x\}$. The set of these points $\{x\}$ then form a manifold (surface), which we may denote by K_F mod F.

The surface K_F mod F obtained in this way from an arbitrary group F subject to the above conditions need not, however,

be of finite connectivity. To obtain this, one more condition must be imposed on the group F, viz. to be generated by a finite number of its elements. As shown in [13], § 11—12 this is equivalent to the condition that there exists a non-euclidean finite region of X, a circle inside E, say, which contains at least one point of every set Fx, x being a point of K_F, in its interior. Under this condition all boundaries of K_F inside X are axes of F and they arise from a finite number r of distinct boundaries by the transformations of F. Then K_F mod F is a surface of finite connectivity with r bounding curves, which are closed geodesics in the sense of the hyperbolic metric imposed on the surface. In case b), $K_F = X$, K_F mod F is a closed surface, $r = 0$. In both cases a certain genus p arises; in case a) p may be zero, provided $r \geq 3$.

To sum up, we start with a transformation group F of X subject to three conditions:

F is not abelian.

All elements of F other than identity are hyperbolic.

F is generated by a finite number of elements.

Then K_F mod F is our orientable surface S of finite connectivity with a certain genus p and a certain number r of boundary curves. S may be illustrated by an image in ordinary space. A hyperbolic metric derived from X is impressed upon S. In this metric every axis of F corresponds to a closed geodesic of S; especially the boundary curves are such geodesics. F is isomorphic to the Poincaré group of S. The minimum number of generators of F is $2p$ in case $r = 0$ and $2p + r - 1$ in case $r > 0$. In the latter case F is a free group.

Some consequences are immediate: Let A be an axis of F. The set of its images under the transformations of F is called the *congruence class* of A and denoted by FA. All axes of FA correspond to one closed geodesic a of S. Let λ be the non-euclidean length of a. There exists an element f of F with the axis A, which displaces the points of A at the distance λ along A. The element f (and likewise its inverse f^{-1}) is called *primary element of F to the axis A*, and λ is called *primary displacement length* belonging to the axis A. All elements of F belonging to A are powers of f, and their displacement lengths are multiples of λ. The class FA does not accumulate in X. All its axes have

the same primary displacement length. The number of elements of F the displacement length of which is inferior to a given positive constant is finite.

The properties of groups F and corresponding surfaces S shortly recalled in this introductory section are investigated at length in my paper [13], to which reference may be made for the proofs. In part I and II of the present paper most of the investigations are carried out in the convex region K_F of X, the universal covering surface of S with its group F, but incidentally we may draw conclusions directly on the illustrative model S.

2. Transformation functions. Let τ denote a topological (i. e. one-to-one and continuous) transformation of S into itself preserving orientation. Let $\{x_0\}$ be any point of S and $\{x_0'\}$ its image under τS. Let x_0 be a point of K_F representing $\{x_0\}$ and x_0' a point representing $\{x_0'\}$. Then by continuity we have one topological transformation of K_F and one only covering the surface transformation τS and carrying x_0 into x_0'. We denote this transformation of K_F by $x' = \varkappa(x)$. The transformation function $\varkappa(x)$ thus defined in K_F satisfies a system of functional equations: Let f be any element of F[1]. As x and $f(x)$ determine the same point $\{x\}$ of S, their images under the transformation $\varkappa$ must correspond to the same point $\{x'\}$ of S:

$$\varkappa(f(x)) = f'(x') = f'(\varkappa(x)), \quad f' \subset F.$$

For reasons of continuity the correspondence $f \to f'$ cannot depend on the choice of x, and it is easily seen that this correspondence constitutes an automorphic transformation of the group F into itself. Denoting this automorphism by the letter I and writing f_I instead of f', we may write the above functional equation in short

$$\varkappa f = f_I \varkappa. \tag{2.1}$$

In (2.1) f and accordingly f_I ranges over the group F and the argument x of the functions (not written explicitly in (2.1)) over the convex region K_F.

[1] We denote this by $f \subset F$, using $\subset$ as a symbol of inclusion, and write likewise $F \supset f$.

Since in defining $\varkappa$ we have chosen the representing points x_0 and x_0' of the points $\{x_0\}$ and $\{x_0'\}$ of S freely within their congruence classes Fx_0 and Fx_0' respectively, $\varkappa$ is not the only transformation function to represent the surface transformation τS. But it is evident that any transformation function covering τS can differ from $\varkappa$ by an element g of F only. Thus

$$g\varkappa = g\,(\varkappa\,(x)), \quad g \subset F,$$

is the totality of transformation functions covering τS, the element g ranging over the entire group F. Since (2.1) may be written

$$\varkappa f \varkappa^{-1} = f_I, \tag{2.2}$$

we have for $g\varkappa$ the functional equation

$$g\varkappa f \varkappa^{-1} g^{-1} = g f_I g^{-1}.$$

The automorphism $f \to g f_I g^{-1}$ corresponding to $g\varkappa$ is said to be *related* to I and is derived from I by applying the *inner* automorphism consisting in transforming by the element g. The totality of related automorphisms obtained by making g range over F is termed a *family of automorphisms* of F.

If the given topological transformation τ of S is made to vary continuously, even so as not to preserve its quality of being one-to-one, this will make $\varkappa$ vary accordingly, but for obvious reasons of continuity it will not alter the functional equation (2.1). Thus the automorphism I induced by $\varkappa$ will be unaltered. So we infer that *the family of automorphisms of F belonging to the surface transformation τS is an invariant of the transformation class of τ.*

In looking for invariants of surface transformation classes the chief means lies in the fact that transformation functions such as $\varkappa$, originally defined in K_F, extend continuously from K_F to $\overline{K}_F$, thus including the set $\overline{G}_F$ of limit points of F within the reach of their definition. For closed surfaces ($r = 0$) this has been proved in [14] I, § 28; in [15], § 4, another proof will be found, which is valid also for $r > 0$. The structure of $\varkappa$ in $\overline{G}_F$ is easily described by first taking into account the set G_F of fundamental points of F. Any point x of G_F is the positive funda-

mental point V_f of exactly one primary element f of F. Then x is the positive fundamental point of all elements f^n, $n>0$, and of no other element of F. Now $\varkappa$ carries the positive fundamental point of any element of F into the positive fundamental point of the element corresponding to it under the automorphism I belonging to $\varkappa$. In symbols:

$$\varkappa\, V_f^n = V_{f_I}^n . \tag{2.3}$$

Since G_F is dense in $\overline{G}_F$, the extension of $\varkappa$ to $\overline{G}_F$ derives from continuity, and it is seen that $\varkappa$ is topological in $\overline{G}_F$ and preserves the order of $\overline{G}_F$ on E. Cf. [14] I, § 9, and [15], § 3.

From (2.3) we infer that the transformation $\varkappa\overline{G}_F$ depends on I only. So it does not vary even if $\varkappa$ varies continuously in K_F. So we have: *The transformations* $g\varkappa$, $g\subset F$, *of the set* $\overline{G}_F$ *of limit points of* F *are invariants of the transformation class.* One of these, say $\varkappa$, is sufficient to determine all the others.

3. The group *T*. Another means needed for thorough investigation of a transformation class is iteration of the transformations of the class. Writing the symbol 1 for the identical transformation of F, an enumeration of the elements of F may be given by

$$1,\ f_1,\ f_2,\ \cdots\cdots \text{ in inf.}$$

Writing τ^2 for the iterated transformation $\tau\tau S$, this transformation is covered by $\varkappa^2 = \varkappa\,(\varkappa(x))$ and likewise by all functions of the sequence

$$\varkappa^2,\ f_1\varkappa^2,\ f_2\varkappa^2,\ \cdots\cdots$$

Supposing τ topological in order that τ^{-1} may be defined, this extends to all positive and negative powers of τ, and we get the following scheme written in full:

$$(T)\qquad \begin{array}{c|l} \cdots & \cdots\cdots\cdots\cdots\cdots \\ [\tau^{-2}] & \varkappa^{-2}\quad f_1\varkappa^{-2}\quad f_2\varkappa^{-2}\quad \cdots \\ [\tau^{-1}] & \varkappa^{-1}\quad f_1\varkappa^{-1}\quad f_2\varkappa^{-1}\quad \cdots \\ [\tau^{0}] & 1\quad f_1\quad f_2\quad \cdots \\ [\tau] & \varkappa\quad f_1\varkappa\quad f_2\varkappa\quad \cdots \\ [\tau^{2}] & \varkappa^{2}\quad f_1\varkappa^{2}\quad f_2\varkappa^{2}\quad \cdots \\ \cdots & \cdots\cdots\cdots\cdots\cdots \end{array}$$

By applying the functional equation (2.1) it is easily seen that these transformation functions form a group; e. g. we get

$$f_\mu z^\alpha \cdot f_\nu z^\beta = f_\mu \left(f_\nu\right)_{I^\alpha} z^{\alpha+\beta},$$

$$\left(f_\mu z^\alpha\right)^{-1} = z^{-\alpha} f_\mu^{-1} = \left(f_\mu^{-1}\right)_{I^{-\alpha}} z^{-\alpha}.$$

This group will be denoted by the letter T. Moreover F is an invariant subgroup of T, as is seen by applying the functional equation in the form (2.2). The lines of the above scheme (T) stand for the elements of the corresponding factor group T/F.

The transformation functions written in the scheme (T) need not be different. Two functions in the same line are always different, since they differ by an element of F. Let $f_\mu z^\alpha$ and $f_\nu z^\beta$ be the same transformation function of K_F. Then $f_\nu^{-1} f_\mu z^{\alpha-\beta} = 1$ is the identical transformation of K_F. Putting $|\alpha-\beta| = n$, we find that z^n is an element of F. So τ^n is the identical transformation of S. Since $n \neq 0$, τ is a *transformation of finite order* (a periodic transformation) of S. In this case T/F is cyclic. In case all functions of the scheme (T) are different, T/F is infinite, viz. a free group generated by one element, and τ is not periodic.

The above scheme is, however, capable of another aspect. In consequence of section 2 all functions of the scheme extend to the set $\overline{G}_F$ of limit points of F. Moreover, all functions of the scheme remain topological in $\overline{G}_F$, even if z by continuous deformation does not remain so in K_F. Therefore the group T always exists as a group of topological transformations of $\overline{G}_F$, and by section 2 it is evident that *the group T defined in $\overline{G}_F$ is an invariant of the transformation class under consideration.*

With this new aspect of the group T we may ask what are the consequences of two elements of the scheme (T) being the same transformation function in $\overline{G}_F$. It means that z^n for some positive n transforms $\overline{G}_F$ in the same way as a certain element f of F; n may be chosen as the smallest positive number with this property. Hence $f^{-1} z^n$, which is a function of the line $[\tau^n]$ of (T), leaves all points of $\overline{G}_F$ fixed. The automorphism induced by $f^{-1} z^n$ therefore is the identical automorphism. This means that $\tau^n S$ belongs to the transformation class of identity, and τ is said to belong to a *transformation class of finite order*. These classes

therefore are characterized by the fact that the factor group T/F is cyclic of some finite order n with respect to $\overline{G}_F$ alone irrespective of the behaviour of the transformation functions in K_F.

Transformation classes of finite order have been investigated at length in [15]. The chief result of this paper is that a class of order n contains a transformation which is itself of order n. So one may always choose periodic transformations as representatives of transformation classes of finite order. We take advantage of this fact later on in this paper.

Periodic transformations of surfaces have been the subject of many investigations. Apart from their rôle in the theory of algebraic functions I quote in the present connection papers of L. E. J. BROUWER [3], [4], [5], B. v. KERÉKJÁRTÓ [8], [9], section 6, § 6, W. SCHERRER [19], [20], [21], F. STEIGER [22] and myself [16]. Later on we will have to enter more fully into the details of such periodic transformations.

4. Principal region and kernel. From what has been said it will be expected that a closer investigation of the behaviour of all transformation functions of the scheme (T) in the set $\overline{G}_F$ of limit points of F will be needed. This investigation has been carried out in [14]II, and we have merely to draw up the results as far as they are required for our present purpose. In one respect a slight addition has to be made: [14] only deals with the case of a closed surface, whereas we here have to take into account the possibility of S being bounded ($r > 0$). This does, however, not affect the validity of the analysis given in [14]. To be short, the difference can be eliminated by first mapping the circumference E continuously on another circumference E' in such a way that all intervals of regularity of E are mapped into single points of E' and the circular order of E is preserved.

With slight variation in formulating the results, the analysis of [14]II may be described in the following way:

Let t denote any element of T and J the automorphism induced by t. If t is unity, all points of $\overline{G}_F$ are left fixed by t, and J is the identical automorphism. We are concerned with the case when t is not unity. Then, in general, the points of a certain true subset M of $\overline{G}_F$ are left fixed by t. M is closed, since t is

continuous on $\overline{G}_F$, and M may contain isolated points. As a special case, M may be empty; we have to deal with this case later on. Also, in general, the elements of a certain subgroup N of F are left fixed under the automorphism J. The fundamental points of the elements of N then belong to M and so does the set $\overline{G}_N$ of limit points of N. Inversely, a fundamental point of F belonging to M is a point of G_N. As a special case, N may consist only of unity, and this may occur even if M is not empty. As another special case, N may be abelian and then consists of all elements of F belonging to a certain axis; in this case, the two fundamental points of this axis are the only fundamental points of F belonging to M. In general, the subgroup N is not abelian and then is of the same character as F itself; the set $\overline{G}_N$ of its limit points then is perfect and contained in M.

Every element of N carries points of M into points of M, thus reproduces M; it also reproduces the complementary set $E-M$.

Since M is a true subset of $\overline{G}_F$, some at least of the intervals forming $E-M$ contain points of $\overline{G}_F$. If i be such an interval, all points of $\overline{G}_F$ inside i are displaced by t in the same direction; this is easily seen to be true even in case $r>0$, when $\overline{G}_F$ is nowhere dense on E; all intervals of regularity of F play the same rôle as single points. A point P of M will be termed an *isolated* point of M, if P is common end point of two intervals of $E-M$ and both contain points of $\overline{G}_F$. It will be termed *attractive* if the direction of displacement in both intervals goes towards P, *repulsive* if the direction of displacement in both intervals goes from P, and *neutral* if the direction of displacement in both intervals are in accordance on E.

If M contains a neutral point, M is made up of exactly two points, which are end points of an axis (fig. 1). The direction of displacement is indicated by arrows.

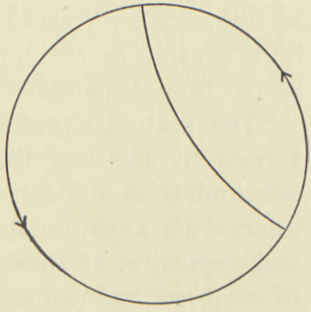

Fig. 1.

We now define a subset M^* of M as follows. Let t belong to the line $[\tau^n]$ of the scheme (T). If $n \geq 0$, M^* is derived from M by removing all repulsive isolated points (if any). If $n<0$, M^* is

derived from M by removing all attractive isolated points (if any). (If $n = 0$, we have $t = f \neq 1$, $f \subset F$; then M consists only of the fundamental points U_f and V_f of f. If the axis of f is not a boundary axis of K_F, the former is repulsive, the latter attractive; so $M^* = V_f$.)

M^* is still a closed set. In all cases in which M^* consists of more than one point a convex region may be built on M^* in the same way as was used in deriving the convex region of F from $\overline{G}_F$ in section 1: We remove from X all non-euclidean half-planes bounded by an interval of $E - M^*$. The convex region obtained in this way will be termed the *principal region* of t. In case M^* only consists of two points, the principal region degenerates to a non-euclidean straight line. This may or may not be an axis of F. In case M^* only consists of one point, there is no principal region at all.

Moreover M^* still contains all points of $\overline{G}_N$, with the only exception of the case in which M is made up of two fundamental points (end points of an axis of F) one of which is repulsive the other attractive; in the latter case, M^* only consists of one point, and there is no principal region. So if a principal region exists, it contains the convex region of N, and this then will be termed the *kernel* of t. Two special cases should be noticed: If N only consists of identity, there is no kernel at all. If N is abelian, $\overline{G}_N$ consists of two points only (end points of an axis): if one of these is repulsive the other attractive, there is no principal region and no kernel; if not, they are either both neutral, or M^* consists of more than these two points; the kernel then degenerates to the axis of N.

The mutual situation of principal region and kernel is governed by the fact that points of M (and so of M^*) do not accumulate in the intervals of $E - \overline{G}_N$. Points of M in such an interval (if any) are therefore isolated and alternately attractive and repulsive. If there is a kernel, the end points of such an interval are end points of an axis bounding the kernel. All elements of F belonging to that axis are elements of N. Hence they reproduce M. If therefore the interval contains a point of M, it contains an infinity of points of M accumulating towards the end points of the interval.

The principal region has cuspidal points in all isolated points of M^*.

To sum up, we review the different cases which may occur. In the figures it is assumed that t belongs to a line $[\tau^n]$, $n > 0$, of the scheme (T).

A. N only consists of identity. ($\overline{G}_N$ is empty.)

A_1. M is empty. t leaves no point of $\overline{G}_F$ fixed.

A_2. M is not empty. t leaves a certain number of points of $\overline{G}_F$ fixed. This number is finite, since M does not accumulate on $E - \overline{G}_N = E$. Fig. 2 shows an example, M consisting of six points, three of which are attractive, the

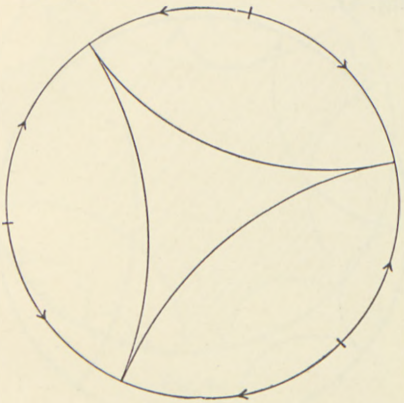

Fig. 2.

others repulsive. There is a principal region but no kernel. If there were but four points in M, the principal region would reduce to a non-euclidean straight line. If there were but two points in M, the subset M^* would reduce to one point, and the principal region would vanish.

B. N is abelian. ($\overline{G}_N$ consists of two points only.)

B_1. M consists of these two points only (the end points of the common axis of all elements of N). If these are neutral points, the axis is both principal region and kernel (fig. 1). If, on the other hand, one is attractive, the other repulsive, M^* consists of one point only, and both kernel and principal region vanish.

B_2. M contains more than these two points. In at least one of the two intervals of $E - \overline{G}_N$ there are cuspidal points of the principal region. These accumulate towards the end points of the axis (fig. 3). This situation may occur in one or in both intervals.

C. N is not abelian. ($\overline{G}_N$ is a perfect set.)

$\mathbf{C}_1$. M coincides with $\overline{G}_N$. Both kernel and principal region are made up of the convex region of the group N. Here is embraced the case in which $N = F$, i. e. t is identity.

$\mathbf{C}_2$. M contains more points than $\overline{G}_N$. In some of the intervals of $E - \overline{G}_N$ we have a series of cuspidal points of the same kind as in fig. 3. The kernel is the convex region of N and orms a part only of the principal region (fig. 4).

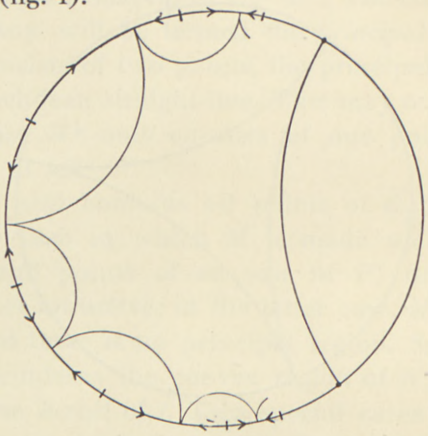

Fig. 3.

From this analysis two numbers may be derived. Let ν denote the minimum number of generators of N. In case **C** we have $\nu > 1$, and N is a free group, if for the present we leave apart the case $N = F$ and S closed. In case **B** we have a free group N with $\nu = 1$ generator. In case **A**, when N is unity, we may agree to call a group consisting of unity only "a free group with $\nu = 0$ generators".

In case **A** the number of cuspidal points of the principal region is finite, say μ. In cases **B** and **C** this number is either zero or infinite, but in the latter case all cuspidal points arise from a certain finite number of cuspidal points by applying the elements of N. So we may speak of μ as the number mod N of cuspidal points.

It is shown in [14] II, that $\nu + \mu$ is limited by some function of the number of connectivity of S. Hence only a finite number

of different types of functions t arise from this analysis. But these considerations are not necessary for our present purpose.

Any fundamental point of F is the positive fundamental point V_f of some element f of F. If V_f belongs to M, the element f is fixed under the automorphism J. So V_f belongs to G_N and hence to $\overline{G}_N$. From this we infer that all cuspidal points of the principal region, which are situated in inter-

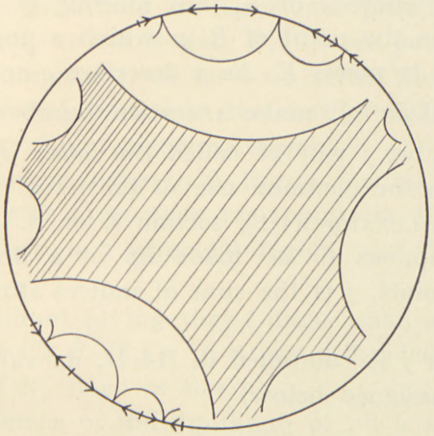

Fig. 4.

vals of $E - \overline{G}_N$, are limit points but not fundamental points of F.

5. Classes of fixed points and index. Let us now consider the function t of the last section not only as a transformation function defined in $\overline{G}_F$ but in $\overline{K}_F = K_F + \overline{G}_F$, and let $\tau^n S$ be the corresponding transformation of the surface S. Let Q denote the set of points of K_F left fixed by t (if any). The set Q covers a certain set q of points of S left fixed by τ^n. This set q is called a *class of fixed points* of $\tau^n S$. There may be other fixed points of $\tau^n S$ than the set q, since other functions of the scheme (T) in the line $[\tau^n]$ of t, functions of the form ft, $f \subset F$, may yield a class. For the moment we are concerned with the class q only. Let x_0 be some point of Q, thus $tx_0 = x_0$. What about fx_0, $f \subset F$? By (2.1) we get immediately

$$tfx_0 = f_J t x_0 = f_J x_0 .$$

So if $f = f_J$, the point fx_0 belongs to Q, and if $f \neq f_J$, it does not. Hence Q is reproduced by the subgroup N of F and by no other element of F.

Let ψ denote a fundamental region of N in K_F, i. e. a region containing exactly one point of each set Nx, $x \subset K_F$. Then the class q will be covered exactly once by the part of Q belonging to ψ. Let us assume ψ to be so chosen as to be bounded by a simple closed curve c of K_F not meeting Q. If x is a point of c, let $\varphi(x)$ be the point of E in which a non-euclidean ray from x through tx meets E. As x describes c once in a positive sense, $\varphi(x)$ will in all make a certain number $j \gtreqless 0$ of tours of E. This number j will be called the *index of the class* q in accordance with the common use of the term "index"; see for instance J. W. ALEXANDER [1], section 2, or S. LEFSCHETZ [12], p. 276: if q happens to be made up of a finite number of isolated fixed points, j is the sum of indices attributed to these single points.

This number j is computed in [14] II, its value being (with one exception assigned below)

$$j = j(t) = 1 - \nu - \mu, \tag{5.1}$$

thus only depending on the numbers ν and μ attributed to t in the preceding section. If the structure of Q be such as not to allow ψ to be so chosen as to be bounded by a simple curve avoiding Q, this may be achieved by a slight variation of t. So we fix the value (5.1) to be the index of q in all cases.

The exceptional case referred to above is a very special one well known from the homology theory of transformations: If S is closed and t belongs to the transformation class of identity, one gets

$$j = 2 - 2p, \tag{5.2}$$

while in that case $\mu = 0$ and $\nu = 2p$. This is the well known formula of BIRKHOFF [2]. The explanation of this difference is simple: In all cases which are not the BIRKHOFF case, the determination of the index of a class of fixed points takes into account an auxiliary surface (so to speak), viz. the surface corresponding to the principal region of t; and this surface in all these cases is not closed. See also [14] II, § 16.

We now examine the different possible values of j in (5.1). Since $\nu \geqq 0$ and $\mu \geqq 0$ the greatest possible value is $j = 1$ arising from $\nu = \mu = 0$. This is the case $\mathbf{A}_1$ of the previous section. The next section will be devoted to closer investigation of this case.

Then we may have $j = 0$. That requires either $\nu = 0$, $\mu = 1$, or $\nu = 1$, $\mu = 0$. If $\nu = 0$, $\mu = 1$, we are in case $\mathbf{A}_2$ with $2\mu = 2$ points in M, and no kernel nor principal region exists. If $\nu = 1$, $\mu = 0$, we are in case $\mathbf{B}_1$. If one point of M is attractive, the other repulsive, we have no kernel nor principal region. If both are neutral, we are in the case of fig. 1 with an axis of F both as kernel and principal region.

Finally we may have $j < 0$, thus $\nu + \mu > 1$. Then we are in the cases $\mathbf{A}_2$ with more than two points in M, $\mathbf{B}_2$ or $\mathbf{C}$. In all these cases there is a principal region, and if $\nu > 0$ there is a kernel.

It goes without saying that t must leave at least one point of K_F fixed, if $j \neq 0$. If $j = 0$, it is not decided whether t leaves some point of K_F fixed or not.

In consequence of the limitation of $\nu + \mu$ mentioned in section 4 there is a limit to the possible negative values of indices of classes of fixed points on a surface of given connectivity. We do not state this limit explicitly, as we do not need it for our purpose.

6. Index $j = 1$. If the set M of fixed points of $\overline{G}_F$ under the transformation t is not empty, let us examine any interval of $E - M$ containing points of $\overline{G}_F$. These are displaced by t in a definite direction common to all points of $\overline{G}_F$ in the interval, only the end points remaining fixed. By the powers $t^2, t^3, \cdots$ this displacement is increased, thus no new fixed point can arise. Hence $t^2, t^3, \cdots$ have the same set M of fixed points as t. The same is true of $t^{-1}, t^{-2}, \cdots$, in which cases the displacement goes in the opposite direction. Moreover, isolated points of M which are repulsive for t are repulsive for $t^2, t^3, \cdots$ and attractive for $t^{-1}, t^{-2}, \cdots$. In view of the definition of M^* in section 4, this set M^* therefore is common to all powers of t (except t^0, of course), and so are the principal region, the kernel, the numbers ν and μ and hence the index j. We thus infer

that *an index $j \leq 0$ of a class of fixed points is stable with respect to iteration of the transformation.*

As to an index $j = 1$, things are different. In this case M is empty, so the successive displacements of a point of $\overline{G}_F$ under the powers of t may eventually carry it back to its original position. In fact, in [14] III, § 1, it has been shown that some power t^n, $n > 0$, of t will have a set M of fixed points, which is not empty, in $\overline{G}_F$. It is true that in the proof given in [14] III the surface was assumed closed, but, as in previous cases, the extension to bounded surfaces is immediate, if one makes the intervals of regularity play the rôle of single points.

Let n be the smallest positive number for which t^n leaves some points of $\overline{G}_F$ fixed, and let M denote the set of these points. Since M is not empty, we have $j(t^n) \leq 0$. Let P be any point of M and $P' = tP$ its image under the transformation t. Then

$$t^n P' = t^n tP = tt^n P = tP = P',$$

hence $P' \subset M$, and M is reproduced by t. Moreover, since $t \cdot t^n \cdot t^{-1} = t^n$, an isolated attractive point of M is carried into an isolated attractive point of M, a repulsive into a repulsive, a neutral into a neutral. Let N be the subgroup of fixed elements belonging to t^n. Since fundamental points are transformed by t into fundamental points, it is seen that G_N and hence $\overline{G}_N$ is reproduced by t. We now examine the different cases of section 4:

A. If t^n is of type $\mathbf{A}_2$, M consists of 2μ points, μ of which are attractive. Since the attractive points of M are interchanged by t, we must have $\mu \geq 2$. Hence there is a principal region for t^n (in case $\mu = 2$ degenerating into one straight line) and, speaking symbolically, this principal region is "rotated" in itself by t.

B. If t^n is of type **B**, M contains two fundamental points, and these are interchanged by t, so $n = 2$. In case $\mathbf{B}_1$ these two points clearly must be neutral. So we are in the case of fig. 1 and, symbolically, the axis, which is at the same time principal region and kernel, is "reversed". In case $\mathbf{B}_2$ the two intervals are interchanged, so the two parts of the principal region separated by the axis (kernel) must have the same number mod N of cuspidal points.

C. In case **C** we merely notice that, symbolically, the principal region of t^n is "rotated" in itself by t, and so is the kernel of t^n.

Thus it is seen that t^n has in all cases a principal region, and we may say that t, though it has not itself a principal region, is *affiliated to the principal region of* t^n. This is of course the principal region of all powers of t^n too. In the same way in cases **B** and **C**, t^n has a kernel, and we may say that t is *affiliated to that kernel.*

So the index of a class of fixed points with index $j = 1$ is not stable with respect to iteration of the transformation. It is affiliated to a class of fixed points with index $j \leq 0$ of some power of the transformation. It should be noticed that several distinct classes with index $j = 1$ may well be affiliated to one and the same class with index $j \leq 0$ of some power of the transformation.

7. Simple axes. Equivalence classes and congruence classes. In the first part of this section we consider T as a group of transformations of $\overline{G}_F$ only, thus abstract from the rôle of the elements of T as transformation functions of the convex region K_F of F.

Let A be any axis of F, f an element of F belonging to A, thus U_f and V_f the end points of A. Let t be any element of T and J the corresponding automorphism. Then t takes U_f and V_f into the points U_{f_J} and V_{f_J} respectively, i. e. into the end points of the axis belonging to the element f_J corresponding to f under the automorphism J. We denote this axis by tA, thus speaking *purely symbolically* of it as the image of A under the transformation t. Making t range over the whole group T we get a totality of axes, denoted by TA and termed the *equivalence class of* A *with respect to* T.

If TA satisfies the condition that any two axes of TA are either identical or have no point in common (thus do not intersect), A and so any axis of TA will be termed *simple with respect to* T. Examples are obvious: If the surface S is bounded, an axis bounding the convex region K_F of F cannot be crossed by any other axis of F; so it is simple with respect to T.

More generally, if A does not mean an axis of F, but merely a non-euclidean straight line joining two points of $\overline{G}_F$, the

straight line joining the images of these to points under t is denoted by tA. Then the same considerations may be applied and simplicity of A with respect to T defined.

Moreover, if T' is any subgroup of T, the meaning of the denotation $T'A$ and of simplicity with respect to T' is immediate. So if F is taken as subgroup of T, simplicity of A with respect to F means that the geodesic a of S corresponding to A does not intersect; if A is an axis, a is a simple closed geodesic (without double points).

Simplicity with respect to T involves simplicity with respect to any subgroup of T, but not vice versa. So if A is simple with respect to T, a is a simple geodesic; if a is a simple geodesic, A is simple with respect to F, but A may be intersected by some tA, $t \subset T$ but not in F, and so need not be simple with respect to T.

Let t_1 and t_2 be two elements $\neq 1$ of T and let a principal region, say $\Omega(t_1)$ and $\Omega(t_2)$, exist for both of them. It is first assumed that t_1 and t_2 belong to the same line of the scheme (T), say to $[\tau^n]$. Then $n \neq 0$, since there is no principal region for an element $\neq 1$ of F. The mutual situation of $\Omega(t_1)$ and $\Omega(t_2)$ in K_F then is one of the following three cases:

1) they are identical,
2) they have no point in common,
3) they have one axis of F in common.

In case 3) both functions of course have a kernel, say $\Gamma(t_1)$ and $\Gamma(t_2)$, the axis is a bounding axis for both of these, and $\Omega(t_1)$ and $\Omega(t_2)$ and so $\Gamma(t_1)$ and $\Gamma(t_2)$ are contiguous along that axis.

The proof of this theorem is to be found in chapter 3 of [14] II with a slight modification: The paper quoted speaks of a principal region $\Omega(t)$ only if t leaves more than two points of $\bar{G}_F$ fixed, whereas we here include the case (fig. 1) of t having exactly two fixed points, these being neutral. It will, however, easily be seen that this case exactly fits into the proof too.—The situation met with later in the present paper makes our present, broader definition of the concept of principal region $\Omega(t)$ necessary. In fact $\Omega(t_2)$, say, may happen to be such an axis as in fig. 1, thus at the same time being

$\Gamma(t_2)$, and may coincide with a boundary axis of $\Omega(t_1)$ (and so of $\Gamma(t_1)$).

The above assumption of t_1 and t_2 belonging to the same line of (T) is readily seen to be superfluous. In fact, since $\Omega(t_1)$ and $\Omega(t_2)$ exist, these regions are, as pointed out in section 6, principal regions of all powers of t_1 and t_2 respectively. So in choosing a line of (T) containing a power of t_1 and of t_2 simultaneously and applying the above theorem we get the same three possibilities of the mutual situation of $\Omega(t_1)$ and $\Omega(t_2)$.

So if we let t range over all elements $\neq 1$ of T for which a principal region $\Omega(t)$ exists, the totality of these regions $\Omega(t)$ has the property that any two of its members do not intersect.

Now, let t and t_1 be any two elements of T. We consider t_1 together with the conjugate element

$$t_2 = tt_1t^{-1}.$$

It is obvious that any point of $\bar{G}_F$ left fixed by t_1 is carried by t into a point left fixed by t_2. So $M(t_2)$ is the image of $M(t_1)$ by t. As the character of being isolated, attractive etc. is preserved for the points of M, and t_1 and t_2 belong to the same line of the scheme (T) (thus $n \geq 0$ or $n < 0$ for both in the definition of M^*) we also have $M^*(t_2) = tM^*(t_1)$. We may therefore say symbolically that $\Omega(t_2)$ is the image of $\Omega(t_1)$ by t and write

$$\Omega(t_2) = t\,\Omega(t_1).$$

The same is valid for the kernels, if any. Making t range over the whole of T we get an *equivalence class* $T\Omega(t_1)$ of principal regions and $T\Gamma(t_1)$ of kernels. All functions tt_1t^{-1} are said to form an *equivalence class of functions.*

We now infer that any non-euclidean straight line, whether axis of F or not, bounding some principal region, is simple with respect to T; this follows at once from the above theorem that two different principal regions do not intersect. Especially such a bounding line is simple with respect to F. Thus the boundaries of a region of the surface corresponding to a principal region are simple geodesics.

Since an equivalence class of principal regions is part of the totality of all such regions, any two of its members are mutually

situated in one of the three possible ways indicated above. We may express this property by saying that *any principal region is simple with respect to T.*

We return once more to the comparison of two conjugate elements of T such as t_1 and $t_2 = tt_1t^{-1}$. If the element $f \subset F$ is left fixed by t_1,

$$t_1 f t_1^{-1} = f,$$

the element tft^{-1}, which also belongs to F, is left fixed by t_2. So we may write

$$N(t_2) = tN(t_1)\, t^{-1}.$$

$N(t_1)$ and $N(t_2)$ need not be conjugate subgroups of F, since t need not belong to F. But they are isomorphic, so they have the same number of generators. Hence

$$\nu(t_1) = \nu(t_2).$$

From this isomorphism and from the homeomorphism of $M^*(t_1)$ and $M^*(t_2)$, thus of $\Omega(t_1)$ and $\Omega(t_2)$, we infer that moreover

$$\mu(t_1) = \mu(t_2).$$

So we find that indices are the same:

$$j(t_1) = j(t_2).$$

We now again take T as a group of transformations of the closed convex region $\bar{K}_F$ of F.

Any two transformation functions conjugate in T such as t_1 and t_2 yield classes of fixed points with the same index j, as we have just seen. Are these classes different classes of fixed points of the surface transformation in question?

To decide this, let t be a transformation function, J the corresponding automorphism and x_0 a point of K_F left fixed by t. No other function of the line of t in the scheme (T) can leave x_0 fixed, since it differs from t by an element of F. Now let $f \neq 1$ be any element of F. The function $ftf^{-1} = ff_J^{-1}t$, which belongs to the line of t, evidently leaves fx_0 fixed; so no other function of the line of t can leave fx_0 fixed. If Q denotes the set of fixed points of t, then fQ is the set of fixed points of

ftf^{-1}. So two functions t_1 and t_2 yield the same class of fixed points, if one is transformed into the other by an element of F, and in that case only.

All functions ftf^{-1}, t being a fixed element of T and f ranging over the entire group F, will be termed a *congruence class of functions* and the corresponding set $F\Omega$ of principal regions a *congruence class of principal regions*. Two functions such as t and $ftf^{-1} = ff_J^{-1}t$ are said to be *congruent*[1].

Any equivalence class is subdivided into congruence classes.

In looking for classes of fixed points of a surface transformation τS, only one representative of each congruence class of functions in the line $[\tau^1]$ has to be examined. These are still in infinite number, but only a finite number of them yield a class of fixed points which is not empty; this is shown in [14] I, § 32.

The principal regions of all functions ftf^{-1} of a congruence class are the images of $\Omega(t)$ by the transformations $f \subset F$. They all cover one and the same region of the surface S.

Part II.

Transformation classes of algebraically finite type.

8. Definition of the transformation classes concerned. The matter of part I was an outlining in brief of the general foundations of the theory of surface transformation classes needed for establishing the main invariants of such classes. We now proceed to the chief subject of this paper, a full investigation of all transformation classes for which *principal region and kernel coincide for every element of T for which a principal region exists.*

The different types of functions t are analyzed at the end of section 4. To make things clear, let us look at the summary of that section with the present assumptions. Cases $\mathbf{B}_1$ and $\mathbf{C}_1$ are clearly in accordance with the present assumptions, whereas $\mathbf{B}_2$ and $\mathbf{C}_2$ are excluded: the existence of cuspidal points makes the principal region contain more than the kernel. In case $\mathbf{A}_2$ there can only be two points in M, one attractive and one repul-

[1] In [14] the term "isogredient" has been used.

sive, since for more than two points in M there would be a principal region without a kernel. Case A_1 is permitted, but it has to be remembered that such a function is affiliated to a principal region corresponding to a certain power of the function, and this principal region must then belong to one of the types permitted.

The characterization of the transformation classes in question may also be put thus: The number μ, defined in section 4, is zero for all elements of T except for the type $\nu = 0$, $\mu = 1$, which is permitted, as it has no principal region.

One may ask whether transformation classes satisfying this condition are to be found at all. It is readily seen that all transformation classes of finite order are embraced. For such classes T/F is a cyclic group of some order n, as pointed out in section 3. It has been shown in §§ 6, 7 of [15], that any element $\neq 1$ of such a group T is *either* of type $j = 0$ with $\nu = 1$, $\mu = 0$, one end point of the axis being attractive, the other repulsive, and so has no principal region, *or* of type $j = 1$ ($\nu = \mu = 0$). In the latter case the principal region to which the element is affiliated is the whole of K_F, as the n-th power of the element is identity. So for the entire group T the convex region K_F is the only existing principal region and obviously is kernel too. Hence the condition imposed above is fulfilled.

We are thus concerned with a rather far-reaching generalization of transformation classes of finite order, for which the term *algebraically finite classes* is proposed for reasons which will be mentioned at the end of this paper.

9. Existence of simple axes. In the rest of this paper τS means a *class of surface transformations*, the corresponding group T of which, *defined in* $\overline{G}_F$, satisfies the condition of section 8.

We first ask whether axes which are simple with respect to T, thus are not intersected by any of their equivalents under T, exist. If S is bounded, the axes forming the boundary of K_F in X are simple with respect to T. So let S be closed. We then use the following theorem: For some power of τ, at least, the algebraic sum of the indices of all fixed points of any transformation belonging to the class is $\neq 0$. This theorem has been

proved in [17] by purely algebraic means of homology theory, using J. W. ALEXANDER's theorem [1] concerning the sum of indices; see also [18]. Now since the sum of indices of all fixed points is equal to the sum of indices of all different classes of fixed points, there must exist some function $t \neq 1$ in T, belonging to τ or to some power of τ, the index of which is $j(t) \neq 0$.

First let $j(t) < 0$. Then we have $1 - \nu - \mu < 0$; now $\mu = 0$, since in the only exceptional case $\nu = 0$, $\mu = 1$, we have $j = 0$. Hence $\nu > 1$ and we are in case **C** of section 4. More precisely, t belongs to the type $\mathbf{C}_1$, since $\mu = 0$ (no cuspidal points).

Then let $j(t) = 1$. As described in section 6, t is affiliated to the principal region of some power t^n. Now t^n must be of one of the types enumerated in section 6. Of these, $\mathbf{A}_2$, $\mathbf{B}_2$ and $\mathbf{C}_2$ clearly cancel on our present assumptions. In case $\mathbf{B}_1$ we only have the situation of an axis with neutral end points (fig. 1), and this axis is kernel. In $\mathbf{C}_1$ we have a kernel too.

To sum up, under the conditions imposed upon the transformation class, the group T contains an element which has a kernel (here coinciding with the principal region). Now if a kernel is bounded, a bounding axis of the kernel (which may make up the entire kernel, case $\mathbf{B}_1$) is simple with respect to T, as shown in section 7.

So we are left with the last possibility of a kernel belonging to some element of T and coinciding with the complete convex region K_F, which for a closed surface is the whole circular disc X. In that case the element 1 belongs to some line $[\tau^n]$, $n \neq 0$, of the scheme (T), and this means that τ is a transformation class of finite order (section 3).

As transformation classes of finite order are fully investigated in [15], we may here assume that τ is not of this special nature. So we have established that an axis, simple with respect to T, always exists for transformation classes of the kind under consideration.

To be precise, even for transformation classes of finite order such simple axes do exist in general. As pointed out in [15], there is only one extremely special case of a transformation class of finite order for which axes simple with respect to T do not exist; see [15], § 23.

10. Decomposition of S by a maximum system of geodesics. Let A_1 be any axis simple with respect to T. We consider the totality TA_1 forming its equivalence class (section 7). As A_1 is simple with respect to the subgroup F of T, it corresponds to a simple closed geodesic a_1 on S, and so do all axes of TA_1. As any two of these simple closed geodesics do not intersect and S is of finite connectivity, their number is finite. For the groups F and T this has the following bearing. $\varkappa$ being chosen as a transformation function of $\overline{G}_F$ corresponding to τS, we recall, that $\varkappa A_1$ is meant symbolically to denote the axis the end points of which are the images of the end points of A_1 under the transformation $\varkappa$. Moreover, if an orientation is assigned to A_1 by taking its end points in a definite order, this is transferred as a definite orientation of $\varkappa A_1$. Then in the sequence

$$A_1, \varkappa A_1, \varkappa^2 A_1, \cdots \tag{10. 1}$$

there is a first axis, $\varkappa^{\alpha_1} A_1$ say, corresponding to A_1 by an element of F,

$$\varkappa^{\alpha_1} A_1 = f A_1, \quad f \subset F,$$

orientation included. If α_1 is an even number, it may happen that $\varkappa^{\frac{\alpha_1}{2}} A_1$ corresponds to A by an element of F with orientation reversed; in that case A_1 will be termed an *amphidrome axis*.

On the surface S we may denote symbolically by

$$a_1, \tau a_1, \tau^2 a_1, \cdots \tag{10. 2}$$

the simple closed geodesics corresponding to the axes (10. 1), although the real image of a_1 by any special transformation of the class τ does not, in general, coincide with the geodesic covered by the axis $\varkappa A_1$, but is only homotopic to it.

With this denotation we get α_1 simple closed geodesics without common points

$$a_1, \tau a_1, \tau^2 a_1, \cdots, \tau^{\alpha_1 - 1} a_1$$

on S from (10. 2) in case A_1 is *not amphidrome*, whilst

$$\tau^{\alpha_1} a_1 = a_1$$

with orientation preserved. These geodesics are covered by the axes

$$A_1, \varkappa A_1, \varkappa^2 A_1, \cdots, \varkappa^{\alpha_1 - 1} A_1.$$

The equivalence class TA_1 then is made up of α_1 *congruence classes*

$$FA_1, F\varkappa A_1, F\varkappa^2 A_1, \cdots, F\varkappa^{\alpha_1 - 1} A_1.$$

(Of course, α_1 may be 1.) If on the other hand A_1 is *amphidrome*, we get $\frac{\alpha_1}{2}$ geodesics

$$a_1, \tau a_1, \cdots, \tau^{\frac{\alpha_1}{2} - 1} a_1,$$

whilst $\tau^{\frac{\alpha_1}{2}} a_1$ coincides with a_1 with orientation reversed. This requires $\alpha_1 \geq 2$ and even. The equivalence class of A_1 is made up of $\frac{\alpha_1}{2}$ congruence classes irrespective of orientation.

Let A_2 be an axis simple with respect to T, not comprised in TA_1 and not crossing any axis of TA_1, if any such A_2 exists. Then TA_1 and TA_2 have no point in common and, α_2 denoting the number analogous to α_1, we have on S in all $\alpha_1 + \alpha_2$ simple closed geodesics without common points, in case both A_1 and A_2 are not amphidrome, and otherwise a smaller number. Then we may look for a third axis A_3 and so on. This process comes to an end in a finite number of steps in view of the finite connectivity of S. Let

$$A_1, A_2, \cdots, A_\xi \tag{10.3}$$

be the *maximum system* finishing the process. This system then has the following property:

1) In the set of axes

$$TA_1 + TA_2 + \cdots + TA_\xi \tag{10.4}$$

any two axes do not intersect.

2) Any axis simple with respect to T and not comprised in the set (10.4) crosses at least one axis of this set.

The numbers $\frac{\alpha_i}{2}$ or α_i denoting the number of congruence classes in TA_i, according as A_i is or is not amphidrome,

$i = 1, 2, \cdots, \xi$, we have on S in all, at most, $\alpha_1 + \alpha_2 + \cdots + \alpha_\xi$ simple closed geodesics without common points. These divide S into a certain number $\geqq 1$ of parts.

In the case of a bounded surface it may be noticed that in whatever way the system (10.3) is chosen, any bounding axis of K_F is comprised in the set (10.4). Otherwise it would contradict condition 2. Moreover, a bounding axis of K_F cannot be amphidrome, since one of the intervals determined by it on E does not contain points of $\overline{G}_F$.

The set (10.4) of axes clearly is reproduced by any element $t \subset T$. Moreover, the arrangement of these axes in K_F is preserved, since t preserves the circular order of the points of $\overline{G}_F$. So the division of K_F by the set (10.4) is reproduced under t: Let B be any region of that division. The boundary of B inside X is made up of a subset of (10.4). If A, A', A'' are any three axes of this subset, none of them separates the two others. If A is an axis not in the subset, axes A' and A'' of the subset may be so chosen that A' separates A and A''. As these separating qualities are preserved by t, the subset of (10.4) into which the subset bounding B is transformed by t, is the boundary of some region of the division. This region will be denoted symbolically by tB. So we may form the concept of equivalence class TB and of congruence class FB of B, and split any equivalence class into congruence classes. In the sequence

$$B, \varkappa B, \varkappa^2 B, \cdots$$

let $\varkappa^\beta B$ be the first to be congruent to B:

$$\varkappa^\beta B = gB, \quad g \subset F. \qquad (\beta \geqq 1)$$

Then TB is made up of β congruence classes

$$FB, F\varkappa B, F\varkappa^2 B, \cdots, F\varkappa^{\beta-1} B. \tag{10.5}$$

If in the division of S corresponding to the division of K_F by the set (10.4) the part covered by B is denoted by b,

$$b, \tau b, \tau^2 b, \cdots, \tau^{\beta-1} b \tag{10.6}$$

will be β different parts, each covered by one of the congruence classes (10.5) of regions of K_F.

11. Transformation class of finite order in the single regions. We now consider some definite region B of the division of K_F by the set (10.4) and denote by T_B the subgroup of T and by F_B the subgroup of F carrying B into itself. F_B is the Poincaré group of the part b of S covered by B, and B is the convex region of the group F_B. If β is the least positive number such that

$$z^\beta B = gB, \quad g \subset F,$$

we put

$$g^{-1} z^\beta = z_B.$$

So $z_B B = B$. It should be noticed that g is not unique but may be replaced by gf_B, f_B being any element of F_B. Then z_B is replaced by $f_B^{-1} z_B$. This replacement has no influence on the following argument.

Elements of T_B are to be found in those lines of the scheme (T) which contain powers of z_B. Moreover, F_B is clearly invariant in T_B, and we get

$$T_B = F_B + F_B z_B + F_B z_B^2 + \cdots + F_B z_B^{-1} + F_B z_B^{-2} + \cdots$$

each of these parts of T_B being contained in some line of the scheme (T). If we assume the factor group T/F to be infinite, τ not being a transformation class of finite order, even the factor group T_B/F_B will be infinite.

One may, however, regard T_B merely as a group of transformations of the set $\bar{G}_{F_B}$ of limit points of F_B; that is the set of all those boundary points of B which are situated on E. Then T_B defines a transformation class τ_b (and all its powers) of the surface $b = B \bmod F_B$ just in the same way as T, given in $\bar{G}_F$, defines a transformation class τ (and all its powers) of the surface $S = K_F \bmod F$. In this respect, an element of T_B being unity only means that it leaves fixed all points of $\bar{G}_{F_B}$ regardless of its behaviour in the rest of $\bar{G}_F$. So in this

view the question as to the order of the factor group T_B/F_B arises anew.

To make this important point quite clear, we may put it in the following way in the language of group theory. Let T_{0B} denote the subset of T_B the elements of which transform $\bar{G}_{F_B}$ in the same way as some element of F_B, i. e. T_{0B} consists of all such elements t of T_B to which an element f of F_B exists, making the element ft leave all points of $\bar{G}_{F_B}$ fixed. This subset T_{0B} forms a group: Let t_1 and t_2 belong to T_{0B} and f_1 and f_2 be the corresponding elements of F_B. Then, if J denotes the automorphism induced by t_1,

$$f_1 t_1 \cdot f_2 t_2 = f_1 f_{2J}\, t_1 t_2$$

leaves all points of $\bar{G}_{F_B}$ fixed and $f_1 f_{2J} \subset F_B$; hence $t_1 t_2 \subset T_{0B}$. Moreover T_{0B} is invariant in T_B: Let $t_1 \subset T_{0B}$ with f as corresponding element, $t \subset T_B$ with J as corresponding automorphism and the point $P \subset \bar{G}_{F_B}$. What is the effect of tt_1t^{-1} upon P? Put $t^{-1}P = P_1 \subset \bar{G}_{F_B}$. Then $t_1 P = f^{-1}P_1$. Finally $tf^{-1}P_1 = f_J^{-1}tP_1 = f_J^{-1}P$. Hence the element $f_J tt_1t^{-1}$ leaves every point P of $\bar{G}_{F_B}$ fixed, and $f_J \subset F_B$. Thus $tt_1t^{-1} \subset T_{0B}$.

The invariant subgroup T_{0B} of T_B evidently contains F_B, but it may contain more. So the corresponding factor group T_B/T_{0B} may well become finite, even if T_B/F_B is not. We set out to prove that it actually does.

We first establish the fact, that *the transformation class τ_b of b satisfies the condition imposed on the class τ of S in section 8,*

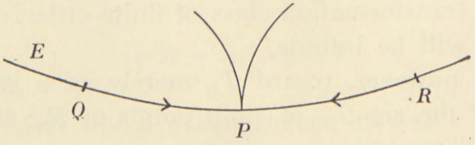

Fig. 5.

viz. that every principal region coincides with its kernel. In fact, assume t to be an element of T_B the principal region of which has a cuspidal point $P \subset \bar{G}_{F_B}$. Let P be attractive, and let Q and R be the neighbouring repulsive points of $\bar{G}_{F_B}$; see fig. 5. All points of $\bar{G}_{F_B}$ contained in the segment QPR are displaced

towards P by t except Q, P and R, which are left fixed. Moreover, Q, P and R are accumulation points of such points of $\overline{G}_{F_B}$. Now let i be any interval of $E - \overline{G}_{F_B}$ belonging to the segment QPR. The end points of i belong to $\overline{G}_{F_B}$, but are not Q, P or R, since these points are accumulation points of $\overline{G}_{F_B}$ on either side. So the end points of i are displaced into the end points of some other interval ti nearer to P. If then i contains points of $\overline{G}_F$ (not in $\overline{G}_{F_B}$) and we regard t as a transformation function in the whole of $\overline{G}_F$, these points are not left fixed by t. So even as we regard t as an element of T, the points Q and R are fixed points neigbouring P and the corresponding principal region would have P as a cuspidal point.—If P is not a cuspidal point, properly speaking, but t leaves only four points of $\overline{G}_{F_B}$ fixed, say P and P' attractive and Q and R repulsive, the principal region degenerates into a simple non-euclidean straight line; but this then is seen by the same argument to be principal region even for t as an element of T in contradiction to the assumptions made in section 8.—So the proof is complete.

Since B is bounded, F_B is a free group with a certain minimum number ν, say, of generators. *Then at least one of the transformation classes*

$$\tau_b, \tau_b^2, \cdots, \tau_b^\nu$$

of b yields a class of fixed points the index of which is not zero. This is seen by the argument of [17], p. 202—203[1].

[1] As the proof given in the paper quoted only takes closed surfaces into account, we shortly indicate the modification required, preserving the notations of the paper quoted: The algebraic sum of the indices in the r-th power of the transformation class is $1 - s_r$ instead of $2 - s_r$, since the surface is bounded. If this sum were to be zero for $\tau_b, \tau_b^2, \cdots, \tau_b^\nu$, we get

$$s_1 = s_2 = \cdots = s_\nu = 1.$$

Now using equations (1), (2), $\cdots$, (ν) of the paper quoted, we get in turn

$$\begin{aligned} a_1 &= -1 \text{ from (1)} \\ a_2 &= 0 \text{ from (2)} \\ &\cdots\cdots\cdots\cdots \\ a_\nu &= 0 \text{ from } (\nu). \end{aligned}$$

But a_ν is the determinant of the matrix Γ and so is $\neq 0$. This completes the proof.

Now, by section 9, the existence of an element of T_B the index of which is not zero involves the existence of a kernel. Such a kernel must be bounded, since B is bounded. Let A be an axis of F_B bounding some kernel. Then by section 7, A is simple with respect to T_B. From this we infer that A is simple with respect to T. Indeed, let t be any element of T. If t belongs to T_B, tA does not cross A, since A is simple with respect to T_B; if t does not belong to T_B, it takes B into some other region tB not intersecting B, so $A \subset B$ and $tA \subset tB$ do not intersect. Hence A is simple with respect to T. If A were interior to B, i. e. not a bounding axis of B, it would not belong to the set (10.4) and so would contradict condition 2, which characterizes (10.4) as a maximum set. So the kernel in question must coincide with B. This means that the unity element of T_B occurs in some set $F_B z_B^n$, $n \neq 0$, and so T_B/F_B is cyclic of some finite order n_B, if these groups are only considered in $\bar{G}_{F_B}$. In other words, using the above notation of the subgroup T_{0B} defined in $\bar{G}_F$, the factor group T_B/T_{0B} is cyclic of order n_B.

Hence the transformation class of $b = B \bmod F_B$ defined by the element z_B is a class of finite order.

12. Screw numbers. Let A be any oriented axis of the set (10.4) and f_A the primary element of F belonging to A, so all powers of f_A forming the subgroup F_A of F with A as axis. Let T_A^* denote the subgroup of T the elements of which leave A fixed, orientation included, thus including the end points of A in their set of fixed points in $\bar{G}_F$. This group T_A^* may be found in a similar way as the group T_B of the preceding section: In the sequence analogous to (10.1)

$$A, zA, z^2A, \cdots$$

we determine the least positive number α for which

$$z^\alpha A = fA, \quad f \subset F,$$

orientation included, and then put

$$f^{-1}z^\alpha = z_A,$$

hence $\varkappa_A A = A$. (The element f is not unique but may be replaced by $f f_A^n$ for any n, thus replacing $\varkappa_A$ by $f_A^{-n}\varkappa_A$. Compare the corresponding remark as to $\varkappa_B$ in the preceding section.) Then we get

$$T_A^* = F_A + F_A\varkappa_A + F_A\varkappa_A^2 + \cdots + F_A\varkappa_A^{-1} + F_A\varkappa_A^{-2} + \cdots$$

Denoting by T_A the subgroup of T the elements of which carry A into itself irrespective of orientation, we have $T_A = T_A^*$,

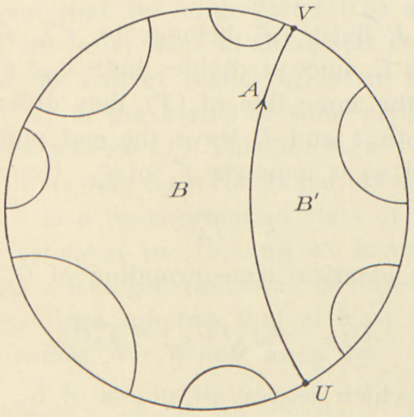

Fig. 6.

if A is not amphidrome, whereas for an amphidrome A there exist elements of T reversing A, and then T_A^* is an (invariant) subgroup of index 2 in T_A. As will be remembered, an amphidrome axis is not boundary axis of K_F.

We now assume A to be an *inner axis* (not boundary axis) of K_F.

Let B and B', (fig. 6[1]), denote the two regions contiguous to A in the division of K_F by the set (10.4), B on the left hand side of A, say. Let the numbers β and β' belong to B and B' respectively in the sense of the preceding section. Clearly T_A^* is a subgroup both of T_B and $T_{B'}$. The elements of T_A^* are contained in those lines $[r^n]$ of the scheme (T) for which n is a multiple of α, the elements of T_B and $T_{B'}$ in the lines for which n is a

[1] The figure is schematic. The number of bounding arcs of B and B' is of course infinite.

multiple of β and β' respectively. Hence α is a common multiple of β and β'. On the other hand, let n_B and $n_{B'}$ denote the order of the transformation class of finite order assigned in the preceding section to B and B' respectively. Then the line $[\tau^{n_B\beta}]$ of (T) contains an element leaving all boundary points of B on E fixed, thus belonging to T_A^*. Hence α divides $n_B\beta$. Likewise α divides $n_{B'}\beta'$.

Denoting by L the least common multiple of $n_B\beta$ and $n_{B'}\beta'$, the line $[\tau^L]$ contains both an element t leaving the boundary points of B on E fixed and an element t' leaving the boundary points of B' on E fixed. ($\varkappa_A^{\frac{L}{\alpha}}$ belongs to $[\tau^L]$, since $\varkappa_A$ belongs to $[\tau^\alpha]$. α divides L, since it divides both $n_B\beta$ and $n_{B'}\beta'$.) Since t and t' are in the same line of (T), they differ by an element f of F. Since both t and t' leave the end points of A fixed, f does so too, and so is a power f_A^e of f_A. Hence

$$t = f_A^e t'. \tag{12.1}$$

Now $t\bar{G}_{F_B}$ is the identical transformation of $\bar{G}_{F_B}$ and

$$t\bar{G}_{F_{B'}} = f_A^e t'\bar{G}_{F_{B'}} = f_A^e \bar{G}_{F_{B'}}.$$

The element t, which leaves all points of $\bar{G}_{F_B}$ fixed, displaces all points of $\bar{G}_{F_{B'}}$ in the same way, as does the element f_A^e of F. The rational number

$$s_A = \frac{e\alpha}{L} \tag{12.2}$$

will be termed the *screw number* of the axis A.

The screw number of an axis remains invariant under the operations of T. [To be sure, replace A by uA, $u \subset T$. Then $\varkappa_A$ is replaced by $u\varkappa_A u^{-1}$, and α remains unaltered. B and B' are replaced by uB and uB', uB being to the left of uA. The numbers $\beta, \beta', n_B, n_{B'}$ and hence L remain unaltered. f_A, t and t' are replaced by uf_Au^{-1}, utu^{-1} and $ut'u^{-1}$ respectively. So e and hence s_A remain unaltered.] Thus the screw number may be said to belong to the equivalence class TA.

Since, in case S is bounded, all boundary axes of K_F are comprised in (10.4), it should be emphasized that screw numbers are only assigned to *inner* axes.

13. Division of S into complete kernels. Now suppose the screw number s_A of A to be zero, thus $e = 0$ and by (12.1) $t = t'$. The element t then leaves both the limit point set of F_B and $F_{B'}$ fixed, thus both B and B' belong to the kernel of t. For all other axes of the equivalence class TA the situation is the same, as they all have their screw number equal to zero. So we may take A to be one of the axes of the set (10.3), A_λ say. *We then omit the subset TA_λ from the set (10.4).* Proceeding so for all values of the subscript λ for which $s_{A_\lambda} = 0$ we reduce (10.3) and so (10.4) to a smaller set, if any. $s = 0$ occurs.

It may happen that the entire set (10.3) and so (10.4) or, if S is bounded, all inner axes of these sets cancel in this way. This means that the convex region K_F is no more subdivided. So the whole of K_F is the kernel of some element $t \subset T$ not in the line $[\tau^0]$ of the scheme (T). This line then is identical with the line $[\tau^0] = F$, as far as only $\overline{G}_F$ is concerned. As stated in section 3, this means that τ is a transformation class of finite order. This case is fully investigated in [15] and we have nothing to add.

In order to get a true generalization of transformation classes of finite order we thus suppose that at least one inner axis of (10.3) does not cancel. We denote anew by

$$A_1, A_2, \cdots, A_i, A_{i+1}, \cdots, A_{i+r} \qquad \begin{pmatrix} i \geqq 1 \\ r \geqq 0 \end{pmatrix} \tag{13.1}$$

the remaining axes and by

$$TA_1 + TA_2 + \cdots + TA_i + TA_{i+1} + \cdots + TA_{i+r} \tag{13.2}$$

the set of their equivalence classes taken together. $A_1, A_2, \cdots, A_i$ are taken to denote inner axes, $A_{i+1}, \cdots, A_{i+r}$ are representatives of the r equivalence classes of boundary axes of K_F corresponding to the r ($\geqq 0$) bounding geodesics of S. The set (13.2) has still property 1) attributed to the set (10.4) but, in general, not property 2), as some axes of (10.4) may have been omitted.

As $i \geqq 1$ we still have a division of K_F by (13.2). We continue to use the letter B to denote some region of that division. So every region B is now the complete kernel of some function of T. Inversely, every kernel of T is someone of the regions B or someone of the axes separating them, since a kernel does not cross any other kernel.

Hence the transformation classes of algebraically finite type constituting the subject of this paper may be characterized as such transformation classes for which K_F is made up of kernels, or, if we transfer the notation of "kernel" to a region b of S covered by some B, for which S *is made up of a finite number of kernels.*

It should not be overlooked that even some or all of the inner axes $A_1, A_2, \cdots, A_i$ of (13.1) and their equivalents by T may play the rôle of independent kernels. Let us look closer at the axis A of fig. 6 together with its neighbouring regions B and B' and use the notations of section 12. As A is to be one of the axes still in (13.2), $e \neq 0$; let us assume $e < -1$. Then under the transformation t all points of $\overline{G}_{F_B}$ are fixed and all points of $\overline{G}_{F_{B'}}$ are displaced in the same way as by f_A^e, thus towards $U = U_{f_A}$. By the element $f_A t \subset T$ all points of $\overline{G}_{F_B}$ are displaced in the same way as by f_A, thus towards $V = V_{f_A}$, whereas all points of $\overline{G}_{F_{B'}}$ are displaced in the same way as by f_A^{e+1}, thus still towards U. So these two directions of displacement coincide on E, both V and U are neutral, and A is the kernel of $f_A t$, being of the type of fig. 1. The index of $f_A t$ is zero, since we have $\nu = 1$, $\mu = 0$.—The case $e > 1$ may be treated accordingly.

A case of special importance is that of A being amphidrome. Let h be an element of T reversing A. Then h clearly leaves no point of $\overline{G}_F$ fixed, so the index of h is 1. The regions B and B' contiguous to A are interchanged by h; so they are equivalent. The element h^2 leaves U and V fixed. Now suppose that h^2 leaves some point P of $\overline{G}_F$ other than U and V fixed. Since

$$h^2 hP = hh^2 P = hP,$$

h^2 also leaves hP fixed. The axis A separates P and hP. Now, since f_A belongs to the subgroup N of elements left fixed by the automorphism induced by h^2, both P and hP are carried into other fixed points by all powers of f_A. So in both intervals determined on E by U and V the points of $\overline{G}_F$ left fixed by h^2 are in infinite number. Thus there exists a principal region for the element h^2, and this region contains A as an inner axis.

This is in contradiction to the fact that the principal region is at the same time a kernel, and that A is not inner axis of the kernel of some element $\neq 1$ of T; we have $h^2 \neq 1$, since T contains no element of finite order. Thus we infer that no point of $\overline{G}_F$ other than U and V is left fixed by h^2.

If the direction of displacement by h^2 to the left of A goes from U to V, say, to the right of A it goes from V to U; this follows immediately by using the equation $h \cdot h^2 \cdot h^{-1} = h^2$. So these two directions coincide on E, and both U and V are neutral (case **B** of section 6). Hence A is the kernel of h^2, belonging to the type of fig. 1. So we see that an amphidrome axis is always an independent kernel.

As we have just seen, in contrast to a non-amphidrome axis A, for which all elements of T with A as their kernel have their index equal to zero, an amphidrome axis A gives rise to an element $h \subset T$ with $j(h) = 1$. One may ask if there are more elements of T with $j = 1$, affiliated to the same kernel A, in the transformation class to which h belongs. As such an element has its place in the line of h in the scheme (T), it has the form fh, $f \subset F$. As fh is affiliated to A and $j(fh) = 1$, fh interchanges U and V, and as h does too, f must leave U and V fixed, thus $f \subset F_A$, $f = f_A^n$ for some $n \neq 0$. Hence all elements

$$f_A^n h, \quad n \text{ arbitrary}, \tag{13.3}$$

and no other elements of the line of h interchange U and V and so are affiliated to A. Each of the elements (13.3) thus defining a class of fixed points with index 1 in the surface transformation class given by h, we have to ask how many of these classes are different, i. e. what is the number of congruence classes (section 7) into which the functions (13.3) fall.

If J denotes the automorphism of F induced by h, J carries F_A into itself, since h interchanges U and V. So J involves an automorphism of F_A, and this is not the identical one. Now, F_A consisting of all powers of the primary element f_A, there is only one non-identical automorphism of F_A, viz. the replacement of f_A by f_A^{-1}. So

$$h f_A h^{-1} = (f_A)_J = f_A^{-1}.$$

Hence we get

$$f_A^m h f_A^{-m} = f_A^m (f_A^{-m})_J h = f_A^{2m} h$$

$$f_A^m (f_A h) f_A^{-m} = f_A^m f_A (f_A^{-m})_J h = f_A^{2m+1} h.$$

Thus all elements of (13.3) with n even belong to the congruence class of h and all elements with n odd belong to the class of $f_A h$. It remains to be seen whether these classes are identical or different. Suppose they are identical. Then an element $f \subset F$ exists such that

$$f_A h = fhf^{-1} = ff_J^{-1} h,$$

hence

$$ff_J^{-1} = f_A \tag{13.4}$$

and by applying J

$$f_J f_J^{-1} = (f_A)_J = f_A^{-1}.$$

From this we get by multiplying these two equations

$$ff_{J^2}^{-1} = 1.$$

So f is left fixed by the automorphism J^2 induced by h^2. Now, as shown above, h^2 leaves only U and V fixed, so J^2 leaves all elements of F_A and no other element of F fixed. Hence

$$f = f_A^m$$

and by (13.4)

$$f_A^{2m} = f_A,$$

which is impossible. Hence the congruence classes of h and $f_A h$ are different.—So we have:

One of the inner axes of the system (13.1) which is amphidrome for some transformation class, τ^n say, and so is reversed by some element of the line $[\tau^n]$ of the scheme (T), gives rise to *exactly two classes of fixed points of the surface transformation class* $\tau^n S$ *each with index 1.*—This may be illustrated by the fact, that if a surface transformation of the class $\tau^n S$ is so chosen as to carry the closed geodesic corresponding to the axis into itself with orientation reversed, exactly two fixed points will arise on the closed curve.

14. Construction of a special transformation. The analysis of the preceding sections enables us to construct a surface transformation of a prescribed class τ of algebraically finite type such that each class of fixed points with index $\neq 0$ is "satisfied" by one single point of the surface and classes of index zero are completely avoided. In order to distinguish between the transformation class τ and the special transformation to be constructed, we denote the latter by ζ.

Let a denote the closed geodesic on S corresponding to some inner axis A of the set (13.2). We assign to a a narrow band $\tilde{a}$ of constant breadth of S enclosing a as its middle line. The part of K_F covering $\tilde{a}$ is a strip $\tilde{A}$ enclosing A and bounded by two circular arcs, all points of which are at the same non-euclidean distance from A; the end points of these arcs coincide with the end points of A. Of course, all strips of the congruence class $F\tilde{A}$ also cover $\tilde{a}$.

This construction is made for all closed geodesics of S corresponding to inner axes of the set (13.2). Since these geodesics are in finite number, the bands may be chosen so narrow as not to have common points. Then also any two of the strips arising in K_F do not interfere. For convenience we may take all bands equally wide.

We then have a division of K_F by the equivalence classes of strips

$$T\tilde{A}_1 + T\tilde{A}_2 + \cdots + T\tilde{A}_i \tag{14.1}$$

instead of by the inner axes of the set (13.2). We continue to use the letter B to denote any region of that division and to denote by b the corresponding region of S. A boundary curve of b which is not a boundary curve of S is then no more a closed geodesic, but a closed simple curve (boundary curve of some band), all points of which are at constant non-euclidean distance from a closed geodesic. This evidently makes no difference in speaking of tB as the region corresponding to B by the element $t \subset T$, of the equivalence class TB, and so on.

Now let b be any region of the division of S, B a corresponding region of K_F and the number β and an element $\varkappa_B$ defined as in section 11. It has been shown in that section that $\varkappa_B$ defines a transformation class of some finite order n_B

(or, as we may write, n_b) of the sub-surface b. By the chief theorem of [15] this class may be represented by a *periodic transformation* of b of order n_b. We construct such a periodic transformation of b by the process outlined in the paper quoted and denote it by $\zeta^\beta b$.

If $\beta > 1$, $\varkappa B = B_1$ (section 10) is a region symbolically equivalent to B (by T), but not congruent to B (by F); so B_1 corresponds to some region b_1 different from b in the division of S. Denoting as in section 2 by I the automorphism corresponding to $\varkappa$, the group F_B is carried into F_{B_1} by I. To this automorphism between F_B and F_{B_1} corresponds a class of transformations of b into b_1. We choose any topological transformation of b into b_1 belonging to that class and denote it by ζb. Then $\zeta\zeta^\beta\zeta^{-1}$ is a periodic transformation of $b_1 = \zeta b$ into itself of order $n_b = n_{b_1}$, which is denoted by $\zeta^\beta b_1$.

If $\beta > 2$, we proceed in the same way for $\varkappa^2 B = B_2$ and the corresponding region $\zeta^2 b = b_2$ and continue this process, till we reach $\zeta^{\beta-1} b = b_{\beta-1}$. Now, since $\varkappa^\beta B = gB$ for some $g \subset F$ (section 11), we have to transform $b_{\beta-1}$ into b by a topological transformation ζ, and there is no choice left; it has to be such that

$$\zeta b_{\beta-1} = \zeta\zeta^{\beta-1} b = \zeta^\beta b$$

is the transformation of b into itself already constructed. Now we have achieved the construction of a group of transformations consisting of all powers of ζ in the set of sub-surfaces $b, b_1, \cdots, b_{\beta-1}$. These regions are interchanged cyclically by $\zeta, \zeta^2, \cdots, \zeta^{\beta-1}$, whereas ζ^β is for all of them a periodic transformation of order n_b. So $\zeta^{\beta n_b}$ is the identical transformation in these β regions.

If there are more than these β regions on S, we choose another one and repeat the process for its equivalence class. After a finite number of steps ζ is defined in all regions of the division of S.

We now have to consider what this construction of the transformation ζ in the regions of S means in K_F. It will be remembered that all elements of F are defined in K_F, but all other elements of T have so far only been defined in the set $\overline{G}_F$ of

limit points by way of the given transformation class τ and its powers. F carries the set (14.1) of strips into itself and so also carries the complementary set of K_F, i. e. the set of regions, into itself. So F is a transformation group of the set of regions of K_F. To extend this property from F to T, take any region B of K_F. The notation $\varkappa B = B_1$ has hitherto been meant symbolically to denote the region of K_F the limit points of which are the images of the limit points of B by $\varkappa$. Now, the region b of S covered by B is subject to a topological transformation ζ into the region b_1 covered by B_1, and this has been so constructed as to correspond to the automorphism I induced by $\varkappa$ and taking F_B into F_{B_1}. So there is one topological transformation, and one only, mapping B into B_1 and covering ζ so as to correspond to I. We may denote this transformation by the same letter $\varkappa$, so that $\varkappa B = B_1$ now literally indicates the mapping of B into B_1 by $\varkappa$. As this applies to all regions B and extends to all powers of $\varkappa$, we have extended T to denote a certain group of topological transformations of the set of regions of K_F. This group satisfies the set of functional equations (2.1) or (2.2).

We now have to extend T to the strips of K_F thus defining ζ in the bands of S.

Let A be an inner axis of the set (13.1) and α the number assigned to it in section 12. We first assume A not to be amphidrome and take $\alpha > 1$. Then $\varkappa A = A_1$[1] means symbolically the axis the end points of which are the images of the end points of A by $\varkappa$. Now, boundary arcs of strips are boundary arcs of regions too, so the mapping function $\varkappa$ is defined on them. Hence the boundary of the strip $\tilde{A}$ imbedding A is mapped by $\varkappa$ upon the boundary of the strip $\tilde{A}_1$ imbedding A_1. We have to extend this mapping function to the interior of $\tilde{A}$.

For convenience we represent the strips $\tilde{A}$ and $\tilde{A}_1$ by the strip $0 \leqq y \leqq 1$ of a euclidean xy-plane and the strip $0 \leqq y' \leqq 1$ of a euclidean $x'y'$-plane respectively (fig. 7). (This may be achieved by some auxiliary mapping function). The axes A and A_1 are represented by the lines $y = \frac{1}{2}$ and $y' = \frac{1}{2}$ respectively. The primary translations f_A and f_{A_1} are both represented by

[1] Here subscripts have no connection with the notation of (13.1), of course.

translations of length 1 of the euclidean strips. So two points of $\tilde{A}$ corresponding by an element of F_A are represented by two points having the same value of y and having values of x the difference of which is an integer.

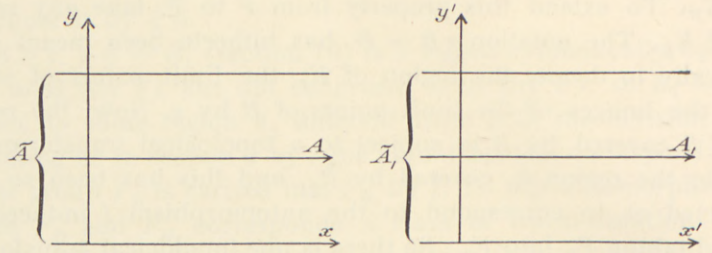

Fig. 7.

On the boundary $y = 0$ of $\tilde{A}$ we have by $\varkappa$ a transformation function $x' = \varkappa_1(x)$ taking this boundary into the boundary $y' = 0$ of $\tilde{A}_1$ and satisfying the functional equation

$$\varkappa_1(x+1) = \varkappa_1(x) + 1,$$

since $\varkappa f_A = f_{A_1}\varkappa$; the element f_{A_1} corresponds to f_A by the automorphism I induced by $\varkappa$. In the same way on $y = 1$ we have a function $x' = \varkappa_2(x)$ taking this boundary into the boundary $y' = 1$ of $\tilde{A}_1$ and such that

$$\varkappa_2(x+1) = \varkappa_2(x) + 1.$$

If now we carry the straight segment joining $(x, 0)$ and $(x, 1)$ into the straight segment joining $(\varkappa_1(x), 0)$ and $(\varkappa_2(x), 1)$ by an affine transformation, we get a topological mapping $\varkappa$ of the strip $\tilde{A}$ upon the strip $\tilde{A}_1$ coinciding with $\varkappa_1$ and $\varkappa_2$ respectively on the boundaries and satisfying the functional equation

$$\varkappa f_A = f_{A_1}\varkappa.$$

(If (x, y) is carried into (x', y'), then $y = y'$ and $(x+1, y)$ is carried into $(x'+1, y')$.) So this transformation $\varkappa$ of the strip $\tilde{A}$ upon $\tilde{A}_1$ covers a topological transformation of the band $\tilde{a}$ of S covered by $\tilde{A}$ upon the band $\tilde{a}_1$ covered by $\tilde{A}_1$. This trans-

formation may be denoted by ζ, since it links up with the transformation ζ of the adjacent regions of S already defined.

If $\alpha > 2$, we define $\varkappa^2\tilde{A}$ and so $\zeta^2\tilde{a}$ in the same way and continue this process until we reach $\varkappa^{\alpha-1}\tilde{A} = \tilde{A}_{\alpha-1}$ covering the band $\tilde{a}_{\alpha-1}$. We now have to define $\varkappa^\alpha\tilde{A} = \varkappa\tilde{A}_{\alpha-1}$. Let us first suppose this to be done in the same way as before. The strip $\tilde{A}_\alpha$, upon which $\tilde{A}$ is mapped by $\varkappa^\alpha$ is congruent to $\tilde{A}$,

$$\varkappa^\alpha\tilde{A} = f\tilde{A}, \quad f \subset F,$$

according to section 12. $\zeta^\alpha\tilde{a}$ is a transformation of the band $\tilde{a}$ into itself. As the values of y are not altered by our construction, a curve of $\tilde{a}$ corresponding to constant y is carried into itself. So fixed points may arise in $\tilde{a}$ under the transformation ζ^α. In order to avoid this we first replace the point (x, y) of $\tilde{A}$ by the point (x, y^2) and then apply the above construction, i. e. the image of (x, y) under $\varkappa^\alpha$ is the image of (x, y^2) by the above construction applied to the strips $\tilde{A}$ and $\tilde{A}_\alpha$. So we get the final definition of $\zeta^\alpha\tilde{a}$ and thus the definition of all powers of ζ in $\tilde{a}$ and in $\zeta\tilde{a}$, $\zeta^2\tilde{a}$, $\cdots$, $\zeta^{\alpha-1}\tilde{a}$ too.—In case $\alpha = 1$, the definition of ζ^α just given is that of ζ itself.

Since $\varkappa$ is now defined in the whole equivalence class $T\tilde{A}$ by means of the functional equation (2.1), the whole group T is defined in that totality of strips $T\tilde{A}$. Let us look at the regions B and B' neighbouring $\tilde{A}$ and use all notations of section 12. The element $\varkappa_A$ transforms $\tilde{A}$ into itself. In the line of $\varkappa_A^{\overline{\alpha}}$ of the scheme (T), which is the line $[\tau^L]$, there is a function t leaving all limit points of B fixed; this element t now is defined in all regions of K_F and in the strip $\tilde{A}$ too. It leaves all points of B fixed, since we have in B a periodic transformation and the limit points of B are left fixed. In the same way t' leaves all points of B' fixed. Then by (12.1) t displaces all points of B' in the same way as does f_A^e. Consider a curve of $\tilde{A}$ joining $(x, 1)$ and $(x, 0)$ in fig. 7, a segment at right angles to A, say. $(x, 1)$ is left fixed by t, since it is on the boundary of B, and $(x, 0)$ is carried into $(x+e, 0)$ by t. For the transformation ζ^L of the band $\tilde{a}$ into itself this means that ζ^L is the identical transformation on both boundaries of the band but carries a straight segment joining two opposite points into a curve

which winds e times round the band. This explains the definition of the screw number given in (12.2). As $\tilde{a}$ is transformed into itself by the powers of ζ^{α} only, we divide e by $\frac{L}{\alpha}$.

M. Dehn calls a transformation such as that just defined in the band $\tilde{a}$ "Verschraubung". Such transformations are the chief means of investigation in his paper [6]. See especially § 2, p. 141—142 of [6].

Finally we have to assume A to be amphidrome. Then we have $\alpha \geqq 2$ and even. In this case the definition of $\varkappa\tilde{A}$, $\varkappa^2\tilde{A}$, $\cdots$ described above goes without limitation, thus the auxiliary transformation replacing (x, y) by (x, y^2), applied in the former case in defining $\varkappa^{\alpha}$ in order to avoid fixed points, does not come into play. The effect is as follows: As to $\varkappa\tilde{A}$, $\varkappa^2\tilde{A}$, $\cdots$, $\varkappa^{\frac{\alpha}{2}-1}\tilde{A}$, there is no difference. $\varkappa^{\frac{\alpha}{2}}A$ is congruent to A by an element of F, say f. Then $f^{-1}\varkappa^{\frac{\alpha}{2}}$ carries the strip $\tilde{A}$ into itself with boundaries interchanged. Then if $\varkappa^{\frac{\alpha}{2}}$ is defined as a transformation of the strip $\tilde{A}$ in the prescribed way, $f^{-1}\varkappa^{\frac{\alpha}{2}}$ carries the middle line A of $\tilde{A}$ into itself with orientation reversed. Thus $\zeta^{\frac{\alpha}{2}}$ transforms a into itself leaving exactly two points of a and no other point of the band fixed. Two fixed points cannot be avoided, since they represent two different classes of fixed points both with index 1 (section 13).

After this construction has been made for all i inner axes of the set (13.1), a topological transformation ζ of the surface S into itself has been established, and ζ belongs to the class r prescribed. What are the fixed points of ζ? As to the bands, there are no fixed points in the interior of a band, if it is not amphidrome, or if it is amphidrome with $\alpha > 2$, since in the latter case $\frac{\alpha}{2}$ bands are interchanged cyclically by ζ. If it is amphidrome with $\alpha = 2$, there are exactly two fixed points each with index 1. As to the regions, there is no fixed point in a region, if $\beta > 1$, since in that case β regions are interchanged cyclically by ζ. If $\beta = 1$, the region b is subject to a periodic transformation into itself. If $n_b > 1$, there may be single invariant

points, each of index 1 (section 8), or there may be none. If $n_b = 1$, all points of the region are fixed by ζ, and their totality forms a class of fixed points of negative index; the index is $1-\nu$, if ν is the minimum number of generators of the Poincaré group of the region. In this case it is easily seen that ζ may be slightly deformed in b so as to leave only one point of b fixed, the index of which then is $1-\nu$; see [14] I, p. 314.

ζS thus satisfies the conditions asked for in the beginning of this section.

15. The equivalence problem. Without going into details we shortly indicate a problem which may be solved by the preceding analysis. Let τ denote a transformation class of S into itself and γ a topological transformation of S upon a surface S^*, which may coincide with S or not. Then $\gamma\tau\gamma^{-1}$ will be a transformation class of S^* into itself. This will be called *equivalent to* τ. The *equivalence problem* then consists in establishing a set of invariants of a transformation class such that it is necessary and sufficient for two classes being equivalent that they agree in this set of invariants. For classes of finite order such a set of invariants has been given in [16], § 11. For classes of algebraically finite type a set of invariants may be derived from the considerations of this paper. Indeed, the division of S into complete kernels, the numbers β and n_b of a kernel, the number α of an axis of the set (13.1), its screw number and its character of being amphidrome or not, are readily seen to be invariants of τ not altered by γ. Moreover, the transformation class of finite order assigned to a region b of S must be equivalent to that assigned to the region γb of S^*, the conditions for which are known from [16]. On the other hand, if two classes of transformations of two homeomorphic surfaces S and S^* agree in these invariants, and we construct special transformations ζ and ζ^* of S and S^* respectively as described in the preceding section, then ζ and ζ^* become equivalent by a suitable transformation γ of S into S^*, and so do the classes to which they belong.

Part III.

Homology theory.

16. Enouncement of the main theorem. Hitherto the Poincaré group F of S has been the chief means of our investigation. In the following sections we fix our attention upon the *homology group* H of S, i. e. the factor group of the commutator group in F. The homology group H is abelian, and we may speak of the elements of F as elements of H provided we make them interchange freely; thus for instance a set of conjugate elements of F yields one element of H. As stated in section 1, the minimum number δ of generators of F is $\delta = 2p$, if S is closed, and $\delta = 2p+r-1$, if F is bounded; in both cases H is a free abelian group with δ generators (for S closed all relations in F are identically satisfied in H). A set of δ free generators of H is called a *homology base.*

Any automorphism of F carries with it an automorphism of H, especially an inner automorphism of F the identical automorphism of H. So a complete family of automorphisms of F, which corresponds to a transformation class of S (section 2), yields one automorphism of H. While I continues to denote the automorphism induced in F by an element $\varkappa$ corresponding to a transformation class τ, let J denote the corresponding automorphism of H. Choosing a homology base of δ elements for H and using the sign of addition to denote the combination of elements of H, we describe J by a linear homogeneous transformation of the δ basic elements. Let $\mathcal{J}$ denote the matrix of that linear transformation and E_δ the unity matrix of δ rows and columns. Then if we put

$$(16.1) \qquad P(x) = (-1)^\delta \left| \mathcal{J} - xE_\delta \right| = x^\delta + \cdots + (-1)^\delta,$$

it is known that $P(x)$ only depends on J irrespective of the choice of homology base. $P(x)$ is a polynomial of degree δ in x and is called the *characteristic polynomial of* J. The roots of the equation $P(x) = 0$ are called the *characteristic roots* (or multipliers) of J. *It is our aim to establish the general form of* $P(x)$, *if* τ *is a class of algebraically finite type.*

A special case of a class of algebraically finite type is a class of finite order. Moreover, by the theorem of [15] already used, such a class contains a periodic transformation, and the general form of $P(x)$ for a periodic transformation has been shown in [16] to be

$$(16.2) \qquad P(x) = \frac{(x-1)^{1+\omega}(x^n-1)^{2q+s-2}}{(x^{m_1}-1)(x^{m_2}-1)\cdots(x^{m_u}-1)},$$

n denoting the order of the periodic transformation and ω being 0 or 1, according as the surface is bounded or closed. As to the numbers $q, s, u, m_1, \cdots, m_u$ a more detailed explanation is needed: In [4] Brouwer has shown that a certain auxiliary surface M, termed *modular surface*, may be assigned to any periodic transformation of order n of a surface S in such a way that S may be looked upon as a regular Riemann surface consisting of n sheets over M, and that the transformation consists in interchanging the sheets of S over M. Then M is closed or bounded according as S is closed or bounded. S may or may not ramify over M. Then q denotes the genus and u the number of ramification points of M; s is the sum of u and the number of boundary curves of M. While S has n distinct points over every ordinary point of M, it has a certain number m of distinct points over a ramification point; this number m is less than n and divides n. The set $m_1, m_2, \cdots, m_u$ denotes these numbers m for all ramification points.

In sections 17—21 we are concerned with the proof of the following generalization of this result concerning classes of finite order:

Theorem: *The characteristic polynomial of a transformation class of algebraically finite type takes the form*

$$(16.3) \qquad P(x) = (x-1)^{1+\omega} \prod_l \frac{\left(x^{\beta_l n_l}-1\right)^{2q_l+s_l-2}}{\left(x^{\beta_l m_{l1}}-1\right)\left(x^{\beta_l m_{l2}}-1\right)\cdots\left(x^{\beta_l m_{lu_l}}-1\right)}$$

Here again ω is 0 or 1 according as S is bounded or closed. l ranges over all equivalence classes of regions and bands, of which S consists. We now discuss the notations in the factor corresponding to the equivalence class of number l. In all cases

β_l is the number of congruence classes into which the equivalence class falls.

First, let this class be made up of regions. Then β_l is the number of regions of S in the class. So if b is one of these regions and B a region of K_F covering b, β_l means the number β assigned to B in section 11. The element $\varkappa_B$ of section 11 defines a transformation class of finite order for b, and n_l means the order of that transformation class. In section 14 this class is represented by a periodic transformation $\zeta^{\beta_l} b$. This periodic transformation gives rise to a modular surface M_l, and the numbers $q_l, u_l, s_l, m_{l1}, \cdots, m_{lu_l}$ are defined as above.

If $\bar{M}_l$ denotes the surface derived from M_l by removing u_l small elements, each containing one ramification point, s_l is the number of boundaries of $\bar{M}_l$. If δ_l denotes the minimum number of generators of the Poincaré group of $\bar{M}_l$, we get for the exponent in the numerator of $P(x)$, provided $s_l > 0$,

$$2q_l + s_l - 2 = \delta_l - 1. \tag{16.4}$$

Then let the equivalence class consist of bands belonging to amphidrome axes. β_l then denotes the number of bands in the class, hence $\beta_l = \frac{\alpha}{2}$, the number α being defined as in section 12. Then by section 14, if $\tilde{a}$ is one of the bands, $\zeta^{\beta_l}\tilde{a} = \zeta^{\alpha/2}\tilde{a}$ is a transformation class of order 2 for $\tilde{a}$. Thus we take n_l to be 2. This class contains a periodic transformation of order 2 interchanging the boundaries of $\tilde{a}$. So the modular surface M_l has only one boundary; M_l is clearly seen to be an element with 2 ramification points. Hence we get

$$q_l = 0, \quad u_l = 2, \quad s_l = 3, \quad m_{l1} = m_{l2} = 1.$$

The factor of $P(x)$ corresponding to such an equivalence class of amphidrome bands thus reduces to

$$\frac{x^{2\beta_l} - 1}{(x^{\beta_l} - 1)^2}. \tag{16.5}$$

Finally, let the equivalence class consist of bands belonging to non-amphidrome axes. β_l denotes the number of bands in the

class, thus $\beta_l = \alpha$, the number of section 12. Now, if $\tilde{a}$ is one of the bands, the transformation $\zeta^{\alpha}\tilde{a}$ of section 14 belongs to the class of identity. The corresponding periodic transformation is the identical transformation, so M_l coincides with $\tilde{a}$ and we have

$$n_l = 1, \quad u_l = 0, \quad q_l = 0, \quad s_l = 2,$$

and no factor arises at all in the numerator or denominator of $P(x)$. So this value of l only yields the factor 1 in $P(x)$.

We may thus restrict l to range over the equivalence classes consisting of regions or of amphidrome bands.

17. Preparations for the proof. The proof of the theorem expressed by (16.3) will be given by induction using the number i of equivalence classes of inner axes in (13.1,2) as number of induction. Since for $i = 0$ no inner axis exists, K_F is not divided and so forms one single kernel. Then l only takes the value $l = 1$. Since K_F is the only region, we have $\beta = 1$. The transformation class considered is a class of finite order, and (16.3) clearly reduces to (16.2). So the theorem is true for $i = 0$. We have to show that it is true for any $i > 0$, if it is true for all smaller values of i.

We pick out one of the inner axes of the set (13.1), denote it by A and fix our attention upon the division of K_F by the equivalence class TA. This division is reproduced by every element of T. If C is any region of that division, we denote by T_C the subgroup of T and by F_C the subgroup of F reproducing C. In the sequence

$$C, \varkappa C, \varkappa^2 C, \cdots$$

let γ be the least positive number such that

$$\varkappa^{\gamma} C = fC, \quad f \subset F,$$

and put

$$f^{-1}\varkappa^{\gamma} = \varkappa_C.$$

Then we have

$$T_C = F_C + F_C \varkappa_C + F_C \varkappa_C^2 + \cdots + F_C \varkappa_C^{-1} + F_C \varkappa_C^{-2} + \cdots.$$

If c denotes the region of S covered by C, a transformation class of c is defined by $\varkappa_C$. This transformation class is of algebraically finite type. To be sure we might repeat the argument of section 11, showing that if the principal region of some element $t \subset T_C$ had a cuspidal point in $\overline{G}_{F_C}$, this would be a cuspidal point in $\overline{G}_F$ too. We may also proceed as follows: If an element $t \subset T_C$, regarded as a transformation function of $\overline{G}_{F_C}$ only, has a kernel, this is at the same time the complete kernel of t regarded as a transformation function of $\overline{G}_F$, since every boundary of C inside K_F belongs to TA and so is boundary of a kernel of T. Inversely, if $t \subset T$ has its kernel inside C, then $t \subset T_C$ with the same kernel. So C is made up of complete kernels of transformation functions belonging to T_C.

If C consists of more than one kernel, the axes dividing C into kernels belong to the set (13.2). If any two of these axes are equivalent with respect to T,

$$A' = tA'', \quad t \subset T,$$

then $t \subset T_C$, since t carries an inner axis of C into another inner axis of C; so A' and A'' are equivalent with respect to T_C; the inverse is obvious. So the distribution of inner axes of C belonging to (13.2) into equivalence classes with respect to T_C is the same as with respect to T. Now the class TA only yields boundary axes of C. *So the number of equivalence classes of inner axes for C is less than the number i of (13.1,2).*

Thus by the assumption of our proof of induction the polynomial $P_c(x)$ belonging to the transformation class of c given by $\varkappa_C$ takes the form (16.3), moreover with $\omega = 0$, since c is bounded. (Even if S happens to be closed, it has been cut along one closed geodesic at least.)

Now suppose γ to be > 1. We then have on S an equivalence class of regions

$$c, \tau c = c_1, \tau^2 c = c_2, \cdots, \tau^{\gamma-1} c = c_{\gamma-1} \tag{17.1}$$

covered by the regions of K_F

$$C, \varkappa C, \varkappa^2 C, \cdots, \varkappa^{\gamma-1} C \tag{17.2}$$

respectively. There may or may not be more regions than (17.1) in the division of S by the geodesics covered by the axes of the class TA. For each of the regions (17.1) we have a transformation class of algebraically finite type defined by

$$\varkappa_C,\ \varkappa\varkappa_C\varkappa^{-1},\ \varkappa^2\varkappa_C\varkappa^{-2},\ \cdots,\ \varkappa^{\gamma-1}\varkappa_C\varkappa^{-(\gamma-1)}$$

respectively, and they all have the same characteristic polynomial $P_c(x)$.

Now we may look upon the subsurfaces (17.1) of S as γ distinct surfaces irrespective of their connection on S. The homology group of this set of surfaces then is defined as the direct sum of the γ isomorphic homology groups belonging to the single subsurfaces. If there are δ generators in the group belonging to c, then the combined homology group is the free abelian group with $\gamma\delta$ generators.

A transformation class of this set of surfaces is given by $\varkappa$. In fact $\varkappa$ defines a transformation class of c upon c_1, of c_1 upon $c_2, \cdots$, of $c_{\gamma-2}$ upon $c_{\gamma-1}$. In applying $\varkappa$ to $\varkappa^{\gamma-1}C$ we get $\varkappa^{\gamma}C = fC$, which covers c and defines the same transformation class of c upon itself as $f^{-1}\varkappa^{\gamma}C = \varkappa_C C$. Since $\varkappa$ represents the transformation class τ, we may prefer to say that a transformation class of the set (17.1) is given by the prescribed class τ; this is expressed in the notation (17.1).

We intend to find the characteristic polynomial of the transformation class of the set (17.1) given by τ. Let δ elements be chosen as a base of the homology group $H(c)$ of c; let A_c be the transformation matrix of this base corresponding to the transformation class τ^{γ} and $P_c(x)$ the corresponding characteristic polynomial (16.3). By τ (i. e. under the isomorphism between $H(c)$ and $H(c_1)$ induced by τ) these δ elements correspond to certain δ elements of $H(c_1)$ forming a homology base of c_1. By τ^2 they correspond to δ elements of $H(c_2)$ forming a homology base of c_2, and so on till we reach $c_{\gamma-1}$. The $\gamma\delta$ elements obtained in this way form a homology base for the set (17.1). The δ elements of $H(c_{\gamma-1})$ correspond by τ to δ elements of $H(c)$, which are the transforms of the elements chosen as homology base for c by the matrix A_c. So the matrix of the automorphism of the homology group $H(c + c_1 + \cdots + c_{\gamma-1})$

of the set (17.1) is easily formed. To find the characteristic polynomial we subtract $xE_{\gamma\delta}$ and take the determinant. In short this determinant may be written

$$\begin{vmatrix} -xE_\delta & E_\delta & 0 & \cdots & 0 & 0 \\ 0 & -xE_\delta & E_\delta & \cdots & 0 & 0 \\ \cdots & \cdots & \cdots & \cdots & \cdots & \cdots \\ 0 & 0 & 0 & \cdots & -xE_\delta & E_\delta \\ A_c & 0 & 0 & \cdots & 0 & -xE_\delta \end{vmatrix}$$

Here every symbol stands for a matrix with δ rows and colums and there are γ symbols in each row and column. To compute the determinant we multiply the first $\gamma-1$ rows by $x^{\gamma-1}$, $x^{\gamma-2}$, $\cdots$, x respectively and add all to the last row; so the determinant reduces to

$$(-1)^{\gamma\delta} \left| A_c - x^\gamma E_\delta \right|.$$

Thus we get:

The characteristic polynomial of the surface set (17.1) belonging to τ is $P_c(x^\gamma)$, if $P_c(x)$ is the polynomial belonging to τ^γ for each separate surface.

It should be noted, that the polynomial of the surface set (17.1) belonging to the transformation class τ^γ is $[P_c(x)]^\gamma$. This is evident.

If there are more equivalence classes of regions in the division of K_F by TA than that of C, all other classes may be treated in the same way.

18. First part of the proof. In this section we assume that the axis A of section 17 is not amphidrome, and that S is not decomposed by the geodesics corresponding to the equivalence class TA. According to the notations of section 12 the number of these geodesics is α, and they are represented by the axes

$$A, \varkappa A, \varkappa^2 A, \cdots, \varkappa^{\alpha-1} A \tag{18.1}$$

of K_F. The corresponding geodesics may be denoted by

$$(18.2) \qquad a,\ \tau a = a_1,\ \tau^2 a = a_2,\ \cdots,\ \tau^{\alpha-1} a = a_{\alpha-1}.$$

We then have $\tau^\alpha a = a$[1].

As S is not decomposed by being cut along these α geodesics, only one region c arises. So there is but one equivalence class and moreover the number γ of (17.1) is 1. It should be noted that in cutting S along the α geodesics the genus p of S decreases by α and the number r of boundary curves increases by 2α. So if S is bounded, the number of generators of the homology group remains unaltered, whereas if S is closed, it decreases by 1.

Now by the assumption of our proof of induction, the polynomial $P_c(x)$ of the transformation class of c given by τ^γ takes the form (16.3), and $\omega = 0$, since c is bounded. The degree of the polynomial is δ, equal to the number of generators of $H(c)$. We intend to find the polynomial $P(x)$ of the transformation class of S given by τ. Its degree is δ, if S is bounded, and $\delta+1$, if S is closed.

If we orient A and transfer its orientation to all curves (18.1) and (18.2), we may speak of α boundary curves

$$(18.3) \qquad a',\ a'_1,\ a'_2,\ \cdots,\ a'_{\alpha-1}$$

of c as left hand borders and of another α boundary curves

$$(18.4) \qquad a'',\ a''_1,\ a''_2,\ \cdots,\ a''_{\alpha-1}$$

of c as right hand borders of $a,\ a_1,\ a_2,\ \cdots,\ a_{\alpha-1}$ respectively.

Now we first assume S to be bounded. Then c has more than these 2α boundary curves. So we may allow both (18.3) and (18.4) to be members of a homology base for c. Let such a homology base be chosen, and let it be arranged so as first to put $\delta-2\alpha$ elements not in (18.3,4) then the α elements (18.3) and finally the α elements (18.4). Then the matrix $\mathcal{A}_c$ describing the automorphism of $H(c)$ corresponding to the transformation class given by $\varkappa_C$ by a linear transformation of the base chosen may be composed of 9 blocks,

[1] To avoid misunderstanding, we recall that the notation $a_1 = \tau a$ etc. is symbolic and means that any closed curve on S homotopic to a is transformed by any transformation of the class τ into a curve homotopic to a_1 (section 7).

$$(18.5) \qquad \mathcal{A}_c = \left\{ \begin{array}{c|c|c} I & IV & V \\ \hline VI & II & VII \\ \hline VIII & IX & III \end{array} \right\},$$

I being a square matrix of $\delta - 2\alpha$ rows and both II and III square matrices of α rows each. Now $\mathcal{A}_c$ is known to interchange the elements (18.3) cyclically and equally for (18.4). So we have

$$(18.6) \qquad II = III = \left\{ \begin{array}{ccccc} 0 & 1 & 0 & \cdots & 0 \\ 0 & 0 & 1 & \cdots & 0 \\ \cdots & \cdots & \cdots & \cdots & \cdots \\ 0 & 0 & 0 & \cdots & 1 \\ 1 & 0 & 0 & \cdots & 0 \end{array} \right\},$$

and all elements of VI, VII, $VIII$, IX are zero. Hence we get irrespective of IV, V

$$\begin{aligned} (-1)^{\delta} P_c(x) &= \left| \mathcal{A}_c - x E_{\delta} \right| \\ &= \left| I - x E_{\delta - 2\alpha} \right| \left| II - x E_{\alpha} \right| \left| III - x E_{\alpha} \right|. \end{aligned}$$

The last two factors are easily computed in the way used in the preceding section, and we get

$$(18.7) \qquad \left| II - x E_{\alpha} \right| = \left| III - x E_{\alpha} \right| = (-1)^{\alpha} (x^{\alpha} - 1).$$

Then let S be closed. So c has exactly 2α boundaries given by (18.3) and (18.4). Thus we have the homology relation

$$(18.8) \qquad a' + a_1' + \cdots + a_{\alpha-1}' - a'' - a_1'' - \cdots - a_{\alpha-1}'' = 0$$

taking the orientation of the curves (18.3) and (18.4) into account. We choose a homology base of c in the same way and in the same order as before, only omitting $a_{\alpha-1}''$. So in (18.5) III now is a square matrix of $\alpha - 1$ rows. II remains equal to (18.6) and all elements of VI and VII are zero. Under the transformation $\mathcal{A}_c$ the element a'' of (18.4) goes into a_1'', this into a_2'', and so on until $a_{\alpha-2}''$. Now $a_{\alpha-2}''$ goes into $a_{\alpha-1}''$, but as this element is not in the base, it has to be replaced by

$$a' + a'_1 + \cdots + a'_{\alpha-1} - a'' - a''_1 - \cdots - a''_{\alpha-2}$$

in consequence of (18.8). So all elements of *VIII* are zero, all elements of *IX* are zero except for the last row of *IX*, which is made up of numbers 1, and for *III* we get the following square matrix of $\alpha - 1$ rows

$$(18.9) \qquad III = \begin{Vmatrix} 0 & 1 & 0 & \cdots & 0 \\ 0 & 0 & 1 & \cdots & 0 \\ \cdot & \cdot & \cdot & \cdots & \cdot \\ 0 & 0 & 0 & \cdots & 1 \\ -1 & -1 & -1 & \cdots & -1 \end{Vmatrix}.$$

Since matrices *VI* and *VIII* and moreover *VII* vanish, we get

$$\begin{aligned} (-1)^{\delta} P_c(x) &= \left| A_c - xE_{\delta} \right| \\ &= \left| I - xE_{\delta-2\alpha+1} \right| \left| II - xE_{\alpha} \right| \left| III - xE_{\alpha-1} \right|. \end{aligned}$$

The last factor is easily computed from (18.9) and we get

$$(18.10) \qquad \left| III - xE_{\alpha-1} \right| = (-1)^{\alpha-1} \frac{x^{\alpha} - 1}{x - 1}.$$

To sum up, we remember that the letter ω means 0 or 1 according as S is bounded or closed. Then we may take both cases together in saying that $\alpha - \omega$ elements of (18.4) enter into the base chosen and that these elements alone yield the factor (from (18.7) and (18.10), irrespective of sign)

$$(18.11) \qquad \frac{x^{\alpha} - 1}{(x-1)^{\omega}}$$

in the polynomial $P_c(x)$ of c.

In order to get S from c we let the boundaries (18.4) of c coincide in turn with the boundaries (18.3). We get a homology base for S by taking the homology base for c, arranged in the same way as before, then cancelling the last $\alpha - \omega$ elements, since these become identical with elements of (18.3) already in the base, and replacing α new homology elements arising from the α new connections. So let

(18.12) $$b, b_1, b_2, \cdots, b_{\alpha-1}$$

denote homology elements corresponding to cycles of S, of which the first, b, crosses a in one point from left to right and does not intersect $a_1, a_2, \cdots, a_{\alpha-1}$, and the same for b_1 and a_1, b_2 and a_2 and so on. These cycles may be taken to have one point of c in common. Evidently there is no homology relation between the elements (18.12), and they make the homology base of S complete.

We may call (18.12) a *homology base of connection*. We now divide the matrix A of S into 9 blocks in the same way as in (18.5):

$$A = \left\{ \begin{array}{c|c|c} I^* & IV^* & V^* \\ \hline VI^* & II^* & VII^* \\ \hline VIII^* & IX^* & III^* \end{array} \right\}.$$

Here III^* is a square matrix with α rows corresponding to the elements (18.12). All other rows of A correspond to the same basic elements as in A_c.

As the elements (18.3) are interchanged cyclically, we have $II^* = II$, and both VI^* and VII^* vanish.—We now look at the basic elements belonging to the rows of I or I^*. Their transformation by A_c depends on the matrices I, IV and V. Now the basic elements (18.4), belonging to the columns of V have been replaced by the corresponding elements of (18.3). This means that $I^* = I$, but IV^* may differ from IV. Moreover these elements of the rows of I have their intersection number with curves (18.2) equal to zero, and this is not changed by the transformation; so their transform by A does not contain any element of (18.12) with a coefficient $\neq 0$; thus V^* vanishes.—Finally we look at the basic elements belonging to the rows of III^*. As b has its intersection number with a equal to 1 and with $a_1, a_2, \cdots, a_{\alpha-1}$ equal to zero, and as (18.2) are interchanged cyclically, we infer that the element corresponding to b by A has its intersection number with a_1 equal to 1 (the transformation class preserves the orientation of S) and with $a_2, \cdots, a_{\alpha-1}, a$ equal to zero. So b_1 is the only element of (18.12) to appear in the transform of b, and b_1 has 1 as its

coefficient. As to the transforms of $b_1, b_2, \cdots, b_{\alpha-1}$, things are analogous. So *III** is equal to (18.6). As to *VIII** and *IX** nothing is known, but that does not matter, since *V** and *VII** are known to vanish. Using the fact that *VI** vanishes too, we get

$$(-1)^{\delta+\omega} P(x) = \left| A - xE_{\delta+\omega} \right|$$

$$= \left| I^* - xE_{\delta-2\alpha+\omega} \right| \left| II^* - xE_{\alpha} \right| \left| III^* - xE_{\alpha} \right|.$$

Since $I^* = I$ and $II^* = II$, the two first factors are the same as before, and since *III** is equal to the matrix (18.6), the last factor is

$$(-1)^{\alpha} (x^{\alpha} - 1)$$

as in (18.7).

Hence we have the following result: The cancelling of $\alpha - \omega$ elements of (18.4) means multiplication of $P_c(x)$ by $\dfrac{(x-1)^{\omega}}{(x^{\alpha}-1)}$ (from 18.11) and the replacement by α new basic elements means multiplication by $(x^{\alpha}-1)$. So the total effect is multiplication by $(x-1)^{\omega}$.

Thus if S is bounded, we have $P(x) = P_c(x)$, and if S is closed, we have $P(x) = (x-1) P_c(x)$.

So we have to ask if this is actually the polynomial $P(x)$ we have to look for according to the description following (16.3). The initial factor, which was $x-1$ in $P_c(x)$, is now $(x-1)^{1+\omega}$. As to the factors of the product $\prod_l$ we recall that such a factor with all its numbers $\beta_l, n_l, q_l, s_l, u_l, m_{l1}, \cdots, m_{lu_l}$ arises from an equivalence class of regions or of amphidrome axes in c. Now every such equivalence class of c is a class of S too with all numbers unchanged. And no new class arises on S. It is true that there is a class of inner axes on S which is not a class of inner axes in c, viz. the class (18.1,2) used for cutting S. But as these axes are not amphidrome, they do not yield a factor in $P(x)$. — So our theorem is proved in the case considered.

19. Second part of the proof. In this section we assume that the geodesic a is not amphidrome, and that S is decomposed by the geodesics (18.2). Let c denote the region of this

decomposition to the left of a; so c has the left hand border a' (18.3) of a as one of its boundaries. c may or may not have some of the right hand borders (18.4) as a boundary. In this section we make the further assumption that it has not. Since τ interchanges the geodesics (18.2), all regions to the left of these geodesics are equivalent by T, and so are all regions to the right of these geodesics. On our present assumption these two equivalence classes are different. As every region of the decomposition has at least one of the geodesics (18.2) as boundary, we have exactly these two equivalence classes of regions of the decomposition of S. If c' denotes the region to the right of a, the two classes are represented by c and c'.

Let γ and γ' denote the number of regions in these equivalence classes (section 17). Then

$$(19.1) \qquad c, \quad \tau c = c_1, \quad \tau^2 c = c_2, \quad \cdots, \quad \tau^{\gamma-1} c = c_{\gamma-1}$$

are all regions of the equivalence class of c and

$$(19.2) \qquad c', \quad \tau c' = c'_1, \quad \tau^2 c' = c'_2, \quad \cdots, \quad \tau^{\gamma'-1} c' = c'_{\gamma'-1}$$

are all regions of the equivalence class of c'. We then have $\tau^{\gamma} c = c$ and $\tau^{\gamma'} c' = c'$. From $\tau^{\alpha} a = a$ we infer that $\tau^{\alpha} c = c$; hence γ divides α and so does γ'.

Let $g = (\gamma, \gamma')$ be the greatest common measure of γ and γ', and put $\gamma = g\gamma_1$, $\gamma' = g\gamma'_1$. Then, if we suppose $g > 1$,

$$(19.3) \qquad c, \quad c_g, \quad c_{2g}, \quad \cdots, \quad c_{(\gamma_1-1)g}$$

is a subset of (19.1) and

$$(19.4) \qquad c', \quad c'_g, \quad c'_{2g}, \quad \cdots, \quad c'_{(\gamma'_1-1)g}$$

is a subset of (19.2). All geodesics

$$(19.5) \qquad a, \quad a_g, \quad a_{2g}, \quad \cdots, \quad a_{\alpha-g}$$

and no other geodesics of the set (18.2) are boundaries of (19.3) and (19.4). So by joining the regions (19.3) and (19.4) along the geodesics (19.5) we get a subsurface S^* of S, and this sub-

surface has no boundary in common with the subsurfaces τS^*, $\tau^2 S^*$, $\cdots$, $\tau^{g-1} S^*$. So S would consist of g distinct surfaces, while throughout this paper we suppose S to be one coherent surface. So we have

$$(\gamma, \gamma') = 1,$$

γ and γ' are relatively prime.

The geodesics (18.2) or, more precisely, their borders (18.3) and (18.4) are so distributed on the subsurfaces (19.1) and (19.2) that

(19.6) $$a'_\nu, a'_{\nu+\gamma}, a'_{\nu+2\gamma}, \cdots, a'_{\nu+\alpha-\gamma}$$

are boundaries of c_ν $(\nu = 0, 1, 2, \cdots, \gamma - 1)$ and

(19.7) $$a''_\nu, a''_{\nu+\gamma'}, a''_{\nu+2\gamma'}, \cdots, a''_{\nu+\alpha-\gamma'}$$

are boundaries of c'_ν $(\nu = 0, 1, 2, \cdots, \gamma' - 1)$.

τ^γ is a transformation class of algebraically finite type for c (section 17) and its characteristic polynomial $P_c(x)$ takes the form (16.3) with $\omega = 0$:

$$P_c(x) = (x-1)\prod_l f_l(x),$$

if we agree to denote the factor corresponding to l by

$$f_l(x) = \frac{(x^{\beta_l n_l} - 1)^{2q_l + s_l - 2}}{(x^{\beta_l m_{l1}} - 1) \cdots (x^{\beta_l m_{lu_l}} - 1)}.$$

Accordingly for $\tau^{\gamma'}$ as a transformation class of c' we have

$$P_{c'}(x) = (x-1)\prod_{l'} f_{l'}(x).$$

τ is a transformation class of the set (19.1) of γ distinct subsurfaces, and the corresponding polynomial is by section 17:

$$P_c(x^\gamma) = (x^\gamma - 1)\prod_l f_l(x^\gamma).$$

τ also is a transformation class of the set (19.2), and the corresponding polynomial is

$$P_{c'}(x^{\gamma'}) = (x^{\gamma'}-1)\prod_{l'} f_{l'}(x^{\gamma'}).$$

We may thus speak of τ as a transformation class of the *decomposed surface* S' (being a set of $\gamma+\gamma'$ distinct subsurfaces); the corresponding polynomial $P_{S'}(x)$ then is the product

$$P_{S'}(x) = P_c(x^{\gamma})\,P_{c'}(x^{\gamma'}) = \tag{19.8}$$

$$= (x^{\gamma}-1)(x^{\gamma'}-1)\prod_{l} f_l(x^{\gamma})\prod_{l'} f_{l'}(x^{\gamma'}).$$

We now ask what is the effect on this polynomial of passing from S' to S by joining the boundaries (18.4) in turn to the boundaries (18.3). This effect is found in two steps as in the preceding section, a) by cancelling some elements of the homology base of S' and b) by introducing new ones by a homology base of connection.

a) First let S be bounded. Then at least one of the subsurfaces c and c' has a boundary not belonging to (18.3,4). Let c have such a boundary; then all subsurfaces (19.1) have. So all elements of (18.3) may be allowed to enter into a homology base of S'. By joining (18.3) to (18.4) these elements (18.3) become equal to the elements (18.4) of the homology group of $c'+c'_1+\cdots+c'_{\gamma'-1}$; these elements may or may not be in the homology base of S' and may even be zero; in all cases they are independent of (18.3). So the elements (18.3) cancel, and as they are interchanged cyclically by τ, this evidently means multiplication of (19.8) by $\frac{1}{x^{\alpha}-1}$; see (18.6,7).

Then let S be closed. Thus (18.3) and (18.4) are the only boundaries of S'. As a preliminary case let us assume $\gamma' = \alpha$; thus (19.2) is a set of the maximum number α of subsurfaces, each bounded by one of the curves (18.4), and these curves are thus all homologous to zero. Then we have $\gamma = 1$, since γ divides α and is relatively prime to γ'. So (19.1) consists only

of one surface c bounded by all curves (18.3). So we may take a', a'_1, $\cdots$, $a'_{\alpha-2}$ into the homology base of S'. The corresponding part of the transformation matrix then is (18.9). Since these $\alpha-1$ basic elements vanish by being identified with (18.4), it is seen from (18.10) that (19.8) is multiplied by $\frac{x-1}{x^\alpha-1}$. Of course it is the same for $\gamma=\alpha$, $\gamma'=1$.

We now consider the general case, both $\gamma<\alpha$ and $\gamma'<\alpha$. The set of subsurfaces (19.1) is made up of γ surfaces, each with $\frac{\alpha}{\gamma}$ boundaries from (18.3), and (19.2) is made up of γ' surfaces, each with $\frac{\alpha}{\gamma'}$ boundaries from (18.4). For each surface the number of boundaries is greater than 1, and their sum is homologous to zero. Thus the sum of the elements of (19.6) is zero for every value of ν and so is the sum of (19.7).

A homology base of (19.1) is now so chosen as to include the *first* $\alpha-\gamma$ elements of (18.3), thus excluding the last γ, as they can be expressed by the first $\alpha-\gamma$. By τ every element is replaced by the following except the last, $a'_{\alpha-\gamma-1}$, which is replaced by the element $a'_{\alpha-\gamma}$ not in the base. So we express it from (19.6) with $\nu=0$:

$$a'_{\alpha-\gamma}=-a'-a'_\gamma-a'_{2\gamma}-\cdots-a'_{\alpha-2\gamma}.$$

We then get the part of the transformation matrix of τ which belongs to the $\alpha-\gamma$ basic elements in question:

$$\left\{\begin{array}{cccccccccccc} 0 & 1 & 0 & \cdots & \cdot & \cdot & \cdot & \cdot & \cdots & \cdot & \cdot & \cdots \\ 0 & 0 & 1 & \cdots & \cdot & \cdot & \cdot & \cdot & \cdots & \cdot & \cdot & \cdots \\ \cdot & \cdot & \cdot & \cdots & \cdot & \cdot & \cdot & \cdot & \cdots & \cdot & \cdot & \cdots \\ -1 & 0 & 0 & \cdots & 0 & -1 & 0 & 0 & \cdots & 0 & -1 & \cdots \end{array}\right\}$$

the last row being alternately -1 and a group of $\gamma-1$ zeros. From this it is easily computed that the corresponding part of the polynomial, denoted above by $P_c(x^\gamma)$, is $\frac{x^\alpha-1}{x^\gamma-1}$. As the same is true for the set (19.2) with γ' instead of γ, we may say that in (19.8) a factor

(19.9) $$\frac{(x^\alpha - 1)^2}{(x^\gamma - 1)(x^{\gamma'} - 1)}$$

is due to the boundaries of S'.

In choosing a homology base for (19.2) we take the $\alpha - \gamma'$ *last* elements of (18.4) into the base. So the part of the basic elements of S' corresponding to boundary curves of S' may be written

$$a' \, a'_1 \cdots a'_{\gamma'-1} \, a'_{\gamma'} \cdots a'_{\alpha-\gamma-1}$$
$$a''_{\gamma'} \cdots a''_{\alpha-\gamma-1} \, a''_{\alpha-\gamma} \cdots a''_{\alpha-1}.$$

These two lines have the subscripts from γ' to $\alpha - \gamma - 1$ in common and that is at least one subscript. Since

$$(\alpha - \gamma - 1) - (\gamma' - 1) = \alpha - (\gamma + \gamma')$$

and both γ and γ' are less than α, divide α and are relatively prime, this is positive. In the empty places of the first line we may substitute linear combinations of the elements written, and likewise in the second line. Then passing from S' to S means equating corresponding members of the two lines and reducing the system. From this it may be directly computed that the elements

$$a', a'_{\gamma'}, \cdots, a'_{\alpha-\gamma-1}$$

may be taken as basic elements of the resulting system, and that they yield the factor

(19.10) $$\frac{(x^\alpha - 1)(x - 1)}{(x^\gamma - 1)(x^{\gamma'} - 1)}$$

in the polynomium of S.

Instead of carrying out this direct computation we may obtain the result more easily in the following way, if we allow the ring of coefficients of the homology group to be complex. We first consider the α boundary curves (18.3) of the surface set (19.1). Putting

$$\varepsilon = e^{\frac{2\pi i}{\alpha}}$$

we introduce the linear transformation

$$(19.11)\qquad \begin{cases} d_0 = a' + a'_1 + a'_2 + \cdots + a'_{\alpha-1} \\ d_1 = a' + \varepsilon^{-1} a'_1 + \varepsilon^{-2} a'_2 + \cdots + \varepsilon^{-(\alpha-1)} a'_{\alpha-1} \\ d_2 = a' + \varepsilon^{-2} a'_1 + \varepsilon^{-4} a'_2 + \cdots + \varepsilon^{-2(\alpha-1)} a'_{\alpha-1} \\ \cdots\cdots\cdots\cdots\cdots\cdots\cdots\cdots\cdots\cdots \\ d_{\alpha-1} = a' + \varepsilon^{-(\alpha-1)} a'_1 + \varepsilon^{-2(\alpha-1)} a'_2 + \cdots + \varepsilon^{-(\alpha-1)^2} a'_{\alpha-1} \end{cases}$$

the determinant of which is $\neq 0$, since it is the product of all differences of $1, \varepsilon, \varepsilon^2, \cdots, \varepsilon^\alpha - 1$. Then τ replaces d_0 by d_0, d_1 by εd_1, d_2 by $\varepsilon^2 d_2$, $\cdots$, $d_{\alpha-1}$ by $\varepsilon^{\alpha-1} d_{\alpha-1}$. So the multipliers of the set (19.11) are $1, \varepsilon, \varepsilon^2, \cdots, \varepsilon^{\alpha-1}$ respectively, i. e. all roots of the polynomial $x^\alpha - 1$. If (18.3) were an independent set, the set (19.11) would be so too. But from (19.6) we have

$$(19.12)\qquad a'_\nu + a'_{\nu+\gamma} + \cdots + a'_{\nu+\alpha-\gamma} = 0, \qquad \nu = 0, 1, \cdots, \gamma - 1.$$

From this we get $d_0 = 0$; moreover, since $\varepsilon^\alpha = 1$:

$$\begin{aligned} d_{\frac{\alpha}{\gamma}} &= a' + \varepsilon^{\frac{\alpha}{\gamma}} a'_1 + \varepsilon^{\frac{2\alpha}{\gamma}} a'_2 + \cdots + \varepsilon^{\frac{(\alpha-1)\alpha}{\gamma}} a'_{\alpha-1} \\ &= a' + a'_\gamma + a'_{2\gamma} + \cdots + a'_{\alpha-\gamma} \\ &\quad + \varepsilon^{\frac{\alpha}{\gamma}} \left[a'_1 + a'_{1+\gamma} + \cdots + a'_{\alpha-\gamma+1}\right] \\ &\quad + \varepsilon^{\frac{2\alpha}{\gamma}} \left[a'_2 + a'_{2+\gamma} + \cdots + a'_{\alpha-\gamma+2}\right] \\ &\quad \cdots\cdots\cdots\cdots\cdots\cdots\cdots\cdots \\ &\quad + \varepsilon^{\frac{(\gamma-1)\alpha}{\gamma}} \left[a'_{\gamma-1} + a'_{2\gamma-1} + \cdots + a'_{\alpha-1}\right], \end{aligned}$$

hence $d_{\frac{\alpha}{\gamma}} = 0$ by (19.12). In the same way we get $d_{\frac{2\alpha}{\gamma}} = 0$, $d_{\frac{3\alpha}{\gamma}} = 0$, $\cdots$, $d_{\frac{(\gamma-1)\alpha}{\gamma}} = 0$. So the multipliers

$$(19.13)\qquad 1, \varepsilon^{\frac{\alpha}{\gamma}}, \varepsilon^{\frac{2\alpha}{\gamma}}, \cdots, \varepsilon^{\frac{(\gamma-1)\alpha}{\gamma}}$$

cancel; they are the roots of $x^{\gamma}-1$. Hence

$$\frac{x^{\alpha}-1}{x^{\gamma}-1}$$

is the corresponding part of $P_c(x^{\gamma})$, as stated before (19.9).

To pass from S' to S we put

$$a'_{\mu} = a''_{\mu}, \quad \mu = 0, 1, \cdots, \alpha-1.$$

Since we have relations from (19.7)

$$a''_{\nu} + a''_{\nu+\gamma'} + \cdots + a''_{\nu+\alpha-\gamma'} = 0, \quad \nu = 0, 1, \cdots, \gamma'-1,$$

we get the corresponding relations

$$a'_{\nu} + a'_{\nu+\gamma'} + \cdots + a'_{\nu+\alpha-\gamma'} = 0, \quad \nu = 0, 1, \cdots, \gamma'-1, \tag{19.12a}$$

besides (19.12). From this we infer in the same way that the multipliers

$$1, \varepsilon^{\frac{\alpha}{\gamma'}}, \varepsilon^{\frac{2\alpha}{\gamma'}}, \cdots, \varepsilon^{\frac{(\gamma'-1)\alpha}{\gamma'}} \tag{19.14}$$

cancel; they are the roots of $x^{\gamma'}-1$. Now (19.13) and (19.14) have only the multiplier 1 in common; for since γ and γ' are relatively prime, $\frac{\alpha}{\gamma}$ and $\frac{\alpha}{\gamma'}$ have α as least common multiple. Hence (19.10) is in fact the factor in the polynomial of S derived from the system (18.2) of geodesics used in decomposing S; the factor $x-1$ in the numerator of (19.10) is due to the fact that the multiplier 1 has been omitted twice.

Comparing (19.9) and (19.10) we see that multiplication by

$$\frac{x-1}{x^{\alpha}-1}$$

is the effect of passing from S' to the closed surface S so far as the bounding geodesics of S' are concerned. For S bounded,

the corresponding factor was $\frac{1}{x^\alpha - 1}$. So we may sum up the effect of the step a) in the following way:

The effect of cancelling some elements of the homology base of S' by joining the boundary curves is multiplication of the polynomial $P_{S'}(x)$ (19.8) by the factor

$$\frac{(x-1)^\omega}{x^\alpha - 1}. \tag{19.15}$$

b) We now have to introduce some new elements in the homology base of S according to the new connections established by joining 2α boundary curves (18.3) and (18.4) of S'. This may be done in the following way. We choose a point in the interior of each region of the decomposition of S and denote the point chosen in the region c by $\{c\}$. Then we join the points $\{c\}$ and $\{c'\}$ by a segment b, crossing a in one point from the left hand side to the right hand side. In this way we join $\{\tau^\mu c\} = \{c_\mu\}$ and $\{\tau^\mu c'\} = \{c'_\mu\}$ by a segment b_μ crossing $\tau^\mu a = a_\mu$ in one point and not meeting any other of the geodesics (18.2); here $\mu = 0, 1, \cdots, \alpha - 1$, and $b_0 = b$. As the equivalence class of c consists of γ regions, we have

$$\{c_\nu\} = \{c_{\nu+\gamma}\} = \{c_{\nu+2\gamma}\} = \cdots = \{c_{\nu+\alpha-\gamma}\}$$

and $\frac{\alpha}{\gamma}$ segments eradiate from this point. Subscripts of c and c' only count modulo γ and modulo γ' respectively.

The totality of these segments form a coherent complex, since S is coherent. This complex consists of $\gamma + \gamma'$ points and α segments. Hence it contains

$$p_1 = 1 + \alpha - (\gamma + \gamma') \tag{19.16}$$

independent cycles. Then any p_1 independent cycles of this complex may be taken as a homology base of connection to complete the homology base of S.

$p_1 = 0$ arises only in the case $\gamma = \alpha$ and hence $\gamma' = 1$ (or inversely). In this case we have one subsurface c' and α subsurfaces $c, c_1, \cdots, c_{\alpha-1}$, each of which is adjacent to c' along one of the α geodesics; so evidently no new element has to be introduced in the base.

So we assume $\gamma < \alpha$, $\gamma' < \alpha$ and hence

$$\gamma \leqq \frac{\alpha}{2}, \quad \gamma' \leqq \frac{\alpha}{2} \quad \text{and} \quad p_1 > 0.$$

Any region c_i of the equivalence class of c neighbours any region c'_j of the equivalence class of c' along at least one geodesic $\tau^n a$. For since γ and γ' are relatively prime, if i is one of the numbers $0, 1, \cdots, \gamma - 1$ and j is one of the numbers $0, 1, \cdots, \gamma' - 1$, then n may be so chosen among the numbers $0, 1, \cdots, \gamma\gamma' - 1$, that $n \equiv i \pmod{\gamma}$ and $n \equiv j \pmod{\gamma'}$, and this in exactly one way. Then $\tau^n c = c_i$ neighbours $\tau^n c' = c'_j$ along $\tau^n a$. Since both γ and γ' divide α and are relatively prime, we have

$$\alpha = \lambda\gamma\gamma' \tag{19.17}$$

and infer that c_i and c'_j have exactly λ of the geodesics (18.2) as common boundary. So λ of the segments b_μ join the points $\{c_i\}$ and $\{c'_j\}$.

We first consider the simplest case $\lambda = 1$. So there goes exactly one segment b_μ from any point $\{c_i\}$ to any point $\{c'_j\}$. Any cycle of the complex consists of an even number of segments as the two equivalence classes of regions or, as we may say, of points, alternate. Thus the simplest cycle consists of four segments. Such a cycle is

$$k_0 = b_0 - b_{\gamma'} + b_{\gamma'+\gamma} - b_\gamma;$$

for b_0 goes from $\{c\}$ to $\{c'\}$, $-b_{\gamma'}$ from $\{c'_{\gamma'}\} = \{c'\}$ to $\{c_{\gamma'}\}$, $b_{\gamma'+\gamma}$ from $\{c_{\gamma'+\gamma}\} = \{c_{\gamma'}\}$ to $\{c'_{\gamma'+\gamma}\} = \{c'_\gamma\}$ and $-b_\gamma$ from $\{c'_\gamma\}$ to $\{c_\gamma\}$, which is the starting point $\{c\}$. From this we get α cycles

$$k_\mu = b_\mu - b_{\mu+\gamma'} + b_{\mu+\gamma'+\gamma} - b_{\mu+\gamma}, \qquad \mu = 0, 1, \cdots, \alpha - 1, \tag{19.18}$$

remembering that subscripts of b only count modulo α. These cycles k_μ are not independent, since their number is $> p_1$.

(19.18) contains a homology base of connection, i. e. p_1 cycles completing the homology base of S. To see this we have to

show that any cycle of the complex, which without restriction may be taken without double points, is a linear combination of the k_μ.

Any cycle with more than four segments is the sum of cycles with four segments each. In fact, let

$$Z = b_x - b_y + b_z - b_u + \cdots$$

be a cycle of n segments. If t is so determined as to satisfy

$$t \equiv z \pmod{\gamma'}, \quad t \equiv x \pmod{\gamma},$$

we may write

$$Z = b_x - b_y + b_z - b_t + b_t - b_u + \cdots.$$

Here the first four segments form a cycle, since $\{c'_z\} = \{c'_t\}$ and $\{c_x\} = \{c_t\}$. Omitting this cycle we reduce Z to $n-2$ segments and continue the same process. ($t \equiv u \pmod{\gamma'}$, since $t \equiv z$ and $z \equiv u \pmod{\gamma'}$.)

So we have to show that any cycle of four segments may be obtained by linear combination of the cycles (19.18). Since the last two segments in k_μ are equal to the first two segments of $k_{\mu+\gamma}$ with opposite sign, we get for any n

$$\begin{aligned} q_\mu &= k_\mu + k_{\mu+\gamma} + k_{\mu+2\gamma} + \cdots + k_{\mu+(n-1)\gamma} \\ &= b_\mu - b_{\mu+\gamma'} + b_{\mu+\gamma'+n\gamma} - b_{\mu+n\gamma}, \end{aligned}$$

from this for any y

$$\begin{aligned} &q_\mu + q_{\mu+\gamma'} + q_{\mu+2\gamma'} + \cdots + q_{\mu+(y-1)\gamma'} \\ &= b_\mu - b_{\mu+y\gamma'} + b_{\mu+y\gamma'+n\gamma} - b_{\mu+n\gamma} \end{aligned}$$

and finally, replacing μ by $\mu + x\gamma$ for any x and putting $x+n = z$,

$$Z = b_{\mu+x\gamma} - b_{\mu+x\gamma+y\gamma'} + b_{\mu+z\gamma+y\gamma'} - b_{\mu+z\gamma}.$$

This cycle Z goes from the point

$$\{c_\mu\} = \{c_{\mu+x\gamma}\} \text{ to } \{c'_{\mu+x\gamma}\} = \{c'_{\mu+x\gamma+y\gamma'}\},$$

from there to $\{c_{\mu+x\gamma+y\gamma'}\} = \{c_{\mu+y\gamma'}\} = \{c_{\mu+z\gamma+y\gamma'}\}$,

from there to $\{c'_{\mu+z\gamma+y\gamma'}\} = \{c'_{\mu+z\gamma}\}$,

from there to $\{c_{\mu+z\gamma}\} = \{c_\mu\}$.

Now, since the four numbers μ, x, y, z, may be chosen arbitrarily and γ and γ' are relatively prime, the points $\{c_\mu\}$, $\{c_{\mu+y\gamma'}\}$ and $\{c'_{\mu+x\gamma}\}$, $\{c'_{\mu+z\gamma}\}$ may be any given points in the equivalence classes of $\{c\}$ and $\{c'\}$ respectively. So Z becomes any cycle composed of four segments. This completes the proof.

Relations between the generating cycles (19.18) are readily found. Taking $n = \frac{\alpha}{\gamma}$ in q_μ and remembering that subscripts of b only count modulo α, we find $q_\mu = 0$ for this particular n, thus

$$k_\mu + k_{\mu+\gamma} + k_{\mu+2\gamma} + \cdots + k_{\mu+\alpha-\gamma} = 0, \qquad (\mu = 0,1,\cdots,\gamma-1), \tag{19.19}$$

and in the same way

$$k_\mu + k_{\mu+\gamma'} + k_{\mu+2\gamma'} + \cdots + k_{\mu+\alpha-\gamma'} = 0 \qquad (\mu = 0,1,\cdots,\gamma'-1). \tag{19.19 a}$$

These $\gamma+\gamma'$ relations between the α generators are, however, not independent, since the sum of all γ left hand members of (19.19) is equal to the sum of all γ' left hand members of (19.20). So one relation is abundant. Hence we may cancel $\gamma+\gamma'-1$ generators properly chosen and so are left with p_1 generators in accordance with (19.16).

We now complete the homology base of S by adding these p_1 new generators derived from the connections. The matrix A corresponding to the transformation class τ of S then takes the form

$$A = \left\{ \begin{array}{c|c} I & II \\ \hline III & IV \end{array} \right\}$$

IV being a matrix with p_1 rows and columns. If there are δ elements in all in the base of S, the transforms of the first $\delta - p_1$ elements (derived from S' by the considerations under a)) do not contain the p_1 new generators. So all elements of II are zero, and we have

$$\left| A - xE_\delta \right| = \left| I - xE_{\delta - p_1} \right| \left| IV - xE_{p_1} \right|.$$

Now take any of the new generators, k_μ say. The intersection numbers of k_μ with a_μ, $a_{\mu+\gamma'}$, $a_{\mu+\gamma'+\gamma}$, $a_{\mu+\gamma}$ are in turn $1, -1$, $1, -1$, and with all other geodesics (18.2) they are zero. The transform of k_μ then must have the same intersection numbers $1, -1, 1, -1$ with $a_{\mu+1}$, $a_{\mu+\gamma'+1}$, $a_{\mu+\gamma'+\gamma+1}$, $a_{\mu+\gamma+1}$, and zero with the rest. From this it follows that it contains $k_{\mu+1}$ with coefficient 1 and all other elements of (19.18) with coefficient zero; if $k_{\mu+1}$ is not in the base, it has of course to be replaced by its expression by the p_1 elements chosen. From this the matrix IV may be derived. III does not matter, since II vanishes.

To compute the polynomial

$$(-1)^{p_1} \left| IV - xE_{p_1} \right| \tag{19.20}$$

we follow the same way as in proving (19.10) by means of the transformation (19.11). In fact, the deduction is literally the same. Instead of the elements $a', a'_1, \cdots, a'_{\alpha-1}$ of (19.11) we have the α elements (19.18). The relations (19.12) and (19.12 a) correspond exactly to the relations (19.19) and (19.19 a). So we find (19.20) equal to (19.10).

We now have the following result: (19.8) was the polynomial $P_{S'}(x)$ belonging to the transformation class τ of the decomposed surface S', and we had to consider the effect on it from joining the boundary curves in order to get the surface S. This means first cancelling some elements of the homology base of S' with the effect of introducing the factor (19.15) into the polynomial, and then introducing new elements into the homology base of S with the effect of introducing the factor (19.10). Hence

$$(19.21) \qquad P(x) = (x-1)^{1+\omega} \prod_{l} f_l(x^{\gamma}) \prod_{l'} f_{l'}(x^{\gamma'})$$

belongs to the transformation class τ of S.

This is in accordance with the theorem stated by (16.3). For since a is not amphidrome, no factor arises from the geodesics (18.2); and all regions of S' and all other geodesics of S' (if any) evidently play the same rôle in S.

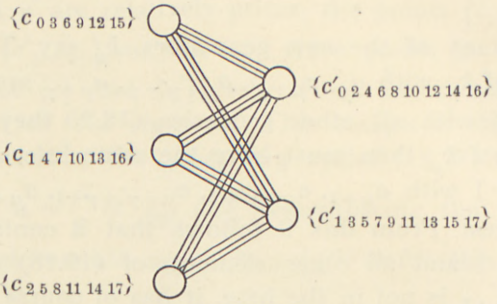

Fig. 8.

Finally an addition has to be made, as we have assumed the factor λ in (19.17) to be 1.

Let λ be greater than 1. Each point $\{c_i\}$ is connected with each point $\{c'_j\}$ by λ segments. In fig. 8 the case $\alpha = 18$, $\gamma = 3$, $\gamma' = 2$, thus $\lambda = 3$, is illustrated in a schematic way; each of the five points carries all subscripts belonging to it; so e. g. $\{c_0\} = \{c_3\} = \{c_6\} = \{c_9\} = \{c_{12}\} = \{c_{15}\}$. Any segment b_μ is one of the segments leading from the c-point with subscript μ to the c'-point with subscript μ. All segments connecting these two points then are

$$(19.22) \qquad b_\mu,\ b_{\mu+\gamma\gamma'},\ b_{\mu+2\gamma\gamma'},\ \cdots,\ b_{\mu+(\lambda-1)\gamma\gamma'}.$$

From these we may form λ cycles

$$(19.23) \qquad \begin{cases} l_\mu = b_\mu - b_{\mu+\gamma\gamma'} \\ l_{\mu+\gamma\gamma'} = b_{\mu+\gamma\gamma'} - b_{\mu+2\gamma\gamma'} \quad (\mu = 0, 1, \cdots, \gamma\gamma'-1) \\ \cdots\cdots\cdots\cdots\cdots\cdots\cdots\cdots \\ l_{\mu+(\lambda-1)\gamma\gamma'} = b_{\mu+(\lambda-1)\gamma\gamma'} - b_\mu. \end{cases}$$

The sum of these λ cycles is zero for every μ. Letting μ range from 0 to $\gamma\gamma' - 1$, we get α cycles in all, which for short we call the l-cycles.

The l-cycles (19.23) together with the the k-cycles (19.18) contain a homology base of connection consisting of p_1 generating cycles of the b-complex: Any segment of a k-cycle may be replaced by another segment connecting the same two points by adding or subtracting some suitable l-cycles. So modulo the subgroup generated by the l-cycles we may look upon the k-cycles as if we join all λ segments (19.22) to one string. The building up of the complex from k-cycles of these strings then is the same as in the case $\lambda = 1$.

If we take $n = \gamma'$ in the cycle q_μ used previously, we get

$$q_\mu = b_\mu - b_{\mu+\gamma'} + b_{\mu+\gamma'+\gamma'\gamma} - b_{\mu+\gamma'\gamma}.$$

Replacing μ in turn by $\mu+\gamma', \mu+2\gamma', \cdots, \mu+(\gamma-1)\gamma'$ and adding we get the cycle

$$\begin{aligned} u_u &= b_\mu - b_{\mu+\gamma\gamma'} + b_{\mu+2\gamma\gamma'} - b_{\mu+\gamma\gamma'} \\ &= l_\iota - l_{\mu+\gamma\gamma'}. \end{aligned}$$

Hence by replacing μ we get the cycles

$$\begin{aligned} u_\mu &= l_\mu - l_{\mu+\gamma\gamma'} \\ u_{\mu+\gamma\gamma'} &= l_{\mu+\gamma\gamma'} - l_{\mu+2\gamma\gamma'} \\ &\cdots\cdots\cdots\cdots\cdots\cdots \\ u_{\mu+(\lambda-1)\gamma\gamma'} &= l_{\mu+(\lambda-1)\gamma\gamma'} - l_\mu, \end{aligned}$$

since $l_{\mu+\alpha} = l_\mu$. Multiplying in turn by $\lambda, \lambda-1, \lambda-2, \cdots, 1$ and adding, we get

$$\lambda u_\mu + (\lambda-1)\, u_{\mu+\gamma\gamma'} + \cdots + u_{\mu+(\lambda-1)\gamma\gamma'} = \lambda\, l_\mu,$$

since the sum of the cycles (19.23) is zero for μ fixed.

So λl_μ is seen to be a linear combination of the k-cycles (19.18) for $\mu = 0, 1, \cdots, \alpha-1$. Now if any cycle Z belongs to a certain multiplier (i. e. root of the characteristic polynomial),

so does λZ, and λZ is expressible by the k-cycles. In other words, if we allow the ring of coefficients of the homology group of connections to consist of all rational numbers, then p_1 of the k-cycles (19.18), properly chosen, may be taken as generators. We thus get the same part IV of the matrix A and the same characteristic polynomial (19.21) as in the case $\lambda = 1$.

20. Third part of the proof. In this section we assume that the geodesic a is not amphidrome, that S is decomposed by the geodesics $a, a_1, \cdots, a_{\alpha-1}$ of (18.2), and that the region c to the left of a (thus with the left hand border a' of (18.3) on its boundary) has also one of the right hand borders (18.4) on its boundary. This is transformed into a by a certain power of τ, and so the region to the right of a is equivalent to c. Hence we get only one equivalence class of regions

$$c, \tau c = c_1, \tau^2 c = c_2, \cdots, \tau^{\gamma-1} c = c_{\gamma-1} \tag{20.1}$$

instead of (19.1) and (19.2). Moreover $\gamma > 1$, since S is decomposed.

Let $\tau^h c = c_h$ be the region of the set (20.1) which is adjacent to c along a. Then, c_μ being the region to the left of a_μ, $c_{\mu+h}$ is the region to the right of a_μ, and $c_{\mu+h} = \tau^h c_\mu$. So we may pass from any region to any other region by a power of τ^h. From this we infer that h and γ are relatively prime. h and α may or may not be relatively prime.

Subscripts of c only counting modulo γ, we may write the set (20.1) in another way:

$$c, c_h, c_{2h}, \cdots, c_{(\gamma-1)h}. \tag{20.2}$$

In this arrangement they form a ring, each region c_μ neighbouring $c_{\mu-h}$ and $c_{\mu+h}$ only.

The α geodesics may be arranged in the following way, if we put

$$\alpha = \gamma\xi,$$

and count their subscripts modulo α:

$$(20.3)\qquad \begin{vmatrix} a & a_\gamma & a_{2\gamma} & \cdots & a_{(\xi-1)\gamma} \\ a_h & a_{h+\gamma} & a_{h+2\gamma} & \cdots & a_{h+(\xi-1)\gamma} \\ a_{2h} & a_{2h+\gamma} & a_{2h+2\gamma} & \cdots & a_{2h+(\xi-1)\gamma} \\ \cdots & \cdots & \cdots & \cdots & \cdots \\ a_{(\gamma-1)h} & a_{(\gamma-1)h+\gamma} & & \cdots & a_{(\gamma-1)h+(\xi-1)\gamma} \end{vmatrix}.$$

The geodesics of the rows beginning with $a_{\mu h}$ and $a_{(\mu-1)h}$ are on the boundary of $c_{\mu h}$, and these two rows bound $c_{\mu h}$ in

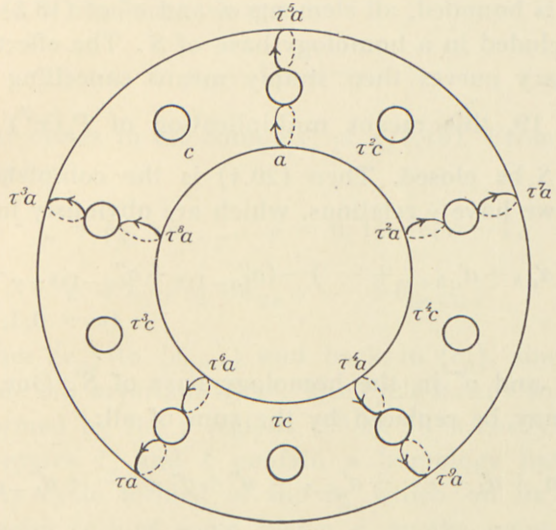

Fig. 9.

opposite senses. Using the notation (18.3) and (18.4) we may say that

$$(20.4)\qquad a'_{\mu h} + a'_{\mu h+\gamma} + \cdots + a'_{\mu h+(\xi-1)\gamma} - (a''_{(\mu-1)h} + \cdots + a''_{(\mu-1)h+(\xi-1)\gamma})$$

is part of the boundary of c_μ.

To illustrate these facts, fig. 9 shows the case $\alpha = 10$, $\gamma = 5$, $h = 2$. One may replace $h = 2$ by $h = 3$ and so obtain a case in which h and α are relatively prime.

The construction of the characteristic polynomial in the case of this section goes along similar lines as in the preceding sections. Let

$$P_c(x) = (x-1)\prod_l \frac{\left(x^{\beta_l n_l}-1\right)^{2q_l+s_l-2}}{\left(x^{\beta_l m_{l1}}-1\right)\cdots}$$

be the polynomial (16.3) belonging to c under the transformation class τ^γ. Then by section 17 $P_c(x^\gamma)$ is the polynomial of the decomposed surface S' under the transformation class τ. We now have to take the same two steps as in the preceding section, a) passing from S' to S by joining boundary curves and b) introducing a homology base of connection.

a) If S is bounded, all elements a' and a'' of (18.3) and (18.4) may be included in a homology base of S'. The effect of joining the boundary curves then simply means cancelling the a''. As in section 19, this means multiplication of $P_c(x^\gamma)$ by $\frac{1}{x^\alpha-1}$.

So let S be closed. Then (20.4) is the complete boundary of c_μ and we have γ relations, which are obviously independent,

$$(20.5)\qquad (a'_{\mu h}+a'_{\mu h+\gamma}+\cdots)-(a''_{(\mu-1)h}+a''_{(\mu-1)h+\gamma}+\cdots)=0 \qquad (\mu=0,1,\cdots,\gamma-1)$$

for the a' and a'' in the homology base of S'. One of these γ relations may be replaced by the sum of all:

$$(20.6)\qquad a'+a'_1+\cdots+a'_{\alpha-1}=a''+a''_1+\cdots+a''_{\alpha-1}.$$

Both the left hand member and the right hand member of this equation are homology elements with the multiplier 1. The effect of putting them equal to one another is to cancel the factor $x-1$. So if (20.6) were not used, $P_c(x^\gamma)$ would have to be multiplied by $(x-1)$.

Now passing from S' to S means replacing every a'' by the corresponding a'. All a'' may be included in the homology base of S', as the relations (20.5) may be used for eliminating some of the a'. The cancelling of the a'' means multiplication by $(x^\alpha-1)^{-1}$. As to the a' the only effect on the polynomial arises from the fact that (20.6) is satisfied identically; thus the factor $x-1$ has to be restored. In all, we get the factor $\frac{x-1}{x^\alpha-1}$, if S is closed.

To sum up for S bounded or closed, the effect of the operation a) is to multiply $P_c(x^\gamma)$ by

$$\frac{(x-1)^\omega}{x^\alpha - 1}. \tag{20.7}$$

b) To set up a homology base of connection we again introduce the segments b_μ, $\mu = 0, 1, \cdots, \alpha - 1$, crossing a_μ from the left hand side to the right hand side; here they connect the points $\{c_\mu\}$ and $\{c_{\mu+h}\}$. As we have a coherent complex of γ points and α segments, we get

$$p_1 = 1 + \alpha - \gamma$$

independent cycles in the complex; cf. (19.16). From the b_μ we form the cycles

$$l_\mu = b_\mu - b_{\mu+\gamma}, \quad \mu = 0, 1, \cdots, \alpha - 1,$$

and

$$k = b_0 + b_h + b_{2h} + \cdots + b_{(\gamma-1)h}.$$

l_μ runs from $\{c_\mu\}$ to $\{c_{\mu+h}\}$ and back to $\{c_\mu\}$, since both c_μ and $c_{\mu+h}$ are left invariant by τ^γ. The cycle k runs once through the ring formed by the γ regions (20.2). It is easily seen that the $\alpha + 1$ cycles l_μ and k contain a homology base of connection: Any cycle formed of the b_μ which on its way runs from the point $\{c_\mu\}$ of some region c_μ to the point $\{c_{\mu\pm h}\}$ of one of the two neighbouring regions $c_{\mu\pm h}$ and then returns to $\{c_\mu\}$ may be reduced to a cycle of fewer segments by adding or subtracting some suitable cycles l_μ. Any cycle which runs once through the ring may be reduced to k by adding a suitable combination of the l_μ.

The l_μ fulfill γ relations

$$l_\mu + l_{\mu+\gamma} + l_{\mu+2\gamma} + \cdots l_{\mu+(\xi-1)\gamma} = 0, \qquad \mu = 0, 1, \cdots, \gamma - 1, \tag{20.8}$$

by means of which γ of the l_μ may be eliminated. The remaining $\alpha - \gamma$ cycles l_μ together with k then are independent and form a homology base of connection of p_1 elements.

The setting up of the part *IV* of the transformation matrix due to these p_1 basic elements is easily performed as in the preceding section and the factor corresponding to (19.20) computed: From the invariance of intersection numbers it is seen that the transform of l_μ contains $l_{\mu+1}$ with coefficient 1 and no other l-cycles nor k. Likewise the transform of k contains k with coefficient 1. So from k the factor $x-1$ is derived, and from the l-cycles we get $\frac{x^\alpha-1}{x^\gamma-1}$ in taking account of the relations (20.8); this follows directly from the computation attached to (19.11) and (19.12).

So in all we have to multiply by

$$\frac{(x^\alpha-1)\,(x-1)}{x^\gamma-1} \tag{20.9}$$

as a result of operations b).

As the final result of both a) and b) we have: In passing from S' to S the polynomial $P_c(x^\gamma)$ of S' has to be multiplied by the factors (20.7) and (20.9), thus giving the polynomial $P(x)$ of S for the transformation class τ:

$$P(x) = (x-1)^{1+\omega} \prod_l \frac{(x^{\gamma/\beta_l n_l}-1)^{2q_l+s_l-2}}{(x^{\gamma/\beta_l m_{l1}}-1)\cdot\cdots}.$$

This is in fact the polynomial set up in (16.3), since a is not amphidrome and any kernel of c passes into kernels of c_1, c_2, $\cdots$, $c_{\gamma-1}$ before returning to c.

In sections 18, 19, 20 we have given the proof of the theorem stated in (16.3), in case the geodesics of the equivalence class used in dividing S are not amphidrome. In the following section we complete the proof by dealing with an amphidrome a.

21. Fourth part of the proof. In this section we assume a to be amphidrome. If again α is the number assigned to a in section 10 or 12, α is even, and there are $\frac{\alpha}{2}$ different geodesics

$$a,\ \tau a = a_1,\ \tau^2 a = a_2,\ \cdots,\ \tau^{\frac{\alpha}{2}-1} a = a_{\frac{\alpha}{2}-1} \tag{21.1}$$

in the equivalence class of a. Let the left hand and right hand borders of a, $a_1, \cdots$ as before be denoted by a', $a'_1, \cdots$ and a'', $a''_1, \cdots$ respectively. They are oriented in the same way as the geodesics (21.1).

We first assume that S is not decomposed by the system (21.1). So S' consists of one region c only. Let

$$P_c(x) = (x-1)\prod_l \frac{(x^{\beta_l n}-1)^{2q+s-2}}{(x^{\beta_l m_{l1}}-1)\cdots}$$

be the characteristic polynomial of c for the transformation class τ. The $\frac{\alpha}{2}$ geodesics (21.1) yield α boundary curves of c.

If S is bounded, we may take the curves

$$(21.2) \qquad a', a'_1, \cdots, a'_{\frac{\alpha}{2}-1}, -a'', -a''_1, \cdots, -a''_{\frac{\alpha}{2}-1}$$

as members of a homology base of S'. As they are interchanged cyclically by τ, we get $x^\alpha - 1$ as the factor in $P_c(x)$ derived from these α boundary curves. If S is closed, the sum of the elements (21.2) is zero. We then get $\frac{x^\alpha - 1}{x-1}$ as the corresponding factor.

Taking both cases together, we get

$$\frac{x^\alpha - 1}{(x-1)^\omega}$$

as the factor of $P_c(x)$ derived from the boundaries (21.1). Compare the corresponding more elaborate proof in section 18.

Now joining the boundary curves in turn, the a''-elements cancel and we retain the a'-elements, which we may denote as a-elements. Then, by τ, a is replaced by $a_1, \cdots, a_{\frac{\alpha}{2}-2}$ by $a_{\frac{\alpha}{2}-1}$ and this by $-a$. No homology relation exists between them. The corresponding polynomial is easily computed to be

$$x^{\frac{\alpha}{2}} + 1.$$

So the effect of joining the boundary curves of S' is to multiply $P_c(x)$ by

$$\frac{(x-1)^{\omega}}{x^{\frac{\alpha}{2}}-1}. \tag{21.3}$$

To introduce a homology base of connection we choose a point $\{c\}$ in c and denote by b_μ ($\mu = 0, 1, \cdots, \alpha-1$) a cycle which starts from $\{c\}$, crosses $\tau^\mu a$ once from left to right, and returns to $\{c\}$. Since

$$\tau^{\mu+\frac{\alpha}{2}} a = -\tau^\mu a,$$

we may choose the cycles b_μ so that

$$b_{\mu+\frac{\alpha}{2}} = -b_\mu.$$

It is seen from intersection numbers that b_μ has the coefficient zero in the transforms of all basic elements derived from S' and in the transforms of all b-cycles except $b_{\mu-1}$; in the transform of $b_{\mu-1}$ the coefficient of b_μ is 1. So the contribution of the b-elements to the polynomial is that of α elements which are interchanged cyclically by τ and which satisfy the condition

$$b_\mu + b_{\mu+\frac{\alpha}{2}} = 0.$$

It then follows (e. g. by a transformation analogous to (19.11)), that the corresponding factor in the polynomial is $\dfrac{x^\alpha-1}{x^{\frac{\alpha}{2}}-1}$.

So the polynomial $P(x)$ of S is found by multiplying $P_c(x)$ by this factor and (21.3):

$$P(x) = \frac{(x-1)^{\omega}}{x^{\frac{\alpha}{2}}-1} \cdot \frac{x^\alpha-1}{x^{\frac{\alpha}{2}}-1} \cdot (x-1)\sqrt{}_l.$$

The part $\dfrac{x^\alpha-1}{\left(x^{\frac{\alpha}{2}}-1\right)^2}$ has to be taken into the sign $\sqrt{}_l$, since it is the factor corresponding to the amphidrome bands arising from the axes (21.1); cf. (16.5) with the notation $\beta_l = \dfrac{\alpha}{2}$. The result

then obviously is in accordance with (16.3) and the explanation attached to that formula.

Secondly we assume that S is decomposed by the system (21.1). Let c be the region to the left and c_1 the region to the right of a. These two regions are not identical, otherwise any two adjacent regions would be identical and S would not be decomposed. Under the transformation class $\tau^{\frac{\alpha}{2}}$ all geodesics (21.1) are inverted, hence $\tau^{\frac{\alpha}{2}} c = c_1$. Thus all those geodesics of the set (21.1) which bound c must bound c_1 too, and vice versa. If these were not all geodesics (21.1), S would not be coherent. So we infer that there are exactly two regions, c and c_1; the number γ of regions in the equivalence class of c is 2, and we have $\tau c = c_1$, $\tau^2 c = c$. Thus $\frac{\alpha}{2}$ must be an odd number.

Let the above polynomial $P_c(x)$ belong to c. Then, as pointed out in section 17, the polynomial

$$P_{S'}(x) = P_c(x^2) = (x^2-1)\prod \frac{(x^{2\beta_i n_i}-1)^{2q_i+s_i-2}}{(x^{2\beta_i m_{i1}}-1)\cdots}$$

belongs to the decomposed surface S'.

The curves (21.2) are on the boundary of S' and are interchanged cyclically by τ. If S is bounded, both c and c_1 have boundaries not belonging to (21.2). So these α curves may be taken as members of a homology base of S' and yield the factor $x^\alpha - 1$ as before. If S is closed, we remember that all even powers of τ transform c into itself and c_1 into itself. So

$$(21.4)\quad a' + a'_2 + a'_4 + \cdots + a'_{\frac{\alpha}{2}-1} - a''_1 - a''_3 - \cdots - a''_{\frac{\alpha}{2}-2} = 0,$$

since these curves constitute the complete boundary of c, and

$$(21.5)\quad a'_1 + a'_3 + a'_5 + \cdots + a'_{\frac{\alpha}{2}-2} - a'' - a''_2 - \cdots - a''_{\frac{\alpha}{2}-1} = 0,$$

since these curves constitute the complete boundary of c_1. Then using a transformation analogous to (19.11) we see that $\frac{x^\alpha - 1}{x^2 - 1}$ is the factor in $P_{S'}(x)$ derived from the boundaries. Taking both cases together

(21.6) $$\frac{x^{\alpha}-1}{(x^2-1)^{\omega}}$$

is the factor of $P_{S'}(x)$ derived from the boundaries (21.2).

We now join the boundaries by putting

$$a''_{\mu} = a'_{\mu}, \quad \mu = 0, 1, \cdots, \frac{\alpha}{2}-1,$$

and denoting it simply by a_{μ}. In the sequence (21.1) each element is by τ replaced by the following and the last element, $a_{\frac{\alpha}{2}-1}$, is replaced by $-a$. If S is bounded, no homology relation has to be observed, and the corresponding factor in the polynomial is as in the first case equal to

$$x^{\frac{\alpha}{2}}+1 = \frac{x^{\alpha}-1}{x^{\frac{\alpha}{2}}-1}.$$

If S is closed, we get from (21.4)

$$a - a_1 + a_2 - a_3 + \cdots + a_{\frac{\alpha}{2}-1} = 0,$$

and the same relation is derived from (21.5). From this we may express $a_{\frac{\alpha}{2}-1}$. The matrix corresponding to the transformation of the set $a, a_1, \cdots, a_{\frac{\alpha}{2}-2}$ then becomes

$$\begin{Vmatrix} 0 & 1 & 0 & 0 & \cdots & 0 \\ 0 & 0 & 1 & 0 & \cdots & 0 \\ 0 & 0 & 0 & 1 & \cdots & 0 \\ \cdot & \cdot & \cdot & \cdot & \cdots & 1 \\ -1 & 1 & -1 & 1 & \cdots & 1 \end{Vmatrix}$$

with $\frac{\alpha}{2}-1$ rows and columns. Subtracting $xE_{\frac{\alpha}{2}-1}$ and then adding the second, third, etc. columns with coefficients x, x^2, etc. to the first, one finds the corresponding polynomial equal to

$$-\left[(1-x)\,x^{\frac{\alpha}{2}-2}-x^{\frac{\alpha}{2}-3}+x^{\frac{\alpha}{2}-4}\cdots+x-1\right]$$

$$=x^{\frac{\alpha}{2}-1}-x^{\frac{\alpha}{2}-2}+x^{\frac{\alpha}{2}-3}-\cdots-x+1$$

$$=\frac{x^{\frac{\alpha}{2}}+1}{x+1}=\frac{(x^{\alpha}-1)\,(x-1)}{\left(x^{\frac{\alpha}{2}}-1\right)(x^2-1)}.$$

Taking both cases together, we find that

$$\frac{(x^{\alpha}-1)\,(x-1)^{\omega}}{\left(x^{\frac{\alpha}{2}}-1\right)(x^2-1)^{\omega}} \tag{21.7}$$

is the factor corresponding to the $\frac{\alpha}{2}-\omega$ basic geodesics after joining the boundary curves.

From a comparison of (21.6) and (21.7) we find that multiplication of $P_{S'}(x)$ by

$$\frac{(x-1)^{\omega}}{x^{\frac{\alpha}{2}}-1} \tag{21.8}$$

is the effect of joining the boundary curves (21.2) of S'.

Finally we have to introduce a homology base of connection. We choose a point $\{c\}$ in c and a point $\{c_1\}$ in c_1 and connect them by α segments, the segment b_μ crossing $\tau^\mu a$ from left to right. Since $a_{\mu+\frac{\alpha}{2}}=-a_\mu$, we take $b_{\mu+\frac{\alpha}{2}}=-b_\mu$. So we have two points and $\frac{\alpha}{2}$ segments in a coherent complex, thus $\frac{\alpha}{2}-1$ independent cycles. (For $\alpha=2$ there is only one common boundary of c and c_1 and no new cycle has to be introduced.) We form the cycles

$$l_\mu=b_\mu+b_{\mu+1},\quad \mu=0,1,\cdots,\alpha-1.$$

This system of α cycles evidently contains a homology base of connection. Relations are obvious: We have

(21.9) $$l_\mu + l_{\mu+\frac{\alpha}{2}} = 0$$

and moreover

(21.10) $$l_\mu - l_{\mu+1} + l_{\mu+2} - \cdots + l_{\mu+\frac{\alpha}{2}-1} = 0.$$

$\frac{\alpha}{2}$ of the relations (21.9) together with one of the relations (21.10) form an independent set of relations, and we are left with $\frac{\alpha}{2}-1$ independent cycles l_μ.

If we introduce

$$\varepsilon = e^{\frac{2\pi i}{\alpha}}$$

and set up the transformation analogous to (19.11), we would get all α powers of ε as multipliers, if the α cycles l_μ were independent. Because of (21.9) all even powers of ε cancel, and because of (21.10) $\varepsilon^{\frac{\alpha}{2}} = -1$ cancels too. So we get

(21.11) $$\frac{x^\alpha - 1}{\left(x^{\frac{\alpha}{2}} - 1\right)(x+1)} = \frac{(x^\alpha - 1)(x-1)}{\left(x^{\frac{\alpha}{2}} - 1\right)(x^2-1)}$$

as the contribution of the homology base of connections. (For $\alpha = 2$ this factor is equal to 1.)

We thus get the following result: In passing from S' to S we get the polynomial $P(x)$ corresponding to the transformation class τ of S by multiplying $P_{S'}(x)$ by (21.8) on account of joining the boundary curves and by (21.11) on account of the new connections thereby established. So we get

$$P(x) = (x-1)^{1+\omega} \cdot \frac{x^\alpha - 1}{\left(x^{\frac{\alpha}{2}} - 1\right)^2} \cdot \left| \begin{array}{c} \\ l \end{array} \right|.$$

The second factor has to be taken under the sign $\left| \begin{array}{c} \\ l \end{array} \right|$ as the contribution of the amphidrome bands corresponding to the amphidrome geodesics (21.1); cf. (16.5). So the result is clearly seen to be in accordance with (16.3) and the explanation attached to it.

This completes the proof of the main homology theorem stated by formula (16.3).

22. Final remarks. In section 14 we have constructed a transformation ζ of S, belonging to a prescribed transformation class τ of algebraically finite type, such that classes of fixed points with index $j = 0$ are completely avoided. We may therefore term such classes *unessential*. Classes with index $j \neq 0$, which we term *essential classes*, cannot, of course, be avoided, but are by ζ "satisfied" by one point each.

The function (16.1)

$$P(x) = (-1)^{\vartheta} \left| A - x E_{\vartheta} \right|$$

is a polynomial in x. So if we write it in the fractional form (16.3), the denominator divides the numerator. It will now be pointed out that one of the advantages of writing $P(x)$ in the fractional form (16.3) is to put all essential classes of fixed points, together with the indices of these classes, into evidence. For this purpose we examine the factors corresponding to the different values of l, which, it will be remembered, ranges over all equivalence classes of kernels, i. e. regions or amphidrome geodesics, of S. — The statement as to the fixed points of ζ at the end of section 14 should be compared.

If $\beta_l > 1$, the β_l kernels of the equivalence class in question are interchanged cyclically by τ, so they do not give rise to any fixed point of the special transformation ζ of section 14 and hence not to any essential class.

If $\beta_l = 1$ and the kernel is an amphidrome geodesic, it is seen from (16.5) that the corresponding factor is $\frac{x^2-1}{(x-1)^2}$. We then associate the two factors $x-1$ of the denominator with the two essential classes of fixed points, each of index $j = 1$, which are known to arise in the amphidrome band in the construction of ζ, each class being represented by one point.

If $\beta_l = 1$ and the kernel is a region, we may first have $n_l > 1$. The region is then mapped into itself by ζ in such a way that ζ^{n_l} is the identical transformation, thus ζ is periodic in the region with n_l as its order. (The region is then kernel of τ^{n_l}.) Fixed points of ζ are such ramification points of the

region over its modular surface M_l for which all n sheets hang together, thus for which the corresponding number m in the set

$$m_{l1}, m_{l2}, \cdots, m_{lu_l} \tag{22.1}$$

has the value 1. Hence we get as many essential classes as the number 1 occurs in the set (22.1), and the index of each class is $j = 1$.

If $\beta_l = 1$ and $n_l = 1$, the region is a kernel of τ itself and so is identical with its modular surface $M_l = \bar{M}_l$. The minimum number δ_l of generators of its Poincaré group is given by (16.4). Putting $\mu = 0$ and δ_l instead of ν in (5.1), we get the index

$$j_l = 2 - s_l - 2q_l < 0.$$

Since there are no ramification points, the set (22.1) is empty, and the factor in (16.3) corresponding to a region with $\beta_l n_l = 1$ is

$$(x-1)^{-j_l}.$$

To sum up, we have the following theorem:

The number of classes of fixed points with index $j = 1$ is equal to the number of factors with $\beta_l m_{li} = 1$ in the denominator of $P(x)$ written in the fractional form (16.3). *The number of classes with negative index is equal to the number of values of l with $\beta_l n_l = 1$, and the corresponding indices are the exponents with the opposite sign $2 - s_l - 2q_l$.*

It is seen that this result is due to a close combination of methods of homotopy with methods of homology. It is easy to deduce from our theorem a well known theorem of pure homology theory concerning the algebraic sum Ξ of all indices. This theorem makes use of the trace of the transformation matrix Δ. This trace does not depend on the choice of the homology base used and is equal to the sum of the roots of the characteristic polynomial $P(x)$. So we have to determine this sum of roots from (16.3). The initial factor $(x-1)^{1+\omega}$ yields $1+\omega$ as its contribution. In $\left[\begin{array}{c}\\ l\end{array}\right]$ a factor of the numerator with $\beta_l n_l > 1$ or of the denominator with $\beta_l m_{li} > 1$ has the sum of its roots equal to zero. A factor of the numerator with $\beta_l n_l = 1$ yields

$$2q_l + s_l - 2 = -j_l$$

as its contribution, a factor of the denominator with $\beta_l m_{li} = 1$ yields 1 and counts for -1, since it is placed in the denominator. So if we denote by Ξ^- the sum of all negative indices and by Ξ^+ the sum of all positive indices, we get

$$\text{trace } \mathcal{A} = 1 + \omega - \Xi^- - \Xi^+,$$

hence

$$\Xi = \Xi^- + \Xi^+ = 1 + \omega - \text{trace } \mathcal{A}.$$

This formula is due to J. W. Alexander [1] in its first form concerning surface transformations. It has received a far-reaching generalization by the investigations of S. Lefschetz [10, 11] and these have been treated in a modified form by H. Hopf [7]. It is seen from the present paper how it is possible for transformation classes of algebraically finite type to split the algebraic sum Ξ given by the trace formula into its different terms, positive or negative, due to the single essential classes of fixed points. To do this requires not only taking into consideration the sum of roots of the characteristic polynomial of the transformation class, but this polynomial itself.

It is seen from (16.3) that all roots of $P(x)$ are roots of unity. Now the roots of the polynomial belonging to τ^n are the n-th powers of the roots of $P(x)$. Owing to this the polynomial of τ^n is easily deduced from the polynomial of τ. Hence trace $\mathcal{A}^n$ is limited for all values of n, and so is $\Xi(\tau^n)$. This justifies the notation "algebraically finite type" for the transformation classes in question. But the full justification lies in a conjecture, which I have so far not been able to prove: It will be remembered that in section 8 classes of algebraically finite type were defined by the character that no principal region possesses cuspidal points. In all cases known to the author the existence of cuspidal points involves the existence of multipliers the numerical value of which is greater than 1, and then Ξ is not limited for the powers of τ. If this were proved to be true in general, then the transformation classes of algebraically finite type would be capable of a purely algebraic definition: They would be the only transformation classes for which all multipliers are roots of unity.

LIST OF PAPERS QUOTED

[1] J. W. Alexander. Invariant points of a surface transformation of given class. Transact. Am. Math. Soc. **25**. 1923.

[2] G. D. Birkhoff. Dynamical systems with two degrees of freedom. Transact. Am. Math. Soc. **18**. 1917.

[3] L. E. J. Brouwer. Über die periodischen Transformationen der Kugel. Math. Ann. **80**. 1919.

[4] L. E. J. Brouwer. Über topologische Involutionen. K. Akad. van Wetensch. te Amsterdam XXI, **9**. 1919.

[5] L. E. J. Brouwer. Aufzählung der periodischen Transformationen des Torus. K. Akad. van Wetensch. te Amsterdam XXI, **10**. 1919.

[6] M. Dehn. Die Gruppe der Abbildungsklassen. Acta math. **69**. 1938.

[7] H. Hopf. Über die algebraische Anzahl von Fixpunkten. Math. Zeitschr. **29**. 1929.

[8] B. v. Kerékjártó. Über die periodischen Transformationen der Kreisscheibe und der Kugelfläche. Math. Ann. **80**. 1919.

[9] B. v. Kerékjártó. Vorlesungen über Topologie. Springer, Berlin. 1923.

[10] S. Lefschetz. Intersections and transformations of complexes and manifolds. Transact. Am. Math. Soc. **28**. 1926.

[11] S. Lefschetz. Manifolds with a boundary and their transformations. Transact. Am. Math. Soc. **29**. 1927.

[12] S. Lefschetz. Topology. Am. Math. Soc. Colloq. Publ. Vol. **12**. 1930.

[13] J. Nielsen. Über Gruppen linearer Transformationen. Mitteil. der math. Gesellschaft in Hamburg. **8**. 1940.

[14] J. Nielsen. Untersuchungen zur Topologie der geschlossenen zweiseitigen Flächen. Acta mathematica.
I. Bd. **50**. 1927.
II. - **53**. 1929.
III. - **58**. 1931.

[15] J. Nielsen. Abbildungsklassen endlicher Ordnung. Acta math. **75**. 1942.

[16] J. Nielsen. Die Struktur periodischer Transformationen von Flächen. D. Kgl. Danske Vidensk. Selskab, Math.- fys. Meddelelser XV, **1**. 1937.

[17] J. Nielsen. Einige Sätze über topologische Flächenabbildungen. Acta litt. ac scient. Szeged. **7**. 1935.

[18] J. Nielsen. Fixpunktfrie Afbildninger. Mat. Tidsskr. B, 1942.

[19] W. SCHERRER. Über topologische Involutionen. Vierteljahrsschr. d. nat. Ges. in Zürich. **70**. 1925.

[20] W. SCHERRER. Über periodische Transformationen von Flächen. (Ibidem).

[21] W. SCHERRER. Zur Theorie der endlichen Gruppen topologischer Abbildungen von geschlossenen Flächen in sich. Commentarii Math. Helv. 1929.

[22] F. STEIGER. Die maximalen Ordnungen periodischer topologischer Abbildungen geschlossener Flächen in sich. Commentarii Math. Helv. 8. 1935.

Indleveret til Selskabet den 12. Oktober 1943.
Færdig fra Trykkeriet den 18. Marts 1944.

DET KGL. DANSKE VIDENSKABERNES SELSKAB
MATEMATISK-FYSISKE MEDDELELSER, BIND XXI, NR. 3

TABLES OF MODEL STELLAR ATMOSPHERES

(MODEL STELLAR ATMOSPHERES. I)

BY

BENGT STRÖMGREN

WITH THE COLLABORATION OF
K. GYLDENKÆRNE, M. RUDKJØBING,
AND K. A. THERNÖE

KØBENHAVN
I KOMMISSION HOS EJNAR MUNKSGAARD
1944

Printed in Denmark.
Bianco Lunos Bogtrykkeri A/S

1. The theoretical analysis of the observations of stellar spectra is carried out with the aid of both inductive and deductive methods. The pioneer work in this field of astrophysics has been done mainly by the former methods, and very important results have been reached by these. During recent years it has become possible, however, to apply deductive methods to an increasing number of problems within the field in question.

Deductive theoretical analysis of stellar spectra is carried out by investigations of so called model stellar atmospheres, cf. (1).

A stellar atmosphere is, by definition, that part of a star which is accessible to observations from the outside. The physical structure of the atmosphere thus determines the spectrum emitted by the star. The structure of the atmosphere is, in its turn, given by 1. its chemical composition, and 2. the influence of the interior star, as described by a number of factors specifying the physical conditions at the lower boundary of the atmosphere.

A model stellar atmosphere is specified by a number of parameters, describing its chemical composition and the physical conditions at its lower boundary. In principle, the structure of such an atmosphere, and the spectrum emitted by it, can be calculated by physical theory. A priori, the parameters of a model stellar atmosphere can be chosen arbitrarily. The ultimate aim of the theoretical study of model stellar atmospheres is, of course, to determine the parameters in such a way that complete agreement is obtained between the various observed stellar spectra and the corresponding theoretically calculated spectra. To achieve this purpose it is necessary to investigate a great number of model stellar atmospheres, varying the parameters systematically. Complete agreement between theoretical and observed spectrum can be assumed to mean identity in structure of the real stellar atmosphere and the considered model stellar atmosphere.

In specifying model stellar atmospheres it is generally necessary to make certain simplifying assumptions. Thus, as a rule, and in particular also in the present investigation, the analysis is restricted by the assumption that the atmosphere is symmetrical with respect to the centre of the star, so that the physical parameters vary with the depth in the atmosphere only. It is further assumed that the atmosphere is in mechanical equilibrium, and that the chemical composition is constant throughout the atmosphere. As far as is known at present these assumptions mean only small departures from the actual conditions of normal stars.

A model stellar atmosphere of the simplified type considered is completely specified by the effective temperature T_e (determined by the outward net-flux of energy per unit area), the gravity g, and the relative abundances of the elements. In practice it is only necessary to consider a rather limited number of the elements, since the structure of actual stellar atmospheres is practically uninfluenced by the great majority of the elements on account of their small abundance.

Given the effective temperature T_e, the gravity g, and the chemical composition of a model stellar atmosphere, the first step in the theoretical calculations leading up to the calculation of the emitted spectrum is the determination of temperature T, total pressure p, electron pressure p_e, and opacity $\bar{\varkappa}$ as a function of the geometrical depth, or the optical depth τ. The next step is the calculation of the coefficients of continuous absorption and emission, and the coefficients of line absorption and emission. These coefficients must be known, for all wave lengths, as functions of the depth. The final step consists in the evaluation of the radiation field, in particular the radiation field on the surface, which gives the emitted spectrum.

In the present investigation we shall consider only the first of the problems mentioned, namely, the calculation of temperature T, total pressure p, electron pressure p_e, and opacity $\bar{\varkappa}$ as functions of the optical depth τ. The final result of the investigations will consist of tables of these functions for a number of model stellar atmospheres. The results here obtained will be utilized in further calculations of the continuous spectrum, and of selected absorption lines, for the model stellar atmospheres considered.

In a previous paper (2) the author has considered the problem of model solar atmospheres, defined by values of T_e and g equal to those valid for the sun ($T_e = 5740°$, $\log g = 4.44$). It was shown that certain discrepancies between theory and observation previously encountered in the study of model solar atmospheres were entirely removed when the opacity of the atmospheric matter was calculated with due regard to the effect, discovered by WILDT (3), of the continuous absorption by the negative hydrogen ion. The comparison of observed and calculated solar spectra led to the determination of a number of the chemical parameters for the solar atmosphere, *viz.* the ratio A between the abundance of hydrogen and all the metals, and the relative abundances of hydrogen, sodium, potassium, calcium and magnesium.

In the present investigation the methods for calculating p, p_e and $\bar{\varkappa}$ as functions of τ developed in the author's paper mentioned above are applied to a number of model stellar atmospheres. The models studied cover the range of effective temperature T_e from that of $G0$ stars like the sun ($T_e = 5740°$) to that of $A5$ stars ($T_e = 8500°$). The range of effective gravity g covered corresponds to a region in the Hertzsprung-Russell-diagram, roughly between a line somewhat below the main series and a line around $M_{\text{bol}} = 0^m$, i. e. slightly above the giant branch. The hydrogen-metal ratio A was varied within the limits $\log A = 3.4$ and $\log A = 4.2$.

The values of the parameters of the model atmospheres are shown in the table below. The value of θ_0, i. e. the value of the temperature function $\theta = \dfrac{5040°}{T}$ at the surface of the star ($T_0 = 0.84\, T_e$), is given instead of T_e. Approximate values of the spectral type and visual absolute magnitude are also inserted for convenience.

For $\theta_0 = 0.7$ a variation of $\log A$ within the range from 3.4 to 4.2 has practically no influence on the structure of the model atmosphere.

In addition to the model atmospheres listed on p. 6 a few special model atmospheres were also considered, namely $\theta_0 = 1.041$, $\log g = 4.44$ (the Sun) for $\log A = 3.0$, 3.4, 3.8, and 4.2, further $\theta_0 = 1.041$, $\log g = 3.0$ (Capella) for $\log A = 3.4$, 3.8, and 4.2, and

θ_0	/ $\log g = 3.0$	3.5	4.0	4.5
1.0	$\log A = 3.4$	$\log A = 3.4$	$\log A = 3.4$	$\log A = 3.4$
	F 7 3.8	F 8 3.8	F 9 3.8	G 0 3.8
	0^m 4.2	$+2^m$ 4.2	$+4^m$ 4.2	$+5^m$ 4.2
0.9		$\log A = 3.4$	$\log A = 3.4$	$\log A = 3.4$
		F 4 3.8	F 4 3.8	F 5 3.8
		$+1^m$ 4.2	$+3^m$ 4.2	$+5^m$ 4.2
0.8		$\log A = 3.4$	$\log A = 3.4$	$\log A = 3.4$
		F 0 3.8	F 0 3.8	F 0 3.8
		0^m 4.2	$+2^m$ 4.2	$+4^m$ 4.2
0.7		$\log A = 3.8$	$\log A = 3.8$	$\log A = 3.8$
		A 5	A 5	A 5
		0^m	$+2^m$	$+3^m$

finally $\theta_0 = 0.7$, $\log g = 4.2$, and $\log g = 2.5$ ($cA\,5$ star) for $\log A = 3.8$. Altogether forty-five model stellar atmospheres have been investigated.

The limits of the range of effective temperatures $0.7 < \theta_0 < 1.04$, corresponding to the range of spectral types $A\,5$—$G\,0$, were fixed according to the following considerations. For stellar atmospheres with temperatures considerably lower than that of the sun it becomes difficult to distinguish between the continuous spectrum and the absorption line spectrum, both observationally and theoretically. Also the influence of molecular bands on the opacity probably becomes of importance. An accurate calculation of the structure of these atmospheres therefore presents additional difficulties, which have not yet been completely solved. On the other hand, for stars with higher temperatures than $A\,5$, electron scattering becomes of importance in the calculation of the opacity. Although it would not have presented very great difficulties to solve the problems arising in this connection, it was thought advisable to reserve the study of high temperature atmospheres for a following investigation.

It is well known that, while the upper layers of a stellar atmosphere are convectively stable, the deeper layers are characterized by convective instability, cf. (4). It has not yet been possible, however, to reach a final solution of the problems connected with the question of the influence of convective instability upon the structure of the unstable layers, cf. (5).

Unsöld and Siedentopf assumed that the structure of the unstable zone is governed by the equations valid in radiational

equilibrium. BIERMANN, on the other hand, assumed that the temperature gradient in the unstable layers is everywhere equal to the adiabatic gradient. The two assumptions clearly represent ideal limiting cases, so that the true structure would be intermediate between the structures calculated according to them.

In the present investigation the structure of the convectively unstable layers is calculated separately according to both assumptions. The calculations have been made according to the methods developed by UNSÖLD, BIERMANN, and SIEDENTOPF (5). In a recent paper RUDKJØBING (6) has adapted these methods to the calculation of model stellar atmospheres of the type considered here. In particular the continuous absorption by the negative hydrogen ion was taken into account. RUDKJØBING's procedure has been employed in calculating the structure of the convectively unstable layer for all the stellar models considered here.

In the following sections 2—4, the procedure of calculation of the opacity and pressure tables is described in somewhat greater detail than in the paper by the author quoted above (2). These, brief summaries of which have been previously given (2), are collected in an appendix. The methods of calculation of the model stellar atmospheres are discussed in sections 5—7. The tables giving the structure of the model stellar atmospheres considered are given in the appendix. The results obtained are discussed in sections 8 and 9.

The calculation of the opacity tables and pressure tables required for the determination of the structure of the model atmospheres considered was made by M. RUDKJØBING, K. A. THERNÖE, and the author. The calculations of the model atmospheres were made by K. GYLDENKÆRNE, M. RUDKJØBING, and the author.

The present investigation was supported by a grant from the CARLSBERG FOUNDATION. The author wishes to express his best thanks to the directors of the FOUNDATION for this subvention.

2. When the chemical composition of a model stellar atmosphere is specified, it is possible to construct tables giving the electron pressure p_e and the opacity $\bar{\varkappa}$ of the stellar atmospheric gas as a function of temperature T and total pressure p.

The chemical composition of the model atmospheres investigated was chosen according to the following considerations. The

analysis of the solar spectrum has shown (cf. RUSSELL (7), WILDT (3), MENZEL (8), B. STRÖMGREN (2), and TEN BRUGGENCATE (9)) that hydrogen is by far the most abundant element in the solar atmosphere. Next follow helium, oxygen, carbon, nitrogen, and perhaps neon. Then follow magnesium, silicon, iron, calcium, aluminum, and sodium. For the rest of the elements the abundance is so small that they need not be considered in this connection.

The analysis of the spectrum of τ Scorpii by UNSÖLD (10) has yielded a similar result.

We now have to consider the contribution of the various elements to the electron pressure and to the opacity. The ionization potential of hydrogen is 13.53 volts. For helium, oxygen, nitrogen and neon the ionization potential is higher and the abundance compared with that of hydrogen so much lower that the contribution of these elements both to the electron pressure and to the opacity can be neglected.

The elements of the metal group have ionization potentials from 5 to 8 volts. In spite of their low abundance they contribute the major part of the electron pressure at low temperatures when the degree of ionization of hydrogen is very small. The contribution of the metal atoms and ions to the opacity may be neglected in comparison with that of the neutral hydrogen atoms and the negative hydrogen ion (cf. (2)).

The case of carbon requires special consideration. The ionization potential is 11.22 volts, or 2.31 volts lower than that of hydrogen. The abundances of hydrogen, carbon and all the metals put together are probably roughly in the ratios 10000 : 10 : 1. Assuming these ratios we find that at high and intermediate temperatures ($\theta < 0.6$) carbon contributes a few per cent. of the electron pressure. For lower temperatures, the contribution is higher, rising to about eighteen per cent. of that of hydrogen at $\theta = 0.9$, and about thirty per cent. at $\theta = 1.0$. At this temperature, however, the metals contribute more to the electron pressure than hydrogen, except for very low pressures ($p_e < 0.1$ bar, i. e. dyne per square centimeter). With the exception of a small part of the relevant pressure-temperature range the relative contribution of carbon to the electron pressure is, therefore, less than ten per cent., generally much less. The relative contribu-

tion of carbon to the opacity is easily seen to be smaller than that of the metals, and therefore negligible.

In the present investigation the influence of carbon upon electron pressure and opacity has been neglected.

The data given above of course depend upon the assumed relative abundance of carbon. Subsequent investigations might possibly lead to a higher value of the abundance, thus making it desirable to consider the influence of carbon. A corresponding revision of the present calculation would present no difficulties. It would, however, be possible to obtain approximate values of the corrections to the model atmosphere tables (for radiative equilibrium) given in the present investigation in the following way. The ratio of the number of free electrons contributed by carbon and by hydrogen on account of the relatively small difference in ionization potential varies relatively little in the relevant part of the atmosphere. It is, therefore, a reasonably good approximation to put the ratio in question equal to a suitably chosen constant, k. Then it can be shown (cf. p. 35) that the corrected values of p, p_e and T as functions of τ are obtained from the tables when these are entered with arguments $(1+k)\,g$ and $(1+k)\,A$ instead of g and A, and the pressure thus obtained is divided by $(1+k)$.

In our investigation we have assumed that practically the whole weight of the atmospheric matter is contributed by hydrogen. This is in agreement with the results obtained so far from the quantitative analysis of stellar atmospheres. It may become desirable, however, to consider model atmospheres with an increased content of helium and oxygen (cf. BIERMANN (5)), in which these two elements contribute appreciably to the weight (without contributing materially to the electron pressure or the opacity). Tables giving the structure of such atmospheres can easily be obtained by a simple transformation of the tables of our investigation. It is in fact easy to prove (cf. p. 34) that correct values of p, p_e and T are obtained when the tables are entered with the argument $\frac{g}{X}$ instead of g, where X is the hydrogen content (relative weight) of the atmospheric matter.

Summarizing, we see that the model atmospheres considered in the present investigation are characterized by a chemical com-

position consisting of a mixture of hydrogen and metals (magnesium, silicon, iron, calcium, aluminum, and sodium). The number of hydrogen atoms and ions per unit volume is equal to A times the total number of metal atoms and ions. The value of the constant A is so large that only hydrogen contributes to the opacity. Both hydrogen and the metals contribute to the electron pressure.

In the relevant range of pressure and temperature the metals are strongly ionized. In calculating the contribution of the metals to the electron pressure it is only necessary to consider singly ionized ions, because the contribution due to higher stages of ionization are always very small as compared with that of hydrogen, since the ionization potentials of the metal ions never are much smaller than that of hydrogen, while the abundances are very much smaller.

In the major part of the range of pressure and temperature it is in fact a very good approximation to put the number of electrons contributed per metal atomic particle equal to 1. In the whole of the relevant range this number is higher than 0.5. From this fact and the fact that the differences between the ionization potentials of the various metals are comparatively small it follows that the contribution of the metals to the electron pressure is not sensitive to changes in the relative abundances of the metals *inter se*. The actual calculations were made with a composition equal to that found by GOLDSCHMIDT (11) for the meteorites. This agrees remarkably well with the result of the quantitative analysis of the solar atmosphere (cf. (2)). The relative abundances assumed are shown in the following table.

Element	Adopted relative number of atoms
Mg	0.30
Si	0.33
Fe	0.30
Ca	0.02
Al	0.03
Na	0.02
	1.00

Thus we see that the only parameter of chemical constitution which it is necessary to vary in the calculation of the ba-

sic tables of electron pressure and opacity, is the ratio A between the number of hydrogen atoms and ions per unit volume and the number of metal atoms and ions per unit volume. The analysis of the solar spectrum leads to a value of A equal to 8000 (cf. (2)). In the present investigation a range of A from 2500 (for some of the tables from 1000) to 16000 is covered.

3. The opacity of the atmospheric gas is calculated as the ROSSELAND mean $\bar{\varkappa}$ of the continuous absorption coefficient $\varkappa_\nu$ (cf. f. inst. (4)). As mentioned above only hydrogen contributes to the latter.

The coefficient $\varkappa_\nu$ of continuous absorption due to hydrogen can be calculated for all frequencies in the required range of frequency ν, when the temperature T and the electron pressure p_e are known. The continuous absorption coefficient for a given frequency is the sum of contributions from the various stationary states of the neutral hydrogen atom and the one existing state of the negative hydrogen ion.

The continuous absorption coefficient per atom or ion in the stationary states mentioned is known from quantum-mechanical calculations. For neutral hydrogen we have (cf. UNSÖLD (4) and the literature quoted there):

$$a_\nu(n) = \frac{64\,\pi^4}{3\sqrt{3}}\,\frac{m_e\,e^{10}}{c\,h^6}\,g_\nu(n)\,\frac{1}{n^5\,\nu^3} \quad (\text{for } \nu > \nu(n)). \tag{1}$$

Here $a_\nu(n)$ is the continuous absorption coefficient per hydrogen atom in the stationary state with principal quantum number n, while $g_\nu(n)$ is a correcting factor depending upon ν and n, which is always very nearly equal to 1. In the present investigation we have, following UNSÖLD, put all $g_\nu(n)$ equal to 1. The quantity $\nu(n)$ is the frequency of the series limit for the stationary state n.

Introducing numerical values of the natural constants m_e, e, c, and h in (1) we get:

$$a_\nu(n) = 1.04 \cdot 10^{-17} \cdot \frac{1}{n^5}\left(\frac{\lambda}{1000\,\text{Å}}\right)^3. \tag{2}$$

The continuous absorption coefficient of the negative hydrogen ion has been calculated by MASSEY and BATES (12). The

resulting value of the continuous absorption coefficient per negative hydrogen ion is shown for the frequency range corresponding to wave lengths between 3000 Å and 18000 Å in the following table.

λ	a_λ
3000 Å	$23 \cdot 10^{-18}$
4000	26
5000	25
6000	22
7000	18
8000	14
10000	9
18000	0

In the range between 3000 Å and 7000 Å the variations of a_λ are less than $\pm$ 20 per cent. Outside this range the value of the continuous absorption coefficient of the negative hydrogen ion has very little influence upon the opacity. This is so because even at the lowest temperatures in question the infra-red part of the spectrum has very little weight when forming the ROSSELAND mean. For the part of the spectrum in the far ultra-violet beyond 3000 Å the same is true for the lower temperatures. For the higher temperatures, on the other hand, the contribution from neutral hydrogen atoms is much greater than that from negative hydrogen ions.

For the range between 3000 Å and 7000 Å observations of the intensity distribution of the continuous spectrum of the sun indicate small variations of the absorption coefficient with wave length (cf. RAUDENBUSCH (13)) which are in the opposite direction of the variation shown by the theoretically calculated values.

In view of these facts it was considered appropriate and sufficiently accurate to adopt an absorption coefficient of the negative hydrogen ion independent of frequency and equal to the maximum value calculated for λ about 4400 Å.

RUDKJØBING (6) has calculated the opacity according to a different assumption, namely, that the absorption coefficient is constant for all wave lengths greater than that of maximum absorption according to MASSEY and BATES, while it follows MASSEY and BATES's curve for the shorter wave lengths. The resulting opacities, as was to be expected, differed only slightly from those

calculated in the present investigation. In a recent investigation RUDKJØBING (14) has revised the quantum-mechanical calculation of the continuous absorption coefficient in the far ultra-violet and thereby obtained values not much below the maximum value in the region 500—1000 Å. In view of this result we have preferred the opacity tables calculated on the assumption of constant absorption coefficient also in the ultra-violet.

The continuous absorption coefficient for any given frequency can now be evaluated if the distribution over the three stages of ionization and over the various stationary states of neutral hydrogen are known. This distribution is governed by the following equations:

$$\frac{N_H}{N_{H^-}} p_e = \frac{(2\pi m_e)^{\frac{3}{2}}}{h^3} \frac{2 g_H}{g_{H^-}} (kT)^{\frac{5}{2}} e^{-\frac{I_{H^-}}{kT}} \tag{3}$$

$$\frac{N_{H^+}}{N_H} p_e = \frac{(2\pi m_e)^{\frac{3}{2}}}{h^3} \frac{2 g_{H^+}}{g_H} (kT)^{\frac{5}{2}} e^{-\frac{I_H}{kT}} \tag{4}$$

$$\frac{N_H(n)}{N_H} = n^2 e^{-\frac{I_H - I(n)}{kT}} \tag{5}$$

Here N_H, N_{H^-}, and N_{H^+} denote the number of neutral hydrogen atoms in the ground state, negative hydrogen ions, and positive hydrogen ions per unit volume, while g_H, g_{H^-}, and g_{H^+} are the corresponding statistical weights, and I_{H^-}, I_H, $I(n)$ the ionization potentials of the negative hydrogen ion, the neutral hydrogen atom in the ground state, and in the stationary state n.

The statistical weights are $g_H = 2$, $g_{H^-} = 1$, $g_{H^+} = 1$, while $I_H = 13.53$ volts and $I(n) = \frac{13.53}{n^2}$ volts. The ionization potential I_{H^-} of the negative hydrogen ion has been evaluated by HYLLERAAS (15) by means of quantum-mechanical calculations. We have adopted the value $I_{H^-} = 0.70$ volts.

Introducing these values, and further the temperature function

$$\theta = \frac{5040^\circ}{T} \tag{6}$$

we can write the ionization equations and equation (5) as follows:

$$\log \frac{N_H^-}{N_H} = -0.12 + 0.70\,\theta - \frac{5}{2}\log T + \log p_e \tag{7}$$

$$\log \frac{N_{H^+}}{N_H} = -0.48 - 13.53\,\theta + \frac{5}{2}\log T - \log p_e \tag{8}$$

$$\log \frac{N_H(n)}{N_H} = 2\log n - 13.53\left(1 - \frac{1}{n^2}\right)\theta. \tag{9}$$

Here the electron pressure must be measured in bars (i. e. dynes per square centimeter). We shall use this unit throughout (1 atm = $1.01 \cdot 10^6$ bar).

With the aid of equations (7), (8), and (9) the distribution over the stationary states in question can be found as a function of the electron pressure p_e and the temperature function θ. The atomic continuous absorption coefficient of the various stationary states being also known, the resulting continuous absorption coefficient $\varkappa_\nu$ per gram hydrogen can be evaluated. The final step is the calculation of the ROSSELAND mean $\bar{\varkappa}$:

$$\frac{1}{\bar{\varkappa}} = \frac{15}{4\pi^4}\int_0^\infty \frac{1}{\varkappa_\nu}\frac{u^4 e^{-u} du}{(1-e^{-u})^3}, \tag{10}$$

where

$$u = \frac{h\nu}{kT} \tag{11}$$

or

$$u = \frac{28400\ \text{Å}}{\lambda}\theta. \tag{12}$$

The actual calculations of the tables giving the opacity $\bar{\varkappa}$ as a function of θ and p_e were carried out as follows. For a given value of the temperature function θ the frequency dependence of the continuous absorption coefficient due to neutral hydrogen is fixed, independently of the electron pressure. The frequency dependence of the continuous absorption coefficient due to the negative hydrogen ion is independent of both θ and p_e. The

resulting absorption coefficient $\varkappa_\nu$, however, shows a run with the frequency which, for given θ, depends upon p_e. Instead of considering immediately the change of the frequency dependence of $\varkappa_\nu$ with p_e, we shall investigate, first, the change of frequency dependence of $\varkappa_\nu$ with the ratio of the absorption by the negative hydrogen ion and that of neutral hydrogen.

In the limiting case of negligible absorption by the negative hydrogen ion (sufficiently small p_e) the frequency dependence of $\varkappa_\nu$ is that of neutral hydrogen for the value of θ considered, and the opacity is equal to $\bar{\varkappa}_H$, the ROSSELAND mean of the neutral hydrogen absorption coefficient:

$$\frac{1}{\bar{\varkappa}_H} = \frac{15}{4\pi^4}\int_0^\infty \frac{1}{\varkappa_\nu(H)}\frac{u^4 e^{-u}du}{(1-e^{-u})^3}. \tag{13}$$

This has been calculated by UNSÖLD (cf. (4)) as a function of θ. The values given by UNSÖLD were used in our calculations (after corrections of an error for $\theta = 0.5$, *viz.* $\log \varkappa_H$ 1.69 instead of 1.59).

The absorption coefficient of the negative hydrogen ion is assumed to be independent of the frequency, equal to $\varkappa_{H^-}$. As a measure of the ratio of the absorption of the negative hydrogen ion and that of neutral hydrogen we use $\frac{\varkappa_{H^-}}{\bar{\varkappa}_H}$. We thus calculate, first, a table giving the ratio $\frac{\bar{\varkappa}}{\bar{\varkappa}_H}$ as a function of θ and $\frac{\varkappa_{H^-}}{\bar{\varkappa}_H}$.

From equations (1) and (5) we obtain the following expression for the absorption coefficient $\varkappa_\nu(H)$ of neutral hydrogen, per gram neutral hydrogen in the ground state:

$$\varkappa_\nu(H) = \frac{1}{m_H}\frac{64\pi^4}{3\sqrt{3}}\frac{m_e e^{10}}{ch^3}\frac{1}{(kT)^3}\frac{e^{-u_H}}{u^3}\sum_{u_n<u}^{7}\frac{1}{n^3}e^{u_n}, \tag{14}$$

where

$$u = \frac{h\nu}{kT} \tag{15}$$

$$u_H = \frac{I_H}{kT} \tag{16}$$

and

$$u_n = \frac{1}{n^2} u_H, \tag{17}$$

while m_H is the mass of the hydrogen atom. For a given ν the sum has to be extended over all n, for which the corresponding absorption edge has a smaller frequency than ν, i. e. $u_n < u$.

Following UNSÖLD (4) we approximate the sum of the terms with $n \geq 5$ in (14) by the corresponding integral. Introducing

$$F = \frac{1}{m_H} \frac{64\pi^4}{3\sqrt{3}} \frac{m_e e^{10}}{ch^3} \frac{1}{(kT)^3} e^{-u_H} \tag{18}$$

and

$$D = \frac{1}{2 u_H} e^{u_5} + \sum_{u_n < u}^{4} \frac{1}{n^3} e^{u_n} \tag{19}$$

we then have

$$\varkappa_\nu(H) = F \frac{D}{u^3} \tag{20}$$

and consequently according to (10)

$$\frac{1}{\bar{\varkappa}_H} = \frac{15}{4\pi^4} \frac{1}{F} \int_0^\infty \frac{1}{D} \frac{u^7 e^{-u} du}{(1-e^{-u})^3}. \tag{21}$$

The following table gives F and D for the required values of the temperature function θ. The table also gives u_n for the absorption edges $n = 1, 2, 3$ and 4. Between successive absorption edges D is constant according to equation (19). The values of D for the frequency region of the LYMAN continuum ($\lambda < 912$ Å) are not given, since for all the temperatures considered the absorption coefficient is here so high that the contribution to the opacity integral in equation (21) is negligible.

The table further contains the contributions of the various frequency regions to the opacity integral (with omission of the factor F), the sum Σ of these contributions, and finally the resulting neutral hydrogen opacity

$$\frac{1}{\bar{\varkappa}_H} = \frac{\Sigma}{F} \tag{22}$$

or

$$\bar{\varkappa}_H = \frac{F}{\Sigma}. \tag{23}$$

$\theta = 0.3$	$\log F = 5.53$		
n	u_n	D	Contr. to Σ
1	9.34		
		1.503	93.3
2	2.34		
		0.210	4.2
3	1.04		
		0.106	0.1
4	0.58		
		0.078	0.0
		$\Sigma =$	97.6

$\log \bar{x}_H = 3.54$

$\theta = 0.4$	$\log F = 4.55$		
n	u_n	D	Contr. to Σ
1	12.46		
		3.066	58.4
2	3.12		
		0.248	14.5
3	1.38		
		0.100	0.6
4	0.78		
		0.066	0.0
		$\Sigma =$	73.5

$\log \bar{x}_H = 2.68$

$\theta = 0.5$	$\log F = 3.49$		
n	u_n	D	Contr. to Σ
1	15.58		
		6.448	28.5
2	3.90		
		0.310	32.0
3	1.73		
		0.101	1.8
4	0.97		
		0.060	0.1
		$\Sigma =$	62.4

$\log \bar{x}_H = 1.69$

$\theta = 0.6$	$\log F = 2.37$		
n	u_n	D	Contr. to Σ
1	18.69		
		13.77	12.7
2	4.67		
		0.402	52.3
3	2.08		
		0.107	4.4
4	1.17		
		0.056	0.4
		$\Sigma =$	69.8

$\log \bar{x}_H = 0.53$

$\theta = 0.7$	$\log F = 1.22$		
n	u_n	D	Contr. to Σ
1	21.80		
		29.66	5.4
2	5.45		
		0.534	69.1
3	2.42		
		0.116	8.7
4	1.36		
		0.055	1.0
		$\Sigma =$	84.2

$\log \bar{x}_H = 9.29 - 10$

$\theta = 0.8$	$\log F = 0.04$		
n	u_n	D	Contr. to Σ
1	24.92		
		64.19	2.2
2	6.23		
		0.719	78.2
3	2.77		
		0.129	15.2
4	1.56		
		0.054	2.0
		$\Sigma =$	97.6

$\log \bar{x}_H = 8.05 - 10$

$\theta = 0.9$	$\log F = 8.84$		
n	u_n	D	Contr. to Σ
1	28.04		
		139.3	0.8
2	7.01		
		0.979	78.5
3	3.12		
		0.145	23.8
4	1.75		
		0.055	3.7
		$\Sigma =$	106.8

$\log \bar{x}_H = 6.81 - 10$

$\theta = 1.0$	$\log F = 7.62$		
n	u_n	D	Contr. to Σ
1	31.15		
		302.6	0.3
2	7.79		
		1.345	72.0
3	3.46		
		0.165	34.0
4	1.95		
		0.056	6.2
		$\Sigma =$	112.5

$\log \bar{x}_H = 5.57 - 10$

Except for $\theta = 0.9$ and $\theta = 1.0$ corresponding values have been given by UNSÖLD (cf. (4), p. 121). Our values agree with UNSÖLD's within a few units of the last decimal.

Considering again the case of both neutral hydrogen and the negative hydrogen ion contributing to the opacity, we now introduce, for each separate temperature, $\bar{\varkappa}_H$ (reckoned per gram neutral hydrogen in the ground state) as the unit of absorption coefficient. From equations (20) and (23) we get

$$\frac{\varkappa_\nu(H)}{\bar{\varkappa}_H} = \frac{D\,\Sigma}{u^3}. \tag{24}$$

The ratio between the resulting continuous absorption coefficients $\varkappa_\nu$ and $\bar{\varkappa}_H$ is

$$\frac{\varkappa_\nu}{\bar{\varkappa}_H} = \frac{\varkappa_\nu(H) + \varkappa_{H^-}}{\bar{\varkappa}_H} = \frac{D\,\Sigma}{u^3} + \frac{\varkappa_{H^-}}{\bar{\varkappa}_H}. \tag{25}$$

Introducing this in the opacity integral we find

$$\frac{\bar{\varkappa}_H}{\bar{\varkappa}} = \frac{15}{4\pi^4}\int_0^\infty \frac{1}{\dfrac{D\,\Sigma}{u^3} + \dfrac{\varkappa_{H^-}}{\bar{\varkappa}_H}} \frac{u^4 e^{-u}}{(1-e^{-u})^3}\,du. \tag{26}$$

By means of equation (26) the required quantity $\dfrac{\bar{\varkappa}}{\bar{\varkappa}_H}$ can be found when $\dfrac{\varkappa_{H^-}}{\bar{\varkappa}_H}$ and θ are known. The calculations were carried out for $\theta = 0.3, 0.4, 0.5, 0.6, 0.7, 0.8, 0.9, 1.0$ and $\log \dfrac{\varkappa_{H^-}}{\bar{\varkappa}_H}$ equal to 8.0, 8.4, 8.8, 9.2, 9.6, 0.0, 0.4, 0.8, 1.2, 1.6, 2.0. In each case the integral was calculated numerically. The integrand was evaluated for the values of u corresponding to the absorption edges (u_1, u_2, u_3, and u_4) and at three additional equidistant points between successive absorption edges, so that the contribution of each interval with constant D to the integral could be found with the aid of Cotes' five-term formula for equidistant abscissae, *viz.*

$$\int_a^b f(x)\,dx = \frac{1}{90}(b-a)\left[7f(a)+32f\left(a+\frac{b-a}{4}\right)+\right.$$

$$\left.+12f\left(a+\frac{b-a}{2}\right)+32f\left(a+\frac{3(b-a)}{4}\right)+7f(b)\right].$$

The final table (Table 2, p. 39) was calculated by interpolation to the interval 0.1 instead of 0.4 for the argument $\log \frac{\varkappa_{H^-}}{\bar{\varkappa}_H}$. A glance at the table shows that the variation of the tabulated quantity $\log \frac{\bar{\varkappa}}{\bar{\varkappa}_H}$ with θ is quite small. This is the principal advantage of the chosen procedure.

With the aid of Table 2 a table of $\log \bar{\varkappa}$ with arguments θ and $\log p_e$ could easily be constructed. First, $\log \bar{\varkappa}_H$ is computed. The number of neutral hydrogen atoms in the ground state per gram is practically equal to

$$\frac{1}{m_H}(1-x_H), \tag{27}$$

where x_H is the degree of ionization of hydrogen. The latter is calculated according to equation (4). In Table 3, p. 40, $-\log(1-x_H)$ is given as a function of θ and $\log p_e$. The opacity per neutral hydrogen atom in the ground state being known as a function of θ, $\log \bar{\varkappa}_H$ follows (cf. Table 1, p. 38).

The number N_{H^-} of negative hydrogen ions per gram follows from equations (7) and (27):

$$\log N_{H^-} = \log \frac{1}{m_H} - 0.12 + 0.70\,\theta - \frac{5}{2}\log T + \log p_e + \log(1-x_H). \tag{28}$$

The continuous absorption coefficient per negative hydrogen ion has been assumed to be equal to $26 \cdot 10^{-18}$ (cf. p. 12). For $\varkappa_{H^-}$ we therefore get

$$\log \varkappa_{H^-} = 7.21 - 0.12 + 0.70\,\theta - \frac{5}{2}\log T + \log p_e + \log(1-x_H). \tag{29}$$

Table 1, p. 38, together with Table 3, p. 40, mentioned above, facilitates the calculation of $\log \bar{\varkappa}_H$, $\log \varkappa_{H^-}$, and $\log \frac{\varkappa_{H^-}}{\bar{\varkappa}_H}$.

With arguments θ and $\log \frac{\varkappa_{H^-}}{\bar{\varkappa}_H}$ we find $\log \frac{\bar{\varkappa}}{\bar{\varkappa}_H}$ from Table 2. Since $\log \bar{\varkappa}_H$ is known, the required value of $\log \bar{\varkappa}$ follows immediately.

Table 4 contains the calculated values of $\log \bar{\varkappa}$ with arguments θ and $\log p_e$. Except for very small p_e ($p_e < 1$ bar) it was not necessary to extend the table beyond $\theta = 0.9$, since absorption by neutral hydrogen is negligible for $\theta > 0.9$, so that $\log \bar{\varkappa}$ is here practically equal to $\log \varkappa_{H^-}$ [corrected for the averaged effect of induced emission by subtracting 0.02 from the logarithm, cf. equation (10)], which is calculated with the aid of Table 1.

It should be emphasized that the table giving the logarithm of the opacity $\log \bar{\varkappa}$ with arguments θ and $\log p_e$, is valid for all values of the hydrogen-metal ratio A.

4. For the calculation of the structure of a model stellar atmosphere the opacity $\bar{\varkappa}$ must be known as a function of θ and the total pressure p. Since $\bar{\varkappa}$ has been calculated as a function of θ and the electron pressure p_e, the next step will be the construction of tables giving the relation between p_e and p, and thus characterizing the degree of ionization of the particular element mixture of the model atmosphere considered.

The following element mixture is adopted in the present investigation (cf. p. 10)

Element	Relative number of atoms
H	A
Mg	0.30
Si	0.33
Fe	0.30
Ca	0.02
Al	0.03
Na	0.02
	1

The mixture is thus characterized by one variable parameter, namely, the ratio A ($A >> 1$) between the number of atomic

particles (atoms and ions) of hydrogen and the corresponding number for all metals together.

Denoting the degree of ionization of hydrogen by x_H, and that of a metal by $x_i (i = 1, 2, \ldots 6)$, and denoting further the relative metal abundances by $\alpha_i \left(\sum_{i=1}^{6} \alpha_i = 1 \right)$, we get the following expression for the number of free electrons N_e per unit volume:

$$N_e = N_H x_H + \frac{N_H}{A} \sum_{i=1}^{6} \alpha_i x_i . \tag{30}$$

Here N_H is the number of hydrogen atoms and ions per unit volume, so that the number of neutral atoms is $N_H(1 - x_H)$, the number of ions $N_H x_H$, and the number of free electrons contributed by hydrogen $N_H x_H$. The number of atoms and singly ionized ions of any metal (the doubly and multiply ionized metal ions can be neglected, cf. p. 8) is $\frac{N_H}{A} \alpha_i$. Hence the corresponding contribution to the number of free electrons is $\frac{N_H}{A} \alpha_i x_i$.

Introducing the average degree of ionization x_M of the metals defined by

$$x_M = \sum_{i=1}^{6} \alpha_i x_i \tag{31}$$

equation (30) becomes

$$N_e = N_H x_H + \frac{N_H}{A} x_M . \tag{32}$$

Now, since A is here always assumed to be greater than 1000, the total number N of particles per unit volume is practically equal to the number N_H of hydrogen atoms and ions plus the number of free electrons contributed by hydrogen

$$N = N_H (1 + x_H). \tag{33}$$

The ratio of electron pressure p_e to total pressure p is equal to the ratio of N_e to N. We thus have

$$\frac{p_e}{p} = \frac{x_H}{1 + x_H} + \frac{1}{A} \frac{x_M}{1 + x_H} . \tag{34}$$

The second term on the right-hand side of (34) is negligible as compared with the first, except when x_H is very small. Hence, it is permissible to substitute 1 for $1 + x_H$ in the term in question,

$$\frac{p_e}{p} = \frac{x_H}{1 + x_H} + \frac{1}{A} x_M . \tag{35}$$

The degree of ionization x_H of hydrogen is given by equation (8). Table 5 gives $\log \frac{1 + x_H}{x_H}$ with arguments θ and $\log p_e$ computed according to this equation.

The degree of ionization of each metal in the assumed metal mixture was computed according to the standard methods (cf. UNSÖLD (4)). The average degree of ionization x_M of the metals then was found according to equation (31). In Table 6 the quantity x_M is given as a function of θ and $\log p_e$.

By means of Table 5 giving x_H and Table 6 giving x_M the ratio $\frac{p_e}{p}$ can be calculated according to equation (35). This means that p can be found corresponding to given values of θ and p_e. The calculation of p, however, has to be made for each separate value of A, since A enters into equation (35).

Table 7 gives $\log p$ with arguments θ and $\log p_e$. It consists of four separate tables valid for $\log A = 3.0$, 3.4, 3.8, and 4.2. The range of θ covered by the table is $0.60 \leq \theta \leq 1.04$. For $\theta < 0.6$ the contribution of the metals to the electron pressure is negligible as compared with that of hydrogen, so that $\log p$ has practically the same value for all four values of A and for pure hydrogen $x_H (A = \infty)$. The range of θ from 0.30 to 0.60 is therefore covered by a single table.

It is sometimes necessary to find $\log p_e$ when $\log p$ and θ are given. This is possible with the aid of Table 7 by backward interpolation. For the sake of convenience, however, a set of tables—Table 8—has been computed giving $\log p_e$ with arguments θ and $\log p$ for $\log A = 3.0$, 3.4, 3.8, and 4.2. The range of θ from 0.30 to 0.60 is covered by a table valid for all four values of A as well as for pure hydrogen.

Table 4 (cf. p. 42) gives the opacity $\bar{z}$ with arguments θ and $\log p_e$, while Table 7, or Table 8, gives the relation between $\log p$

and log p_e for each θ and A. By combining these tables it is therefore possible to construct tables—Table 9—giving log $\bar{z}$ with arguments θ and log p_e. For $0.60 \leqq \theta \leqq 1.04$ there are four separate tables for log A = 3.0, 3.4, 3.8, and 4.2. For $0.30 \leqq \theta \leqq 0.60$ there is again only one table, valid also for pure hydrogen.

Table 9 completes the series of auxiliary tables.

We have previously considered the case of carbon contributing appreciably to the electron pressure (cf. p. 8). In this case we have instead of equation (32)

$$N_e = N_H x_H + N_C x_C + \frac{N_H}{A} x_M . \tag{36}$$

Putting

$$\frac{N_H}{N_C} = B,$$

we get from equations (33) and (36), neglecting again x_H in comparison with 1 in the last term,

$$\frac{p_e}{p} = \frac{x_H}{1 + x_H} + \frac{1}{B} \frac{x_C}{1 + x_H} + \frac{1}{A} x_M , \tag{37}$$

or

$$\frac{p_e}{p} = \frac{x_H}{1 + x_H} \left(1 + \frac{1}{B} \frac{x_C}{x_H} \right) + \frac{1}{A} x_M . \tag{38}$$

Now $\frac{1}{B} \frac{x_C}{x_H}$ can be put equal to a constant $k = \frac{1}{B} \frac{\overline{x_C}}{x_H}$ equal to the average value of $\frac{1}{B} \frac{x_C}{x_H}$ in the relevant layers of the atmosphere (cf. p. 9). With

$$K = 1 + \frac{1}{B} \frac{\overline{x_C}}{x_H} = 1 + k \tag{39}$$

equation (38) then becomes

$$\frac{p_e}{p} = \frac{x_H}{1 + x_H} K + \frac{1}{A} x_M , \tag{40}$$

or

$$\frac{p_e}{Kp} = \frac{x_H}{1 + x_H} + \frac{1}{KA} x_M . \tag{41}$$

We shall make use of this equation later on (cf. p. 35) in a discussion of the influence of an appreciable carbon admixture upon the structure of model stellar atmospheres.

5. The model stellar atmospheres here considered are assumed to be in mechanical equilibrium. The gravity g is set constant throughout the atmosphere. Radiation pressure can be neglected. For the atmospheres considered its gradient is generally quite small as compared with that of gas pressure. The corresponding reduction of gravity (cf. UNSÖLD (4)) is less than five per cent. except for the $cA\,5$ atmosphere tabulated on p. 85.

Under these circumstances the equation expressing mechanical equilibrium is

$$\frac{dp}{dh} = -g\varrho\,, \tag{42}$$

where p, as before, is the total gas pressure, ϱ is the density of the atmospheric gas, while h is the height of the point considered over some arbitrarily chosen fixed level.

In this section we shall consider only the case of the temperature gradient being everywhere given by the equations valid in radiational equilibrium (cf. p. 6). We then define the optical depth τ through

$$d\tau = -\bar{\varkappa}\varrho\, dh \tag{43}$$

and the additional condition that τ is zero at the top of the atmosphere. Here $\bar{\varkappa}$ is the opacity defined by equation (10) as the ROSSELAND mean of the continuous absorption coefficient.

From equations (42) and (43) one obtains

$$\frac{dp}{d\tau} = \frac{g}{\bar{\varkappa}}\,. \tag{44}$$

This means that by introducing the optical depth instead of the geometrical depth it is possible to eliminate the density from the problem.

In radiational equilibrium the standard equation connecting optical depth and temperature is valid,

$$T^4 = T_e^4\left(\frac{1}{2} + \frac{3}{4}\tau\right), \tag{45}$$

or

$$T^4 = T_0^4\left(1+\frac{3}{2}\tau\right), \tag{46}$$

where

$$T_0 = \sqrt[4]{\frac{1}{2}}\,T_e$$

is the surface temperature, while T_e is the effective temperature.

Equation (45) is only approximately correct, but the approximation was considered sufficient for our purposes.

Introducing again the temperature function

$$\theta = \frac{5040^\circ}{T}, \tag{47}$$

equation (46) becomes

$$\theta = \theta_0\left(1+\frac{3}{2}\tau\right)^{-\frac{1}{4}}, \tag{48}$$

where θ_0 is the value of the temperature function θ on the surface of the atmosphere.

In the previous section we have considered the problem of calculating the opacity $\bar{\varkappa}$ as a function of θ and p. Tables of $\log \bar{\varkappa}$ with arguments θ and $\log p$ are given in the appendix (Table 9). We can, therefore, consider $\bar{\varkappa}$ as a known function of θ and p,

$$\bar{\varkappa} = \bar{\varkappa}(\theta, p). \tag{49}$$

Comparing now equations (44), (48), and (49), we see that for a given model atmosphere—for which θ_0, g and A are specified—p can be found as a function of τ by integrating the differential equation (44). The solution is fixed by the boundary condition that $p = 0$ for $\tau = 0$. In general the solution has to be calculated by means of numerical integration.

In carrying out the numerical integration it is convenient to introduce $\log p$ as the independent variable. From (44) we get

$$\frac{d\tau}{d\log p} = \frac{1}{g\log e}\bar{\varkappa}p, \tag{50}$$

where e is the base of the natural logarithms, while log means the logarithm with base 10, or, with regard to the boundary condition,

$$\tau(\log p) = \frac{1}{g \log e} \int_{-\infty}^{\log p} \bar{\varkappa}(\theta, p)\, p\, d \log p . \qquad (51)$$

The numerical integration for a model stellar atmosphere with given values of θ_0, g, and A, is now carried out as follows. It is started at a point, where the optical depth is so small that θ according to equation (48) is practically equal to θ_0. Then

$$\tau(\log p) = \frac{1}{g \log e} \int_{-\infty}^{\log p} \bar{\varkappa}(\theta_0, p)\, p\, d \log p \quad (\tau << 1), \qquad (52)$$

which means that τ can be found as a function of $\log p$ by a quadrature, use being made of the $\bar{\varkappa}$-table, with $\theta = \theta_0$. The quadrature starts at a suitably chosen value of $\log p$, for which the integrand is practically zero. It is carried further up to a point, where τ is so large that θ begins to deviate from θ_0.

The numerical integration is now continued step by step in the usual way. With an extrapolated value of θ one finds $\bar{\varkappa}$ from the $\bar{\varkappa}$-table and the corresponding value of the integrand in (52) is calculated. From this the integral, and thus τ, is found. Finally θ follows by the insertion of τ in (48). Should this value of θ deviate appreciably from the extrapolated value, the whole process is repeated. The interval of integration was chosen so small, however, that repetition was usually unnecessary.

The integral was determined with the aid of the standard formula

$$\frac{1}{w} \int_{a}^{a+nw} f(x)\, dx = \frac{1}{2} f(a) + f(a+w) + \cdots + f(a+(n-1)w) + \\ + \frac{1}{2} f(a+nw) + \frac{1}{12} f^I(a) - \frac{1}{12} f^I(a+nw) + \cdots \qquad (53)$$

Here $f^I(a)$ denotes the first difference at a, i.e. the average of the first differences $f(a) - f(a-w)$ and $f(a+w) - f(a)$, and $f^I(a+nw)$ the same quantity at $a+nw$. The interval w was chosen so small that the terms involving differences of the third and higher orders were negligible.

For small and moderate values of τ the integration interval of $\log p$ could be taken equal to 0.1. With increasing τ the interval was gradually decreased to 0.002. A glance at the resulting tables given in the appendix shows that this was necessary,

because the increase of p with τ gradually becomes very small. The difficulty could also have been overcome by introducing, from a suitably chosen point, τ as the independent variable instead of $\log p$, i. e. calculating

$$\log p(\tau) = \log p(\tau_0) + g \log e \int_{\tau_0}^{\tau} \frac{1}{\bar{\varkappa} p} d\tau. \tag{54}$$

The frequent changes of intervals required in the adopted method, however, are not very inconvenient.

After the completion of the integration the required values of $\log p$ as a function of τ were found by interpolation. Finally the corresponding values of $\log \bar{\varkappa}$ and $\log p_e$ were found with the aid of the auxiliary tables, Table 8 and Table 9.

The results of the integrations are collected in Tables 10, 11, 12, and 13 of the appendix. The integrations were made with one more figure than given in the tables. The computational errors of the tabular values should not exceed one or two units of the last decimal given.

6. A glance at the tables of model stellar atmospheres given in the appendix suffices to show that in the deeper atmospheric layers the relative increase of temperature is more rapid than that of total pressure. This means that in the layers in question the density decreases with depth in the atmosphere.

Already before the density gradient becomes negative, however, convectional instability sets in. The criterion for convectional instability, due to K. SCHWARZSCHILD, is

$$\left|\frac{dT}{dh}\right|_{\text{adiab.}} < \left|\frac{dT}{dh}\right|_{\text{rad.}} \tag{55}$$

Here $\left|\frac{dT}{dh}\right|_{\text{adiab.}}$ means the numerical value of the adiabatic temperature gradient and $\left|\frac{dT}{dh}\right|_{\text{rad.}}$ the numerical value of the actual temperature gradient in radiational equilibrium. With regard to equation (42) expressing the condition of mechanical equilibrium this can be written in the form

$$\left(\frac{d\log T}{d\log p}\right)_{\text{adiab.}} < \left(\frac{d\log T}{d\log p}\right)_{\text{rad.}} \tag{56}$$

With the aid of equations (44) and (46) one finds the following expression for $\left(\frac{d\log T}{d\log p}\right)_{\text{rad.}}$,

$$\left(\frac{d\log T}{d\log p}\right)_{\text{rad.}} = \frac{3}{8}\frac{1}{g}\frac{p\bar{\varkappa}}{1+\frac{3}{2}\tau}. \tag{57}$$

For the model stellar atmospheres tabulated in the appendix this expression can easily be found as a function of τ.

The adiabatic gradient has been determined by UNSÖLD (4) for a two-component gas. Identifying the two components with hydrogen and an average metal we get an expression sufficiently accurate for our purposes. With our notation the expression is (cf. RUDKJØBING (6))

$$\left(\frac{d\log T}{d\log p}\right)_{\text{adiab.}} = \frac{\left(1+x_H+\frac{1}{A}x_M+\frac{x_H(1-x_H)}{x_H+\frac{1}{A}x_M}\right)+x_H(1-x_H)\left(\frac{5}{2}+\frac{I_H}{kT}\right)}{\frac{5}{2}\left(1+x_H+\frac{1}{A}x_M+\frac{x_H(1-x_H)}{x_H+\frac{1}{A}x_M}\right)+x_H(1-x_H)\left(\frac{5}{2}+\frac{I_H}{kT}\right)^2}. \tag{58}$$

Both for x_H nearly equal to 0 and for x_H nearly equal to 1 this expression tends toward 0.4. For intermediate values of x_H, it is, however, considerably smaller. This, in connection with an increase of the radiative gradient, leads to convective instability in the layers where hydrogen becomes appreciably ionized, as was first shown by UNSÖLD.

For a given value of A expression (58) for $\left(\frac{d\log T}{d\log p}\right)_{\text{adiab.}}$ can be calculated as a function of θ and $\log p$ by using the auxiliary tables of the appendix.

For any model stellar atmosphere that has been calculated on the assumption of radiational equilibrium it is thus possible to compute $\left(\frac{d\log T}{d\log p}\right)_{\text{adiab.}}$ and $\left(\frac{d\log T}{d\log p}\right)_{\text{rad.}}$ and apply the criterion (56). In this way the upper boundary of the zone of convectional instability is determined. If it is assumed that the temperature gradient in the unstable zone is equal to the value given by the

equations of radiative equilibrium (cf. p.6), then the lower boundary of the zone is determined in the same way.

As an example we consider the model atmosphere for $\theta_0 = 0.7$, $\log g = 4.0$, $\log A = 3.8$ in radiational equilibrium (cf. p. 78). The numerical values of the radiative and adiabatic gradients are given below as a function of τ.

τ	$\left(\frac{d \log T}{d \log p}\right)_{\text{rad.}}$	$\left(\frac{d \log T}{d \log p}\right)_{\text{adiab.}}$
0.01	0.006	0.11
0.10	0.05	0.14
0.15	0.09	0.14
0.2	0.11	0.13
0.4	0.28	0.11
0.6	0.46	0.10
0.8	0.68	0.09
1.0	0.93	0.09
2	1.95	0.08
3	2.24	0.08
4	1.91	0.09
5	1.51	0.11
6	1.12	0.14
7	0.89	0.17
8	0.71	0.20
9	0.59	0.23
10	0.49	0.26

The convectively unstable zone is seen to extend from about $\tau = 0.2$ to somewhat below $\tau = 10$. It should be noted that for lower effective temperatures, such as e. g. that of the sun, the unstable zone extends to much greater optical depths (cf. RUDKJØBING (6)).

In the tables of the appendix the upper boundaries of the convectively unstable regions are marked with horizontal lines. With increasing effective temperature T_e and decreasing surface gravity g the upper boundary moves towards higher atmospheric levels. An increase of the hydrogen-metal ratio A has the same effect.

The structure of the convectively unstable zones has also been determined according to the assumption that the temperature gradient is equal to the adiabatic value (cf. p. 6). Since for a given model stellar atmosphere $\left(\frac{d \log T}{d \log p}\right)_{\text{adiab.}}$ can be calculated

according to (58) as a function of T and p, it is comparatively simple to find $\log T$ as a function of $\log p$ by numerical integration (cf. RUDKJØBING (6)). The results of these calculations are given at the foot of each model atmosphere table of the appendix. The much slower increase of T with p, compared with that characterizing the atmospheres in radiational equilibrium, is obvious. As a consequence of this the zone of convectional instability extends to very great depths in this case (cf. BIERMANN (5) and RUDKJØBING (6)).

7. The density ϱ and the height h over a suitably chosen level are not given in the model atmosphere tables in the appendix. If required they can be found from the tabulated data as follows.

The equation of state of the atmospheric gas is

$$p = NkT, \tag{59}$$

where k is the Boltzmann constant. Since practically the whole total pressure is contributed by hydrogen, this becomes

$$p = \frac{k}{m_H}(1 + x_H)\ \varrho\, T, \tag{60}$$

if the degree of ionization of hydrogen is x_H. The logarithm of the gas constant $\frac{k}{m_H}$ is 7.916.

The values of θ, p and p_e are given in the model atmosphere tables of the appendix. The degree of ionization x_H of hydrogen can be found from Table 3 with arguments θ and $\log p_e$. The density ϱ can thus be determined. The following table may facilitate the calculations.

θ	$\log p = 0.0$	1.0	2.0	3.0	4.0	5.0	6.0
0.3	12.14	11.14	10.14	9.14	8.14	7.14	6.14
0.4	12.02	11.02	10.02	9.02	8.02	7.02	6.02
0.5	11.92	10.92	9.92	8.92	7.92	6.92	5.92
0.6	11.84	10.84	9.84	8.84	7.84	6.84	5.84
0.7	11.77	10.77	9.77	8.77	7.77	6.77	5.77
0.8	11.72	10.72	9.72	8.72	7.72	6.72	5.72
0.9	11.66	10.66	9.66	8.66	7.66	6.66	5.66
1.0	11.62	10.62	9.62	8.62	7.62	6.62	5.62

The table gives $-\log \varrho(1 + x_H)$

The geometrical height h can be found as a function of the optical depth τ by means of the tabulated data. From equation (42) we get

$$-\frac{dh}{d\log p} = \frac{1}{g\log e}\frac{p}{\varrho}. \tag{61}$$

Making use of the equation of state (60) we get

$$-\frac{dh}{d\log p} = \frac{k\cdot 5040^\circ}{m_H \log e}\frac{1}{g}\frac{1+x_H}{\theta}, \tag{62}$$

or

$$h_0 - h = \frac{9.57\cdot 10^{11}}{g}\int_{p_0}^{p}\frac{1+x_H}{\theta}\,d\log p \tag{63}$$

Use being made of the tabulated data and Table 3 the integral can easily be evaluated by numerical quadrature.

The following table is given as an example. It is valid for the solar atmosphere ($\theta_0 = 1.041$, $\log g = 4.44$, $\log A = 3.8$) assumed to be in radiational equilibrium.

τ	θ	T	$\log p$	$\log p_e$	$\log \bar{z}$	$1-x_H$	$\log \varrho$	h
0.01	1.037	4860	4.02	0.15	8.74	1.00	2.42 − 10	427 km
0.1	1.005	5010	4.54	0.64	9.17	1.00	2.92	251
0.3	0.949	5310	4.80	0.95	9.38	1.00	3.16	159
0.5	0.905	5570	4.92	1.15	9.50	1.00	3.26	114
1.0	0.828	6090	5.06	1.56	9.77	1.00	3.36	59
2.0	0.736	6850	5.16	2.19	0.23	1.00	3.41	15
3.0	0.681	7400	5.19	2.60	0.56	1.00	3.40	0

It follows from equation (62) that the geometrical height of a stellar atmosphere is roughly proportional to the effective temperature T_e, and roughly inversely proportional to the gravity g.

8. We shall now discuss some of the features shown by the data tabulated in the model atmosphere tables of the appendix.

Since the tables have four arguments, *viz.* θ_0, $\log g$, $\log A$, and τ, an intercomparison cannot be conveniently made. We have therefore made extracts from the tables for two values of τ, namely, for $\tau = 0.3$ as a point representative of conditions influencing absorption lines (cf. (2)), and $\tau = 0.7$ similarly as a representative point with regard to the continuous spectrum. Separate tables are given below for $\log p$, $\log p_e$, and $\log \bar{z}$.

		$\tau = 0.3$, $\log A = 3.4$				$\tau = 0.3$, $\log A = 3.8$				$\tau = 0.3$, $\log A = 4.2$			
θ_0	θ	$\log g = 3.0$	3.5	4.0	4.5	3.0	3.5	4.0	4.5	3.0	3.5	4.0	4.5
1.0	0.911	3.86	4.13	4.39	4.66	4.00	4.27	4.56	4.83	4.10	4.40	4.69	4.98
0.9	0.820		4.05	4.35	4.64		4.11	4.42	4.73		4.13	4.46	4.79
0.8	0.729						3.71	4.07	4.42				
0.7	0.638						3.13	3.54	3.93				

		$\tau = 0.7$, $\log A = 3.4$				$\tau = 0.7$, $\log A = 3.8$				$\tau = 0.7$, $\log A = 4.2$			
θ_0	θ	$\log g = 3.0$	3.5	4.0	4.5	3.0	3.5	4.0	4.5	3.0	3.5	4.0	4.5
1.0	0.836	4.03	4.31	4.59	4.86	4.15	4.44	4.73	5.01	4.22	4.53	4.83	5.13
0.9	0.752		4.18	4.50	4.80		4.23	4.55	4.87		4.25	4.59	4.92
0.8	0.669						3.83	4.19	4.55				
0.7	0.585						3.25	3.66	4.06				

The tables above give $\log p$

		$\tau = 0.3$, $\log A = 3.4$				$\tau = 0.3$. $\log A = 3.8$				$\tau = 0.3$, $\log A = 4.2$			
θ_0	θ	$\log g = 3.0$	3.5	4.0	4.5	3.0	3.5	4.0	4.5	3.0	3.5	4.0	4.5
1.0	0.911	0.55	0.76	0.99	1.22	0.45	0.64	0.86	1.06	0.40	0.59	0.77	0.97
0.9	0.820		1.07	1.26	1.46		1.05	1.22	1.40		1.03	1.20	1.38
0.8	0.729						1.49	1.67	1.85				
0.7	0.638						1.86	2.07	2.27				

		$\tau = 0.7$, $\log A = 3.4$				$\tau = 0.7$, $\log A = 3,8$				$\tau = 0.7$, $\log A = 4.2$			
θ_0	θ	$\log g = 3.0$	3.5	4.0	4.5	3.0	3.5	4.0	4.5	3.0	3.5	4.0	4.5
1.0	0.836	0.97	1.16	1.36	1.55	0.97	1.13	1.30	1.48	0.97	1.13	1.30	1.47
0.9	0.752		1.58	1.76	1.93		1.59	1.75	1.93		1.59	1.76	1.93
0.8	0.669						1.99	2.18	2.37				
0.7	0.585						2.29	2.52	2.73				

The tables above give $\log p_e$.

		$\tau = 0.3$, $\log A = 3.4$				$\tau = 0.3$, $\log A = 3.8$				$\tau = 0.3$, $\log A = 4.2$			
θ_0	θ	$\log g = 3.0$	3.5	4.0	4.5	3.0	3.5	4.0	4.5	3.0	3.5	4.0	4.5
1.0	0.911	8.91	9.13	9.35	9.58	8.82	9.00	9.22	9.42	8.77	8.95	9.14	9.33
0.9	0.820		9.29	9.47	9.66		9.26	9.43	9.60		9.24	9.40	9.58
0.8	0.729						9.65	9.78	9.93				
0.7	0.638						0.23	0.32	0.42				

		$\tau = 0.7$, $\log A = 3.4$				$\tau = 0.7$, $\log A = 3.8$				$\tau = 0.7$, $\log A = 4.2$			
θ_0	θ	$\log g = 3.0$	3.5	4.0	4.5	3.0	3.5	4.0	4.5	3.0	3.5	4.0	4.5
1.0	0.836	9.21	9.38	9.57	9.77	9.19	9.36	9.53	9.71	9.20	9.35	9.52	9.68
0.9	0.752		9.70	9.85	0.01		9.71	9.85	0.00		9.71	9.86	0.00
0.8	0.669						0.14	0.26	0.39				
0.7	0.585						0.76	0.84	0.91				

The tables above give $\log \bar{\varkappa}$.

A glance at these tables shows that the variation of the tabulated quantities with the arguments is quite regular. In fact, linear interpolation will everywhere give sufficient accuracy.

The variation of p, p_e, and $\bar{z}$ with θ, g, and A is seen to be quite similar for the two optical depths.

With increasing effective temperature, i. e. decreasing θ_0, p decreases, while p_e and $\bar{z}$ increase. From $\theta_0 = 1.0$ to $\theta_0 = 0.7$ these quantities change by factors between 10 and 30.

A qualitative interpretation of the variation of p, p_e, and $\bar{z}$ with g and A can be derived as follows. At low temperatures the free electrons are contributed mainly by the metals. As the temperature rises, they are contributed mainly by hydrogen, which to begin with is little ionized, and finally strongly ionized. Further, the opacity is at low temperatures mainly due to H^-, and at high temperatures mainly to H. We consider, therefore, the simplified cases specified in the following table.

Electron pressure	Opacity	$\bar{z}$	p_e	p	p_e	$\bar{z}$
Metals ($x_M \gtrsim 1$) ..	H^-	$A^{-1}p$	$A^{-1}p$	$A^{\frac{1}{2}} g^{\frac{1}{2}}$	$A^{-\frac{1}{2}} g^{\frac{1}{2}}$	$A^{-\frac{1}{2}} g^{\frac{1}{2}}$
$H(x_H << 1)$	H^-	$p^{\frac{1}{2}}$	$p^{\frac{1}{2}}$	$g^{\frac{2}{3}}$	$g^{\frac{1}{3}}$	$g^{\frac{1}{3}}$
$H(x_H << 1)$	H	p^0	$p^{\frac{1}{2}}$	g	$g^{\frac{1}{2}}$	g^0
$H(1-x_H << 1)$ ...	H	p	p	$g^{\frac{1}{2}}$	$g^{\frac{1}{2}}$	$g^{\frac{1}{2}}$

In the four cases considered the dependence of $\bar{z}$ and p_e upon A and p is easily seen to be as stated in the third and fourth column.

Assuming now

$$\bar{z} = C f(\tau)\, p^n, \tag{64}$$

where $f(\tau)$ is some function of τ (and therefore of T), and n a positive constant, we get from the equation (44) expressing mechanical equilibrium,

$$\frac{dp}{d\tau} = \frac{g}{C} \frac{1}{f(\tau)}\, p^{-n}, \tag{65}$$

or

$$\frac{p^{1+n}}{1+n} = \frac{g}{C} \int_0^{\tau} \frac{d\tau}{f(\tau)}. \tag{66}$$

This shows that

$$p \sim \left(\frac{g}{C}\right)^{\frac{1}{1+n}}. \tag{67}$$

From this the dependences of p, p_e, and $\bar{\varkappa}$ upon A and g given in the three last columns of the schedule are easily derived.

As an example we shall consider the dependence of p_e upon g. This is seen to lie always between $g^{\frac{1}{3}}$ and $g^{\frac{1}{2}}$. In fact the tables on p. 32 show that this is the case, and that the dependence is never far from $g^{0.4}$.

The first of the four simplified cases has been considered in greater detail in the author's previous paper (2). The equations resulting from the discussion of this case are good approximations in the case of the solar atmosphere.

9. We have seen (cf. p. 9) that it might become desirable to calculate the effect of a higher content of helium, oxygen, and nitrogen than that assumed in the model stellar atmospheres considered in the present investigation.

We consider the case that these elements contribute to the weight, but not appreciably to the opacity or the electron pressure. We denote the relative weight of hydrogen by X, so that 1 gram of matter contains very nearly $(1-X)$ gram helium, oxygen, and nitrogen, X gram hydrogen, and a negligible weight of the rest of the elements. This means that the opacity $\bar{\varkappa}$, which is due to hydrogen (neutral hydrogen atoms and negative hydrogen ions) alone, is reduced in the ratio $X:1$ as compared with the case of the model stellar atmospheres previously considered.

Now in the calculation of the atmospheric structure (p, p_e, and $\bar{\varkappa}$ as functions of τ), $\bar{\varkappa}$ enters only in the differential equation expressing mechanical equilibrium,

$$\frac{d\tau}{dp} = \frac{\bar{\varkappa}}{g}. \tag{68}$$

It is therefore immediately seen that a reduction of $\bar{\varkappa}$ by the factor X is equivalent to a multiplication of the gravity g by the factor $\frac{1}{X}$. We thus derive the rule stated on p. 9 that a hydrogen content $X\,(X<1)$ is allowed for by entering the tables given in the appendix with argument $\frac{g}{X}$ instead of g. Correct values of $\log p$, and $\log p_e$ are thus obtained. The value of $\bar{\varkappa}$ obtained from the tables must, of course, be multiplied by X.

It might also become desirable (cf. p. 9) to correct approximately for the influence of an appreciable admixture of carbon. We assume that the contributions of carbon to the weight and to the opacity are negligible, while the contribution to the electron pressure is appreciable. This means (cf. p. 23) that instead of the equation

$$\frac{p_e}{p} = \frac{x_H}{1+x_H} + \frac{x_M}{A} \tag{69}$$

assumed in the calculation of the model stellar atmospheres, we now have [cf. equation (41)]

$$\frac{p_e}{Kp} = \frac{x_H}{1+x_H} + \frac{x_M}{KA} \quad (K = 1+k). \tag{70}$$

Consequently, if the ionization tables (Table 7) used in the calculation of the model stellar atmospheres are entered with argument KA instead of A, a quantity p' is obtained, which is equal to the true corrected pressure multiplied by K, i. e.

$$p' = p'(\theta, p_e; KA) \quad \text{(Table 7)} \tag{71}$$

with

$$p' = Kp. \tag{72}$$

Now equation (44) expressing mechanical equilibrium can be written

$$d\tau = \bar{\varkappa}\frac{1}{Kg}\,dp'. \tag{73}$$

If therefore the structure of a model stellar atmosphere be calculated with the use of the standard Table 7 and with Kg instead of g, this will give the true values of τ for a model stellar atmosphere with a carbon admixture characterized by K, and gravity g.

We thus derive the rule stated on p. 9 that the influence of the carbon admixture is allowed for by entering the model atmosphere tables of the appendix with arguments KA and Kg instead of A and g, and finally dividing the values in the p-column by K.

References.

(1) Earlier work on model stellar atmospheres: E. A. MILNE, Phil. Trans. Roy. Soc. A **228**, 421, 1929, Bakerian Lecture; W. H. MC CREA, M. N. **91**, 836, 1931; S. CHANDRASEKHAR and E. A. MILNE, M. N. **92**, 150, 1932; S. CHANDRASEKHAR, M. N. **92**, 186, 1932; H. N. RUSSELL, Ap. J. **78**, 239, 1933; A. UNSÖLD, Z. f. Ap. **8**, 225, 1934; A. PANNEKOEK, Publ. Astr. Inst. Univ. Amsterdam Nr. 4, 1935.

(2) B. STRÖMGREN, Festschrift für ELIS STRÖMGREN, København 1940 (Publ. Kbhvn. Obs. Nr. 127).

(3) R. WILDT, Ap. J. **89**, 295, 1939; **90**, 611, 1939.

(4) A. UNSÖLD, Physik der Sternatmosphären, Berlin 1938.

(5) A. UNSÖLD, Z. f. Ap. **1**, 138, 1931; **2**, 209, 1931; loc. cit. 4; H. SIEDENTOPF, A. N. **247**, 297, 1933; **249**, 53, 1933; **255**, 157, 1935; L. BIERMANN, A. N. **264**, 361, 395, 1938; A. S. EDDINGTON, M. N. **101**, 177, 1941; **102**, 154, 1942; A. UNSÖLD, Z. f. Ap. **21**, 307, 1942; L. BIERMANN, Z. f. Ap. **21**, 320, 1942; M. SCHWARZSCHILD, M. N. **102**, 152, 1942; J. WASIUTYNSKI, unpublished; R. v. d. R. WOOLLEY, M. N. **103**, 191, 1943.

(6) M. RUDKJØBING, Z. f. Ap. **21**, 254, 1942 (Publ. Kbhvn. Obs. Nr. 133).

(7) H. N. RUSSELL, Ap. J. **78**, 239, 1933.

(8) D. H. MENZEL, Pop. Astr. **47**, 6, 66, 124, 1939.

(9) P. TEN BRUGGENCATE, V. J. S. **76**, 172, 1941.

(10) A. UNSÖLD, Z. f. Ap. **21**, 22, 1941.

(11) V. M. GOLDSCHMIDT, Norske Videnskaps-Akademi Oslo, Mat.-Naturv. Klasse, 1937, No. 4.

(12) H. S. W. MASSEY and D. R. BATES, Ap. J. **91**, 202, 1940.

(13) H. RAUDENBUSCH, A. N. **270**, 39, 1940.

(14) M. RUDKJØBING, D. Kgl. Danske Vidensk. Selskab, Mat.-fys. Medd. XX, Nr. 16, 1943 (Publ. Kbhvn. Obs. Nr. 136).

(15) E. HYLLERAAS, Z. f. Phys. **60**, 624, 1930.

Indleveret til Selskabet den 19. November 1943.
Færdig fra Trykkeriet den 15. September 1944.

APPENDIX

Table 1.

θ	$\log \bar{\varkappa}_H$	$\log \varkappa_{H^-}$	$\log \frac{\varkappa_{H^-}}{\bar{\varkappa}_H}$
0.30....	$3.52 + \log (1-x)$	$6.74-10 + \log p_e + \log (1-x)$	$3.22-10 + \log p_e$
32....	3.36	6.82	3.46
34....	3.20	6.90	3.70
36....	3.04	6.98	3.94
38....	2.86	7.05	4.19
0.40....	2.68	7.12	4.44
42....	2.49	7.18	4.69
44....	2.30	7.25	4.95
46....	2.11	7.31	5.20
48....	1.90	7.37	5.47
0.50....	1.69	7.43	5.74
52....	1.46	7.49	6.03
54....	1.23	7.54	6.31
56....	1.00	7.60	6.60
58....	0.76	7.65	6.89
0.60....	0.52	7.70	7.18
62....	0.27	7.75	7.48
64....	0.03	7.80	7.77
66....	9.78—10	7.85	8.07
68....	9.54	7.89	8.35
0.70....	9.29	7.94	8.65
72....	9.04	7.98	8.94
74....	8.79	8.03	9.24
76....	8.55	8.07	9.52
78....	8.30	8.11	9.81 — 10
0.80....	8.05	8.15	0.10
82....	7.80	8.19	0.39
84....	7.55	8.23	0.68
86....	7.30	8.27	0.97
88....	7.05	8.31	1.26
0.90....	6.81 — 10	8.35 — 10	1.54

θ	$\log \varkappa_{H^-}$
0.90....	$8.35-10 + \log p_e + \log (1-x)$
92....	8.39
94....	8.42
96....	8.46
98....	8.49
1.00....	8.53
02....	8.57
04....	8.60
06....	8.64
08....	8.67
1.10....	8.71

Table 2.

$\log \frac{\varkappa_H}{\bar{\varkappa}_H}$	θ = 0.3	0.4	0.5	0.6	0.7	0.8	0.9
8.0—10	0.01	0.01	0.01	0.01	0.01	0.01	0.01
8.1.....	0.01	0.01	0.01	0.01	0.01	0.01	0.01
8.2.....	0.01	0.01	0.01	0.01	0.01	0.01	0.01
8.3.....	0.02	0.02	0.02	0.02	0.02	0.02	0.02
8.4.....	0.02	0.02	0.02	0.02	0.02	0.02	0.02
8.5.....	0.02	0.02	0.02	0.02	0.02	0.02	0.02
8.6.....	0.03	0.03	0.03	0.03	0.03	0.03	0.03
8.7.....	0.04	0.03	0.03	0.03	0.03	0.03	0.03
8.8.....	0.05	0.04	0.04	0.04	0.04	0.04	0.04
8.9.....	0.06	0.05	0.05	0.05	0.05	0.05	0.05
9.0.....	0.08	0.07	0.07	0.07	0.07	0.07	0.07
9.1.....	0.10	0.09	0.08	0.08	0.08	0.08	0.08
9.2.....	0.12	0.11	0.10	0.10	0.10	0.10	0.10
9.3.....	0.14	0.13	0.12	0.12	0.12	0.12	0.12
9.4.....	0.17	0.15	0.15	0.15	0.15	0.15	0.15
9.5.....	0.20	0.18	0.17	0.17	0.17	0.17	0.17
9.6.....	0.23	0.21	0.20	0.20	0.20	0.20	0.20
9.7.....	0.27	0.24	0.24	0.24	0.24	0.24	0.24
9.8.....	0.31	0.28	0.28	0.28	0.28	0.28	0.28
9.9—10	0.35	0.32	0.32	0.32	0.33	0.33	0.32
0.0.....	0.40	0.37	0.37	0.37	0.38	0.38	0.37
0.1.....	0.45	0.42	0.42	0.42	0.43	0.43	0.43
0.2.....	0.51	0.48	0.48	0.48	0.49	0.49	0.49
0.3.....	0.57	0.54	0.54	0.54	0.55	0.56	0.55
0.4.....	0.63	0.60	0.60	0.60	0.61	0.62	0.61
0.5.....	0.70	0.67	0.67	0.67	0.68	0.69	0.68
0.6.....	0.78	0.75	0.75	0.75	0.76	0.77	0.76
0.7.....	0.85	0.82	0.82	0.82	0.83	0.84	0.83
0.8.....	0.93	0.90	0.90	0.90	0.91	0.92	0.91
0.9.....	1.00	0.98	0.98	0.98	0.99	1.00	0.99
1.0.....	1.09	1.07	1.07	1.07	1.07	1.08	1.07
1.1.....	1.17	1.15	1.15	1.15	1.15	1.16	1.15
1.2.....	1.26	1.24	1.24	1.24	1.24	1.25	1.24
1.3.....	1.34	1.33	1.33	1.33	1.33	1.34	1.33
1.4.....	1.43	1.43	1.43	1.43	1.43	1.43	1.43
1.5.....	1.52	1.52	1.52	1.52	1.52	1.52	1.52
1.6.....	1.62	1.62	1.62	1.62	1.62	1.62	1.62
1.7.....	1.71	1.71	1.71	1.71	1.71	1.71	1.71
1.8.....	1.81	1.81	1.81	1.81	1.81	1.81	1.81
1.9.....	1.90	1.90	1.90	1.90	1.90	1.90	1.90
2.0.....	1.99	1.99	1.99	1.99	1.99	1.99	1.99

The table gives $\log \frac{\bar{\varkappa}}{\varkappa_H}$

Table 3. Ionization

θ	$\log p_e$	0.0	0.2	0.4	0.6	0.8	1.0	1.2	1.4	1.6	1.8	2.0	2.2	2.4
0.30		6.02	5.82	5.62	5.42	5.22	5.02	4.82	4.62	4.42	4.22	4.02	3.82	3.62
	32	5.68	5.48	5.28	5.08	4.88	4.68	4.48	4.28	4.08	3.88	3.68	3.48	3.28
	34	5.35	5.15	4.95	4.75	4.55	4.35	4.15	3.95	3.75	3.55	3.35	3.15	2.95
	36	5.01	4.81	4.61	4.41	4.21	4.01	3.81	3.61	3.41	3.21	3.01	2.81	2.61
	38	4.68	4.48	4.28	4.08	3.88	3.68	3.48	3.28	3.08	2.88	2.68	2.48	2.28
0.40		4.35	4.15	3.95	3.75	3.55	3.35	3.15	2.95	2.75	2.55	2.35	2.15	1.95
	42	4.03	3.83	3.63	3.43	3.23	3.03	2.83	2.63	2.43	2.23	2.03	1.84	1.64
	44	3.71	3.51	3.31	3.11	2.91	2.71	2.51	2.31	2.11	1.92	1.72	1.52	1.33
	46	3.39	3.19	2.99	2.79	2.59	2.39	2.19	1.99	1.80	1.60	1.41	1.22	1.03
	48	3.07	2.87	2.67	2.47	2.27	2.07	1.88	1.68	1.48	1.29	1.11	0.92	0.75
0.50		2.76	2.56	2.36	2.16	1.96	1.77	1.57	1.38	1.19	1.01	0.83	0.67	0.52
	52	2.45	2.25	2.05	1.86	1.66	1.47	1.27	1.09	0.91	0.74	0.58	0.44	0.33
	54	2.14	1.94	1.75	1.55	1.36	1.17	0.99	0.81	0.65	0.50	0.38	0.27	0.19
	56	1.84	1.64	1.45	1.25	1.07	0.89	0.72	0.57	0.43	0.32	0.22	0.15	0.10
	58	1.53	1.34	1.15	0.97	0.80	0.63	0.49	0.37	0.26	0.18	0.12	0.08	0.05
0.60		1.24	1.05	0.87	0.71	0.55	0.42	0.31	0.22	0.15	0.10	0.07	0.04	0.03
	62	0.96	0.79	0.63	0.48	0.36	0.26	0.18	0.12	0.08	0.05	0.03	0.02	0.01
	64	0.70	0.55	0.41	0.30	0.21	0.15	0.10	0.06	0.04	0.03	0.02	0.01	0.01
	66	0.48	0.35	0.25	0.18	0.12	0.08	0.05	0.03	0.02	0.01	0.01	0.01	0.00
	68	0.30	0.21	0.15	0.10	0.06	0.04	0.03	0.02	0.01	0.01	0.00	0.00	0.00
0.70		0.17	0.12	0.08	0.05	0.03	0.02	0.01	0.01	0.01	0.00	0.00	0.00	0.00
	72	0.10	0.06	0.04	0.03	0.02	0.01	0.01	0.00	0.00	0.00	0.00	0.00	0.00
	74	0.05	0.03	0.02	0.01	0.01	0.01	0.00	0.00	0.00	0.00	0.00	0.00	0.00
	76	0.03	0.02	0.01	0.01	0.00	0.00	0.00	0.00	0.00	0.00	0.00	0.00	0.00
	78	0.01	0.01	0.01	0.00	0.00	0.00	0.00	0.00	0.00	0.00	0.00	0.00	0.00
0.80		0.01	0.00	0.00	0.00	0.00	0.00	0.00	0.00	0.00	0.00	0.00	0.00	0.00

The table gives

of *H*. I.

2.6	2.8	3.0	θ	$\log p_e$	3.0	3.2	3.4	3.6	3.8	4.0	4.2	4.4	4.6	4.8	5.0
3.42	3.22	3.02	0.30	.....	3.02	2.82	2.62	2.42	2.22	2.02	1.83	1.63	1.44	1.25	1.06
3.08	2.88	2.68	32	.....	2.68	2.48	2.28	2.08	1.89	1.69	1.49	1.30	1.11	0.93	0.76
2.75	2.55	2.35	34	.....	2.35	2.15	1.95	1.76	1.56	1.37	1.18	1.00	0.82	0.66	0.51
2.41	2.21	2.01	36	.....	2.01	1.82	1.62	1.43	1.24	1.06	0.87	0.70	0.55	0.42	0.31
2.08	1.89	1.69	38	.....	1.69	1.49	1.30	1.11	0.93	0.76	0.60	0.46	0.34	0.25	0.17
1.76	1.56	1.37	0.40	.....	1.37	1.18	1.00	0.82	0.66	0.51	0.38	0.28	0.19	0.13	0.09
1.45	1.25	1.07	42	.....	1.07	0.89	0.72	0.57	0.43	0.32	0.23	0.16	0.10	0.07	0.04
1.14	0.96	0.79	44	.....	0.79	0.63	0.48	0.36	0.26	0.18	0.12	0.08			
0.86	0.69	0.54	46	.....	0.54	0.41	0.30	0.21	0.14	0.10	0.06				
0.60	0.46	0.34	48	.....	0.34	0.24	0.17	0.11	0.07	0.05	0.03				
0.39	0.28	0.20	0.50	.....	0.20	0.13	0.09	0.06	0.04	0.02					
0.23	0.16	0.11	52	.....	0.11	0.07	0.05	0.03	0.02	0.01					
0.13	0.09	0.06	54	.....	0.06	0.04	0.02	0.01	0.01	0.01					
0.07	0.04	0.03	56	.....	0.03	0.02	0.01	0.01	0.00	0.00					
0.03	0.02	0.01	58	.....	0.01	0.01	0.01	0.00	0.00	0.00					
0.02	0.01	0.01	0.60	.....	0.01	0.00	0.00	0.00	0.00	0.00					
0.01	0.01	0.00													
0.00	0.00	0.00													
0.00	0.00	0.00													
0.00	0.00	0.00													
0.00	0.00	0.00													
0.00	0.00	0.00													
0.00	0.00	0.00													
0.00	0.00	0.00													
0.00	0.00	0.00													

$-\log(1-x_H)$

Table 4. Opacity $\bar{\varkappa}$. I.

θ	$\log p_e$ 9.0—10	9.2	9.4	9.6	9.8	0.0	0.2	0.4	0.6	0.8	1.0	1.2	1.4	1.6	1.8	2.0
0.30...						7.50	7.70	7.90	8.10	8.30	8.50	8.70	8.90	9.10	9.30	9.50
32...						7.68	7.88	8.08	8.28	8.48	8.68	8.88	9.08	9.28	9.48	9.68
34...						7.85	8.05	8.25	8.45	8.65	8.85	9.05	9.25	9.45	9.65	9.85
36...						8.03	8.23	8.43	8.63	8.83	9.03	9.23	9.43	9.63	9.83	0.03
38...						8.18	8.38	8.58	8.78	8.98	9.18	9.38	9.58	9.78	9.98	0.18
0.40...						8.33	8.53	8.73	8.93	9.13	9.33	9.53	9.73	9.93	0.13	0.33
42...						8.46	8.66	8.86	9.06	9.26	9.46	9.66	9.86	0.06	0.26	0.46
44...						8.59	8.79	8.99	9.19	9.39	9.59	9.79	9.99	0.19	0.38	0.58
46...						8.72	8.92	9.12	9.32	9.52	9.72	9.92	0.12	0.31	0.51	0.70
48...						8.83	9.03	9.23	9.43	9.63	9.83	0.02	0.22	0.42	0.61	0.79
0.50...						8.93	9.13	9.33	9.53	9.73	9.92	0.12	0.31	0.50	0.68	0.86
52...						9.01	9.21	9.41	9.60	9.80	9.99	0.19	0.37	0.55	0.72	0.89
54...						9.09	9.29	9.48	9.68	9.87	0.06	0.24	0.42	0.58	0.74	0.87
56...						9.16	9.36	9.55	9.75	9.93	0.11	0.28	0.43	0.58	0.70	0.81
58...						9.22	9.41	9.60	9.78	9.95	0.12	0.27	0.40	0.51	0.60	0.68
0.60...						9.28	9.47	9.65	9.81	9.97	0.11	0.23	0.33	0.41	0.48	0.55
62...						9.31	9.48	9.64	9.80	9.93	0.03	0.12	0.20	0.27	0.33	0.40
64...						9.33	9.48	9.63	9.75	9.85	9.92	9.99	0.06	0.13	0.19	0.27
66...						9.31	9.45	9.55	9.63	9.71	9.78	9.84	9.91	9.98	0.08	0.18
68...						9.26	9.35	9.42	9.50	9.57	9.63	9.69	9.78	9.88	9.98	0.11
0.70...						9.15	9.21	9.28	9.35	9.42	9.49	9.58	9.68	9.79	9.93	0.08
72...						9.00	9.07	9.13	9.19	9.27	9.37	9.48	9.61	9.74	9.89	0.05
74...						8.85	8.92	8.98	9.08	9.18	9.29	9.42	9.57	9.72	9.88	0.06
76...						8.69	8.77	8.88	8.98	9.12	9.25	9.40	9.56	9.72	9.90	0.08
78...						8.57	8.67	8.78	8.92	9.07	9.22	9.38	9.55	9.73	9.92	0.12
0.80...						8.46	8.60	8.73	8.88	9.04	9.20	9.38	9.56	9.76	9.95	0.14
82...						8.41	8.55	8.70	8.86	9.03	9.21	9.40	9.60	9.79	9.98	0.18
84...						8.37	8.53	8.69	8.86	9.04	9.24	9.43	9.62	9.82	0.02	0.22
86...						8.34	8.50	8.69	8.88	9.08	9.27	9.46	9.66	9.86	0.06	0.26
88...						8.33	8.53	8.72	8.91	9.10	9.30	9.50	9.70	9.90	0.10	0.30
90...	7.51	7.66	7.82	7.99	8.17	8.36	8.56	8.75	8.94	9.14	9.34	9.54	9.74	9.94	0.14	0.34

The table gives $\log \bar{\varkappa}$

Table 4 (continued). Opacity $\bar{\varkappa}$. I.

θ	$\log p_e$ 2.0	2.2	2.4	2.6	2.8	3.0	3.2	3.4	3.6	3.8	4.0	4.2	4.4	4.6	4.8	5.0
0.30...	9.50	9.70	9.90	0.10	0.30	0.50	0.70	0.90	1.10	1.30	1.50	1.69	1.89	2.08	2.28	2.47
32...	9.68	9.88	0.08	0.28	0.48	0.68	0.88	1.08	1.28	1.47	1.67	1.87	2.06	2.26	2.44	2.62
34...	9.85	0.05	0.25	0.45	0.65	0.85	1.05	1.25	1.44	1.64	1.83	2.02	2.21	2.40	2.56	2.72
36...	0.03	0.23	0.43	0.63	0.83	1.03	1.22	1.42	1.61	1.80	1.98	2.18	2.36	2.51	2.66	2.79
38...	0.18	0.38	0.58	0.78	0.97	1.17	1.37	1.56	1.75	1.93	2.11	2.28	2.43	2.56	2.68	2.79
0.40...	0.33	0.53	0.73	0.92	1.12	1.31	1.50	1.68	1.87	2.03	2.19	2.33	2.44	2.57	2.67	2.75
42...	0.46	0.65	0.85	1.04	1.24	1.42	1.60	1.78	1.94	2.08	2.20	2.31	2.42	2.52	2.59	2.68
44...	0.58	0.78	0.97	1.16	1.34	1.51	1.68	1.84	1.96	2.07	2.18	2.26	2.36			
46...	0.70	0.89	1.08	1.25	1.42	1.58	1.72	1.84	1.94	2.04	2.11	2.20				
48...	0.79	0.97	1.15	1.31	1.46	1.58	1.69	1.78	1.87	1.94	2.01	2.09				
0.50...	0.86	1.02	1.18	1.32	1.43	1.52	1.61	1.69	1.76	1.83	1.92					
52...	0.89	1.03	1.15	1.26	1.34	1.42	1.49	1.56	1.64	1.73	1.83					
54...	0.87	0.98	1.07	1.15	1.22	1.29	1.36	1.45	1.54	1.64	1.76					
56...	0.81	0.89	0.97	1.03	1.11	1.17	1.26	1.36	1.46	1.59	1.74					
58...	0.68	0.75	0.82	0.89	0.97	1.06	1.16	1.27	1.41	1.56	1.72					
0.60...	0.55	0.62	0.68	0.77	0.87	0.97	1.10	1.25	1.40	1.56	1.73					
62...	0.40	0.48	0.57	0.66	0.78	0.92	1.07	1.23	1.40	1.57	1.76					
64...	0.27	0.37	0.48	0.61	0.75	0.90	1.06	1.23	1.42	1.61	1.81					
66...	0.18	0.30	0.43	0.58	0.74	0.90	1.07	1.26	1.46	1.65	1.84					
68...	0.11	0.25	0.40	0.56	0.73	0.91	1.10	1.30	1.49	1.68	1.88					
0.70...	0.08	0.23	0.39	0.57	0.76	0.95	1.15	1.33	1.53	1.73	1.93					
72...	0.05	0.22	0.40	0.59	0.79	0.98	1.17	1.37	1.57	1.77	1.97					
74...	0.06	0.25	0.44	0.63	0.82	1.02	1.22	1.42	1.62	1.82	2.02					
76...	0.08	0.28	0.47	0.66	0.86	1.06	1.26	1.46	1.66	1.86	2.06					
78...	0.12	0.31	0.50	0.70	0.90	1.10	1.30	1.50	1.70	1.90	2.10					
0.80...	0.14	0.34	0.54	0.74	0.94	1.14	1.34	1.54	1.74	1.94	2.14					
82...	0.18	0.38	0.58	0.78	0.98	1.18	1.38	1.58	1.78	1.98	2.18					
84...	0.22	0.42	0.62	0.82	1.02	1.22	1.42	1.62	1.82	2.02	2.22					
86...	0.26	0.46	0.66	0.86	1.06	1.26	1.46	1.66	1.86	2.06	2.26					
88...	0.30	0.50	0.70	0.90	1.10	1.30	1.50	1.70	1.90	2.10	2.30					
0.90...	0.34	0.54	0.74	0.94	1.14	1.34	1.54	1.74	1.94	2.14	2.34					

The table gives $\log \bar{\varkappa}$

Table 5. Ionization

θ	log p_e 0.0	0.2	0.4	0.6	0.8	1.0	1.2	1.4	1.6	1.8	2.0	2.2	2.4
0.30.....	0.30	0.30	0.30	0.30	0.30	0.30	0.30	0.30	0.30	0.30	0.30	0.30	0.30
32.....	0.30	0.30	0.30	0.30	0.30	0.30	0.30	0.30	0.30	0.30	0.30	0.30	0.30
34.....	0.30	0.30	0.30	0.30	0.30	0.30	0.30	0.30	0.30	0.30	0.30	0.30	0.30
36.....	0.30	0.30	0.30	0.30	0.30	0.30	0.30	0.30	0.30	0.30	0.30	0.30	0.30
38.....	0.30	0.30	0.30	0.30	0.30	0.30	0.30	0.30	0.30	0.30	0.30	0.30	0.30
0.40.....	0.30	0.30	0.30	0.30	0.30	0.30	0.30	0.30	0.30	0.30	0.30	0.30	0.30
42.....	0.30	0.30	0.30	0.30	0.30	0.30	0.30	0.30	0.30	0.30	0.30	0.31	0.31
44.....	0.30	0.30	0.30	0.30	0.30	0.30	0.30	0.30	0.30	0.31	0.31	0.31	0.31
46.....	0.30	0.30	0.30	0.30	0.30	0.30	0.30	0.30	0.31	0.31	0.31	0.32	0.32
48.....	0.30	0.30	0.30	0.30	0.30	0.30	0.31	0.31	0.31	0.31	0.32	0.33	0.35
0.50.....	0.30	0.30	0.30	0.30	0.30	0.31	0.31	0.31	0.32	0.33	0.34	0.36	0.39
52.....	0.30	0.30	0.30	0.31	0.31	0.31	0.31	0.32	0.33	0.35	0.37	0.41	0.46
54.....	0.30	0.30	0.31	0.31	0.31	0.32	0.33	0.34	0.36	0.39	0.44	0.50	0.58
56.....	0.31	0.31	0.31	0.31	0.32	0.33	0.35	0.38	0.41	0.47	0.54	0.63	0.75
58.....	0.31	0.31	0.32	0.33	0.34	0.36	0.39	0.44	0.50	0.59	0.70	0.83	0.98
0.60.....	0.32	0.32	0.33	0.35	0.38	0.42	0.48	0.55	0.65	0.77	0.92	1.07	1.25
62.....	0.33	0.34	0.37	0.39	0.44	0.51	0.60	0.71	0.84	0.99	1.15	1.33	1.51
64.....	0.35	0.38	0.42	0.48	0.55	0.66	0.78	0.92	1.08	1.25	1.44	1.62	1.82
66.....	0.40	0.44	0.51	0.60	0.71	0.85	1.00	1.16	1.34	1.52	1.72	1.92	2.10
68.....	0.48	0.55	0.66	0.78	0.92	1.08	1.25	1.44	1.62	1.82	2.00	2.20	2.40
0.70.....	0.60	0.72	0.86	1.01	1.17	1.35	1.53	1.73	1.93	2.11	2.31	2.51	2.71
72.....	0.79	0.92	1.09	1.26	1.45	1.63	1.83	2.01	2.21	2.41	2.61	2.81	3.01
74.....	1.01	1.17	1.35	1.53	1.73	1.93	2.11	2.31	2.51	2.71	2.91	3.11	3.31
76.....	1.26	1.45	1.63	1.83	2.01	2.21	2.41	2.61	2.81	3.01	3.21	3.41	3.61
78.....	1.52	1.72	1.92	2.11	2.31	2.51	2.71	2.91	3.11	3.31	3.51	3.71	3.91
0.80.....	1.82	2.00	2.20	2.40	2.60	2.80	3.00	3.20	3.40	3.60	3.80	4.00	4.20
82.....	2.10	2.30	2.50	2.70	2.90	3.10	3.30	3.50	3.70	3.90	4.10	4.30	4.50
84.....	2.40	2.60	2.80	3.00	3.20	3.40	3.60	3.80	4.00	4.20	4.40	4.60	4.80
86.....	2.70	2.90	3.10	3.30	3.50	3.70	3.90	4.10	4.30	4.50	4.70	4.90	5.10
88.....	2.99	3.19	3.39	3.59	3.79	3.99	4.19	4.39	4.59	4.79	4.99	5.19	5.39
0.90.....	3.29	3.49	3.69	3.89	4.09	4.29	4.49	4.69	4.89	5.09	5.29	5.49	5.69
92.....	3.58	3.78	3.98	4.18	4.38	4.58	4.78	4.98	5.18	5.38	5.58	5.78	5.98
94.....	3.88	4.08	4.28	4.48	4.68	4.88	5.08	5.28	5.48	5.68	5.88	6.08	6.28
96.....	4.17	4.37	4.57	4.77	4.97	5.17	5.37	5.57	5.77	5.97	6.17	6.37	6.57
98.....	4.46	4.66	4.86	5.06	5.26	5.46	5.66	5.86	6.06	6.26	6.46	6.66	6.86
1.00.....	4.75	4.95	5.15	5.35	5.55	5.75	5.95	6.15	6.35	6.55	6.75	6.95	7.15
02.....	5.04	5.24	5.44	5.64	5.84	6.04	6.24	6.44	6.64	6.84	7.04	7.24	7.44
04.....	5.33	5.53	5.73	5.93	6.13	6.33	6.53	6.73	6.93	7.13	7.33	7.53	7.73

The table gives

of *H*. II.

2.6	2.8	3.0	θ	log p_e	3.0	3.2	3.4	3.6	3.8	4.0	4.2	4.4	4.6	4.8	5.0
0.30	0.30	0.30	0.30	.....	0.30	0.30	0.30	0.30	0.30	0.30	0.31	0.31	0.31	0.32	0.32
0.30	0.30	0.30	32	.....	0.30	0.30	0.30	0.30	0.31	0.31	0.31	0.31	0.32	0.33	0.34
0.30	0.30	0.30	34	.....	0.30	0.30	0.30	0.31	0.31	0.31	0.32	0.33	0.34	0.36	0.39
0.30	0.30	0.30	36	.....	0.30	0.31	0.31	0.31	0.32	0.33	0.33	0.35	0.38	0.42	0.48
0.30	0.31	0.31	38	.....	0.31	0.31	0.31	0.32	0.33	0.35	0.37	0.40	0.45	0.52	0.61
0.31	0.31	0.31	0.40	.....	0.31	0.32	0.33	0.34	0.36	0.39	0.43	0.50	0.57	0.68	0.81
0.32	0.32	0.32	42	.....	0.32	0.33	0.35	0.38	0.41	0.47	0.55	0.65	0.75	0.90	1.05
0.32	0.33	0.34	44	.....	0.34	0.37	0.40	0.44	0.51	0.60	0.71	0.84			
0.33	0.35	0.38	46	.....	0.38	0.42	0.48	0.56	0.66	0.79	0.93				
0.37	0.41	0.46	48	.....	0.46	0.52	0.62	0.73	0.87	1.02	1.19				
0.43	0.49	0.57	0.50	.....	0.57	0.67	0.80	0.95	1.11	1.28					
0.53	0.63	0.75	52	.....	0.75	0.88	1.04	1.21	1.39	1.57					
0.69	0.82	0.97	54	.....	0.97	1.13	1.30	1.48	1.68	1.88					
0.90	1.05	1.23	56	.....	1.23	1.41	1.59	1.79	1.98	2.17					
1.14	1.32	1.50	58	.....	1.50	1.70	1.90	2.08	2.28	2.48					
1.43	1.61	1.81	0.60	.....	1.81	1.99	2.19	2.39	2.59	2.79					
1.71	1.91	2.10	62	.....	2.10	2.29	2.49	2.69	2.89	3.09					
2.00	2.20	2.40	64	.....	2.40	2.60	2.80	3.00	3.20	3.40					
2.30	2.50	2.70	66	.....	2.70	2.90	3.10	3.30	3.50	3.70					
2.60	2.80	3.00	68	.....	3.00	3.20	3.40	3.60	3.80	4.00					
2.91	3.11	3.31	0.70	.....	3.31	3.51	3.71	3.91	4.11	4.31					
3.21	3.41	3.61	72	.....	3.61	3.81	4.01	4.21	4.41	4.61					
3.51	3.71	3.91	74	.....	3.91	4.11	4.31	4.51	4.71	4.91					
3.81	4.01	4.21	76	.....	4.21	4.41	4.61	4.81	5.01	5.21					
4.11	4.31	4.51	78	.....	4.51	4.71	4.91	5.11	5.31	5.51					
4.40	4.60	4.80	0.80	.....	4.80	5.00	5.20	5.40	5.60	5.80					
4.70	4.90	5.10	82	.....	5.10	5.30	5.50	5.70	5.90	6.10					
5.00	5.20	5.40	84	.....	5.40	5.60	5.80	6.00	6.20	6.40					
5.30	5.50	5.70	86	.....	5.70	5.90	6.10	6.30	6.50	6.70					
5.59	5.79	5.99	88	.....	5.99	6.19	6.39	6.59	6.79	6.99					
5.89	6.09	6.29	0.90	.....	6.29	6.49	6.69	6.89	7.09	7.29					
6.18	6.38	6.58													
6.48	6.68	6.88													
6.77	6.97	7.17													
7.06	7.26	7.46													
7.35	7.55	7.75													
7.64	7.84	8.04													
7.93	8.13	8.33													

$$\log \frac{1 + x_H}{x_H} = \log \frac{p}{p_e} \text{ for pure hydrogen}$$

Table 6. Ionization of metal mixture.

θ \ $\log p_e$	0.0	0.2	0.4	0.6	0.8	1.0	1.2	1.4	1.6	1.8	2.0	2.2	2.4
0.70...	1.00	1.00	1.00	1.00	1.00	1.00	1.00	1.00	1.00	0.99	0.99	0.99	0.98
72...	1.00	1.00	1.00	1.00	1.00	1.00	1.00	1.00	0.99	0.99	0.99	0.98	0.97
74...	1.00	1.00	1.00	1.00	1.00	1.00	1.00	0.99	0.99	0.98	0.98	0.96	0.94
76...	1.00	1.00	1.00	1.00	1.00	1.00	0.99	0.99	0.99	0.97	0.96	0.93	0.90
78...	1.00	1.00	1.00	1.00	1.00	0.99	0.99	0.98	0.98	0.96	0.93	0.89	0.86
0.80...	1.00	1.00	1.00	1.00	0.99	0.98	0.98	0.97	0.96	0.93	0.89	0.85	0.81
82...	1.00	1.00	1.00	1.00	0.98	0.98	0.97	0.96	0.93	0.89	0.85	0.80	0.75
84...	1.00	1.00	0.99	0.99	0.98	0.97	0.96	0.94	0.90	0.85	0.80	0.74	0.68
86...	1.00	0.99	0.99	0.99	0.97	0.96	0.94	0.91	0.86	0.81	0.74	0.67	0.60
88...	0.99	0.99	0.98	0.98	0.96	0.94	0.91	0.87	0.81	0.75	0.67	0.60	0.52
0.90...	0.99	0.98	0.98	0.96	0.95	0.92	0.88	0.83	0.75	0.68	0.60	0.52	0.44
92...	0.98	0.98	0.97	0.94	0.93	0.89	0.84	0.77	0.69	0.60	0.52	0.44	0.37
94...	0.98	0.97	0.95	0.92	0.89	0.84	0.78	0.70	0.62	0.53	0.44	0.37	0.30
96...	0.96	0.95	0.93	0.89	0.85	0.79	0.73	0.63	0.54	0.45	0.37	0.30	0.24
98...	0.95	0.93	0.90	0.85	0.80	0.73	0.65	0.57	0.48	0.38	0.30	0.24	0.19
1.00...	0.93	0.90	0.86	0.80	0.74	0.67	0.58	0.50	0.41	0.32	0.25	0.19	0.15
02...	0.90	0.86	0.81	0.74	0.67	0.60	0.51	0.43	0.35	0.27	0.20	0.14	0.11
04...	0.86	0.81	0.75	0.68	0.60	0.52	0.44	0.37	0.29	0.22	0.16	0.11	0.08
06...	0.82	0.75	0.69	0.61	0.53	0.45	0.37	0.30	0.24	0.18	0.12	0.09	0.06
08...	0.78	0.69	0.62	0.53	0.45	0.38	0.30	0.24	0.19	0.14	0.10	0.07	0.05
1.10...	0.73	0.63	0.54	0.46	0.38	0.31	0.24	0.19	0.14	0.11	0.08	0.06	0.04

θ \ $\log p_e$	9.0—10	9.2	9.4	9.6	9.8	0.0
0.90...	1.00	1.00	1.00	1.00	0.99	0.99
92...	1.00	1.00	1.00	1.00	0.99	0.98
94...	1.00	1.00	1.00	0.99	0.98	0.98
96...	1.00	1.00	0.99	0.99	0.97	0.96
98...	1.00	0.99	0.99	0.97	0.96	0.95
1.00...	0.99	0.99	0.99	0.97	0.95	0.93
02...	0.99	0.99	0.98	0.95	0.92	0.90
04...	0.99	0.97	0.96	0.93	0.90	0.86
06...	0.98	0.96	0.94	0.90	0.86	0.82
08...	0.96	0.95	0.91	0.87	0.82	0.78
1.10...	0.95	0.92	0.88	0.83	0.78	0.73

The table gives x_M

Table 7. Ionization of matter in stellar atmospheres.
$\log A = 3.0, 3.4, 3.8, 4.2$ and pure H.

θ	$\log p_e$ 0.0	0.2	0.4	0.6	0.8	1.0	1.2	1.4	1.6	1.8	2.0	2.2	2.4	2.6	2.8	3.0
0.30...	0.30	0.50	0.70	0.90	1.10	1.30	1.50	1.70	1.90	2.10	2.30	2.50	2.70	2.90	3.10	3.30
32...	0.30	0.50	0.70	0.90	1.10	1.30	1.50	1.70	1.90	2.10	2.30	2.50	2.70	2.90	3.10	3.30
34...	0.30	0.50	0.70	0.90	1.10	1.30	1.50	1.70	1.90	2.10	2.30	2.50	2.70	2.90	3.10	3.30
36...	0.30	0.50	0.70	0.90	1.10	1.30	1.50	1.70	1.90	2.10	2.30	2.50	2.70	2.90	3.10	3.30
38...	0.30	0.50	0.70	0.90	1.10	1.30	1.50	1.70	1.90	2.10	2.30	2.50	2.70	2.90	3.11	3.31
0.40...	0.30	0.50	0.70	0.90	1.10	1.30	1.50	1.70	1.90	2.10	2.30	2.50	2.70	2.91	3.11	3.31
42...	0.30	0.50	0.70	0.90	1.10	1.30	1.50	1.70	1.90	2.10	2.30	2.51	2.71	2.92	3.12	3.32
44...	0.30	0.50	0.70	0.90	1.10	1.30	1.50	1.70	1.90	2.11	2.31	2.51	2.71	2.92	3.13	3.34
46...	0.30	0.50	0.70	0.90	1.10	1.30	1.50	1.70	1.91	2.11	2.31	2.52	2.72	2.93	3.15	3.38
48...	0.30	0.50	0.70	0.90	1.10	1.30	1.51	1.71	1.91	2.11	2.32	2.53	2.75	2.97	3.21	3.46
0.50...	0.30	0.50	0.70	0.90	1.10	1.31	1.51	1.71	1.92	2.13	2.34	2.56	2.79	3.03	3.29	3.57
52...	0.30	0.50	0.70	0.91	1.11	1.31	1.51	1.72	1.93	2.15	2.37	2.61	2.86	3.13	3.43	3.75
54...	0.30	0.50	0.71	0.91	1.11	1.32	1.53	1.74	1.96	2.19	2.44	2.70	2.98	3.29	3.62	3.97
56...	0.31	0.51	0.71	0.91	1.12	1.33	1.55	1.78	2.01	2.27	2.54	2.83	3.15	3.50	3.85	4.23
58...	0.31	0.51	0.72	0.93	1.14	1.36	1.59	1.84	2.10	2.39	2.70	3.03	3.38	3.74	4.12	4.50
0.60...	0.32	0.52	0.73	0.95	1.18	1.42	1.68	1.95	2.25	2.57	2.92	3.27	3.65	4.03	4.41	4.81

The table gives $\log p$

θ	$\log p_e$ 3.0	3.2	3.4	3.6	3.8	4.0	4.2	4.4	4.6	4.8	5.0
0.30...	3.30	3.50	3.70	3.90	4.10	4.30	4.51	4.71	4.91	5.12	5.32
32...	3.30	3.50	3.70	3.90	4.11	4.31	4.51	4.71	4.92	5.13	5.34
34...	3.30	3.50	3.70	3.91	4.11	4.31	4.52	4.73	4.94	5.16	5.39
36...	3.30	3.51	3.71	3.91	4.12	4.33	4.53	4.75	4.98	5.22	5.48
38...	3.31	3.51	3.71	3.92	4.13	4.35	4.57	4.80	5.05	5.32	5.61
0.40...	3.31	3.52	3.73	3.94	4.16	4.39	4.63	4.90	5.17	5.48	5.81
42...	3.32	3.53	3.75	3.98	4.21	4.47	4.75	5.06	5.35	5.70	6.05
44...	3.34	3.57	3.80	4.04	4.31	4.60	4.91	5.24			
46...	3.38	3.62	3.88	4.16	4.46	4.79	5.13				
48...	3.46	3.72	4.02	4.33	4.67	5.02	5.39				
0.50...	3.57	3.87	4.20	4.55	4.91	5.28					
52...	3.75	4.08	4.44	4.81	5.19	5.57					
54...	3.97	4.33	4.70	5.08	5.48	5.88					
56...	4.23	4.61	4.99	5.39	5.78	6.17					
58...	4.50	4.90	5.30	5.68	6.08	6.48					
0.60...	4.81	5.19	5.59	5.99	6.39	6.79					

The table gives $\log p$

Table 7 (continued).

Ionization of matter in stellar atmospheres. $\log A = 3.0$.

θ	$\log p_e$ 0.0	0.2	0.4	0.6	0.8	1.0	1.2	1.4	1.6	1.8	2.0	2.2	2.4	2.6	2.8	3.0
0.60...	0.32	0.52	0.73	0.95	1.18	1.42	1.68	1.95	2.25	2.57	2.92	3.26	3.64	4.02	4.39	4.78
62...	0.33	0.54	0.77	0.99	1.24	1.51	1.80	2.11	2.44	2.79	3.14	3.52	3.90	4.29	4.68	5.05
64...	0.35	0.58	0.82	1.08	1.35	1.66	1.98	2.32	2.67	3.04	3.43	3.80	4.19	4.56	4.94	5.30
66...	0.40	0.64	0.91	1.20	1.51	1.85	2.20	2.55	2.93	3.31	3.70	4.09	4.45	4.82	5.18	5.52
68...	0.48	0.75	1.06	1.38	1.72	2.08	2.44	2.83	3.20	3.59	3.96	4.34	4.70	5.06	5.39	5.70
0.70...	0.60	0.92	1.26	1.61	1.96	2.34	2.72	3.11	3.50	3.86	4.23	4.59	4.92	5.26	5.55	5.83
72...	0.79	1.12	1.49	1.86	2.24	2.61	3.00	3.37	3.74	4.11	4.46	4.80	5.11			
74...	1.01	1.37	1.75	2.13	2.51	2.90	3.26	3.63	3.99	4.33	4.66	4.96	5.28			
76...	1.25	1.64	2.01	2.40	2.77	3.14	3.51	3.86	4.20	4.51	4.80	5.08				
78...	1.51	1.90	2.29	2.66	3.03	3.39	3.73	4.06	4.35	4.64	4.91	5.17				
0.80...	1.79	2.16	2.54	2.90	3.26	3.59	3.90	4.20	4.47	4.73	4.98	5.22				
82...	2.05	2.42	2.78	3.12	3.45	3.75	4.03	4.29	4.55	4.79	5.03	5.27				
84...	2.30	2.65	2.99	3.30	3.59	3.86	4.12	4.36	4.60	4.84	5.08	5.32				
86...	2.52	2.85	3.15	3.43	3.69	3.94	4.17	4.40	4.64	4.87	5.12	5.37				
88...	2.67	2.99	3.26	3.51	3.76	3.98	4.21	4.44	4.68	4.92	5.17	5.42				
0.90...	2.82	3.09	3.33	3.56	3.79	4.01	4.24	4.47	4.72	4.96	5.22	5.48				
92...	2.91	3.14	3.37	3.60	3.81	4.04	4.27	4.51	4.76	5.02	5.28					
94...	2.95	3.18	3.40	3.62	3.84	4.07	4.30	4.55	4.81	5.07	5.36					
96...	2.99	3.20	3.42	3.64	3.86	4.10	4.33	4.60	4.87	5.15	5.43					
98...	3.01	3.22	3.44	3.67	3.89	4.13	4.38	4.64	4.92	5.22	5.52					
1.00...	3.02	3.24	3.46	3.69	3.93	4.17	4.44	4.70	4.99	5.29	5.60					
02...	3.04	3.26	3.49	3.73	3.97	4.22	4.49	4.77	5.06	5.37	5.70					
04...	3.06	3.29	3.52	3.77	4.02	4.28	4.56	4.83	5.14	5.46	5.80					

The table gives $\log p$

Table 7 (continued).

Ionization of matter in stellar atmospheres. $\log A = 3.4$.

θ	$\log p_e$ 0.0	0.2	0.4	0.6	0.8	1.0	1.2	1.4	1.6	1.8	2.0	2.2	2.4	2.6	2.8	3.0
0.60...	0.32	0.52	0.73	0.95	1.18	1.42	1.68	1.95	2.25	2.57	2.92	3.27	3.65	4.02	4.40	4.80
62...	0.33	0.54	0.77	0.99	1.24	1.51	1.80	2.11	2.44	2.79	3.15	3.53	3.90	4.30	4.70	5.08
64...	0.35	0.58	0.82	1.08	1.35	1.66	1.98	2.32	2.68	3.05	3.44	3.81	4.20	4.58	4.97	5.36
66...	0.40	0.64	0.91	1.20	1.51	1.85	2.20	2.56	2.94	3.31	3.71	4.11	4.48	4.87	5.25	5.62
68...	0.48	0.75	1.06	1.38	1.72	2.08	2.45	2.84	3.21	3.61	3.98	4.37	4.76	5.14	5.50	5.85
0.70...	0.60	0.92	1.26	1.61	1.97	2.35	2.72	3.12	3.52	3.89	4.28	4.66	5.03	5.39	5.73	6.05
72...	0.79	1.12	1.49	1.86	2.24	2.62	3.02	3.39	3.78	4.17	4.55	4.91	5.27			
74...	1.01	1.37	1.75	2.13	2.52	2.92	3.29	3.68	4.06	4.43	4.79	5.14	5.47			
76...	1.26	1.64	2.02	2.42	2.79	3.18	3.57	3.95	4.31	4.67	5.00	5.32				
78...	1.51	1.91	2.31	2.69	3.08	3.46	3.83	4.19	4.53	4.86	5.17	5.46				
0.80...	1.81	2.18	2.57	2.96	3.34	3.71	4.06	4.39	4.71	5.01	5.29	5.56				
82...	2.08	2.47	2.85	3.22	3.58	3.93	4.25	4.56	4.84	5.12	5.38	5.63				
84...	2.36	2.74	3.10	3.45	3.78	4.11	4.40	4.67	4.94	5.20	5.45	5.69				
86...	2.62	2.98	3.32	3.65	3.95	4.24	4.50	4.76	5.01	5.25	5.50	5.75				
88...	2.85	3.18	3.50	3.79	4.06	4.32	4.57	4.81	5.06	5.30	5.56	5.81				
0.90...	3.04	3.35	3.63	3.89	4.14	4.38	4.62	4.86	5.11	5.35	5.61	5.88				
92...	3.19	3.45	3.71	3.96	4.19	4.42	4.65	4.90	5.15	5.41	5.68					
94...	3.28	3.53	3.77	4.00	4.23	4.46	4.70	4.95	5.20	5.47	5.75					
96...	3.35	3.58	3.80	4.03	4.26	4.49	4.73	5.00	5.26	5.54	5.83					
98...	3.38	3.61	3.83	4.06	4.29	4.53	4.78	5.04	5.32	5.62	5.92					
1.00...	3.41	3.63	3.86	4.09	4.33	4.57	4.83	5.10	5.39	5.70	6.00					
02...	3.44	3.66	3.89	4.13	4.37	4.62	4.89	5.17	5.46	5.77	6.10					
04...	3.46	3.69	3.92	4.17	4.42	4.68	4.96	5.23	5.54	5.86	6.19					

The table gives $\log p$

Table 7 (continued).

Ionization of matter in stellar atmospheres. $\log A = 3.8$.

θ	$\log p_e$ 0.0	0.2	0.4	0.6	0.8	1.0	1.2	1.4	1.6	1.8	2.0	2.2	2.4	2.6	2.8	3.0
0.60...	0.32	0.52	0.73	0.95	1.18	1.42	1.68	1.95	2.25	2.57	2.92	3.27	3.65	4.03	4.41	4.80
62...	0.33	0.54	0.77	0.99	1.24	1.51	1.80	2.11	2.44	2.79	3.15	3.53	3.91	4.31	4.70	5.09
64...	0.35	0.58	0.82	1.08	1.35	1.66	1.98	2.32	2.68	3.05	3.44	3.82	4.21	4.59	4.99	5.38
66...	0.40	0.64	0.91	1.20	1.51	1.85	2.20	2.56	2.94	3.32	3.71	4.11	4.49	4.89	5.28	5.67
68...	0.48	0.75	1.06	1.38	1.72	2.08	2.45	2.84	3.22	3.62	3.99	4.39	4.78	5.17	5.56	5.94
0.70...	0.60	0.92	1.26	1.61	1.97	2.35	2.73	3.13	3.52	3.90	4.30	4.69	5.08	5.46	5.83	6.19
72...	0.79	1.12	1.49	1.86	2.25	2.63	3.02	3.40	3.80	4.19	4.58	4.97	5.35			
74...	1.01	1.37	1.75	2.13	2.53	2.92	3.30	3.70	4.09	4.48	4.86	5.23	5.59			
76...	1.26	1.65	2.03	2.42	2.80	3.20	3.59	3.98	4.37	4.75	5.11	5.47				
78...	1.52	1.92	2.31	2.70	3.10	3.49	3.88	4.26	4.63	4.99	5.34	5.67				
0.80...	1.82	2.19	2.59	2.98	3.37	3.76	4.14	4.51	4.86	5.20	5.52	5.83				
82...	2.09	2.49	2.88	3.27	3.65	4.02	4.38	4.73	5.06	5.37	5.67	5.95				
84...	2.38	2.77	3.16	3.54	3.90	4.26	4.59	4.91	5.22	5.51	5.78	6.05				
86...	2.67	3.05	3.42	3.78	4.13	4.45	4.76	5.05	5.33	5.60	5.86	6.12				
88...	2.93	3.30	3.65	3.98	4.30	4.60	4.88	5.15	5.41	5.67	5.94	6.20				
0.90...	3.17	3.52	3.84	4.15	4.44	4.71	4.97	5.22	5.48	5.74	6.00	6.27				
92...	3.38	3.69	3.99	4.27	4.52	4.78	5.02	5.28	5.54	5.80	6.07					
94...	3.54	3.83	4.09	4.35	4.59	4.84	5.08	5.34	5.60	5.87	6.15					
96...	3.66	3.91	4.16	4.40	4.64	4.88	5.12	5.39	5.66	5.94	6.23					
98...	3.73	3.97	4.21	4.44	4.68	4.93	5.18	5.44	5.71	6.01	6.33					
1.00...	3.78	4.02	4.24	4.48	4.72	4.97	5.23	5.50	5.79	6.09	6.40					
02...	3.82	4.05	4.28	4.52	4.77	5.02	5.29	5.57	5.86	6.17	6.49					
04...	3.85	4.08	4.32	4.57	4.82	5.09	5.35	5.64	5.94	6.26	6.60					

The table gives $\log p$

Table 7 (continued).

Ionization of matter in stellar atmospheres. $\log A = 4.2$.

θ	$\log p_e$ 0.0	0.2	0.4	0.6	0.8	1.0	1.2	1.4	1.6	1.8	2.0	2.2	2.4	2.6	2.8	3.0	3.2
0.60..	0.32	0.52	0.73	0.95	1.18	1.42	1.68	1.95	2.25	2.57	2.92	3.27	3.65	4.03	4.41	4.81	5.19
62..	0.33	0.54	0.77	0.99	1.24	1.51	1.80	2.11	2.44	2.79	3.15	3.53	3.91	4.31	4.71	5.10	5.49
64..	0.35	0.58	0.82	1.08	1.35	1.66	1.98	2.32	2.68	3.05	3.44	3.82	4.22	4.60	5.00	5.39	5.78
66..	0.40	0.64	0.91	1.20	1.51	1.85	2.20	2.56	2.94	3.32	3.71	4.12	4.50	4.90	5.29	5.69	6.08
68..	0.48	0.75	1.06	1.38	1.72	2.08	2.45	2.84	3.22	3.62	4.00	4.40	4.79	5.19			
0.70..	0.60	0.92	1.26	1.61	1.97	2.35	2.73	3.13	3.53	3.91	4.30	4.70	5.10	5.49			
72..	0.79	1.12	1.49	1.86	2.25	2.63	3.03	3.41	3.81	4.20	4.60	4.99	5.38				
74..	1.01	1.37	1.75	2.13	2.53	2.93	3.31	3.70	4.10	4.50	4.89	5.28	5.66				
76..	1.26	1.65	2.03	2.43	2.81	3.21	3.60	4.00	4.39	4.78	5.17	5.55					
78..	1.52	1.92	2.32	2.71	3.10	3.50	3.90	4.29	4.68	5.06	5.43	5.80					
0.80..	1.82	2.20	2.60	2.99	3.39	3.79	4.17	4.56	4.94	5.31	5.67	6.01					
82..	2.10	2.49	2.89	3.29	3.68	4.07	4.45	4.82	5.19	5.54	5.88	6.20					
84..	2.39	2.79	3.19	3.57	3.96	4.34	4.71	5.06	5.40	5.73	6.04	6.34					
86..	2.69	3.08	3.47	3.85	4.22	4.58	4.93	5.26	5.58	5.88	6.18	6.46					
88..	2.97	3.35	3.73	4.10	4.45	4.79	5.11	5.42	5.71	6.00	6.28	6.55					
0.90..	3.24	3.61	3.98	4.32	4.65	4.96	5.26	5.54	5.82	6.09	6.37	6.64					
92..	3.49	3.84	4.18	4.50	4.80	5.09	5.36	5.63	5.89	6.18	6.44						
94..	3.71	4.04	4.35	4.64	4.91	5.18	5.44	5.71	5.98	6.26	6.54						
96..	3.90	4.19	4.47	4.74	4.99	5.24	5.50	5.77	6.04	6.34	6.62						
98..	4.02	4.29	4.55	4.80	5.06	5.31	5.57	5.83	6.11	6.40	6.72						
1.00..	4.11	4.37	4.61	4.86	5.10	5.36	5.62	5.88	6.19	6.50	6.80						
02..	4.18	4.42	4.66	4.91	5.16	5.41	5.68	5.97	6.26	6.57	6.89						
04..	4.23	4.47	4.71	4.96	5.21	5.48	5.75	6.04	6.34	6.65	7.00						

The table gives $\log p$

Table 8. Ionization of matter in stellar atmospheres.

θ	log p 0.0	0.2	0.4	0.6	0.8	1.0	1.2	1.4
0.30	—0.30	—0.10	0.10	0.30	0.50	0.70	0.90	1.10
32	—0.30	—0.10	0.10	0.30	0.50	0.70	0.90	1.10
34	—0.30	—0.10	0.10	0.30	0.50	0.70	0.90	1.10
36	—0.30	—0.10	0.10	0.30	0.50	0.70	0.90	1.10
38	—0.30	—0.10	0.10	0.30	0.50	0.70	0.90	1.10
0.40	—0.30	—0.10	0.10	0.30	0.50	0.70	0.90	1.10
42	—0.30	—0.10	0.10	0.30	0.50	0.70	0.90	1.10
44	—0.30	—0.10	0.10	0.30	0.50	0.70	0.90	1.10
46	—0.30	—0.10	0.10	0.30	0.50	0.70	0.90	1.10
48	—0.30	—0.10	0.10	0.30	0.50	0.70	0.90	1.10
0.50	—0.30	—0.10	0.10	0.30	0.50	0.70	0.90	1.09
52	—0.30	—0.10	0.10	0.30	0.50	0.69	0.89	1.09
54	—0.30	—0.10	0.10	0.30	0.49	0.69	0.89	1.08
56	—0.30	—0.11	0.09	0.29	0.49	0.69	0.88	1.06
58	—0.30	—0.11	0.09	0.29	0.48	0.67	0.85	1.03
0.60	—0.31	—0.11	0.08	0.28	0.46	0.64	0.82	0.98

The table gives

θ	log p 3.0	3.2	3.4	3.6	3.8	4.0	4.2	4.4
0.30	2.70	2.90	3.10	3.30	3.50	3.70	3.90	4.1(
32	2.70	2.90	3.10	3.30	3.50	3.70	3.89	4.0
34	2.70	2.90	3.10	3.30	3.50	3.69	3.89	4.0
36	2.70	2.90	3.10	3.29	3.49	3.69	3.88	4.0
38	2.70	2.89	3.09	3.29	3.49	3.68	3.86	4.0
0.40	2.69	2.89	3.09	3.28	3.47	3.65	3.83	4.0
42	2.68	2.88	3.08	3.26	3.44	3.62	3.79	3.9
44	2.68	2.87	3.05	3.23	3.40	3.57	3.72	3.8(
46	2.66	2.84	3.02	3.18	3.34	3.49	3.63	3.7(
48	2.62	2.79	2.95	3.11	3.25	3.39	3.52	3.6
0.50	2.58	2.73	2.88	3.02	3.15	3.28	3.40	3.5
52	2.50	2.65	2.78	2.91	3.03	3.15	3.27	3.3
54	2.41	2.54	2.67	2.79	2.90	3.02	3.13	3.2
56	2.31	2.43	2.54	2.66	2.77	2.88	2.98	3.0
58	2.18	2.30	2.41	2.52	2.63	2.74	2.84	2.9
0.60	2.05	2.16	2.27	2.37	2.48	2.58	2.69	2.7

The table give

$\log A = 3.0,\ 3.4,\ 3.8,\ 4.2$ and pure H.

1.6	1.8	2.0	2.2	2.4	2.6	2.8	3.0	θ
1.30	1.50	1.70	1.90	2.10	2.30	2.50	2.70	.....0.30
1.30	1.50	1.70	1.90	2.10	2.30	2.50	2.70	 32
1.30	1.50	1.70	1.90	2.10	2.30	2.50	2.70	 34
1.30	1.50	1.70	1.90	2.10	2.30	2.50	2.70	 36
1.30	1.50	1.70	1.90	2.10	2.30	2.50	2.70	 38
1.30	1.50	1.70	1.90	2.10	2.30	2.50	2.69	.....0.40
1.30	1.50	1.70	1.90	2.10	2.29	2.49	2.68	 42
1.30	1.50	1.70	1.89	2.09	2.29	2.49	2.68	 44
1.30	1.50	1.69	1.89	2.09	2.28	2.48	2.66	 46
1.29	1.49	1.69	1.89	2.08	2.26	2.45	2.62	 48
1.29	1.49	1.68	1.87	2.05	2.23	2.41	2.58	.....0.50
1.29	1.48	1.66	1.85	2.02	2.19	2.35	2.50	 52
1.27	1.45	1.63	1.81	1.97	2.12	2.27	2.41	 54
1.24	1.42	1.59	1.75	1.90	2.04	2.18	2.31	 56
1.21	1.37	1.52	1.67	1.81	1.94	2.06	2.18	 58
1.14	1.29	1.43	1.57	1.69	1.82	1.93	2.05	.....0.60

$\log p_e$

4.6	4.8	5.0	5.2	5.4	θ
4.29	4.49	4.69	4.88		.....0.30
4.29	4.49	4.68	4.87		 32
4.28	4.47	4.65	4.83		 34
4.26	4.44	4.62	4.78	4.94	 36
4.23	4.40	4.56	4.71	4.86	 38
4.18	4.33	4.47	4.62	4.75	.....0.40
4.09	4.23	4.36	4.50	4.63	 42
4.00	4.13	4.25	4.38	4.49	 44
3.88	4.01	4.12	4.24	4.35	 46
3.76	3.87	3.99	4.10	4.21	 48
3.63	3.74	3.85	3.96	4.06	.....0.50
3.45	3.59	3.70	3.81	3.91	 52
3.39	3.45	3.56	3.66	3.76	 54
3.19	3.30	3.40	3.50	3.61	 56
3.05	3.15	3.25	3.35	3.45	 58
3.00	3.10	3.20	3.30	2.90	.....0.60

$\log p_e$

Table 8 (continued). Ionization of matter

θ \ $\log p$	0.4	0.6	0.8	1.0	1.2	1.4	1.6	1.8	2.0
0.60	0.08	0.28	0.46	0.64	0.82	0.98	1.14	1.29	1.43
62	0.07	0.25	0.43	0.61	0.77	0.92	1.06	1.20	1.33
64	0.04	0.22	0.38	0.54	0.69	0.83	0.96	1.09	1.21
66	0.00	0.17	0.32	0.46	0.60	0.73	0.85	0.97	1.09
68		0.09	0.23	0.36	0.49	0.61	0.73	0.84	0.95
0.70		0.00	0.13	0.25	0.36	0.48	0.59	0.71	0.82
72			0.01	0.13	0.24	0.35	0.46	0.57	0.67
74				−0.01	0.11	0.22	0.32	0.43	0.53
76						0.08	0.18	0.29	0.39
78							0.05	0.15	0.25
0.80								0.01	0.11
82									
84									
86									
88									
0.90					−1.00	−0.89	−0.78	−0.67	−0.55
92						−1.02	−0.91	−0.79	−0.66
94								−0.89	−0.76
96									−0.84
98									−0.90
1.00									−0.94
02									−0.97
04									−0.98

The table gives

θ \ $\log p$	4.0	4.2	4.4	4.6	4.8	5.0	5.2
0.60	2.59	2.70	2.81	2.91	3.01		
62	2.45	2.55	2.66	2.76	2.86	2.97	
64	2.30	2.41	2.51	2.62	2.73	2.83	2.94
66	2.15	2.26	2.37	2.48	2.59	2.70	2.81
68	2.02	2.13	2.23	2.34	2.46	2.57	2.68
0.70	1.88	1.98	2.09	2.21	2.33	2.45	2.56
72	1.74	1.85	1.97	2.08	2.20	2.33	2.45
74	1.61	1.72	1.84	1.96	2.09	2.22	2.35
76	1.48	1.60	1.73	1.86	2.00	2.14	2.28
78	1.36	1.50	1.63	1.78	1.92	2.07	2.22
0.80	1.27	1.40	1.55	1.70	1.86	2.02	2.18
82	1.18	1.33	1.48	1.64	1.81	1.98	2.14
84	1.11	1.27	1.43	1.60	1.77	1.93	2.10
86	1.05	1.23	1.40	1.57	1.74	1.90	2.06
88	1.02	1.19	1.37	1.53	1.70	1.86	2.02
0.90	0.99	1.17	1.34	1.50	1.67	1.83	1.98
92	0.97	1.14	1.31	1.47	1.63	1.78	1.94
94	0.94	1.11	1.28	1.44	1.59	1.75	1.89
96	0.92	1.09	1.25	1.40	1.55	1.69	1.84
98	0.89	1.06	1.22	1.37	1.51	1.65	1.79
1.00	0.86	1.02	1.17	1.32	1.47	1.61	1.74
02	0.82	0.98	1.13	1.28	1.43	1.56	1.69
04	0.78	0.94	1.09	1.23	1.38	1.51	1.64

The table gives

in stellar atmospheres. $\log A = 3.0$.

2.2	2.4	2.6	2.8	3.0	3.2	3.4	3.6	3.8	4.0	θ
1.57	1.69	1.82	1.93	2.05	2.16	2.27	2.38	2.48	2.59	....0.60
1.46	1.58	1.69	1.81	1.92	2.03	2.14	2.24	2.35	2.45	 62
1.33	1.45	1.56	1.67	1.78	1.88	1.98	2.09	2.20	2.30	 64
1.20	1.31	1.43	1.53	1.64	1.74	1.85	1.95	2.05	2.15	 66
1.07	1.18	1.28	1.38	1.49	1.60	1.70	1.81	1.91	2.02	 68
0.93	1.03	1.14	1.24	1.34	1.45	1.55	1.66	1.77	1.88	....0.70
0.78	0.89	0.99	1.10	1.20	1.31	1.42	1.52	1.63	1.74	 72
0.64	0.74	0.85	0.95	1.06	1.17	1.28	1.38	1.49	1.61	 74
0.50	0.60	0.71	0.82	0.92	1.03	1.14	1.25	1.37	1.48	 76
0.35	0.46	0.57	0.68	0.78	0.89	1.01	1.12	1.24	1.36	 78
0.22	0.33	0.43	0.54	0.66	0.77	0.88	1.01	1.13	1.27	....0.80
0.08	0.19	0.30	0.41	0.53	0.65	0.77	0.90	1.04	1.18	 82
	0.06	0.17	0.29	0.41	0.53	0.67	0.81	0.96	1.11	 84
		0.05	0.17	0.30	0.44	0.58	0.73	0.89	1.05	 86
			0.08	0.21	0.36	0.51	0.67	0.84	1.02	 88
−0.42	−0.29	−0.15	−0.01	0.13	0.29	0.46	0.63	0.81	0.99	....0.90
−0.52	−0.38	−0.24	−0.08	0.08	0.25	0.43	0.60	0.79	0.97	 92
−0.61	−0.46	−0.30	−0.13	0.04	0.22	0.40	0.58	0.76	0.94	 94
−0.68	−0.52	−0.35	−0.17	0.01	0.20	0.38	0.56	0.75	0.92	 96
−0.73	−0.56	−0.38	−0.20	−0.01	0.18	0.36	0.54	0.72	0.89	 98
−0.76	−0.57	−0.39	−0.22	−0.02	0.16	0.35	0.52	0.69	0.86	....1.00
−0.78	−0.59	−0.41	−0.23	−0.04	0.15	0.32	0.49	0.66	0.82	 02
−0.80	−0.61	−0.43	−0.24	−0.06	0.12	0.30	0.46	0.62	0.78	 04

$\log p_e$

$\log p_e$

Table 8 (continued). Ionization of matter

θ \ log p	0.4	0.6	0.8	1.0	1.2	1.4	1.6	1.8	2.0
0.60	0.08	0.28	0.46	0.64	0.82	0.98	1.14	1.29	1.43
62	0.07	0.25	0.43	0.61	0.77	0.92	1.06	1.20	1.33
64	0.04	0.22	0.38	0.54	0.69	0.83	0.96	1.09	1.21
66	0.00	0.17	0.32	0.46	0.60	0.73	0.85	0.97	1.09
68		0.09	0.23	0.36	0.49	0.61	0.73	0.84	0.95
0.70		0.00	0.13	0.25	0.36	0.48	0.59	0.70	0.81
72			0.01	0.13	0.24	0.35	0.46	0.57	0.67
74				−0.01	0.11	0.22	0.32	0.43	0.53
76						0.07	0.18	0.28	0.39
78							0.04	0.14	0.25
0.80								−0.01	0.10
82									−0.04
84									
86									
88									
0.90						−0.93	−0.82	−0.71	−0.61
92							−0.96	−0.85	−0.74
94								−0.98	−0.86
96									−0.98
98									
1.00									
02									
04									

The table gives

θ \ log p	4.0	4.2	4.4	4.6	4.8	5.0	5.2	5.4
0.60	2.59	2.70	2.80	2.90	3.00	3.11		
62	2.45	2.55	2.65	2.75	2.85	2.96		
64	2.30	2.40	2.51	2.61	2.71	2.81	2.92	
66	2.14	2.25	2.36	2.46	2.56	2.67	2.77	2.88
68	2.01	2.11	2.22	2.32	2.42	2.52	2.63	2.74
0.70	1.86	1.96	2.06	2.17	2.27	2.38	2.49	2.61
72	1.71	1.81	1.92	2.03	2.14	2.25	2.36	2.48
74	1.56	1.67	1.78	1.89	2.01	2.12	2.24	2.36
76	1.43	1.54	1.65	1.76	1.88	2.00	2.12	2.26
78	1.29	1.41	1.52	1.64	1.76	1.89	2.02	2.16
0.80	1.16	1.28	1.40	1.53	1.66	1.79	1.94	2.08
82	1.04	1.17	1.30	1.43	1.57	1.71	1.86	2.01
84	0.93	1.06	1.20	1.35	1.50	1.65	1.80	1.96
86	0.83	0.97	1.12	1.28	1.43	1.59	1.76	1.92
88	0.76	0.91	1.06	1.22	1.39	1.56	1.72	1.88
0.90	0.69	0.85	1.02	1.18	1.35	1.51	1.68	1.84
92	0.63	0.81	0.98	1.15	1.32	1.48	1.64	1.79
94	0.60	0.77	0.95	1.12	1.28	1.44	1.60	1.75
96	0.58	0.75	0.92	1.09	1.25	1.40	1.55	1.70
98	0.55	0.72	0.89	1.06	1.21	1.37	1.51	1.65
1.00	0.52	0.69	0.86	1.02	1.18	1.33	1.46	1.61
02	0.48	0.66	0.82	0.98	1.13	1.28	1.42	1.56
04	0.46	0.62	0.78	0.94	1.09	1.23	1.38	1.51

The table gives

in stellar atmospheres. $\log A = 3.4$.

2.2	2.4	2.6	2.8	3.0	3.2	3.4	3.6	3.8	4.0	θ
1.57	1.69	1.82	1.93	2.05	2.16	2.27	2.37	2.48	2.59	....0.60
1.46	1.58	1.69	1.81	1.92	2.03	2.13	2.24	2.35	2.45	 62
1.33	1.44	1.56	1.66	1.77	1.88	1.98	2.09	2.20	2.30	 64
1.20	1.31	1.42	1.53	1.63	1.74	1.84	1.94	2.04	2.14	 66
1.06	1.17	1.28	1.38	1.49	1.59	1.70	1.80	1.90	2.01	 68
0.92	1.02	1.13	1.24	1.34	1.44	1.54	1.64	1.75	1.86	....0.70
0.78	0.88	0.99	1.09	1.19	1.29	1.40	1.50	1.61	1.71	 72
0.64	0.74	0.84	0.94	1.04	1.15	1.26	1.36	1.46	1.56	 74
0.49	0.59	0.70	0.81	0.91	1.01	1.11	1.22	1.32	1.43	 76
0.35	0.45	0.55	0.66	0.76	0.86	0.97	1.08	1.18	1.29	 78
0.21	0.31	0.42	0.52	0.62	0.73	0.83	0.94	1.05	1.16	....0.80
0.06	0.16	0.27	0.37	0.48	0.59	0.70	0.81	0.92	1.04	 82
	0.02	0.12	0.23	0.34	0.46	0.57	0.69	0.81	0.93	 84
		−0.01	0.10	0.21	0.33	0.45	0.57	0.70	0.83	 86
				0.09	0.21	0.33	0.47	0.61	0.76	 88
−0.49	−0.38	−0.27	−0.15	−0.02	0.10	0.23	0.38	0.53	0.69	....0.90
−0.62	−0.51	−0.39	−0.26	−0.13	0.01	0.16	0.31	0.47	0.63	 92
−0.74	−0.62	−0.49	−0.36	−0.21	−0.06	0.10	0.26	0.43	0.60	 94
−0.85	−0.72	−0.59	−0.44	−0.29	−0.13	0.04	0.21	0.40	0.58	 96
−0.95	−0.81	−0.65	−0.50	−0.34	−0.16	0.02	0.19	0.37	0.55	 98
	−0.88	−0.71	−0.54	−0.37	−0.19	−0.01	0.17	0.35	0.52	....1.00
	−0.92	−0.75	−0.57	−0.40	−0.22	−0.04	0.15	0.31	0.48	 02
	−0.96	−0.78	−0.60	−0.42	−0.24	−0.05	0.12	0.30	0.46	 04

$\log p_e$

$\log p_e$

Table 8 (continued). Ionization of matter

θ \ log p	0.4	0.6	0.8	1.0	1.2	1.4	1.6	1.8	2.0
0.60	0.08	0.28	0.46	0.64	0.82	0.98	1.14	1.29	1.43
62	0.07	0.25	0.43	0.61	0.77	0.92	1.06	1.20	1.33
64	0.04	0.22	0.38	0.54	0.69	0.83	0.96	1.09	1.21
66	0.00	0.17	0.32	0.46	0.60	0.73	0.85	0.97	1.09
68		0.09	0.23	0.36	0.49	0.61	0.73	0.84	0.95
0.70		0.00	0.13	0.25	0.36	0.48	0.59	0.70	0.81
72			0.01	0.13	0.24	0.35	0.46	0.56	0.67
74				—0.01	0.11	0.22	0.32	0.43	0.53
76						0.07	0.17	0.28	0.38
78							0.04	0.14	0.24
0.80								—0.01	0.10
82									
84									
86									
88									
0.90						—0.94	—0.84	—0.73	—0.63
92							—0.97	—0.87	—0.77
94								—1.02	—0.91
96									
98									
1.00									
02									
04									

The table gives

θ \ log p	4.0	4.2	4.4	4.6	4.8	5.0	5.2	5.4	5.6
0.60	2.58	2.69	2.79	2.90	3.00	3.10	3.21	3.31	
62	2.45	2.55	2.65	2.75	2.85	2.95	3.06	3.16	
64	2.29	2.40	2.50	2.61	2.71	2.81	2.91	3.01	
66	2.14	2.25	2.35	2.45	2.55	2.65	2.76	2.86	2.96
68	2.00	2.11	2.21	2.31	2.41	2.51	2.61	2.72	2.82
0.70	1.85	1.95	2.05	2.15	2.25	2.36	2.46	2.57	2.68
72	1.71	1.81	1.91	2.01	2.11	2.22	2.32	2.43	2.54
74	1.55	1.66	1.76	1.86	1.97	2.08	2.18	2.29	2.40
76	1.41	1.51	1.62	1.72	1.83	1.94	2.05	2.16	2.28
78	1.26	1.37	1.47	1.58	1.70	1.81	1.92	2.04	2.16
0.80	1.13	1.23	1.34	1.45	1.57	1.68	1.80	1.92	2.05
82	0.99	1.10	1.21	1.33	1.44	1.56	1.69	1.82	1.95
84	0.85	0.97	1.08	1.20	1.33	1.46	1.59	1.72	1.87
86	0.73	0.84	0.97	1.09	1.23	1.36	1.50	1.65	1.80
88	0.61	0.74	0.87	1.00	1.14	1.29	1.44	1.59	1.75
0.90	0.50	0.64	0.78	0.92	1.07	1.22	1.38	1.54	1.69
92	0.41	0.55	0.70	0.86	1.02	1.18	1.34	1.49	1.65
94	0.33	0.49	0.64	0.81	0.97	1.13	1.29	1.45	1.60
96	0.27	0.44	0.60	0.77	0.93	1.10	1.26	1.41	1.56
98	0.22	0.39	0.57	0.73	0.90	1.06	1.22	1.37	1.52
1.00	0.18	0.36	0.53	0.70	0.87	1.02	1.18	1.33	1.47
02	0.16	0.33	0.50	0.66	0.82	0.98	1.13	1.28	1.42
04	0.13	0.30	0.46	0.62	0.78	0.93	1.08	1.23	1.37

The table gives

in stellar atmospheres. $\log A = 3.8$.

2.2	2.4	2.6	2.8	3.0	3.2	3.4	3.6	3.8	4.0	θ
1.57	1.69	1.82	1.93	2.05	2.16	2.27	2.37	2.48	2.58	....0.60
1.46	1.58	1.69	1.81	1.92	2.03	2.13	2.24	2.34	2.45	 62
1.33	1.44	1.56	1.67	1.78	1.88	1.98	2.08	2.19	2.29	 64
1.20	1.31	1.42	1.53	1.63	1.74	1.84	1.94	2.04	2.14	 66
1.06	1.17	1.28	1.38	1.48	1.59	1.69	1.79	1.89	2.00	 68
0.92	1.03	1.13	1.23	1.33	1.44	1.54	1.64	1.74	1.85	....0.70
0.77	0.88	0.98	1.08	1.19	1.29	1.40	1.50	1.60	1.71	 72
0.63	0.73	0.84	0.94	1.04	1.15	1.25	1.35	1.45	1.55	 74
0.49	0.59	0.69	0.80	0.90	1.00	1.10	1.21	1.31	1.41	 76
0.34	0.45	0.55	0.65	0.75	0.85	0.95	1.06	1.16	1.26	 78
0.20	0.30	0.40	0.51	0.61	0.71	0.81	0.92	1.02	1.13	....0.80
0.06	0.16	0.26	0.36	0.46	0.56	0.67	0.77	0.88	0.99	 82
	0.01	0.11	0.21	0.32	0.42	0.53	0.63	0.74	0.85	 84
			0.07	0.17	0.28	0.39	0.50	0.61	0.73	 86
				0.04	0.15	0.26	0.37	0.49	0.61	 88
—0.53	—0.42	—0.31	—0.21	—0.09	0.02	0.13	0.25	0.38	0.50	....0.90
—0.66	—0.56	—0.45	—0.34	—0.22	—0.11	0.01	0.14	0.27	0.41	 92
—0.80	—0.69	—0.58	—0.46	—0.35	—0.22	—0.08	0.04	0.18	0.33	 94
—0.93	—0.82	—0.70	—0.58	—0.46	—0.32	—0.19	—0.04	0.11	0.27	 96
	—0.94	—0.81	—0.68	—0.55	—0.41	—0.26	—0.10	0.06	0.22	 98
		—0.91	—0.78	—0.63	—0.48	—0.32	—0.16	0.02	0.18	....1.00
		—1.01	—0.85	—0.70	—0.53	—0.37	—0.20	—0.02	0.16	 02
			—0.91	—0.75	—0.57	—0.40	—0.22	—0.04	0.13	 04

$\log p_e$

$\log p_e$

Table 8 (continued). Ionization of matter

θ \ log p	0.4	0.6	0.8	1.0	1.2	1.4	1.6	1.8	2.0
0.60	0.08	0.28	0.46	0.64	0.82	0.98	1.14	1.29	1.43
62	0.07	0.25	0.43	0.61	0.77	0.92	1.06	1.20	1.33
64	0.04	0.22	0.38	0.54	0.69	0.83	0.96	1.09	1.21
66	0.00	0.17	0.32	0.46	0.60	0.73	0.85	0.97	1.09
68		0.09	0.23	0.36	0.49	0.61	0.73	0.84	0.95
0.70		0.00	0.13	0.25	0.36	0.48	0.59	0.70	0.81
72			0.01	0.13	0.24	0.35	0.46	0.56	0.67
74				−0.01	0.11	0.22	0.32	0.43	0.53
76						0.07	0.17	0.28	0.38
78							0.04	0.14	0.24
0.80								−0.01	0.10
82									
84									
86									
88									
0.90						−0.94	−0.84	−0.74	−0.64
92							−0.98	−0.88	−0.78
94									−0.93
96									
98									
1.00									
02									
04									

The table gives

θ \ log p	4.0	4.2	4.4	4.6	4.8	5.0	5.2	5.4	5.6
0.60	2.58	2.69	2.79	2.89	3.00	3.10	3.20	3.30	
62	2.45	2.55	2.65	2.75	2.85	2.95	3.05	3.15	
64	2.29	2.40	2.50	2.60	2.70	2.80	2.90	3.01	3.11
66	2.14	2.24	2.34	2.45	2.55	2.65	2.76	2.86	2.96
68	2.00	2.10	2.20	2.30	2.41	2.51	2.61	2.71	2.81
0.70	1.84	1.95	2.05	2.15	2.25	2.35	2.45	2.55	2.65
72	1.70	1.80	1.90	2.00	2.10	2.21	2.31	2.41	2.51
74	1.55	1.65	1.75	1.85	1.95	2.06	2.16	2.26	2.36
76	1.40	1.50	1.61	1.71	1.81	1.91	2.02	2.12	2.23
78	1.25	1.35	1.46	1.56	1.67	1.77	1.88	1.98	2.09
0.80	1.11	1.21	1.32	1.42	1.53	1.63	1.74	1.85	1.96
82	0.96	1.07	1.17	1.28	1.39	1.50	1.61	1.72	1.84
84	0.82	0.93	1.03	1.14	1.25	1.36	1.48	1.60	1.72
86	0.68	0.79	0.90	1.01	1.12	1.24	1.36	1.49	1.61
88	0.55	0.66	0.77	0.89	1.01	1.13	1.26	1.39	1.52
0.90	0.41	0.53	0.65	0.77	0.90	1.03	1.16	1.30	1.44
92	0.29	0.41	0.54	0.67	0.80	0.94	1.08	1.23	1.38
94	0.17	0.30	0.44	0.58	0.72	0.86	1.01	1.17	1.32
96	0.07	0.21	0.35	0.50	0.65	0.81	0.97	1.12	1.27
98	−0.01	0.14	0.29	0.44	0.60	0.75	0.91	1.07	1.22
1.00	−0.09	0.07	0.23	0.39	0.55	0.72	0.88	1.03	1.18
02	−0.15	0.02	0.18	0.35	0.51	0.67	0.83	0.99	1.14
04	−0.19	−0.02	0.14	0.31	0.47	0.63	0.79	0.94	1.09

The table gives

in stellar atmospheres. $\log A = 4.2$.

2.2	2.4	2.6	2.8	3.0	3.2	3.4	3.6	3.8	4.0	θ
1.57	1.69	1.82	1.93	2.05	2.16	2.27	2.37	2.48	2.58	....0.60
1.46	1.58	1.69	1.81	1.92	2.03	2.13	2.24	2.34	2.45	 62
1.33	1.44	1.56	1.67	1.78	1.88	1.98	2.08	2.19	2.29	 64
1.20	1.31	1.42	1.53	1.63	1.74	1.84	1.94	2.04	2.14	 66
1.06	1.17	1.28	1.38	1.48	1.59	1.69	1.79	1.89	2.00	 68
0.92	1.03	1.13	1.23	1.33	1.43	1.54	1.64	1.74	1.84	....0.70
0.77	0.88	0.98	1.08	1.19	1.29	1.39	1.50	1.60	1.70	 72
0.63	0.73	0.84	0.94	1.04	1.14	1.25	1.35	1.45	1.55	 74
0.48	0.58	0.69	0.79	0.90	1.00	1.10	1.20	1.30	1.40	 76
0.34	0.44	0.54	0.65	0.75	0.85	0.95	1.05	1.15	1.25	 78
0.20	0.30	0.40	0.50	0.60	0.70	0.80	0.90	1.01	1.11	....0.80
0.05	0.16	0.26	0.36	0.45	0.55	0.66	0.76	0.86	0.96	 82
	0.00	0.11	0.21	0.31	0.41	0.51	0.61	0.72	0.82	 84
			0.06	0.16	0.26	0.36	0.47	0.57	0.68	 86
				0.02	0.12	0.23	0.33	0.44	0.55	 88
−0.54	−0.44	−0.33	−0.23	−0.13	−0.02	0.09	0.19	0.30	0.41	....0.90
−0.68	−0.57	−0.47	−0.37	−0.26	−0.16	−0.05	0.06	0.18	0.29	 92
−0.83	−0.72	−0.62	−0.51	−0.41	−0.29	−0.18	−0.06	0.05	0.17	 94
−0.96	−0.86	−0.75	−0.64	−0.53	−0.42	−0.30	−0.18	−0.06	0.07	 96
	−0.99	−0.88	−0.77	−0.66	−0.54	−0.42	−0.29	−0.16	−0.01	 98
		−1.01	−0.89	−0.77	−0.65	−0.52	−0.39	−0.24	−0.09	....1.00
			−1.01	−0.88	−0.74	−0.61	−0.46	−0.31	−0.15	 02
				−0.97	−0.83	−0.68	−0.52	−0.36	−0.19	 04

$\log p_e$

$\log p_e$

Table 9. Opacity $\bar{\varkappa}$. II. $\log A = 3.0$, 3.4, 3.8 4.2 and pure H.

θ	$\log p$	1.2	1.4	1.6	1.8	2.0	2.2	2.4	2.6	2.8	3.0	3.2	3.4
0.30		8.40	8.60	8.80	9.00	9.20	9.40	9.60	9.80	0.00	0.20	0.40	0.60
32		8.58	8.78	8.98	9.18	9.38	9.58	9.78	9.98	0.18	0.38	0 58	0.78
34		8.75	8.95	9.15	9.35	9.55	9.75	9.95	0.15	0.35	0.55	0.75	0.95
36		8.93	9.13	9.33	9.53	9.73	9.93	0.13	0.33	0.53	0.73	0.93	1.12
38		9.08	9.28	9.48	9.68	9.88	0.08	0.28	0.48	0.68	0.88	1.06	1.26
0.40		9.23	9.43	9.63	9.83	0.03	0.23	0.43	0.63	0.82	1.01	1.20	1.39
42		9.36	9.56	9.76	9.96	0.16	0.36	0.55	0.74	0.94	1.13	1.32	1.49
44		9.49	9.69	9.89	0.09	0.28	0.47	0.67	0.87	1.05	1.23	1.40	1.55
46		9.62	9.82	0.02	0.21	0.40	0.60	0.78	0.97	1.14	1.30	1.45	1.59
48		9.73	9.92	0.11	0.31	0.50	0.69	0.86	1.03	1.19	1.33	1.45	1.55
0.50		9.82	0.01	0.21	0.39	0.57	0.74	0.90	1.05	1.19	1.30	1.39	1.47
52		9.89	0.08	0.27	0.44	0.60	0.76	0.91	1.02	1.12	1.21	1.28	1.33
54		9.95	0.13	0.30	0.46	0.61	0.75	0.85	0.94	1.01	1.08	1.13	1.17
56		0.00	0.16	0.31	0.44	0.57	0.67	0.75	0.83	0.88	0.93	0.98	1.01
58		0.00	0.15	0.28	0.38	0.47	0.54	0.60	0.65	0.70	0.74	0.79	0.82
0.60			0.10	0.19	0.27	0.34	0.40	0.44	0.49	0.53	0.57	0.61	0.64

The table gives $\log \bar{\varkappa}$

θ	$\log p$	3.4	3.6	3.8	4.0	4.2	4.4	4.6	4.8	5.0
0.30		0.60	0.80	1.00	1.20	1.40	1.59	1.78	1.98	2.17
32		0.78	0.98	1.18	1.37	1.56	1.76	1.96	2.15	2.34
34		0.95	1.15	1.34	1.53	1.72	1.91	2.10	2.27	2.44
36		1.12	1.31	1.51	1.69	1.87	2.05	2.24	2.39	2.52
38		1.26	1.46	1.64	1.82	1.99	2.15	2.30	2.43	2.53
0.40		1.39	1.57	1.74	1.91	2.06	2.20	2.31	2.40	2.49
42		1.49	1.66	1.82	1.95	2.07	2.17	2.25	2.33	2.40
44		1.55	1.70	1.84	1.94	2.03	2.11	2.18	2.23	2.29
46		1.59	1.71	1.81	1.88	1.95	2.02	2.07	2.11	2.17
48		1.55	1.64	1.71	1.77	1.83	1.88	1.93	1.97	2.01
0.50		1.47	1.53	1.59	1.64	1.69	1.73	1.77	1.81	1.85
52		1.33	1.38	1.43	1.47	1.51	1.55	1.59	1.64	1.68
54		1.17	1.22	1.26	1.30	1.33	1.38	1.43	1.47	1.52
56		1.01	1.05	1.10	1.13	1.17	1.21	1.26	1.31	1.36
58		0.82	0.86	0.90	0.94	0.99	1.04	1.09	1.14	1.19
0.60		0.64	0.67	0.71	0.76	0.81	0.87	0.92	0.97	1.03

The table gives $\log \bar{\varkappa}$

Table 9 (continued). Opacity $\bar{\varkappa}$. II. $\log A = 3.0$.

θ	$\log p$ 2.0	2.2	2.4	2.6	2.8	3.0	3.2	3.4	3.6	3.8	4.0	4.2	4.4	4.6	4.8	5.0	5.2
0.60..	0.34	0.40	0.44	0.49	0.53	0.57	0.61	0.64	0.67	0.72	0.77	0.82	0.87	0.92	0.98	1.04	
62..	0.17	0.22	0.26	0.30	0.33	0.37	0.41	0.45	0.50	0.55	0.59	0.64	0.69	0.76	0.83	0.90	
64..	9.99	0.04	0.08	0.12	0.15	0.18	0.22	0.26	0.32	0.37	0.43	0.48	0.55	0.62	0.70	0.77	
66..	9.81	9.84	9.88	9.92	9.96	0.00	0.05	0.10	0.15	0.21	0.27	0.34	0.41	0.49	0.57	0.66	
68..	9.61	9.65	9.68	9.73	9.77	9.83	9.88	9.93	9.98	0.05	0.12	0.20	0.27	0.36	0.44	0.53	
0.70..						9.65	9.71	9.76	9.83	9.91	9.99	0.07	0.15	0.23	0.33	0.43	
72..						9.48	9.55	9.62	9.69	9.76	9.85	9.93	0.02	0.12	0.22	0.34	
74..						9.33	9.40	9.48	9.56	9.64	9.72	9.82	9.92	0.03	0.15	0.27	
76..						9.20	9.27	9.36	9.44	9.53	9.63	9.72	9.84	9.96	0.08	0.22	
78..						9.06	9.14	9.22	9.32	9.42	9.52	9.64	9.76	9.89	0.04	0.19	
0.80..						8.92	9.01	9.11	9.21	9.32	9.44	9.56	9.71	9.85	0.00	0.16	
82..						8.80	8.90	9.00	9.12	9.24	9.38	9.53	9.68	9.83	9.99	0.16	0.32
84..						8.70	8.81	8.92	9.05	9.20	9.34	9.50	9.65	9.82	9.99	0.15	0.32
86..						8.60	8.72	8.86	9.01	9.16	9.32	9.49	9.66	9.83	0.00	0.16	0.32
88..						8.54	8.68	8.83	8.98	9.14	9.32	9.49	9.67	9.83	0.00	0.16	0.32
0.90..	7.86	7.97	8.09	8.22	8.35	8.49	8.65	8.81	8.97	9.15	9.33	9.51	9.68	9.84	0.01	0.17	0.32
92..	7.77	7.89	8.02	8.16	8.30	8.46	8.63	8.81	8.98	9.17	9.35	9.52	9.69	9.85	0.01	0.16	0.32
94..	7.68	7.82	7.97	8.12	8.28	8.45	8.63	8.81	8.99	9.17	9.35	9.52	9.69	9.85	0.00	0.16	0.30
96..	7.63	7.79	7.95	8.11	8.28	8.46	8.65	8.83	9.01	9.20	9.37	9.54	9.70	9.85	0.00	0.14	0.29
98..	7.60	7.76	7.93	8.10	8.29	8.47	8.66	8.84	9.02	9.20	9.37	9.54	9.69	9.85	9.99	0.13	0.27
1.00..	7.58	7.76	7.95	8.13	8.31	8.49	8.68	8.87	9.04	9.21	9.38	9.54	9.69	9.84	9.99	0.13	0.26
02..	7.59	7.78	7.97	8.15	8.33	8.52	8.70	8.88	9,05	9.22	9.38	9.54	9.69	9.84	9.98	0.12	0.25
04..	7.61	7.79	7.98	8.16	8.35	8.54	8.71	8.89	9.05	9.21	9.37	9.53	9.68	9.82	9.97	0.10	0.23

The table gives $\log \bar{\varkappa}$

Table 9 (continued). Opacity $\bar{\varkappa}$. II. $\log A = 3.4$.

θ	$\log p$ 2.0	2.2	2.4	2.6	2.8	3.0	3.2	3.4	3.6	3.8	4.0	4.2	4.4	4.6	4.8	5.0	5.2
0.60..	0.34	0.40	0.44	0.49	0.53	0.57	0.61	0.64	0.67	0.71	0.77	0.82	0.87	0.92	0.97	1.03	
62..	0.17	0.22	0.26	0.30	0.33	0.37	0.41	0.45	0.50	0.55	0.59	0.64	0.69	0.75	0.82	0.89	
64..	9.99	0.04	0.08	0.11	0.15	0.18	0.22	0.26	0.31	0.37	0.42	0.48	0.55	0.62	0.69	0 76	
66..	9.81	9.84	9.88	9.92	9.95	0.00	0.05	0.10	0.15	0.21	0.27	0.33	0.40	0.48	0.55	0.63	
68..	9.61	9.65	9.68	9.72	9.77	9.82	9.88	9.93	9.98	0.05	0.12	0.19	0.26	0.34	0.42	0.50	
0.70..	9.43	9.46	9.50	9.55	9.60	9.65	9.70	9.76	9.82	9.90	9.97	0.05	0.13	0.21	0.29	0.38	0.48
72..						9.47	9.54	9.61	9.68	9.75	9.82	9.90	9.99	0.08	0.17	0.26	0.36
74..						9.32	9.39	9.46	9.54	9.62	9.70	9.78	9.87	9.97	0.07	0.17	0.28
76..						9.19	9.26	9.34	9.42	9.50	9.58	9.67	9.76	9.86	9.97	0.08	0.20
78..						9.04	9.12	9.20	9.28	9.37	9.46	9.56	9.67	9.77	9.88	0.01	0.14
0.80..						8.90	8.98	9.07	9.15	9.25	9.35	9.46	9.57	9.69	9.82	9.94	0.08
82..						8.76	8.85	8.94	9.04	9.15	9.26	9.37	9.49	9.63	9.76	9.90	0.04
84..						8.64	8.74	8.84	8.94	9.05	9.17	9.30	9.43	9.57	9.72	9.87	0.02
86..						8.51	8.62	8.74	8.85	8.98	9.11	9.24	9.39	9.54	9.69	9.85	0.02
88..						8.42	8.54	8.66	8.79	8.92	9.06	9.21	9.37	9.53	9.69	9.85	0.02
0.90..	7.82	7.91	8.01	8.11	8.22	8.34	8.46	8.59	8.73	8.88	9.03	9.19	9.36	9.52	9.69	9.85	0.02
92..	7.70	7.80	7.91	8.02	8.14	8.26	8.39	8.54	8.70	8.85	9.01	9.19	9.36	9.53	9.70	9.86	0.02
94..	7.58	7.69	7.81	7.94	8.07	8.21	8.36	8.51	8.67	8.84	9.01	9.18	9.36	9.53	9.69	9.85	0.01
96..	7.50	7.62	7.75	7.88	8.02	8.17	8.33	8.49	8.67	8.85	9.02	9.20	9.37	9.54	9.70	9.85	0.00
98..		7.55	7.68	7.84	7.99	8.14	8.32	8.50	8.67	8.85	9.02	9.20	9.37	9.54	9.70	9.85	9.99
1.00..			7.64	7.81	7.98	8.15	8.33	8.51	8.69	8.87	9.04	9.21	9.38	9.54	9.70	9.85	9.99
02..			7.64	7.81	7.99	8.16	8.34	8.52	8.71	8.87	9.04	9.22	9.38	9.54	9.69	9.84	9.98
04..			7.63	7.81	7.99	8.17	8.35	8.53	8.71	8.88	9.05	9.21	9.37	9.53	9.68	9.82	9.97

The table gives $\log \bar{\varkappa}$

Table 9 (continued). Opacity $\bar{\varkappa}$. II. $\log A = 3.8$.

θ \ $\log p$	2.0	2.2	2.4	2.6	2.8	3.0	3.2	3.4	3.6	3.8	4.0	4.2	4.4	4.6	4.8	5.0	5.2
0.60..	0.34	0.40	0.44	0.49	0.53	0.57	0.61	0.64	0.67	0.71	0.76	0.81	0.87	0.92	0.97	1.03	
62..	0.17	0.22	0.26	0.30	0.33	0.37	0.41	0.45	0.50	0.54	0.59	0.64	0.69	0.75	0.82	0.89	
64..	9.99	0.04	0.08	0.11	0.15	0.18	0.22	0.26	0.31	0.36	0.42	0.47	0.54	0.61	0.68	0.75	
66..	9.81	9.84	9.88	9.92	9.96	0.00	0.05	0.10	0.15	0.21	0.27	0.33	0.40	0.47	0.55	0.63	
68..	9.62	9.65	9.68	9.73	9.77	9.82	9.87	9.92	9.98	0.04	0.11	0.18	0.25	0.33	0.41	0.49	
0.70..	9.43	9.46	9.50	9.55	9.60	9.65	9.70	9.76	9.82	9.89	9.97	0.04	0.12	0.20	0.28	0.36	0.45
72..						9.47	9.54	9.61	9.67	9.74	9.82	9.89	9.98	0.06	0.15	0.23	0.33
74..						9.32	9.39	9.46	9.53	9.61	9.69	9.77	9.85	9.94	0.03	0.13	0.23
76..						9.18	9.25	9.33	9.40	9.49	9.57	9.65	9.73	9.83	9.92	0.02	0.13
78..						9.03	9.11	9.19	9.27	9.35	9.43	9.52	9.62	9.72	9.82	9.93	0.04
0.80..						8.89	8.97	9.05	9.13	9.22	9.31	9.41	9.51	9.61	9.73	9.84	9.95
82..						8.75	8.85	8.92	9.01	9.10	9.20	9.31	9.42	9.53	9.64	9.76	9.88
84..						8.62	8.71	8.80	8.89	8.99	9.10	9.21	9.32	9.44	9.55	9.68	9.81
86..						8.48	8.58	8.68	8.79	8.89	9.01	9.12	9.24	9.36	9.49	9.63	9.77
88..						8.37	8.48	8.58	8.69	8.81	8.92	9.04	9.17	9.30	9.44	9.59	9.74
0.90..	7.80	7.88	7.97	8.06	8.17	8.27	8.38	8.49	8.61	8.73	8.85	8.97	9.11	9.26	9.41	9.56	9.72
92..	7.67	7.76	7.86	7.96	8.07	8.17	8.28	8.39	8.52	8.65	8.79	8.93	9.08	9.24	9.40	9.56	9.72
94..	7.54	7.64	7.74	7.85	7.97	8.08	8.20	8.32	8.45	8.59	8.74	8.89	9.05	9.22	9.38	9.54	9.70
96..		7.55	7.65	7.77	7.89	8.01	8.13	8.26	8.41	8.56	8.72	8.88	9.05	9.22	9.38	9.55	9.71
98..			7.55	7.68	7.81	7.94	8.07	8.22	8.38	8.54	8.70	8.87	9.05	9.22	9.38	9.54	9.70
1.00..				7.61	7.74	7.89	8.04	8.20	8.37	8.54	8.70	8.88	9.05	9.22	9.38	9.54	9.70
02..				7.55	7.71	7.86	8.03	8.19	8.36	8.54	8.71	8.89	9.06	9.22	9.38	9.54	9.69
04..					7.68	7.84	8.02	8.19	8.37	8.55	8.72	8.89	9.05	9.21	9.37	9.52	9.67

The table gives $\log \bar{\varkappa}$

Table 9 (continued).

θ \ $\log p$	2.0	2.2	2.4	2.6	2.8	3.0	3.2	3.4	3.6
0.60.....	0.34	0.40	0.44	0.49	0.53	0.57	0.61	0.64	0.67
62.....	0.17	0.22	0.26	0.30	0.33	0.37	0.41	0.45	0.50
64.....	9.99	0.04	0.08	0.11	0.15	0.18	0.22	0.26	0.31
66.....	9.81	9.84	9.88	9.92	9.95	0.00	0.05	0.10	0.15
68.....	9.62	9.65	9.68	9.73	9.77	9.82	9.87	9.92	9.98
0.70.....	9.43	9.46	9.50	9.55	9.60	9.65	9.70	9.75	9.82
72.....	9.22	9.26	9.31	9.36	9.42	9.47	9.54	9.61	9.67
74.....	9.05	9.10	9.15	9.20	9.25	9.31	9.38	9.45	9.53
76.....	8.87	8.92	8.97	9.04	9.11	9.18	9.25	9.32	9.40
78.....	8.69	8.75	8.81	8.88	8.95	9.03	9.11	9.18	9.26
0.80.....	8.53	8.60	8.66	8.73	8.81	8.88	8.96	9.04	9.12
82.....		8.44	8.51	8.59	8.67	8.74	8.82	8.91	9.00
84.....			8.37	8.45	8.53	8.61	8.69	8.78	8.87
86.....						8.47	8.56	8.66	8.76
88.....						8.35	8.45	8.56	8.66
0.90.....	7.79	7.87	7.96	8.05	8.14	8.24	8.34	8.45	8.55
92.....	7.66	7.75	7.84	7.94	8.04	8.14	8.24	8.34	8.44
94.....	7.52	7.62	7.72	7.81	7.92	8.02	8.13	8.24	8.35
96.....		7.52	7.62	7.72	7.83	7.94	8.05	8.16	8.27
98.....			7.51	7.61	7.72	7.83	7.95	8.06	8.19
1.00.....					7.63	7.74	7.87	8.00	8.13
02.....					7.55	7.68	7.82	7.95	8.10
04.....						7.62	7.76	7.91	8.07

The table gives

Opacity $\bar{\varkappa}$. II. $\log A = 4.2$.

3.8	4.0	4.2	4.4	4.6	4.8	5.0	5.2	5.4	θ
0.71	0.76	0.81	0.87	0.92	0.97	1.03	1.10	1.18	.....0.60
0.54	0.59	0.64	0.69	0.75	0.82	0.88	0.96	1.04	 62
0.36	0.42	0.47	0.54	0.61	0.68	0.75	0.83	0.90	 64
0.21	0.27	0.33	0.40	0.47	0.54	0.62	0.70	0.78	 66
0.04	0.11	0.18	0.25	0.33	0.40	0.48	0.56	0.65	 68
9.89	9.96	0.04	0.12	0.19	0.27	0.35	0.44	0.53	.....0.70
9.74	9.81	9.89	9.97	0.05	0.14	0.22	0.32	0.42	 72
9.61	9.68	9.76	9.84	9.93	0.02	0.11	0.21	0.31	 74
9.48	9.56	9.64	9.72	9.82	9.91	0.00	0.10	0.20	 76
9.34	9.42	9.51	9.60	9.69	9.79	9.89	0.00	0.10	 78
9.20	9.30	9.39	9.49	9.58	9.69	9.79	9.89	0.00	.....0.80
9.09	9.18	9.28	9.38	9.48	9.59	9.69	9.80	9.90	 82
8.97	9.06	9.17	9.27	9.37	9.48	9.59	9.70	9.82	 84
8.86	8.96	9.07	9.18	9.28	9.39	9.50	9.62	9.75	 86
8.76	8.86	8.96	9.07	9.19	9.31	9.43	9.56	9.69	 88
8.66	8.76	8.87	8.99	9.11	9.24	9.37	9.50	9.64	.....0.90
8.56	8.67	8.79	8.92	9.05	9.18	9.32	9.46	9.62	 92
8.46	8.59	8.71	8.84	8.98	9.13	9.28	9.43	9.58	 94
8.39	8.52	8.66	8.80	8.95	9.10	9.26	9.42	9.57	 96
8.32	8.47	8.61	8.76	8.92	9.08	9.23	9.40	9.55	 98
8.28	8.43	8.59	8.74	8.91	9.07	9.23	9.40	9.55	.....1.00
8.25	8.41	8.58	8.74	8.91	9.07	9.23	9.38	9.55	 02
8.23	8.40	8.57	8.73	8.90	9.06	9.22	9.38	9.53	 04

$\log \bar{\varkappa}$

Table 10. Model stellar

	$\log g = 3.0$			$\log g = 3.5$		
τ	θ	$\log p$	$\log p_e$	$\log \bar{\varkappa}$	θ	$\log p$	$\log p_e$	$\log \bar{\varkappa}$
0.00	1.000				1.000			
0.01	0.996	3.08			0.996	3.34		
0.02	0.993	3.22			0.993	3.50	0.09	8.60
0.03	0.989	3.31			0.989	3.59	0.17	8.67
0.04	0.985	3.38	9.99		0.985	3.65	0.23	8.71
0.05	0.982	3.44	0.05	8.53	0.982	3.70	0.28	8.76
0.06	0.978	3.48	0.09	8.57	0.978	3.75	0.33	8.80
0.07	0.975	3.52	0.13	8.61	0.975	3.78	0.36	8.83
0.08	0.972	3.55	0.16	8.63	0.972	3.81	0.39	8.86
0.09	0.968	3.58	0.19	8.65	0.968	3.84	0.42	8.88
0.10	0.965	3.60	0.21	8.67	0.965	3.86	0.45	8.90
0.15	0.950	3.69	0.32	8.75	0.950	3.96	0.55	8.98
0.2	0.936	3.76	0.40	8.81	0.936	4.03	0.63	9.04
0.3	0.911	3.86	0.55	8.91	0.911	4.13	0.76	9.13
0.4	0.889	3.92	0.67	8.99	0.889	4.19	0.87	9.19
0.5	0.869	3.97	0.78	9.07	0.869	4.24	0.97	9.26
0.6	0.852	4.00	0.87	9.13	0.852	4.28	1.06	9.32
0.7	0.836	4.03	0.97	9.21	0.836	4.31	1.16	9.38
0.8	0.821	4.05	1.07	9.29	0.821	4.34	1.25	9.45
0.9	0.808	4.07	1.16	9.35	0.808	4.36	1.34	9.52
1.0	0.795	4.08	1.24	9.42	0.795	4.37	1.42	9.57
1.5	0.745	4.13	1.60	9.72	0.745	4.43	1.77	9.86
2	0.707	4.15	1.88	9.98	0.707	4.45	2.04	0.10
3	0.653	4.17	2.28	0.37	0.653	4.48	2.44	0.48
4	0.614	4.18	2.58	0.69	0.614	4.49	2.74	0.77
5	0.585	4.19	2.80	0.95	0.585	4.49	2.96	1.02
6	0.562	4.19	2.97	1.15	0.562	4.50	3.13	1.21
7	0.543	4.19	3.11	1.31	0.543	4.50	3.27	1.38
8	0.527	4.19	3.21	1.45	0.527	4.50	3.38	1.51
9	0.512	4.19	3.31	1.58	0.512	4.50	3.49	1.64
10	0.500	4.20	3.40	1.69	0.500	4.50	3.57	1.75

θ	$\log p$	$\log p_e$	θ	$\log p$	$\log p_e$
0.823	4.05	1.06	0.808	4.35	1.33
0.790	4.10	1.28	0.776	4.40	1.55
0.733	4.20	1.72	0.720	4.50	1.98
0.688	4.30	2.10	0.674	4.60	2.35
0.650	4.40	2.44	0.636	4.70	2.69
0.620	4.50	2.70	0.605	4.80	2.96
0.595	4.60	2.94	0.579	4.90	3.21
0.574	4.70	3.14	0.557	5.00	3.42

atmospheres. $\theta_0 = 1.0$. $\log A = 3.4$

	$\log g = 4.0$				$\log g = 4.5$			
θ	$\log p$	$\log p_e$	$\log \bar{\varkappa}$	θ	$\log p$	$\log p_e$	$\log \bar{\varkappa}$	τ
1.000				1.000				..... 0.00
0.996	3.60	0.17	8.69	0.996	3.90	0.44	8.94	..... 0.01
0.993	3.76	0.32	8.82	0.993	4.05	0.56	9.07	..... 0.02
0.989	3.85	0.41	8.90	0.989	4.14	0.66	9.15	..... 0.03
0.985	3.92	0.47	8.95	0.985	4.21	0.72	9.21	..... 0.04
0.982	3.97	0.52	8.99	0.982	4.25	0.76	9.24	..... 0.05
0.978	4.01	0.56	9.03	0.978	4.29	0.80	9.27	..... 0.06
0.975	4.05	0.60	9.06	0.975	4.32	0.83	9.30	..... 0.07
0.972	4.08	0.63	9.09	0.972	4.35	0.86	9.33	..... 0.08
0.968	4.11	0.66	9.12	0.968	4.38	0.89	9.35	..... 0.09
0.965	4.13	0.68	9.14	0.965	4.40	0.91	9.37	..... 0.10
0.950	4.23	0.79	9.22	0.950	4.50	1.02	9.45	..... 0.15
0.936	4.29	0.86	9.26	0.936	4.57	1.10	9.50	..... 0.2
0.911	4.39	0.99	9.35	0.911	4.66	1.22	9.58	..... 0.3
0.889	4.46	1.10	9.42	0.889	4.73	1.32	9.63	..... 0.4
0.869	4.51	1.18	9.47	0.869	4.79	1.41	9.68	..... 0.5
0.852	4.55	1.27	9.51	0.852	4.83	1.48	9.72	..... 0.6
0.836	4.59	1.36	9.57	0.836	4.86	1.55	9.77	..... 0.7
0.821	4.62	1.44	9.64	0.821	4.89	1.63	9.82	..... 0.8
0.808	4.64	1.51	9.70	0.808	4.92	1.71	9.87	..... 0.9
0.795	4.65	1.59	9.74	0.795	4.94	1.78	9.92	..... 1.0
0.745	4.72	1.93	0.00	0.745	5.01	2.09	0.16	..... 1.5
0.707	4.75	2.20	0.23	0.707	5.04	2.36	0.36	 2
0.653	4.78	2.59	0.59	0.653	5.07	2.75	0.71	 3
0.614	4.79	2.89	0.86	0.614	5.09	3.04	0.96	 4
0.585	4.80	3.11	1.10	0.585	5.10	3.27	1.17	 5
0.562	4.80	3.28	1.29	0.562	5.11	3.45	1.37	 6
0.543	4.81	3.44	1.45	0.543	5.11	3.60	1.53	 7
0.527	4.81	3.55	1.58	0.527	5.12	3.71	1.65	 8
0.512	4.81	3.66	1.71	0.512	5.12	3.82	1.77	 9
0.500	4.81	3.74	1.81	0.500	5.12	3.92	1.87	10

θ	$\log p$	$\log p_e$	θ	$\log p$	$\log p_e$
.795	4.65	1.59	0.786	4.96	1.83
.763	4.70	1.80	0.759	5.00	2.01
.707	4.80	2.22	0.701	5.10	2.42
.660	4.90	2.62	0.650	5.20	2.84
.621	5.00	2.95	0.610	5.30	
.589	5.10	3.23	0.578	5.40	3.47
.563	5.20	3.48	0.550	5.50	3.74
.540	5.30	3.71	0.527	5.60	3.96

Table 10 (continued). Model stellar

	log g = 3.0				log g = 3.5			
τ	θ	log p	log p_e	log $\bar{\varkappa}$	θ	log p	log p_e	log $\bar{\varkappa}$
0.00.....	1.000				1.000			
0.01.....	0.996	3.22	9.55	8.06	0.996	3.47	9.75	8.26
0.02.....	0.993	3.36	9.67	8.17	0.993	3.65	9.91	8.41
0.03.....	0.989	3.46	9.76	8.26	0.989	3.74	9.99	8.49
0.04.....	0.985	3.53	9.83	8.31	0.985	3.80	0.05	8.54
0.05.....	0.982	3.59	9.88	8.36	0.982	3.85	0.10	8.58
0.06.....	0.978	3.63	9.93	8.40	0.978	3.89	0.14	8.61
0.07.....	0.975	3.67	9.97	8.43	0.975	3.93	0.18	8.64
0.08.....	0.972	3.71	0.00	8.47	0.972	3.96	0.21	8.67
0.09.....	0.968	3.74	0.05	8.49	0.968	3.99	0.24	8.70
0.10.....	0.965	3.76	0.07	8.52	0.965	4.01	0.27	8.73
0.15.....	0.950	3.85	0.18	8.61	0.950	4.11	0.39	8.81
0.2	0.936	3.92	0.29	8.69	0.936	4.18	0.48	8.88
0.3	0.911	4.00	0.45	8.82	0.911	4.27	0.64	9.00
0.4	0.889	4.06	0.60	8.93	0.889	4.33	0.78	9.09
0.5	0.869	4.09	0.73	9.02	0.869	4.38	0.91	9.20
0.6	0.852	4.12	0.85	9.10	0.852	4.41	1.02	9.28
0.7	0.836	4.15	0.97	9.19	0.836	4.44	1.13	9.36
0.8	0.821	4.17	1.07	9.28	0.821	4.46	1.24	9.44
0.9	0.808	4.18	1.17	9.36	0.808	4.47	1.33	9.51
1.0	0.795	4.19	1.27	9.43	0.795	4.48	1.42	9.57
1.5	0.745	4.22	1.63	9.75	0.745	4.52	1.78	9.87
2	0.707	4.24	1.92	0.01	0.707	4.54	2.07	0.12
3	0.653	4.26	2.33	0.40	0.653	4.56	2.49	0.52
4	0.614	4.26	2.62	0.70	0.614	4.57	2.78	0.77
5	0.585	4.27	2.84	0.97	0.585	4.58	3.00	1.04
6	0.562	4.27	3.01	1.16	0.562	4.58	3.17	1.22
7	0.543	4.27	3.15	1.33	0.543	4.58	3.32	1.40
8	0.527	4.27	3.26	1.46	0.527	4.58	3.43	1.53
9	0.512	4.27	3.36	1.59	0.512	4.58	3.53	1.65
10	0.500	4.27	3.44	1.70	0.500	4.58	3.61	1.77

θ	log p	log p_e	θ	log p	log p_e
0.844	4.14	0.88	0.832	4.44	1.16
0.804	4.20	1.20	0.794	4.50	1.43
0.743	4.30	1.69	0.735	4.60	1.90
0.696	4.40	2.08	0.686	4.70	2.31
0.656	4.50	2.43	0.644	4.80	2.68
0.624	4.60	2.72	0.610	4.90	2.98
0.598	4.70	2.96	0.582	5.00	3.24
0.575	4.80	3.19	0.557	5.10	3.47

atmospheres. $\theta_0 = 1.0$. $\log A = 3.8$.

	$\log g = 4.0$				$\log g = 4.5$				
θ	$\log p$	$\log p_e$	$\log \bar{\varkappa}$	θ	$\log p$	$\log p_e$	$\log \bar{\varkappa}$		τ
1.000				1.000				.....	0.00
0.996	3.78	0.01	8.52	0.996	4.00	0.19	8.70	.....	0.01
0.993	3.95	0.15	8.66	0.993	4.18	0.35	8.86	.....	0.02
0.989	4.05	0.25	8.74	0.989	4.29	0.44	8.95	.....	0.03
0.985	4.11	0.31	8.79	0.985	4.36	0.52	9.01	.....	0.04
0.982	4.16	0.36	8.84	0.982	4.41	0.57	9.06	.....	0.05
0.978	4.20	0.39	8.87	0.978	4.45	0.61	9.09	.....	0.06
0.975	4.23	0.43	8.90	0.975	4.49	0.65	9.12	.....	0.07
0.972	4.26	0.46	8.93	0.972	4.52	0.68	9.15	.....	0.08
0.968	4.29	0.49	8.96	0.968	4.55	0.71	9.18	.....	0.09
0.965	4.31	0.52	8.98	0.965	4.57	0.73	9.19	.....	0.10
0.950	4.41	0.63	9.06	0.950	4.67	0.84	9.28	.....	0.15
0.936	4.47	0.71	9.12	0.936	4.73	0.92	9.32	.....	0.2
0.911	4.56	0.86	9.22	0.911	4.83	1.06	9.42	.....	0.3
0.889	4.62	0.98	9.30	0.889	4.89	1.18	9.50	.....	0.4
0.869	4.67	1.10	9.38	0.869	4.94	1.28	9.57	.....	0.5
0.852	4.70	1.20	9.46	0.852	4.98	1.39	9.64	.....	0.6
0.836	4.73	1.30	9.53	0.836	5.01	1.48	9.71	.....	0.7
0.821	4.75	1.40	9.60	0.821	5.03	1.57	9.78	.....	0.8
0.808	4.77	1.50	9.67	0.808	5.05	1.66	9.84	.....	0.9
0.795	4.78	1.58	9.74	0.795	5.07	1.75	9.90	.....	1.0
0.745	4.83	1.95	0.02	0.745	5.12	2.11	0.15	.....	1.5
0.707	4.85	2.23	0.25	0.707	5.15	2.39	0.39	.....	2
0.653	4.87	2.64	0.63	0.653	5.18	2.80	0.75	.....	3
0.614	4.88	2.94	0.90	0.614	5.19	3.09	1.01	.....	4
0.585	4.90	3.16	1.12	0.585	5.19	3.32	1.21	.....	5
0.562	4.90	3.34	1.31	0.562	5.20	3.49	1.39	.....	6
0.543	4.91	3.49	1.48	0.543	5.20	3.64	1.56	.....	7
0.527	4.91	3.60	1.61	0.527	5.20	3.76	1.68	.....	8
0.512	4.91	3.71	1.73	0.512	5.21	3.87	1.80	.....	9
0.500	4.91	3.80	1.83	0.500	5.21	3.97	1.90	.....	10

θ	$\log p$	$\log p_e$	θ	$\log p$	$\log p_e$
0.823	4.75	1.40	0.812	5.05	1.64
0.788	4.80	1.65	0.777	5.10	1.88
0.726	4.90	2.12	0.717	5.20	2.34
0.675	5.00	2.54	0.664	5.30	2.78
0.633	5.10	2.91	0.620	5.40	3.16
0.598	5.20	3.22	0.586	5.50	3.46
0.569	5.30	3.49	0.556	5.60	3.74
0.544	5.40	3.73	0.529	5.70	

Tabel 10 (continued). Model stellar

	$\log g = 3.0$			$\log g = 3.5$			
τ	θ	$\log p$	$\log p_e$	$\log \bar{\varkappa}$	θ	$\log p$	$\log p_e$	$\log \bar{\varkappa}$
0.00.....	1.000				1.000			
0.01.....	0.996	3.30	9.44	7.95	0.996	3.60	9.64	8.15
0.02.....	0.993	3.47	9.57	8.08	0.993	3.77	9.77	8.27
0.03.....	0.989	3.57	9.65	8.15	0.989	3.87	9.86	8.35
0.04.....	0.985	3.65	9.71	8.20	0.985	3.94	9.92	8.42
0.05.....	0.982	3.70	9.76	8.25	0.982	4.00	9.98	8.47
0.06.....	0.978	3.75	9.82	8.30	0.978	4.04	0.03	8.51
0.07.....	0.975	3.78	9.86	8.33	0.975	4.08	0.07	8.54
0.08.....	0.972	3.82	9.90	8.36	0.972	4.11	0.10	8.57
0.09.....	0.968	3.84	9.93	8.39	0.968	4.14	0.13	8.60
0.10.....	0.965	3.87	9.96	8.42	0.965	4.16	0.16	8.62
0.15.....	0.950	3.96	0.10	8.52	0.950	4.25	0.29	8.72
0.2	0.936	4.02	0.21	8.61	0.936	4.32	0.40	8.80
0.3	0.911	4.10	0.40	8.77	0.911	4.40	0.59	8.95
0.4	0.889	4.15	0.57	8.89	0.889	4.45	0.75	9.06
0.5	0.869	4.18	0.72	9.01	0.869	4.48	0.89	9.16
0.6	0.852	4.21	0.85	9.11	0.852	4.51	1.01	9.26
0.7	0.836	4.22	0.97	9.20	0.836	4.53	1.13	9.35
0.8	0.821	4.24	1.08	9.28	0.821	4.55	1.24	9.44
0.9	0.808	4.25	1.18	9.36	0.808	4.56	1.34	9.52
1.0	0.795	4.26	1.28	9.44	0.795	4.57	1.44	9.60
1.5	0.745	4.29	1.66	9.77	0.745	4.60	1.82	9.90
2	0.707	4.30	1.95	0.03	0.707	4.62	2.11	0.15
3	0.653	4.32	2.36	0.42	0.653	4.63	2.53	0.53
4	0.614	4.32	2.65	0.72	0.614	4.64	2.81	0.81
5	0.585	4.33	2.87	0.98	0.585	4.64	3.03	1.06
6	0.562	4.33	3.04	1.18	0.562	4.65	3.21	1.25
7	0.543	4.33	3.18	1.34	0.543	4.65	3.35	1.41
8	0.527	4.33	3.29	1.48	0.527	4.65	3.46	1.54
9	0.512	4.33	3.40	1.61	0.512	4.65	3.56	1.67
10	0.500	4.33	3.48	1.72	0.500	4.65	3.65	1.78

θ	$\log p$	$\log p_e$	θ	$\log p$	$\log p_e$
0.860	4.20	0.79	0.850	4.51	1.03
0.792	4.30	1.32	0.794	4.60	1.46
0.735	4.40	1.79	0.730	4.70	1.98
0.690	4.50	2.18	0.680	4.80	2.41
0.649	4.60	2.53	0.638	4.90	2.76
0.617	4.70	2.82	0.605	5.00	3.06
0.591	4.80	3.07	0.576	5.10	3.33
0.569	4.90	3.28	0.553	5.20	3.52

atmospheres. $\theta_0 = 1.0$. $\log A = 4.2$.

	$\log g = 4.0$				$\log g = 4.5$				
θ	$\log p$	$\log p_e$	$\log \varkappa$	θ	$\log p$	$\log p_e$	$\log \varkappa$		τ
1.000				1.000				.....	0.00
0.996	3.90	9.85	8.36	0.996	4.20	0.09	8.59	.....	0.01
0.993	4.07	9.99	8.50	0.993	4.36	0.22	8.72	.....	0.02
0.989	4.17	0.08	8.58	0.989	4.45	0.30	8.79	.....	0.03
0.985	4.24	0.15	8.64	0.985	4.52	0.37	8.86	.....	0.04
0.982	4.29	0.20	8.68	0.982	4.57	0.41	8.90	.....	0.05
0.978	4.33	0.24	8.71	0.978	4.62	0.45	8.94	.....	0.06
0.975	4.37	0.28	8.74	0.975	4.65	0.49	8.97	.....	0.07
0.972	4.40	0.32	8.77	0.972	4.68	0.53	8.99	.....	0.08
0.968	4.43	0.35	8.80	0.968	4.71	0.56	9.02	.....	0.09
0.965	4.45	0.37	8.83	0.965	4.73	0.58	9.04	.....	0.10
0.950	4.54	0.49	8.93	0.950	4.83	0.71	9.13	.....	0.15
0.936	4.60	0.60	9.00	0.936	4.89	0.81	9.21	.....	0.2
0.911	4.69	0.77	9.14	0.911	4.98	0.97	9.33	.....	0.3
0.889	4.74	0.92	9.24	0.889	5.03	1.10	9.42	.....	0.4
0.869	4.78	1.06	9.34	0.869	5.08	1.24	9.51	.....	0.5
0.852	4.81	1.18	9.44	0.852	5.11	1.36	9.60	.....	0.6
0.836	4.83	1.30	9.52	0.836	5.13	1.47	9.68	.....	0.7
0.821	4.85	1.40	9.60	0.821	5.15	1.57	9.76	.....	0.8
0.808	4.86	1.50	9.68	0.808	5.17	1.66	9.83	.....	0.9
0.795	4.87	1.60	9.75	0.795	5.18	1.76	9.90	.....	1.0
0.745	4.91	1.98	0.04	0.745	5.22	2.14	0.19	.....	1.5
0.707	4.93	2.27	0.27	0.707	5.24	2.42	0.41	.....	2
0.653	4.95	2.68	0.65	0.653	5.26	2.84	0.77	.....	3
0.614	4.95	2.97	0.91	0.614	5.27	3.14	1.03	.....	4
0.585	4.96	3.20	1.13	0.585	5.27	3.35	1.23	.....	5
0.562	4.96	3.37	1.33	0.562	5.28	3.53	1.41	.....	6
0.543	4.96	3.52	1.49	0.543	5.28	3.69	1.57	.....	7
0.527	4.96	3.63	1.62	0.527	5.28	3.80	1.69	.....	8
0.512	4.97	3.74	1.74	0.512	5.28	3.91	1.81	.....	9
0.500	4.97	3.83	1.84	0.500	5.28	4.01	1.92	.....	10

θ	$\log p$	$\log p_e$	θ	$\log p$	$\log p_e$
0.842	4.83	1.25	0.832	5.14	1.50
0.792	4.90	1.64	0.790	5.20	1.81
0.730	5.00	2.14	0.725	5.30	2.32
0.677	5.10	2.58	0.670	5.40	2.78
0.633	5.20	2.95	0.626	5.50	3.16
0.596	5.30	3.28	0.587	5.60	3.50
0.566	5.40	3.56	0.556	5.70	3.79
0.540	5.50	3.81	0.529	5.80	

Table 11. Model stellar atmospheres.

$\theta_0 = 0.9$. $\log A = 3.4$.

	$\log g = 3.5$				$\log g = 4.0$				$\log g = 4.5$			
τ	θ	$\log p$	$\log p_e$	$\log \varkappa$	θ	$\log p$	$\log p_e$	$\log \varkappa$	θ	$\log p$	$\log p_e$	$\log \varkappa$
0.00...	0.900				0.900				0.900			
0.01...	0.896	3.23	0.14	8.50	0.896	3.54	0.35	8.70	0.896	3.87	0.60	8.94
0.02...	0.893	3.42	0.29	8.62	0.893	3.72	0.50	8.83	0.893	4.03	0.73	9.06
0.03...	0.890	3.52	0.37	8.70	0.890	3.82	0.58	8.91	0.890	4.12	0.81	9.14
0.04...	0.887	3.59	0.43	8.76	0.887	3.89	0.65	8.97	0.887	4.19	0.88	9.20
0.05...	0.884	3.65	0.48	8.81	0.884	3.95	0.71	9.02	0.884	4.24	0.93	9.24
0.06...	0.881	3.69	0.53	8.85	0.881	3.99	0.75	9.05	0.881	4.29	0.98	9.28
0.07...	0.878	3.73	0.57	8.88	0.878	4.03	0.79	9.08	0.878	4.32	1.01	9.31
0.08...	0.875	3.76	0.60	8.91	0.875	4.06	0.82	9.11	0.875	4.35	1.04	9.34
0.09...	0.872	3.79	0.64	8.93	0.872	4.09	0.85	9.15	0.872	4.38	1.07	9.36
0.10...	0.869	3.81	0.67	8.96	0.869	4.11	0.88	9.17	0.869	4.40	1.10	9.38
0.15...	0.853	3.90	0.80	9.06	0.853	4.20	1.01	9.26	0.853	4.49	1.22	9.47
0.2 ...	0.843	3.97	0.90	9.14	0.843	4.27	1.10	9.34	0.843	4.56	1.31	9.54
0.3 ...	0.820	4.05	1.07	9.29	0.820	4.35	1.26	9.47	0.820	4.64	1.46	9.66
0.4 ...	0.800	4.10	1.22	9.40	0.800	4.41	1.41	9.58	0.800	4.70	1.59	9.75
0.5 ...	0.782	4.14	1.36	9.52	0.782	4.44	1.54	9.68	0.782	4.74	1.72	9.84
0.6 ...	0.767	4.16	1.47	9.61	0.767	4.47	1.65	9.77	0.767	4.77	1.82	9.92
0.7 ...	0.752	4.18	1.58	9.70	0.752	4.50	1.76	9.85	0.752	4.80	1.93	0.01
0.8 ...	0.739	4.20	1.68	9.79	0.739	4.51	1.85	9.93	0.739	4.82	2.03	0.08
0.9 ...	0.727	4.21	1.77	9.87	0.727	4.53	1.94	0.01	0.727	4.84	2.11	0.15
1.0 ...	0.716	4.22	1.85	9.94	0.716	4.54	2.02	0.08	0.716	4.85	2.20	0.21
1.5 ...	0.670	4.25	2.21	0.28	0.670	4.57	2.37	0.40	0.670	4.89	2.54	0.52
2 ...	0.636	4.27	2.46	0.54	0.636	4.59	2.63	0.65	0.636	4.91	2.80	0.75
3 ...	0.588	4.28	2.82	0.94	0.588	4.61	3.00	1.02	0.588	4.93	3.16	1.11
4 ...	0.553	4.29	3.08	1.25	0.553	4.62	3.26	1.32	0.553	4.94	3.43	1.40
5 ...	0.527	4.29	3.27	1.47	0.527	4.62	3.45	1.54	0.527	4.94	3.62	1.61
6 ...	0.506	4.29	3.40	1.66	0.506	4.62	3.60	1.72	0.506	4.94	3.77	1.79
7 ...	0.489	4.30	3.53	1.79	0.489	4.62	3.72	1.86	0.489	4.95	3.90	1.93
8 ...	0.474	4.30	3.61	1.89	0.474	4.63	3.82	1.98	0.474	4.95	4.01	2.05
9 ...	0.461	4.30	3.69	1.98	0.461	4.63	3.90	2.07	0.461	4.95	4.09	2.14
10 ...	0.450	4.30	3.74	2.03	0.450	4.63	3.96	2.13	0.450	4.95	4.15	2.21

θ	$\log p$	$\log p_e$	θ	$\log p$	$\log p_e$	θ	$\log p$	$\log p_e$
0.776	4.15	1.41	0.768	4.47	1.64	0.756	4.79	1.90
0.747	4.20	1.62	0.756	4.50	1.73	0.749	4.80	1.95
0.699	4.30	2.02	0.699	4.60	2.18	0.691	4.90	2.39
0.661	4.40	2.35	0.657	4.70	2.53	0.648	5.00	2.75
0.631	4.50	2.62	0.623	4.80	2.82	0.613	5.10	3.06
0.605	4.60	2.86	0.593	4.90	3.10	0.583	5.20	3.33
0.582	4.70	3.08	0.569	5.00	3.33	0.557	5.30	3.58
0.561	4.80	3.28	0.548	5.10	3.54	0.534	5.40	3.80
0.543	4.90	3.48	0.530	5.20	3.74	0.512	5.50	

Table 11 (continued). Model stellar atmospheres.

$\theta_0 = 0.9$. $\log A = 3.8$.

	$\log g = 3.5$				$\log g = 4.0$				$\log g = 4.5$			
τ	θ	$\log p$	$\log p_e$	$\log \varkappa$	θ	$\log p$	$\log p_e$	$\log \varkappa$	θ	$\log p$	$\log p_e$	$\log \varkappa$
0.00...	0.900				0.900				0.900			
0.01...	0.896	3.29	0.10	8.45	0.896	3.60	0.28	8.63	0.896	3.90	0.46	8.81
0.02...	0.893	3.47	0.22	8.56	0.893	3.78	0.40	8.75	0.893	4.08	0.59	8.92
0.03...	0.890	3.58	0.30	8.64	0.890	3.89	0.49	8.82	0.890	4.19	0.68	9.00
0.04...	0.887	3.65	0.36	8.69	0.887	3.96	0.55	8.88	0.887	4.27	0.75	9.07
0.05...	0.884	3.71	0.41	8.74	0.884	4.02	0.60	8.92	0.884	4.33	0.80	9.11
0.06...	0.881	3.75	0.45	8.78	0.881	4.06	0.64	8.96	0.881	4.37	0.84	9.15
0.07...	0.878	3.79	0.49	8.81	0.878	4.10	0.68	8.99	0.878	4.41	0.88	9.19
0.08...	0.875	3.82	0.53	8.84	0.875	4.13	0.72	9.02	0.875	4.44	0.92	9.22
0.09...	0.872	3.85	0.57	8.87	0.872	4.16	0.76	9.05	0.872	4.47	0.95	9.25
0.10...	0.869	3.87	0.60	8.89	0.869	4.19	0.79	9.07	0.869	4.49	0.98	9.26
0.15...	0.853	3.96	0.75	9.02	0.853	4.28	0.93	9.20	0.853	4.59	1.13	9.38
0.2 ...	0.843	4.03	0.85	9.11	0.843	4.34	1.03	9.28	0.843	4.66	1.22	9.46
0.3 ...	0.820	4.11	1.05	9.26	0.820	4.42	1.22	9.43	0.820	4.73	1.40	9.60
0.4 ...	0.800	4.16	1.21	9.39	0.800	4.47	1.38	9.55	0.800	4.79	1.56	9.72
0.5 ...	0.782	4.19	1.35	9.51	0.782	4.51	1.52	9.67	0.782	4.82	1.70	9.82
0.6 ...	0.767	4.21	1.47	9.61	0.767	4.53	1.64	9.76	0.767	4.85	1.82	9.91
0.7 ...	0.752	4.23	1.59	9.71	0.752	4.55	1.75	9.85	0.752	4.87	1.93	0.00
0.8 ...	0.739	4.25	1.69	9.80	0.739	4.57	1.85	9.94	0.739	4.89	2.03	0.08
0.9 ...	0.727	4.26	1.79	9.88	0.727	4.58	1.95	0.02	0.727	4.90	2.12	0.16
1.0 ...	0.716	4.27	1.87	9.95	0.716	4.59	2.04	0.09	0.716	4.92	2.21	0.23
1.5 ...	0.670	4.29	2.23	0.28	0.670	4.62	2.40	0.41	0.670	4.95	2.55	0.54
2 ...	0.636	4.31	2.48	0.54	0.636	4.64	2.65	0.65	0.636	4.97	2.82	0.77
3 ...	0.588	4.32	2.85	0.95	0.588	4.65	3.01	1.03	0.588	4.98	3.19	1.13
4 ...	0.553	4.32	3.10	1.25	0.553	4.66	3.28	1.34	0.553	4.99	3.45	1.42
5 ...	0.527	4.33	3.29	1.48	0.527	4.66	3.47	1.56	0.527	5.00	3.65	1.62
6 ...	0.506	4.33	3.44	1.66	0.506	4.66	3.62	1.73	0.506	5.00	3.80	1.80
7 ...	0.489	4.33	3.55	1.79	0.489	4.67	3.75	1.87	0.489	5.00	3.93	1.94
8 ...	0.474	4.33	3.63	1.90	0.474	4.67	3.84	1.98	0.474	5.00	4.03	2.06
9 ...	0.461	4.33	3.71	1.99	0.461	4.67	3.92	2.07	0.461	5.00	4.11	2.16
10 ...	0.450	4.33	3.76	2.04	0.450	4.67	3.99	2.14	0.450	5.01	4.19	2.23

θ	$\log p$	$\log p_e$	θ	$\log p$	$\log p_e$	θ	$\log p$	$\log p_e$
0.783	4.19	1.34						
0.777	4.20	1.39	0.777	4.52	1.56	0.768	4.85	1.81
0.723	4.30	1.84	0.726	4.60	1.96	0.735	4.90	2.06
0.680	4.40	2.21	0.680	4.70	2.36	0.683	5.00	2.49
0.643	4.50	2.53	0.642	4.80	2.69	0.640	5.10	2.86
0.613	4.60	2.80	0.610	4.90	2.98	0.606	5.20	3.16
0.589	4.70	3.03	0.580	5.00	3.25	0.574	5.30	3.45
0.567	4.80	3.25	0.556	5.10	3.48	0.548	5.40	3.70
0.547	4.90	3.45	0.534	5.20	3.70	0.526	5.50	3.92

Table 11 (continued). Model stellar atmospheres.

$\theta_0 = 0.9$. $\log A = 4.2$.

	$\log g = 3.5$				$\log g = 4.0$				$\log g = 4.5$			
τ	θ	$\log p$	$\log p_e$	$\log \varkappa$	θ	$\log p$	$\log p_e$	$\log \varkappa$	θ	$\log p$	$\log p_e$	$\log \varkappa$
0.00...	0.900				0.900				0.900			
0.01...	0.896	3.30	0.06	8.42	0.896	3.66	0.26	8.60	0.896	3.97	0.42	8.76
0.02...	0.893	3.49	0.18	8.53	0.893	3.84	0.37	8.71	0.893	4.16	0.55	8.88
0.03...	0.890	3.60	0.26	8.60	0.890	3.94	0.45	8.78	0.890	4.26	0.63	8.95
0.04...	0.887	3.67	0.32	8.65	0.887	4.01	0.50	8.83	0.887	4.33	0.69	9.00
0.05...	0.884	3.73	0.37	8.70	0.884	4.07	0.55	8.87	0.884	4.39	0.74	9.05
0.06...	0.881	3.77	0.41	8.74	0.881	4.11	0.60	8.91	0.881	4.43	0.78	9.09
0.07...	0.878	3.81	0.45	8.78	0.878	4.15	0.64	8.95	0.878	4.47	0.82	9.13
0.08...	0.875	3.84	0.49	8.81	0.875	4.18	0.68	8.98	0.875	4.51	0.86	9.16
0.09...	0.872	3.87	0.53	8.84	0.872	4.21	0.71	9.01	0.872	4.54	0.90	9.19
0.10...	0.869	3.90	0.57	8.86	0.869	4.23	0.74	9.03	0.869	4.57	0.94	9.22
0.15...	0.853	3.99	0.73	8.99	0.853	4.33	0.91	9.17	0.853	4.66	1.09	9.34
0.2 ...	0.843	4.05	0.83	9.07	0.843	4.39	1.01	9.25	0.843	4.71	1.18	9.42
0.3 ...	0.820	4.13	1.03	9.24	0.820	4.46	1.20	9.40	0.820	4.79	1.38	9.58
0.4 ...	0.800	4.18	1.20	9.38	0.800	4.51	1.37	9.54	0.800	4.84	1.55	9.71
0.5 ...	0.782	4.21	1.35	9.50	0.782	4.54	1.52	9.66	0.782	4.87	1.69	9.81
0.6 ...	0.767	4.23	1.47	9.60	0.767	4.57	1.64	9.76	0.767	4.90	1.81	9.91
0.7 ...	0.752	4.25	1.59	9.71	0.752	4.59	1.76	9.86	0.752	4.92	1.93	0.00
0.8 ...	0.739	4.26	1.69	9.79	0.739	4.60	1.86	9.94	0.739	4.93	2.03	0.09
0.9 ...	0.727	4.27	1.78	9.87	0.727	4.61	1.95	0.01	0.727	4.94	2.13	0.16
1.0 ...	0.716	4.28	1.87	9.95	0.716	4.62	2.04	0.09	0.716	4.95	2.21	0.23
1.5 ...	0.670	4.31	2.23	0.29	0.670	4.65	2.40	0.42	0.670	4.98	2.57	0.54
2 ...	0.636	4.32	2.49	0.54	0.636	4.66	2.66	0.66	0.636	5.00	2.83	0.78
3 ...	0.588	4.33	2.85	0.95	0.588	4.68	3.03	1.04	0.588	5.01	3.19	1.13
4 ...	0.553	4.34	3.11	1.26	0.553	4.68	3.29	1.34	0.553	5.02	3.47	1.42
5 ...	0.527	4.34	3.30	1.48	0.527	4.69	3.48	1.56	0.527	5.03	3.67	1.64
6 ...	0.506	4.34	3.45	1.67	0.506	4.69	3.63	1.74	0.506	5.03	3.82	1.81
7 ...	0.489	4.34	3.55	1.80	0.489	4.69	3.76	1.88	0.489	5.03	3.94	1.95
8 ...	0.474	4.35	3.65	1.91	0.474	4.69	3.86	2.00	0.474	5.03	4.05	2.07
9 ...	0.461	4.35	3.72	1.99	0.461	4.69	3.93	2.08	0.461	5.03	4.13	2.17
10 ...	0.450	4.35	3.78	2.04	0.450	4.69	4.00	2.14	0.450	5.03	4.21	2.24

θ	$\log p$	$\log p_e$	θ	$\log p$	$\log p_e$	θ	$\log p$	$\log p_e$
0.785	4.21	1.32	0.781	4.54	1.52	0.776	4.89	1.74
0.738	4.30	1.72	0.749	4.60	1.79	0.768	4.90	1.80
0.693	4.40	2.10	0.696	4.70	2.23	0.710	5.00	2.28
0.655	4.50	2.43	0.652	4.80	2.61	0.661	5.10	2.70
0.623	4.60	2.73	0.619	4.90	2.91	0.620	5.20	3.05
0.598	4.70	2.97	0.589	5.00	3.18	0.586	5.30	3.36
0.575	4.80	3.19	0.565	5.10	3.41	0.558	5.40	3.62
0.554	4.90	3.40	0.543	5.20	3.64	0.534	5.50	3.86
0.536	5.00	3.59	0.523	5.30	3.80			

Table 12. Model stellar atmospheres.

$\theta_0 = 0.8$. $\log A = 3.8$.

	$\log g = 3.5$				$\log g = 4.0$				$\log g = 4.5$			
τ	θ	$\log p$	$\log p_e$	$\log \varkappa$	θ	$\log p$	$\log p_e$	$\log \varkappa$	θ	$\log p$	$\log p_e$	$\log \varkappa$
0.00...	0.800				0.800				0.800			
0.01...	0.796	2.84	0.56	8.86	0.796	3.20	0.74	9.00	0.796	3.54	0.92	9.14
0.02...	0.793	3.04	0.68	8.96	0.793	3.40	0.87	9.10	0.793	3.75	1.05	9.25
0.03...	0.790	3.16	0.76	9.02	0.790	3.52	0.95	9.17	0.790	3.86	1.12	9.31
0.04...	0.787	3.24	0.82	9.08	0.787	3.60	1.01	9.22	0.787	3.94	1.18	9.37
0.05...	0.785	3.30	0.87	9.12	0.785	3.66	1.05	9.25	0.785	4.00	1.23	9.40
0.06...	0.782	3.34	0.91	9.16	0.782	3.70	1.09	9.30	0.782	4.05	1.28	9.44
0.07...	0.779	3.38	0.95	9.19	0.779	3.74	1.14	9.34	0.779	4.09	1.32	9.48
0.08...	0.777	3.41	0.99	9.22	0.777	3.78	1.17	9.36	0.777	4.12	1.35	9.50
0.09...	0.774	3.44	1.02	9.25	0.774	3.81	1.21	9.39	0.774	4.15	1.38	9.54
0.10...	0.772	3.47	1.05	9.28	0.772	3.83	1.23	9.42	0.772	4.18	1.42	9.56
0.15...	0.760	3.57	1.19	9.39	0.760	3.92	1.37	9.54	0.760	4.28	1.56	9.68
0.2 ...	0.749	3.63	1.30	9.48	0.749	3.99	1.49	9.63	0.749	4.34	1.67	9.78
0.3 ...	0.729	3.71	1.49	9.65	0.729	4.07	1.67	9.78	0.729	4.42	1.85	9.93
0.4 ...	0.711	3.76	1.65	9.80	0.711	4.12	1.84	9.93	0.711	4.47	2.01	0.07
0.5 ...	0.695	3.79	1.78	9.93	0.695	4.15	1.97	0.05	0.695	4.50	2.14	0.19
0.6 ...	0.681	3.82	1.90	0.04	0.681	4.17	2.08	0.16	0.681	4.53	2.27	0.29
0.7 ...	0.669	3.83	1.99	0.14	0.669	4.19	2.18	0.26	0.669	4.55	2.37	0.39
0.8 ...	0.657	3.85	2.09	0.25	0.657	4.21	2.27	0.35	0.657	4.56	2.46	0.48
0.9 ...	0.646	3.86	2.18	0.34	0.646	4.22	2.36	0.44	0.646	4.57	2.54	0.56
1.0 ...	0.636	3.86	2.25	0.42	0.636	4.23	2.44	0.51	0.636	4.58	2.62	0.63
1.5 ...	0.596	3.89	2.56	0.77	0.596	4.25	2.74	0.86	0.596	4.61	2.93	0.95
2 ...	0.566	3.90	2.78	1.05	0.566	4.27	2.98	1.13	0.566	4.63	3.17	1.22
3 ...	0.522	3.91	3.09	1.43	0.522	4.28	3.29	1.51	0.522	4.64	3.50	1.58
4 ...	0.492	3.91	3.27	1.67	0.492	4.28	3.50	1.76	0.492	4.65	3.72	1.84
5 ...	0.468	3.92	3.39	1.81	0.468	4.28	3.64	1.93	0.468	4.65	3.86	2.02
6 ...	0.450	3.92	3.47	1.88	0.450	4.29	3.74	2.03	0.450	4.65	3.98	2.13
7 ...	0.434	3.92	3.52	1.90	0.434	4.29	3.81	2.08	0.434	4.66	4.06	2.21
8 ...	0.421	3.92	3.55	1.90	0.421	4.29	3.86	2.12	0.421	4.66	4.13	2.27
9 ...	0.410	3.92	3.57	1.88	0.410	4.29	3.89	2.12	0.410	4.66	4.17	2.31
10 ...	0.400	3.93	3.59	1.85	0.400	4.29	3.91	2.12	0.400	4.66	4.22	2.34

θ	$\log p$	$\log p_e$	θ	$\log p$	$\log p_e$	θ	$\log p$	$\log p_e$
0.718	3.75	1.59	0.710	4.12	1.84	0.707	4.49	2.05
0.701	3.80	1.73						
0.672	3.90	2.00	0.678	4.20	2.12	0.702	4.50	2.09
0.646	4.00	2.24	0.645	4.30	2.42	0.660	4.60	2.45
0.621	4.10	2.49	0.619	4.40	2.66	0.624	4.70	2.77
0.600	4.20	2.69	0.595	4.50	2.88	0.596	4.80	3.03
0.582	4.30	2.89	0.575	4.60	3.08	0.572	4.90	3.26
0.565	4.40	3.06	0.557	4.70	3.26	0.550	5.00	3.48
0.549	4.50	3.23	0.539	4.80	3.45	0.532	5.10	3.67
			0.523	4.90	3.62	0.514	5.20	3.86

Table 13. Model stellar atmospheres.

$\theta_0 = 0.7$. $\log A = 3.8$.

	$\log g = 3.5$				$\log g = 4.0$				$\log g = 4.5$			
τ	θ	$\log p$	$\log p_e$	$\log \varkappa$	θ	$\log p$	$\log p_e$	$\log \varkappa$	θ	$\log p$	$\log p_e$	$\log \varkappa$
0.00...	0.700				0.700				0.700			
0.01...	0.696	2.11	0.90	9.49	0.696	2.59	1.15	9.59	0.696	3.04	1.38	9.69
0.02...	0.693	2.35	1.05	9.55	0.693	2.80	1.28	9.66	0.693	3.23	1.50	9.77
0.03...	0.690	2.50	1.14	9.61	0.690	2.92	1.36	9.71	0.690	3.35	1.59	9.83
0.04...	0.688	2.59	1.21	9.66	0.688	3.01	1.43	9.75	0.688	3.43	1.65	9.87
0.05...	0.686	2.67	1.27	9.69	0.686	3.08	1.48	9.79	0.686	3.50	1.70	9.90
0.06...	0.684	2.73	1.31	9.73	0.684	3.14	1.52	9.82	0.684	3.55	1.74	9.93
0.07...	0.682	2.78	1.35	9.75	0.682	3.18	1.56	9.85	0.682	3.59	1.78	9.96
0.08...	0.680	2.82	1.39	9.77	0.680	3.22	1.60	9.87	0.680	3.63	1.81	9.99
0.09...	0.678	2.85	1.42	9.80	0.678	3.25	1.63	9.90	0.678	3.66	1.84	0.02
0.10...	0.676	2.87	1.45	9.83	0.676	3.28	1.66	9.93	0.676	3.69	1.87	0.04
0.15...	0.666	2.98	1.58	9.95	0.666	3.39	1.79	0.05	0.666	3.79	2.00	0.16
0.2 ...	0.656	3.05	1.69	0.05	0.656	3.46	1.90	0.14	0.656	3.85	2.10	0.25
0.3 ...	0.638	3.13	1.86	0.23	0.638	3.54	2.07	0.32	0.638	3.93	2.27	0.42
0.4 ...	0.622	3.18	2.00	0.39	0.622	3.59	2.22	0.48	0.622	3.98	2.42	0.57
0.5 ...	0.609	3.21	2.11	0.52	0.609	3.62	2.33	0.59	0.609	4.02	2.53	0.69
0.6 ...	0.596	3.23	2.21	0.65	0.596	3.64	2.43	0.72	0.596	4.04	2.63	0.81
0.7 ...	0.585	3.25	2.29	0.76	0.585	3.66	2.52	0.83	0.585	4.06	2.73	0.91
0.8 ...	0.575	3.26	2.36	0.85	0.575	3.67	2.60	0.93	0.575	4.07	2.81	1.01
0.9 ...	0.565	3.27	2.44	0.94	0.565	3.68	2.67	1.03	0.565	4.08	2.89	1.10
1.0 ...	0.557	3.28	2.50	1.01	0.557	3.69	2.73	1.10	0.557	4.09	2.95	1.18
1.5 ...	0.521	3.30	2.71	1.30	0.521	3.71	2.97	1.40	0.521	4.11	3.21	1.48
2 ...	0.495	3.32	2.84	1.46	0.495	3.72	3.13	1.60	0.495	4.13	3.39	1.70
3 ...	0.457	3.34	2.97	1.54	0.457	3.74	3.31	1.78	0.457	4.14	3.60	1.94
4 ...	0.430	3.36	3.03	1.49	0.430	3.75	3.38	1.80	0.430	4.15	3.71	2.03
5 ...	0.410	3.38	3.06	1.42	0.410	3.77	3.43	1.76	0.410	4.16	3.78	2.04
6 ...	0.394	3.40	3.09	1.35	0.394	3.78	3.46	1.70	0.394	4.17	3.82	2.02
7 ...	0.380	3.43	3.12	1.29	0.380	3.80	3.48	1.64	0.380	4.18	3.85	1.97
8 ...	0.369	3.45	3.15	1.23	0.369	3.81	3.50	1.58	0.369	4.19	3.87	1.91
9 ...	0.359	3.48	3.18	1.19	0.359	3.83	3.52	1.53	0.359	4.20	3.88	1.86
10 ...	0.350	3.51	3.21	1.14	0.350	3.85	3.54	1.47	0.350	4.21	3.89	1.81

θ	$\log p$	$\log p_e$	θ	$\log p$	$\log p_e$	θ	$\log p$	$\log p_e$
0.658	3.04	1.67	0.649	3.50	1.97	0.643	3.92	2.23
0.649	3.10	1.76						
0.634	3.20	1.92	0.631	3.60	2.15	0.626	4.00	2.40
0.619	3.30	2.09	0.614	3.70	2.32	0.606	4.10	2.59
0.605	3.40	2.24	0.598	3.80	2.49	0.588	4.20	2.78
0.592	3.50	2.38	0.583	3.90	2.65	0.571	4.30	2.96
0.580	3.60	2.52	0.569	4.00	2.82	0.556	4.40	3.12
0.568	3.70	2.66	0.556	4.10	2.96	0.540	4.50	3.30
0.556	3.80	2.80	0.543	4.20	3.11	0.526	4.60	3.45
0.544	3.90	2.93	0.530	4.30	3.26	0.512	4.70	3.60
0.533	4.00	3.07	0.518	4.40	3.39	0.499	4.80	3.75

SPECIAL STELLAR ATMOSPHERES

Table 14. Model solar atmospheres.

	log A = 3.0				log A = 3.4			
τ	θ	log p	log p_e	log $\bar{\bar{\varkappa}}$	θ	log p	log p_e	log $\bar{\varkappa}$
0.00	1.041				1.041			
0.01	1.037	3.66	0.52	9.10	1.037	3.84	0.33	8.91
0.02	1.034	3.81	0.64	9.22	1.034	4.00	0.47	9.05
0.03	1.030	3.90	0.72	9.29	1.030	4.09	0.55	9.12
0.04	1.027	3.96	0.78	9.35	1.027	4.15	0.60	9.17
0.05	1.023	4.02	0.83	9.39	1.023	4.20	0.65	9.22
0.06	1.019	4.06	0.87	9.43	1.019	4.24	0.69	9.25
0.07	1.015	4.10	0.91	9.46	1.015	4.28	0.73	9.28
0.08	1.012	4.12	0.93	9.48	1.012	4.31	0.76	9.31
0.09	1.009	4.15	0.97	9.50	1.009	4.34	0.79	9.33
0.10	1.005	4.18	1.00	9.52	1.005	4.36	0.82	9.35
0.2	0.975	4.34	1.20	9.64	0.975	4.52	1.00	9.47
0.3	0.949	4.44	1.30	9.72	0.949	4.62	1.12	9.55
0.4	0.925	4.51	1.39	9.78	0.925	4.69	1.22	9.61
0.5	0.905	4.57	1.47	9.82	0.905	4.75	1.30	9.65
0.6	0.887	4.61	1.53	9.85	0.887	4.79	1.38	9.68
0.7	0.870	4.65	1.59	9.87	0.870	4.83	1.44	9.71
0.8	0.855	4.68	1.64	9.90	0.855	4.86	1.50	9.74
0.9	0.841	4.71	1.69	9.91	0.841	4.89	1.56	9.79
1.0	0.828	4.74	1.74	9.94	0.828	4.91	1.62	9.82
1.1	0.816	4.76	1.79	9.96	0.816	4.93	1.68	9.86
1.2	0.805	4.78	1.83	9.98	0.805	4.95	1.74	9.90
1.3	0.794	4.80	1.88	0.01	0.794	4.96	1.80	9.94
1.4	0.784	4.82	1.92	0.05	0.784	4.98	1.86	9.98
1.5	0.775	4.84	1.97	0.08	0.775	4.99	1.91	0.02
1.6	0.767	4.85	2.01	0.10	0.767	5.00	1.96	0.06
1.7	0.758	4.86	2.05	0.13	0.758	5.01	2.02	0.09
1.8	0.751	4.87	2.09	0.16	0.751	5.02	2.07	0.13
1.9	0.743	4.88	2.13	0.19	0.743	5.03	2.12	0.17
2.0	0.736	4.90	2.18	0.22	0.736	5.03	2.16	0.20
2.5								
3.0								

$\theta_0 = 1.041.\ \log g = 4.44.$

	$\log A = 3.8$				$\log A = 4.2$			
θ	$\log p$	$\log p_e$	$\log \varkappa$	θ	$\log p$	$\log p_e$	$\log \varkappa$	τ
1.041				1.041				.....0.00
1.037	4.02	0.15	8.74	1.037	4.23	0.01	8.60	.....0.01
1.034	4.17	0.28	8.86	1.034	4.37	0.13	8.71	.....0.02
1.030	4.26	0.37	8.94	1.030	4.45	0.20	8.78	.....0.03
1.027	4.33	0.43	8.99	1.027	4.51	0.26	8.83	.....0.04
1.023	4.38	0.48	9.04	1.023	4.56	0.31	8.87	.....0.05
1.019	4.42	0.52	9.08	1.019	4.61	0.36	8.92	.....0.06
1.015	4.45	0.55	9.10	1.015	4.64	0.39	8.94	.....0.07
1.012	4.49	0.59	9.13	1.012	4.66	0.42	8.96	.....0.08
1.009	4.51	0.61	9.15	1.009	4.69	0.45	8.98	.....0.09
1.005	4.54	0.64	9.17	1.005	4.72	0.48	9.01	.....0.10
0.975	4.70	0.82	9.30	0.975	4.87	0.67	9.14	.....0.2
0.949	4.80	0.95	9.38	0.949	4.97	0.82	9.25	.....0.3
0.925	4.86	1.05	9.44	0.925	5.04	0.95	9.34	.....0.4
0.905	4.92	1.15	9.50	0.905	5.08	1.06	9.41	.....0.5
0.887	4.96	1.24	9.55	0.887	5.11	1.17	9.48	.....0.6
0.870	4.99	1.32	9.60	0.870	5.14	1.28	9.55	.....0.7
0.855	5.02	1.40	9.66	0.855	5.16	1.37	9.62	.....0.8
0.841	5.04	1.48	9.70	0.841	5.18	1.46	9.69	.....0.9
0.828	5.06	1.56	9.77	0.828	5.20	1.56	9.77	.....1.0
0.816	5.08	1.64	9.82	0.816	5.21	1.64	9.83	.....1.1
0.805	5.09	1.71	9.87	0.805	5.22	1.72	9.88	.....1.2
0.794	5.11	1.78	9.93	0.794	5.23	1.80	9.94	.....1.3
0.784	5.11	1.85	9.97	0.784	5.24	1.87	0.00	.....1.4
0.775	5.12	1.91	0.02	0.775	5.25	1.94	0.05	.....1.5
0.767	5.13	1.97	0.06	0.767	5.25	1.99	0.09	.....1.6
0.758	5.14	2.03	0.11	0.758	5.26	2.06	0.14	.....1.7
0.751	5.15	2.08	0.15	0.751	5.26	2.11	0.18	.....1.8
0.743	5.16	2.13	0.19	0.743	5.27	2.17	0.23	.....1.9
0.736	5.16	2.19	0.23	0.736	5.27	2.23	0.27	.....2.0
0.707	5.18	2.41	0.40					.....2.5
0.681	5.19	2.60	0.56					.....3.0

Table 15.

Model solar atmospheres. $\theta_0 = 1.041$. $\log g = 4.44$.
(Calculated with Rudkjøbing's opacity tables, cf. p. 12).

	$\log A = 3.4$				$\log A = 3.8$				$\log A = 4.2$			
τ	θ	$\log p$	$\log p_e$	$\log \varkappa$	θ	$\log p$	$\log p_e$	$\log \varkappa$	θ	$\log p$	$\log p_e$	$\log \varkappa$
0.00...	1.041				1.041				1.041			
0.01...	1.037	3.84	0.33	8.87	1.037	4.04	0.17	8.70	1.037	4.20	9.99	8.53
0.02...	1.034	4.00	0.47	9.01	1.034	4.19	0.30	8.83	1.034	4.36	0.13	8.66
0.03...	1.030	4.09	0.55	9.08	1.030	4.27	0.37	8.91	1.030	4.45	0.20	8.74
0.04...	1.027	4.16	0.61	9.15	1.027	4.33	0.43	8.96	1.027	4.52	0.27	8.80
0.05...	1.023	4.22	0.67	9.19	1.023	4.39	0.47	9.01	1.023	4.57	0.32	8.84
0.06...	1.019	4.26	0.71	9.23	1.019	4.43	0.53	9.04	1.019	4.61	0.36	8.88
0.07...	1.015	4.30	0.75	9.26	1.015	4.47	0.56	9.07	1.015	4.65	0.40	8.91
0.08...	1.012	4.33	0.78	9.28	1.012	4.50	0.59	9.10	1.012	4.68	0.43	8.93
0.09...	1.009	4.36	0.81	9.30	1.009	4.53	0.62	9.12	1.009	4.71	0.46	8.95
0.10...	1.005	4.38	0.83	9.32	1.005	4.55	0.65	9.14	1.005	4.73	0.48	8.97
0.15...	0.989	4.47	0.93	9.40	0.989	4.66	0.77	9.23	0.989	4.83	0.62	9.05
0.2 ...	0.975	4.54	1.02	9.45	0.975	4.73	0.85	9.28	0.975	4.90	0.69	9.11
0.3 ...	0.949	4.64	1.14	9.53	0.949	4.82	0.97	9.36	0.949	4.99	0.83	9.20
0.4 ...	0.925	4.71	1.24	9.58	0.925	4.89	1.08	9.41	0.925	5.05	0.96	9.30
0.5 ...	0.905	4.77	1.32	9.62	0.905	4.94	1.17	9.46	0.905	5.10	1.07	9.38
0.6 ...	0.887	4.82	1.39	9.66	0.887	4.99	1.26	9.52	0.887	5.14	1.19	9.45
0.7 ...	0.870	4.85	1.45	9.68	0.870	5.02	1.34	9.57	0.870	5.17	1.29	9.52
0.8 ...	0.855	4.89	1.52	9.72	0.855	5.05	1.42	9.63	0.855	5.19	1.38	9.58
0.9 ...	0.841	4.91	1.59	9.76	0.841	5.07	1.50	9.67	0.841	5.21	1.48	9.65
1.0 ...	0.828	4.94	1.65	9.80	0.828	5.09	1.58	9.72	0.828	5.22	1.57	9.72
1.5 ...	0.775	5.02	1.93	9.99	0.775	5.16	1.93	9.97	0.775	5.27	1.95	0.00
2 ...	0.736	5.06	2.18	0.16	0.736	5.19	2.20	0.20	0.736	5.29	2.24	0.23
3 ...	0.680	5.11	2.58	0.51	0.680	5.22	2.62	0.54	0.680	5.32	2.67	0.57
4 ...	0.640	5.13	2.88	0.76	0.640	5.24	2.93	0.79	0.640	5.33	2.97	0.82
5 ...	0.610	5.14	3.11	0.97	0.610	5.25	3.16	1.01	0.610	5.34	3.20	1.01
6 ...	0.585	5.15	3.29	1.14	0.585	5.25	3.34	1.18	0.585	5.34	3.38	1.18
7 ...	0.565	5.16	3.44	1.29	0.565	5.26	3.49	1.32	0.565	5.34	3.53	1.33
8 ...	0.548	5.16	3.58	1.43	0.548	5.26	3.63	1.45	0.548	5.35	3.67	1.47
9 ...	0.533	5.16	3.69	1.55	0.533	5.26	3.74	1.57	0.533	5.35	3.78	1.59
10 ...	0.520	5.16	3.79	1.65	0.520	5.26	3.84	1.67	0.520	5.35	3.88	1.68

θ	$\log p$
0.816	5.11
0.753	5.20
0.695	5.30
0.647	5.40
0.605	5.50
0.570	5.60
0.542	5.70
0.518	5.80

Table 16.

Model stellar atmospheres. $\theta_0 = 1.041$. $\log g = 3.0$.
(Calculated with Rudkjøbing's opacity tables, cf. p. 12).

	$\log A = 3.4$				$\log A = 3.8$				$\log A = 4.2$			
τ	θ	$\log p$	$\log p_e$	$\log \varkappa$	θ	$\log p$	$\log p_e$	$\log \varkappa$	θ	$\log p$	$\log p_e$	$\log \varkappa$
0.00...	1.041				1.041				1.041			
0.01...	1.037	3.12	9.66	8.25	1.037	3.27	9.49	8.07	1.037	3.36	9.30	7.93
0.02...	1.034	3.26	9.82	8.36	1.034	3.41	9.62	8.18	1.034	3.51	9.43	8.04
0.03...	1.030	3.35	9.91	8.44	1.030	3.50	9.70	8.25	1.030	3.62	9.53	8.10
0.04...	1.027	3.41	9.95	8.50	1.027	3.57	9.77	8.31	1.027	3.69	9.59	8.16
0.05...	1.023	3.46	0.01	8.54	1.023	3.62	9.82	8.35	1.023	3.74	9.64	8.19
0.06...	1.019	3.50	0.06	8.58	1.019	3.66	9.86	8.39	1.019	3.79	9.69	8.22
0.07...	1.015	3.53	0.09	8.60	1.015	3.70	9.90	8.42	1.015	3.83	9.73	8.25
0.08...	1.012	3.56	0.12	8.63	1.012	3.73	9.94	8.44	1.012	3.86	9.77	8.28
0.09...	1.009	3.59	0.15	8.65	1.009	3.76	9.97	8.46	1.009	3.89	9.80	8.30
0.10...	1.005	3.61	0.16	8.67	1.005	3.78	9.99	8.48	1.005	3.91	9.83	8.32
0.15...	0.989	3.71	0.28	8.73	0.989	3.88	0.11	8.56	0.989	4.02	9.97	8.42
0.2 ...	0.975	3.78	0.36	8.78	0.975	3.94	0.18	8.62	0.975	4.09	0.08	8.50
0.3 ...	0.949	3.87	0.48	8.85	0.949	4.04	0.34	8.72	0.949	4.18	0.25	8.62
0.4 ...	0.925	3.94	0.57	8.91	0.925	4.10	0.46	8.80	0.925	4.24	0.41	8.73
0.5 ...	0.905	4.00	0.67	8.98	0.905	4.15	0.58	8.88	0.905	4.27	0.54	8.83
0.6 ...	0.887	4.04	0.76	9.03	0.887	4.19	0.70	8.96	0.887	4.30	0.67	8.91
0.7 ...	0.870	4.07	0.85	9.09	0.870	4.22	0.80	9.04	0.870	4.32	0.79	9.00
0.8 ...	0.855	4.10	0.92	9.15	0.855	4.24	0.90	9.11	0.855	4.34	0.90	9.10
0.9 ...	0.841	4.12	1.00	9.20	0.841	4.25	0.99	9.18	0.841	4.36	1.00	9.18
1.0 ...	0.828	4.14	1.09	9.25	0.828	4.27	1.09	9.25	0.828	4.37	1.10	9.26
1.5 ...	0.775	4.20	1.44	9.54	0.775	4.31	1.46	9.55	0.775	4.40	1.50	9.59
2 ...	0.736	4.23	1.71	9.76	0.736	4.34	1.76	9.81	0.736	4.42	1.79	9.84
3 ...	0.680	4.26	2.14	0.17	0.680	4.36	2.19	0.20	0.680	4.43	2.23	0.23
4 ...	0.640	4.27	2.44	0.47	0.640	4.36	2.48	0.49	0.640	4.44	2.52	0.50
5 ...	0.610	4.28	2.66	0.71	0.610	4.37	2.70	0.74	0.610	4.44	2.74	0.74
6 ...	0.585	4.28	2.84	0.93	0.585	4.37	2.89	0.95	0.585	4.44	2.93	0.96
7 ...	0.565	4.28	2.99	1.10	0.565	4.37	3.04	1.13	0.565	4.45	3.08	1.14
8 ...	0.548	4.28	3.11	1.24	0.548	4.37	3.16	1.27	0.548	4.45	3.21	1.28
9 ...	0.533	4.28	3.22	1.36	0.533	4.37	3.27	1.39	0.533	4.45	3.32	1.40
10 ...	0.520	4.28	3.31	1.48	0.520	4.37	3.36	1.49	0.520	4.45	3.41	1.51

θ	$\log p$
0.856	4.24
0.813	4.30
0.750	4.40
0.700	4.50
0.658	4.60
0.624	4.70
0.596	4.80
0.571	4.90

Table 17.

Model stellar atmosphere. $\theta_0 = 0.7$. $\log g = 4.2$. $\log A = 3.8$. (Calculated with Rudkjøbing's opacity tables, cf. p. 12).

τ	θ	$\log p$	$\log p_e$	$\log \bar{\varkappa}$
0.00	0.700			
0.01	0.696	2.76	1.24	9.59
0.02	0.693	2.97	1.37	9.67
0.03	0.690	3.10	1.46	9.72
0.04	0.688	3.19	1.52	9.78
0.05	0.686	3.27	1.58	9.82
0.06	0.684	3.32	1.62	9.86
0.07	0.682	3.36	1.66	9.89
0.08	0.680	3.40	1.69	9.91
0.09	0.678	3.43	1.72	9.94
0.10	0.676	3.46	1.75	9.96
0.15	0.666	3.56	1.88	0.08
0.2	0.656	3.63	1.98	0.17
0.3	0.638	3.71	2.16	0.34
0.4	0.622	3.76	2.30	0.50
0.5	0.609	3.79	2.41	0.62
0.6	0.596	3.81	2.51	0.75
0.7	0.585	3.83	2.61	0.86
0.8	0.575	3.84	2.69	0.95
0.9	0.565	3.85	2.76	1.03
1.0	0.557	3.86	2.82	1.11
1.5	0.521	3.89	3.09	1.41
2	0.495	3.90	3.24	1.60
3	0.457	3.92	3.44	1.83
4	0.430	3.93	3.53	1.88
5	0.410	3.94	3.58	1.86
6	0.394	3.95	3.61	1.81
7	0.380	3.96	3.64	1.76
8	0.369	3.98	3.67	1.71
9	0.359	3.99	3.68	1.66
10	0.350	4.00	3.69	1.61

θ	$\log p$
0.648	3.67
0.641	3.70
0.621	3.80
0.604	3.90
0.587	4.00
0.513	4.50

Table 18.

Model stellar atmosphere. $\theta_0 = 0.7$. $\log g = 2.5$. $\log A = 3.8$
(Calculated with Rudkjøbing's opacity tables, cf. p. 12).

τ	θ	$\log p$	$\log p_e$	$\log \bar{\varkappa}$
0.00	0.700			
0.01	0.696	1.37	0.48	9.30
0.02	0.693	1.57	0.60	9.36
0.03	0.690	1.70	0.71	9.42
0.04	0.688	1.79	0.77	9.46
0.05	0.686	1.86	0.83	9.49
0.06	0.684	1.92	0.87	9.52
0.07	0.682	1.96	0.91	9.55
0.08	0.680	2.00	0.95	9.59
0.09	0.678	2.03	0.99	9.62
0.10	0.676	2.06	1.02	9.64
0.15	0.666	2.17	1.15	9.77
0.2	0.656	2.23	1.25	9.87
0.3	0.638	2.31	1.40	0.06
0.4	0.622	2.36	1.54	0.20
0.5	0.609	2.39	1.64	0.33
0.6	0.596	2.41	1.72	0.44
0.7	0.585	2.43	1.79	0.55
0.8	0.575	2.44	1.85	0.62
0.9	0.565	2.45	1.91	0.69
1.0	0.557	2.46	1.95	0.75
1.5	0.521	2.50	2.11	0.93
2	0.495	2.52	2.17	0.96
3	0.457	2.57	2.25	0.91
4	0.430	2.61	2.30	0.82
5	0.410	2.67	2.36	0.74
6	0.394	2.72	2.42	0.68
7	0.380	2.77	2.47	0.63
8	0.369	2.83	2.53	0.61
9	0.359	2.88	2.58	0.58
10	0.350	2.93	2.63	0.55

θ	$\log p$
0.667	2.15
0.661	2.20
0.651	2.30
0.638	2.40
0.628	2.50
0.618	2.60
0.607	2.70
0.597	2.80
0.588	2.90
0.577	3.00
0.568	3.10
0.557	3.20

DET KGL. DANSKE VIDENSKABERNES SELSKAB
MATEMATISK-FYSISKE MEDDELELSER, BIND XXI, Nr. 4

A NEW OPTICAL PRINCIPLE FOR THE INVESTIGATION OF STEP EQUILIBRIA

BY

JANNIK BJERRUM

KØBENHAVN
I KOMMISSION HOS EJNAR MUNKSGAARD
1944

Printed in Denmark.
Bianco Lunos Bogtrykkeri A/S

The term "step equilibria" is applied to reciprocal reactions of the type

$$M + A \rightleftarrows MA$$

$$MA + A \rightleftarrows MA_2$$

$$\cdots\cdots\cdots\cdots\cdots$$

$$MA_{N-1} + A \rightleftarrows MA_N,$$

where an ion (or a molecule) M is in chemical equilibrium with a series of compounds (complexes) MA_1, $MA_2 \cdots MA_N$ formed from M (the central group) by addition of one or several ligands A (molecules or ions). Step reactions of this type play an important rôle in complex chemistry. They are best investigated by methods which make it possible to determine the equilibrium concentrations of the free ligand or of one of the central group compounds involved. From this point of view the author has previously[1] maintained that determinations of the light absorption are rarely suited for the establishment of the equilibrium constants of the step system, and that they are better applicable when it is a question of proving the correctness of a set of constants obtained from the determination of one of the individual concentrations involved. This point of view is not entirely adequate, however, and, as it is the main purpose of the present paper to show, it is quite possible to determine the free ligand concentration, and hence the equilibrium constants of the system, solely by means of measurements of the light absorption. An accurate determination, however, is only possible if the following conditions are satisfied: (1) The ligand's own absorption must be infinitesimal in relation to that of the complexes, and (2)

[1] J. Bjerrum: Metal Ammine Formation in Aqueous Solution — Theory of the Reversible Step Reactions. Doctoral thesis, Copenhagen 1941. See p. 23.

the measurements must be carried out in a salt medium at a high and constant concentration of a neutral salt, so that (a) the law of mass action applies in its classical form, and (b) Beer's law applies to the individual complexes.

The theory of step equilibria is dealt with in detail in the above cited paper by the author, and only some of its main features will be recalled in the present paper. In accordance with the nomenclature of the paper in question we shall here introduce the following quantities and designations:

$[A]$ = concentration of free ligand.

$[MA_n]$ = concentration of the molecule type MA_n.

N = maximum value of n.

$$C_M = \sum_0^N [MA_n],$$

total concentration of central group.

$$C_A = [A] + \sum_0^N n[MA_n],$$

total ligand concentration.

$$\bar{n} = \frac{C_A - [A]}{C_M} = \frac{\sum_0^N n\,[MA_n]}{\sum_0^N [MA_n]},$$

the formation function of the system = the average number of ligands bound per central group.

$$\alpha_n = \frac{[MA_n]}{C_M},$$

the degree of formation of the compound MA_n or the fraction of the total central group concentration present as the compound MA_n.

$$k_n = \frac{[MA_n]}{[MA_{n-1}][A]},$$

consecutive complexity constant corresponding to the equilibrium $MA_{n-1} + A \rightleftarrows MA_n$.

$$K_n = k_1 k_2 \cdots k_n = \frac{[MA_n]}{[M][A]^n},$$

gross complexity constant corresponding to the equilibrium $M + nA \rightleftarrows MA_n$.

If the gross complexity constant is introduced into the summation expression for the formation function, we get, after eliminating the free central group concentration:

$$\bar{n} = \frac{\sum_{0}^{N} nK_n [A]^n}{\sum_{0}^{N} K_n [A]^n} = \frac{K_1 [A] + 2 K_2 [A]^2 + \cdots N K_N [A]^N}{1 + K_1 [A] + K_2 [A]^2 + \cdots K_N [A]^N}, \quad (1)$$

K_0 being = 1. From this expression it follows that the formation function depends on the concentration of free ligand only, and is independent of the central group concentration. Of course, this is not something here derived for the first time, but no one seems to have noticed that this rule makes it possible to establish the equilibrium constants of the step system by investigating the properties of the system which in an unequivocal manner permit us to ascertain a change in the formation function $\bar{n}$, or, what amounts to the same thing, enable us to decide whether 2 solutions, with different total concentrations, have the same percentage distribution of the complexes. Solutions meeting this requirement will in the following be called "corresponding solutions." It follows from (1) that corresponding solutions also have the same concentration of free ligand. Hence it is possible to establish the following set of equations for the calculation of the formation function and the unknown ligand concentration:

$$\bar{n} = \frac{C'_A - [A]}{C'_M} = \frac{C''_A - [A]}{C''_M}. \quad (2)$$

The total concentrations indicated refer to the composition of the two corresponding solutions. Of methods suitable for deciding whether two solutions are corresponding, several may be considered, but the only one of practical significance is that based on the measurements of light absorption. The present paper shows how it is possible with the aid of the new principle and the measurement of light absorption to establish the formation curve for the cupric ammonia system in good agreement with the results of the many other methods by which this system has previously been investigated. It is further shown how a coloured system (the copper ammonia system) may be employed as indicator system in the investigation of analogous colourless systems (the zinc ammonia system). Finally, an attempt is made at using the method for an investigation of the complex formation in concentrated solutions of cupric chloride.

The measurements may be carried out either by means of a colorimeter, as a kind of colorimetric titration, or by means of a spectrophotometer. These procedures are described in chapters one and two which also include the examples of the practical application. The third and last chapter discusses the possibilities of using optical measurements for a direct determination of the number of compounds in the chemical equilibrium. This determination is but rarely possible. It is always possible, however, if the formation curve is known, to calculate the equilibrium constants of the system and thus obtain information regarding the number of complexes present and their mutual proportions.

1. Determination of the Formation Curve by Means of Colorimetric Titration.

In the case of most complexes Beer's law is usually valid with good approximation, and if the investigation deals especially with conditions in aqueous solution at a high and constant concentration of a neutral salt we may with great accuracy consider the molar extinction coefficients ε_n of the complexes present as being perfectly constant. The molar extinction coefficient ε of the system, inasmuch as we confine ourselves to systems where only the complexes absorb, is connected with the molar extinction coefficients and the degrees of formation of the individual complexes by the equation

$$\varepsilon = \sum_{0}^{N} \alpha_n \varepsilon_n = \alpha_0 \varepsilon_0 + \alpha_1 \varepsilon_1 + \alpha_2 \varepsilon_2 \cdots + \alpha_N \varepsilon_N. \qquad (3)$$

In contrast to the extinction coefficients of the complexes ε is a variable which depends on the composition of the solution, but if we limit ourselves to corresponding solutions it is immediately apparent from (3) that ε, too, is constant. In other words, for step equilibria of the type in question Beer's law must be satisfied at constant concentration of the free ligand. This rule may without application of the equations (2) be used in the determination of free ligand, the procedure being as follows: The colorimeter employed has two vertical cylindrical tubes with plate glass bottoms, the only requirement being that the cross section of one of the tubes (the dilution

tube) has the same area throughout. A suitable amount of the coloured solution to be investigated is poured into both tubes (in the case of complete symmetry the same amount in each) so that the solutions when observed in the colorimeter look identical. The actual measurements now are carried out as a kind of titration to the same tone of colour. A suitable amount of the solvent is added from a burette to one of the tubes, this causing a change not only in the intensity, but also in the tone of colour. The effect of the dilution then is neutralized by adding from another burette so much of a ligand solution of known concentration that the solutions when observed in the colorimeter once more give the same colour impression. If, to achieve this, x ml of solvent and y ml of ligand solution with concentration a are added, the concentration of free ligand in the complex solution in question must be given by the expression

$$[A] = \frac{a \cdot y}{(x+y)}. \qquad (4)$$

The formation function or the average number of ligands per central atom is calculated as

$$\bar{n} = \frac{C_A - [A]}{C_M}. \qquad (5)$$

Should it be found impossible, by dilution and subsequent addition of ligand to a coloured complex solution, to make the two solutions in the colorimeter assume the same colour tone and colour intensity, this can only mean that the complex formation does not proceed according to the usual scheme and that the solutions presumably contain multinuclear complexes. On the other hand, if the method functions it is a sign that we have to do with step equilibria of the simple type. The method cannot be applied to all coloured step systems, but only to systems of a suitable complexity and colour intensity. If the complexity is too great, the complexes will not dissociate noticeably upon dilution, and if too small ($C_A \sim [A]$) it will be impossible to calculate $\bar{n}$ according to (5).

a. Experimentally. A Wolff colorimeter was used for the measurements, with the modification that the usual measuring

tubes for this colorimeter (the height of the liquid column being changed by drawing water through a side tap at the bottom of the tube) were replaced by tubes from a König-Martens spectrophotometer. The tubes for this apparatus had almost the same cross-sectional area throughout their entire length, and further had a sufficiently large diameter (3 cm) to ensure a plane surface; in return, they required a relatively large amount of liquid (7 ml per 1 cm of layer). The 25 cm tube was used as dilution tube and the 5 cm tube as the tube with the constant solution. Both tubes were used with only one of the plate glass covers screwed on, thus being open at the top. In some instances correction was made for the difference in the height of the liquid column by placing the 12 cm tube, filled with an amount of solvent corresponding to the dilution, on top of the 5 cm tube; in order to get the same number of reflections of the light, a glass was at the same time placed on top of the dilution tube. With the reasonably dust-free solutions used, however, this correction played a rôle only with the highest dilutions. In the case of low colour intensity it might be practical to interpose a colour filter in the path of the rays. Thus by using a green colour filter, transparent for light in the wave range 495 — 573 mμ, placed immediately below the ocular, it was possible to measure only weakly coloured solutions like 6 in table 1 with about the same accuracy as the other solutions.

b. Determination of the formation curve for the cupric ammonia system in 2 N ammonium nitrate. The results of the measurements are recorded in table 1. The concentrations[1] of free ammonia in the 6th column are mean values calculated according to (4) on the basis of titrations of solutions having the total copper and total ammonia concentrations stated. The diluent was a 2 N ammonium nitrate solution, and the ligand solution (all according to the concentration of free ammonia in the solution investigated) was a 0.02 or a 0.1 N aqueous ammonia which likewise was 2 N with respect to ammonium nitrate. For orientation the table gives the number of mls which to begin with were introduced into the absorption

[1] When nothing else is said, all concentrations in this paper are moles per liter.

Table 1. Investigation of some cupric ammonia solutions in 2 N ammonium nitrate by the colorimetric method.

No.	C_{Cu}	C_{NH_3}	Initial volume	Final volume	$[NH_3]_{exp.}$	$\log [NH_3]$	$\bar{n}_{exp.}$
1...	0.02016	0.0518	10	71	0.0016 ± 0.0003	-2.80 ± 0.09	2.49 ∓ 0.02
2...	0.02016	0.0830	5	69	0.0064 ± 0.0015	-2.19 ± 0.10	3.80 ∓ 0.08
3...	0.1012	0.310	4	70	0.0029 ± 0.0005	-2.54 ± 0.08	3.03 ∓ 0.01
4...	0.1015	0.3725	5	64	0.0058 ± 0.0015	-2.24 ± 0.12	3.61 ∓ 0.02
5...	0.1015	0.413	3	55	0.020 ± 0.005	-1.70 ± 0.11	3.87 ∓ 0.05
6...	0.00159	0.00506	20	51	0.0009 ± 0.0002	-3.05 ± 0.10	2.62 ∓ 0.13
7...	0.0248	0.1016	5	17	0.006 ± 0.002	-2.22 ± 0.15	3.85 ∓ 0.08

tubes (the initial volume), and the total volume in the dilution tube at the conclusion of the titration (the final volume). Before the final volume was reached, 3 or 4 adjustments to the same colour tone had usually been made. The recorded uncertainty of the concentrations of free ammonia found should not be taken too literally, but as an estimate of the accuracy with which it was possible to reproduce a determination. The table also shows how the uncertainty of the ammonia determination influences the $\bar{n}$-values calculated according to (5). Fig. 1 (upper part) shows a graphical representation of the colorimetrically determined values of $\bar{n}$ and $\log [NH_3]$ with accompanying range of uncertainty. The fully drawn curves represent the formation curves for the cupric ammonia system in 2 N ammonium nitrate at 18° and 22°, on the basis of ammonia tension[1] and glass electrode[2] measurements. In the colorimetric measurements the temperature is about 18°. The figure directly shows that on the whole the colorimetric method, within the supposed experimental uncertainty, gives the correct result.

c. Use of the cupric ammonia system as an indicator system. The colorimetric method can be used not only in the case of coloured systems, but also for investigating colourless systems when a suitable indicator system is added to the solutions in question. To illustrate this application, an investigation was made of a couple of ammoniacal zinc salt solutions with

[1] Untersuch. über Kupferammoniakverb. I, D. Kgl. Danske Vidensk. Selskab, Math.-fys. Medd. XI, No. 5 (1931), p. 16.
[2] Metal Ammine Formation in Aqueous Solution, p. 125.

Table 2. The use of the cupric ammonia system as indicator system in the investigation of two ammoniacal zinc salt solutions in 2 N ammonium nitrate solution.

No.	C_{Cu}	C_{Zn}	C_{NH_3}	Initial volume	Final volume
1...	0.00993	0.01987	0.1111	10	55
2...	0.00159	0.00498	0.01004	20	84

No.	$[NH_3]_{exp.}$	log $[NH_3]$	$\bar{n}_{Cu}$	$\bar{n}_{Zn_{exp.}}$
1...	0.0065	2.19	3.47	3.53
2...	0.0013	2.89	2.67	0.90

No.	$[NH_3]_{calc.}$	log $[NH_3]$	$\bar{n}_{Cu}$	$\bar{n}_{Zn_{calc.}}$
1...	0.0089	2.05	3.59	3.35
2...	0.00148	2.83	2.75	0.84

a suitable content of cupric salt. In these determinations the green filter was interposed.

The upper part of table 2 gives the total concentrations of the solutions measured as well as the initial and final volumes in the two titrations. The middle section gives the experimentally determined data for the concentration of free ammonia, and the formation function for the zinc system calculated from this concentration with the use of our knowledge of the formation curve for the cupric ammonia system. The bottom part of the table finally gives the same quantities calculated on the basis of the total concentrations with the use of our knowledge of the formation curves for both the cupric and the zinc system.[1] The temperature at the measurements is about 18°, and accordingly the formation curves corresponding to 18° are used in these calculations. The values found and those calculated are in very good agreement, and the experiments show directly the pronounced steepness of the formation curve for the zinc ammonia system.

d. Some experiments with strong cupric chloride solutions. An attempt was also made at using the colorimetric method to obtain some information on the formation of complexes in strong solutions of cupric chloride. The green solutions were diluted, whereby the colour changed in the direction of

[1] As regards the formation curve of the zinc system, see Metal Ammine Formation in Aqueous Solution, p. 158.

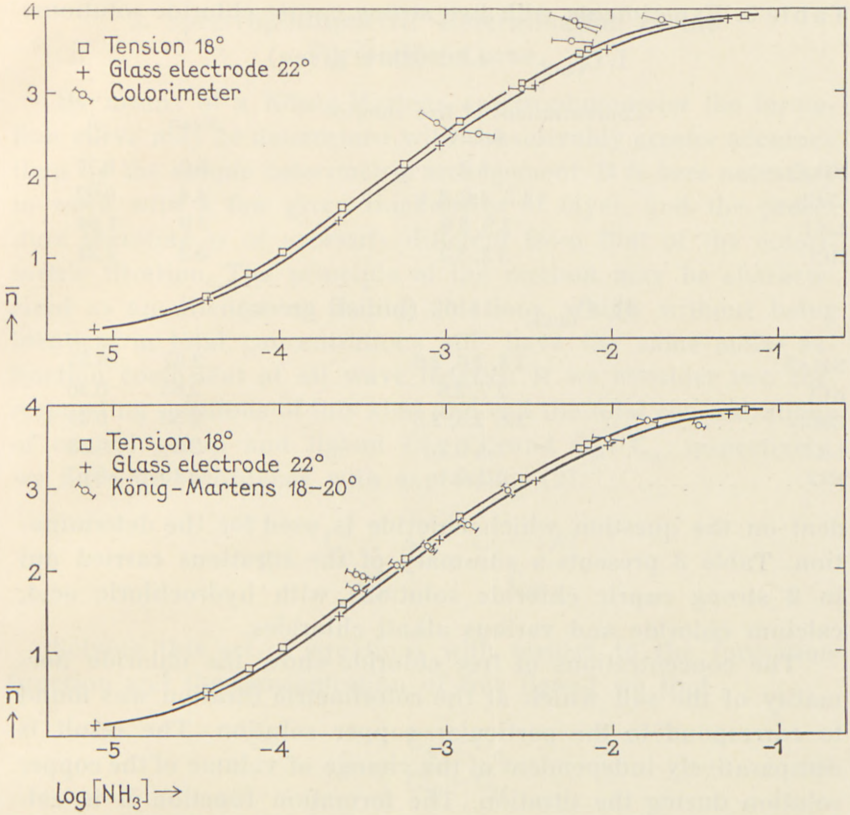

Fig. 1. Optical determination of the formation curve for the cupric ammonia system in 2 N ammonium nitrate. For the significance of the indicated uncertainty of the colorimetrically determined points (upper part of the figure) and the spectrophotometrically determined points (lower part of the figure), see the text.

blue, and the original colour then was reestablished by the addition of strong solutions of chlorides. The eye is especially sensitive to green, and the adjustment itself could be made with considerable accuracy. Nevertheless, this method gives only qualitative information regarding the complex formation, since the large copper concentrations make it impossible to work under conditions of the medium being but approximately constant. It is always possible to strike the same colour tone within the limits of experimental accuracy. This shows that, in the main, only mononuclear complexes are present, but the concentrations of free chlorine ion found are on the other hand strongly depen-

Table 3. Experiments with two strong cupric chloride solutions.

I. $C_{CuCl_2} = 4.06$ (dark green)

	Concentrations of free chloride found	Mean	$\bar{n}$
NH_4Cl	5.0	5.0	0.77
$CaCl_2$	4.3, 4.6, 4.4	4.4	0.92
LiCl	3.9, 3.9	3.9	1.04
HCl	3.2, 3,2	3.2	1.21

II. $C_{CuCl_2} = 1.62$ (bluish green)

NH_4Cl	2.8, 2.6, 2.6	2.67	0.35
KCl	2.7, 2.6	2.65	0.36
$CaCl_2$	2.6, 2.5, 2.5	2.53	0.44
LiCl	2.4, 2.2	2.3	0.58
HCl	2.2, 2.1	2.15	0.67

dent on the question which chloride is used for the determination. Table 3 presents a summary of the titrations carried out in 2 strong cupric chloride solutions with hydrochloric acid, calcium chloride and various alkali chlorides.

The concentrations of free chloride show the chloride normality of the salt which at the colorimetric titration was found to correspond to the particular copper solution. The result is comparatively independent of the change of volume of the copper solution during the titration. The formation function $\bar{n}$ is calculated, according to (5), from the mean value of the chloride normality for each salt. The table shows directly how largely the complex formation is dependent on the kind of chloride used in the determination. In the order NH_4Cl, KCl, $CaCl_2$, LiCl and HCl, we find an increasing tendency to produce complex formation, and it is worth noting that the mean activity coefficients of the salts in question rise in the same consecutive order (see table 4).

Table 4. Mean activity coefficients (at 25°) for the chlorides used at the chlorine ion normalities 2 and 4.

	NH_4Cl	KCl	$CaCl_2$	LiCl	HCl
2 N	0.57	0.58	0.72	0.95	1.02
4 N	0.59	0.58	1.57	1.56	1.76

The figures are from Landolt-Börnstein's tables.

2. Spectrophotometric Determination of the Formation Curve.

By means of a König-Martens spectrophotometer the formation curve may be determined with considerably greater accuracy than by the simple colorimetric arrangement. It is here necessary to work with a few given thicknesses of layer, and the procedure therefore is of necessity different from that of the colorimetric titration. The principle of the method may be characterized as an attempt at finding solutions which without being identical in total concentrations still have the same molar extinction coefficient at all wave lengths. If we consider two corresponding solutions of this kind and call the total concentrations of central group and ligand C_M^0, C_A^0 and C_M, C_A, respectively, we have in accordance with expression (2):

$$\bar{n} = \frac{C_A^0 - [A]}{C_M^0} = \frac{C_A - [A]}{C_M}.$$

Solving this set of equations with respect to the formation function and the concentration of free ligand we find

$$\bar{n} = \frac{C_A^0 - C_A}{C_M^0 - C_M} \tag{6}$$

$$[A] = \frac{C_M^0 C_A - C_M C_A^0}{C_M^0 - C_M}. \tag{7}$$

a. The formation curve for the cupric ammonia system. The application of (6) and (7) may be elucidated in connection with some measurements of the cupric ammonia system in 2 N ammonium nitrate. At a wave length of 590 mμ, where the absorption continuously increased with the ammonia concentration, measurements were made, for a constant copper concentration ($C_{Cu}^0 = 0.01972$), of the molar extinction coefficient (ε_{590}) with a series of different ammonia concentrations. The results are recorded graphically in fig. 2. By means of such an adjustment curve it is possible to arrive at corresponding solutions. If we measure ε_{590} for an arbitrary solution having a copper

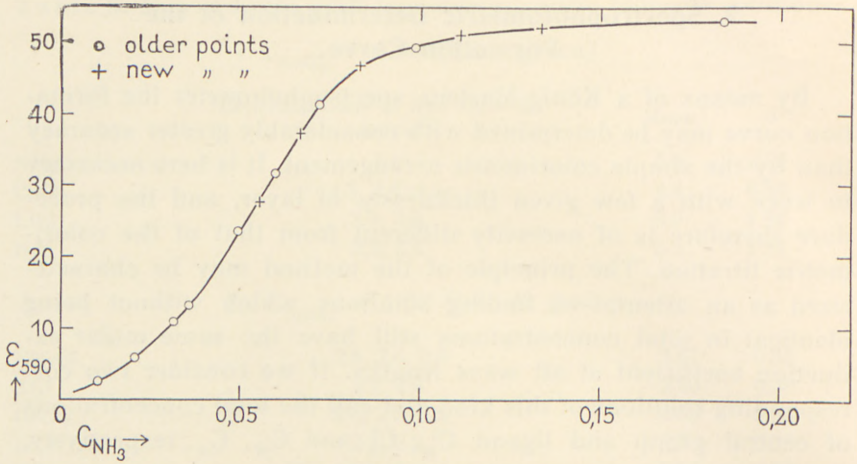

Fig. 2. Adjustment curve giving the connection between the molar extinction coefficient at the wave length 590 mμ and the total ammonia concentration for cupric ammonia solutions with a total copper concentration of 0.01972 molar.

concentration (C_{Cu}) different from 0.01972, the adjustment curve will directly give the ammonia concentration ($C^0_{NH_3}$) corresponding to the copper concentration 0.01972, so that the gross composition of two corresponding solutions is known. The concentration of free ammonia and the average number of ammonia molecules bound may then be calculated directly by means of the expressions (6) and (7).

The measurements forming the basis for the adjustment curve were mainly taken from an earlier paper[1] and supplemented by new measurements. In the new measurements the copper concentration was not exactly 0.01972, but the total ammonia concentration corresponding to this concentration was calculated with the aid of (6), the formation function being known in this special case. The supplementary measurements for the adjustment curve are recorded in table 5 a. It will be seen from the adjustment curve that there is exceptionally good agreement between the earlier and the new measurements (points o and +, respectively).

The actual measurements for the determination of the formation curve are recorded in table 5 b. The first part of this table gives the gross composition of the solution investigated,

[1] Untersuch. über Kupferammoniakverb. II, D. Kgl. Danske Vidensk. Selskab, Math.-fys. Medd. XI, No. 10 (1932), p. 47.

Table 5. Measurements by means of the König-Martens spectrophotometer of the cupric ammonia system in 2 N NH_4NO_3 at 18—20°.

a. Supplementary measurements for the adjustment curve.

C_{Cu}	C_{NH_3}	$\bar{n}$	C_{NH_3} (corresponding to C_{Cu} 0.01972)	ε_{590}
0.02016	0.1352	3.96	0.1335	52.2
0.02016	0.1126	3.92	0.1109	51.1
0.01972	0.0830	3.65	0.0830	46.7
0.02016	0.0678	3.25	0.0664	37.2
0.02016	0.0564	2.80	0.0552	27.75

b. Actual measurements.

No.	C_{Cu}	C_{NH_3}	ε_{590}	$C^0_{NH_3}$ (graph.) (C^0_{Cu} 0.01972)
1...	0.1015	0.413	50.7	0.107
2...	0.1015	0.401	48.35	0.0910
3...	0.1015	0.3725	45.7	0.0800
4...	0.00253	0.00982	32.5	0.0605
5...	0.00253	0.00776	25.0	0.0512
6...	0.001018	0.003106	20.35	0.0452
7...	0.001018	0.003106	20.9	0.0459
8...	0.001018	0.002587	17.12	0.0408
9...	0.001018	0.002270	15.1	0.0381
10...	0.001018	0.002250	15.3	0.0383
11...	0.001018	0.002080	13.0	0.0350

No.	$\bar{n}$	$[NH_3]$	$-\log [NH_3]$	$\frac{\Delta \bar{n}}{\bar{n}} \Big/ \frac{\Delta C^0_{NH_3}}{C^0_{NH_3}}$	$\frac{\Delta [NH_3]}{[NH_3]} \Big/ \frac{\Delta C^0_{NH_3}}{C^0_{NH_3}}$
1...	3.74	0.0332	1.479	0.35	4.0
2...	3.79	0.0162	1.790	0.29	7.0
3...	3.58	0.00947	2.024	0.27	10.5
4...	2.95	0.00236	2.627	1.19	3.8
5...	2.53	0.00137	2.863	1.18	5.5
6...	2.25	0.000816	3.088	1.07	3.0
7...	2.29	0.000777	3.109	1.07	3.2
8...	2.044	0.000507	3.294	1.07	4.4
9...	1.916	0.000320	3.495	1.07	6.5
10...	1.928	0.000287	3.542	1.06	6.6
11...	1.761	0.000288	3.541	1.06	7.3

the molar extinction coefficient measured, and, finally, the corresponding ammonia concentration $C^0_{NH_3}$ determined graphically by means of this quantity and the adjustment curve. In the measurements of the least absorbing solutions with copper concentrations of the order of magnitude 0.001 it was necessary to use the 12 cm and 25 cm tubes in order to measure sufficiently large extinctions. With such long tubes the dispersion of light by the particles of dust gives rise to a comparatively large error (cf. p. 8). This source of error was reduced as much as possible by continuously measuring the solution in question against a freshly prepared solution with the same ammonia and ammonium concentrations, but with no cupric salt added. The addition of cupric salt was carried out by pipetting from a carefully filtered stock solution of cupric nitrate. The approximately one molar ammonia stock solution, in order to secure a completely CO_2-free and almost dust-free solution, was prepared with ammonia from a steel cylinder after passing through a long tube with pieces of potassium hydroxide and then a cotton filter before being led into water.

The continuation of table 5 b gives the formation function and the concentration of free ammonia as calculated from the formulae (6) and (7). The figures in the last two columns finally show the magnitude of the relative uncertainty of these two quantities in proportion to the relative uncertainty of the experimentally determined $C^0_{NH_3}$-concentration, with the tacit understanding that the uncertainty of this concentration is solely responsible for the uncertainty of the calculated formation function and the concentration of free ammonia. The calculation is carried out by means of the expressions

$$\frac{\frac{\Delta \bar{n}}{\bar{n}}}{\frac{\Delta C^0_{NH_3}}{C^0_{NH_3}}} = \left| \frac{C^0_{NH_3}}{(C^0_{Cu} - C_{Cu})\,\bar{n}} \right| \quad \text{and} \quad \frac{\frac{\Delta [NH_3]}{[NH_3]}}{\frac{\Delta C^0_{NH_3}}{C^0_{NH_3}}} = \left| \frac{C^0_{NH_3}}{\left(\frac{C^0_{Cu}}{C_{Cu}} - 1\right)[NH_3]} \right| \tag{8}$$

which under the above assumption are easely derived from (6) and (7). The experimental material is graphically reproduced in fig. 1, lower part. As in the upper part of fig. 1, the fully drawn curves are the formation curves for the copper ammonia

system in the same medium at 18° and 22° on the basis of the earlier ammonia tension and glass electrode measurements. The range of uncertainty attending the spectrophotometrically determined points is traced so as to show how an uncertainty of 2 per cent. in the graphically determined $C^0_{NH_3}$-concentration affects the formation curve. The extinction coefficients are presumably determined with an accuracy of about 1 per cent., but this entails a somewhat higher uncertainty in the graphically determined $C^0_{NH_3}$-concentration, especially on the upper part of the adjustment curve, where the extinction coefficient changes comparatively little with the ammonia concentration. The uncertain temperature recording (room temperature) further contributes towards an increase of the inaccuracy of the spectrophotometrically determined points, but as a whole fig. 1 shows that the estimated uncertainty is of the right order of magnitude.

b. On the field of application of the method. The formulae (8) give us some information as to the conditions the most favourable to the application of the new method. It will be seen, for example, that if $C_{Cu} > C^0_{Cu}$ (solutions 1 to 3 in table 5), nothing special is gained, as regards the determination of the concentration of free ammonia, by making the ratio $\frac{C^0_{Cu}}{C_{Cu}} <$ about $^1/_5$, while in the opposite case (solutions Nos. 4 and 11), provided it is possible for other reasons, it is of distinct advantage to make the ratio $\frac{C^0_{Cu}}{C_{Cu}}$ large. For the ammonia determination it is first of all necessary to work with solutions so dilute that the concentration of free ammonia is not too small in proportion to the smallest of the total ammonia concentrations. Hence there is a limit to the applicability of the method, depending, besides on the complexity, also on the magnitude of the absorption of the complexes. Thus it is not only because of a too large complexity, but also because of the light absorption of the particular complexes being rather small, that the first stretch of the formation curve for the copper ammonia system cannot be determined by the new method. With respect to the determination of the formation function there is conversely a limit to the application of the method in the case of slight complexity, or, expressed

differently, when the concentration of free ammonia and the total ammonia concentrations are of the same order of magnitude. We may try to remedy this by using large concentrations. On the last stretch of the formation curve, where the complexity is not particularly great, the $\bar{n}$-determination has been assured by means of large total concentrations, but this is not without consequences for the determination of the concentration of free ammonia (see solution 3 in table 5). The fact is that if we wish to determine the formation function with a high degree of certainty, the determination of the concentration of free ligand will become correspondingly more uncertain, and vice versa.

It will be understood from the above that the method is not always applicable, but that it has an optimum depending on the magnitude of the complexity constants and the light absorption. Finally, we shall call attention to a fact which is of significance in some cases. For a step system where the ligand is a base and which is investigated in a medium containing a large concentration of the corresponding acid, the absolutely correct expression for the formation function is

$$\bar{n} = \frac{C_A - [A] + [H^+]}{C_M}. \qquad (9)$$

Hence, with the method described, it is not actually the concentration of free ligand itself that is determined, but the ligand concentration minus the hydrogen ion concentration of the solution. In the copper ammonia system this circumstance does not give rise to any noticeable correction, but in other cases, *e. g.* in the copper pyridine system, it may be a question of rather large corrections. It should be added that in the case of the last mentioned system conditions are so favourable that the whole formation curve may be determined by the spectrophotometric method. Measurements of this kind were carried out at 3 different wave lengths, and gave the same result within the range of experimental accuracy; they will be described in a separate paper. We shall only mention here that when applying the spectrophotometric method to a system unknown beforehand it is necessary to make the investigation at several wave lengths. Otherwise we cannot be certain that we have to do with a simple step equilibrium so that the basis for the method is in order.

3. On the Possibility of Optical Identification of the Individual Compounds in the Equilibrium.

If in a step system the ratio between the consecutive constants is sufficiently large (more than 4 times the statistical ratio[1]), the wave-like appearance of the formation curve will show directly the number of intermediate compounds in the equilibrium. In complex step systems the consecutive constants usually follow so closely upon one another that the individual steps have disappeared completely for the benefit of a single S-shaped curve, as in the formation curve for the copper ammonia system investigated here. Thus we do not get a direct proof of the existence of the intermediate complexes, but have to draw our conclusions on the basis of the calculated complexity constants. It may be asked whether there is any possibility of identifying the individual compounds in the equilibrium by optical means. In a comprehensive paper Otto Ruff[2] has dealt with this question. His calculations, which are quite general in form, show with reference to the case in question that for a step system having a coloured central group, colourless ligand and N coloured complexes, a curve representing the extinction coefficient ε at a certain wave length plotted against the total ligand concentration at constant total concentration of central group will have $N-1$ maxima and minima at the most. If instead of the plotting employed by Ruff we use a diagram with ε being plotted against the formation function $\bar{n}$ it is easily seen that according to the above the number of maxima and minima in such an ε, $\bar{n}$-diagram cannot exceed the number of the intermediate compounds. As to the positions of the maxima and minima nothing can be said with absolute certainty, but in general they will be close to the whole value of the formation function corresponding to the composition of the complex in question, and the closer the more pronounced the particular maxima and minima. Fig. 3, as an example, shows the molar extinction coefficient ε for the cupric ammonia system at wave length 676 mμ plotted against the formation function. The particular curve has a maximum for $\bar{n}$ approximately 3 and a minimum for $\bar{n}$ approximately 4, and

[1] See Metal Ammine Formation in Aqueous Solutions, pp. 31 and 35.
[2] Otto Ruff, Zeitschr. physik. Chem. **76** (1911) 21.

thus it is possible on a purely optical basis to deduce the existence of 2 out of the 4 complexes intermediate between the cupric ion and the pentammine ion. The existence of the tetrammine ion follows directly from the shape of the formation curve, and further it follows from the slope of the curve that at least one of the remaining complexes exists. Thus there is not very much in the line of extra information to be gained from knowledge of the light absorption of the system, and on the whole it may be said that this method rarely gives direct information regarding the number of complexes in the equilibrium. To get a maximum or minimum corresponding to each complex the extinction coefficient of consecutive compounds must be alternately large and small, and of course we rarely find a wave length where this is the case, or we may find several wave lengths so as to have in all a maximum or minimum corresponding to the existence of each complex and located in accordance herewith. The possibility of establishing the presence of complexes is not always dependent on maxima or minima, however. If the ratio between the consecutive constants is very large, the extinction curve will abruptly change its slope at each whole $\bar{n}$-value corresponding to the existence of a complex. Reference is made to fig. 3 where the dotted broken line shows the course of the curve when the ratio between the consecutive constants is infinitely large.

The material used for fig. 3 is taken from »Untersuchungen über Kupferammoniakverbindungen II«[1], except for the data recorded in table 6.

A small quantity of nitric acid has been added to solution No. 1 in order to suppress the ammine formation completely so

Table 6.

The extinction coefficient at 676 mμ for some cupric solutions (very poor in ammonia) in 2 N NH_4NO_3 at approximately 20°.

No.	C_{Cu}	C_{HNO_3}	C_{NH_3}	$[H^+]$	$[NH_3]$	$\bar{n}$	ε_{676}
1...	0.0505	0.01995	0	0.01995	0.000000024	0	4.88
2...	0.0505	—	0.00409	0.000104	0.0000046	0.083	5.80
3...	0.0505	—	0.01018	0.000040	0.0000120	0.202	6.89

[1] D. Kgl. Danske Vidensk. Selskab, Math.-fys. Medd. XI, No. 10 (1932), p. 46.

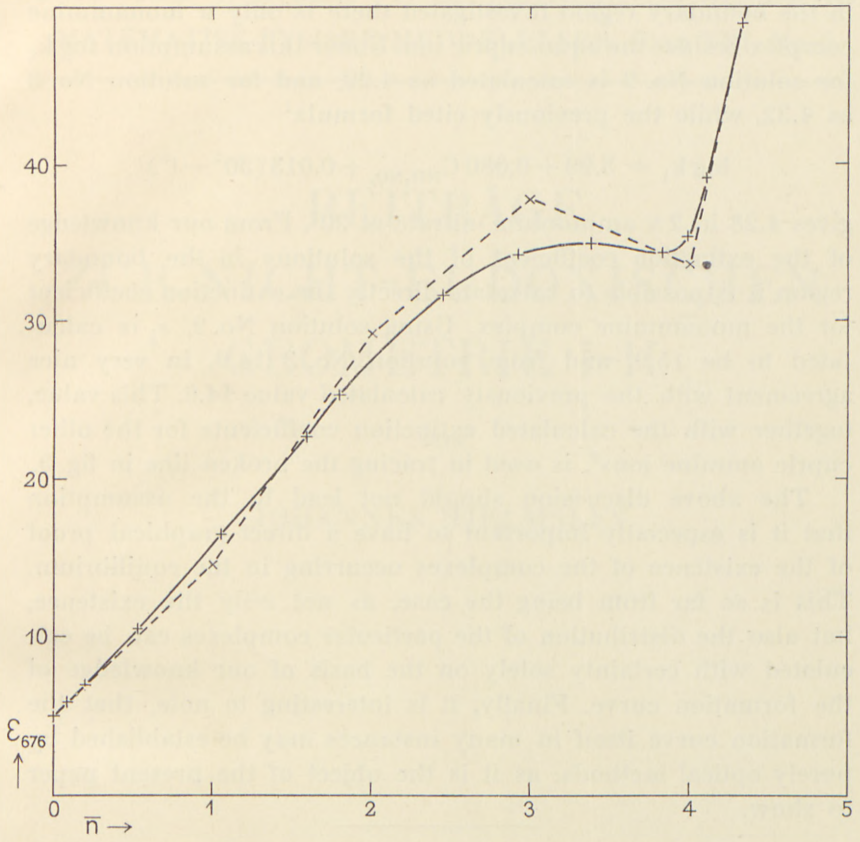

Fig. 3. The connection between the extinction coefficient and the formation function for the cupric ammonia system at wave length 676 mμ. The dotted broken line connects the extinction coefficients corresponding to the pure complexes.

that the extinction coefficient measured directly gives the absorption of the aquo-cupric ion[1]. In the case of the other solutions the formation function is calculated with the aid of (9). The recorded concentrations of hydrogen ion and free ammonia are in the usual way determined by means of the glass electrode[2]. The concentrations of free ammonia found in the case of solutions Nos. 2 and 3 are almost proportional to the corresponding values of the formation function, and this actually proves that

[1] Cf. loc. cit. p. 56.
[2] See Metal Ammine Formation in Aqueous Solution, p. 123 ff.

in the boundary region investigated there is only a monammine complex besides the aquo-cupric ion. Under this assumption $\log k_1$ for solution No. 2 is calculated as 4.29, and for solution No. 3 as 4.32, while the previously cited formula[1]

$$\log k_1 = 3.99 + 0.080\, C_{NH_4NO_3} + 0.013\,(30° - t°)$$

gives 4.28 in 2 N ammonium nitrate at 20°. From our knowledge of the extinction coefficient of the solutions in the boundary region it is possible to calculate directly the extinction coefficient for the monammine complex. Using solution No. 2, ε_1 is calculated to be 15.9, and from solution No. 3 14.9, in very nice agreement with the previously calculated value 14.6. This value, together with the calculated extinction coefficients for the other cupric ammine ions[2], is used in tracing the broken line in fig. 3.

The above discussion should not lead to the assumption that it is especially important to have a direct graphical proof of the existence of the complexes occurring in the equilibrium. This is so far from being the case, as not only the existence, but also the distribution of the particular complexes can be calculated with certainty solely on the basis of our knowledge of the formation curve. Finally, it is interesting to note, that the formation curve itself in many instances may be established by purely optical methods, as it is the object of the present paper to show.

The author wishes to thank Professor, Dr. Niels Bjerrum for permission to use a König-Martens spectrophotometer and a Wolff colorimeter from the Chemical Laboratory of the Royal Veterinary and Agricultural College.

[1] Loc. cit. p. 127.
[2] Untersuch. über Kupferammoniakverb. II, p. 52.

The Chemical Laboratory
of the University of Copenhagen.

Indleveret til Selskabet den 18. November 1943.
Færdig fra Trykkeriet den 17. Marts 1944.

DET KGL. DANSKE VIDENSKABERNES SELSKAB
MATEMATISK-FYSISKE MEDDELELSER, BIND XXI, NR. 5

BEITRÄGE ZUR NICHT-EUDOXISCHEN GEOMETRIE I–II

VON

JOHANNES HJELMSLEV

KØBENHAVN
I KOMMISSION HOS EJNAR MUNKSGAARD
1944

Printed in Denmark.
Bianco Lunos Bogtrykkeri A/S

Einleitung.

§ 1. Den folgenden Untersuchungen über nicht-Eudoxische Geometrie legen wir eine Kongruenzlehre zugrunde, die beispielsweise durch Hilberts Axiomgruppen I—III (Grundlagen der Geometrie, 2.—7. Auflage), eventuell ohne die räumlichen Axiome[1], festgelegt werden kann. Dies bringt mit sich, dass es in der Ebene stets sich nicht treffende Geraden gibt, z. B. Lote auf derselben Geraden. Die Ebene wird daher als offene Ebene bezeichnet.

Hierzu kommt nun als Ausdruck dafür, dass die Geometrie nicht-Eudoxisch ist:

Es gibt zwei Strecken von der Beschaffenheit, dass die eine von ihnen grösser als jedes Vielfache der anderen ist.

Innerhalb des hiermit gegebenen Rahmens hat man den »Euklidischen« Fall, wo die Winkelsumme eines jeden Dreiecks gleich $2R$ ist, den »elliptischen«, wo sie grösser, und endlich den »hyperbolischen«, wo sie kleiner als $2R$ ist.

In allen drei Fällen gilt der Satz vom Aussenwinkel (Euklid I, 16) und, dass die Summe zweier beliebiger Winkel eines Dreiecks kleiner als $2R$ ist (Euklid I, 17).

§ 2. Zwei Strecken a und b, $a<b$, heissen ebenbürtig, $a \sim b$, wenn ein Vielfaches der kleineren grösser als die grössere ist, d. h. wenn eine ganze Zahl n derart existiert, dass $na>b$ ist. Selbstverständlich sollen auch zwei gleich grosse Strecken ebenbürtig genannt werden. Ist dagegen $na<b$ für jede positive ganze Zahl n, so wird a als b unterlegen ($a \prec b$), b als a überlegen ($b \succ a$) bezeichnet. Aus $a \sim b$, $b \sim c$ folgt $a \sim c$. Aus $a \prec b$, $b \precsim c$ folgt $a \prec c$.

[1] Die räumlichen Axiome sind ja in dem Sinne überflüssig, dass sie stets durch konstruktive Erweiterung erfüllt werden können.

Die entsprechenden Bezeichnungen werden beim Vergleichen von Winkeln verwendet. Die Existenz der entsprechenden Relationen, Unterlegenheit und Überlegenheit, bei Winkeln wird im folgenden nachgewiesen.

Ein Winkel wird ordinär genannt, wenn er einem rechten Winkel ebenbürtig ist; er kann dann spitz, recht oder stumpf sein. Ein nicht ordinärer Winkel ist dem rechten Winkel unterlegen ($\prec R$) und wird singulär genannt. Zwei ordinäre Winkel sind stets ebenbürtig. Zwei ebenbürtige Winkel sind entweder beide ordinär oder beide singulär.

Im Euklidischen und elliptischen Fall besitzt jedes Dreieck wenigstens einen ordinären Winkel, während im hyperbolischen Fall alle drei Winkel singulär sein können.

§ 3. Die die nicht-Eudoxischen Geometrien betreffenden Untersuchungen fallen naturgemäss in drei Gruppen:

A. Die erste Gruppe besteht aus den vom Eudoxischen Axiom vollständig unabhängigen Untersuchungen, die somit sowohl in der Eudoxischen als auch in der nicht-Eudoxischen Geometrie Gültigkeit haben. Hierzu gehören viele Sätze bei Euklid, alle Untersuchungen unter den Axiomgruppen I-III bei Hilbert, die Einführung der Halbdrehungen und die daran anschliessenden Definitionen idealer Elemente usw.[1]. Als spezielle Beispiele aus dieser Gruppe sollen hier die folgenden fundamentalen Sätze angeführt werden, die in gewissem Sinne alle Untersuchungen dieser Art beherrschen:

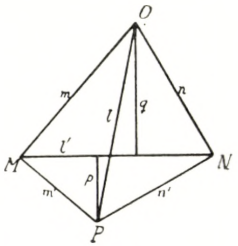

Fig. 1.

1°. Lotsatz. Auf zwei Geraden m und n durch einen Punkt O (Fig. 1) werden von einem Punkt P aus die Lote $PM = m'$ und $PN = n'$ gefällt. Auf die Verbindungsgerade $MN = l'$ der Fusspunkte werden die Lote p von P aus und q von O aus gefällt, und es wird die Gerade $PO = l$ gezogen. Es bestehen dann die Winkelrelationen $ml = qn$, $m'p = ln'$ und die Abstandsrelation $Mp = qN$.

Diese Relationen gelten zugleich als Spiegelungsrelationen, und als solche sind sie auch ursprünglich abgeleitet worden[2].

[1] Vgl. die Abhandlung des Verf. in Math. Ann. 64 sowie die weitergehenden Untersuchungen in »Einleitung in die allgemeine Kongruenzlehre« I, II, III, Kgl. Danske Vidensk. Selskab, Math.-fys. Medd. VIII (1929), X (1929), XIX (1942).

[2] Einleitung in die allgemeine Kongruenzlehre, I, S. 24—25, II, S. 4.

2°. Sätze über Quersummen von Strecken.

Unter der Quersumme c zweier Strecken a, b soll die Hypotenuse c eines rechtwinkligen Dreiecks mit den Katheten a und b verstanden werden. Wir schreiben dies

$$a + b = c.$$

Die hierdurch definierte Operation (Queraddition) ist nicht nur kommutativ sondern auch assoziativ, d.h. für drei Strecken p, q, r gilt

$$(p + q) + r = p + (q + r).$$

Dies erkennt man unmittelbar mittels einer räumlichen Betrachtung, indem man p, q, r als Seiten eines windschiefen Streckenzuges auffasst, bei dem die Winkel zwischen p und q, zwischen q und r sowie zwischen den Ebenen pq und qr recht sind. Der Satz kann natürlich auch mittels ebener Betrachtungen bewiesen werden.

Die umgekehrte Operation (Quersubtraktion), die dadurch definiert ist, dass

$$c - b = a$$

mit $a + b = c$ gleichbedeutend ist, ist eindeutig, wenn sie ausführbar ist. Dies folgt daraus, dass das gleichschenklige Dreieck eine Symmetrieachse besitzt.

Dafür, dass die Quersubtraktion $c - b$ möglich ist, ist notwendig, dass $c > b$ ist; wenn man kein Schnittpostulat für Kreis und Gerade einführt, kann man diese Bedingung aber nicht als hinreichend voraussetzen. Es ist indessen möglich, Rechenoperationen für Streckenpaare (a, b), (p, q), (r, s), $\cdots$ einzuführen, indem Gleichheit zweier Paare durch

$$(a, b) = (c, d),$$

wenn

$$a + d = b + c,$$

und Addition und Subtraktion durch

$$(p, q) + (r, s) = (p + r, q + s)$$
$$(p, q) - (r, s) = (p + s, q + r)$$

definiert werden. Wir wollen hierbei auch solche Grössenpaare in Betracht ziehen, bei denen 0 auf einer der Stellen oder auf beiden (Nullelement) steht.

Die üblichen Regeln der Addition und Subtraktion sind dann erfüllt.

Ist $p > q$ und existiert $p - q$, so hat man

$$(p, q) = (p - q, 0),$$

und ist $p < q$ und existiert $q - p$, so hat man

$$(p, q) = (0, q - p).$$

Hat man aber das elementare Schnittpostulat für Kreis und Gerade nicht, so kann das Paar (p, q) nicht immer auf eine Form gebracht werden, die 0 an einer der Stellen hat, da weder $p - q$ noch $q - p$ zu existieren braucht.

Nimmt man indessen die Strecken in dem Sinne unter die Grössenpaare auf, dass die beliebige Strecke x durch das Paar $(x, 0)$ vertreten wird, und untersucht man die Bedeutung der Addition und Subtraktion für diese speziellen Grössenpaare, so sieht man, dass

$$(x, 0) + (y, 0) = (x + y, 0)$$
$$(x, 0) - (y, 0) = (x, y)$$

gilt, wo das letzte Paar eventuell auf $(x - y, 0)$ oder $(0, y - x)$ reduziert werden kann. Auf diese Weise ist es möglich einer beliebigen Reihe von Queradditionen und -subtraktionen eine Bedeutung beizulegen, die die Anwendung der gewöhnlichen Umformungen von (additiv und subtraktiv gebildeten) mehrgliedrigen Grössen gestattet.

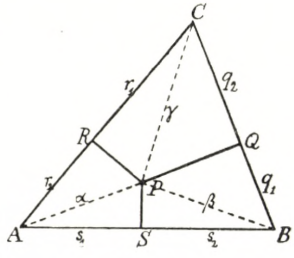

Fig 2.

Ein paar Anwendungen seien angeführt.

1) Von einem Punkt P werden die Lote PQ, PR, PS auf die Seiten eines Dreiecks ABC (Fig. 2) gefällt. Bezeichnen q_1, q_2; r_1, r_2; s_1, s_2 die Stücke, in welche die Seiten hierbei geteilt werden, so gilt

$$q_1 + r_1 + s_1 = q_2 + r_2 + s_2.$$

Dies folgt aus den Gleichungen

$$\begin{aligned} \beta - q_1 &= \gamma - q_2 \\ \gamma - r_1 &= \alpha - r_2 \\ \alpha - s_1 &= \beta - s_2 \end{aligned}$$

durch Queraddition.

2) Hat man umgekehrt auf den Seiten eines Dreiecks ABC drei Punkte Q, R, S, die die Seiten in Stücke q_1, q_2; r_1, r_2; s_1, s_2 teilen, die der Relation

$$q_1 + r_1 + s_1 = q_2 + r_2 + s_2$$

genügen, so gehen die auf den Seiten in den Punkten Q, R, S errichteten Lote durch denselben Punkt, falls sich überhaupt zwei von ihnen schneiden. Der Beweis wird indirekt geführt, indem man beachtet, dass die Quersumme wächst mit den Addenden, und dass $a + b < a + b$. Der Satz kann so erweitert werden, dass auch ideale Schnittpunkte einbezogen werden, worauf wir jedoch nicht eingehen wollen.

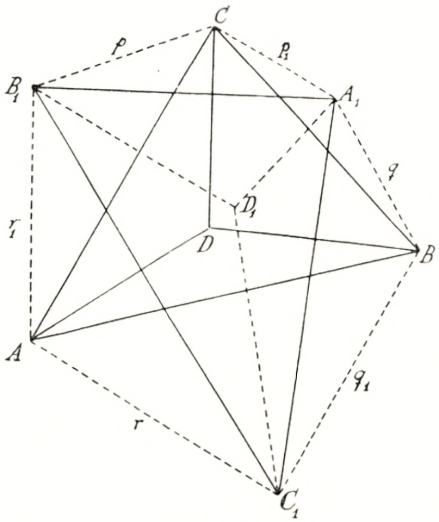

Fig. 3.

3) Der Satz von den orthologen Dreiecken (Fig 3).

Gehen die von den Ecken A, B, C eines Dreiecks ABC auf die Seiten B_1C_1, C_1A_1, A_1B_1 eines anderen Dreiecks gefällten Lote durch denselben Punkt D, so gehen auch die von den Ecken A_1, B_1, C_1 des zweiten Dreiecks auf die Seiten BC, CA, AB des ersten gefällten Lote durch einen und denselben Punkt D_1 (vorausgesetzt, dass sich überhaupt zwei von ihnen schneiden).

Der Beweis ergibt sich leicht aus den unter 1) und 2) angeführten Sätzen. Man hat nämlich nach 1)

$$p + q + r = p_1 + q_1 + r_1$$

woraus nach 2) folgt, dass die von A_1, B_1, C_1 auf BC, CA, AB gefällen Lote durch denselben Punkt gehen.

Der Satz kann natürlich so erweitert werden, dass auch ideale Punkte einbezogen werden, worauf aber nicht eingegangen werden soll.

Der gefundene Satz kann auch so ausgesprochen werden:

Wenn zwei vollständige Vierecke $ABCD$ und $A_1B_1C_1D_1$ so gelegen sind, dass die fünf Seiten AD, BD, CD, AB und BC des einen auf den Seiten B_1C_1, A_1C_1, A_1B_1, C_1D_1 bzw. A_1D_1 des anderen senkrecht stehen, so stehen auch die sechsten Seiten AC und B_1D_1 aufeinander senkrecht.

Im Euklidischen Fall ist dieser Satz dem Pappus-Pascalschen Satz äquivalent.

Wir machen darauf aufmerksam, dass der Beweis unabhängig davon gilt, ob die Figur eben ist oder nicht, sodass der Satz in der folgenden Form auch im Raume gilt:

Wenn zwei Tetraeder $ABCD$ und $A_1B_1C_1D_1$ so gelegen sind, dass die fünf Kanten AD, BD, CD, AB und BC des einen auf den »gegenüberliegenden« Kanten B_1C_1, A_1C_1, A_1B_1, C_1D_1 bzw. A_1D_1 des anderen senkrecht stehen, so stehen auch die sechsten »einander gegenüberliegenden« Kanten AC und B_1D_1 aufeinander senkrecht[1].

Auf ganz analoge Weise beweist man den folgenden Satz über orthologe Vierecke im Raume:

Wenn zwei windschiefe Vierecke $ABCD$ und $A_1B_1C_1D_1$ so gelegen sind, dass die vier durch A, B, C bzw. D gehenden, auf A_1B_1, B_1C_1, C_1D_1 bzw. D_1A_1 senkrechten Ebenen durch denselben Punkt gehen, so gehen auch die vier entsprechenden, durch A_1, B_1, C_1 bzw. D_1 gehenden und auf AB, BC, CD bzw. DA senkrechten Ebenen durch einen Punkt (vorausgesetzt, dass überhaupt drei dieser Ebenen einen Punkt gemein haben; anderenfalls kann man den Satz durch Einführung idealer Elemente retten).

Aus diesem Satz folgert man nun leicht den Satz von den orthologen Tetraedern:

Wenn zwei Tetraeder $ABCD$ und $A_1B_1C_1D_1$ so gelegen sind, dass die Lote von den Ecken A, B, C, D des einen auf die »gegenüberliegenden« Seitenflächen $B_1C_1D_1$, $C_1D_1A_1$, $D_1A_1B_1$, $A_1B_1C_1$ durch denselben Punkt gehen, so gehen auch die Lote von den Ecken A_1, B_1, C_1, D_1 des

[1] Dass zwei Geraden im Raume aufeinander senkrecht stehen, soll bedeuten, dass eine der Geraden einer auf der anderen senkrechten Ebene angehört.

zweiten auf die »gegenüberliegenden« Seitenflächen BCD, CDA, DAB, ABC des ersten durch einen und denselben Punkt.

Schliesslich ergibt sich aus diesem Satz unmittelbar die Existenz von vollständigen Fünfecken $ABCDE$ und $A_1B_1C_1D_1E_1$ im Raume, die derart miteinander verknüpft sind, dass jede Seite des einen auf der »gegenüberliegenden« Seitenebene des anderen senkrecht steht, also $AB \perp C_1D_1E_1$, $BC \perp A_1D_1E_1$ usw., $A_1B_1 \perp CDE$, $B_1C_1 \perp ADE$ usw.

Die angeführten Sätze können natürlich durch Einführung idealer Elemente auf bekannte Weise in den projektiven Raum eingeordnet werden; hier war jedoch beabsichtigt, ihre Gültigkeit in den unmittelbar durch die Axiome festgelegten Raum und ihren einfachen Zusammenhang mit dem assoziativen Gesetz der Queraddition hervorzuheben.

B. Eine zweite, die nicht-Eudoxische Geometrie betreffende Gruppe von Untersuchungen läuft auf den Nachweis hinaus, dass gewisse Sätze, die aus einem das Eudoxische Axiom enthaltenden Axiomsystem Σ ableitbar sind, nicht ohne Anwendung dieses Axioms bewiesen werden können. Dieser Nachweis besteht in der Konstruktion einer Geometrie, in welcher das Eudoxische Axiom nicht gilt, während alle übrigen Axiome aus Σ gelten, und in der Angabe eines Beispiels, das zeigt, dass der betreffende Satz in dieser Geometrie nicht richtig ist. Die Einführung derartiger Untersuchungen verdankt man David Hilbert.

Ein bekanntes Beispiel hat man in den Ausführungen über Satz 46 in Hilberts »Grundlagen der Geometrie«, 7. Aufl., S. 72—73, wo nachgewiesen wird, dass der Satz, dass Parallelogramme mit gleichen Grundlinien und gleichen Höhen zerlegungsgleich sind, nicht ohne Heranziehung des Eudoxischen Axioms bewiesen werden kann.

Ein weiteres Beispiel hat man in dem Beweis dafür, dass das Saccheri-Lambertsche Axiom von der Existenz eines Rechtecks zusammen mit den Hilbertschen Axiomgruppen I—III das V. Postulat Euklids nicht ohne Hinzufügung des Eudoxischen Axioms zu beweisen gestattet. Der Beweis wird in folgender Weise geführt: In der durch die vorgelegten Axiome definierten Geometrie Π betrachte man ein rechtwinkliges Dreieck ABC (Fig. 4) mit den Katheten $a = BC$, $b = CA$, $a \prec b$, und definiere

eine Untergeometrie, die den Bereich Π' umfasst, der aus allen den Punkten von Π besteht, deren Abstand von C kleiner als oder ebenbürtig mit a ist, und zwar so, dass unter den Geraden in Π' die Durchschnitte der ursprünglichen Geraden mit Π' verstanden werden. Alle für Π vorgeschriebenen Axiome einschliesslich des Saccheri-Lambertschen gelten dann auch in Π'. Der Durchschnitt des Dreiecks ABC mit Π' ist jedoch eine Figur, die unmittelbar zeigt, dass das V. Postulat in Π' nicht gilt, und damit ist unser Nachweis beendet.

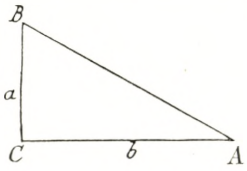

Fig. 4.

C. Die dritte Gruppe von Untersuchungen läuft schliesslich darauf hinaus, die nicht-Eudoxische Geometrie selbst in Bezug auf solche Eigenschaften zu untersuchen, die direkt keine Bedeutung oder keine Gültigkeit in der Eudoxischen Geometrie haben. Sätze dieser Art scheinen auf der hier gewählten Grundlage bisher keine Rolle in der mathematischen Literatur gespielt zu haben, wenn man von Sätzen rein negativer Form, die eine direkte Folge von Untersuchungen der Gruppe B sind, absieht.

Im folgenden sollen einige der naheliegendsten Fragen dieser Art, die einerseits die Ebenbürtigkeit oder Nicht-Ebenbürtigkeit von Seiten und Winkeln eines Dreiecks o. a., andererseits die Zerlegungsgleichheit von Polygonen betreffen, behandelt werden[1].

[1] G. Veronese hat in seinem gross angelegten, aber schwer zugänglichen Werk »Fondamenti di geometria a più dimensioni e a più spezie di unità rettilinee esposti in forma elementare«, Padova 1891 (deutsche Ausgabe von A. Schepp: »Grundzüge der Geometrie von mehreren Dimensionen und mehreren Arten geradliniger Einheiten . . .«, Leipzig 1894) die erste umfassende Behandlung einer nicht-Eudoxischen Geometrie gegeben. Es liegt in der Natur der Sache, dass gewisse Betrachtungen dieses Werkes Berührungspunkte mit den vorliegenden Untersuchungen aufweisen. Axiomatische Einstellung, Grundlage und Ziele sind jedoch wesentlich verschieden.

Bestimmte Definitionen von Zahlsystemen, die dem Nachweis der Existenz der Geometrien, mit denen Veronese arbeitet, dienen können, sind von T. Levi-Civita in einer Arbeit aus dem Jahre 1893: Sugli infiniti ed infinitesimi attuali quali elementi analitici, Atti Ist. Veneto (7) IV. S. 1765—1815, sowie in einer späteren Arbeit: Sui numeri transfiniti, Rend. Acc. Lincei (5) 7₁, S. 91—96, 113—121 (1898) aufgestellt worden.

Aber erst durch Hilberts epochemachendes Werk »Grundlagen der Geometrie«, 1899, haben die nicht-Eudoxischen Gebilde einen fundamentalen Platz in der mathematischen Forschung erhalten.

I. Allgemeine Sätze über Ebenbürtigkeit.

§ 4. Zunächst soll es sich um Sätze handeln, die innerhalb des in der Einleitung angegebenen Rahmens in allen drei Hauptfällen (dem Euklidischen, dem elliptischen und dem hyperbolischen) gelten.

Aus der Gültigkeit der Dreiecksungleichung entnimmt man, dass die beiden grössten Seiten eines Dreiecks stets ebenbürtig sind.

Satz 1. Ebenbürtigen Winkeln eines Dreiecks liegen ebenbürtige Seiten gegenüber.

Das gegebene Dreieck sei ABC. Der Winkel A sei kleiner als und ebenbürtig mit $\angle B$ (Fig. 5). Man konstruiere das gleichschenklige Dreieck ABB_1 ($AB_1 = BB_1$), indem man an AB in B den Winkel A abträgt. Ferner konstruiere man das gleichschenklige Dreieck B_1BB_2 ($BB_2 = B_1B_2$), und so fahre man fort. Die Winkel, die man hierbei nacheinander bei B abträgt, sind zuerst A, dann ein Winkel grösser als A, danach ein noch grösserer usw. Hieraus geht hervor, dass die abgetragenen Winkel zusammen schliesslich $\angle B$ überdecken müssen, so dass man einmal eine Strecke BB_{r-1} erhält, die innerhalb des Winkels B verläuft, während die folgende BB_r ausserhalb fällt (und möglicherweise überhaupt keinen Schnittpunkt B_r liefert). Hieraus folgt, dass $\angle B_{r-1}BC$ kleiner als $\angle BB_{r-1}C$ ist, also

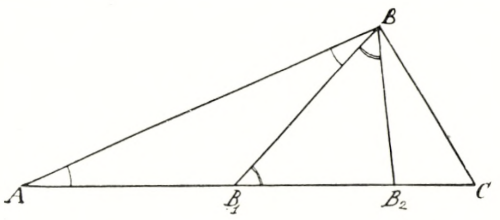

Fig. 5.

$$B_{r-1}C < BC,\ BB_{r-1} < BC + B_{r-1}C < 2\,BC,$$

$$BB_{r-2} < 4\,BC,\ \cdots,\ BB_1 < 2^{r-1}BC,\ AB < 2^rBC,$$

$$AC < AB + BC < (2^r + 1)\,BC.$$

Da zugleich $AC > BC$ ist, sind folglich AC und BC ebenbürtig, was zu beweisen war.

Beim Beweis ist, von gewöhnlichen, einfachen Kongruenzbetrachtungen abgesehen, nur der Satz vom Aussenwinkel benutzt

worden. Satz 1 gilt daher auch für sphärische Dreiecke, deren Seiten kleiner als 90° sind.

Aus Satz 1 folgert man sofort

Satz 2. Die Seiten eines Dreiecks mit lauter ordinären Winkeln sind untereinander ebenbürtig.

Ferner hat man den spezielleren

Satz 3. In einem rechtwinkligen Dreieck mit einem ordinären spitzen Winkel ist dessen gegenüberliegende Kathete der Hypotenuse ebenbürtig.

Aus dem folgert man weiter

Satz 4. In einem gleichschenkligen Dreieck, dessen Winkel an der Spitze ordinär ist, ist die Grundlinie den Schenkeln ebenbürtig.

Bemerkung: Auf der Kugel gilt ein entsprechender Satz mit dem Vorbehalt, dass die Schenkel $\leq 90°$ sind.

Schliesslich erhält man aus Satz 1 durch einen indirekten Schluss:

Satz 5. Wenn eine Seite eines Dreiecks einer der anderen Seiten (und damit beiden) unterlegen ist, so ist ihr Gegenwinkel den beiden anderen Winkeln unterlegen und somit gewiss singulär.

Hierin liegt ein Beweis für die Existenz nicht ebenbürtiger Winkel und somit die von singulären Winkeln.

Ferner kann man im Anschluss hieran zeigen:

Satz 6. Zu einem gegebenen Winkel α lässt sich stets ein Winkel $\beta \prec \alpha$ konstruieren.

Der Winkel α habe den Scheitel A (Fig. 6). Auf seinem einen Schenkel werde die beliebige Strecke AC und auf dem anderen

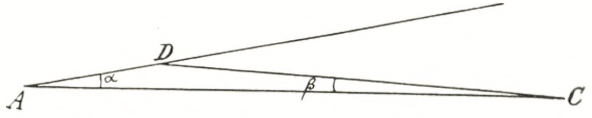

Fig. 6.

eine Strecke $AD \prec AC$ abgetragen. Im Dreieck ADC ist $AD \prec DC$ und daher $\beta = \angle ACD \prec \alpha$.

Hierdurch wird man weiter auf einen entsprechenden Satz über Strecken geführt:

Satz 7. Zu einer gegebenen Strecke a lässt sich stets eine Strecke $b \prec a$ konstruieren.

Beim Beweise können wir davon ausgehen, dass eine Strecke $k \succ a$ existiert, da Satz 7 anderenfalls nur ein neuer Ausdruck für die allgemeine nicht-Eudoxische Voraussetzung (§ 1) ist. Wir konstruieren ein rechtwinkliges Dreieck ABC (Fig. 7) mit den Katheten $BC = a$, $AC = k$. Der Gegenwinkel α von a ist dann singulär. Man trage nun einen Winkel $\beta \prec \alpha$ in der aus der Figur ersichtlichen Weise ab. Dieser schneidet auf a die Strecke CB_1 aus. Man trage nun den Winkel β wiederholt derart ab, dass $\angle CAB_1 = B_1AB_2 = B_2AB_3 = \cdots$. Da α durch diese Winkel, die alle gleich β sind, niemals überdeckt werden kann, können die Strecken $CB_1, B_1B_2, B_2B_3, \cdots$, die eine wachsende Folge bilden, die Strecke a niemals überdecken, d. h. es ist $CB_1 \prec a$. Als die gewünschte Strecke b kann also CB_1 gewählt werden.

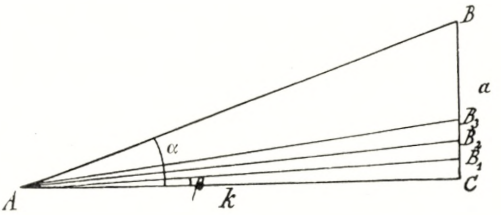

Fig. 7.

Die Sätze 6 und 7 gelten auch auf der Kugel, da man die betreffenden Untersuchungen auf einen Oktanten beschränken kann.

In der nicht-Eudoxischen Geometrie gibt es also keine niedrigste Grössenstufe in dem Sinne, dass zu jeder Strecke und zu jedem Winkel eine unterlegene Strecke bzw. ein unterlegener Winkel existiert. Dagegen kann es sehr wohl eine höchste Stufe geben. Was die Winkel betrifft, so repräsentiert der rechte Winkel stets die höchste Stufe. Falls es für Strecken keine höchste Stufe gibt, kann man zu einer vorgegebenen Strecke a stets eine Untergeometrie angeben, in der a die höchste Stufe repräsentiert. Man grenze nämlich um einen beliebig gewählten Punkt O den sogenannten Eudoxischen Bereich $E(a)$ ab, der aus allen den Punkten besteht, deren Abstand von O kleiner als oder ebenbürtig mit a ist. In diesem Bereich $E(a)$ gelten sämtliche vorausgesetzten Axiome, und damit hat man die gesuchte Untergeometrie.

Auf der Kugel hat man immer eine höchste Stufe, die durch den Quadranten k repräsentiert wird. Auch hier kann man natür-

lich zu jedem Abstand $a \prec k$ eine Untergeometrie $E(a)$ konstruieren, und jede solche Untergeometrie ist eine schwache elliptische Geometrie, d. h. eine Geometrie, in der alle Exzesse singulär sind (vgl. den folgenden § 5).

§ 5. Wir gehen nun zur spezielleren Untersuchung des elliptischen Falles innerhalb der Geometrie der nicht-Eudoxischen Ebene über und beweisen zunächst

Satz 8. Alle Exzesse von Dreiecken, und damit auch von Polygonen, sind singulär.

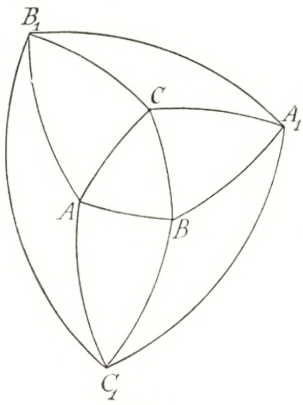

Fig. 8.

Die Winkel des Dreiecks seien A, B, C. Man betrachte die drei dem gegebenen kongruenten Dreiecke, die aus ihm durch Umwendung (Drehung um 180°) um die Mittelpunkte seiner Seiten hervorgehen (Fig. 8). Hierbei entstehen an den Ecken A, B, C drei Gruppen von Winkeln, von denen jede $A+B+C>2R$ ausmacht. Daraus folgt, dass ein grosses Dreieck $A_1B_1C_1$ entsteht, das alle übrigen umschliesst und dessen Exzess also mehr als viermal so gross wie der Exzess ε des gegebenen Dreiecks ist. Der Prozess kann wiederholt werden, woraus man ersieht, dass es ein Dreieck geben muss, dessen Exzess $4^r\varepsilon$ übersteigt, wo r eine beliebig grosse ganze Zahl ist. Da der Exzess jedoch stets kleiner als $4R$ ist, hat man $4^r\varepsilon < 4R$, d. h. ε ist singulär, was zu beweisen war.

Die Geometrie kann daher naturgemäss als schwache elliptische Geometrie bezeichnet werden[1].

§ 6. Danach gehen wir zu den Schnittkriterien im elliptischen und Euklidischen Fall über.

Satz 9. Wenn zwei Geraden l und m mit einer sie schneidenden Geraden innere Winkel bilden, von denen der eine recht und der andere spitz mit ordinärem Komplementwinkel ε ist, so schneiden sie sich (Fig. 9).

[1] Diesen geometrischen Systemen ordnet sich die von M. Dehn aufgestellte »Nicht-Legendresche Geometrie« (Math. Ann. 53, S. 431) unter. Ebenso gehört die dort aufgestellte »Semi-Euklidische Geometrie« zu den hier S. 13 genannten Untergeometrien.

Zum Beweise konstruiere man die gleichschenkligen Dreiecke ABB_1 ($BB_1 = AB$), AB_1B_2 ($B_1B_2 = AB_1$) usw. Deren Basiswinkel sind bzw.

$$\geqq \frac{R}{2}, \quad \geqq \frac{R}{4}, \ldots .$$

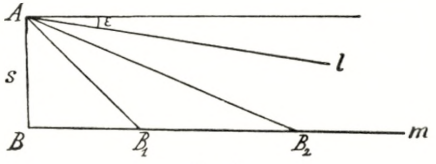

Fig. 9.

Hieraus folgt, dass die Strecke AB_r einmal innerhalb des Winkels ε fallen muss, da ε ordinär und daher grösser als $\frac{R}{2^n}$ für ein passendes n ist. Man sieht also, dass m von l zwischen B_{r-1} und B_r geschnitten wird.

Der Satz lässt sich verallgemeinern:

Satz 10. Wenn zwei Geraden l und m von einer dritten s so geschnitten werden, dass zwei auf derselben Seite von s gelegene Innenwinkel eine Summe haben, die um einen ordinären Winkel kleiner als $2R$ ist, so schneiden sie sich.

Der Beweis kann ganz wie der vorige geführt werden. Der Satz kann aber auch direkt auf den vorigen zurückgeführt werden, indem das Lot AC von A auf m gefällt wird (Fig. 10): Gegeben ist, das $\varepsilon = 2R-(\alpha+\beta)$ ordinär ist. Die Winkelsumme des Dreiecks ABC ist $2R+\eta$, wo η singulär oder 0 ist, und man hat

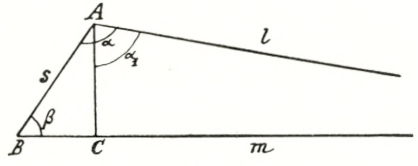

Fig. 10.

$$R+\beta+(\alpha-\alpha_1) = 2R+\eta$$

oder

$$\alpha_1 = R-(\varepsilon+\eta),$$

wo $\varepsilon+\eta$ ordinär ist. Nach Satz 9 schneiden sich also l und m.

Man kann dies auch formulieren als

Satz 11. Wenn die Differenz der Wechselwinkel ordinär ist, so schneiden sich die Geraden.

Anwendung: Bei einem Dreieck mit ordinären Winkeln existieren der einbeschriebene und die drei anbeschriebenen Kreise.

§ 7. Wir führen ferner einige Dreiecks- und Polygonsätze an, deren Gültigkeit auf den elliptischen und den Euklidischen Fall beschränkt ist.

Satz 12. Ist in einem Dreieck ein Winkel ordinär, und sind dessen anliegende Seiten ebenbürtig, so sind die beiden anderen Winkel ebenbürtig.

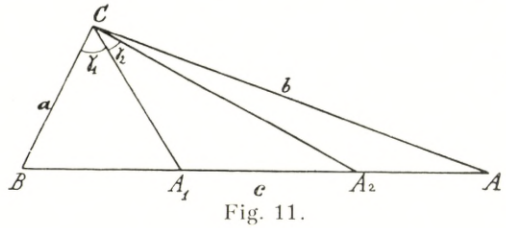

Fig. 11.

Das Dreieck sei ABC (Fig. 11), $\angle B$ ordinär, und die Seiten a und c, wo $a < c$, seien ebenbürtig. Man konstruiere nacheinander die gleichschenkligen Dreiecke BCA_1 ($BA_1 = a$), CA_1A_2 ($A_1A_2 = CA_1$) usw. Die Strecke BA_r muss dann einmal grösser als BA werden; denn man hat $BA_1 = a$, und $A_1A_2 = CA_1$ ist a ebenbürtig (Satz 4), ferner gilt $A_2A_3 = CA_2 > A_1A_2$ usw. Da nun $A_{r-1}A < CA_{r-1}$ ist, hat man $\angle A_{r-1}CA < A$. Bezeichnet man die Winkel bei C der Reihe nach mit $\gamma_1, \gamma_2, \cdots$, so hat man aber $\gamma_1 > \frac{C}{2}$ (halbiert nämlich die Strecke CD den Winkel C (Fig. 12), so entnimmt man dem Dreieck CDA, dass $u > \frac{C}{2}$ ist, und danach dem Dreieck BCD, dass $BC > BD$, also $BA_1 > BD$, d. h. $\gamma_1 > \frac{C}{2}$ ist). Ferner hat man wegen $2\gamma_2 \geqq \gamma_1$, $2\gamma_3 \geqq \gamma_2, \cdots$

$$\gamma_2 > \frac{C}{4}, \quad \gamma_3 > \frac{C}{8}, \cdots, \quad \gamma_{r-1} > \frac{C}{2^{r-1}}.$$

Der Winkel γ_r wird von CA in zwei Teile geteilt, die beide kleiner als A sind. Folglich ist

$$A > \frac{\gamma_r}{2} > \frac{C}{2^{r+1}},$$

und da gleichzeitig $A < C$ gilt, folgt hieraus, dass A und C ebenbürtig sind.

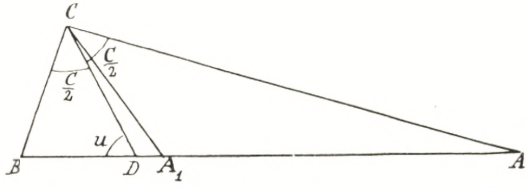

Fig. 12.

Bemerkung: Satz 12 gilt auch in der sphärischen Geometrie innerhalb eines beschränkten Bereichs, z. B. eines Oktanten, nämlich soweit der Satz vom Aussenwinkel gilt.

Definition: Ein Winkel soll regulär genannt werden, wenn sowohl er selbst als auch sein Nebenwinkel ordinär sind.

Ein Winkel ist regulär, wenn er seinem Nebenwinkel ebenbürtig ist.

Satz 13. Ist in einem Dreieck ein Winkel regulär, und sind dessen anliegende Seiten ebenbürtig, so sind alle Winkel regulär und alle Seiten ebenbürtig.

Im Dreieck ABC sei der Winkel A regulär, und die Seiten b und c seien ebenbürtig. Nach Satz 12 sind dann auch die Winkel B und C ebenbürtig. Da aber ihre Summe grösser oder gleich dem Nebenwinkel von A, also ordinär ist, muss jeder dieser Winkel ordinär sein. Ferner sind die Nebenwinkel von B und C beide grösser als A, also ordinär, d. h. die Winkel B und C sind regulär. Aus Satz 1 folgt hiernach, dass alle Seiten des Dreiecks ebenbürtig sind.

Im elliptischen oder Euklidischen Fall ist die Summe der Nebenwinkel eines konvexen Polygons $ABC \cdots K \leqq 4R$. Hieraus folgt unmittelbar

Satz 14. Hat ein konvexes Polygon der elliptischen oder Euklidischen Ebene zwei singuläre Winkel, so haben alle übrigen Polygonwinkel singuläre Nebenwinkel.

Mit Hilfe einfacher Anwendungen der obigen Sätze schliesst man hieraus weiter

Satz 15. Wenn ein konvexes Polygon (der elliptischen oder Euklidischen Ebene) lauter ordinäre Aussenwinkel hat, so sind auch die Innenwinkel ordinär (und daher regulär). Hat das Polygon ausserdem untereinander ebenbürtige Seiten, so sind alle Diagonalen und die Stücke, in die sie einander teilen, den Seiten ebenbürtig; ferner sind alle Winkel zwischen den von einer Ecke ausgehenden Seiten und Diagonalen sowie zwischen Diagonalen, die sich innerhalb des Polygons schneiden, ordinär.

Auf der Kugel gelten die entsprechenden Sätze innerhalb eines derart abgegrenzten Bereichs, dass der Satz vom Aussenwinkel zur Verfügung steht.

II. Betrachtungen zur Flächeninhaltslehre[1].

§ 8. Die geläufige Verwandlungsfigur (Fig. 13) zeigt, dass ein Dreieck ABC mit spitzen Winkeln bei A und B einem zweirechtwinkligen Viereck $APQB$ zerlegungsgleich ist, in dem $AP = BQ = CR$ (Scheitelhöhe) und $PQ = 2\,MN$ ist. Man ersieht hieraus: wird das Dreieck ABC derart abgeändert, dass MN dabei auf der Geraden PQ beliebig innerhalb der Strecke PQ verschoben wird, so bleibt es dem Viereck, und daher auch dem ursprünglichen Dreieck zerlegungsgleich. Die folgende Figur (Fig. 14) zeigt, dass das Dreieck ABC dem Dreieck ABD zerlegungsgleich ist, das

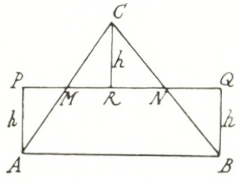

Fig. 13.

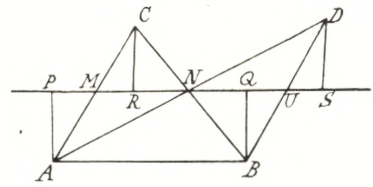

Fig. 14.

entsteht, wenn $ND = AN$ abgetragen wird. Die Verbindungsstrecke NU der Seitenmitten des neuen Dreiecks fällt in die Verlängerung von MN und ist gleich dieser Strecke ($AP = BQ$, $AP = DS$, $NU = \frac{1}{2}\,PQ$).

Durch Fortsetzung des letztgenannten Prozesses und Anwendung des erstgenannten gelangt man zu

Satz 16. Ein Dreieck ABC ist jedem Dreieck zerlegungsgleich, das dadurch entsteht, dass die Grundlinie AB beibehalten wird, während der Mittelpunkt M der Seite AC längs MN, wo N der Mittelpunkt von BC ist, ein beliebiges Stück verschoben wird, das kleiner als ein Vielfaches von MN ist.

Man erkennt auch leicht die Richtigkeit von

Satz 17. Ein Dreieck ABC ist, auch wenn es bei A und B nicht spitzwinklig ist, dem zugehörigen Verwand-

[1] Von früheren, die allgemeine Grundlage der Flächeninhaltslehre behandelnden Arbeiten sei ausser auf Hilbert's »Grundlagen« verwiesen auf: M. Dehn, Über den Inhalt sphärischer Dreiecke (Math. Ann. 60, S. 166—174), A. Finzel, Die Lehre vom Flächeninhalt in der allgemeinen Geometrie (Math. Ann. 72, S. 262—284).

lungsviereck $APQB$ zerlegungsgleich, falls nur PM kleiner als ein Vielfaches von MN ist. (Fig. 15).

Es ist also hinreichend, dass AM, und damit AC (oder BC) kleiner als ein Vielfaches von MN ist.

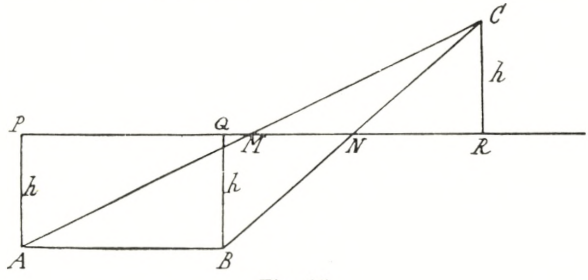

Fig. 15.

§ 9. Wir gehen nun zu Betrachtungen über, die allein den Euklidischen Fall betreffen. Indem wir als Inhaltsmass des Dreiecks (mit HILBERT) das halbe Produkt von Höhe und Grundlinie einführen, müssen wir beachten, dass die Existenz dieses Produktes von der zu wählenden Einheit abhängt. Wir setzen voraus, dass diese Einheit so gewählt ist, dass sie der grössten Strecke ebenbürtig ist, mit der wir es in den zu betrachtenden Figuren zu tun haben. Man kann dann ebenso wie bei HILBERT nachweisen, dass die gewöhnlichen Regeln der Addition und Multiplikation gültig sind. Die Division ist stets eindeutig, sobald sie möglich ist. Ferner kann man zeigen, dass Polygone mit gleichem Inhaltsmass stets ergänzungsgleich sind.

Wir untersuchen nun die Bedingungen für Zerlegungsgleichheit, zunächst für zwei Dreiecke. Diesbezüglich beweisen wir

Satz 18. Zwei Dreiecke, die dasselbe Inhaltsmass haben und deren grösste Seiten ebenbürtig sind, sind zerlegungsgleich.

Dass die genannten Bedingungen notwendig sind leuchtet ein. Dass sie hinreichend sind, sieht man so: Die Dreiecke seien ABC und $A_1B_1C_1$, ihre grössten Seiten $AB = c$ und $A_1B_1 = c_1$, $c \geqq c_1$, $AC \geqq BC$, $A_1C_1 \geqq B_1C_1$ (Fig. 16—17). Man führt das Doppelte der Strecke

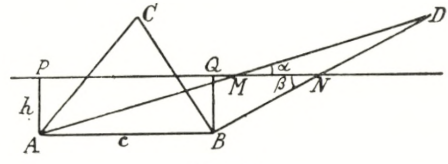

Fig. 16.

$$h + h_1 + c,$$

die kleiner als $3c$ ist, als Seite AD eines neuen Dreiecks ABD ein, das dem ursprünglichen ABC zerlegungsgleich ist und bei A einen spitzen Winkel hat. Dieselbe Grösse verwende man als Seite A_1D_1 eines Dreiecks $A_1B_1D_1$, das dem Dreieck $A_1B_1C_1$ zerlegungsgleich ist und bei A_1 einen spitzen Winkel hat. Die erforderlichen Konstruktionen werden ausgeführt, indem man

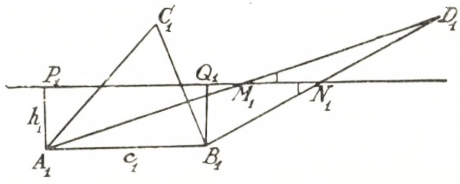

Fig. 17.

$$PM = h_1 + c, \quad P_1M_1 = h + c$$

abträgt, wodurch man die Mittelpunkte der Seiten AD und A_1D_1 erhält.

Die beiden neuen Dreiecke haben nun den gleichen Inhalt, und ihre grössten Seiten AD und A_1D_1 (Fig. 16: $AM > BN$, weil $\beta > \alpha$, also $AD > BD$) stimmen überein. Sie sind daher demselben Rechteck zerlegungsgleich. Hieraus folgt, dass auch die ursprünglichen Dreiecke zerlegungsgleich sind, was zu beweisen war.

Der Satz soll nun auf konvexe Polygone erweitert werden. Für Rechtecke erhält man sofort

Satz 19. Rechtecke mit gleichem Inhalt und ebenbürtigen Diagonalen (oder auch nur einem Paar ebenbürtiger Seiten) sind zerlegungsgleich.

Ferner gilt für zwei beliebige konvexe Vierecke:

Satz 20. Zwei konvexe Vierecke mit gleichem Inhaltsmass und ebenbürtigen grössten Seiten sind zerlegungsgleich.

Das eine der Vierecke sei $ABCD$ (Fig. 18) mit der grössten Seite AD. Die beiden Diagonalen mögen sich in O schneiden. Die Strecken AO und OD können nicht beide AD unterlegen sein; eine von ihnen, etwa OD, muss AD ebenbürtig sein. Das gleiche gilt dann von der Strecke BD, da diese grösser als OD und kleiner als $2\,AD$ ist. Das Viereck wird nun durch BD in zwei Dreiecke mit der Grundlinie BD zerlegt und ist also einem Rechteck mit der Grundlinie BD und demselben Inhalt zerlegungsgleich.

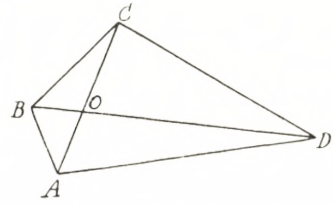

Fig. 18.

Analog schliesst man für das andere Viereck, wonach man den gefundenen Satz über Rechtecke anwenden kann.

Fünfecke können auf ähnliche Weise behandelt werden, und durch Induktion gelangt man dann zu dem Satz für beliebige konvexe Polygone:

Satz 21. Zwei konvexe Polygone mit gleichem Inhaltsmass und ebenbürtigen grössten Seiten sind zerlegungsgleich.

Es erhebt sich nun die Frage, ob dieser Satz auf nicht-konvexe Polygone erweitert werden kann. Das ist im allgemeinen

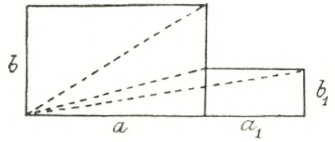

Fig. 19.

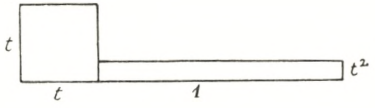

Fig. 20.

nicht der Fall. Ein Polygon, das aus zwei Rechtecken zusammengesetzt ist, von denen eines kleinere Dimensionen als das andere hat, kann in ein Rechteck verwandelt werden, indem es einfach in Dreiecke zerlegt wird, wie in der Figur angegeben (Fig. 19, wo $a > b > a_1 > b_1$). Das zweite Polygon (Fig. 20), das aus einem Rechteck mit den Seiten 1, t^2 und einem Quadrat mit der Seite t ($t \prec 1$) besteht und somit den Inhalt $2t^2$ hat, kann jedoch nicht in ein Rechteck verwandelt werden. Der Inhalt eines solchen Rechtecks müsste $2t^2$, seine grösste Dimension ebenbürtig mit 1 und seine kleinste Dimension ebenbürtig mit t^2 sein. Dann kann es aber kein rechtwinkliges Dreieck enthalten, dessen Katheten beide mit t ebenbürtig sind. Wenigstens eine der Projektionen der Katheten auf die kurze Seite des Rechtecks würde nämlich mit t ebenbürtig sein und folglich keiner Strecke, die höchstens gleich der kurzen Seite des Rechtecks ist, angehören können. Das gegebene Quadrat mit der Seite t kann aber nicht in rechtwinklige Dreiecke zerlegt werden, deren eine Kathete $\succsim t$ und deren andere $\prec t$ ist; denn mit einer endlichen Anzahl solcher Dreiecke kann das Quadrat t^2 nicht ausgefüllt werden, da jedes der Dreiecke einen Inhalt $\prec t^2$ hat.

§ 10. Um die Zerlegungsgleichheit von Dreiecken in den beiden anderen Geometrien, dem elliptischen und dem hyperbolischen Fall zu untersuchen, wählen wir wieder die grösste

Seite des Dreiecks als Grundlinie, so dass auch hier die Basiswinkel spitz sind. Ein solches Dreieck ist dem zugehörigen zweirechtwinkligen Verwandlungsviereck (vgl. Fig. 13, S. 18) zerlegungsgleich. Haben zwei solche Dreiecke dieselbe Grundlinie und dieselbe Winkelsumme, so sind die zugehörigen Vierecke kongruent und die Dreiecke selbst folglich untereinander zerlegungsgleich. Also:

Satz 22. Im elliptischen und im hyperbolischen Fall sind zwei Dreiecke zerlegungsgleich, wenn sie dieselbe Winkelsumme haben und die beiden grössten Seiten einander gleich sind.

Um in der gemeinsamen Untersuchung der beiden Geometrien weiter zu kommen, wollen wir voraussetzen, dass die zu betrachtenden Dreiecke lauter ordinäre Winkel haben. Sei ABC (Fig. 21) ein solches Dreieck mit der grössten Seite AB. Seine Seiten sind untereinander ebenbürtig (Satz 2). Die Scheitelhöhe $h = CH$ teilt den Winkel C in zwei Winkel α und β, für die man leicht die Werte

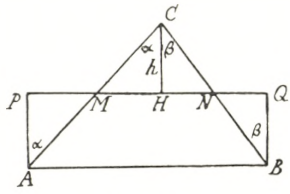

Fig. 21.

$$\alpha = \frac{B+C-A}{2}, \quad \beta = \frac{A+C-B}{2}$$

findet. Beide sind ordinär. Die Strecken MH und NH sind dann ebenbürtig mit MC und NC und daher auch mit AB. Also hat man auch $MN \sim AB$.

Es seien nun zwei Dreiecke ABC und $A_1B_1C_1$ mit lauter ordinären Winkeln, gleicher Winkelsumme und ebenbürtigen grössten Seiten c und c_1, $c > c_1$, vorgelegt. Indem wir $AC \geqq BC$, $A_1C_1 \geqq B_1C_1$ annehmen können, gehen wir ebenso wie im Euklidischen Fall vor (vgl. Fig. 16—17, S. 19—20). Wir tragen die Seiten AD und A_1D_1 gleich dem Doppelten der Strecke $h + h_1 + c$ (die kleiner als $3c$ ist) ab, so dass zwei Dreiecke ABD und $A_1B_1D_1$ mit den grössten Seiten AD und A_1D_1 entstehen. Diese sind den gegebenen Dreiecken zerlegungsgleich, da die Verbindungsstrecken der Seitenmitten der obigen Betrachtung zufolge mit c und c_1 ebenbürtig sind. Da nun die beiden Dreiecke dieselbe Winkelsumme haben, sind sie nach Satz 22 auch untereinander zerlegungsgleich, und dies gilt somit auch für die ursprünglichen

Dreiecke. Hieraus geht hervor, dass zwei Dreiecke mit derselben Winkelsumme, lauter ordinären Winkeln und ebenbürtigen grössten Seiten zerlegungsgleich sind.

Man kann indessen zeigen, dass die letztgenannte Bedingung, dass die grössten Seiten ebenbürtig sind, eine Folge der übrigen ist. Wenn nämlich die Dreiecke lauter ordinäre Winkel haben, so sind die Seiten jedes einzelnen Dreiecks untereinander ebenbürtig. Dann müssen aber auch die Seiten des einen Dreiecks denen des anderen ebenbürtig sein. Anderenfalls wären beispielsweise die Seiten von ABC denen von $A_1B_1C_1$ unterlegen. Daraus würde aber folgen, dass $\triangle ABC$ als Teil von $\triangle A_1B_1C_1$ angebracht werden kann, z. B. indem man das erste Dreieck so legt, dass sein kleinster Winkel einen Teil des grössten Winkels des zweiten Dreiecks ausmacht, was stets möglich ist, da die Dreiecke die gleiche Winkelsumme haben. Andrerseits wäre dies aber unvereinbar damit, dass die Dreiecke die gleiche Winkelsumme haben, da ein Dreieck, das einen Teil eines andren ausmacht, kleineren Exzess bzw. Defekt als dieses hat.

Damit ist man zu folgendem Resultat gelangt:

Satz 23. Im elliptischen und im hyperbolischen Fall sind zwei Dreiecke mit lauter ordinären Winkeln und gleicher Winkelsumme stets zerlegungsgleich.

Aus der obigen Betrachtung geht zugleich hervor, dass man den folgenden Satz aussprechen kann:

Satz 24. Zwei Dreiecke mit derselben ordinären Winkelsumme und ebenbürtigen grössten Seiten sind zerlegungsgleich.

Im elliptischen Fall, wo die Winkelsumme ja stets ordinär ist, da sie grösser als $2R$ ist, ist der Wortlaut wie folgt abzuändern:

Zwei Dreiecke mit derselben Winkelsumme und ebenbürtigen grössten Seiten sind zerlegungsgleich.

Wir bemerken ferner, dass ein Dreieck ABC, dessen Seite AB den anderen Seiten nicht unterlegen ist, im elliptischen Fall stets einem gleichschenkligen Dreieck mit der Grundlinie AB zerlegungsgleich ist. Die Verbindungsstrecke MN der Mittelpunkte von AC und BC ist nämlich grösser als $\frac{1}{2}AB$ und zugleich kleiner als $\frac{1}{2}(BC + CA)$, also mit AB ebenbürtig.

Für konvexe Polygone können wir nun im elliptischen Fall den folgenden Satz aufstellen:

Satz 25. Zwei konvexe Polygone mit demselben Exzess und ebenbürtigen grössten Seiten sind zerlegungsgleich.

Zunächst mögen zwei Vierecke $ABCD$ und $A_1B_1C_1D_1$ mit den grössten Seiten AB und A_1B_1 betrachtet werden. Die Schnittpunkte der Diagonalen seien O und O_1. Wenigstens eine der Strecken AO und BO ist mit AB ebenbürtig. Sei dies AO. Dann sind AC und AB ebenbürtig, und das Viereck ist somit in zwei Dreiecke mit der mit AB ebenbürtigen gemeinsamen Seite AC zerlegt. Diese Dreiecke können, da keine ihrer Seiten AC überlegen ist, in ihnen zerlegungsgleiche, gleichschenklige Dreiecke mit gemeinsamer Basis verwandelt werden; und diese machen ein Viereck aus, das aus zwei kongruenten Dreiecken zusammengesetzt ist. Diese Dreiecke können wiederum in gleichschenklige verwandelt werden. Auf dieselbe Weise kann das andere Viereck in die Summe zweier kongruenter gleichschenkliger Dreiecke, die denselben Exzess wie die vorigen haben, verwandelt werden. Hiermit ist für zwei Vierecke mit demselben Exzess alles klar.

Bei Fünf- und Sechsecken kann man in ähnlicher Weise vorgehen, z. B. für Sechsecke so: Man zerlegt das eine Sechseck in zwei Vierecke und verwandelt diese in zwei Paare T_1 und T_2 von kongruenten Dreiecken. Eines der Dreiecke T_1 und eines der Dreiecke T_2 zusammen werden durch gleichschenklige Dreiecke mit gemeinsamer Seite ersetzt, womit das Sechseck auf die Summe von vier kongruenten Dreiecken reduziert ist. Analog behandelt man das andere Sechseck. Auch hier entstehen vier kongruente Dreiecke, von denen jedes einem der vorigen zerlegungsgleich ist.

Auf diese Weise geht man weiter, und die Untersuchung führt dann gerade auf den obigen Satz.

Was den hyperbolischen Fall betrifft, so ist man genötigt, weitergehende Vorbehalte zu machen, z. B. indem man die Untersuchung auf solche konvexen Polygone beschränkt, bei denen alle Dreipunktswinkel (das sind die Winkel der durch drei Polygonecken bestimmten Dreiecke) ordinär sind. Hier zeigen den obigen ähnliche Betrachtungen, dass Polygone dieser Art zerlegungsgleich sind, wenn sie denselben Defekt haben. Übrigens gilt der analoge Satz auch in der elliptischen Ebene.

§ 11. Zum Schluss führen wir die entsprechenden Untersuchungen für die Lehre vom Flächeninhalt auf der Kugel durch.

Wir verwenden auch hier die gewöhnliche Verwandlungsfigur für ein Dreieck ABC, und die der früheren analoge, die Verschiebung der Verbindungsstrecke MN der Seitenmittelpunkte längs ihres Grosskreises betreffende Betrachtung führt sofort zu dem Satz: Dreieck ABC ist einem anderen Dreieck ABD mit derselben Grundlinie AB zerlegungsgleich, wenn nur die Verbindungsstrecke der Mittelpunkte der beiden anderen Seiten des zweiten Dreiecks aus der entsprechenden Strecke MN des ersten durch eine Verschiebung längs des Grosskreises MN hervorgeht, deren Grösse der Strecke MN selbst ebenbürtig ist. Hieraus folgt zugleich, dass das Dreieck ABC einem Zweieck zerlegungsgleich ist, wenn MN ordinär, d. h. dem ganzen Grosskreis der Kugel ebenbürtig ist.

Die einzigen sphärischen Dreiecke, die keinem Zweieck zerlegungsgleich sind, sind also solche mit singulären Verbindungsstrekken der Seitenmittelpunkte. Das von diesen Strecken gebildete Dreieck ist in dem Sinne singulär, dass alle Abstände zwischen seinen Punkten singulär sind. Das ursprüngliche Dreieck selbst ist dann auch singulär. Die einzigen Dreiecke, die durch endliche Zerlegung und Zusammensetzung nicht in ein Zweieck verwandelt werden können, sind die singulären, die Dreiecke mit singulären Seiten; und dass dies bei diesen Dreiecken nicht möglich ist, ist von vornherein einleuchtend.

Aus diesen Betrachtungen ergibt sich

Satz 26. Zwei sphärische Dreiecke sind zerlegungsgleich, wenn sie denselben Exzess ε und jedes wenigstens eine ordinäre Seite besitzt.

Beide sind nämlich einem Zweieck mit dem Winkel $\frac{\varepsilon}{2}$ zerlegungsgleich.

Satz 27. Zwei sphärische Dreiecke mit demselben Exzess ε sind stets dann zerlegungsgleich, wenn ε ordinär ist.

Ein singuläres Dreieck hat nämlich stets singulären Exzess. Dies erkennt man ganz wie in der offenen elliptischen Ebene.

Überhaupt macht jeder singuläre Bereich auf der Kugel, d. h. die Menge aller Punkte, deren Abstand von einem festen Punkt

kleiner oder ebenbürtig einem vorgegebenen singulären Abstand ist, eine offene elliptische Ebene aus, so dass in einem solchen Bereich alle Sätze dieser Ebene gelten.

Was die sphärischen Polygone betrifft, können wir ganz wie früher vorgehen. Hat ein konvexes sphärisches Viereck eine ordinäre Seite, so bestimmt diese zusammen mit den Diagonalen ein Dreieck, dessen andere Seiten nicht beide singulär sein können. Eine Diagonale, die eine ordinäre dieser Seiten enthält, ist selbst ordinär und teilt das Viereck in zwei Dreiecke, die beide durch Zerlegung und Zusammensetzung in Zweiecke verwandelt werden können. Damit wird auch das ganze Viereck in ein Zweieck verwandelt, also: Ein konvexes sphärisches Viereck, das wenigstens eine ordinäre Seite (und daher mindestens noch eine) besitzt, ist stets einem Zweieck zerlegungsgleich. Der Satz lässt sich leicht auf Polygone mit mehr Seiten erweitern. Die einzigen konvexen sphärischen Polygone, die nicht in Zweiecke verwandelt werden können, sind die singulären, deren sämtliche Seiten und somit auch ihr Exzess singulär sind. Man hat also die folgenden Sätze:

Satz 28. Zwei konvexe sphärische Polygone mit demselben Exzess, von denen jedes wenigstens eine ordinäre Seite besitzt, sind zerlegungsgleich.

Satz 29. Zwei konvexe sphärische Polygone mit demselben ordinären Exzess sind zerlegungsgleich.

Man kann diese Resultate auch zu folgendem Satz zusammenfassen:

Satz 30. Nicht-singuläre, konvexe sphärische Polygone mit demselben Exzess sind zerlegungsgleich.

Für singuläre sphärische Polygone hat man, wie bereits bemerkt, dieselben Sätze wie in der schwachen elliptischen Geometrie.

Indleveret til Selskabet den 10. Januar 1944.
Færdig fra Trykkeriet den 26. Maj 1944.

DET KGL. DANSKE VIDENSKABERNES SELSKAB
MATEMATISK-FYSISKE MEDDELELSER, BIND XXI, NR. 6

LIBRATIONSPUNKTE IM RESTRINGIERTEN VIERKÖRPER-PROBLEM

VON

PEDER PEDERSEN

KØBENHAVN
I KOMMISSION HOS EJNAR MUNKSGAARD
1944

INHALT

Printed in Denmark.
Bianco Lunos Bogtrykkeri A/S

EINLEITUNG

In einer Abhandlung aus dem Jahre 1924 hat M. LINDOW[1] die Librationspunkte in dem speziellen Fall des Vierkörperproblems bestimmt, wo drei gleich grosse Massen in der relativen Bewegung in den Eckpunkten eines gleichseitigen Dreiecks fest liegen, und die vierte Masse unendlich klein ist und sich in derselben Ebene bewegt wie die drei endlichen Massen. In diesem Falle findet man 10 Librationspunkte. Diese zu bestimmen ist eine recht mühsame Aufgabe, da die Bestimmung von der Lösung von Gleichungen recht hohen Grades abhängig ist.

Die vorliegende Abhandlung beabsichtigt, die Librationspunkte für willkürliche Massenverhältnisse zu bestimmen. In Analogie mit der Bezeichnung des problème restreint als das restringierte Dreikörperproblem wollen wir dieses Problem das restringierte Vierkörperproblem nennen.

Die gestellte Aufgabe wäre nicht zu bewältigen, wenn sie nach derselben Methode gelöst werden sollte, die LINDOW in dem speziellen Fall mit drei gleich grossen, endlichen Massen hat anwenden müssen. Indessen liegt die Sache nun so, dass man im allgemeinen Falle, wo die Massen willkürlich sind, die Problemstellung mit Erfolg umkehren kann: Statt die Librationspunkte von gegebenen Massenverhältnissen aus zu bestimmen, kann man die Massenverhältnisse von gegebenen Librationspunkten aus bestimmen. Denn während bei der Anwendung des erstgenannten Verfahrens die Lösung von Gleichungen recht hohen Grades verlangt wird, wird bei der Verwendung des zweiten Verfahrens nur die Lösung von Gleichungen ersten Grades verlangt.

Bei der Anwendung dieser Methode in Praxis kann man Schritt für Schritt die Librationspunkte durch die ganze Ebene

[1] Der Kreisfall im Problem der 3 + 1 Körper, A. N. 220, 369 und in den Publikationen der Kopenhagener Sternwarte Nr. 46.

verschieben; die entsprechende Änderung der Massenverhältnisse kann dann auf eine anschauliche Weise durch die Verschiebung des gemeinsamen Schwerpunktes der Massen ausgedrückt werden. Aus einer solchen Untersuchung wird es dann hervorgehen, dass die Librationspunkte nur innerhalb bestimmter Gebiete der Ebene fallen können, und die Bestimmung dieser Gebiete wird eins der wichtigsten Resultate der Untersuchung sein.

Im Abschnitt I wird das Problem ganz allgemein behandelt werden, und es zeigt sich, dass für einen gegebenen Librationspunkt die Koordinaten des entsprechenden Schwerpunktes durch zwei Gleichungen ersten Grades bestimmt werden können.

Mit den Resultaten des Abschnitts I als Grundlage wird im Abschnitt II eine theoretische Untersuchung einer Reihe von speziellen Fällen ausgeführt.

Ebenfalls mit den Resultaten im Abschnitt I als Grundlage wird endlich im Abschnitt III eine eingehende numerische Behandlung des Problems vorgenommen.

Im allgemeinen werden nur positive Werte der endlichen Massen berücksichtigt werden, so dass ihr gemeinsamer Schwerpunkt in das von den Massen gebildete gleichseitige Dreieck fällt. In gewissen speziellen Fällen wird es jedoch der Übersicht wegen notwendig sein, auch negative Werte der Massen zu berücksichtigen, so dass ihr gemeinsamer Schwerpunkt in diesen Fällen ausserhalb des gleichseitigen Dreiecks fallen wird.

Wenn eine der endlichen Massen gegen Null strebt, wird das Problem auf das problème restreint reduziert, und in diesem Falle werden die Librationspunkte in die fünf bekannten Librationspunkte L_1, L_2, L_3, L_4 und L_5 hineinwandern. Dieser Übergang vom allgemeinen zum speziellen Fall wird gewisse Aufschlüsse über den verschiedenen Charakter dieser fünf Librationspunkte geben können.

Die vorliegende Abhandlung ist durch eine pekuniäre Unterstützung seitens des Carlsbergfonds, dem ich zu grossem Dank verpflichtet bin, ermöglicht worden. Es ist mir auch eine liebe Pflicht, an dieser Stelle Herrn Professor E. Strömgren für gute Ratschläge und andere Hilfe, die für die Durchführung meiner Arbeit von wesentlicher Bedeutung waren, meinen herzlichsten Dank auszusprechen.

I. Der allgemeine Fall.

1. Die Differentialgleichungen der Bewegung.

Die drei endlichen Massen m_1, m_2 und m_3 und eine vierte unendlich kleine Masse befinden sich in einem gegebenen Augenblick in derselben Ebene, mit Geschwindigkeiten, die in dieser Ebene liegen. Die vier Massen werden dann, wenn sie keinen anderen Einwirkungen als ihren gegenseitigen Anziehungen ausgesetzt sind, für immer in dieser Ebene bleiben. Wir wählen nun in dieser Ebene ein festes, rechtwinkliges Koordinatensystem und bezeichnen die Koordinaten der drei endlichen Massen in diesem Koordinatensystem mit (X_1, Y_1), (X_2, Y_2) und (X_3, Y_3), während die unendlich kleine Masse die Koordinaten (X, Y) hat. Wir bezeichnen ferner die Distanzen zwischen den endlichen Massen mit $\varrho_{1,2}$, $\varrho_{2,3}$ und $\varrho_{1,3}$, während ϱ_1, ϱ_2 und ϱ_3 die Distanzen zwischen den drei endlichen Massen und der unendlich kleinen Masse bezeichnen. Indem k^2 die Gravitationskonstante bezeichnet, erhalten wir die folgenden Differentialgleichungen für die Bewegung der drei endlichen Massen:

$$\left.\begin{aligned}
X_1'' &= -k^2 m_2 (X_1 - X_2) / \varrho_{1,2}^3 - k^2 m_3 (X_1 - X_3) / \varrho_{1,3}^3, \\
Y_1'' &= -k^2 m_2 (Y_1 - Y_2) / \varrho_{1,2}^3 - k^2 m_3 (Y_1 - Y_3) / \varrho_{1,3}^3, \\
X_2'' &= -k^2 m_1 (X_2 - X_1) / \varrho_{1,2}^3 - k^2 m_3 (X_2 - X_3) / \varrho_{2,3}^3, \\
Y_2'' &= -k^2 m_1 (Y_2 - Y_1) / \varrho_{1,2}^3 - k^2 m_3 (Y_2 - Y_3) / \varrho_{2,3}^3, \\
X_3'' &= -k^2 m_1 (X_3 - X_1) / \varrho_{1,3}^3 - k^2 m_2 (X_3 - X_2) / \varrho_{2,3}^3, \\
Y_3'' &= -k^2 m_1 (Y_3 - Y_1) / \varrho_{1,3}^3 - k^2 m_2 (Y_3 - Y_2) / \varrho_{2,3}^3,
\end{aligned}\right\} \quad (1)$$

während die Bewegung der unendlich kleinen Masse durch die folgenden Differentialgleichungen bestimmt wird:

$$\left.\begin{aligned} X'' &= -k^2 m_1 (X - X_1)/\varrho_1^3 - k^2 m_2 (X - X_2)/\varrho_2^3 - k^2 m_3 (X - X_3)/\varrho_3^3, \\ Y'' &= -k^2 m_1 (Y - Y_1)/\varrho_1^3 - k^2 m_2 (Y - Y_2)/\varrho_2^3 - k^2 m_3 (Y - Y_3)/\varrho_3^3. \end{aligned}\right\} \quad (2)$$

Wir ersetzen jetzt das feste Koordinatensystem X, Y durch ein mit der konstanten Winkelgeschwindigkeit n rotierendes Koordinatensystem x, y. Wir erhalten dann die Transformationsgleichungen:

$$\left.\begin{aligned} X &= x \cos nt - y \sin nt, \\ Y &= x \sin nt + y \cos nt. \end{aligned}\right\} \quad (3)$$

Die Differentialgleichungen für die Bewegung der drei endlichen Massen in dem rotierenden Koordinatensystem werden nun:

$$\left.\begin{aligned} x_1'' - 2ny_1' - n^2 x_1 &= -k^2 m_2 (x_1 - x_2)/\varrho_{1,2}^3 - k^2 m_3 (x_1 - x_3)/\varrho_{1,3}^3, \\ y_1'' + 2nx_1' - n^2 y_1 &= -k^2 m_2 (y_1 - y_2)/\varrho_{1,2}^3 - k^2 m_3 (y_1 - y_3)/\varrho_{1,3}^3, \\ x_2'' - 2ny_2' - n^2 x_2 &= -k^2 m_1 (x_2 - x_1)/\varrho_{1,2}^3 - k^2 m_3 (x_2 - x_3)/\varrho_{2,3}^3, \\ y_2'' + 2nx_2' - n^2 y_2 &= -k^2 m_1 (y_2 - y_1)/\varrho_{1,2}^3 - k^2 m_3 (y_2 - y_3)/\varrho_{2,3}^3, \\ x_3'' - 2ny_3' - n^2 x_3 &= -k^2 m_1 (x_3 - x_1)/\varrho_{1,3}^3 - k^2 m_2 (x_3 - x_2)/\varrho_{2,3}^3, \\ y_3'' + 2nx_3' - n^2 y_3 &= -k^2 m_1 (y_3 - y_1)/\varrho_{1,3}^3 - k^2 m_2 (y_3 - y_2)/\varrho_{2,3}^3, \end{aligned}\right\} \quad (4)$$

während die Bewegung der unendlich kleinen Masse durch folgende Differentialgleichungen bestimmt wird:

$$\left.\begin{aligned} x'' - 2ny' - n^2 x &= -k^2 m_1 (x - x_1)/\varrho_1^3 - k^2 m_2 (x - x_2)/\varrho_2^3 \\ &\quad - k^2 m_3 (x - x_3)/\varrho_3^3, \\ y'' + 2nx' - n^2 y &= -k^2 m_1 (y - y_1)/\varrho_1^3 - k^2 m_2 (y - y_2)/\varrho_2^3 \\ &\quad - k^2 m_3 (y - y_3)/\varrho_3^3. \end{aligned}\right\} \quad (5)$$

Wir betrachten jetzt den speziellen Fall, wo die drei endlichen Massen in dem rotierenden Koordinatensystem feste Lagen einnehmen, indem sie sich in den Eckpunkten eines gleichseitigen Dreiecks mit der Seite ϱ befinden; ihre Geschwindigkeit und Akzeleration müssen dann zu jeder Zeit gleich Null sein. Wir haben deshalb:

$$\left.\begin{aligned} x_1' = x_2' = x_3' = 0, \quad x_1'' = x_2'' = x_3'' = 0, \\ y_1' = y_2' = y_3' = 0, \quad y_1'' = y_2'' = y_3'' = 0, \end{aligned}\right\} \quad (6)$$

$$\varrho_{1,2} = \varrho_{2,3} = \varrho_{1,3} = \varrho. \quad (7)$$

Aus (4) in Verbindung mit (6) und (7) erhalten wir dann:

$$\left.\begin{aligned} n^2\varrho^3 x_1 &= k^2 m_2 (x_1 - x_2) + k^2 m_3 (x_1 - x_3), \\ n^2\varrho^3 x_2 &= k^2 m_1 (x_2 - x_1) + k^2 m_3 (x_2 - x_3), \\ n^2\varrho^3 x_3 &= k^2 m_1 (x_3 - x_1) + k^2 m_2 (x_3 - x_2), \end{aligned}\right\} \quad (8)$$

$$\left.\begin{aligned} n^2\varrho^3 y_1 &= k^2 m_2 (y_1 - y_2) + k^2 m_3 (y_1 - y_3), \\ n^2\varrho^3 y_2 &= k^2 m_1 (y_2 - y_1) + k^2 m_3 (y_2 - y_3), \\ n^2\varrho^3 y_3 &= k^2 m_1 (y_3 - y_1) + k^2 m_2 (y_3 - y_2), \end{aligned}\right\} \quad (9)$$

wo (8) zur Bestimmung von x_1, x_2 und x_3 dienen kann, während y_1, y_2 und y_3 mit Hilfe von (9) bestimmt werden können.

Wenn wir nun die drei Gleichungen (8) mit bzw. m_1, m_2 und m_3 multiplizieren und die drei Gleichungen (9) auf entsprechende Weise behandeln, gibt Addition die zwei Gleichungen:

$$\left.\begin{aligned} m_1 x_1 + m_2 x_2 + m_3 x_3 &= 0, \\ m_1 y_1 + m_2 y_2 + m_3 y_3 &= 0. \end{aligned}\right\} \quad (10)$$

Es ergibt sich aus (10), dass der gemeinsame Schwerpunkt der drei endlichen Massen in den Anfangspunkt des Koordinatensystems fallen muss.

Mit Hilfe von (10) können (8) und (9) auf folgende Gleichungssysteme reduziert werden:

$$\left.\begin{aligned} (k^2 M - n^2\varrho^3)\, x_1 &= 0, \\ (k^2 M - n^2\varrho^3)\, x_2 &= 0, \\ (k^2 M - n^2\varrho^3)\, x_3 &= 0, \end{aligned}\right\} \quad (11)$$

$$\left.\begin{aligned} (k^2 M - n^2\varrho^3)\, y_1 &= 0, \\ (k^2 M - n^2\varrho^3)\, y_2 &= 0, \\ (k^2 M - n^2\varrho^3)\, y_3 &= 0, \end{aligned}\right\} \quad (12)$$

wo

$$M = m_1 + m_2 + m_3. \quad (13)$$

Wir setzen jetzt voraus, dass nicht sämtliche sechs Koordinaten gleich Null sind, wonach die sechs Bedingungsgleichungen (11) und (12) auf eine einzelne Bedingungsgleichung

$$k^2M - n^2\varrho^3 = 0 \tag{14}$$

reduziert werden.

Unter den im vorhergehenden gemachten Voraussetzungen gilt also folgendes System von Bedingungsgleichungen:

$$\left.\begin{aligned} x_1' = x_2' = x_3' &= 0, \\ y_1' = y_2' = y_3' &= 0, \\ \varrho_{1,2} = \varrho_{2,3} = \varrho_{1,3} &= \varrho, \\ m_1x_1 + m_2x_2 + m_3x_3 &= 0, \\ m_1y_1 + m_2y_2 + m_3y_3 &= 0, \\ k^2M - n^2\varrho^3 &= 0. \end{aligned}\right\} \tag{15}$$

2. Librationspunkte.

Nachdem wir nun nachgewiesen haben, dass die drei endlichen Massen unter ihren gegenseitigen Anziehungen für immer in den Eckpunkten eines gleichseitigen Dreiecks verbleiben können, so dass sie in einem Koordinatensystem, das seinen Anfangspunkt in dem gemeinsamen Schwerpunkt der Massen hat, und das mit einer passenden Winkelgeschwindigkeit rotiert, feste Stellungen einnehmen, wollen wir die Bedingung dafür finden, dass die unendlich kleine Masse auch eine feste Stellung in dem rotierenden Koordinatensystem einnimmt; wir wollen mit anderen Worten die Librationspunkte, die den drei endlichen Massen entsprechen, bestimmen. Ist der Punkt (x, y) ein Librationspunkt, so haben wir zu jeder Zeit

$$\left.\begin{aligned} x' = 0, \quad x'' &= 0, \\ y' = 0, \quad y'' &= 0, \end{aligned}\right\} \tag{16}$$

die, in die Differentialgleichungen (5) für die Bewegung der unendlich kleinen Masse eingesetzt, folgende zwei Bedingungsgleichungen ergeben:

$$\left.\begin{aligned} k^2m_1(x-x_1)/\varrho_1^3 + k^2m_2(x-x_2)/\varrho_2^3 + k^2m_3(x-x_3)/\varrho_3^3 &= n^2x, \\ k^2m_1(y-y_1)/\varrho_1^3 + k^2m_2(y-y_2)/\varrho_2^3 + k^2m_3(y-y_3)/\varrho_3^3 &= n^2y, \end{aligned}\right\} \tag{17}$$

wo

$$\left.\begin{aligned} \varrho_1^2 &= (x-x_1)^2+(y-y_1)^2, \\ \varrho_2^2 &= (x-x_2)^2+(y-y_2)^2, \\ \varrho_3^2 &= (x-x_3)^2+(y-y_3)^2. \end{aligned}\right\} \quad (18)$$

Wird in (17) der Wert für n^2 aus der Gleichung (14) eingesetzt, so kann die Gravitationskonstante k^2 aus den zwei Gleichungen fortdividiert werden, und hierdurch entstehen die Gleichungen

$$\left.\begin{aligned} m_1(x-x_1)/\varrho_1^3+m_2(x-x_2)/\varrho_2^3+m_3(x-x_3)/\varrho_3^3 &= Mx/\varrho^3, \\ m_1(y-y_1)/\varrho_1^3+m_2(y-y_2)/\varrho_2^3+m_3(y-y_3)/\varrho_3^3 &= My/\varrho^3. \end{aligned}\right\} \quad (19)$$

Wir führen nun in die zwei Bedingungsgleichungen die relativen Massen μ_1, μ_2 und μ_3 ein, die durch die Gleichungen

$$\mu_1 = m_1/M, \quad \mu_2 = m_2/M, \quad \mu_3 = m_3/M \quad (20)$$

definiert werden, so dass wir

$$\mu_1+\mu_2+\mu_3 = 1 \quad (21)$$

haben.

Hierdurch entstehen die zwei neuen Bedingungsgleichungen

$$\left.\begin{aligned} \mu_1(x-x_1)/\varrho_1^3+\mu_2(x-x_2)/\varrho_2^3+\mu_3(x-x_3) &= x/\varrho^3, \\ \mu_1(y-y_1)/\varrho_1^3+\mu_2(y-y_2)/\varrho_2^3+\mu_3(y-y_3) &= y/\varrho^3. \end{aligned}\right\} \quad (22)$$

Das Problem, die Librationspunkte zu bestimmen, ist damit von einem dynamischen Problem auf ein rein mathematisches Problem reduziert worden. Das zeigt sich u. a. dadurch, dass die zwei Bedingungsgleichungen von den Einheiten der Masse und der Zeit unabhängig sind. Was die Einheit der Länge betrifft, werden wir später eine für das vorliegende Problem bequeme Längeneinheit wählen.

3. Lösung der Bedingungsgleichungen.

Bei der Behandlung der zwei Bedingungsgleichungen (22) in Verbindung mit den Gleichungen (18) und (21) kann man nach zwei verschiedenen Verfahren vorgehen.

In die erwähnten Gleichungen gehen ein:

1. Die Koordinaten der drei endlichen Massen; diese Koordinaten sind bekannte Grössen.
2. Die Koordinaten x und y der Librationspunkte.
3. Die relativen Massen μ_1, μ_2 und μ_3.

Wenn die relativen Massen bekannt sind, werden die zwei Bedingungsgleichungen dazu dienen können, die Koordinaten x und y der Librationspunkte zu bestimmen. Da aber x und y sowohl explicite in die Zähler als implicite in die Nenner der Brüche eingehen, wird die Bestimmung von x und y sehr schwierig werden, und es werden sich gewöhnlich viele Lösungen ergeben. Einem bestimmten Satz von Werten der relativen Massen entspricht indessen eine bestimmte Lage des gemeinsamen Schwerpunktes, und wir erhalten deshalb das folgende Resultat: Einer bestimmten Lage des Schwerpunktes entsprechen gewöhnlich mehrere Librationspunkte.

Ist dagegen die Lage eines Librationspunktes und damit x und y bekannt, werden die zwei Bedingungsgleichungen in Verbindung mit Gleichung (21) zur Bestimmung der relativen Massen μ_1, μ_2 und μ_3 dienen können. Da die drei Gleichungen in diesen Grössen linear sind, werden die Gleichungen leicht gelöst werden können, und sie werden im allgemeinen einen und nur einen Satz von Werten der relativen Massen und damit eine bestimmte Lage des Schwerpunktes ergeben. Wir erhalten deshalb: Einer bestimmten Lage eines Librationspunktes entspricht gewöhnlich ein und nur ein Schwerpunkt.

Hiermit ist die Grundlage für die folgende Behandlung der zwei Bedingungsgleichungen gegeben. Wir wollen in diesen Gleichungen x und y als bekannte Grössen auffassen, während μ_1, μ_2 und μ_3 unbekannte Grössen sind. Die in μ_1, μ_2 und μ_3 linearen Gleichungen wollen wir auf eine möglichst einfache Form zu bringen suchen.

Wir denken uns das gleichseitige Dreieck (Massendreieck) auf einfache Weise in dem rotierenden Koordinatensystem x, y orientiert, indem die Verbindungslinie M_2M_3 zwischen den Massen m_2 und m_3 als parallel mit der Ordinatenachse vorausgesetzt wird (Abb. 1). Mit dem Anfangspunkt im Mittelpunkt des Massendreiecks und mit Achsen, die mit der x-Achse und der y-Achse parallel sind, wird ein neues Koordinatensystem ξ, η eingeführt.

Wir bezeichnen die Koordinaten des Anfangspunktes des Koordinatensystems x, y in dem neuen Koordinatensystem mit σ, τ; der Übergang von dem einen System von Koordinaten zum anderen findet dann mit Hilfe der Gleichungen

$$\left.\begin{aligned} \xi &= \sigma + x, \\ \eta &= \tau + y \end{aligned}\right\} \quad (23)$$

statt.

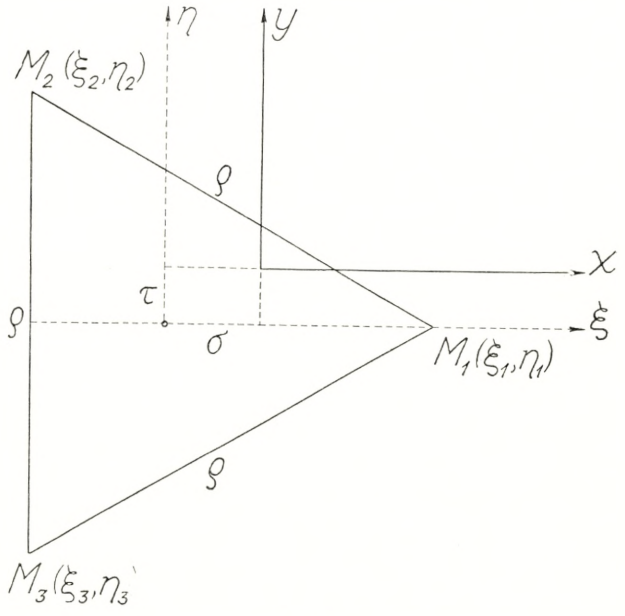

Abb. 1.

σ und τ, d. h. die Koordinaten des Schwerpunktes im neuen Koordinatensystem ξ, η, können mit Hilfe der relativen Massen μ_1, μ_2 und μ_3 ausgedrückt werden. Man findet leicht:

$$\left.\begin{aligned} \sigma &= \frac{1}{6}\sqrt{3}\,(3\mu_1 - 1)\,\varrho, \\ \tau &= \frac{1}{2}\,(\mu_2 - \mu_3)\,\varrho. \end{aligned}\right\} \quad (24)$$

Umgekehrt können μ_1, μ_2 und μ_3 mit Hilfe der Koordinaten des Schwerpunktes σ und τ ausgedrückt werden:

$$\left.\begin{aligned} \mu_1 &= \frac{1}{3} + \frac{2}{3}\sqrt{3}\,\sigma/\varrho, \\ \mu_2 &= \frac{1}{3} - \frac{1}{3}\sqrt{3}\,\sigma/\varrho + \tau/\varrho, \\ \mu_3 &= \frac{1}{3} - \frac{1}{3}\sqrt{3}\,\sigma/\varrho - \tau/\varrho. \end{aligned}\right\} \quad (25)$$

Statt μ_1, μ_2 und μ_3 als unbekannte Grössen zu behandeln können wir σ und τ als Unbekannte betrachten. Aus den zwei Bedingungsgleichungen (22) in Verbindung mit (23) und (25) erhalten wir zur Bestimmung von σ und τ folgende zwei Gleichungen:

$$\left.\begin{aligned} &\left[\frac{1}{3}\sqrt{3}\left(2\frac{\xi-\xi_1}{\varrho_1^3} - \frac{\xi-\xi_2}{\varrho_2^3} - \frac{\xi-\xi_3}{\varrho_3^3}\right) + \frac{1}{\varrho^2}\right]\sigma + \left[\frac{\xi-\xi_2}{\varrho_2^3} - \frac{\xi-\xi_3}{\varrho_3^3}\right]\tau \\ &\qquad = \frac{\xi}{\varrho^2} - \frac{\varrho}{3}\left[\frac{\xi-\xi_1}{\varrho_1^3} + \frac{\xi-\xi_2}{\varrho_2^3} + \frac{\xi-\xi_3}{\varrho_3^3}\right], \\ &\left[\frac{1}{3}\sqrt{3}\left(2\frac{\eta-\eta_1}{\varrho_1^3} - \frac{\eta-\eta_2}{\varrho_2^3} - \frac{\eta-\eta_3}{\varrho_3^3}\right)\right]\sigma + \left[\frac{\eta-\eta_2}{\varrho_2^3} - \frac{\eta-\eta_3}{\varrho_3^3} + \frac{1}{\varrho^2}\right]\tau \\ &\qquad = \frac{\eta}{\varrho^2} - \frac{\varrho}{3}\left[\frac{\eta-\eta_1}{\varrho_1^3} + \frac{\eta-\eta_2}{\varrho_2^3} + \frac{\eta-\eta_3}{\varrho_3^3}\right], \end{aligned}\right\} \quad (26)$$

wo

$$\left.\begin{aligned} \varrho_1^2 &= (\xi-\xi_1)^2 + (\eta-\eta_1)^2, \\ \varrho_2^2 &= (\xi-\xi_2)^2 + (\eta-\eta_2)^2, \\ \varrho_3^2 &= (\xi-\xi_3)^2 + (\eta-\eta_3)^2. \end{aligned}\right\} \quad (27)$$

Der Kürze wegen schreiben wir jetzt

$$\left.\begin{aligned} \alpha_1 &= \frac{\xi-\xi_1}{\varrho_1^3}, \quad \alpha_2 = \frac{\xi-\xi_2}{\varrho_2^3}, \quad \alpha_3 = \frac{\xi-\xi_3}{\varrho_3^3}, \\ \beta_1 &= \frac{\eta-\eta_1}{\varrho_1^3}, \quad \beta_2 = \frac{\eta-\eta_2}{\varrho_2^3}, \quad \beta_3 = \frac{\eta-\eta_3}{\varrho_3^3}, \end{aligned}\right\} \quad (28)$$

wonach die Gleichungen zur Bestimmung von σ und τ die einfachere Form

$$\left.\begin{aligned}\left[\frac{1}{3}\sqrt{3}\,(2\alpha_1-\alpha_2-\alpha_3)+\frac{1}{\varrho^2}\right]\sigma+\left[\alpha_2-\alpha_3\right]\tau &= \frac{\xi}{\varrho^2}-\frac{\varrho}{3}\left[\alpha_1+\alpha_2+\alpha_3\right],\\ \left[\frac{1}{3}\sqrt{3}\,(2\beta_1-\beta_2-\beta_3)\right]\sigma+\left[\beta_2-\beta_3+\frac{1}{\varrho^2}\right]\tau &= \frac{\eta}{\varrho^2}-\frac{\varrho}{3}\left[\beta_1+\beta_2+\beta_3\right]\end{aligned}\right\} \quad (29)$$

erhalten.

Eine weitere Vereinfachung kann jetzt dadurch stattfinden, dass eine bestimmte Längeneinheit festgelegt wird. Es wird bequem sein, als Längeneinheit den Radius des dem Massendreieck umschriebenen Kreises zu wählen; für die Seite ϱ des Massendreiecks erhalten wir dann

$$\varrho = \sqrt{3}. \quad (30)$$

Die Koordinaten der drei endlichen Massen werden:

$$\left.\begin{aligned}\xi_1 &= 1, \quad \xi_2 = -\frac{1}{2}, \quad \xi_3 = -\frac{1}{2},\\ \eta_1 &= 0, \quad \eta_2 = \frac{1}{2}\sqrt{3}, \quad \eta_3 = -\frac{1}{2}\sqrt{3},\end{aligned}\right\} \quad (31)$$

während die Gleichungen zur Bestimmung von σ und τ jetzt die einfachere Form

$$\left.\begin{aligned}\left[1+\sqrt{3}\,(2\alpha_1-\alpha_2-\alpha_3)\right]\sigma+3\left[\alpha_2-\alpha_3\right]\tau &= \xi-\sqrt{3}\,(\alpha_1+\alpha_2+\alpha_3), \quad \text{(I)}\\ \left[\sqrt{3}\,(2\beta_1-\beta_2-\beta_3)\right]\sigma+\left[1+3\,(\beta_2-\beta_3)\right]\tau &= \eta-\sqrt{3}\,(\beta_1+\beta_2+\beta_3) \quad \text{(II)}\end{aligned}\right\} \quad (32)$$

erhalten.

Diese zwei Gleichungen, die die Grundlage sowohl der theoretischen als der numerischen Behandlung des vorliegenden Problems bilden, werden im folgenden mit römisch I und II bezeichnet werden. Der Übersicht wegen geben wir jetzt eine Zusammenstellung der Formeln in der Reihenfolge, in der sie benutzt werden sollen, wenn man für einen gegebenen Librationspunkt mit den Koordinaten ξ und η den entsprechenden Schwerpunkt mit den Koordinaten σ und τ bestimmen will.

$$\left.\begin{aligned}\varrho_1^2 &= (\xi-1)^2+\eta^2,\\ \varrho_2^2 &= \left(\xi+\frac{1}{2}\right)^2+\left(\eta-\frac{1}{2}\sqrt{3}\right)^2,\\ \varrho_3^2 &= \left(\xi+\frac{1}{2}\right)^2+\left(\eta+\frac{1}{2}\sqrt{3}\right)^2.\end{aligned}\right\} \quad (33)$$

$$\left.\begin{aligned} \alpha_1 &= \frac{\xi-1}{\varrho_1^3}, \quad \alpha_2 = \frac{\xi+\frac{1}{2}}{\varrho_2^3}, \quad \alpha_3 = \frac{\xi+\frac{1}{2}}{\varrho_3^3}, \\ \beta_1 &= \frac{\eta}{\varrho_1^3}, \quad \beta_2 = \frac{\eta-\frac{1}{2}\sqrt{3}}{\varrho_2^3}, \quad \beta_3 = \frac{\eta+\frac{1}{2}\sqrt{3}}{\varrho_3^3}. \end{aligned}\right\} \quad (34)$$

$$\left.\begin{aligned} A_1 &= 1+\sqrt{3}\,(2\alpha_1-\alpha_2-\alpha_3), \\ B_1 &= 3\,(\alpha_2-\alpha_3), \\ C_1 &= \xi-\sqrt{3}\,(\alpha_1+\alpha_2+\alpha_3), \\ A_2 &= \sqrt{3}\,(2\beta_1-\beta_2-\beta_3), \\ B_2 &= 1+3\,(\beta_2-\beta_3), \\ C_2 &= \eta-\sqrt{3}\,(\beta_1+\beta_2+\beta_3). \end{aligned}\right\} \quad (35)$$

$$\left.\begin{aligned} A_1\sigma+B_1\tau &= C_1, \\ A_2\sigma+B_2\tau &= C_2. \end{aligned}\right\} \quad (36)$$

Die Bestimmung von σ und τ erfolgt, wie es sich aus dieser Zusammenstellung ergibt, in vier Schritten. Zunächst werden ϱ_1, ϱ_2 und ϱ_3 aus (33), dann α_1, α_2, α_3, β_1, β_2 und β_3 aus (34) bestimmt; nachher können A_1, B_1, C_1, A_2, B_2 und C_2 aus (35) abgeleitet werden; zum Schluss werden σ und τ durch Lösung der zwei linearen Gleichungen (36) bestimmt.

II. Spezialfälle.

1. Der Librationspunkt auf einer Symmetrieachse.

Wir wollen jetzt den speziellen Fall betrachten, wo der Librationspunkt auf eine der Symmetrieachsen des Massendreiecks fällt. Liegt der Librationspunkt auf der Symmetrieachse durch M_1 (der ξ-Achse), haben wir $\eta = 0$, woraus folgt:

$$\left.\begin{aligned} \varrho_1^2 &= (\xi-1)^2, \\ \varrho_2^2 &= \varrho_3^2 = 1+\xi+\xi^2, \end{aligned}\right\} \quad (1)$$

$$\left.\begin{aligned} \alpha_1 &= \frac{\xi - 1}{\varrho_1^3}, \quad \alpha_2 = \alpha_3 = \frac{\xi + \frac{1}{2}}{\varrho_2^3}, \\ \beta_1 &= 0, \quad \beta_2 = -\beta_3 = -\frac{\frac{1}{2}\sqrt{3}}{\varrho_2^3}, \end{aligned}\right\} \tag{2}$$

$$\left.\begin{aligned} A_1 &= 1 + 2\sqrt{3}\,(\alpha_1 - \alpha_2), \\ B_1 &= 0, \\ C_1 &= \xi - \sqrt{3}\,(\alpha_1 + 2\alpha_2), \\ A_2 &= 0, \\ B_2 &= 1 + 6\beta_2, \\ C_2 &= 0. \end{aligned}\right\} \tag{3}$$

Die Gleichungen zur Bestimmung von σ und τ werden deshalb auf

$$\left.\begin{aligned} [1 + 2\sqrt{3}\,(\alpha_1 - \alpha_2)]\,\sigma &= \xi - \sqrt{3}\,(\alpha_1 + 2\alpha_2), \quad \text{(I)} \\ [1 + 6\beta_2]\,\tau &= 0 \qquad\qquad\qquad\qquad\quad \text{(II)} \end{aligned}\right\} \tag{4}$$

reduziert, so dass σ aus I und τ aus II bestimmt werden können. Wird $1 + 6\beta_2 \neq 0$ vorausgesetzt, erhalten wir aus Gleichung II $\tau = 0$, und dies bedeutet, dass der Schwerpunkt, ebenso wie der Librationspunkt, auf der Symmetrieachse liegt. Die Abszisse des Schwerpunktes wird dann durch die Gleichung

$$\left.\sigma = \frac{\xi - \sqrt{3}\,(\alpha_1 + 2\alpha_2)}{1 + 2\sqrt{3}\,(\alpha_1 - \alpha_2)}\right\} \tag{5}$$

bestimmt.

Ist $1 + 6\beta_2 = 0$, braucht τ nicht gleich Null zu sein, und der Schwerpunkt kann dann ausserhalb der Symmetrieachse fallen. Aus $1 + 6\beta_2 = 0$ folgt $\varrho_2 = \sqrt{3}$, was wiederum zur Folge hat, dass entweder $\xi = 1$ oder $\xi = -2$ ist. Sowohl für $\xi = 1$ als für $\xi = -2$ erhalten wir aus (5) $\sigma = -\frac{1}{2}$. Es geht hieraus hervor, dass, wenn der Librationspunkt mit den Massen m_2 und m_3 die Eckpunkte eines gleichseitigen Dreiecks bildet, der Schwerpunkt

auf der Verbindungslinie zwischen m_2 und m_3 liegen wird. Die Masse m_1 ist in diesem Falle Null, und das Vierkörperproblem ist auf einen bekannten Spezialfall des Dreikörperproblems (das problème restreint) reduziert worden. Die Librationspunkte in $\xi = 1$ und $\xi = -2$ auf der Symmetrieachse entsprechen den Librationspunkten L_4 und L_5 im problème restreint.

Verhältnisse, die den für die Symmetrieachse durch die Masse m_1 gefundenen entsprechen, müssen auch für die Symmetrieachsen durch die Massen m_2 und m_3 gelten. Es gilt deshalb folgende Regel:

Wenn der Librationspunkt auf eine der Symmetrieachsen des Massendreiecks fällt, wird der entsprechende Schwerpunkt im allgemeinen auf dieselbe Symmetrieachse fallen. Nur wenn der Librationspunkt mit zwei der endlichen Massen die Eckpunkte eines gleichseitigen Dreiecks bildet, kann der entsprechende Schwerpunkt ausserhalb der Symmetrieachse fallen, und er wird dann auf die Seite des Dreiecks fallen, welche die zwei endlichen Massen verbindet.

2. Der Librationspunkt auf einer Verbindungslinie zwischen zwei Massen.

Wir gehen jetzt dazu über, den Fall zu behandeln, wo der Librationspunkt auf eine der drei Verbindungslinien zwischen den drei endlichen Massen fällt. Die Rechnung wird am einfachsten, wenn der Librationspunkt sich auf der Verbindungslinie zwischen den Massen m_2 und m_3 befindet, in welchem Falle $\xi = -\frac{1}{2}$ ist.

Es wird praktisch sein, die Untersuchung in 5 Teile einzuteilen, je nachdem

$$1^\circ. \quad -\frac{1}{2}\sqrt{3} < \eta < \frac{1}{2}\sqrt{3},$$

$$2^\circ. \quad \eta > \frac{1}{2}\sqrt{3},$$

$$3^\circ. \quad \eta < -\frac{1}{2}\sqrt{3},$$

$$4^\circ. \qquad \eta = \frac{1}{2}\sqrt{3},$$

$$5^\circ. \qquad \eta = -\frac{1}{2}\sqrt{3}.$$

In dem ersten Fall liegt der Librationspunkt zwischen m_2 und m_3, im zweiten und dritten Fall auf den Verlängerungen der Dreiecksseite, während er im vierten und fünften Fall in den Massen m_2 und m_3 selbst liegt.

Die Bestimmung von σ wird in den drei ersten Fällen dieselbe sein, weshalb diese Bestimmung ausgeführt werden wird, ehe die einzelnen Fälle jede für sich betrachtet werden.

In den drei ersten Fällen erhalten wir:

$$\alpha_2 = 0, \quad \alpha_3 = 0, \tag{6}$$

so dass Gleichung I zur Bestimmung von σ

$$(1 + 2\sqrt{3}\,\alpha_1)\,\sigma = -\frac{1}{2} - \sqrt{3}\,\alpha_1 \tag{7}$$

wird, woraus sich

$$\sigma = -\frac{1}{2} \tag{8}$$

ergibt.

$1^\circ.$ $\underline{-\frac{1}{2}\sqrt{3} < \eta < \frac{1}{2}\sqrt{3}.}$

Für $\xi = -\frac{1}{2}$ und unter der gegebenen Voraussetzung erhalten wir

$$\left.\begin{aligned} \varrho_1^2 &= \frac{9}{4} + \eta^2, \\ \varrho_2 &= \frac{1}{2}\sqrt{3} - \eta, \\ \varrho_3 &= \frac{1}{2}\sqrt{3} + \eta, \end{aligned}\right\} \tag{9}$$

$$\beta_1 = \frac{\eta}{\varrho_1^3}, \quad \beta_2 = -\frac{1}{\varrho_2^2}, \quad \beta_3 = \frac{1}{\varrho_3^2}. \tag{10}$$

Aus Gleichung II findet man danach den folgenden Wert für τ:

$$\tau = \frac{16\eta^5 - 24\eta^3 + 153\eta}{16\eta^4 - 120\eta^2 - 63}. \tag{11}$$

2°. $\eta > \frac{1}{2}\sqrt{3}$.

Für $\xi = -\frac{1}{2}$ und unter der gegebenen Voraussetzung erhalten wir

$$\left.\begin{aligned} \varrho_1^2 &= \frac{9}{4} + \eta^2, \\ \varrho_2 &= \eta - \frac{1}{2}\sqrt{3}, \\ \varrho_3 &= \eta + \frac{1}{2}\sqrt{3}, \end{aligned}\right\} \tag{12}$$

$$\beta_1 = \frac{\eta}{\varrho_1^3}, \quad \beta_2 = \frac{1}{\varrho_2^2}, \quad \beta_3 = \frac{1}{\varrho_3^2}. \tag{13}$$

Aus Gleichung II findet man danach den folgenden Wert für τ:

$$\tau = \eta - \frac{27\left(\eta^2 + \frac{1}{4}\right)}{\sqrt{3}\left(\eta^2 - \frac{3}{4}\right)^2 + 18\eta}. \tag{14}$$

3°. $\eta < -\frac{1}{2}\sqrt{3}$.

Für $\xi = -\frac{1}{2}$ und unter der gegebenen Voraussetzung erhalten wir

$$\left.\begin{aligned} \varrho_1^2 &= \frac{9}{4} + \eta^2, \\ \varrho_2 &= \frac{1}{2}\sqrt{3} - \eta, \\ \varrho_3 &= -\frac{1}{2}\sqrt{3} - \eta, \end{aligned}\right\} \tag{15}$$

$$\beta_1 = \frac{\eta}{\varrho_1^3}, \quad \beta_2 = -\frac{1}{\varrho_2^2}, \quad \beta_3 = -\frac{1}{\varrho_3^2}. \tag{16}$$

Aus Gleichung II findet man danach den folgenden Wert für τ:

$$\tau = \eta + \frac{27\left(\eta^2 + \frac{1}{4}\right)}{\sqrt{3}\left(\eta^2 - \frac{3}{4}\right)^2 - 18\,\eta}. \tag{17}$$

4°. $\eta = \frac{1}{2}\sqrt{3}$.

Mit den Werten $\xi = -\frac{1}{2}$ und $\eta = \frac{1}{2}\sqrt{3}$ erhalten wir

$$\varrho_1 = \sqrt{3}, \quad \varrho_2 = 0, \quad \varrho_3 = \sqrt{3}, \tag{18}$$

$$\left.\begin{aligned} \alpha_1 &= -\frac{1}{6}\sqrt{3}, \quad \alpha_3 = 0, \\ \beta_1 &= \frac{1}{6}, \qquad\quad \beta_3 = \frac{1}{3}, \end{aligned}\right\} \tag{19}$$

während α_2 und β_2 unbestimmt bleiben.

Wenn wir die Werte für α_1 und α_3 in I einsetzen, erhalten wir die Gleichung

$$-\sqrt{3}\,\alpha_2\,\sigma + 3\,\alpha_2\,\tau = -\sqrt{3}\,\alpha_2, \tag{20}$$

die nach Division durch die unbestimmte Grösse α_2 in

$$\sigma - \sqrt{3}\,\tau = 1 \tag{21}$$

umschrieben werden kann. Dies ist die Gleichung für die Verbindungslinie zwischen den Massen m_1 und m_3.

Wenn wir dann die Werte für β_1 und β_3 in II einsetzen, erhalten wir die Gleichung

$$-\sqrt{3}\,\beta_2\,\sigma + 3\,\beta_2\,\tau = -\sqrt{3}\,\beta_2, \tag{22}$$

die nach Division durch die unbestimmte Grösse β_2 in

$$\sigma - \sqrt{3}\,\tau = 1 \tag{23}$$

umschrieben werden kann, d. h. dieselbe Gleichung, die sich aus Gleichung I ergab. Hieraus geht hervor, dass, wenn der Librationspunkt in der Masse m_2 liegt, der Schwerpunkt in einem willkürlichen Punkt auf der Verbindungslinie zwischen den Massen m_1 und m_3 liegen kann. Dieses Resultat ist in Übereinstimmung mit dem früher gefundenen.

5°. $\eta = -\frac{1}{2}\sqrt{3}$.

Mit den Werten $\xi = -\frac{1}{2}$ und $\eta = -\frac{1}{2}\sqrt{3}$ erhalten wir

$$\varrho_1 = \sqrt{3}, \quad \varrho_2 = \sqrt{3}, \quad \varrho_3 = 0, \tag{24}$$

$$\left.\begin{aligned} \alpha_1 &= -\frac{1}{6}\sqrt{3}, \quad \alpha_2 = 0, \\ \beta_1 &= -\frac{1}{6}, \qquad \beta_2 = -\frac{1}{3}, \end{aligned}\right\} \tag{25}$$

während α_3 und β_3 unbestimmt bleiben.

Setzen wir die gefundenen Werten in I und II ein, erhalten wir in beiden Fällen die Gleichung

$$\sigma + \sqrt{3}\,\tau = 1, \tag{26}$$

das ist die Gleichung für die Verbindungslinie zwischen den Massen m_1 und m_2. Hieraus geht hervor, dass, wenn der Librationspunkt in der Masse m_3 liegt, der Schwerpunkt in einem willkürlichen Punkte auf der Verbindungslinie zwischen den Massen m_1 und m_2 liegen kann.

Verhältnisse, die den für die Verbindungslinie zwischen den Massen m_2 und m_3 gefundenen entsprechen, müssen auch für die zwei anderen Verbindungslinien zwischen den Massen gelten.

Es gilt deshalb folgende Regel:

Wenn der Librationspunkt auf eine der Verbindungslinien zwischen den Massen fällt, wird der Schwerpunkt im allgemeinen auf dieselbe Linie fallen. Nur wenn der Librationspunkt in einen der Eckpunkte des Massendreiecks fällt, kann der Schwerpunkt ausserhalb dieser Linie fallen, und er wird dann in einen willkürlichen Punkt auf der Seite fallen können, die die zwei anderen Eckpunkte des Dreiecks verbindet.

3. Der Librationspunkt in der Nähe des Mittelpunktes des Massendreiecks.

Wenn der Librationspunkt sich im Mittelpunkt des Massendreiecks befindet, wird der Schwerpunkt mit dem Librationspunkt zusammenfallen. Für $\xi = 0$ und $\eta = 0$ erhalten wir nämlich:

$$\varrho_1 = \varrho_2 = \varrho_3 = 1, \tag{27}$$

$$\left.\begin{aligned} \alpha_1 = -1, \quad \alpha_2 = \frac{1}{2}, \quad \alpha_3 = \frac{1}{2}, \\ \beta_1 = 0, \quad \beta_2 = -\frac{1}{2}\sqrt{3}, \quad \beta_3 = \frac{1}{2}\sqrt{3}, \end{aligned}\right\} \tag{28}$$

$$\left.\begin{aligned} A_1 = 1-3\sqrt{3}, \quad B_1 = 0, \quad C_1 = 0, \\ A_2 = 0, \quad B_2 = 1-3\sqrt{3}, \quad C_2 = 0, \end{aligned}\right\} \tag{29}$$

so dass die Gleichungen zur Bestimmung von σ und τ

$$\left.\begin{aligned} (1-3\sqrt{3})\,\sigma = 0, \\ (1-3\sqrt{3})\,\tau = 0 \end{aligned}\right\} \tag{30}$$

oder

$$\sigma = 0, \quad \tau = 0 \tag{31}$$

werden.

Wir denken uns jetzt, dass sich der Librationspunkt in unmittelbarer Nähe des Mittelpunkts des Massendreiecks befindet, und setzen

$$\left.\begin{aligned} \xi &= r\cos\varphi, \\ \eta &= r\sin\varphi, \end{aligned}\right\} \quad (32)$$

wo r die Distanz des Librationspunktes vom Mittelpunkt bezeichnet. Wir betrachten r als eine unendlich kleine Grösse erster Ordnung. Da die Koordinaten σ und τ des Schwerpunktes, die auch unendlich kleine Grössen erster Ordnung sind, aus den zwei Gleichungen

$$\left.\begin{aligned} A_1\sigma + B_1\tau &= C_1, \\ A_2\sigma + B_2\tau &= C_2 \end{aligned}\right\} \quad (33)$$

bestimmt werden sollen, sieht man, dass die Ordnung, bis zu welcher C_1 und C_2 berechnet werden sollen, um 1 grösser sein muss als die Ordnung, bis zu der die vier Koeffizienten berechnet werden sollen. Wir wollen A_1, B_1, A_2 und B_2 bis zu Gliedern zweiter Ordnung, C_1 und C_2 bis zu Gliedern dritter Ordnung berechnen. Wir finden:

$$\left.\begin{aligned} \varrho_1^2 &= 1 - 2\cos\varphi\cdot r + r^2, \\ \varrho_2^2 &= 1 + (\cos\varphi - \sqrt{3}\sin\varphi)\, r + r^2, \\ \varrho_3^2 &= 1 + (\cos\varphi + \sqrt{3}\sin\varphi)\, r + r^2, \end{aligned}\right\} \quad (34)$$

$$\left.\begin{aligned} \alpha_1 &= -1 - 2\cos\varphi\cdot r - \frac{3}{4}(1 + 3\cos 2\varphi)\, r^2 \\ &\qquad - \frac{1}{2}(3\cos\varphi + 5\cos 3\varphi)\, r^3, \\ \alpha_2 &= \frac{1}{2} + \frac{1}{4}(\cos\varphi + 3\sqrt{3}\sin\varphi)\, r + \frac{3}{16}(2 - 9\cos 2\varphi - \sqrt{3}\sin 2\varphi)\, r^2 \\ &\quad + \frac{1}{32}(-3\cos\varphi + 15\sqrt{3}\sin\varphi + 40\cos 3\varphi - 30\sqrt{3}\sin 3\varphi) r^3, \\ \alpha_3 &= \frac{1}{2} + \frac{1}{4}(\cos\varphi - 3\sqrt{3}\sin\varphi)\, r + \frac{3}{16}(2 - 9\cos 2\varphi + \sqrt{3}\sin 2\varphi)\, r^2 \\ &\quad + \frac{1}{32}(-3\cos\varphi - 15\sqrt{3}\sin\varphi + 40\cos 3\varphi + 30\sqrt{3}\sin 3\varphi)\, r^3, \end{aligned}\right\} \quad (35)$$

$$
\left.\begin{aligned}
\beta_1 &= \sin\varphi\cdot r+\frac{3}{2}\sin 2\varphi\cdot r^2+\frac{3}{8}(\sin\varphi+5\sin 3\varphi)r^3,\\
\beta_2 &= -\frac{1}{2}\sqrt{3}+\frac{1}{4}(3\sqrt{3}\cos\varphi-5\sin\varphi)\,r\\
&\quad -\frac{3}{16}(2\sqrt{3}-\sqrt{3}\cos 2\varphi-11\sin 2\varphi)\,r^2\\
&\quad +\frac{1}{32}(15\sqrt{3}\cos\varphi-33\sin\varphi\\
&\quad -40\sqrt{3}\cos 3\varphi-30\sin 3\varphi)\,r^3,\\
\beta_3 &= \frac{1}{2}\sqrt{3}-\frac{1}{4}(3\sqrt{3}\cos\varphi+5\sin\varphi)\,r\\
&\quad +\frac{3}{16}(2\sqrt{3}-\sqrt{3}\cos 2\varphi+11\sin 2\varphi)\,r^2\\
&\quad -\frac{1}{32}(15\sqrt{3}\cos\varphi+33\sin\varphi\\
&\quad -40\sqrt{3}\cos 3\varphi+30\sin 3\varphi)\,r^3,
\end{aligned}\right\}\qquad (36)
$$

$$
\left.\begin{aligned}
A_1 &= 1-3\sqrt{3}\left(1+\frac{3}{2}\cos\varphi\cdot r+\frac{3}{8}(2+\cos 2\varphi)\,r^2\right),\\
B_1 &= \frac{9}{2}\sqrt{3}\left(\sin\varphi\cdot r-\frac{1}{4}\sin 2\varphi\cdot r^2\right),\\
C_1 &= \left(1+\frac{3}{2}\sqrt{3}\right)\cos\varphi\cdot r+\frac{45}{8}\sqrt{3}\cos 2\varphi\cdot r^2+\frac{27}{16}\sqrt{3}\cos\varphi\cdot r^3,
\end{aligned}\right\}\qquad (37)
$$

$$
\left.\begin{aligned}
A_2 &= \frac{9}{2}\sqrt{3}\left(\sin\varphi\cdot r-\frac{1}{4}\sin 2\varphi\cdot r^2\right),\\
B_2 &= 1-3\sqrt{3}\left(1-\frac{3}{2}\cos\varphi\cdot r+\frac{3}{8}(2-\cos 2\varphi)\,r^2\right),\\
C_2 &= \left(1+\frac{3}{2}\sqrt{3}\right)\sin\varphi\cdot r-\frac{45}{8}\sqrt{3}\sin 2\varphi\cdot r^2+\frac{27}{16}\sqrt{3}\sin\varphi\cdot r^3.
\end{aligned}\right\}\qquad (38)
$$

Die zwei unbekannten Grössen σ und τ können jetzt aus den Gleichungen I und II durch wiederholte Annäherungen bestimmt werden. Nimmt man in erster Annäherung nur Glieder erster Ordnung in Gleichung I mit, kann das Glied $B_1\tau$, das zweiter

Ordnung wird, weggelassen werden, wonach das Glied erster Ordnung in der Reihenentwicklung für σ durch Gleichung I bestimmt werden kann. Mit dem gefundenen Wert für σ kann das Glied zweiter Ordnung in $A_2\sigma$ berechnet werden, wonach Gleichung II das Glied erster Ordnung in der Reihenentwicklung für τ ergibt. Den gefundenen Wert für τ setzt man dann in Gleichung I ein, wobei σ bis zu Gliedern zweiter Ordnung bestimmt werden kann, und in der Weise fährt man fort, bis σ und τ bis zu Gliedern dritter Ordnung bestimmt sind. Das Resultat wird:

$$\left.\begin{aligned}\sigma &= -\frac{29+9\sqrt{3}}{52}\cos\varphi\cdot r-\frac{2673-405\sqrt{3}}{2704}\cos 2\varphi\cdot r^2\\ &\quad+\frac{56133+5184\sqrt{3}}{35152}\cos\varphi\cdot r^3,\\ \tau &= -\frac{29+9\sqrt{3}}{52}\sin\varphi\cdot r+\frac{2673-405\sqrt{3}}{2704}\sin 2\varphi\cdot r^2\\ &\quad+\frac{56133+5184\sqrt{3}}{35152}\sin\varphi\cdot r^3.\end{aligned}\right\}\quad(39)$$

Es sei bemerkt, dass die Zahlenkoeffizienten in den zwei Reihenentwicklungen numerisch dieselben sind. Wenn wir die Zahlenkoeffizienten mit 6 Dezimalen berechnen, so erhalten wir folgende zwei Reihenentwicklungen:

$$\left.\begin{aligned}\sigma &= -0.857470\cos\varphi\cdot r-0.729112\cos 2\varphi\cdot r^2\\ &\quad+1.852297\cos\varphi\cdot r^3,\\ \tau &= -0.857470\sin\varphi\cdot r+0.729112\sin 2\varphi\cdot r^2\\ &\quad+1.852297\sin\varphi\cdot r^3.\end{aligned}\right\}\quad(40)$$

Wird r als konstant betrachtet, während φ variiert, so wird der Librationspunkt einen Kreis mit dem Zentrum im Mittelpunkt des Massendreiecks und mit dem Radius r durchlaufen. Der Schwerpunkt wird dann in erster Annäherung einen mit dem Kreise des Librationspunktes konzentrischen Kreis durchlaufen, jedoch mit einem etwas kleineren Radius; ferner werden die Lagen des Librationspunktes und des Schwerpunktes in den Kreisen um 180° gegeneinander verschoben sein. Das Resultat wird mit anderen Worten:

Eine kleine Verschiebung des Librationspunktes vom Mittelpunkt des Dreiecks hat eine Verschiebung des Schwerpunktes zur Folge, die in entgegengesetzter Richtung vor sich geht, und die $\frac{29+9\sqrt{3}}{52}$ mal so gross ist wie die Verschiebung des Librationspunktes.

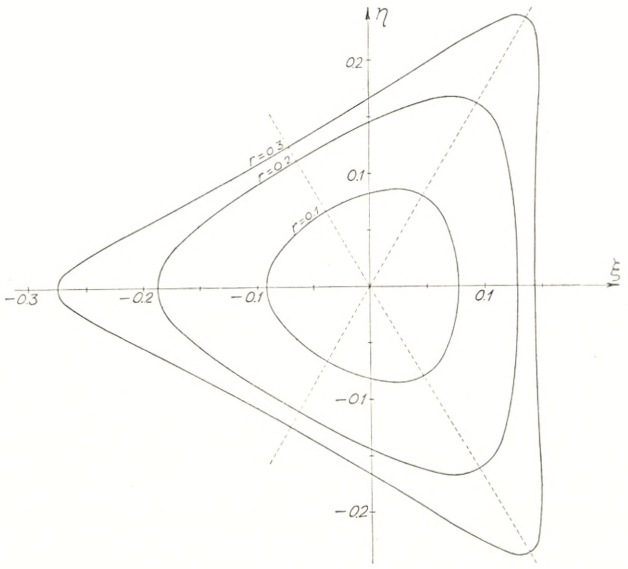

Abb. 2.

Abb. 2 zeigt drei Schwerpunktskurven, die drei verschiedenen r-Werten entsprechen; die Kurvenpunkte sind mit Hilfe von den Gleichungen (40) berechnet. Die Kurven haben, ebenso wie das Massendreieck, 3 Symmetrieachsen. Bei der äussersten der drei Kurven ist die Abweichung zwischen der berechneten Kurve und der wirklichen Kurve schon ziemlich bedeutend. Numerische Berechnungen, die in Abschnitt III erwähnt werden, zeigen, wie sich die weitere Entwicklung der Kurve gestaltet. Für einen gewissen Wert von r zwischen 0.3 und 0.4 erhält die Kurve drei Spitzen, die gegen die Mittelpunkte der Dreiecksseiten gerichtet sind, und für noch grössere Werte von r ergeben sich drei Schleifen.

4. Der Librationspunkt in der Nähe einer der endlichen Massen.

Wenn der Librationspunkt gerade mit einer der drei endlichen Massen zusammenfällt, muss, wie wir früher gesehen haben, diese Masse gleich Null sein, und der Schwerpunkt muss auf derjenigen Dreiecksseite liegen, die die zwei anderen Massen verbindet. Wir wollen jetzt die Lage des Schwerpunktes untersuchen, wenn der Librationspunkt sich in der Nähe der Masse m_1 befindet. Wir setzen in diesem Fall

$$\left.\begin{aligned} \xi &= 1 + r\cos\varphi, \\ \eta &= r\sin\varphi, \end{aligned}\right\} \tag{41}$$

wo wir r als eine unendlich kleine Grösse erster Ordnung betrachten. Mit diesen Werten für ξ und η erhalten wir

$$\left.\begin{aligned} \varrho_1 &= r, \\ \varrho_2^2 &= 3 + (3\cos\varphi - \sqrt{3}\sin\varphi)\, r + r^2, \\ \varrho_3^2 &= 3 + (3\cos\varphi + \sqrt{3}\sin\varphi)\, r + r^2. \end{aligned}\right\} \tag{42}$$

Hieraus ergibt sich ferner, indem in den Reihenentwicklungen nur Glieder erster Ordnung mitgenommen werden:

$$\left.\begin{aligned} \alpha_1 &= \cos\varphi \cdot r^{-2}, \\ \alpha_2 &= \frac{1}{6}\sqrt{3} + \frac{1}{36}(-5\sqrt{3}\cos\varphi + 9\sin\varphi)\, r, \\ \alpha_3 &= \frac{1}{6}\sqrt{3} + \frac{1}{36}(-5\sqrt{3}\cos\varphi - 9\sin\varphi)\, r, \end{aligned}\right\} \tag{43}$$

$$\left.\begin{aligned} \beta_1 &= \sin\varphi \cdot r^{-2}, \\ \beta_2 &= -\frac{1}{6} + \frac{1}{36}(9\cos\varphi + \sqrt{3}\sin\varphi)\, r, \\ \beta_3 &= \frac{1}{6} + \frac{1}{36}(-9\cos\varphi + \sqrt{3}\sin\varphi)\, r, \end{aligned}\right\} \tag{44}$$

$$\left.\begin{aligned} A_1 &= 2\sqrt{3}\cos\varphi\cdot r^{-2}+\frac{5}{6}\cos\varphi\cdot r,\\ B_1 &= \qquad\qquad \frac{3}{2}\sin\varphi\cdot r,\\ C_1 &= -\sqrt{3}\cos\varphi\cdot r^{-2}+\frac{11}{6}\cos\varphi\cdot r, \end{aligned}\right\} \tag{45}$$

$$\left.\begin{aligned} A_2 &= 2\sqrt{3}\sin\varphi\cdot r^{-2}-\frac{1}{6}\sin\varphi\cdot r,\\ B_2 &= \qquad\qquad \frac{3}{2}\cos\varphi\cdot r,\\ C_2 &= -\sqrt{3}\sin\varphi\cdot r^{-2}+\frac{5}{6}\sin\varphi\cdot r. \end{aligned}\right\} \tag{46}$$

Es geht aus den gefundenen Ausdrücken hervor, dass B_1 und B_2 erster Ordnung werden, A_1, C_1, A_2 und C_2 aber der Ordnung -2. Da sowohl σ als τ in diesem speziellen Fall endliche Grössen — also von der Ordnung 0 — sind, werden die Glieder $B_1\tau$ und $B_2\tau$ in den Gleichungen I und II einer Ordnung werden, die um 3 höher ist als die der übrigen Glieder. Diese zwei Glieder können deshalb in der ersten Annäherung weggelassen werden, wonach σ aus jeder Gleichung für sich bestimmt werden kann. Wir finden in beiden Fällen:

$$\sigma = -\frac{1}{2}. \tag{47}$$

Um einen genaueren Wert für σ zu finden, und um den Wert von τ zu bestimmen, nehmen wir jetzt in I und II Glieder erster Ordnung mit, d. h. wir benutzen die in (45) und (46) gegebenen Ausdrücke für die Koeffizienten. Durch Multiplikation von I mit $\cos\varphi$ und von II mit $-\sin\varphi$ und darauffolgende Addition wird τ eliminiert, und für σ erhalten wir dann nach einer kleinen Reduktion:

$$\sigma = -\frac{1}{2}+\frac{\sqrt{3}\,(1+2\cos 2\varphi)}{8\cos 2\varphi}\,r^3. \tag{48}$$

Wenn wir den Wert von σ in eine der zwei Bedingungsgleichungen einsetzen, erhalten wir:

$$\tau = -\frac{1}{2}\operatorname{tg} 2\varphi . \tag{49}$$

Soll der gefundene Schwerpunkt in das Massendreieck oder auf seine Begrenzung fallen, müssen die folgenden zwei Bedingungen gleichzeitig erfüllt sein:

$$1^\circ. \qquad \sigma \geqq -\frac{1}{2} . \tag{50}$$

$$2^\circ. \qquad -\frac{1}{2}\sqrt{3} \leqq \tau \leqq \frac{1}{2}\sqrt{3} . \tag{51}$$

Die erste Bedingung kann in

$$\frac{1 + 2\cos 2\varphi}{\cos 2\varphi} \geqq 0 \tag{52}$$

umschrieben werden, woraus wir

$$\left.\begin{aligned} 0^\circ \leqq \varphi \leqq\ & 45^\circ, \\ 60^\circ \leqq \varphi \leqq\ & 120^\circ, \\ 135^\circ \leqq \varphi \leqq\ & 225^\circ, \\ 240^\circ \leqq \varphi \leqq\ & 300^\circ, \\ 315^\circ \leqq \varphi <\ & 360^\circ \end{aligned}\right\} \tag{53}$$

erhalten.

Die zweite Bedingung kann in

$$-\sqrt{3} \leqq \operatorname{tg} 2\varphi \leqq \sqrt{3} \tag{54}$$

umschrieben werden, woraus wir

$$\left.\begin{aligned} 0^\circ \leqq \varphi \leqq\ & 30^\circ, \\ 60^\circ \leqq \varphi \leqq\ & 120^\circ, \\ 150^\circ \leqq \varphi \leqq\ & 210^\circ, \\ 240^\circ \leqq \varphi \leqq\ & 300^\circ, \\ 330^\circ \leqq \varphi <\ & 360^\circ \end{aligned}\right\} \tag{55}$$

erhalten.

Fassen wir nun die zwei Sätze von Bedingungen zusammen, die φ gleichzeitig befriedigen muss, erhalten wir als Bedingung dafür, dass der Schwerpunkt in das Massendreieck fallen soll:

$$\left.\begin{aligned} 0^\circ \leqq \varphi \leqq 30^\circ, \\ 60^\circ \leqq \varphi \leqq 120^\circ, \\ 150^\circ \leqq \varphi \leqq 210^\circ, \\ 240^\circ \leqq \varphi \leqq 300^\circ, \\ 330^\circ \leqq \varphi < 360^\circ. \end{aligned}\right\} \quad (56)$$

Abb. 3 zeigt das Gebiet um die Masse m_1. Die schraffierten Ausschnitte bezeichnen die verbotenen Gebiete. Die für den Librationspunkt erlaubten Gebiete bestehen aus vier Ausschnitten, jeder von 60°, durch vier Ausschnitte — jeder von 30° — von einander getrennt. Das Massendreieck selbst liegt in einem der erlaubten Ausschnitte.

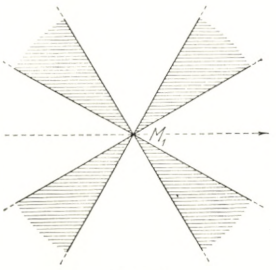

Abb. 3.

In der folgenden Tabelle sind σ und τ für spezielle Werte von φ angegeben.

φ		σ	τ
0°	180°	$-\frac{1}{2}+\frac{3}{8}\sqrt{3}\,r^3$	0
30	210	$-\frac{1}{2}+\frac{1}{2}\sqrt{3}\,r^3$	$-\frac{1}{2}\sqrt{3}$
60	240	$-\frac{1}{2}$	$\frac{1}{2}\sqrt{3}$
90	270	$-\frac{1}{2}+\frac{1}{8}\sqrt{3}\,r^3$	0
120	300	$-\frac{1}{2}$	$-\frac{1}{2}\sqrt{3}$
150	330	$-\frac{1}{2}+\frac{1}{2}\sqrt{3}\,r^3$	$\frac{1}{2}\sqrt{3}$

Es kann nun gezeigt werden, dass einem bestimmten Schwerpunkt in der Nähe einer Seite des Massendreiecks vier Librationspunkte in der Nähe derjenigen Masse entsprechen, die in dem der Seite gegenüberliegenden Eckpunkt liegt. Wir setzen

$$\left.\begin{aligned} \sigma &= -\frac{1}{2} + \frac{1}{8}\sqrt{3}\,\varepsilon^3, \\ \tau &= \tau_0, \end{aligned}\right\} \tag{57}$$

wo ε eine positive, unendlich kleine Grösse erster Ordnung ist, während τ_0 eine endliche Grösse ist. φ kann dann aus der Gleichung

$$\operatorname{tg} 2\varphi = -2\tau_0 \tag{58}$$

bestimmt werden, welche die vier Lösungen

$$\varphi = \left\{\begin{array}{l} \varphi_0 \\ \varphi_0 + 90^\circ \\ \varphi_0 + 180^\circ \\ \varphi_0 + 270^\circ \end{array}\right\} \tag{59}$$

ergibt.

Die entsprechenden Werte von r finden sich aus der Gleichung

$$r = \sqrt[3]{\frac{\cos 2\varphi}{1 + 2\cos 2\varphi}} \cdot \varepsilon. \tag{60}$$

Aus (59) und (60) geht jetzt hervor:

Wenn der Schwerpunkt in der Nähe einer Seite des Massendreiecks liegt, werden vier Librationspunkte in der Nähe derjenigen Masse liegen, die sich in dem der Seite gegenüberliegenden Eckpunkt befindet, und zwar **ein** Librationspunkt in jedem der vier erlaubten Gebiete.

Wird der Koeffizient für ε in der Gleichung (60) mit k bezeichnet, so erhalten wir

$$k = \sqrt[3]{\frac{\cos 2\varphi}{1 + 2\cos 2\varphi}}. \tag{61}$$

In der folgenden Tabelle sind die Werte von k für die φ-Werte von 0° bis 90° angegeben.

φ	k
0°	0.6934
5	6922
10	6885
15	6818
20	6713
25	6552
30	6300
35	5878
40	5051
45	0.0000
50	—0.6432
55	—1.0268
60	∞
65	1.311
70	1.129
75	1.058
80	1.022
85	1.005
90	1.000

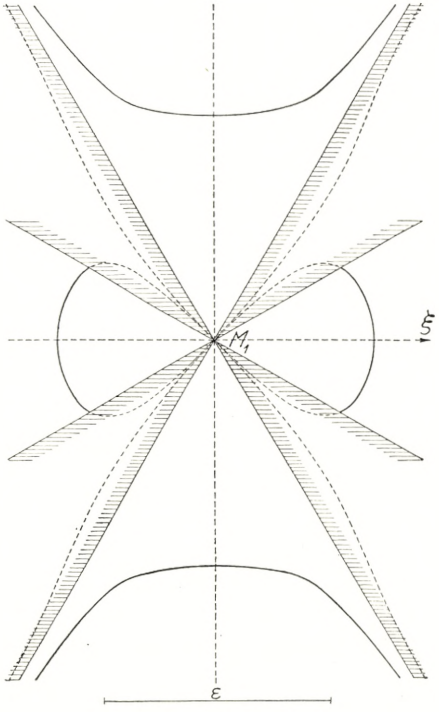

Abb. 4.

Abb. 4 zeigt, wie sich die vier Librationspunkte in den vier Gebieten verschieben, wenn ε konstant gehalten wird, während τ_0 variiert, d. h. wenn der Schwerpunkt parallel der Seite des Massendreiecks verschoben wird.

5. Der Librationspunkt in der Nähe eines der Punkte, die mit den Eckpunkten des Massendreiecks in Bezug auf dessen Seiten symmetrisch liegen.

Wenn der Librationspunkt auf eine der Symmetrieachsen des Massendreiecks fällt, so dass er mit den zwei Massen, die nicht auf der Symmetrieachse liegen, ein gleichseitiges Dreieck bildet, wird, wie wir früher gesehen haben, der Schwerpunkt auf die Seite des Dreiecks fallen, die senkrecht zur Symmetrieachse steht.

Von den zwei Lagen, die der Librationspunkt in diesem Falle auf der Symmetrieachse einnehmen kann, wird die eine mit einer der Massen zusammenfallen, während die andere ausserhalb des Massendreiecks fallen wird (Abb. 5). Wir haben schon früher die Lage des Schwerpunktes bestimmt, wenn sich der Librationspunkt in der Nähe eines dieser Punkte (M_1) befand, und gehen

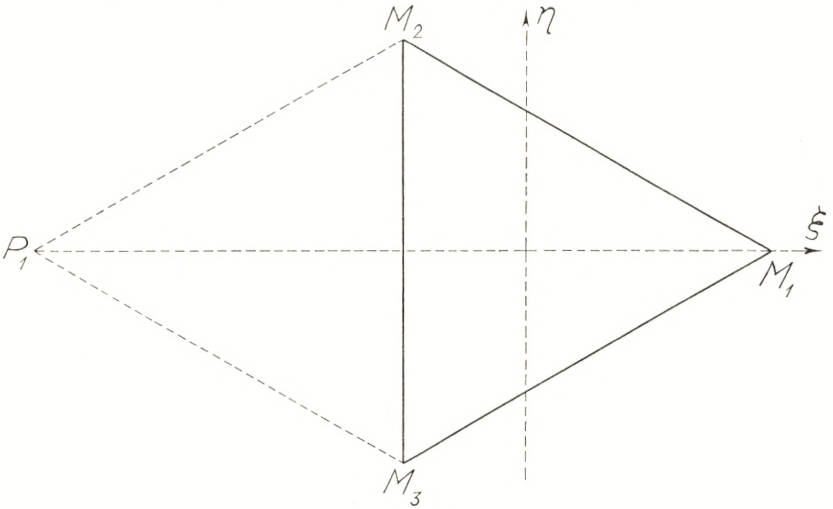

Abb. 5.

nun dazu über, die Lage des Schwerpunktes zu bestimmen, wenn sich der Librationspunkt in der Nähe des anderen Punktes (P_1) befindet.

Wir setzen in diesem Fall

$$\left.\begin{aligned} \xi &= -2 + r\cos\varphi, \\ \eta &= r\sin\varphi, \end{aligned}\right\} \qquad (62)$$

wo r eine unendlich kleine Grösse erster Ordnung ist. Mit diesen Werten für ξ und η erhalten wir:

$$\left.\begin{aligned} \varrho_1^2 &= 9 - 6\cos\varphi \cdot r + r^2, \\ \varrho_2^2 &= 3 - (3\cos\varphi + \sqrt{3}\sin\varphi)\, r + r^2, \\ \varrho_3^2 &= 3 - (3\cos\varphi - \sqrt{3}\sin\varphi)\, r + r^2. \end{aligned}\right\} \qquad (63)$$

Hieraus finden wir, indem nur Glieder bis zur ersten Ordnung mitgenommen werden:

$$\left.\begin{aligned}
\alpha_1 &= -\frac{1}{9}\left(1+\frac{2}{3}\cos\varphi\cdot r\right),\\
\alpha_2 &= -\frac{1}{6}\sqrt{3}\left(1+\left(\frac{5}{6}\cos\varphi+\frac{1}{2}\sqrt{3}\sin\varphi\right)r\right),\\
\alpha_3 &= -\frac{1}{6}\sqrt{3}\left(1+\left(\frac{5}{6}\cos\varphi-\frac{1}{2}\sqrt{3}\sin\varphi\right)r\right),
\end{aligned}\right\} \quad (64)$$

$$\left.\begin{aligned}
\beta_1 &= \frac{1}{27}\sin\varphi\cdot r,\\
\beta_2 &= -\frac{1}{6}\left(1+\left(\frac{3}{2}\cos\varphi-\frac{1}{6}\sqrt{3}\sin\varphi\right)r\right),\\
\beta_3 &= \frac{1}{6}\left(1+\left(\frac{3}{2}\cos\varphi+\frac{1}{6}\sqrt{3}\sin\varphi\right)r\right),
\end{aligned}\right\} \quad (65)$$

$$\left.\begin{aligned}
A_1 &= 2-\frac{2}{9}\sqrt{3}+\left(\frac{5}{6}-\frac{4}{27}\sqrt{3}\right)\cos\varphi\cdot r,\\
B_1 &= -\frac{3}{2}\sin\varphi\cdot r,\\
C_1 &= -1+\frac{1}{9}\sqrt{3}+\left(\frac{11}{6}+\frac{2}{27}\sqrt{3}\right)\cos\varphi\cdot r,
\end{aligned}\right\} \quad (66)$$

$$\left.\begin{aligned}
A_2 &= \left(-\frac{1}{6}+\frac{2}{27}\sqrt{3}\right)\sin\varphi\cdot r,\\
B_2 &= -\frac{3}{2}\cos\varphi\cdot r,\\
C_2 &= \left(\frac{5}{6}-\frac{1}{27}\sqrt{3}\right)\sin\varphi\cdot r.
\end{aligned}\right\} \quad (67)$$

Die Koordinaten des Schwerpunktes werden dann aus den Gleichungen I und II bestimmt. Durch Multiplikation von I mit $\cos\varphi$ und von II mit $-\sin\varphi$ und darauffolgende Addition wird τ eliminiert, und für σ erhalten wir dann nach Reduktion:

$$\sigma = -\frac{1}{2}+\frac{9\,(9+\sqrt{3})\,(1+2\cos 2\varphi)}{208\cos\varphi}\,r. \quad (68)$$

Setzen wir den Wert für σ in eine der zwei Gleichungen ein, so erhalten wir:

$$\tau = -\frac{1}{2}\operatorname{tg}\varphi. \tag{69}$$

Wenn der gefundene Schwerpunkt innerhalb des Massendreiecks oder auf dessen Begrenzung fallen soll, müssen folgende zwei Bedingungen gleichzeitig erfüllt sein:

$$1°. \quad \sigma \geqq -\frac{1}{2}. \tag{70}$$

$$2°. \quad -\frac{1}{2}\sqrt{3} \leqq \tau \leqq \frac{1}{2}\sqrt{3}. \tag{71}$$

Die erste Bedingung kann in

$$\frac{1+2\cos 2\varphi}{\cos\varphi} \geqq 0 \tag{72}$$

umschrieben werden, woraus sich wieder

$$\left.\begin{aligned} 0° &\leqq \varphi \leqq 60°, \\ 90° &\leqq \varphi \leqq 120°, \\ 240° &\leqq \varphi \leqq 270°, \\ 300° &\leqq \varphi < 360° \end{aligned}\right\} \tag{73}$$

ergibt.

Die zweite Bedingung kann in

$$-\sqrt{3} \leqq \operatorname{tg}\varphi \leqq \sqrt{3} \tag{74}$$

umschrieben werden, woraus sich

$$\left.\begin{aligned} 0° &\leqq \varphi \leqq 60°, \\ 120° &\leqq \varphi \leqq 240°, \\ 300° &\leqq \varphi < 360° \end{aligned}\right\} \tag{75}$$

ergibt.

Fassen wir nun die zwei Sätze von Bedingungen, die φ gleichzeitig befriedigen muss, zusammen, so erhalten wir als Bedin-

gung dafür, dass der Schwerpunkt innerhalb des Massendreiecks fallen soll:

$$\left.\begin{aligned} 0^\circ \leqq \varphi \leqq 60^\circ, \\ 300^\circ \leqq \varphi < 360^\circ. \end{aligned}\right\} \quad (76)$$

Abb. 6 zeigt das Gebiet um P_1. Der schraffierte Teil bezeichnet das verbotene Gebiet. Das für den Librationspunkt erlaubte Gebiet ist ein Ausschnitt von 120°.

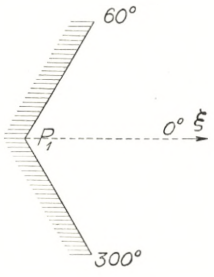

Abb. 6.

Es kann nun gezeigt werden, dass einem bestimmten Schwerpunkt in der Nähe der Seite M_2M_3 im Massendreieck ein Librationspunkt in der Nähe von P_1 entspricht. Wir setzen

$$\left.\begin{aligned} \sigma &= -\frac{1}{2} + \frac{9(9+\sqrt{3})}{208}\varepsilon, \\ \tau &= \tau_0, \end{aligned}\right\} \quad (77)$$

wo ε eine positive, unendlich kleine Grösse erster Ordnung ist, während τ_0 eine endliche Grösse ist. φ kann dann aus der Gleichung

$$\operatorname{tg}\varphi = -2\tau_0 \quad (78)$$

bestimmt werden, die folgende zwei Lösungen ergibt:

$$\varphi = \begin{cases} \varphi_0 \\ \varphi_0 + 180^\circ. \end{cases} \quad (79)$$

Wegen der Bedingungen, die φ befriedigen muss, kann doch nur der eine Wert von φ angewandt werden.

Den entsprechenden Wert von r findet man aus der Gleichung

$$r = \frac{\cos\varphi}{1 + 2\cos 2\varphi}\varepsilon. \quad (80)$$

Aus dem Vorhergehenden geht jetzt hervor:

Wenn der Schwerpunkt in der Nähe einer Seite des Massendreiecks liegt, wird ein Librationspunkt in der

Nähe des Punktes liegen, der mit dem gegenüberstehenden Eckpunkt der Seite in Bezug auf die betreffende Seite symmetrisch liegt.

Wird der Koeffizient von ε in der Gleichung (80) mit k bezeichnet, erhalten wir:

$$k = \frac{\cos \varphi}{1 + 2 \cos 2 \varphi}. \tag{81}$$

In der Tabelle ist der Wert von k für φ-Werte von 0° bis 60° angegeben.

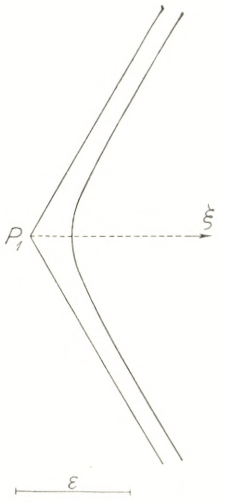

Abb. 7.

φ	k
0°	0.3333
5	3355
10	3420
15	3536
20	3711
25	3965
30	4330
35	4864
40	5686
45	7071
50	0.9847
55	1.8154
60	∞

Abb. 7 zeigt, wie sich der Librationspunkt verschiebt, wenn man ε konstant hält, während τ_0 variiert, d. h. wenn der Schwerpunkt parallel der Seite des Massendreiecks verschoben wird.

6. Der Librationspunkt in der Nähe eines Librationskreises.

Unter einem Librationskreis wollen wir einen Kreis verstehen, der sein Zentrum in einem der Eckpunkte des Massendreiecks hat und durch die zwei anderen Eckpunkte geht. Abb. 8 zeigt das Massendreieck $M_1 M_2 M_3$ und die drei Librationskreise l_1, l_2

und l_3. Die Schnittpunkte zwischen den Librationskreisen sind einerseits die Punkte M_1, M_2 und M_3 und andererseits die im Vorhergehenden erwähnten Punkte P_1, P_2 und P_3. Auf jedem einzelnen der drei Librationskreise liegen vier der erwähnten sechs Punkte, so auf l_1 die Punkte M_2, M_3, P_2 und P_3. Wir haben im Vorhergehenden (II, 4; II, 5) den Fall näher untersucht, wo der Librationspunkt in der Nähe dieser Punkte liegt, und wir gehen

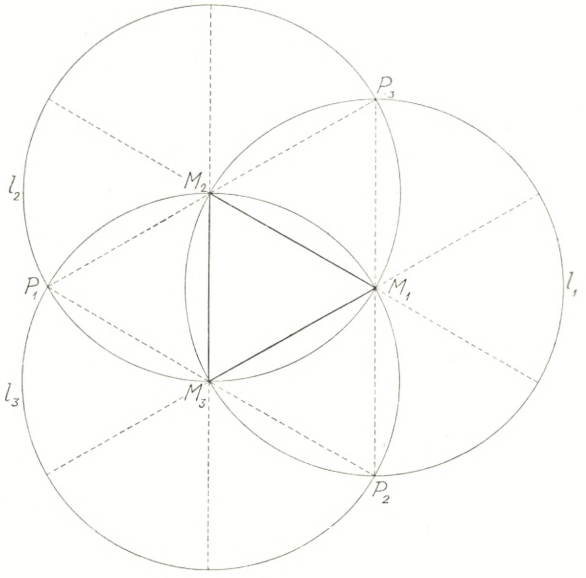

Abb. 8.

nun dazu über, den allgemeineren Fall zu studieren, wo der Librationspunkt in der Nähe eines Librationskreises liegt, entweder etwas ausserhalb oder etwas innerhalb des Kreises.

Wenn der Librationspunkt sich in der Nähe des Librationskreises l_1 befindet, können wir, da der Radius des Kreises $\sqrt{3}$ ist,

$$\left.\begin{aligned} \xi &= 1 + (\sqrt{3} + \varepsilon)\cos\varphi, \\ \eta &= \quad (\sqrt{3} + \varepsilon)\sin\varphi \end{aligned}\right\} \quad (82)$$

setzen, wo die unendlich kleine Grösse ε die Distanz zwischen dem Librationspunkt und dem Librationskreis bezeichnet. Mit diesen Werten für ξ und η erhalten wir:

$$\left.\begin{aligned} \varrho_1 &= \sqrt{3}\left(1+\frac{1}{3}\sqrt{3}\,\varepsilon\right), \\ \varrho_2^2 &= \left(6+3\sqrt{3}\cos\varphi-3\sin\varphi\right)\left(1+\frac{1}{3}\sqrt{3}\,\varepsilon\right)+\varepsilon^2, \\ \varrho_3^2 &= \left(6+3\sqrt{3}\cos\varphi+3\sin\varphi\right)\left(1+\frac{1}{3}\sqrt{3}\,\varepsilon\right)+\varepsilon^2. \end{aligned}\right\} \quad (83)$$

Die Grössen $6+3\sqrt{3}\cos\varphi-3\sin\varphi$ und $6+3\sqrt{3}\cos\varphi+3\sin\varphi$, die von 0 bis 12 variieren können, wollen wir mit f_2^2 und f_3^2 bezeichnen:

$$\left.\begin{aligned} f_2^2 &= 6+3\sqrt{3}\cos\varphi-3\sin\varphi = 6\left[1+\cos\left(\varphi+30^\circ\right)\right], \\ f_3^2 &= 6+3\sqrt{3}\cos\varphi+3\sin\varphi = 6\left[1+\cos\left(\varphi-30^\circ\right)\right]. \end{aligned}\right\} \quad (84)$$

Indem nur Glieder erster Ordnung in den Reihenentwicklungen mitgenommen werden, erhalten wir:

$$\left.\begin{aligned} \varrho_1 &= \sqrt{3}\,(1+\frac{1}{3}\sqrt{3}\,\varepsilon), \\ \varrho_2 &= f_2\,(1+\frac{1}{6}\sqrt{3}\,\varepsilon), \\ \varrho_3 &= f_3\,(1+\frac{1}{6}\sqrt{3}\,\varepsilon), \end{aligned}\right\} \quad (85)$$

$$\left.\begin{aligned} \alpha_1 &= \frac{1}{3}\cos\varphi-\frac{2}{9}\sqrt{3}\cos\varphi\cdot\varepsilon, \\ \alpha_2 &= \frac{1}{f_2^3}\left[\frac{3}{2}+\sqrt{3}\cos\varphi-\left(\frac{3}{4}\sqrt{3}+\frac{1}{2}\cos\varphi\right)\varepsilon\right], \\ \alpha_3 &= \frac{1}{f_3^3}\left[\frac{3}{2}+\sqrt{3}\cos\varphi-\left(\frac{3}{4}\sqrt{3}+\frac{1}{2}\cos\varphi\right)\varepsilon\right], \end{aligned}\right\} \quad (86)$$

$$\left.\begin{aligned} \beta_1 &= \frac{1}{3}\sin\varphi-\frac{2}{9}\sqrt{3}\sin\varphi\cdot\varepsilon, \\ \beta_2 &= \frac{1}{f_2^3}\left[-\frac{1}{2}\sqrt{3}+\sqrt{3}\sin\varphi+\left(\frac{3}{4}-\frac{1}{2}\sin\varphi\right)\varepsilon\right], \\ \beta_3 &= \frac{1}{f_3^3}\left[\frac{1}{2}\sqrt{3}+\sqrt{3}\sin\varphi-\left(\frac{3}{4}+\frac{1}{2}\sin\varphi\right)\varepsilon\right], \end{aligned}\right\} \quad (87)$$

$$
\left.\begin{aligned}
A_1 &= 1+\frac{2}{3}\sqrt{3}\cos\varphi-\frac{4}{3}\cos\varphi\cdot\varepsilon \\
&\quad -\left[\frac{3}{2}\sqrt{3}+3\cos\varphi-\left(\frac{9}{4}+\frac{1}{2}\sqrt{3}\cos\varphi\right)\varepsilon\right]\cdot\left[\frac{1}{f_2^3}+\frac{1}{f_3^3}\right], \\
B_1 &= \left[\frac{9}{2}+3\sqrt{3}\cos\varphi-\left(\frac{9}{4}\sqrt{3}+\frac{3}{2}\cos\varphi\right)\varepsilon\right]\cdot\left[\frac{1}{f_2^3}-\frac{1}{f_3^3}\right], \\
C_1 &= 1+\frac{2}{3}\sqrt{3}\cos\varphi+\frac{5}{3}\cos\varphi\cdot\varepsilon \\
&\quad -\left[\frac{3}{2}\sqrt{3}+3\cos\varphi-\left(\frac{9}{4}+\frac{1}{2}\sqrt{3}\cos\varphi\right)\varepsilon\right]\cdot\left[\frac{1}{f_2^3}+\frac{1}{f_3^3}\right],
\end{aligned}\right\} \quad (88)
$$

$$
\left.\begin{aligned}
A_2 &= \frac{2}{3}\sqrt{3}\sin\varphi-\frac{4}{3}\sin\varphi\cdot\varepsilon+\left[\frac{3}{2}-\frac{3}{4}\sqrt{3}\,\varepsilon\right]\cdot\left[\frac{1}{f_2^3}-\frac{1}{f_3^3}\right] \\
&\quad -\left[3\sin\varphi-\frac{1}{2}\sqrt{3}\sin\varphi\cdot\varepsilon\right]\cdot\left[\frac{1}{f_2^3}+\frac{1}{f_3^3}\right], \\
B_2 &= 1+\left[-\frac{3}{2}\sqrt{3}+\frac{9}{4}\varepsilon\right]\cdot\left[\frac{1}{f_2^3}+\frac{1}{f_3^3}\right] \\
&\quad +\left[3\sqrt{3}\sin\varphi-\frac{3}{2}\sin\varphi\cdot\varepsilon\right]\cdot\left[\frac{1}{f_2^3}-\frac{1}{f_3^3}\right], \\
C_2 &= \frac{2}{3}\sqrt{3}\sin\varphi+\frac{5}{3}\sin\varphi\cdot\varepsilon+\left[\frac{3}{2}-\frac{3}{4}\sqrt{3}\,\varepsilon\right]\cdot\left[\frac{1}{f_2^3}-\frac{1}{f_3^3}\right] \\
&\quad -\left[3\sin\varphi-\frac{1}{2}\sqrt{3}\sin\varphi\cdot\varepsilon\right]\cdot\left[\frac{1}{f_2^3}+\frac{1}{f_3^3}\right].
\end{aligned}\right\} \quad (89)
$$

Der Kürze wegen führen wir die Bezeichnungen

$$
\left.\begin{aligned}
g_1 &= \frac{1}{f_2^3}+\frac{1}{f_3^3}, \\
g_2 &= \frac{1}{f_2^3}-\frac{1}{f_3^3}
\end{aligned}\right\} \quad (90)
$$

ein; ferner setzen wir

$$
\sigma = 1+\delta, \quad (91)
$$

wo δ eine unendlich kleine Grösse erster Ordnung ist. Gleichung I und II können dann nach Reduktion auf folgende einfache Form gebracht werden:

$$\left.\begin{aligned} &\left[1+\frac{2}{3}\sqrt{3}\cos\varphi\right]\cdot\left[\left(1-\frac{3}{2}\sqrt{3}\,g_1\right)\delta+\frac{9}{2}g_2\tau\right] = 3\cos\varphi\cdot\varepsilon,\\ &\left[\frac{2}{3}\sqrt{3}\sin\varphi\left(1-\frac{3}{2}\sqrt{3}\,g_1\right)+\frac{3}{2}g_2\right]\delta\\ &\qquad+\left[1-\frac{3}{2}\sqrt{3}\,g_1+3\sqrt{3}\sin\varphi\cdot g_2\right]\tau = 3\sin\varphi\cdot\varepsilon. \end{aligned}\right\} \quad (92)$$

Da g_1 nur im Ausdruck $1-\frac{3}{2}\sqrt{3}\,g_1$ auftritt, wollen wir

$$g_3 = 1-\frac{3}{2}\sqrt{3}\,g_1 \quad (93)$$

setzen, wonach die Gleichungen I und II folgende Form erhalten:

$$\left.\begin{aligned} \left[1+\frac{2}{3}\sqrt{3}\cos\varphi\right]\cdot\left[g_3\delta+\frac{9}{2}g_2\tau\right] &= 3\cos\varphi\cdot\varepsilon,\\ \left[\frac{2}{3}\sqrt{3}\sin\varphi\cdot g_3+\frac{3}{2}g_2\right]\delta+\left[g_3+3\sqrt{3}\sin\varphi\cdot g_2\right]\tau &= 3\sin\varphi\cdot\varepsilon. \end{aligned}\right\} \quad (94)$$

Die Determinante des Systems wird

$$D = \left[1+\frac{2}{3}\sqrt{3}\cos\varphi\right]\cdot\left[g_3^2-\frac{27}{4}g_2^2\right]. \quad (95)$$

Diese Determinante wird Null, wenn

$$1°. \quad 1+\frac{2}{3}\sqrt{3}\cos\varphi = 0, \quad (96)$$

$$2°. \quad g_3^2-\frac{27}{4}g_2^2 = 0. \quad (97)$$

Aus (96) erhalten wir

$$\varphi = \begin{cases} 150^\circ \\ 210^\circ. \end{cases} \tag{98}$$

Die zwei gefundenen Werte von φ entsprechen den Punkten M_2 und M_3 auf dem Librationskreis l_1.

Aus (97) erhalten wir

$$\left.\begin{matrix} f_2 \\ f_3 \end{matrix}\right\} = \sqrt{3}. \tag{99}$$

Da f_2 und f_3 die Distanzen des Librationspunktes von M_2 bzw. M_3 bezeichnen, wenn $\varepsilon = 0$ ist, wird $f_2 = \sqrt{3}$ den Punkten M_3 und P_3 auf dem Librationskreis l_1 entsprechen, während $f_3 = \sqrt{3}$ den Punkten M_2 und P_2 entspricht.

Hieraus geht hervor, dass die Determinante der Gleichungen für die Punkte M_2, M_3, P_2 und P_3 auf dem Librationskreis l_1 Null wird. Diese vier Punkte sind gerade die Schnittpunkte zwischen dem Librationskreis l_1 und den zwei anderen Librationskreisen. Für andere Punkte auf diesem Kreis ist die Determinante von Null verschieden, und das Gleichungssystem kann dann zur Bestimmung der Koordinaten des Schwerpunktes dienen. Man findet:

$$\left.\begin{aligned} D\delta &= \left[3\cos\varphi \cdot g_3 - \frac{27}{2}\sin\varphi \cdot g_2\right]\varepsilon, \\ D\tau &= \left[3\sin\varphi \cdot g_3 - \frac{9}{2}\cos\varphi \cdot g_2\right]\varepsilon. \end{aligned}\right\} \tag{100}$$

Wir stellen zum Schluss die Formeln zur Berechnung von σ und τ in der Reihenfolge zusammen, in der sie angewandt werden sollen.

$$f_2^2 = 6\,[1 + \cos(\varphi + 30°)],$$

$$f_3^2 = 6\,[1 + \cos(\varphi - 30°)],$$

$$g_1 = \frac{1}{f_2^3} + \frac{1}{f_3^3},$$

$$g_2 = \frac{1}{f_2^3} - \frac{1}{f_3^3},$$

$$g_3 = 1 - \frac{3}{2}\sqrt{3}\, g_1,$$

$$h_1 = 3\cos\varphi \cdot g_3 - \frac{27}{2}\sin\varphi \cdot g_2,$$

$$h_2 = 3\sin\varphi \cdot g_3 - \frac{9}{2}\cos\varphi \cdot g_2,$$

$$D = \left[1 + \frac{2}{3}\sqrt{3}\cos\varphi\right] \cdot \left[g_3^2 - \frac{27}{4} g_2^2\right],$$

$$k_1 = \frac{h_1}{D},$$

$$k_2 = \frac{h_2}{D},$$

$$\underline{\sigma = 1 + k_1 \varepsilon,} \qquad \underline{\tau = k_2 \varepsilon.}$$

Zur numerischen Berechnung sind jedoch folgende Formeln geeigneter:

$$a = \left|\operatorname{cosec}^3\left(75^\circ - \frac{\varphi}{2}\right)\right|,$$

$$b = \left|\operatorname{cosec}^3\left(105^\circ - \frac{\varphi}{2}\right)\right|,$$

$$h_1 = 3\left[\cos\varphi - \left(\frac{a}{8}\sin\left(30^\circ + \varphi\right) + \frac{b}{8}\sin\left(30^\circ - \varphi\right)\right)\right],$$

$$h_2 = 3\left[\sin\varphi - \frac{1}{3}\sqrt{3}\left(\frac{a}{8}\sin\left(30^\circ + \varphi\right) - \frac{b}{8}\sin\left(30^\circ - \varphi\right)\right)\right],$$

$$D = \left[1 + \frac{2}{3}\sqrt{3}\cos\varphi\right]\cdot\left[\frac{a}{8} - 1\right]\cdot\left[\frac{b}{8} - 1\right].$$

In der folgenden Tabelle sind die Werte von k_1 und k_2 für die φ-Werte von 0° bis 180° angegeben.

φ	k_1	k_2
0°	+1.616	+0.000
10	1.603	0.273
20	1.562	0.555
30	1.485	0.857
40	1.355	1.195
50	1.135	1.597
60	+0.737	2.124
70	−0.118	2.947
80	−2.849	+4.903
90	—	—
100	+9.096	−0.955
110	6.713	+1.222
120	6.633	2.510
130	8.021	4.052
140	+13.497	+7.642
150	—	—
160	−9.479	−5.307
170	4.136	1.678
180	−3.123	−0.000

Abb. 9 zeigt, wie sich der Schwerpunkt im Verhältnis zu M_1 verschiebt, wenn ε eine positive Konstante ist, während φ variiert, d. h. wenn der Librationspunkt auf der äusseren Seite des

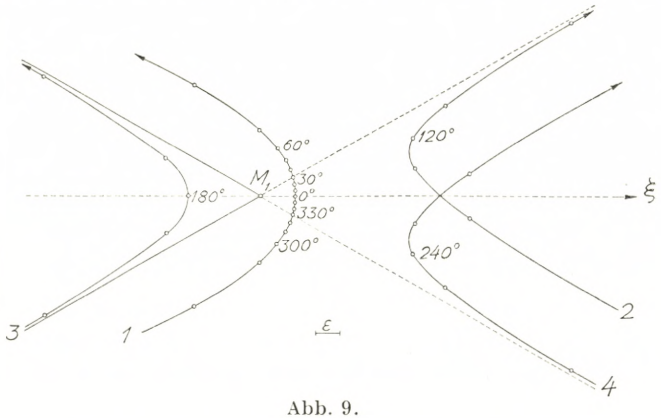

Abb. 9.

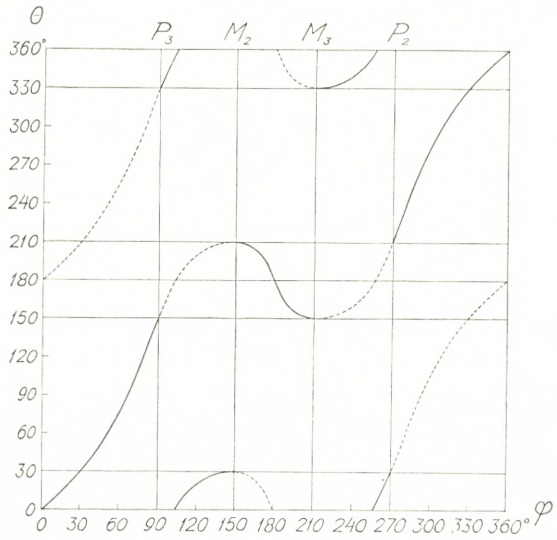

Abb. 10.

Librationskreises, in konstanter Entfernung von diesem, verschoben wird. Wenn ε aber eine negative Konstante ist, so dass der Librationspunkt auf der inneren Seite des Kreises verschoben wird, so wird die Kurve der Verschiebung des Schwerpunktes

zu der in der Abbildung gezeigten Kurve mit M_1 als Symmetriezentrum symmetrisch liegen.

Setzen wir

$$\left.\begin{aligned} \sigma &= 1 + k_1 \varepsilon = 1 + q\cos\theta, \\ \tau &= \quad k_2 \varepsilon = \quad q\sin\theta, \end{aligned}\right\} \quad (101)$$

so ist θ damit als Funktion von φ definiert. Abb. 10 zeigt das Abhängigkeitsverhältnis zwischen θ und φ. Die voll ausgezogenen Teile der Kurven entsprechen positiven Werten von ε (der Librationspunkt ausserhalb des Librationskreises), die gestrichelten Teile entsprechen negativen Werten von ε (der Librationspunkt innerhalb des Librationskreises). Es geht aus der Abbildung hervor, dass einem bestimmten Wert von φ zwei Werte von θ (θ_0 und $\theta_0 + 180°$) bzw. auf einem voll ausgezogenen oder einem gestrichelten Kurventeil entsprechen, der Tatsache gemäss, dass der Librationspunkt für einen bestimmten Wert von φ entweder ausserhalb oder innerhalb des Librationskreises liegen kann.

Einem bestimmten Wert von θ entsprechen entweder zwei oder vier Werte von φ, wie aus der folgenden Übersicht hervorgeht.

θ	Anzahl von Librationspunkten		
	Ausserhalb des Librationskreises	Innerhalb des Librationskreises	Insgesamt
0°— 30°	3	1	4
30°—150°	1	1	2
150°—210°	1	3	4
210°—330°	1	1	2
330°—360°	3	1	4

Wenn man nur mit positiven Massen rechnet, muss der Schwerpunkt im Massendreieck liegen, so dass $150° < \theta < 210°$. Aus dieser Übersicht ersieht man, dass dann vier Librationspunkte in der Nähe des Librationskreises liegen.

Es sei bemerkt, dass in der Übersicht eventuelle Librationspunkte in der Nähe der kritischen Punkte M_2, M_3, P_2 und P_3 nicht berücksichtigt sind. In der Tat liegen, wie aus den nu-

merischen Berechnungen in Abschnitt III hervorgehen wird, im ganzen acht Librationspunkte in der Nähe des Librationskreises; ausser den oben genannten vier Librationspunkten liegen zwei Librationspunkte in der Nähe von M_2 und zwei in der Nähe von M_3.

7. Die Gebiete der Librationspunkte.

Mit Hilfe der vorhergehenden theoretischen Untersuchung ist es jetzt möglich, zu entscheiden, in welchen Gebieten der Ebene der Librationspunkt liegen kann, wenn dem Librationspunkt positive Massen entsprechen sollen, d. h. wenn der Schwerpunkt innerhalb des Massendreiecks fallen soll. Die Begrenzung der erwähnten Gebiete wird man dadurch finden können, dass man den Schwerpunkt den Umkreis des Massendreiecks durchlaufen lässt und die Kurven bestimmt, die die entsprechenden Librationspunkte dabei durchlaufen.

So lange sich der Schwerpunkt auf einer Seite des Massendreiecks befindet, ohne in einem der Eckpunkte zu liegen, haben wir einen Spezialfall des Dreikörperproblems (problème restreint). In diesem Spezialfall gibt es fünf Librationspunkte, nämlich:

L_1 auf der Linie, die die zwei endlichen Massen verbindet, und zwar zwischen diesen zwei Massen liegend,

L_2 und L_3 auf der Linie, die die zwei endlichen Massen verbindet, jeder auf einer der Verlängerungen der Linie über die Massen hinaus liegend,

L_4 und L_5 in den zwei Punkten, die mit den zwei Massen Eckpunkte gleichseitiger Dreiecke bilden.

Abb. 11 zeigt die Verschiebungen der Librationspunkte, wenn der Schwerpunkt den Seiten des Massendreiecks entlang verschoben wird, jedoch von den Eckpunkten des Massendreiecks abgesehen. Die Pfeile geben die Bewegungsrichtungen der Librationspunkte an, wenn wir uns denken, dass der Schwerpunkt in der positiven Umdrehungsrichtung um das Massendreieck verschoben wird. Die Pfeile auf den Seiten des Massendreiecks geben die Bewegungsrichtung des Librationspunktes L_1 an, während die Pfeile auf den Verlängerungen der Seiten die Bewegungsrichtungen der Librationspunkte L_2 und L_3 angeben. Für

die Librationspunkte L_4 und L_5 wechselt die Lage zwischen den sechs Punkten M_1, P_1, M_2, P_2, M_3 und P_3.

Es geht nun aus der Abbildung klar hervor, dass — von dem Gebiet abgesehen, das von den Seiten des Massendreiecks begrenzt wird — keine bestimmten Gebiete der Ebene durch die gegebenen Linienstücke und Punkte begrenzt sind. Wir haben aber auch bis jetzt vorausgesetzt, dass der Schwerpunkt sich nicht gerade in den Eckpunkten des Massendreiecks befand; sollte dies der Fall sein, werden zwei der Massen Null sein, und das Problem ist jetzt auf ein Zweikörperproblem reduziert. Es existiert dann keine endliche Anzahl von Librationspunkten mehr; für die gegebene Winkelgeschwindigkeit, womit das Koordinatensystem rotiert, haben die Librationspunkte als geometrischen Ort einen Kreis mit dem Zentrum in der endlichen Masse und mit dem Radius $\sqrt{3}$. Es werden somit insgesamt drei Kreise (die Librationskreise l_1, l_2 und l_3) zu berücksichtigen sein. Es sind indessen nur Teile der Peripherie der Librationskreise, die die gesuchten Gebiete begrenzen. Denken wir uns, dass der Schwerpunkt nicht den Umkreis des Massendreiecks selbst durchläuft, sich aber längs der inneren Seite des Umkreises bewegt, so wird der Schwerpunkt, indem er in positiver Umdrehungsrichtung M_1 passiert, im Verhältnis zu M_1 Positionswinkel θ durchlaufen, die von 210° bis 150° variieren. Die entsprechenden Werte des Positionswinkels φ des Librationspunktes gehen aus Abb. 10 hervor; aus dieser Abbildung geht auch hervor, ob sich der Librationspunkt längs der äusseren oder der inneren Seite des Librationskreises bewegt. Vom Librationskreis l_1 werden folgende vier Bogen Grenzkurven:

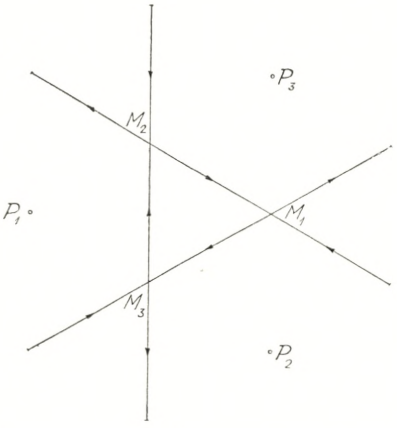

Abb. 11.

$-30° < \varphi < 30°$ (Innere Seite), $150° < \varphi < 210°$ (Äussere Seite),

$90° < \varphi < 150°$ (Innere Seite), $210° < \varphi < 270°$ (Innere Seite).

Für die Librationskreise l_2 und l_3 gelten entsprechende Verhältnisse.

Abb. 12 zeigt, wie die 9 geradlinigen Stücke auf den Seiten des Massendreiecks und auf den Verlängerungen der Seiten in

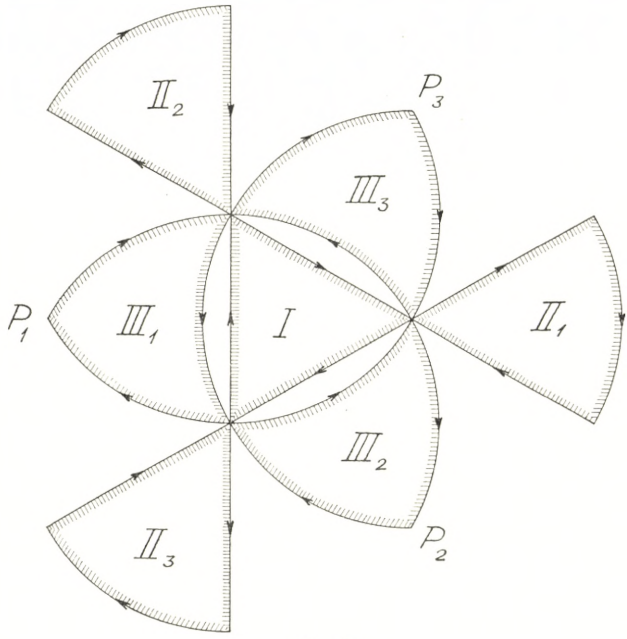

Abb. 12.

Verbindung mit den 12 Bogen auf den 3 Librationskreisen im ganzen 7 Gebiete der Ebene begrenzen, nämlich:

1 Gebiet von den Seiten des Massendreiecks begrenzt (I),

3 Gebiete von zwei Verlängerungsstücken und einem Kreisbogen begrenzt (II),

3 Gebiete von drei Kreisbogen begrenzt (III).

Die auf den Begrenzungsstücken angebrachten Pfeile geben diejenige Umlaufsrichtung auf der Gebietsbegrenzung an, die der positiven Umlaufsrichtung des Schwerpunktes in der Bewegung längs der Begrenzung des Massendreiecks entspricht. Man sieht, dass die Bewegung des Librationspunktes für alle 7 Gebiete in einer der Umlaufsrichtung des Schwerpunktes entgegengesetzten Richtung erfolgt.

III. Numerische Berechnungen.

1. Der Librationspunkt auf einer Symmetrieachse.

Im Abschnitt II, 1 haben wir den Spezialfall behandelt, wo der Librationspunkt auf eine der Symmetrieachsen des Massendreiecks fällt. Der Schwerpunkt wird dann im allgemeinen auch auf die betreffende Symmetrieachse fallen. Für die Symmetrieachse, die mit der ξ-Achse zusammenfällt, haben wir früher gefunden, dass die Abszisse σ des Schwerpunktes durch die Gleichung

$$\sigma = \frac{\xi - \sqrt{3}\,(\alpha_1 + 2\alpha_2)}{1 + 2\sqrt{3}\,(\alpha_1 - \alpha_2)} \tag{1}$$

bestimmt werden kann, wo

$$\alpha_1 = \frac{\xi - 1}{\varrho_1^3}, \qquad \alpha_2 = \frac{\xi + \frac{1}{2}}{\varrho_2^3}, \tag{2}$$

$$\varrho_1^2 = (\xi - 1)^2, \quad \varrho_2^2 = 1 + \xi + \xi^2. \tag{3}$$

Wenn man nun ξ bestimmte Werte gibt, können die entsprechenden Werte von σ berechnet werden. In der folgenden Tabelle I ist σ für ξ-Werte von -2.0 bis 2.7 angegeben. Für $\xi < -2$

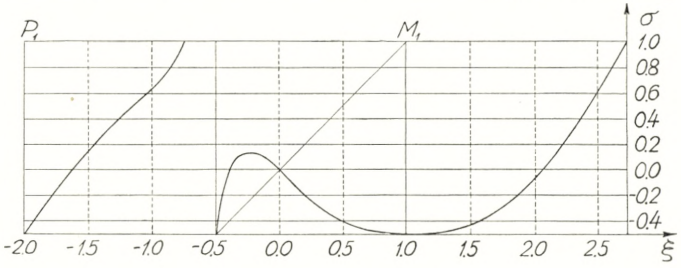

Abb. 13.

und $\xi > 1 + \sqrt{3}$ fällt der Schwerpunkt ausserhalb des Massendreiecks, und es ist deshalb bei der Rechnung nicht notwendig gewesen, diese Werte von ξ zu berücksichtigen; auch für ein kleines Gebiet innerhalb des Intervalls $-2 < \xi < 1 + \sqrt{3}$ fällt der Schwerpunkt ausserhalb des Massendreiecks, des Zusammenhangs wegen sind jedoch diese Werte in der Tabelle mitgenommen.

Eine gute Übersicht darüber, wie sich die Librationspunkte verschieben, wenn der Schwerpunkt die ξ-Achse durchläuft, er-

Tabelle I.

ξ	σ	ξ	σ
−2.0	−0.5000	+0.1	−0.0912
1.9	0.3623	0.2	0.1864
1.8	0.2285	0.3	0.2762
1.7	−0.0994	0.4	0.3533
1.6	+0.0239	0.5	0.4133
1.5	0.1408	0.6	0.4554
1.4	0.2506	0.7	0.4813
1.3	0.3528	0.8	0.4946
1.2	0.4479	0.9	0.4993
1.1	0.5373	1.0	0.5000
1.0	0.6244	1.1	0.4994
0.9	0.7186	1.2	0.4951
0.8	0.8468	1.3	0.4838
0.7	1.1243	1.4	0.4628
0.6	+3.5331	1.5	0.4298
0.5	−0.5000	1.6	0.3831
0.4	+0.0303	1.7	0.3218
0.3	0.1286	1.8	0.2456
0.2	0.1259	1.9	0.1547
−0.1	+0.0765	2.0	−0.0500
0.0	0.0000	2.1	+0.0674
		2.2	0.1959
		2.3	0.3340
		2.4	0.4798
		2.5	0.6318
		2.6	0.7884
		+2.7	+0.9483

halten wir durch Betrachtung der Abb. 13. Die waagerechten Linien stellen die Symmetrieachse für verschiedene Werte von σ dar, die schräge Gerade markiert die Lage des Schwerpunktes auf der Symmetrieachse, und endlich bezeichnen die Schnittpunkte zwischen den waagerechten Linien und der Kurve die Lage der Librationspunkte auf der Symmetrieachse.

Für $\sigma = 0$ gibt es vier Schnittpunkte zwischen der Achse und der Kurve; diese vier Schnittpunkte entsprechen gerade den Lindowschen Librationspunkten L_0, L_2, L_4 und L_6. Wenn jetzt der Schwerpunkt auf der Abbildung nach rechts und die Achse gleichzeitig nach oben rückt, so geht aus der Abbildung deutlich her-

Tabelle II.

No.	ξ	σ
1	-2	-0.5
2	-1.619790	0
3	-0.732051	$+1$
4	-0.5	-0.5
5	-0.413888	0
6	-0.257	$+0.135171$
7	0	0
8	$+1$	-0.5
9	$+2.043817$	0
10	$+2.732051$	$+1$

No. 1. Der Librationspunkt L_4 im problème restreint.
No. 2. Der Lindowsche Librationspunkt L_6.
No. 3. Der Librationspunkt auf dem Librationskreis l_1 ($\xi = 1-\sqrt{3}$).
No. 4. Der Librationspunkt L_1 im problème restreint.
No. 5. Der Lindowsche Librationspunkt L_4.
No. 6. Der Zusammenschmelzungspunkt für L_0 und L_4.
No. 7. Der Lindowsche Librationspunkt L_0.
No. 8. Der Librationspunkt L_5 im problème restreint.
No. 9. Der Lindowsche Librationspunkt L_2.
No. 10. Der Librationspunkt auf dem Librationskreis l_1 ($\xi = 1+\sqrt{3}$).

vor, dass sich L_0 und L_4 einander nähern werden, während L_2 sich vom Mittelpunkt entfernen und L_6 sich dem Mittelpunkt nähern wird. Für einen bestimmten Wert von σ ($\sigma = 0.135171$) schmelzen L_0 und L_4 zusammen ($\xi = -0.257$), und für grössere Werte von σ liegen auf der Achse nur die zwei Librationspunkte L_2 und L_6. Für $\sigma = 1$ hat man für $L_2 : \xi = 1+\sqrt{3}$ und für $L_6 : \xi = 1-\sqrt{3}$. Wenn dagegen der Schwerpunkt vom Mittelpunkt nach links und die Achse gleichzeitig nach unten rückt, werden stets vier Schnittpunkte zwischen der Achse und der Kurve, also vier Librationspunkte vorhanden sein. Während σ sich -0.5 nähert, werden L_0 und L_2 sich einander nähern, um schliesslich im Punkt $\xi = 1\,(M_1)$ zusammenzuschmelzen; gleichzeitig wird sich L_4 dem Schwerpunkt nähern und mit diesem im Punkt $\xi = -0.5$ zusammenschmelzen, während die Bewegung von L_6 im Punkt $\xi = -2\,(P_1)$ enden wird.

In der Tabelle II sind ξ und σ für gewisse Spezialfälle angegeben. Wenn die Zahlenwerte irrational sind, sind sie mit 6 De-

zimalen angegeben; doch ist im Falle No. 6 ξ nur mit 3 Dezimalen angegeben, weil eine Angabe von σ mit 6 Dezimalen in diesem Falle nur einer Angabe von ξ mit 3 Dezimalen entspricht.

2. Der Librationspunkt auf einer Verbindungslinie zwischen zwei Massen.

Ebenso wie bei der theoretischen Behandlung dieses Falles (II, 2), denken wir uns auch hier, dass der Librationspunkt auf die Linie $M_2 M_3$ (die Verbindungslinie zwischen den Massen m_2 und m_3) fällt. Wenn wir von den zwei Spezialfällen, wo der Librationspunkt in M_2 und M_3 fällt, absehen, so wird der entsprechende Schwerpunkt auch auf diese Linie fallen, und seine Ordinate τ wird durch die Gleichungen

$$\tau = \frac{16\,\eta^5 - 24\,\eta^3 + 153\,\eta}{16\,\eta^4 - 120\,\eta^2 - 63}, \quad -\frac{1}{2}\sqrt{3} < \eta < \frac{1}{2}\sqrt{3}, \tag{4}$$

$$\tau = \eta - \frac{27\left(\eta^2 + \frac{1}{4}\right)}{\sqrt{3}\left(\eta^2 - \frac{3}{4}\right)^2 + 18\,\eta}, \quad \eta > \frac{1}{2}\sqrt{3}, \tag{5}$$

$$\tau = \eta + \frac{27\left(\eta^2 + \frac{1}{4}\right)}{\sqrt{3}\left(\eta^2 - \frac{3}{4}\right)^2 - 18\,\eta}, \quad \eta < -\frac{1}{2}\sqrt{3} \tag{6}$$

bestimmt sein.

In der Tabelle III ist τ für η-Werte von 0 bis 2.6 angegeben. Aus den Gleichungen für τ ersieht man, dass, wenn η gegen $-\eta$ vertauscht wird, τ durch $-\tau$ ersetzt werden wird; die Tabelle gibt deshalb gleichzeitig τ für η-Werte von 0 bis -2.6.

Abb. 14 zeigt, wie die Librationspunkte verschoben werden, wenn sich der Schwerpunkt auf der Linie $M_2 M_3$ bewegt. Die senkrechten Linien der Abbildung zeigen die Linie $M_2 M_3$ für verschiedene Werte von τ; die schräge Gerade markiert die Lage des Schwerpunktes auf dieser Linie, während die Schnittpunkte zwischen den senkrechten Linien und der Kurve die Librationspunkte bezeichnen.

Tabelle III.

η	τ	η	τ
0.00	—0.0000	0.9	—0.8660
0.05	0.1208	1.0	0.8638
0.10	0.2380	1.1	0.8547
0.15	0.3481	1.2	0.8349
0.20	0.4487	1.3	0.8010
0.25	0.5379	1.4	0.7514
0.30	0.6148	1.5	0.6847
0.35	0.6791	1.6	0.6008
0.40	0.7315	1.7	0.5002
0.45	0.7728	1.8	0.3844
0.50	0.8043	1.9	0.2547
0.55	0.8275	2.0	—0.1135
0.60	0.8438	2.1	+0.0374
0.65	0.8545	2.2	0.1959
0.70	0.8610	2.3	0.3600
0.75	0.8644	2.4	0.5278
0.80	—0.8657	2.5	0.6981
		2.6	+0.8694

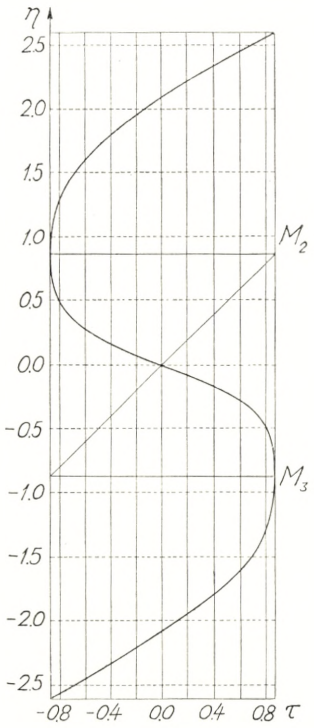

Abb. 14.

Man sieht aus der Abbildung, dass immer drei Schnittpunkte zwischen der Kurve und einer der senkrechten Linien existieren. Es werden deshalb immer drei Librationspunkte auf der Linie $M_2 M_3$ liegen. Der Librationspunkt, der zwischen M_2 und M_3 liegt, entspricht dem Librationspunkt L_1 im problème restreint, während die zwei anderen Librationspunkte den Librationspunkten L_2 und L_3 im problème restreint entsprechen.

3. Der Librationspunkt innerhalb des Massendreiecks (Gebiet I).

Den allgemeinen Fall, wo der Librationspunkt innerhalb der Seiten des Massendreiecks liegt, wollen wir jetzt einer genaueren numerischen Untersuchung unterziehen. Wenn nach und nach der Librationspunkt in einer grossen Anzahl von Punkten innerhalb des Massendreiecks angebracht wird und die entsprechenden Schwerpunkte bestimmt werden, wird man eine gute Übersicht darüber erhalten können, wie der Schwerpunkt verschoben wird, wenn der Librationspunkt sich bewegt.

Von grosser Bedeutung für die Durchführung dieser Rechenarbeit ist es, die Verschiebung des Librationspunktes auf eine bequeme Weise zu wählen. Man könnte daran denken, mit dem Librationspunkt im Mittelpunkt des Massendreiecks zu beginnen, um ihn nachher in gleich langen Schritten auf Linien durch den Startpunkt zu verschieben. Es ist jedoch ein Nachteil bei dieser Methode, dass die Punkte am dichtesten um den Mittelpunkt liegen werden, ebenso wie die Methode keine gebührende Rücksicht auf die fundamentale Rolle nimmt, welche die Dreiecksseiten im Problem spielen. Das Verfahren ist identisch mit der Methode, nach der der Librationspunkt auf Kreisen mit dem Zentrum im Mittelpunkt des Dreiecks verschoben wird.

Die soeben skizzierte Methode wurde im Anfang der Berechnung angewandt, und eine grosse Arbeit wurde ausgeführt, ehe es klar wurde, dass die Methode unbefriedigend war. Die Rechenarbeit wurde deshalb auf einer ganz neuen Grundlage wieder aufgenommen und nach einer Methode, welche die Bedeutung der Dreiecksseiten berücksichtigt. Der Librationspunkt wird auch bei dieser Methode um den Mittelpunkt verschoben; statt in Kreisen verschoben zu werden, wird er aber jetzt auf den Seiten gleichseitiger Dreiecke verschoben, deren Seiten mit den Seiten des Massendreiecks parallel sind, und deren Mittelpunkte in den Mittelpunkt des Massendreiecks fallen. Dadurch entsteht die enge Beziehung zu den Seiten des Massendreiecks.

Wegen der Symmetrie in Bezug auf die drei Symmetrieachsen des Massendreiecks ist es bei der Berechnung nicht notwendig, den Librationspunkt auf dem ganzen Umkreis der erwähnten Dreiecke zu verschieben. Es genügt, den Librationspunkt auf $^1/_6$ des Umkreises zu verschieben, z. B. vom Seitenmittelpunkt bis zum Eckpunkt, indem wir die Schwerpunkte, die den übrigen Librationspunkten entsprechen, mit Hilfe der Symmetrie in Bezug auf die drei Symmetrieachsen finden können. Dieses Verhältnis kann auch so ausgedrückt werden, dass es genügt, den Librationspunkt innerhalb eines der sechs kongruenten Dreiecke, worin das Massendreieck durch die drei Symmetrieachsen geteilt wird, zu verschieben.

Abb. 15 zeigt die Lage der Librationspunkte, die bei der Berechnung benutzt sind. Die sechs kongruenten Dreiecke, in die das Massendreieck geteilt ist, sind mit den Zahlen 1-6 numeriert.

Die gewählten Librationspunkte befinden sich alle im Dreieck 3. Wie aus der Abbildung hervorgeht, sind die Librationspunkte auf den Dreiecksseiten in Schritten von der Grösse 0.05 verschoben worden, ebenso wie die Distanz zwischen den Dreiecksseiten 0.05 ist; jedoch ist zwischen der Dreiecksseite $\xi = -0.45$ und der Seite $\xi = -0.50$ des Massendreiecks eine besondere Dreiecksseite $\xi = -0.48$ eingeschoben, indem es sich, als die Berechnung vorwärtsschritt, zeigte, dass in dem erwähnten Gebiet eine ganz geringe Verschiebung des Librationspunktes senkrecht auf die Dreiecksseite eine grosse Verschiebung des Schwerpunktes zur Folge haben wird. Die in der Abbildung angegebenen 84 Librationspunkte sind über die verschiedenen Abszissen so verteilt, wie die folgende Übersicht zeigt.

ξ	Anzahl
−0.05	1
10	3
15	4
20	6
25	8
30	9
35	11
40	13
45	14
−0.48	15
Summe	84

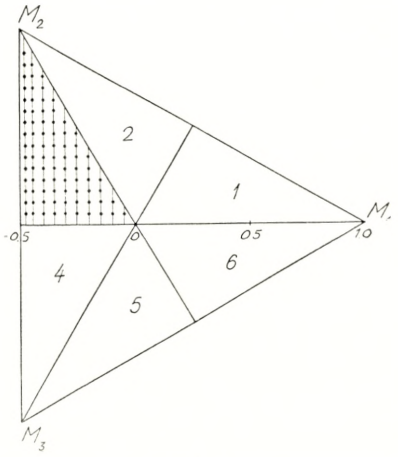

Abb. 15.

Nach Vollendung der Berechnung wurden dann unter Verwertung der Symmetrie in Bezug auf die Symmetrieachse durch M_2 die entsprechenden Librationspunkte im Dreieck 2 behandelt, wonach unter Verwertung der Symmetrie in Bezug auf die Symmetrieachse durch M_3 die entsprechenden Librationspunkte im Dreieck 1 behandelt wurden. Damit waren die Librationspunkte oberhalb der ξ-Achse behandelt. Die symmetrischen Librationspunkte unterhalb der ξ-Achse erfordern keine spezielle Behandlung, da es sich hier um Symmetrie in Bezug auf eine Koordinatenachse handelt.

Mit 84 Librationspunkten in jedem der kleinen Dreiecke wird die Gesamtzahl der Librationspunkte innerhalb dieser Dreiecke 504. Hierzu kommen noch 61 Librationspunkte, die auf den drei Symmetrieachsen liegen, so dass die Gesamtzahl der Librationspunkte innerhalb des Massendreiecks, deren Schwerpunkt bestimmt ist, die Anzahl von 565 erreicht.

Im folgenden sind die numerischen Resultate der Berechnungen in Tabellenform angegeben. In diesen Tabellen sind nur die Librationspunkte oberhalb der ξ-Achse berücksichtigt, indem wir die Schwerpunktskoordinaten, welche den in Bezug auf die ξ-Achse symmetrischen Librationspunkten entsprechen, durch Wechsel des Vorzeichens der Ordinaten finden können. Die Koordinaten sind in den Tabellen Dreieck für Dreieck angegeben, so dass in der ersten Tabelle diejenigen Koordinaten angegeben sind, die dem kleinsten der Dreiecke entsprechen, auf deren Seiten der Librationspunkt verschoben wird; dieses Dreieck wird durch $\xi = -0.05$ gekennzeichnet. In der letzten Tabelle findet man die Koordinaten, die dem grössten der Dreiecke entsprechen; dieses Dreieck wird durch $\xi = -0.48$ gekennzeichnet.

Die numerischen Rechnungen sind mit einer Rechenmaschine ausgeführt und zwar im allgemeinen fünfstellig; in gewissen kritischen Fällen sind jedoch die Berechnungen mit noch mehr Stellen ausgeführt. Dennoch führt die ziemlich komplizierte Rechnung in der fünften Stelle des Resultats oft Unsicherheit mit sich. Ich habe es deshalb vorgezogen, die Koordinaten der Librationspunkte und Schwerpunkte nur mit 4 Dezimalen anzugeben.

Tabelle IV.

$\xi = -0.05$.

ξ	η	σ	τ
+0.10	+0	−0.0912	−0
0.0683	0.0183	0.0611	0.0137
+0.0250	0.0433	−0.0204	0.0354
−0.0183	0.0683	+0.0187	0.0598
0.05	0.0866	0.0456	0.0790
0.05	0 05	0.0424	0.0461
−0.05	+0	+0.0408	−0

Tabelle V.

$\xi = -0.10.$

ξ	η	σ	τ
+0.20	+0	−0.1864	−0
0.1799	0.0116	0.1674	0.0060
0.1366	0.0366	0.1249	0.0225
0.0933	0.0616	0.0815	0.0429
0.0500	0.0866	−0.0383	0.0663
+0.0067	0.1116	+0.0036	0.0920
−0.0366	0.1366	0.0430	0.1194
0.0799	0.1616	0.0785	0.1480
0.10	0.1732	0.0932	0.1614
0.10	0.15	0.0889	0.1419
0.10	0.10	0.0819	0.0969
0.10	0.05	0.0779	0.0492
−0.10	+0	+0.0765	−0

Tabelle VI.

$\xi = -0.15.$

ξ	η	σ	τ
+0.30	+0	−0.2762	−0
0.2482	0.0299	0.2300	0.0102
0.2049	0.0549	0.1881	0.0248
0.1616	0.0799	0.1439	0.0438
0.1183	0.1049	0.0984	0.0663
0.0750	0.1299	0 0528	0.0914
+0.0317	0.1549	−0.0082	0.1184
−0.0116	0.1799	+0.0340	0.1465
0.0549	0.2049	0.0725	0.1753
0.0982	0.2299	0.1062	0.2043
0.15	0.2598	0.1381	0.2392
0.15	0.20	0.1239	0.1941
0.15	0.15	0.1155	0.1505
0.15	0.10	0.1099	0.1027
0.15	0.05	0.1066	0.0521
−0.15	+0	+0.1056	−0

Tabelle VII.

$\xi = -0.20.$

ξ	η	σ	τ
+0.40	+0	−0.3533	0
0.3598	0.0232	0.3237	+0.0005
0.3165	0.0482	0.2877	−0.0061
0.2732	0.0732	0.2477	0.0187
0.2299	0.0982	0.2044	0.0362
0.1866	0.1232	0.1585	0.0577
0.1433	0.1482	0.1110	0.0823
0.1000	0.1732	0.0630	0.1090
0.0567	0.1982	−0.0158	0.1373
+0.0134	0.2232	+0.0293	0.1661
−0.0299	0.2482	0.0709	0.1951
0.0732	0.2732	0.1077	0.2239
0.1165	0.2982	0.1386	0.2522
0.1598	0.3232	0.1622	0.2801
0.20	0.3464	0.1767	0.3060
0.20	0.30	0.1614	0 2805
0.20	0.25	0.1491	0.2461
0.20	0.20	0.1400	0.2052
0.20	0.15	0.1336	0.1589
0.20	0.10	0.1292	0.1084
0.20	0.05	0.1268	0.0550
−0.20	+0	+0.1259	−0

Tabelle VIII.

$\xi = -0.25.$

ξ	η	σ	τ
+0.50	+0	−0.4133	+0
0.4714	0.0165	0.3977	0.0082
0.4281	0.0415	0.3704	0.0126
0.3848	0.0665	0.3383	+0.0089
0.3415	0.0915	0.3016	−0.0013
0.2982	0.1165	0.2606	0.0172
0.2549	0.1415	0.2157	0.0376
0.2116	0.1665	0.1679	0.0616
0.1683	0.1915	0.1181	0.0884
0.1250	0.2165	0.0675	0.1169
0.0817	0.2415	−0.0175	0.1465
+0.0384	0.2665	+0.0306	0.1762
−0.0049	0.2915	0.0753	0.2056
0.0482	0.3165	0.1154	0.2342
0.0915	0.3415	0.1496	0.2619
0.1348	0.3665	0.1769	0.2885
0.1781	0.3915	0.1961	0.3144
0.2214	0.4165	0.2060	0.3404
0.25	0.4330	0.2067	0.3579
0.25	0.40	0.1918	0.3486
0.25	0.35	0.1743	0.3270
0.25	0.30	0.1614	0.2974
0.25	0.25	0.1520	0.2605
0.25	0.20	0.1452	0.2171
0.25	0.15	0.1404	0.1680
0.25	0.10	0.1373	0.1146
0.25	0.05	0.1356	0.0581
−0.25	+0	+0.1350	−0

Tabelle IX.

$\xi = -0.30.$

ξ	η	σ	τ
+0.60	+0	−0.4554	+0
0.5397	0.0348	0.4312	0.0308
0.4964	0.0598	0.4085	0.0393
0.4531	0.0848	0.3808	0.0390
0.4098	0.1098	0.3481	0.0314
0.3665	0.1348	0.3104	+0.0176
0.3232	0.1598	0.2678	−0.0015
0.2799	0.1848	0.2210	0.0248
0.2366	0.2098	0.1707	0.0516
0.1933	0.2348	0.1180	0.0807
0.1500	0.2598	0.0643	0.1114
0.1067	0.2848	−0.0109	0.1426
0.0634	0.3098	+0.0407	0.1736
+0.0201	0.3348	0.0890	0.2038
−0.0232	0.3598	0.1326	0.2327
0.0665	0.3848	0.1704	0.2600
0.1098	0.4098	0.2013	0.2858
0.1531	0.4348	0.2242	0.3103
0.1964	0.4598	0.2382	0.3341
0.2397	0.4848	0.2422	0.3580
0.30	0.5196	0.2277	0.3944
0.30	0.45	0.1889	0.3888
0.30	0.40	0.1702	0.3734
0.30	0.35	0.1567	0.3493
0.30	0.30	0.1469	0.3172
0.30	0.25	0.1400	0.2776
0.30	0.20	0.1352	0.2312
0.30	0.15	0.1320	0.1790
0.30	0.10	0.1300	0.1220
0.30	0.05	0.1289	0.0619
−0.30	+0	+0.1286	−0

Tabelle X.

$\xi = -0.35.$

ξ	η	σ	τ
+0.70	+0	−0.4813	+0
0.6513	0.0281	0.4701	0.0488
0.6080	0.0531	0.4562	0.0742
0.5647	0.0781	0.4379	0.0876
0.5214	0.1031	0.4149	0.0913
0.4781	0.1281	0.3864	0.0870
0.4348	0.1531	0.3525	0.0757
0.3915	0.1781	0.3129	0.0585
0.3482	0.2031	0.2679	0.0361
0.3049	0.2281	0.2180	+0.0095
0.2616	0.2531	0.1642	−0.0203
0.2183	0.2781	0.1076	0.0524
0.1750	0.3031	−0.0495	0.0857
0.1317	0.3281	+0.0084	0.1194
0.0884	0.3531	0.0645	0.1524
0.0451	0.3781	0.1173	0.1840
+0.0018	0.4031	0.1652	0.2139
−0.0415	0.4281	0.2071	0.2417
0.0848	0.4531	0.2418	0.2674
0.1281	0.4781	0.2685	0.2912
0.1714	0.5031	0.2865	0.3136
0.2147	0.5281	0.2948	0.3355
0.2580	0.5531	0.2924	0.3580
0.3013	0.5781	0.2773	0.3827
0.35	0.6062	0.2407	0.4168
0.35	0.55	0.1928	0.4315
0.35	0.50	0.1638	0.4322
0.35	0.45	0.1431	0.4231
0.35	0.40	0.1284	0.4049
0.35	0.35	0.1179	0.3782
0.35	0.30	0.1107	0.3431
0.35	0.25	0.1058	0.3002
0.35	0.20	0.1027	0.2500
0.35	0.15	0.1008	0.1936
0.35	0.10	0.0997	0.1320
0.35	0.05	0.0992	0.0669
−0.35	+0	+0.0990	−0

Tabelle XI.

$\xi = -0.40.$

ξ	η	σ	τ
+0.80	+0	−0.4946	+0
0.7629	0.0214	0.4907	0.0695
0.7196	0.0464	0.4838	0.1216
0.6763	0.0714	0.4736	0.1544
0.6330	0.0964	0.4594	0.1736
0.5897	0.1214	0.4405	0.1822
0.5464	0.1464	0.4162	0.1819
0.5031	0.1714	0.3860	0.1738
0.4598	0.1964	0.3494	0.1589
0.4165	0.2214	0.3064	0.1380
0.3732	0.2464	0.2572	0.1118
0.3299	0.2714	0.2023	0.0812
0.2866	0.2964	0.1428	0.0472
0.2433	0.3214	0.0799	+0.0111
0.2000	0.3464	−0.0152	−0.0262
0.1567	0.3714	+0.0495	0.0636
0.1134	0.3964	0.1123	0.1001
0.0701	0.4214	0.1715	0.1346
+0.0268	0.4464	0.2254	0.1669
−0.0165	0.4714	0.2727	0.1964
0.0598	0.4964	0.3123	0.2231
0.1031	0.5214	0.3435	0.2473
0.1464	0.5464	0.3656	0.2695
0.1897	0.5714	0.3781	0.2904
0.2330	0.5964	0.3801	0.3111
0.2763	0.6214	0.3705	0.3330
0.3196	0.6464	0.3472	0.3582
0.3629	0.6714	0.3055	0.3902
0.40	0.6928	0.2473	0.4283
0.40	0.65	0.1852	0.4597
0.40	0.60	0.1366	0.4798
0.40	0.55	0.1031	0.4874
0.40	0.50	0.0794	0.4847
0.40	0.45	0.0625	0.4726
0.40	0.40	0.0506	0.4514
0.40	0.35	0.0424	0.4212
0.40	0.30	0.0371	0.3820
0.40	0.25	0.0337	0.3343
0.40	0.20	0.0318	0.2786
0.40	0.15	0.0309	0.2158
0.40	0.10	0.0305	0.1473
0.40	0.05	0.0304	0.0747
−0.40	+0	+0.0303	−0

Tabelle XII.

$\xi = -0.45$.

ξ	η	σ	τ
+0.90	+0	−0.4993	+0
0.8312	0.0397	0.4963	0.2137
0.7879	0.0647	0.4919	0.2786
0.7446	0.0897	0.4847	0.3199
0.7013	0.1147	0.4738	0.3452
0.6580	0.1397	0.4582	0.3586
0.6147	0.1647	0.4372	0.3623
0.5714	0.1897	0.4098	0.3574
0.5281	0.2147	0.3753	0.3448
0.4848	0.2397	0.3333	0.3252
0.4415	0.2647	0.2835	0.2991
0.3982	0.2897	0.2261	0.2673
0.3549	0.3147	0.1618	0.2307
0.3116	0.3397	0.0916	0.1902
0.2683	0.3647	−0.0172	0.1472
0.2250	0.3897	+0.0594	0.1029
0.1817	0.4147	0.1361	0.0587
0.1384	0.4397	0.2106	+0.0158
0.0951	0.4647	0.2807	−0.0248
0.0518	0.4897	0.3446	0.0622
+0.0085	0.5147	0.4008	0.0960
−0.0348	0.5397	0.4483	0.1261
0.0781	0.5647	0.4863	0.1526
0.1214	0.5897	0.5144	0.1762
0.1647	0.6147	0.5323	0.1974
0.2080	0.6397	0.5397	0.2175
0.2513	0.6647	0.5359	0.2377
0.2946	0.6897	0.5194	0.2598
0.3379	0.7147	0.4873	0.2867
0.3812	0.7397	0.4332	0.3230
0.45	0.7794	0.2497	0.4324
0.45	0.70	0.0631	0.5367
0.45	0.65	+0.0047	0.5654
0.45	0.60	−0.0347	0.5797
0.45	0.55	0.0621	0.5829
0.45	0.50	0.0815	0.5761
0.45	0.45	0.0952	0.5597
0.45	0.40	0.1047	0.5336
0.45	0.35	0.1110	0.4975
0.45	0.30	0.1150	0.4513

(fortgesetzt).

Tabelle XII (fortgesetzt).

ξ	η	σ	τ
0.45	0.25	0.1173	0.3951
0.45	0.20	0.1185	0.3295
0.45	0.15	0.1189	0.2554
0.45	0.10	0.1189	0.1745
0.45	0.05	0.1189	0.0885
−0.45	+0	−0.1188	−0

Tabelle XIII.

$\xi = -0.48.$

ξ	η	σ	τ
+0.96	+0	−0.5000	+0
0.8895	0.0407	0.4988	0.3970
0.8462	0.0657	0.4963	0.4792
0.8029	0.0907	0.4915	0.5269
0.7596	0.1157	0.4834	0.5551
0.7163	0.1407	0.4711	0.5704
0.6730	0.1657	0.4535	0.5757
0.6297	0.1907	0.4296	0.5726
0.5864	0.2157	0.3983	0.5618
0.5431	0.2407	0.3588	0.5438
0.4998	0.2657	0.3103	0.5189
0.4565	0.2907	0.2527	0.4874
0.4132	0.3157	0.1859	0.4497
0.3699	0.3407	0.1108	0.4066
0.3266	0.3657	−0.0287	0.3593
0.2833	0.3907	+0.0585	0.3089
0.2400	0.4157	0.1484	0.2570
0.1967	0.4407	0.2383	0.2051
0.1534	0.4657	0.3255	0.1548
0.1101	0.4907	0.4076	0.1073
0.0668	0.5157	0.4824	0.0639
+0.0235	0.5407	0.5484	+0.0249
−0.0198	0.5657	0.6046	−0.0093
0.0631	0.5907	0.6504	0.0388
0.1064	0.6157	0.6857	0.0640
0.1497	0.6407	0.7107	0.0858
0.1930	0.6657	0.7253	0.1049

(fortgesetzt).

Tabelle XIII (fortgesetzt).

ξ	η	σ	τ
0.2363	0.6907	0.7295	0.1228
0.2796	0.7157	0.7224	0.1411
0.3229	0.7407	0.7020	0.1622
0.3662	0.7657	0.6631	0.1902
0.4095	0.7907	0.5932	0.2335
0.48	0.8314	+ 0.2500	0.4330
0.48	0.75	— 0.0944	0.6305
0.48	0.70	0.1668	0.6694
0.48	0.65	0.2105	0.6890
0.48	0.60	0.2390	0.6962
0.48	0.55	0.2584	0.6931
0.48	0.50	0.2718	0.6806
0.48	0.45	0.2811	0.6583
0.48	0.40	0.2874	0.6259
0.48	0.35	0.2916	0.5826
0.48	0.30	0.2943	0.5282
0.48	0.25	0.2958	0.4625
0.48	0.20	0.2965	0.3859
0.48	0.15	0.2968	0.2993
0.48	0.10	0.2968	0.2045
0.48	0.05	0.2968	0.1038
— 0.48	+ 0	— 0.2967	— 0

Zur Veranschaulichung des Inhalts der Tabellen dienen folgende drei Abbildungen. Abb. 16 zeigt die Kurven, die der Schwerpunkt durchläuft, wenn der Librationspunkt den Umkreis der vier kleinsten Dreiecke durchläuft. Bis zum Auftreten der Schleifenbildung findet die Bewegung des Schwerpunktes in derselben Umlaufsrichtung statt wie die Bewegung des Librationspunktes, die Lage der Punkte auf den Kurven aber wird ungefähr um 180° im Verhältnis zu einander verschoben sein. — Abb. 17 zeigt die Schwerpunktskurven, die den drei folgenden Dreiecken entsprechen. Die Schleifen haben sich hier entwickelt und nähern sich stark den Seiten des Massendreiecks. — Endlich zeigt Abb. 18 die Schwerpunktskurven, die den drei grössten Dreiecken entsprechen. Gleichzeitig damit, dass die Schleifen grösser werden, nähern sich diese

immer mehr den Seiten des Massendreiecks und gleiten nach und nach übereinander. Wenn wir die Kurve betrachten, die dem grössten Dreieck entspricht, werden wir sehen, dass

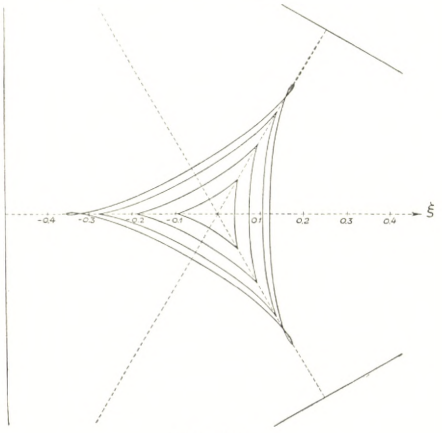

Abb. 16.

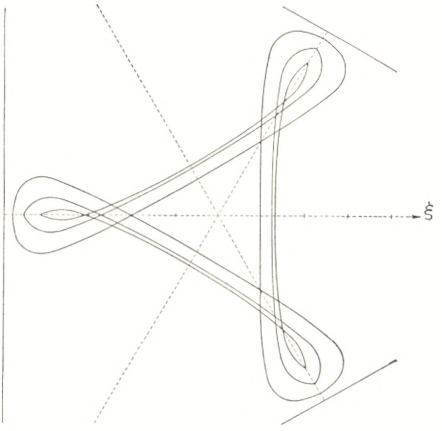

Abb. 17.

jedem Umlauf des Librationspunktes zwei Umläufe des Schwerpunktes in entgegengesetzter Richtung entsprechen. Denken wir uns die Entwicklung fortgesetzt, so dass die Bewegung des Librationspunktes immer näher an den Seiten des Massendreiecks stattfindet, so wird das Resultat augenscheinlich, dass auch die

Bewegung des Schwerpunktes immer näher an den Seiten des Massendreiecks verlaufen wird; wenn sich der Librationspunkt aber einen Umlauf bewegt, wird sich der Schwerpunkt zwei Umläufe in entgegengesetzter Umlaufsrichtung bewegen.

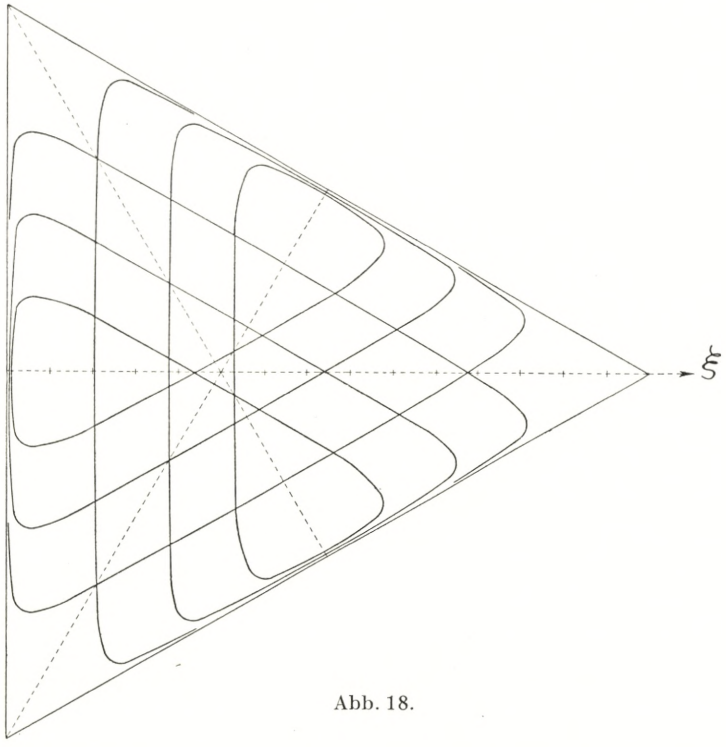

Abb. 18.

Aus dem Vorhergehenden geht nun folgendes hervor: Einem Librationspunkt *innerhalb* des Massendreiecks entspricht ein Schwerpunkt *innerhalb* des Massendreiecks.

Da es ferner einleuchtend ist, dass, gleichzeitig damit, dass der Librationspunkt das ganze Areal des Massendreiecks durchläuft, der Schwerpunkt mindestens ein Mal dieses Areal durchlaufen wird, erhalten wir folgendes Resultat: Einem Schwerpunkt *innerhalb* des Massendreiecks entspricht mindestens ein Librationspunkt *innerhalb* des Massendreiecks.

Dass einem Schwerpunkt innerhalb des Massendreiecks mehrere Librationspunkte innerhalb dieses Dreiecks entsprechen können, geht schon aus dem Lindowschen Spezialfall hervor; in diesem Fall liegen vier Librationspunkte innerhalb des Massendreiecks.

4. Der Librationspunkt ausserhalb des Massendreiecks (Gebiet II).

Bei der numerischen Untersuchung des Falles, wo der Librationspunkt im Gebiet II liegt, können wir uns bei den Berechnungen auf die Behandlung eines einzelnen der drei kongruenten Teile, woraus das Gebiet besteht, beschränken. Es wird deshalb wegen der Symmetrie in Bezug auf die ξ-Achse am praktischsten sein, den Teil des Gebietes, der bei M_1 (II_1) liegt, zu behandeln.

Da der Zusammenhang zwischen der Bewegung des Librationspunktes und des Schwerpunktes für Gebiet II nicht so komplizierter Natur ist wie für Gebiet I, steht dem nichts im Wege, hier den Librationspunkt in grösseren Schritten zu verschieben. Um die Verschiebung des Librationspunktes auf einfache Weise der Begrenzung des Gebietes anzupassen, wollen wir die Verschiebung auf geraden Linien durch M_1 erfolgen lassen. Die Länge der Schritte ist mit 0.2 gewählt, so dass für jede Linie Berechnungen für acht Librationspunkte ausgeführt werden müssen ($\varrho_1 = 0.2; 0.4; 0.6; 0.8; 1.0; 1.2; 1.4; 1.6$). Als Linien für die Verschiebung des Librationspunktes sind die vier Linien gewählt worden, die mit der ξ-Achse die Winkel $-20°$, $-10°$, $10°$ und $20°$ bilden. Die ξ-Achse selbst und die zwei Linien, die einen Teil der Begrenzung des Gebietes bilden, müssen noch hinzugefügt werden; die Verhältnisse auf diesen Linien sind jedoch schon im Vorhergehenden behandelt worden (III, 1; III, 2). Dadurch wird die Gesamtzahl der Librationspunkte innerhalb des Gebietes II_1, für die der Schwerpunkt bestimmt ist, 57; wenn die entsprechenden Librationspunkte in den zwei anderen Gebieten mitgerechnet werden, erreichen wir im Gebiet II eine Gesamtzahl von 171.

Die Tabellen XIV—XVI enthalten die numerischen Resultate für die Librationspunkte auf den drei Linien: $\varphi = 10°$, $\varphi = 20°$

Tabelle XIV.

$\varphi = 10°$.

ϱ_1	σ	τ
0.2	— 0.4950	— 0.2034
0.4	0.4622	0.2140
0.6	0.3816	0.2123
0.8	0.2430	0.1975
1.0	— 0.0464	0.1703
1.2	+ 0.1997	0.1325
1.4	0.4830	0.0868
1.6	+ 0.7900	— 0.0356

Tabelle XV.

$\varphi = 20°$.

ϱ_1	σ	τ
0.2	— 0.4947	— 0.4535
0.4	0.4602	0.4664
0.6	0.3763	0.4550
0.8	0.2340	0.4178
1.0	— 0.0346	0.3562
1.2	+ 0.2122	0.2746
1.4	0.4931	0.1783
1.6	+ 0.7949	— 0.0726

und $\varphi = 30°$. Wegen der Symmetrie in Bezug auf die ξ-Achse ist es nicht notwendig, in den Tabellen die Librationspunkte unterhalb der ξ-Achse mitzunehmen. Für die Librationspunkte auf der ξ-Achse wird auf Tabelle I verwiesen.

Abb. 19 zeigt das Gebiet II_1 mit eingezeichneten Librationspunkten, sowie das Massendreieck mit eingezeichneten Schwer-

Tabelle XVI.

$\varphi = 30°$.

ϱ_1	σ	τ
0.2	— 0.4938	— 0.8624
0.4	0.4551	0.8401
0.6	0.3642	0.7876
0.8	0.2144	0.7011
1.0	— 0.0100	0.5831
1.2	+ 0.2372	0.4404
1.4	0.5130	0.2812
1.6	+ 0.8043	— 0.1130

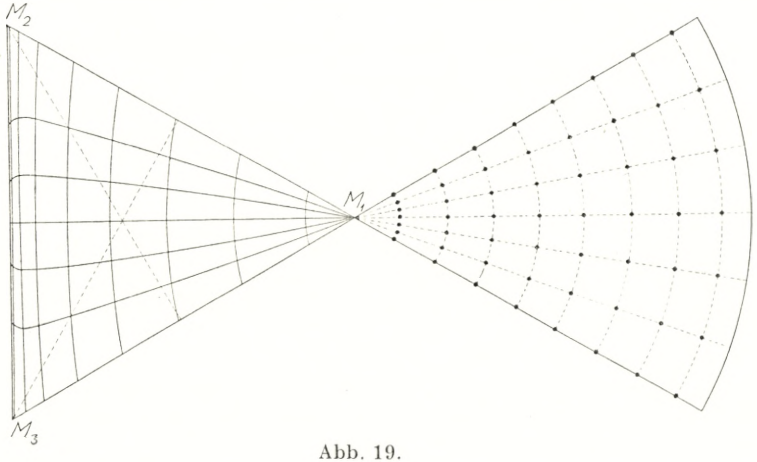

Abb. 19.

punkten. Wenn der Librationspunkt von M_1 aus auf einer geraden Linie bis zum Librationskreis l_1 verschoben wird, geht gleichzeitig eine Verschiebung des Schwerpunktes von einem Punkt auf $M_2 M_3$ bis M_1 auf einer Kurve vor sich, die in dem grössten Teil ihres Laufes wenig von einer geraden Linie abweicht. Es geht deutlich aus dem Lauf der Schwerpunktskurven hervor, dass, wenn der Librationspunkt das ganze Gebiet II_1 durchläuft, der Schwerpunkt gleichzeitig das Gebiet des Massendreiecks ein und nur ein Mal durchlaufen wird. Hieraus folgt:

Einem Schwerpunkt innerhalb des Massendreiecks entspricht ein und nur ein Librationspunkt innerhalb jedes der drei Gebiete II_1, II_2 und II_3.

5. Der Librationspunkt ausserhalb des Massendreiecks (Gebiet III).

In ähnlicher Weise wie bei der Behandlung des Gebiets II können wir uns hier mit der Behandlung eines einzelnen der drei kongruenten Gebiete, die zusammen das Gebiet III ausmachen, begnügen. Es wird dann am leichtesten sein, das Gebiet zu behandeln, das in Bezug auf die ξ-Achse symmetrisch liegt (III_1).

Auch in diesem Fall wird der Zusammenhang zwischen den Verschiebungen des Librationspunktes und des Schwerpunktes ziemlich einfacher Natur sein, so dass man sich bei der Behandlung damit begnügen kann, eine verhältnismässig kleine Anzahl von Librationspunkten zu betrachten. Abb. 20 zeigt das Gebiet III_1 mit den Librationspunkten, die bei der Berechnung angewandt sind. Diese liegen auf Kreisbogen mit dem Zentrum in M_1 und mit den Radien $\varrho_1 = 1.8; 2.0; 2.2; 2.4; 2.6; 2.8$. Jeder einzelne Kreisbogen des Gebietes ist von den Librationspunkten in acht gleich grosse Bogen geteilt. Hierdurch werden die Librationspunkte um P_1 herum am dichtesten liegen, was der Streuung der entsprechenden Schwerpunkte zum Teil entgegenwirkt. Auf jedem einzelnen der sechs Kreisbogen liegen 9 Librationspunkte, so dass die Gesamtzahl der Librationspunkte im Gebiet III_1 54 beträgt; wenn die entsprechenden Librationspunkte in den zwei anderen Gebieten mitgerechnet werden, so erhalten wir im Gebiet III 162 Librationspunkte.

Die Tabellen XVII—XXII enthalten die Koordinaten der Librationspunkte und der Schwerpunkte. Wegen der Symmetrie in Bezug auf die ξ-Achse ist es nicht notwendig, in den Tabellen die Librationspunkte unterhalb der ξ-Achse mitzunehmen; berücksichtigt sind auch nicht die Librationspunkte auf dem Librationskreis l_3, weil der entsprechende Schwerpunkt in M_3 liegt. Die Librationspunkte auf der ξ-Achse sind schon früher behan-

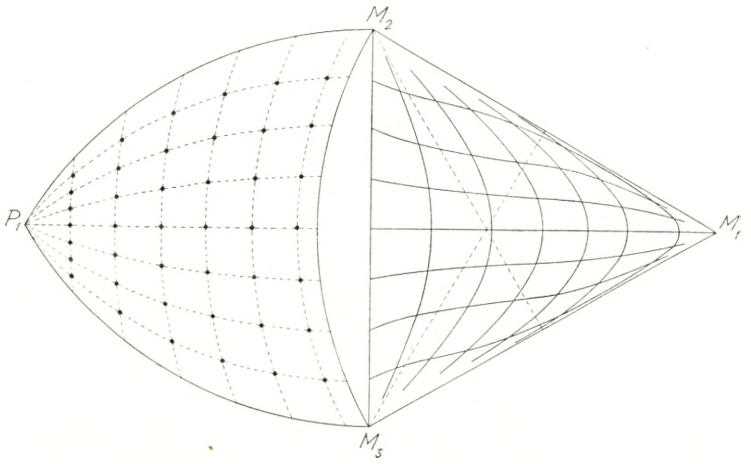

Abb. 20.

delt worden (III,1); der Vollständigkeit wegen sind jedoch auch diese Punkte in den Tabellen mit aufgenommen.

Die den Librationspunkten entsprechenden Schwerpunkte sind im Massendreieck in der Abb. 20 gezeigt. Wenn der Librationspunkt längs eines der Kreisbogen vom Librationskreis l_2 nach l_3 verschoben wird, so wird der Schwerpunkt gleichzeitig

Tabelle XVII.

$\varrho_1 = 1.8.$

ξ	η	σ	τ
−0.8	+0	+0.8468	−0
0.7859	0.2248	0.8262	0.0550
0.7439	0.4460	0.7545	0.1234
−0.6745	+0.6603	+0.5821	−0.2371

Tabelle XVIII.

$\varrho_1 = 2.0.$

ξ	η	σ	τ
−1.0	+0	+0.6244	−0
0.9884	0.2154	0.5928	0.1115
0.9536	0.4284	0.4905	0.2339
−0.8961	+0.6363	+0.2747	−0.3964

Tabelle XIX.

$\varrho_1 = 2.2.$

ξ	η	σ	τ
−1.2	+0	+0.4479	−0
1.1911	0.1972	0.4167	0.1317
1.1646	0.3929	0.3146	0.2754
−1.1207	+0.5854	+0.0987	−0.4625

Tabelle XX.

$\varrho_1 = 2.4.$

ξ	η	σ	τ
−1.4	+0	+0.2506	−0
1.3941	0.1690	0.2223	0.1442
1.3762	0.3371	+0.1297	0.3032
−1.3466	+0.5035	−0.0625	−0.5074

Tabelle XXI.

$\varrho_1 = 2.6.$

ξ	η	σ	τ
−1.6	+0	+0.0239	−0
1.5968	0.1288	+0.0011	0.1580
1.5872	0.2574	−0.0727	0.3318
−1.5713	+0.3853	−0.2187	−0.5471

Tabelle XXII.

$\varrho_1 = 2.8.$

ξ	η	σ	τ
−1.8	+0	−0.2285	−0
1.7990	0.0742	0.2425	0.1796
1.7961	0.1483	0.2863	0.3715
−1.7912	+0.2223	−0.3669	−0.5916

einer der gezeigten Kurven entlang von M_2 nach M_3 verschoben. Der Kreisbogen, der l_1 am nächsten liegt, entspricht der Schwerpunktskurve, die M_1 am nächsten liegt, während der Kreisbogen, der P_1 am nächsten liegt, der Schwerpunktskurve entspricht, die $M_2 M_3$ am nächsten liegt. Der Punkt P_1 selbst entspricht der Linie $M_2 M_3$, ebenso wie der Kreisbogen l_1 dem Punkt M_1 entspricht. Es geht aus der Abbildung hervor, dass, wenn der Librationspunkt das ganze Gebiet III_1 durchläuft, der Schwerpunkt gleichzeitig das Gebiet des Massendreiecks ein und nur ein Mal durchlaufen wird. Hieraus folgt:

Einem Schwerpunkt innerhalb des Massendreiecks entspricht ein und nur ein Librationspunkt innerhalb jedes der drei Gebiete III_1, III_2 und III_3.

6. Übersicht über die numerischen Resultate.

Nachdem nun eine vollständige Übersicht über die Verschiebungen des Schwerpunktes, die bestimmten gegebenen Verschiebungen des Librationspunktes entsprechen, zustandegebracht ist, liegt es nahe, das Problem umzukehren, indem man — von den numerischen Resultaten ausgehend — versucht, die Verschiebungen der Librationspunkte für bestimmte gegebene Verschiebungen des Schwerpunktes zu bestimmen.

Dieses Problem ist gewissermassen von komplizierterer Natur als das ursprüngliche Problem, da es sich hier darum handelt, die gleichzeitige Bewegung einer grösseren Anzahl von Librationspunkten klarzulegen. Dies lässt sich an und für sich schon machen, wegen der verwickelten Verhältnisse wird eine solche Untersuchung aber kaum von grösserem Wert sein. Dagegen wird man eine gute Übersicht über die Verhältnisse bekommen,

wenn man den Schwerpunkt bestimmte Gebiete innerhalb des Massendreiecks durchlaufen lässt und dann die Gebiete bestimmt, die gleichzeitig von den entsprechenden Librationspunkten durchlaufen werden.

Die im folgenden gefundenen Kurven, die diese Verhältnisse veranschaulichen sollen, sind alle durch Interpolation zwischen den in früheren Tabellen gegebenen Zahlenwerten gefunden worden.

Die Untersuchung wird nun zunächst für diejenigen Librationspunkte durchgeführt werden, die sich im Gebiet I befinden.

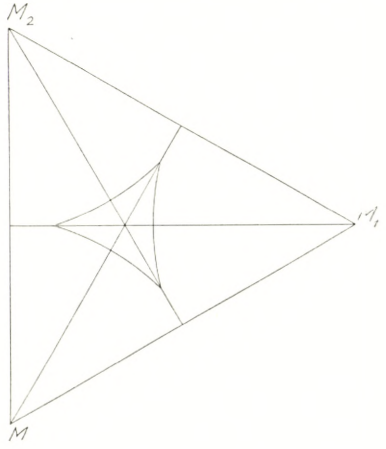

Abb. 21.

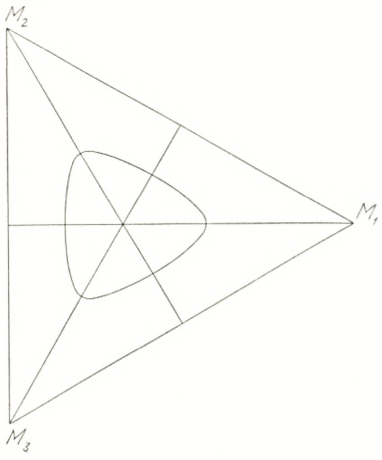

Abb. 22.

Wie schon früher erwähnt, wird in diesem Gebiet mehr als ein Librationspunkt einem bestimmten Schwerpunkt entsprechen können. Dies Verhältnis beruht darauf, dass, gleichzeitig damit, dass der Librationspunkt ein einzelnes Mal durch das ganze Gebiet I verschoben wird, der Schwerpunkt jedenfalls durch gewisse Teile des Gebietes mehr als ein Mal verschoben wird. Eine nähere Untersuchung zeigt, dass ein kleiner Teil des Massendreiecks um den Mittelpunkt des Dreiecks viermal vom Schwerpunkt durchlaufen wird, während der übrige Teil des Dreiecks nur zweimal durchlaufen wird. Die Kurve, welche die zwei Teile des Dreiecks trennt, sieht man auf Abb. 21; sie wird im folgenden als die Schwerpunktsgrenzkurve bezeichnet werden. Die zwei Schnittpunkte zwischen der Kurve und der ξ-Achse haben die Abszissen

0.135171 und −0.320605. Liegt der Schwerpunkt innerhalb dieser Grenzkurve, gibt es also vier Librationspunkte im Gebiet I; wenn er dagegen ausserhalb der Grenzkurve liegt, gibt es nur zwei Librationpunkte im Gebiet I. Denkt man sich eine Verschiebung des Schwerpunktes aus dem inneren ins äussere Gebiet, wird der Übergang von vier auf zwei Librationspunkte dadurch geschehen, dass zwei der Librationspunkte sich einander nähern, um sich in einen Doppelpunkt zu vereinen, wenn der Schwerpunkt auf der Grenzkurve selbst liegt; dieser Doppelpunkt verschwindet, sobald die Grenzkurve passiert ist.

Dem Schwerpunkt in einem bestimmten Punkt der Grenzkurve muss deshalb eine bestimmte Lage des Librationsdoppelpunktes entsprechen, oder mit anderen Worten: der Schwerpunktsgrenzkurve muss eine Kurve der Librationsdoppelpunkte entsprechen. Diese Kurve sieht man in Abb. 22. Ihre Schnittpunkte mit der ξ-Achse haben die Abszissen 0.355111 und −0.257, die den oben erwähnten Schwerpunktsabszissen entsprechen, wie im Schema gezeigt ist.

ξ	σ
0.355111	−0.320605
−0.257	0.135171

Der untere Satz von Werten ist schon während der Behandlung des Spezialfalles erwähnt, wo der Schwerpunkt sich auf einer Symmetrieachse befindet (III, 1). Wenn der Schwerpunkt auf der ξ-Achse von M_1 aus verschoben wird, wird es, wie aus Abb. 13 hervorgeht, anfangs keine Librationspunkte auf dem Teil der ξ-Achse geben, der innerhalb des Massendreiecks liegt; die zwei Librationspunkte, die im Gebiet I liegen, müssen also ausserhalb der ξ-Achse liegen. Wenn aber der Schwerpunkt den Punkt mit der Abszisse 0.135171 erreicht hat, taucht ein Librationsdoppelpunkt mit der Abzisse −0.257 auf, dem Maximum der Kurve in Abb. 13 entsprechend. Wenn der Schwerpunkt danach innerhalb der Grenzkurve wandert, entstehen im Gebiet I vier Librationspunkte, und zwar zwei auf der ξ-Achse und zwei ausserhalb der ξ-Achse. Erreicht dann der Schwerpunkt die Spitze der Schwerpunktsgrenzkurve mit der Abszisse −0.320605, so werden, wie wir später sehen werden, die zwei ausserhalb der

ξ-Achse liegenden Librationspunkte zu einem Librationsdoppelpunkt auf der ξ-Achse selbst und mit der Abszisse 0.355111 zusammenschmelzen. Dieser Librationsdoppelpunkt, der im Verschwinden begriffen ist, fällt übrigens mit einem der zwei auf der ξ-Achse liegenden Librationspunkte zusammen, so dass in der Tat von einem Librationstripelpunkt die Rede ist. Bei der weiteren Verschiebung des Schwerpunktes bleiben nur zwei Librationspunkte zurück, die beide auf der ξ-Achse liegen.

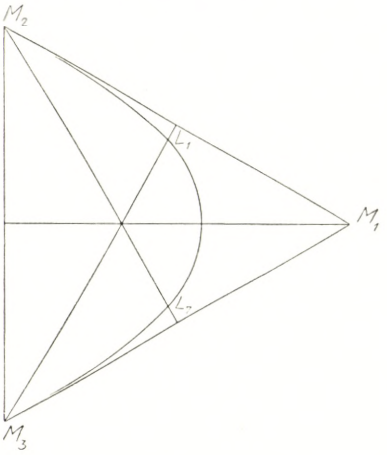

Abb. 23.

Die Kurve, die von den zwei ausserhalb der ξ-Achse liegenden Librationspunkten durchlaufen wird, wenn der Schwerpunkt die ξ-Achse durchläuft, sehen wir in Abb. 23. Beim Starten des Schwerpunktes von M_1 aus liegen die zwei Librationspunkte in M_2 und M_3. Während der Verschiebung des Schwerpunktes von M_1 nach dem Mittelpunkt des Dreiecks werden die zwei Librationspunkte von den Eckpunkten des Dreiecks nach den Lindowschen Librationspunkten L_1 und L_7 verschoben. Während der weiteren Verschiebung des Schwerpunktes vom Mittelpunkt des Dreiecks nach dem Punkt mit der Abszisse -0.320605 wandern die Librationspunkte weiter auf der gezeigten Kurve, um sich auf der ξ-Achse im Punkt mit der Abszisse 0.355111 zu vereinen.

Die Übersicht, die wir jetzt über die Verschiebungen der vier Librationspunkte als Folge der Verschiebung des Schwerpunktes auf der Symmetrieachse durch M_1 erlangt haben, kann direkt auf die Verschiebungen des Schwerpunktes auf den zwei Symmetrieachsen durch M_2 und M_3 übertragen werden. Die Schwerpunktsgrenzkurve und die Kurve der Librationsdoppelpunkte werden selbstverständlich bei den drei Symmetrieachsen dieselben sein; dagegen wird die Kurve der ausserhalb der Symmetrieachse liegenden Librationspunkte in den drei Fällen verschieden sein. In Abb. 24 sehen wir alle drei Librationspunktkurven. Diese drei Kurven werden jetzt mit den drei Symmetrieachsen

und den drei Dreiecksseiten zusammen das Dreieck in 18 Abschnitte teilen. Für diese Abschnitte gilt es, dass, wenn der Schwerpunkt auf den drei Dreiecksseiten oder den drei Symmetrieachsen verschoben wird, der Librationspunkt sich gleichzeitig auf den Linien oder Kurven, die die Grenze der Abschnitte bilden, verschiebt. Wenn also der Schwerpunkt auf dem Umkreis des in Abb. 25 gezeigten Dreiecks 1 verschoben wird, werden die Librationspunkte sich gleichzeitig auf den Umkreis der drei Ab-

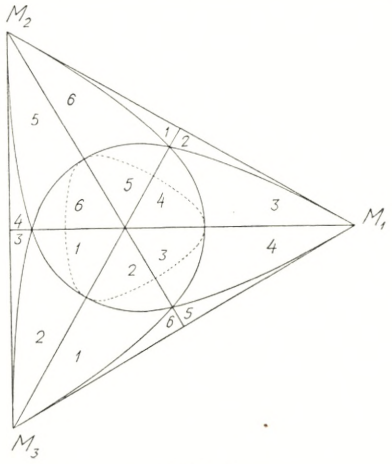

Abb. 24.

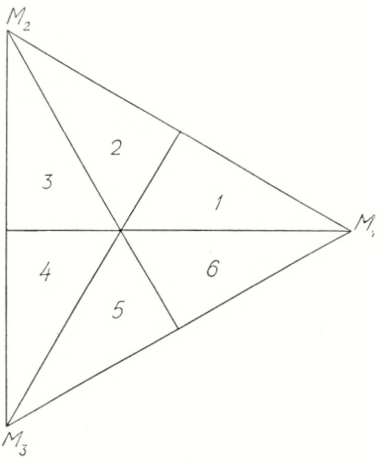

Abb. 25.

schnitte 1 in Abb. 24 verschieben. Die zwei äusseren Abschnitte werden beide einen Librationspunkt auf dem Umkreis haben, während der innere Abschnitt entweder zwei Librationspunkte (wenn der Schwerpunkt innerhalb der Schwerpunktsgrenzkurve liegt) oder keine Librationspunkte auf dem Umkreis hat. Liegt dagegen der Schwerpunkt innerhalb des Dreiecks 1, wird ein Librationspunkt innerhalb jedes der zwei äusseren Abschnitte liegen, während innerhalb des inneren Abschnittes entweder zwei Librationspunkte (wenn der Schwerpunkt innerhalb der Schwerpunktsgrenzkurve liegt) oder keine Librationspunkte liegen. Wenn zwei Librationspunkte im inneren Abschnitt liegen, so werden sie jeder auf seiner Seite der gestrichelten Kurve liegen, die die Kurve der Librationsdoppelpunkte darstellt. Diese Kurve darf als eine Verschwindungskurve der Librationspunkte aufgefasst werden. Wenn zwei Librationspunkte verschwinden sollen, wandern

sie nach dieser Kurve hin. Auf der Kurve werden sie sich in einem Librationsdoppelpunkt vereinen und dort verschwinden.

In derselben Weise wie drei Abschnitte dem Dreieck 1 entsprechen, werden drei Abschnitte jedem der anderen fünf Dreiecke im Gebiet I entsprechen. Vergleicht man Abb. 24 mit Abb. 25, so sieht man, wie die 18 Abschnitte für die Librationspunkte in Abb. 24 den Dreiecken in Abb. 25 entsprechen. Ein näheres Studium der Lage und der Form der Abschnitte kann zu vielen interessanten Beobachtungen Anlass geben. Hier soll nur auf zwei Tatsachen aufmerksam gemacht werden: 1°. Die drei Schnittpunkte zwischen den drei Librationspunktkurven sind gerade die Lindowschen Librationspunkte L_1, L_4 und L_7. — 2°. Es geht aus der Rechnung ziemlich sicher hervor, dass die Kurve der Librationsdoppelpunkte die drei Librationspunktkurven berührt.

Die Librationspunkte im Gebiet II können in derselben Weise wie die Librationspunkte im Gebiet I behandelt werden. Wegen der Symmetrieverhältnisse genügt es, die Verhältnisse in II_1 zu behandeln.

Wird der Schwerpunkt von M_1 auf der Symmetrieachse des Massendreiecks verschoben, so wird der Librationspunkt, der in II_1 liegt, gleichzeitig vom Librationskreis l_1 nach M_1 auf der ξ-Achse verschoben. Wird dagegen der Schwerpunkt auf den anderen zwei Symmetrieachsen verschoben, so wird der Librationspunkt auf den zwei Kurven, die in Abb. 26 gezeigt sind, verschoben. Diese zwei Kurven in Verbindung mit der ξ-Achse werden II_1 in sechs Abschnitte teilen, die den sechs kongruenten Dreiecken des Massendreiecks entsprechen, wie die Zahlen in der Abbildung zeigen.

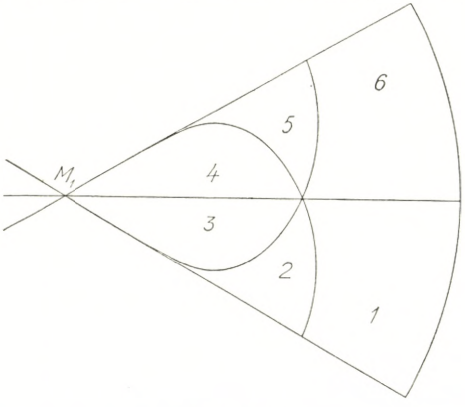

Abb. 26.

Der Schnittpunkt zwischen den zwei Kurven, die innerhalb II_1 liegen, ist der Lindowsche Librationspunkt L_2. Es geht aus

der Rechnung ziemlich deutlich hervor, dass die zwei Kurven die geradlinigen Grenzen des Gebietes im Punkt M_1 berühren.

Für die bei M_2 und M_3 liegenden Teile des Gebietes II (II_2 und II_3) gelten ähnliche Verhältnisse wie bei II_1.

Auch die Librationspunkte im Gebiet III können in derselben Weise wie die Librationspunkte in den Gebieten I und II behandelt werden. Hier wollen wir der Symmetrieverhältnisse wegen den Teil des Gebietes behandeln, der bei der Dreiecksseite $M_2 M_3$ (III_1) liegt.

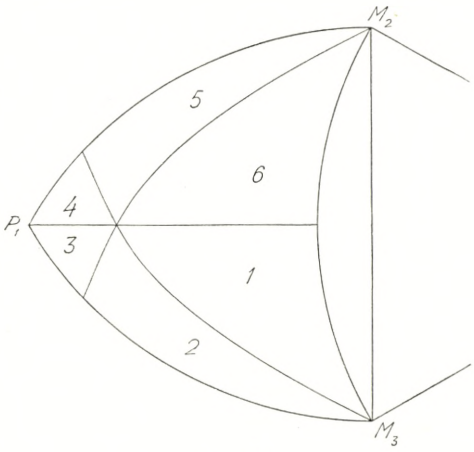

Abb. 27.

Wird der Schwerpunkt von M_1 längs der Symmetrieachse des Massendreiecks verschoben, so wird der Librationspunkt, der in III_1 liegt, gleichzeitig längs der ξ-Achse vom Librationskreis l_1 nach P_1, der den einen Schnittpunkt zwischen den Librationskreisen l_2 und l_3 bildet, verschoben. Wird dagegen der Schwerpunkt längs der zwei anderen Symmetrieachsen verschoben, so wird der Librationspunkt auf den zwei Kurven, die in Abb. 27 gezeigt sind, verschoben werden. Diese zwei Kurven in Verbindung mit der ξ-Achse werden III_1 in sechs Abschnitte teilen, die den sechs kongruenten Dreiecken des Massendreiecks entsprechen, wie die Zahlen in der Abbildung zeigen.

Der Schnittpunkt zwischen den zwei Kurven ist der Lindowsche Librationspunkt L_6. Die Schnittpunkte zwischen den Kurven und den Librationskreisen l_2 und l_3 haben eine solche Lage auf den Librationskreisen, dass die zwei Bogen von den Schnittpunkten nach P_1 13° 12′ ausmachen.

Die bei $M_1 M_2$ und $M_1 M_3$ liegenden Teile des Gebietes III (III_2 und III_3) werden in entsprechender Weise in sechs Abschnitte geteilt werden können.

Was die mögliche Anzahl von Librationspunkten in dem vorliegenden Problem betrifft, geht nun folgendes Hauptresultat aus dem Vorhergehenden hervor:

In dem behandelten Spezialfall des Vierkörperproblems, wo die drei endlichen Massen in einem rotierenden Koordinatensystem feste Stellungen in den Eckpunkten eines gleichseitigen Dreiecks einnehmen, werden 8, 9 oder 10 Librationspunkte bestehen, je nachdem der Schwerpunkt der drei endlichen Massen *ausserhalb*, *auf* oder *innerhalb* der Schwerpunktsgrenzkurve liegt. Ausserhalb des Massendreiecks liegen immer 6 Librationspunkte.

Indleveret til Selskabet den 2. December 1943.
Færdig fra Trykkeriet den 17. August 1944

DET KGL. DANSKE VIDENSKABERNES SELSKAB
MATEMATISK-FYSISKE MEDDELELSER, BIND XXI, NR. 7

INVESTIGATIONS ON THE SOLUBILITY OF CALCIUM PHYTATE

BY

E. HOFF-JØRGENSEN

KØBENHAVN
I KOMMISSION HOS EJNAR MUNKSGAARD
1944

Printed in Denmark
Bianco Lunos Bogtrykkeri A/S

Phytic acid is the hexaphosphoric ester of inositol (Posternak (1921)): $C_6H_6(O \cdot PO(OH)_2)_6$,

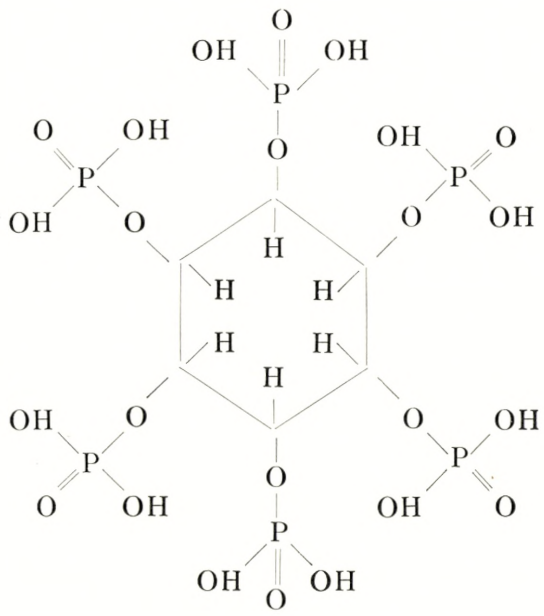

and is thus a 12-basic acid; this acid is found particularly in cereals, 60 to 85 per cent. of the phosphorus here occurring as phytic acid (J. G. A. Pedersen (1940)). Phytic acid is not absorbed from the alimentary canal, and in the intestine of animals and man it is only to a slight extent split into inositol and phosphate (Starkenstein (1910)).

In 1920 Mellanby demonstrated that cereals contain varying amounts of an "anticalcifying factor" which favours the development of rickets. Bruce and Callow (1934) experimented with a diet which was rich in cereals, but poor in phosphate; their

results implied that the rachitogenic action of the cereals depends on their content of phytic acid, and that the rickets developed was due to lack of absorbable phosphate. In 1939 HARRISON and MELLANBY put forth a new theory regarding the effect of phytic acid. Their experiments support the assumption that the solubility of the calcium salt of phytic acid is so slight, that the absorption of calcium is impaired, because calcium phytate is precipitated in the intestine. Experiments on pigs by PEDERSEN (*l. c.*) have further supported both theories; he found that the former mode of action prevailed on a diet high in calcium, whilst the latter effect was the most pronounced on a diet low in calcium.

BRUCE and CALLOW's theory has been supported by various experiments, whilst MELLANBY's theory still rests on an assumption, as determinations of the solubility of calcium phytate have not so far been published.

It has been the aim of the present work first to determine the compositions of the calcium salts of phytic acid, when precipitated under conditions similar to those found in the intestine, and secondly to determine the solubility of the said salts.

1. Composition of the Calcium Salts of Phytic Acid.

The raw material used was sodium phytate, prepared from wheat bran according to the method of POSTERNAK (1921). The colourless crystalline sodium salt was recrystallised three times from water. For analysis it was dried at 120° C., by which 35 out of the 38 molecules of crystal water disappear.

	C	H	P	Na	H_2O (120° C.)
Found per cent.	7.48	1.22	19.14	28,2	38.8
Calculated for $C_6H_6O_{24}P_6Na_{12}, 3\ H_2O$ per cent....	7.36	1.23	19.02	28.2	39.2

Preparation of the Barium Salt of Phytic Acid.

A solution of sodium phytate, about 0.1 M, was brought to $p_H = 1$ with 1 N HCl. An equal volume of barium chloride solution, about 0.5 M, was added. After some time a white, crystalline precipitate began to form. The precipitation was

finished in about twelve hours. The salt was analysed after drying at 120° C.

	P	Ba
Found per cent.	17.62	38.3
Calculated for $C_6H_{12}O_{24}P_6Ba_3$ per cent.	17.45	38.6

If crystallization takes place at p_H above 2, the barium content is higher than corresponding to the above formula.

Preparation of Phytic Acid.

The barium salt was suspended in water and heated to 60° C. 0.5 M H_2SO_4 in a quantity determined by calculation, was added slowly during vigorous stirring. The barium sulphate formed was separated by filtration, and the clear filtrate was evaporated in vacuo until it was 1 M in phosphorus. This solution does not give the inorganic phosphate reaction with molybdate reagent. The phosphorus content was determined after destruction of the organic matter, and the solution then was diluted to be 0.6 M in phosporus, i. e. 0.1 M in phytic acid.

Preparation of the Calcium Salt of Phytic Acid.

30 ml. 0.1 M phytic acid were mixed with 100 ml. 1.0 M NaCl. The p_H of the solution was adjusted to 3.7 (glass electrode) by adding 0.5 M NaOH. Addition of 10 ml. 1.8 M $CaCl_2$ now caused a drop in p_H to about 2.7, without precipitation occurring. During vigorous mechanical stirring and aeration with CO_2-free air, 0.5 M NaOH was slowly added until the desired p_H was reached. Stirring and aeration was continued for one hour. The precipitate was filtered off by means of a Jena glass filter No. 11 G 3 and washed with three times 15 ml. boiling distilled water and dried at 105° C.

Analytical methods.

About 300 mg. of calcium phytate were ashed with sulphuric acid, nitric acid, and perchloric acid; the mixture was aerated during the ashing in order to prevent bumping. The precipitated calcium sulphate was dissolved by boiling with about 50 ml. 2 per cent. hydrochloric acid. The calcium content of this

solution was determined gravimetrically as CaC_2O_4, H_2O, and the phosphorus as NH_4MgPO_4, $6\,H_2O$, according to the methods of WASHBURN and SHEAR (1932). The accuracy of the methods was determined through eight analyses on solutions with known contents of calcium and phosphorus. The standard deviation of 8 calcium determinations was 0.25 per cent., and the standard deviation of 8 phosphorus determinations 0.30 per cent. The water content was determined by drying over P_2O_5 in vacuo at 200° C. (boiling benzyl alcohol). The compound was not discoloured.

Table 1 gives the results of the analyses of the calcium salt precipitated at varying p_H.

Table 1.

Precipitation of Calcium Phytate at Varying p_H.

Precipitation conditions	p_H	Ca p.c.	P p.c.	H_2O p.c.	P/Ca Mol
Precipitated at room temperature Stirred for one hour after precipitation	2.75	19.04	21.72	—	1.475
	3.01	19.25	21.30	—	1.430
	3.45	19.90	21.06	—	1.366
	3.70	20.12	21.37	4.66	1.370
	4.11	21.15	20.74	5.22	1.267
	4.25	21.76	20.60	5.38	1.223
	4.79	22.10	20.65	5.47	1.208
	5.30	21.86	20.62	5.82	1.216
	5.52	21.49	19.81	7.38	1.190
	6.03	21.79	20.11	5.67	1.192
	6.50	21.82	20.23	6.21	1.196
	6.92	21.95	20.21	5.81	1.188
	7.27	22.06	19.61	6.42	1.149
	7.85	22.45	18.72	6.90	1.077
	8.31	22.68	18.44	6.60	1.051
Precipitated at room temperature Stirred for 12 hours at 37° C.	3.72	20.06	21.27	—	1.370
	4.19	20.61	20.89	—	1.308
	4.85	21.21	20.05	—	1.220
	5.58	21.21	19.88	—	1.210
Precipitated at 100° C. Stirred for one hour at 100° C.	3.94	19.15	20.10	—	1.355
	4.12	21.24	20.72	—	1.260
	4.82	21.92	20.53	—	1.210
	5.47	22.10	20.37	—	1.190

Table 2 gives the results of some experiments in which the ratio P/Ca was varied in the solution. The table shows that the composition of the salt is independent of this ratio.

Table 2.
Precipitation of Pentacalcium Phytate, the Ratio P/Ca being Varied in Precipitation Solutions.

Precipitation conditions	P/Ca[1] Mol	p_H	Ca p.c.	P p.c.	P/Ca[2] Mol
Precipitated at	$^2/_1$	5.05	22.10	20.71	1 209
room temperature	$^1/_2$	5.05	22.00	20.64	1.211
Stirred for one hour	$^1/_3$	5.05	21.94	20.32	1.194
after precipitation	$^1/_4$	5.05	22.01	20.37	1.193

[1] In precipitation solution.
[2] In precipitate.

Fig. 1 shows that the ratio P/Ca in the salt is constant and corresponds to the formula $C_6H_8O_{24}P_6Ca_5$ when precipitation takes place in the p_H-interval $4.6 < p_H < 6.9$. Outside this interval

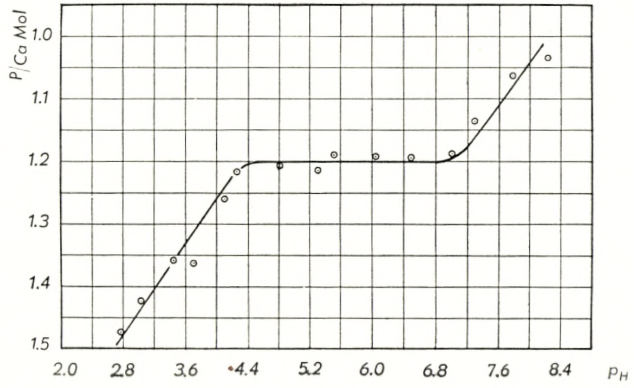

Fig. 1. Correlation between p_H in the solution and the ratio P/Ca in the precipitated salt.

the composition of the salt changes. The precipitation of other salts with a simple P/Ca ratio has failed.

As the pentacalcium phytate precipitate is fairly easily filtered off and as its composition is constant in a fairly large p_H-interval, it was to be expected that the salt was crystalline. This, however, is not the case. Mr. A. Tovborg Jensen has kindly pre-

pared X-ray powder diagrams of a series of precipitations, precipitated under various conditions. They were all amorphous. An example is shown in Fig. 2.

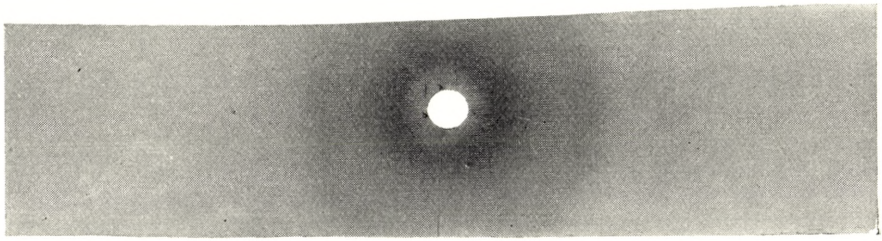

Fig. 2. X-ray powder diagram of pentacalcium phytate precipitated at p_H 5. Experimental conditions: Camera diameter 57,4 mm. Co-radiation, Fe-filter. Exposure 6 hours, pinhole diameter 0.6 mm. The two diffraction rings by registration with the Zeiss Photometer were found to correspond to glancing angles of 5°.7 and 16°.4.

2. Determination of the Dissociation Constants of Phytic Acid in 0.2 M and 1.0 M NaCl.

The dissociation constants have been determined by measurements with the H_2-electrode in 0.2 and 1.0 M sodium chloride solutions. The electrode vessel used was one constructed by K. J. PEDERSEN (1936); it consists of two Jena glass filters through which the hydrogen was passed into the solution. The bridge solution was 3.5 M potassium chloride. The hydrogen was taken from a steel flask and was washed in pyrogallol-potassium hydroxide and in a solution of sodium chloride of the same concentration as that to be examined. All readings were made at a temperature of 37° C ± 0°.1 C. Potentiometer: Wolff. Sensitivity of galvanometer: 2 mm. for 0.01 millivolt. The reference electrode was a hydrogen electrode in a solution which was 0.01 M in HCl and 0.2 and 1.0 M, respectively, in NaCl.

Preparation of Solutions.

10 ml. 0.01 M sodium phytate, 5 or 25 ml. 4.0 M sodium chloride and the amount of 0.02 N HCl entered in the tables was pipetted into a 100 ml. volumetric flask. The flask was filled to the mark with CO_2-free water. The figures given are the averages of two readings differing 0.2 millivolt at most.

$-\log[H^+]$ was calculated from the voltage difference π by the equation: $-\log[H^+] = 2.00 + \frac{\pi}{0.0615}$; $-\log[OH^-]$ was calculated from: $p_{K_c} = -\log[H^+] - \log[OH^-]$, where $p_{K_c} = 13.38$ in 1 M NaC and $p_{K_c} = 13.57$ in 0.2 M NaCl (BJERRUM and UNMACK (1929)). $\bar{n} = \frac{C_{HCl} - [H^+] + [OH^-]}{C_{phytate}}$ represents the average number of acidic hydrogen atoms of the phytate molecule at the p_H in question.

Table 3.

$C_{phytate} = 10^{-3}$ M; $C_{NaCl} = 0.2$ M; Reference Electrode: 0.01 N HCl, 0.2 M NaCl; 37° C.

$C_{HCl} \cdot 10^{-3}$	π Volt	$-\log[H^+]$	$-\log[OH^-]$	$\bar{n}$
0	0.5012	10.15	3.42	0.38
0.5	0.4914	9.99	3.58	0.76
1.5	0.4569	9.43	4.16	1.56
2.5	0.4193	8.82	4.75	2.52
3.5	0.3623	7.89	5.68	3.50
4.5	0.2696	6.38	7.21	4.50
5.5	0.1916	5.12	—	5.49
6.5	0.1017	3.65	—	6.26
7.5	0.0647	3.05	—	6.61
8.5	0.0486	2.79	—	6.88
9.5	0.0373	2.61	—	7.04
10.5	0.0292	2.47	—	7.11
11.5	0.0231	2.38	—	7.33
12	0.0201	2.33	—	7.32

$-\log[H^+]$ for $\bar{n} = 7.5$, 6.5, 5.5, 4.5, 3.5, 2.5, 1.5 and 0.5 was read by graphical interpolation (see Fig. 3) from the corresponding values of $\bar{n}$ and $-\log[H^+]$, which have been given in Table 3:

$\bar{n} =$	7.5	6.5	5.5	4.5	3.5	2.5	1.5	0.5
$-\log[H^+] =$	2.20	3.22	5.10	6.42	7.85	8.80	9.48	10.13

These values of $-\log[H^+]$ form a preliminary approximation to eight of the twelve dissociation constants of phytic acid.

Table 3 shows that determination of the remaining four preliminary constants is impossible, as this would require knowledge of $-\log[H^+]$ from $\bar{n} = 7.5$ to $\bar{n} = 12$.

Table 4.

$C_{phytate} = 10^{-3}$ M; $C_{NaCl} = 1.0$ M; Reference Electrode: 0.01 n HCl, 1.0 M NaCl; 37° C.

$C_{HCl} \cdot 10^{-3}$	π Volt	$-\log [H^+]$	$-\log [OH^-]$	$\bar{n}$
0	0.4631	9.53	3.85	0.14
0.5	0.4446	9.23	4.15	0.57
1.5	0.4096	8.66	4.72	1.52
2.5	0.3764	8.12	5.26	2.51
3.5	0.3255	7.29	—	3.50
4.5	0.2333	5.79	—	4.50
5.5	0.1585	4.58	—	5.47
6.5	0.0902	3.47	—	6.16
7.5	0.0587	2.95	—	6.38
8.5	0.0437	2.71	—	6.55
9.5	0.0335	2.54	—	6.62
10.5	0.0262	2.43	—	6.78
11.5	0.0203	2.33	—	6.82
12	0.0179	2.29	—	6.87

Table 5.

$C_{phytate} = 10^{-2}$ M; $C_{NaCl} = 1.0$ M; Reference Electrode: 0.1 M HCl, 1.0 M NaCl; 37° C.

$C_{HCl} \cdot 10^{-2}$	π Volt	$-\log [H^+]$	$-\log [OH^-]$	$\bar{n}$
0	0.5352	9.70	3.68	0.02
0.5	0.5176	9.42	3.96	0.51
1.5	0.4872	8.92	4.46	1.50
2.5	0.4477	8.28	5.13	2.50
3.5	0.3841	7.25	—	3.50
4.5	0.2904	5.72	—	4.50
5.5	0.2151	4.50	—	5.50
6.5	0.1242	3.02	—	6.40
7.5	0.0763	2.24	—	6.92
8.5	0.0567	1.92	—	7.30
9.5	0.0437	1.71	—	7.55
10.5	0.0345	1.56	—	7.75
11.5	0.0273	1.44	—	7.87
12	0.0242	1.39	—	7.93

Exactly similar measurements were made in 1.0 M sodium chloride. The results have been entered in Table 4.

Table 4 shows that corresponding values of $\bar{n}$ and $-\log[H^+]$ only allow determination of seven out of the twelve dissociation constants of phytic acid. Determination of another one or two constants was attempted by making a series of measurements in a ten times stronger concentration of phytic acid. The results of the measurements have been given in Table 5.

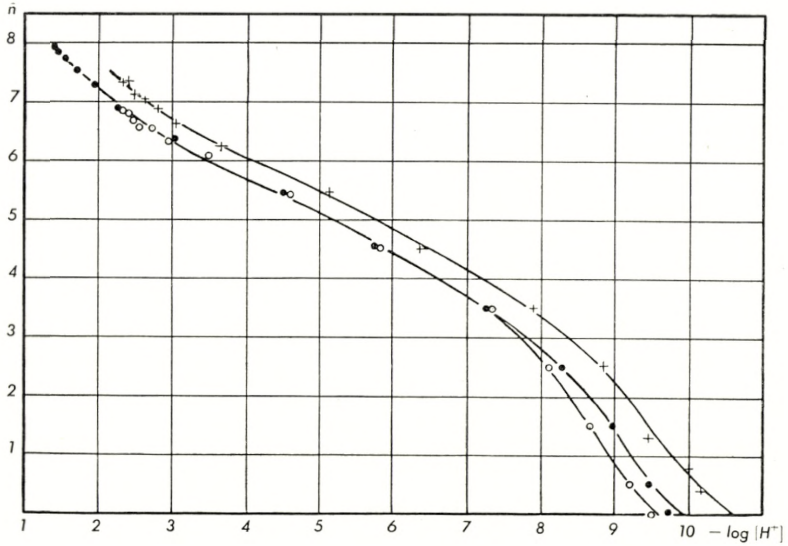

Fig. 3. Corrected titration curve for phytic acid.
+——+ $C_{phytate} = 10^{-3}$; $C_{Na\,Cl} = 0.2$
●——● - $= 10^{-2}$; - $= 1.0$
○——○ - $= 10^{-3}$; - $= 1.0$

When corresponding values of $\bar{n}$ and $-\log[H^+]$ are plotted in a diagram, we see that the curves from Table 4 and Table 5 are identical for values of $\bar{n}$ larger than 3.5, i. e. in the acid and neutral region. The values of $-\log[H^+]$ corresponding to n = 7.5, 6.5, 5.5, 4.5, and 3.5 have therefore been read from the joint curve, the values for n = 2.5, 1.5 and 0.5 from the curve plotted from Table 4 (0.001 M phytate). In this way preliminary values were found for the eight dissociation constants in 1.0 M NaCl:

$\bar{n} =$	7.5	6.5	5.5	4.5	3.5	2.5	1.5	0.5
$-\log[H^+] =$	1.75	2.77	4.53	5.76	7.28	8.12	8.68	9.25

From the corresponding values of $\bar{n}$ and $-\log[H^+]$ it is possible to calculate a set of dissociation constants which mutually agree. The calculation may be carried out in several ways. In the present paper the procedure worked out by J. BJERRUM (1941) for complexity constants has been adapted to dissociation constants; according to this method the constants are computed by successive approximation of the preliminary constants, according to the following formula:

$$(1) \quad K_n = [H^+]_{N-\left(n-\frac{1}{2}\right)} \cdot \frac{1+\sum_{t=1}^{t=n-1} \frac{(1+2t)\,[H^+]^t}{K_{n-1} \cdot K_{n-2} \cdots K_{n-t}}}{1+\sum_{t=1}^{t=N-n} \frac{(1+2t)\,K_{n+1} \cdot K_{n+2} \cdot \cdots \cdot K_{n+t}}{[H^+]^t}}$$

K_n is the n^{th} of the n consecutive dissociation constants. N is the total number of dissociation constants = 12, and t is a parameter which must take all integer values between the fixed limits. The terms dealing with one or more of the four unknown preliminary dissociation constants have been disregarded. The following two sets of dissociation constants were determined after three successive approximations according to the above formula (K_5 has not been corrected, as the correction would be unilateral):

	$-\log K_5$	$-\log K_6$	$-\log K_7$	$-\log K_8$	$-\log K_9$	$-\log K_{10}$	$-\log K_{11}$	$-\log K_{12}$
In 1.0 M NaCl...	1.75	2.68	4.59	5.71	7.34	8.19	8.78	8.95
In 0.2 M NaCl...	2.20	3.24	5.15	6.39	7.96	8.82	9.61	9.83

In order to calculate the solubility product of pentacalcium phytate it is neccessary to know the concentration of the phytate ion with ten negative charges. The total phytate concentration may be determined analytically, and the ratio (phytate ion with ten charges)/(total phytate concentration) may be calculated from the dissociation constants.

$[Py_0]$ represents the concentration of non-dissociated phytic acid, and $[Py_n]$ the concentration of phytate ions with n negative charges.

$$[Py_t] = [Py_0] + [Py_1] + \cdots\cdots [Py_{12}]$$

from the dissociation equations we have:

$$[Py_n] = K_1 \cdot K_2 \cdots\cdots K_n \cdot \frac{1}{[H^+]^n} \cdot [Py_0],$$

and from this:

$$(2) \qquad \frac{[Py_{10}]}{[Py_t]} = \frac{K_1 \cdot K_2 \cdots\cdots K_{10} \cdot \frac{1}{[H^+]^{10}} \cdot [Py_0]}{[Py_0] + K_1 \cdot \frac{1}{[H^+]} \cdot [Py_0] + \cdots + K_1 \cdot K_2 \cdots K_{12} \cdot \frac{1}{[H^+]^{12}} \cdot [Py_0]}.$$

If we put $K_1 = K_2 = K_3 = K_4 = K_5$, a simple substitution of the values determined for $K_5 \cdots\cdots K_{12}$ shows that if only $-\log[H^+]$ is larger than 4, the four first constants, which we have not been able to determine, may be disregarded. In this special case the formula may therefore be written

$$(3) \qquad \frac{[Py_{10}]}{[Py_t]} = \frac{K_5 \cdot K_6 \cdot K_7 \cdot \cdots\cdots K_{10} \cdot \frac{1}{[H^+]^{10}}}{\frac{1}{[H^+]^4} + \frac{K_5}{[H^+]^5} + \frac{K_5 \cdot K_6}{[H^+]^6} + \cdots + \frac{K_5 \cdot K_6 \cdots K_{12}}{[H^+]^{12}}}.$$

Corresponding to the values of $-\log[H^+]$, at which the solubility of pentacalcium phytate has been determined experimentally, Py_{10}/Py_t has been calculated by this formula. The results have been given in Tables 8 and 9.

3. The Solubility of Pentacalcium Phytate in 0.2 and 1.0 M Sodium Chloride.

The calcium phytate used for solubility determinations was prepared as described on p. 5; precipitation took place at p_H 5, and the salt was dried at room temperature. Before analysis the preparation was dried in vacuo over P_2O_5 at 105° C. The water content after drying in this manner was determined by further drying at 200° C. in vacuo over P_2O_5.

	C	H	P	Ca	H_2O	Ash	P/Ca
Found per cent.	8.08	1.78	20.68	22.06	6.14	71.3	1.210
Calculated for $C_6H_8O_{24}P_6Ca_5$, $3\,H_2O$ per cent.	7.97	1.55	20.58	22.12	5.87	—	1.200

5 or 25 ml. 4.0 M sodium chloride were measured into a 100 ml. volumetric flask and a suitable quantity of 0.1 M HCl or NaOH was added; the flask was filled to the mark with CO_2-free water. About 1 grm. calcium phytate was added and the flask was rotated for about 24 hours at 37° C. ± 0.1° C. Before samples were taken, the flask was left to stand in the thermostat for about one hour in order to let the precipitate set. The desired quantity of the clear supernatant fluid was sucked off through a filterstick G 3.

Analytical Methods.

Calcium was determined by the methods of LARSON and GREENBERG (1938) as oxalate by oxidation with ceri sulphate and titration with ferrous ammonium sulphate, using ferroin as indicator. This method is more accurate than the usual titration with potassium permanganate. 10 determinations of 1 mg. calcium show a standard deviation of 0.8 per cent.

Phosphorus was determined according to WIDMARK and WAHLQUIST (1931). The organic matter is ashed with sulphuric acid and nitric acid and the phosphorus precipitated as ammonium phosphorus molybdate, which is titrated with sodium hydroxide. 10 determinations of 0.5 mg. phosphorus show a standard deviation of 1.2 per cent.

The hydrogen ion concentration was determined with the glass electrode. 0.01 M HCl in 0.2 or 1.0 M sodium chloride was used as standard solution ($-\log[H^+] = 2.00$).

The Solubility is Independent of the Quantity of Solid Calcium Phytate Present.

a. A suspension of 0.2 grm. calcium phytate in 100 ml. 1.0 M NaCl, containing 1.5 ml. 0.1 N HCl.

b. A suspension of 2.0 grm. calcium phytate in 100 ml. of the same solution.

The following values were found after rotation at 37° C. for 24 hours:

	a	b
$-\log [H^+]$	5.37	5.38
C_{Ca} mM per l.	5.98	6.02

Connection between Solubility and Temperature.

Fig. 4 shows that the solubility of calcium phytate decreases rapidly as the temperature increases.

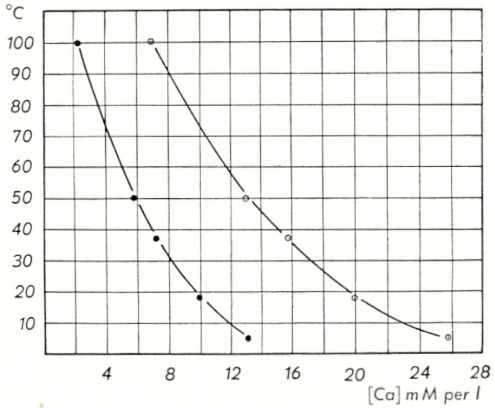

Fig. 4. The solubility of calcium phytate at various temperatures.
○——○ In 1 M NaCl
●——● In 0.2 M NaCl

Reversibility of Solubility.

The solubility of calcium phytate was determined in the following solutions:

a. 0.2 M sodium acetate, 0.15 M acetic acid.

b. 0.2 M sodium acetate, 0.15 M acetic acid, 0.8 M sodium chloride.

The solubility was first determined at 37° C.; the temperature was then lowered to 18° C., and the solubility determined at this temperature. The temperature was again raised to 37° C., so that the equilibrium now was approached from the supersaturated side. The following results show that the same values of solubility were reached from the supersaturated as from the undersaturated side:

	a	b
C_{Ca} mM per l., 37° C.	7.22	15.80
— 18° C.	9.85	20.00
— 37° C.	7.27	15.75

Connection between Solubility and Hydrogen Ion Concentration.

Table 6.
The Solubility of Pentacalcium Phytate in 1.0 M NaCl at 37° C.

$-\log [H^+]$	C_{Ca} m M per l.	C_P m M per l.	P/Ca Mol
4.20	37.8	—	—
4.52	22.5	25.8	1.15
4.74	15.05	—	—
5.02	9.05	10.70	1.18
5.40	5.85	—	—
5.89	3.47	4.12	1.19
6.30	2.48	—	—
6.62	1.86	2.18	1.17
7.03	1.18	1.48	1.25
7.64	0.685	—	—

The tables show that in the interval $5 < -\log [H^+] < 7$ the ratio P/Ca is the same in the solution as in the salt.

Tab e 7.
The Solubility of Pentacalcium Phytate in 0.2 M NaCl at 37° C.

$-\log [H^+]$	C_{Ca} m M per l.	P_P m M per l.	P/Ca Mol
4.15	28.9	30.0	1.04
4.57	14.25	—	—
4.81	8.25	—	—
5.03	5.45	6.32	1.16
5.44	3.10	—	—
5.87	1.65	2.02	1.22
6.24	1.03	—	—
6.70	0.595	0.693	1.17
7.05	0.320	—	—
7.43	0.185	—	—

Calculation of the Solubility Product of Pentacalcium Phytate in 0.2 M and 1.0 M NaCl.

The solubility product $[Ca]^5 \cdot [Py_{10}] = L$ has been calculated as follows: [Ca] was taken from Tables 6 and 7; $[Py_{10}]/[Py_t]$

was calculated from the formula (3); $[Py_t]$ was calculated from: $5 \cdot [Py_t] = [Ca]$.

Table 8.
Calculation of the Solubility Product of Pentacalcium Phytate in 1 M NaCl at 37° C.

$-\log [H^+]$	4.20	4.52	4.74	5.02	5.40	5.89	6.30	6.62	7.03	7.64
$-\log \frac{[Py_{10}]}{[Py_t]}$	9.216	8.059	7.283	6.379	5.256	3.987	3.127	2.409	1.663	0.807
$-\log [Ca]$	1.423	1.648	1.823	2.043	2.233	2.460	2.606	2.731	2.928	3.164
$-\log [Py_t]$	2.122	2.347	2.522	2.742	2.932	3.159	3.305	3.430	3.627	3.863
$-\log [Py_{10}]$	11.338	10.406	9.805	9.121	8.188	7.146	6.432	5.839	5.290	4.670
$-\log L$	18.453	18.646	18.920	**19.336**	**19.353**	**19.446**	**19.462**	**19.494**	19.930	20.490

The table shows that the solubility product in 1.0 M NaCl is almost constant in the interval $5.02 < -\log [H^+] < 6.62$. In this interval the average of our five determinations was:

$$-\log L = 19.4 \text{ (1.0 M NaCl)}$$

The solubility product has been determined in the same manner in 0.2 M NaCl.

The calculations have been entered in Table 9.

Table 9.
Calculation of the Solubility Product of Pentacalcium Phytate in 0.2 M NaCl at 37° C.

$-\log [H^+]$	4.15	4.57	4.81	5.03	5.44	5.87	6.24	6.70	7.05	7.43
$-\log \frac{[Py_{10}]}{[Py_t]}$	11.797	10.152	9.245	8.448	7.057	5.724	4.697	3.563	2.800	2.056
$-\log [Ca]$	1.539	1.846	2.084	2.264	2.509	2.783	2.987	3.226	3.495	3.733
$-\log [Py_{10}]$	2.238	2.545	2.783	2.963	3.208	3.482	3.686	3.925	4.194	4.432
$-\log [Py_t]$	14.035	12.697	12.028	11.411	10.265	9.206	8.383	7.488	6.994	6.488
$-\log L$	21.730	21.927	22.448	**22.731**	**22.810**	**23.121**	**23.318**	**23.618**	24.469	25.153

The values of $-\log L$ are not quite so constant as in 1.0 M NaCl. In the interval $5.03 < -\log [H^+] < 6.70$ the average of five determinations was:

$$-\log L = 23.0 \text{ (0.2 M NaCl)}.$$

4. Formation of Calcium Phytate Complex Ions.

The experiments described on p. 5 show that solutions of calcium phytate are considerably more acid than the corresponding solutions of sodium phytate. Similar relations are found in solutions of calcium phosphate and are explained by a pronounced acidity of the calcium complexes formed (N. Bjerrum et al. (1936)). They state that in solutions of calcium phosphates the complex formation is usually less than 10 per cent. The experiments described above, however, render it likely that in solutions of calcium phytate a considerably larger part of the dissolved calcium is found as a calcium phytate complex ion. Like precipitated calcium, complex bound calcium is probably not absorbed at all from the intestine, and we have therefore tried to determine the degree of complexity in solutions of calcium phytate.

In order to examine this, solutions with varying contents of calcium and phytate were rotated with solid calcium iodate (Kilde (1934)). From the solubility product of calcium iodate: $[Ca^{++}] \cdot [JO_3^-]^2 = K$, the concentration of calcium ions may be calculated from the iodate concentration. The total quantity of dissolved calcium was determined in the usual manner. The fact that the solubility of calcium iodate is fairly large as compared with that of calcium phytate presents a difficulty, as it is necessary to avoid precipitation of calcium phytate. The experiments therefore can only be carried out within a fairly limited interval of the concentrations of hydrogen ions, phytate and calcium ions. Contrary to calcium iodate, calcium phytate has its greatest solubility at low temperatures. The principal experiments therefore have been made at 18° C., instead of at 37° C.

Table 10 gives the results of the complexity determinations made at 18° C., $p_H = 4.3$ and μ about 0.2. The solubility product of the calcium iodate has been calculated from the average of the iodate analyses in the last two experiments. The calcium ion concentration has been calculated from the equation: $[Ca^{++}] = \frac{K}{[JO_3^-]^2}$.

Table 11 gives the results of a similar series of experiments at μ about 1.

Table 10.

Solution A: 0.02 M sodium phytate, 0.12 M HCl.

Solution B: 0.05 M calcium nitrate, 0.07 M sodium acetate, 0.14 M acetic acid.

Solution C: 0.1 M sodium acetate, 0.12 M sodium chloride, 0.2 M acetic acid.

18° C; p_H 4.3.

$[Ca^{++}] \cdot [JO_3^-]^2 = K = 3.00 \cdot 10^{-6}$ ($\mu = 0.247$)

ml. A	ml. B	ml. C	$C_{phytate}$ m M per l.	$C_{Ca_{total}}$ m M per l.	$C_{JO_3^-}$ m M per l.	C_{Ca++} m M per l.	$C_{Ca_{complex}}$ m M per l.	$\frac{C_{Ca_{complex}}}{C_{phytate}}$
50	0	0	20.00	12.78	30.90	3.14	9.64	0.48
25	10	0	14.28	22.05	19.45	7.93	14.12	0.97
25	25	0	10.00	29.77	13.67	16.06	13.71	1.37
10	25	0	5.71	39.80	9.93	30.41	9.39	1.65
10	40	0	4.00	43.75	9.05	36.62	7.13	1.78
5	45	0	2.00	48.55	8.18	44.80	3.75	1.88
0	0	50	0	9.20	18.16	(9.08)	—	—
0	0	50	0	9.25	18.20	(9.10)	—	—

In order to examine the connection between complex formation and p_H, a short series of experiments was made at $p_H = 5$

Table 11.

Solution A, B, and C as in Table 10, but with 0.78 M NaCl added pr l.

18° C; $p_H = 4.3$.

$[Ca^{++}] \cdot [JO_3^-]^2 = K = 10.2 \cdot 10^{-6}$ ($\mu = 1.041$)

ml. A	ml. B	ml. C	$C_{phytate}$ m M per l.	$C_{Ca_{total}}$ m M per l.	$C_{JO_3^-}$ m M per l.	C_{Ca++} m M per l.	$C_{Ca_{complex}}$ m M per l.	$\frac{C_{Ca_{complex}}}{C_{phytate}}$
50	0	0	20.00	14.40	33.30	9.19	5.21	0.26
20	10	0	13.33	26.60	23.20	18.95	7.65	0.57
15	15	0	10.00	33.58	19.75	26.22	7.36	0.74
10	20	0	6.67	41.75	17.02	35.18	6.57	0.99
5	20	0	4.00	48.50	15.20	44.12	4.38	1.09
3	20	0	2.61	52.30	14.40	49.15	3.15	1.20
0	0	50	0	13.80	27.30	(13.65)	—	—
0	0	50	0	13.85	27.40	(13.70)	—	—

and μ about 0.2. On account of the solubilities of the salt in question the investigation cannot be made at higher p_H.

Table 12.

Solution A: 0.02 M sodium phytate, 0.01 M HCl, 0.01 M NaCl.

Solution B: 0.05 M calcium nitrate, 0.07 M sodium acetate, 0.35 M acetic acid.

Solution C: 0.10 M sodium acetate, 0.12 M sodium chloride, 0.2 M acetic acid.

18° C; $p_H = 5.0$

$[Ca^{++}] \cdot [JO_3^-]^2 = K = 3.08 \cdot 10^{-6}$ ($\mu = 0.248$)

ml. A	ml. B	ml. C	$C_{phytate}$ m M per l.	$C_{Ca_{total}}$ m M per l.	$C_{JO_3^-}$ m M per l.	$C_{Ca^{++}}$ m M per l.	$C_{Ca_{complex}}$ m M per l.	$\frac{C_{Ca_{complex}}}{C_{phytate}}$
10	0	40	4.0	11.03	22.55	6.06	4.97	1.24
10	10	30	4.0	17.35	16.74	11.00	6.35	1.59
5	10	35	2.0	17.05	15.08	13.55	3.50	1.75
0	0	50	0	9.25	18.36	(9.18)	—	—

In order to find the connection between complex formation and temperature, experiments were also made at 30° C. At temperatures higher than 32° C. calcium iodate is decomposed.

Table 13.

Solution A, B and C as in Table 12.

30°C. $p_H = 4.3$.

$[Ca^{++}] \cdot [JO_3^-]^2 = K = 11.6 \cdot 10^{-6}$ ($\mu = 0.263$)

ml. A	ml. C	ml. C	$C_{phytate}$ m M per l.	$C_{Ca_{total}}$ m M per l.	$C_{JO_3^-}$ m M per l.	$C_{Ca^{++}}$ m M per l.	$C_{Ca_{complex}}$ m M per l.	$\frac{C_{Ca_{complex}}}{C_{phytate}}$
20	0	10	13.33	19.16	40.08	7.21	11.95	0.90
10	10	10	6.67	28.50	25.05	18.49	10.01	1.51
10	15	10	5.71	33.00	21.78	24.25	8.80	1.54
0	0	30	0	14.05	28.50	(14.25)	—	—

In Fig. 5 a graph has been plotted, showing the connection between $\bar{n} = \frac{C_{Ca_{complex}}}{C_{phytate}}$ and $-\log [Ca^{++}]$. The graph shows how many calcium atoms are on an average bound in the

Table 14.

Solution A, B and C as in Table 11.

30° C; $p_H = 4.3$.

$[Ca^{++}] \cdot [JO_3^-]^2 = K = 38.7 \cdot 10^{-6}$ ($\mu = 1.064$)

ml. A	ml. B	ml. C	$C_{phytate}$ m M per l.	$C_{Ca_{total}}$ m M per l.	$C_{JO_3^-}$ m M per l.	C_{Ca++} m M per l.	$C_{Ca_{complex}}$ m M per l.	$\frac{C_{Ca_{complex}}}{C_{phytate}}$
20	0	0	20	25.50	50.79	15.02	10.48	0.52
10	5	15	6.67	28.42	40.55	23.55	4.97	0.74
10	15	5	6.67	41.10	33.35	34.78	6.32	0.95
0	0	30	0	21.35	42.60	(21.30)	—	—

calcium phytate complex ion at a certain concentration of calcium ions.

Fig. 5 shows that the degree of complexity changes only slightly with variation in temperature; on the other hand it decreases with increasing ionic strength and increases with in-

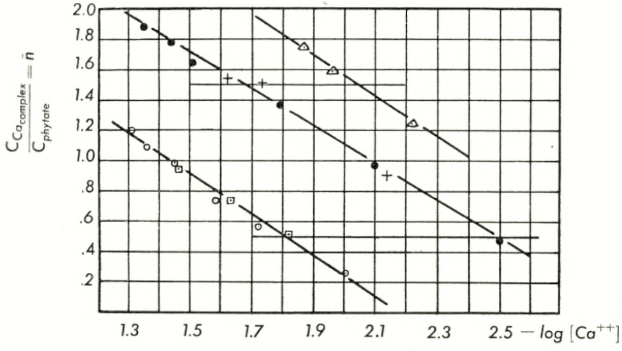

Fig. 5. Formation curves for calcium phytate complex ion.

● ——— ● 18° C. $p_H = 4.3$, μ about 0.2
○ ——— ○ 18° C. $p_H = 4.3$, - - 1
△ ——— △ 18° C. $p_H = 5.0$, - - 0.2
\+ ——— \+ 30° C. $p_H = 4.3$, - - 0.2
□ ——— □ 30° C. $p_H = 4.3$, - - 1

creasing p_H. This explains that the calculated solubility product (Tables 6 and 7) decreases as p_H increases.

Proceeding as we did for the dissociation constants (see Fig. 3) we may derive approximate values for the first two complexity constants, K_1 and K_2, from the values of $-\log [Ca^{++}]$, which correspond to $\bar{n} = 0.5$ and $\bar{n} = 1.5$;

	$-\log K_1$	$-\log K_2$
$p_H = 4.3$, μ about 0.2	2.50	1.67
$p_H = 4.3$, μ - 1	1.83	—
$p_H = 5.0$, μ - 0.2	—	2.04

From the results in Table 11 it can be calculated that in saturated solutions of calcium phytate, at p_H about 5 and μ about 3, approximately 0.20 per cent. of the dissolved calcium will be complex bound.

5. Comparative Investigations on the Solubility of Calcium Phytate and Some Calcium Phosphates.

In the p_H-interval which is most important as far as precipitation of calcium in the intestine is concerned, hydroxyl apatite, $Ca_5(PO_4)_3OH$, is the least soluble of the calcium phosphates. BJERRUM et al. (*l. c.*) have determined the solubility of hydroxyl apatite in much diluted salt solutions; their investigations thus are not exactly comparable with the measurements of the solubility of calcium phytate described above. The author therefore has determined the solubility of hydroxyl apatite in 0.2 M sodium chloride solutions in the same manner as described for calcium phytate, the hydroxyl apatite being precipitated *ad modum* BJERRUM et al. (*l. c.*). The solubility of secondary calcium phosphate, $CaHPO_4$, $2\,H_2O$, has also been measured in 0.2 M NaCl. The results of these measurements are shown in Fig. 6.

Fig. 6 shows that when equilibrium is approached from the under-saturated side, the calcium concentration in the saturated solution of hydroxyl apatite is slightly below the calcium concentration in the saturated solution of calcium phytate. Thus, if the calcium phosphate is precipitated in the intestine as hydroxyl apatite, there seems to be no reason to assume that calcium absorption should be more impaired by the presence of phytic acid in the food than by the presence of phosphate.

This mode of reasoning, however, does not consider the fact that when the acid contents of the stomach enter the intestine the solubility equilibrium is approached from the supersaturated side. In order to examine whether this is of any importance the following experiments were made:

a. A solution of hydroxyl apatite was made by rotating solid hydroxyl apatite in a solution which was 0.2 M in NaCl and 0.07 M in HCl; quantities of this solution sufficient to dissolve all the hydroxyl apatite were used. The solution obtained was 0.067 M in Ca and $p_H = 3.5$.

b. A solution of calcium phytate was made in the same manner; it was 0.074 M in Ca and $p_H = 3.4$.

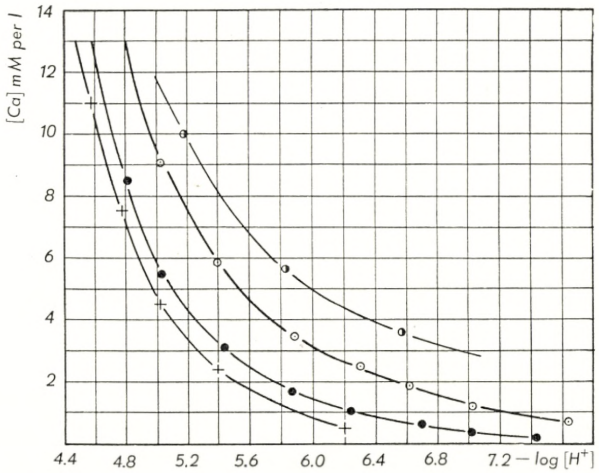

Fig. 6. Solubility of calcium phytate, hydroxyl apatite, and secondary calcium phosphate.

⊙——⊙ Calcium phytate in 1 M NaCl
●——● Calcium phytate in 0.2 M NaCl
+——+ Hydroxyl apatite in 0.2 M NaCl
◑——◑ Secondary calcium phosphate in 02 M NaCl.

Each of these solutions was mixed at a temperature of 37° C. with equal parts of a solution which was 0.2 M in sodium acetate and 0.02 M in acetic acid. Two 100 ml. samples were taken from each of these mixtures, making four samples in all. 1 grm. hydroxyl apatite was added to one of the hydroxyl apatite samples, and 1 grm. calcium phytate to one of the phytate samples. All four samples were rotated at 37° C. In each experiment the quantities of calcium dissolved at different points of time were determined. The results have been plotted in Fig. 7.

Fig. 7 shows that whether a supersaturated solution of calcium phytate contains solid calcium phytate or not, the equilibrium is reached instantly. In the solution of hydroxyl apatite,

calcium is precipitated slowly when solid hydroxyl apatite is present. The solution of hydroxyl apatite, which did not contain solid hydroxyl apatite, did not show turbidity until about

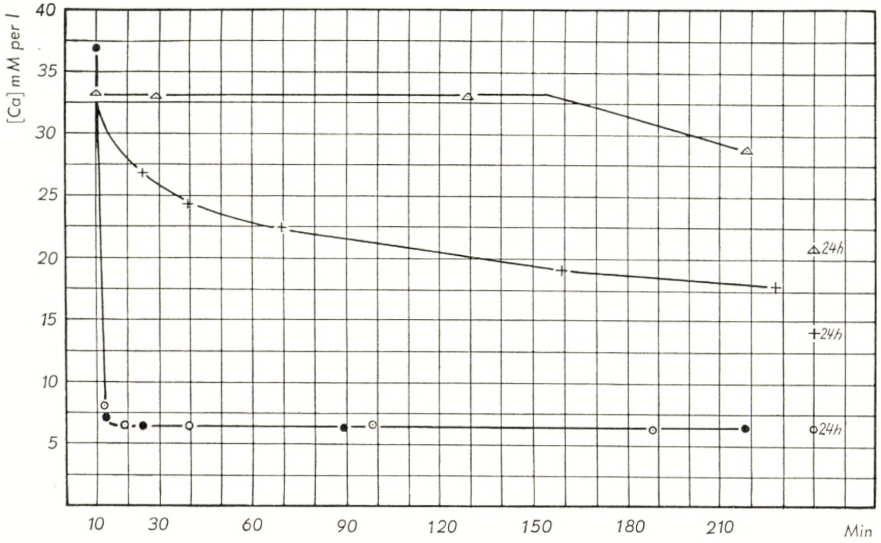

Fig. 7. Precipitation of calcium in solutions of calcium phytate and hydroxyl apatite.

⊙——⊙ Calcium phytate at p_H 5.08
●——● - - with solid calcium phytate at p_H 5.04
△——△ Hydroxyl apatite at p_H 5.28
+——+ - - with solid hydroxyl apatite at p_H 5.20.

two hours had passed. After 24 hours the sediment was clearly crystalline. The X-ray powder diagram (A. Tovborg Jensen) together with the analyses given below showed that the sediment was secondary calcium phosphate.

	Ca	P	Loss at 600° C.
Found per cent.....	23.32	18.25	26.15
Calculated for $CaHPO_4$, $2H_2O$, per cent....	23.50	18.12	26.15

In a series of experiments with varying contents of calcium and phosphate in diluted acid solutions, which were brought to a p_H about 5 at 37° C., the precipitate formed likewise consisted of crystalline secondary calcium phosphate.

These experiments seem to indicate that when the acid stomach contents containing calcium and phosphate are emptied

into the intestine, a precipitate of secondary calcium phosphate will form. The precipitation, however, is slow. According to the present investigations it therefore seems probable that the presence of phytic acid in the food reduces the concentration of calcium ions in the intestine considerably. This is due to the fact that calcium phytate is only slightly soluble, and particularly to the fact that calcium phytate is not liable to form supersaturated solutions. It is moreover of importance that a considerable part of the dissolved calcium will be complex bound in the presence of phytic acid.

Summary.

(1) In solutions of phytic acid and calcium ions, amorphous pentacalcium phytate precipitates in the p_H-interval $5 < p_H < 7$.

(2) Eight of the dissociation constants of phytic acid have been determined in 0.2 and 1.0 M NaCl.

(3) The solubility of pentacalcium phytate has been determined at various hydrogen ion concentrations in 0.2 and 1.0 M NaCl, respectively.

(4) The solubility product of pentacalcium phytate (complex formation having been disregarded) was calculated to be $10^{-19.4}$ in 1.0 M NaCl and $10^{-23.0}$ in 0.2 M NaCl in the interval $5 < -\log H^+ < 6.6$.

(5) The formation of calcium phytate complex ions has been examined.

(6) The calcium phosphate precipitated in the intestine is probably $CaHPO_4$, $2\,H_2O$.

(7) Pentacalcium phytate is less soluble than secondary calcium phosphate. The former salt is precipitated instantly, whilst the latter precipitates slowly.

(8) Calcium absorption is more likely to be impaired when the food contains large quantities of phytic acids than when it contains a surplus of phosphate. The present investigations thus support the theory of HARRISON and MELLANBY (*l. c.*).

The author wishes to express his thanks to Professor Dr. N. BJERRUM and Dr. J. BJERRUM for valuable discussions on the subject of this paper, and to Teknisk Kemisk Fond for a grant.

From the Biochemical Institute of the University of Copenhagen, Denmark.

Bibliography.

BJERRUM, J. (1941): Metal Ammine Formation in Aqueous Solution. Diss. Copenhagen.

BJERRUM, N. et al. (1936): Undersøgelser over Kalciumfosfaters Opløselighed. 19th. „Skandinaviske Naturforskermøde" in Helsingfors (see the proceedings, p. 308.

BJERRUM, N. and A. UNMACK (1929): Det Kgl. Danske Videnskabernes Selskab, Mat.-fys. Meddelelser IX, **1**.

BRUCE and CALLOW (1934): Biochem. J. **28**, 517.

HARRISON and MELLANBY (1939): Biochem. J. **33**. 1660.

KILDE (1934): Z. für anorg. a. allgem. C. **218**, 113.

LARSON and GREENBERG (1938): J. biol. Chem. **123**, 199.

MELLANBY (1920): Lancet **1**, 1290.

PEDERSEN, J. G. A. (1940): Experimentel Rakitis hos Svin. 193. Beretning fra Landøkonomisk Forsøgslaboratorium. København.

PEDERSEN, K. J. (1936): J. Amr. Chem. Soc. **58**, 240.

POSTERNAK (1921): Helv. Chim. Acta **4**, 150.

STARKENSTEIN (1910): Biochem. Z. **30**, 56.

WASHBURN and SHEAR (1932): J. biol. Chem. **99**, 21.

WIDMARK and WAHLQUIST (1931): Biochem. Z. **330**, 246.

Indleveret til Selskabet den 6. Marts 1944.
Færdig fra Trykkeriet den 11. August 1944.

DET KGL. DANSKE VIDENSKABERNES SELSKAB
MATEMATISK-FYSISKE MEDDELELSER, BIND XXI, Nr. 8

A HIGH INTENSITY MASS-SPECTROGRAPH FOR EXPERIMENTS ON THE SEPARATION OF ISOTOPES

BY

JØRGEN KOCH AND BØRGE BENDT-NIELSEN

KØBENHAVN
I KOMMISSION HOS EJNAR MUNKSGAARD
1944

Printed in Denmark.
Bianco Lunos Bogtrykkeri A/S

Introduction.

In recent years a great number of different methods for the separation of isotopes has been developed. This technique has assumed increasing importance, the entirely or partly separated isotopes being used more and more in experimental investigations in both nuclear physics, spectroscopy, and biology.

Among the different methods the mass-spectrographic separation of isotopes holds a special position, inasmuch as by this means it is possible to produce extremely pure samples, the quantities separated, however, being exceedingly small.[1]

Only very few elements, however, have been subjected to mass-spectrographic separation. In the first place the alkalis Li, K, and Rb must be mentioned (Na and Cs possess only one stable isotope each, cf. 5, 17, 18, 19, 20, 21, 22, 23, 27). This is due to the fact that for the production of alkali ions especially efficient ion sources are available, the ions evaporating at thermal energies from a hot equipotential surface (8, 11, 24). Next, using a low voltage arc of special design it has been possible to produce samples of the pure boron isotopes ^{10}B and ^{11}B and of the carbon isotope ^{12}C (27).[2]

For all these experiments special apparatus (high intensity mass-spectrographs) have been used which on many points differ materially from the well-known high precision mass-spec-

[1] In a treatise by J. KOCH, *Mass-Spectrographic Separation of Isotopes. With a Special View to the Production of Isotopes for Experimental Research*, these methods have been subjected to a critical survey in conjunction with experiments on the same subject. In the following this paper is referred to as (J. K.). See also reference (9) page 28.

[2] The experiments for the separation of the uranium isotopes must also be mentioned on account of their great importance for the study of the fission processes despite the fact that the mass-spectrographs used are capable of working only with currents considerably smaller than those used in the above-mentioned experiments (2, 6, 7, 15, 16).

trographs. For instance, ion-optical systems are used instead of narrow slits for the collimation of the ions.

As there was strong reason to assume that a limit for the methods of mass-spectrographic separation of isotopes was far from being reached, a number of experiments has in recent years been carried out at the Institute of Theoretical Physics (J. K.). More particularly experiments have been made on the application of the Lamar, Samson, and Compton ion source (12), which in advance must be considered especially suitable for this purpose. It was found that by means of this ion source

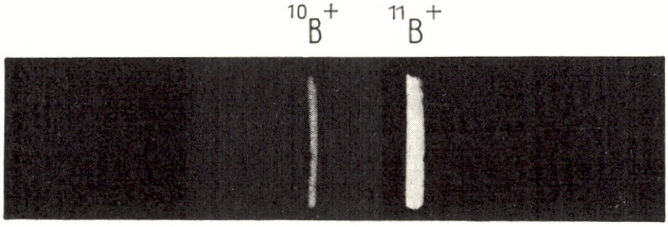

Fig. 1. Mass-spectrum of boron.

and a suitable system of electrostatic lenses using high voltages, it was possible to produce ion beams of exceptional homogeneity. A mass-spectrographic analysis of the ion beam undertaken preliminarily with a magnet of small resolving power ($\Delta m/m \approx 1/50$) further proved that by adding to the ion source various gases or vapours of chemical compounds it was possible to produce large quantities of atomic ions. By adding borontrifluoride it was thus possible to produce intensive beams of atomic boron ions. A specimen mass-spectrum is shown in Fig. 1. In this case boron ions with an energy of 43 kev impinge on a fluorescent screen and the light emitted is photographed from the opposite side. It further proved that C^+-ions might be produced from CO_2, CCl_4 and CS_2. The last-mentioned compound was used also for the production of S^+-ions. Ions of chlorine were produced from both CCl_4 and $TiCl_4$. By adding bromium vapour mixed with a small quantity of argon, ions of atomic bromium were produced. The atomic ion currents, measured by means of a Faraday cylinder which did not allow secondary electrons to escape, ranged between 1 and 10 μa.

With a view to continued experiments a large electromagnet has now been erected in the Institute, whereby the resolving power of the mass-spectrograph has been increased to more than 1:238, according to the acceleration voltage and the ion current used. By this construction a basis has been created for further experiments on the effective separation of isotopes, it being now possible to extend the experiments to even the heaviest elements. Experiments on the collection of separated isotopes have already been commenced.

The method developed for the production of beams containing a given species of ions with practically the same energy ($\Delta E/E < 3.5 \cdot 10^{-6}$) must further be considered especially suitable for a study of the interaction between ions and other atomic particles for primary energies from about 20 kev and upwards. In view of this versatility the following description of the mass-spectrograph may already at this stage be of interest.

The Resolving Power of a Homogeneous Magnetic Field.

The acceleration- and lens-system for the formation of the ion beam was developed empirically. In the planning of the construction of the magnet the following considerations of the course of the ion paths in a homogeneous magnetic field were used, the data of the ion beam (diameter d, energy spread ΔE, and the maximum angle α of the ion paths with the axis of the beam) being known approximately.

The ion beam is deflected 90° in the analyzing system of the mass-spectrograph. In what follows the resolving effect of the magnetic field will be calculated and a survey given of the main quantities determining the breadth of the lines (cf. 23 and (J. K.)). In this connection the effect of the magnetic stray field and space charges within the beam are left out of consideration. In order to make it easier to follow the course of the ions we may consider them emitted from a circular area of diameter d at the entrance to the magnetic field at any angle with the normal of the plane within the limit α and at energies within the interval $e\,(E \pm \frac{1}{2}\Delta E)$.

First, we shall consider the course of a beam of very small diameter ($d \to 0$) containing ions with absolutely parallel paths and

of mass M and energy eE, entering the magnetic field H at P (Fig. 2 a). The ions will move in a circle with centre O and radius $r = H^{-1}\sqrt{2EM/e}$. Ions of mass $(M+\Delta M)$ will move in a somewhat larger circle and at P' we shall have a mass-dispersion of

$$\Delta r = r\left(\sqrt{1+\frac{\Delta M}{M}}-1\right) \approx \frac{r}{2}\cdot\frac{\Delta M}{M};\ \Delta M \ll M. \qquad [1]$$

If we introduce the mass-number A, we have

$$\Delta r \approx \frac{r}{2}\cdot\frac{\Delta A}{A}. \qquad [2]$$

In Fig. 3 Δr is plotted as a function of the mass-number A for $\Delta A = 1, 2, 3$, and 4 for the mean radius of curvature of the ion beam of $r = 80$ cm. as used in the experiments.

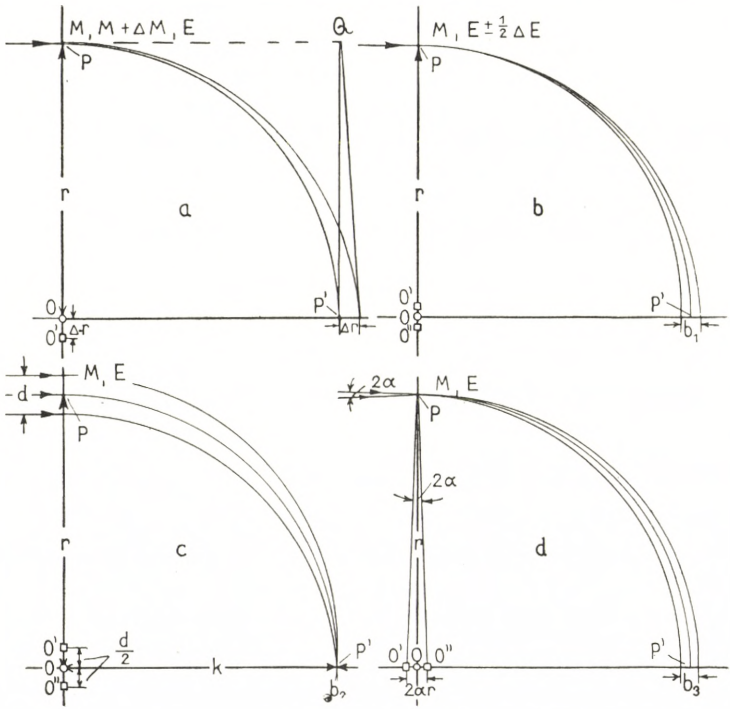

Fig. 2. Ion beams in a homogeneous magnetic field. Ions of mass M and energy eE moving on circles with radius r.

As appears from Fig. 2 a, the ions apparently emerge from a virtual source Q. If, therefore, we let the ions continue on

their paths outside the magnetic field, we shall obtain a mass-dispersion between the two beams increasing proportionally with

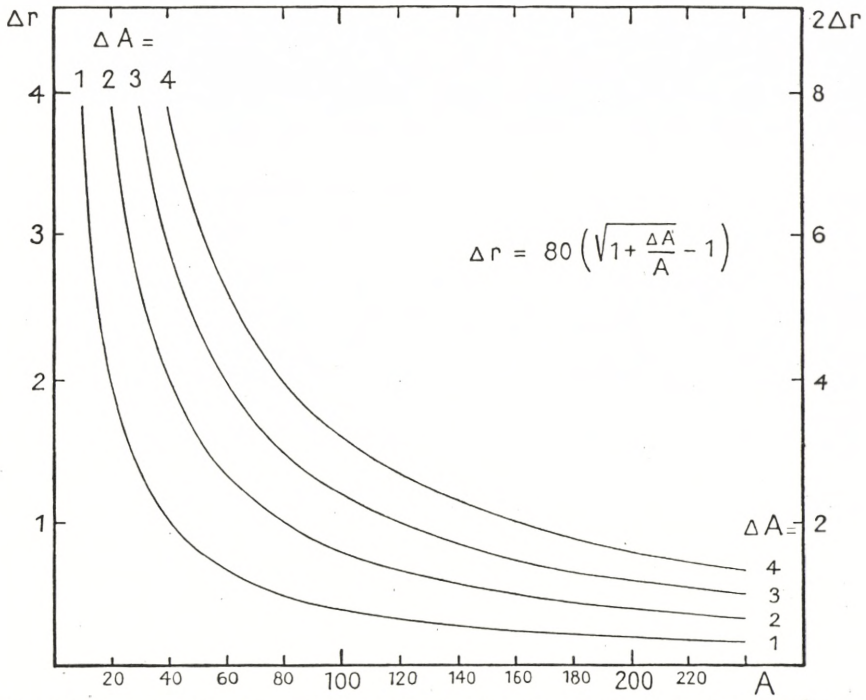

Fig. 3. The mass-dispersion Δr (in cm.) of an ion beam after deflection of 90° in a homogeneous magnetic field as a function of the mass-number A with ΔA as parameter (r = 80 cm.).

the distance from Q. In the present apparatus collecting cylinders and fluorescent screens are placed at a distance of $2r$ from Q and the mass-dispersion will thus be twice as large as at the exit from the magnetic field (cf. the ordinate on the right in Fig. 3).

As the most favourable place for collecting the ions depends on the ratio between the mass-dispersion and the breadth of the lines (the 'reduced mass-dispersion'), the course of the ions during the passage through the field must be further examined. The extent of the beam in the direction of the radius vector (r, Fig. 2) is called its breadth, the extent in the direction of the magnetic field force its height.

If the ions have an energy spread of $e\Delta E$ (Fig. 2 *b*), we shall consequently at P' have a breadth of the ion beam of

$$b_1 \approx \frac{r}{2} \cdot \frac{\Delta E}{E}; \quad \Delta E \ll E. \qquad [3]$$

(The ripple of the high voltage generator is considered small in relation to ΔE).

By means of Fig. 2*c* we shall now consider the course of an ion beam of diameter d. The ions are still assumed to have parallel paths at P ($\alpha \to 0$) and to have mass M and energy eE. At P' the beam is focussed as will be seen from the figure. The breadth of the beam at this place is

$$b_2 \approx \frac{d^2}{8r}; \quad \frac{d^2}{4r^2} \ll 1. \qquad [4]$$

Finally, we shall consider Fig. 2 *d*, showing ions being emitted from the point P at all angles within the limit α. The resultant breadth at P' is

$$b_3 \approx 2\alpha r; \quad \alpha \ll 1. \qquad [5]$$

In the direction of the magnetic field force the ions will not be affected, and the height of the beam at P' will therefore be $h = d + \pi\alpha r$.

We can now state the condition for ions of mass-numbers A and $(A + \Delta A)$ being separated at the exit from the magnetic field. The total breadth B of the lines must satisfy the condition

$$B = b_1 + b_2 + b_3 \leq \Delta r. \qquad [6]$$

According to these considerations the line breadth may be expected to increase when receding from P', which fact is especially apparent from Fig. 2. The question as to whether the reduced mass-dispersion will increase or decrease, however, may be settled only by consideration of an actual example in which the values b_1, b_2 and b_3 may be calculated. It will subsequently be shown that in the present experiments b_3 makes the largest contribution to the total breadth. In order to ascertain the exact course of the ion paths, regard must also be paid to the effect of the magnetic stray field. As already indicated especially favourable conditions were empirically found at the distance $2r$ from Q.

In the calculation of the line breadth the further simplification was made, that the effect of space charges on the course

of the ion beam could be disregarded. An exact calculation of their influence is not quite simple, partly because of the focussing properties of the magnetic field and partly because of the fact that the beam is split up into several parts.[1] Hitherto we thus have only made use of the following simple considerations, which are based on results of WATSON (26, see also (J. K.)), in

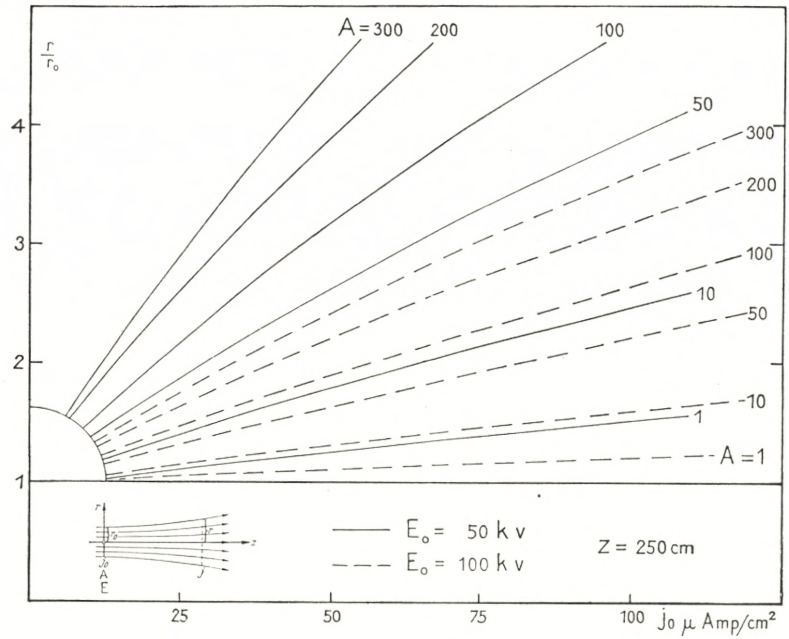

Fig. 4. Dispersion of ion beams on account of the mutual repulsion of the ions; $\left(\frac{r}{r_0}\right)$ as a function of j_0 for different values of A and E.

order to obtain a rough idea of the influence of space charges in the present experiments.

Let us consider a beam of parallel ions with the current density j_0 (cf. in what follows the drawing in the lower left corner of Fig. 4) passing at $z = 0$ through a circular aperture with radius r_0, moving thereafter into a field-free space. As a consequence of the mutual repulsion between the ions the beam will diverge and, having passed through a distance z, have

[1] Recently WALCHER (25) has investigated the influence of space charges on the focussing properties of a homogeneous field. These considerations must, however, be further extended in order to be utilised for the discussion of the present apparatus.

a somewhat greater radius r. Assuming that the ions have the same energy eE and mass-number A, we can calculate the divergence r/r_0 of the ion beam from the equation:

$$I\left(\frac{r}{r_0}\right) = 1.137 \cdot 10^{-2} \cdot \left(\frac{A \cdot j_0^2}{E^3}\right)^{1/4} \cdot z \approx \frac{r}{r_0}, \qquad [7]$$

when j_0 is given in $\mu a/\text{cm}^2$, E in kv and z in cm.[1]

In Fig. 4 r/r_0 is plotted as a function of the current density j_0 within the interval of special interest with A and E as parameters. The value of z used corresponds to the distance passed by the ion beam in the mass-spectrograph later described from the centre of the electrostatic lens until it hits the fluorescent screen. If the current density is e. g. $j_0 = 50\,\mu a$ at an acceleration voltage of $E = 50$ kv, as generally used in the experiments, we may expect a considerable divergence of the ion beam in the case of heavy ions. Notwithstanding that a higher acceleration voltage of e. g. 100 kv will reduce the space charge effect somewhat, there can be no doubt that this effect will impose a practical limit on the mass-spectrographic separation of isotopes even if it might be possible to construct ion sources with higher yields of atomic ions than known hitherto.

In order to make it possible to work later on with higher voltages than 50 kv (the preliminary operating voltage of the electrostatic lens) at which space charge effects are reduced, the magnet of the mass-spectrograph was dimensioned so as to deflect uranium ions of an energy as high as 80 kev; for lighter ions the energy used may be correspondingly higher.

Design of the Mass-Spectrograph.

The mass-spectrograph is shown in cross-section in Fig. 5. The ion source and the lens system are placed on top of a casing with openings to the high vacuum pumps and mounted on the massive magnet. By means of a strong electric field the

[1] In the interval $1.3 < I < 5$ we have $I \approx r/r_0$ with an accuracy of less than 10 per cent. The correct expression on which the curves in Fig. 4 are based, is

$$I\left(\frac{r}{r_0}\right) = \int_1^{\frac{r}{r_0}} \frac{d\left(\frac{r}{r_0}\right)}{\sqrt{ln\left(\frac{r}{r_0}\right)}}. \qquad [8]$$

ions are drawn from the plasma of the arc, and by passing through the tubular lens consisting of three cylinders a beam of ions with almost parallel paths is formed. When the ions have passed through the casing they enter the magnetic field, where they are deflected 90°. Finally, the beam proceeds some way outside the magnet until the ions hit the collecting cylinders or the fluorescent screen.

The ion source is a low voltage arc built on the Lamar, Samson, and Compton principle (9, 12, 14).[1] The length and diameter of the capillary are 10 mm. and 4 mm., respectively, and the aperture in the side of the capillary through which the ions are emitted has a diameter of ab. 1 mm. The anode and the cathode holders, which carry an 0.7 mm. tungsten filament, are water-cooled. The gas supply from two glass containers is regulated by means of two valves provided with vacuum-tight bellows. The gas pressure in the ion source must be $0.6 \cdot 10^{-2}$ — $6 \cdot 10^{-2}$ mm. Hg. The arc current as a rule was less than 1 ampere at an arc voltage of 50—60 volts. The energy for operating the ion source which is connected with the high voltage generator is delivered from a belt-driven power stack and from a cathode current transformer insulated for 60 kv.

The electrostatic lens consists of three brass cylinders. According to earlier experiments sufficiently good conditions could be obtained with a fairly simple arrangement (10). In order to obviate aberrations of the lens, the diameter of the cylinders was made a great deal larger than that of the ion beam. The cylinders D_1 and D_3 are earthed, whereas the middle one has a "lens-potential" of about two-thirds of the acceleration potential (retardation lens).

The lens potential is derived from a high voltage potentiometer of 67 $M\Omega$ (Siemens resistances type 4 a) immersed in oil. By interposing a further, variable resistance of up to 20 $M\Omega$ on the earthed side of the potentiometer a precision adjustment of the lens-potential for focussing the ion beam may be obtained. The different parts of the lens were aligned by rule of thumb, no later changes being possible, whereas an adjustment of the ion source in relation to the lens might be made during the

[1] The ion source has been constructed by J. M. Lyshede, M. Sc., of the Physical Institute of the University of Aarhus, and has kindly been put at our disposal.

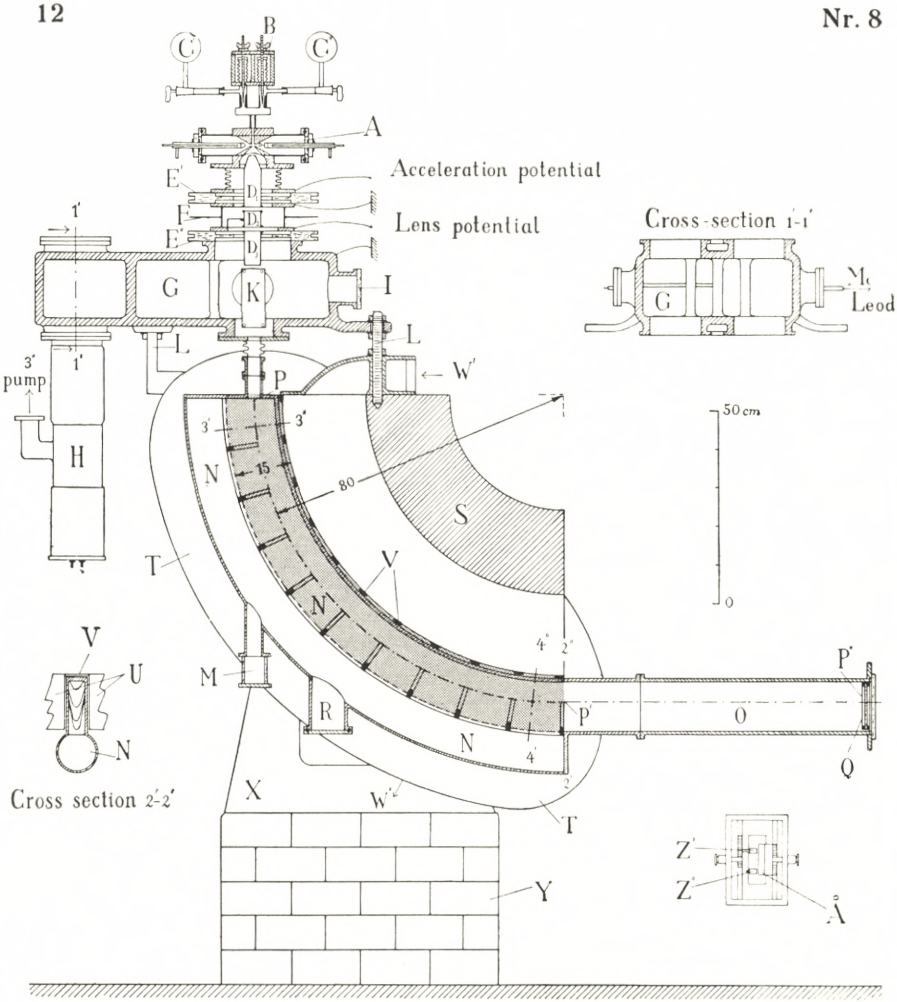

Fig. 5. Drawing of the mass-spectrograph. *A*: ion source. *B*: valves for control of gas from the containers *C'*, *C''*. D_1, D_2 and D_3: elements of the tubular electrostatic lens, isolated from each other by plates of glass *E'*, *E''* and a glass cylinder with a Pertinax screen *F*. *G*: casing on which the ion source and the diffusion pumps *H* are mounted. *I*: glass window for observation of the ion beam. *K*: plate condenser for deflection of the beam at right angles to the plane of the paper. *L*: stay-bolts with threads for adjustment of the lens system in relation to the magnetic field. The undeflected ion beam can be observed in the glass cylinder *M*. *N*: analyzing chamber with extension *O*, on which the fluorescent screen *Q* (or the Faraday cylinders) is (are) placed. *R*: connection for diffusion pump. *S*: yoke of the magnet. *T*: guard screens for protection of the magnet coils. Between the pole pieces *U* a number of distance pieces, *V*, are inserted. *W'* and *W''*: Air admission and air exhaust, respectively. *X*: iron base of magnet resting on concrete pillars *Y*. In the lower right corner is shown the arrangement for measurements with the moveable Faraday cylinders *Z'*, *Z''* in connection with observation of the beam on the fluorescent screen *Å*, to which the beam can be bent by the plate condenser *K*.

experiments by interposing another large vacuum-tight bellows. Glass plates and a glass cylinder with a pertinax shield to prevent surface discharges were used as insulators.

The oil diffusion pumps are mounted on the casing as close to the ion source as possible (cf. the drawing of cross-section $1' - 1''$). The pump system consists of two 5″ pumps in parallel, backed by a 3″ and a 2″ pump of the type ordinarily used in the Institute (1). To produce the forevacuum a Pfeiffer mechanical pump Type 30100 was used. During the experiments the pressure measured by both a McLeòd manometer and a Pirani manometer amounted to less than 10^{-5} mm. Hg.

The analyzing chamber is also connected with the casing by a bellows. As the latter is mounted on the magnet by means of threaded stay-bolts, the whole upper part of the apparatus may easily be adjusted so that the ion beam may be correctly aligned against the magnetic field.

The analyzing chamber consists of a flat, circular box to the outside of which a wide tube is attached (cf. the drawing of cross-section $2' - 2''$). This arrangement was made to facilitate the removal of the gases given off by the metal walls. In order to keep the gas pressure extremely low, the chamber is provided with a flange for connection of a 5″ diffusion pump, but so far this arrangement has not been used. On the analyzing chamber in continuation of the axis of the lens a glass cylinder is placed for observation and adjustment of the undeflected ion beam.

Outside the magnetic field the analyzing chamber extends into a flat box provided at the end with a large flange, on which Faraday cylinders and fluorescent screens are mounted. The fluorescent screens are made of glass coated with a thin layer of fluorescent material (mainly ZnS), and in order to avoid electrical charges on the screen preventing the ion beam from remaining stationary, thin molybdenum wires are drawn across the surface of the glass at intervals of 4 mm.

When ion currents are measured by means of the Faraday cylinders it is convenient to be able to check the form and position of the lines of the mass-spectrum on a fluorescent screen without the nesessity of changing the magnetic field. A fluorescent screen was therefore mounted next to the Faraday-cylinders as will be seen in the lower right corner of Fig. 5. In order to give

the ion beam the necessary deflection in direction of the magnetic field force a plate condenser (length of plates 17 cm., spacing 2,5 cm.) was interposed just below the electrostatic lens. The required deflection voltage amounted to a few hundred volts only.

The magnet producing the magnetic deflection field is also partly shown in cross-section in Fig. 5. The pole pieces whose shape correspond to the stippled area in the drawing have a mean radius of curvature of 80 cm., a width of 15 cm. and are spaced 6 cm. apart. The cores on which the two magnetizing coils are mounted are not carried all the way to the ends of the pole pieces at P and P', but only cover a sector of 76° corresponding to the area within the two dotted lines $3'-3''$ and $4'-4''$. The coils consist of 50 layers containing 11 windings each of 3×7 mm. copper ribbon. The windings are continued right up to the pole faces in order to decrease stray fields.

The coils are encased in guard screens indicated in Fig. 5. The magnetic circuit is closed by a heavy yoke also partly shown in cross-section in the figure. To prevent reduction in the space between the pole-pieces by a bending of the yoke due to attraction between the poles of the magnet a series of distance-pieces have been interposed between them. The energy consumption in the coils at maximum current amounts to about 4400 watts. In order to keep the temperature at a suitable level when working for a considerable length of time, ventilation must be provided by means of a forge bellows capable of delivering up to 12 m^3 per minute. The temperature of the air then will rise by about 20° when passing through the magnet. The whole apparatus, which weighs about 4500 kg., is mounted on two concrete pillars. This arrangement facilitates access to the various parts and observation of the mass-spectra. The maximum field force that may be produced is about 8000 Ørsted, enabling uranium ions of an energy of 80 kev to be deflected.

As the magnetic field force is almost of the same value for increasing and decreasing values of the magnetizing current, it is easy to identify a definite ion species. The current for the magnet is supplied by a dynamo, the magnetizing current of which is controlled from the operator's post.

The magnetic field is exceedingly homogeneous near the middle of the centre line. In order that good results may be

obtained the most essential point is, that the field force is kept constant within each cross-section at right angles to the direction of the beam. A smaller variation along the path of the beam

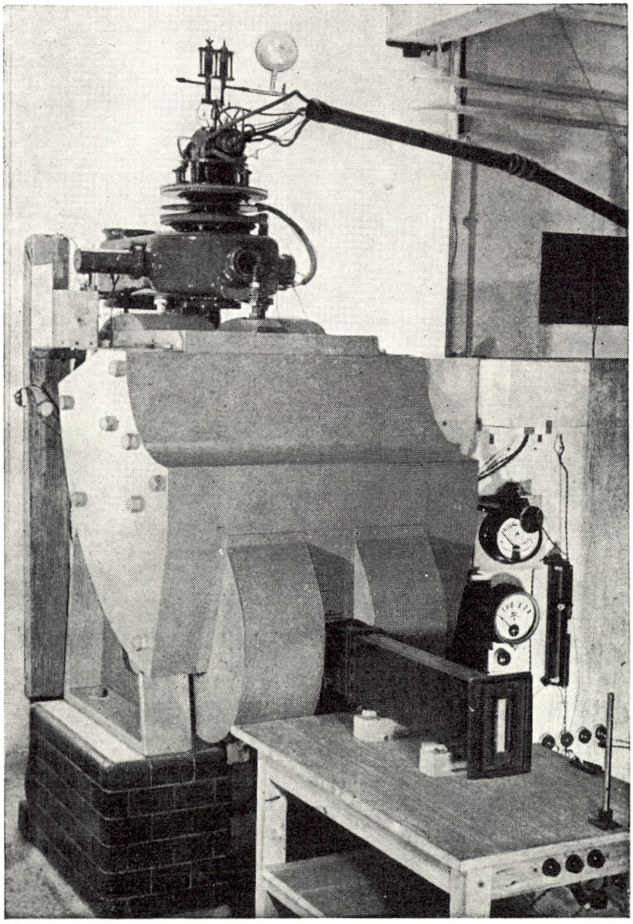

Fig. 6. Photograph of mass-spectrograph.

is of less importance. Measurements have shown that the magnetic field within the space passed by the ion beam deviates less than 1 per 1000 from the maximum field force in the centre line. Deviations of about 1 per cent. are found only at a distance of 3—4 cm. from the centre line. No further measurements of the field force have been made, as the preliminary measurements yielded satisfactory results and the most important

information concerning the properties of the field was obviously to be obtained through experiments with the ion beam, which is exposed to the full effect of the field during its passage through the magnet.

The voltage for accelerating the ions was produced by an ordinary Greinacher generator with two rectifiers. In order to reduce the ripple sufficiently a filter consisting of resistances and condensers was interposed. The constancy thereby obtained was so great that the influence of the ripple on the breadth of the lines ($\sim 10^{-2}$cm.) might be disregarded. The high voltage was measured on a micro-ammeter combined with a 50 cm. long resistance of 400 $M\Omega$. (Vitrohm resistances) immersed in oil. A photograph of the mass-spectrograph is shown in Fig. 6.

Experimental Results.

As the focussing of the ion beam was of decisive importance for the computation of the resolving power of the mass-spectrograph, the properties of the electrostatic lens system had been subjected to previous investigation (J. K.). In these experiments the fact was utilized that the ion beam at the prevailing current densities and gas pressures could be observed as a faintly luminous stripe. For the purpose of comparing the focussing of the lens at varying conditions a series of photographs of the beam was taken.[1] An example of such a photograph of the ion beam is shown in Fig. 7. In this photograph the fluorescent light from the glass around the electrostatic lens is seen at the extreme top, further down the ion beam can first be observed through a small window in the casing bearing the lens system, and subsequently its path may be followed over a considerable length in a glass tube the wall of which is covered with metal netting in order to obviate electrical surface charges. At the bottom of this tube a Faraday cylinder was placed for measuring the ion current. In the present experiment the acceleration potential was

[1] In a brief note in the *Physical Review* BUECHNER and LAMAR (3) state that they have independently photographed ion beams in highly evacuated tubes for the purpose of studying the focussing with ion lenses. According to the *Physikalische Berichte* (22, 2462 (1941)) a detailed treatise on this work has been published in an American periodical (4). We have not, however, been able to provide a copy.

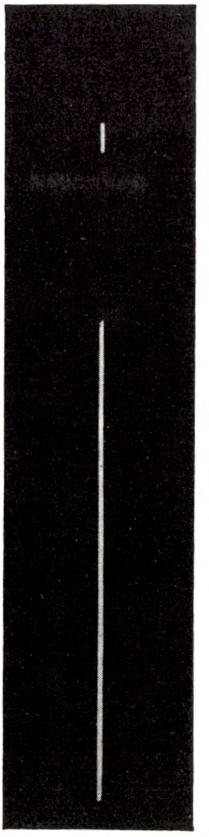

Fig. 7. Photographic record of the focussing of the ion beam. From the middle of the electrostatic lens at the very top of the apparatus and until it disappears into the Faraday cylinder at the bottom the beam passes through a length of ab. 117 cm. Measurement of the original negative shows that the diameter of the beam is about 1 cm. The records were taken with a *Leica* camera with *Summitar* objective. Exposure 10 minutes with diaphragm 2 and *Super-pan* film.

45.5 kv and the ion current 30.8 μa (with an arc current of the ion source of 0.37 amp.), corresponding to the adjustment used for the recording of the mass-spectra. Hydrogen was added to the ion source and the mass-spectrographic analysis subsequently showed that in this case the ion beam mainly consisted of H_2^+ ions, whereas protons and H_3^+ ions were present in somewhat smaller quantities.[1]

As will be seen, the focussing was good, no divergence of the ion beam being observable. In conformity with the curves in Fig. 4 no appreciable divergence of the beam by space charges was to be expected under the prevailing conditions. In the case of stronger currents or heavier ions such an effect, however, could be observed.

In the first mass-spectrographic experiments with the large magnet, the fluorescent screen was placed at the exit from the magnetic field (at P' in Fig. 2 and Fig. 5). Experiments with several screens at increasing distances from the end of the pole pieces, which alternately might be turned into the path of the beam, however, soon showed that the reduced mass-dispersion increased with the distance from the virtual source Q of the beams (cf. Fig. 2 a). At distance $2r$ (P'' in Fig. 5) it was of sufficient magnitude to enable the experiments to be extended to include even the heaviest elements. This does not, however, prove that still better results cannot be obtained at greater distances under suitable focussing conditions.

[1] Further, on account of impurities, very small quantities of the following ions were found: O^+, $(H_2O)^+$, $(H_3O)^+$, $(CO)^+$, $(COH)^+$, and $(CO_2)^+$.

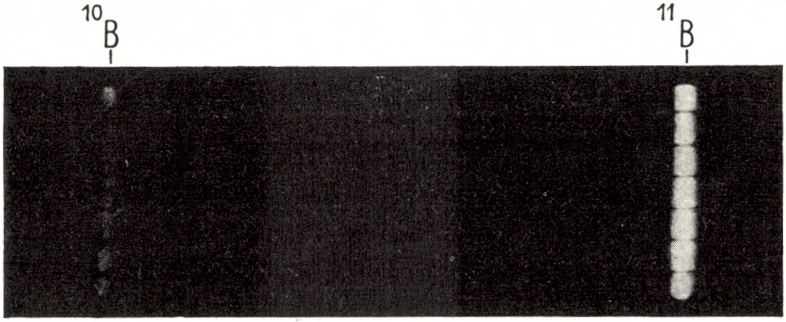

Fig. 8. Mass-spectrum of boron. Isotopes: ^{10}B (20.6 %) and ^{11}B (79.4 %). Photograph of the light from the fluorescent screen. *Leica* camera with *Summitar* objective and *Isopan-Ultra* film. Exposure: ab. 10 sec. Natural size. During the exposure the ion source was supplied with borontrifluoride.

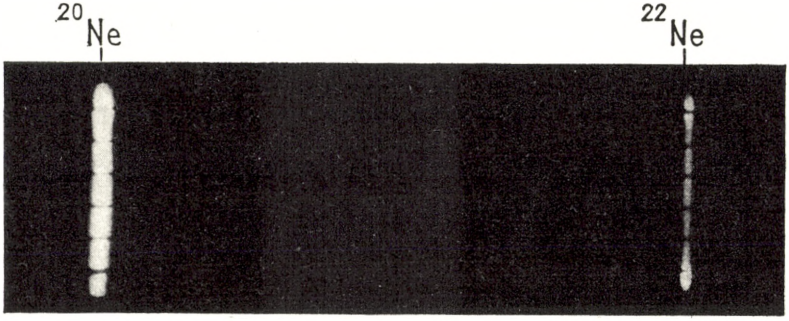

Fig. 9. Mass-spectrum of neon. Isotopes: ^{20}Ne (90.00 %), ^{21}Ne (0.27 %), and ^{22}Ne (9.73 %).

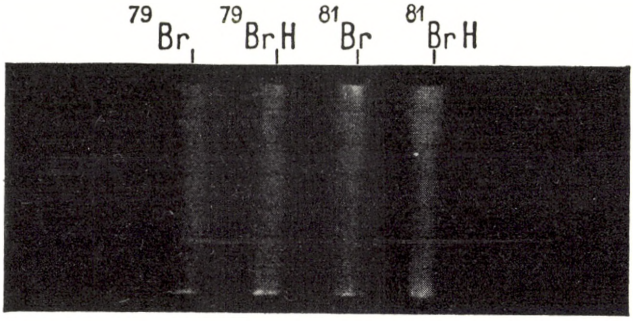

Fig. 10. Mass-spectrum of bromium. Isotopes: ^{79}Br (50.7 %), and ^{81}Br (49.3 %).

In order to demonstrate the resolving power of the mass-spectrograph the mass-spectra of various elements have been photographed. Figs. 8—12 show as typical examples the spectra of boron, neon, bromium, krypton and xenon. At these record-

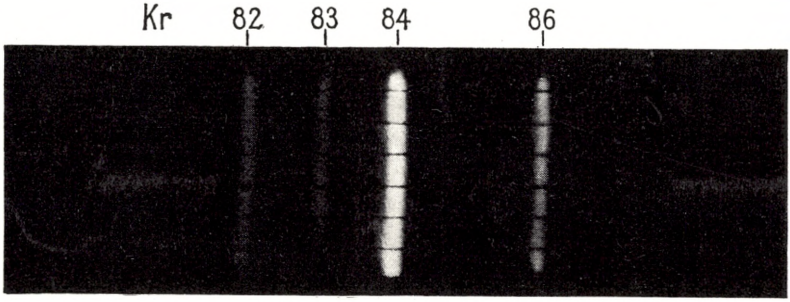

Fig. 11. Mass-spectrum of krypton. Isotopes: ^{78}Kr (0.42 %), ^{80}Kr (2.45 %), ^{82}Kr (11.79 %), ^{83}Kr (11.79 %), ^{84}Kr (56.85 %), and ^{86}Kr (16.70 %).

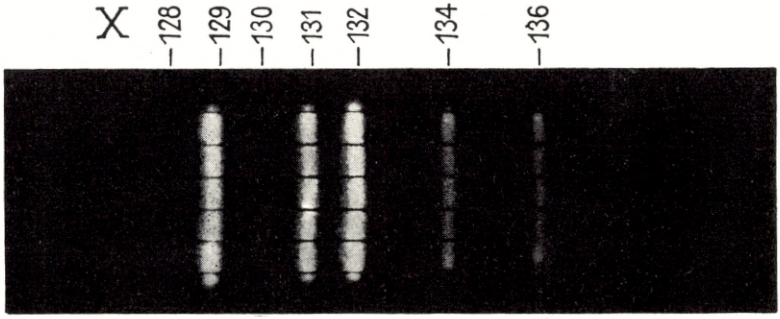

Fig. 12. Mass-spectrum of xenon. Isotopes: ^{124}X (0.08 %), ^{126}X (0.08 %), ^{128}X (2.30 %), ^{129}X (27.13 %), ^{130}X (4.18 %), ^{131}X (20.67 %), ^{132}X (26.45 %), ^{134}X (10.31 %), and ^{136}X (8.79 %).

ings the acceleration voltage was about 50 kv, the arc current ab. 0.3 amp., and the ion currents between 1 and 10 μa. The somewhat different luminosity within the individual lines is due to the irregular thickness of the fluorescent coating. The black stripes across the lines originate from the molybdenum wires stretched across the surface of the glass in order to remove electrical charges.

The boron spectrum shows the two boron isotopes ^{10}B and ^{11}B at a distance of about 72 mm. The luminosity of the lines approximately indicates the ratio between their abundance of ab. 1 : 4. Such an estimate, however, may be very deceptive if the ions hit a charred piece of the screen. The photograph shows that beams hitting the screen even at a considerable distance from the centre line (Point P'' in Fig. 5) are satisfactorily focussed.

In the following table the mass-dispersion measured is compared with the values computed according to [2]. No correction

Table of comparisons between measured and calculated values of the mass-dispersion of the mass-spectrograph.

Isotopes	$2\Delta r$ (meas.)	$2\Delta r$ (calc.)
$^{10}B - ^{11}B$	72	80
$^{20}Ne - ^{22}Ne$	74	80
$^{79}Br - ^{81}Br$	20	20,3
$^{82}Kr - ^{86}Kr$	37	39
$^{129}X - ^{136}X$	41,5	43,4

has been applied for the fact that the light isotope does not impinge on the fluorescent screen at P'', as assumed in the calculations. It will be noticed that the mass-dispersion of $^{10}B - ^{11}B$ is somewhat smaller than the calculated value. This must be due to the fact that the magnetic field diminishes at the ends of the pole pieces.

The measurement of the mass-spectrum of neon also shows a mass-dispersion somewhat smaller than that calculated. The weak isotope ^{21}Ne cannot be observed on the fluorescent screen. Besides the two equally frequent isotopes ^{79}Br and ^{81}Br, the mass-spectrum of bromium shows the presence of the respective hydrides. Such hydride formation would make it impossible to separate isotopes only one mass-unit apart. The possibility, however, exists that the hydrogen may be removed from the ion source by connecting the latter direct to a powerful pumping system, at the same time admitting large quantities of the gas the ions of which it is desired to produce, in order to maintain the necessary pressure to keep the arc burning.

The mass-spectrum of krypton shows only the four most frequent isotopes; thus, ^{78}Kr and ^{80}Kr could not be observed. The mass-spectrum of xenon shows seven of the nine known isotopes; ^{128}X, however, can only just be discerned. In this experiment the resolving power of the mass-spectrograph is obviously higher than $\Delta A/A = 1/238$. At weaker currents or higher acceleration voltage than in this case, both the breadth and height of the lines, however, will decrease and the resolving power will therefore increase still more. If the above data are reversed the resolving power will be decreased. This must, no

doubt, be attributed to the mutual repulsion of the ions; for according to Fig. 4 we have here conditions in which this space charge effect becomes important on account of the heavy ions. For experiments of long duration the lens would not be able to stand acceleration potentials much higher than 50 kv, but

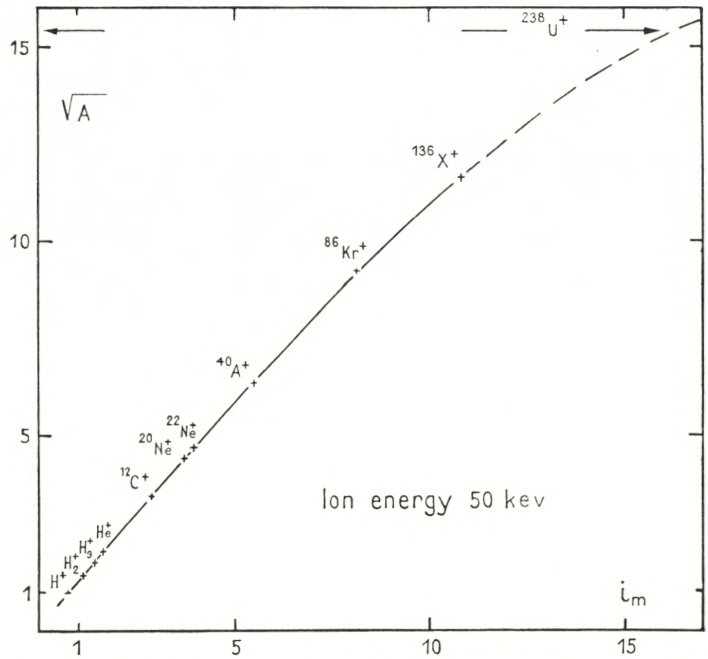

Fig. 13. Curve of adjustment taken with an acceleration voltage of 50 kv.

probably it will not be difficult to build a system which may be used for much higher voltages.

If we plot $\sqrt{A}$ as a function of that magnetizing current i_m which will deflect the ions sufficiently to hit the point P'' on the fluorescent screen (cf. Fig. 5), we shall obtain an adjustment curve as shown in Fig. 13 for an acceleration potential of 50 kv. This curve is extremely useful as a preliminary indication of the region within which a definite ion species may be found. Generally, there will be no doubt as to the identification of the lines, the mass-spectra often being very characteristic and, furthermore, only on rare occasions other ions will be found in the immediate proximity of those wanted.

We shall now show that from a measurement of the line breadths at the exit from the magnetic field, which in the case of medium ion currents and an acceleration voltage of 50 kv was ab. 0.3 cm., it is possible to derive important information as to the paths of the ions in the beam and also as to their mean energy when emitted from the ion source.

According to [3], [4], [5], and [6], the line breadth may be expressed as follows:

$$B \approx \frac{d^2}{8r} + \frac{r}{2} \cdot \frac{\Delta E}{E} + 2r\alpha. \qquad [9]$$

As the diameter of the ion beam at the entrance to the magnetic field according to the photograph (Fig. 7) is only 1 cm., we may disregard the contribution of the first term inasmuch as

$$\frac{d^2}{8r} \approx \frac{1}{8 \cdot 80} = 1.56 \cdot 10^{-3} \text{ cm}. \qquad [10]$$

Already from the previous focussing experiments (J. K.) it was possible to conclude that the ions are emitted from the source at very small energies (< 1.6 ev). In what follows we shall try to determine this energy more accurately, and it is therefore presumed that the ions participating in the formation of the beam are emitted from the plasma of the arc with a Maxwell distribution or a similar energy distribution the energy spread $e\Delta E$ of which is of the same order as the mean energy $e\varepsilon$. Further, we make use of the well-known result (23) that on having passed through an electrostatic lens ions of energy eE will in the most favourable case move along paths the angle of which with the axis of the beam is

$$\alpha < \sqrt{\frac{\varepsilon}{E}}. \qquad [11]$$

On these assumptions the term [9] may be given in the following form

$$B \approx \frac{r}{2} \alpha^2 + 2r\alpha. \qquad [12]$$

As, however, $\alpha \ll 1$, we have

$$B \approx 2r\alpha. \qquad [13]$$

By introducing the numerical values we obtain:

$$\alpha \approx \frac{0.3}{2 \cdot 80} = 1.88 \cdot 10^{-3}. \qquad [14]$$

In other words, the maximum angle of the ion paths with the axis of the beam at the entrance to the magnetic field will be about 0.1°. A further, appreciable diminution of α and thereby of the line breadth B will for technical reasons be difficult, as in that case, in conformity with [11], we should have to use very high acceleration voltages.

From [11] and [14] we may compute the mean energy of the ions at departure from the ion source. It will be

$$e\varepsilon = e\alpha^2 E = e3.53 \cdot 10^{-6} \cdot 5 \cdot 10^4 = 0.176 \text{ ev}. \qquad [15]$$

This means that the ions are emitted with initial energies approximately corresponding to the ion temperature in the arc (0.1 ev $\approx$ 900°K). The process of emission must therefore be assumed to take place in such a way that the ions are drawn straight from the plasma of the arc without subsequently colliding with other atoms, as such collisions would impart to the ions considerable velocity components at right angles to the direction of the beam, which would prevent focussing.

In view of these considerations, the Lamar, Samson, and Compton ion source is seen to be especially suitable for the present investigations. Hence, in designing other types of ion sources for similar purposes, it would obviously be reasonable to choose an experimental arrangement so that discharge and emission conditions approach those obtained in these experiments.

In conclusion it may be pointed out, that low voltage arcs provided with a probe to draw the ions out of the arc must be considered unsuitable for the present investigations, the ions being exposed to collisions in the canal of the probe with a consequent loss of energy. YATES (27) has used this form of ion source for the separation of the boron isotopes, but the mentioned influence of the probe on the emission conditions appeared very plainly from the fact that the mass-spectrum was not completely dissolved.

The high intensity mass-spectrograph described in what precedes will in the near future be used for experiments on the separation of isotopes in such quantities, it is to be expected, as to enable experiments to be made on pure samples. The apparatus for collecting isotopes is already finished. Certain difficulties will, no doubt, be encountered, such as e. g. impurities from the gases present in the apparatus. It has been found, however, that the oil diffusion pumps are capable of maintaining sufficiently low pressures with any of the gases hitherto used. By suitable placing of metal surfaces cooled by means of liquid air it may be possible entirely to prevent impurities from entering the collecting cylinders.

Other Applications.

On account of the great homogeneity of the ion beams obtained, both in respect of mass and energy ($\Delta E/E \approx 3.5 \cdot 10^{-6}$), the mass-spectrograph described may be used for a number of experiments for which the means have hitherto been lacking.

In the first instance the most obvious experiment would be the simple one of determining the yield of secondary electrons from metallic surfaces by bombardment with various ions with primary energies from about 20 kev and upwards. Preliminary experiments on these lines have already been carried out (J. K.) and inter alia, showed, extraordinarily high yields ($i^-/i^+ \sim 20$) for certain molecular ions. By observing the fluorescent light from glass or from the substances covering its surface, it was further found that the colour of the light depended upon the ion species and the nature of the screens. Thus, the light from a glass screen when bombarded with H^+- and A^+-ions was blue and red, respectively. However, so far these experiments have not been continued.

It must, further, be possible to investigate the interaction between high velocity ions and atoms by letting the ions pass through a canal into a chamber with higher pressure than that of the analyzing chamber. It would be of importance for certain astro-physical calculations to obtain approximate values of the cross-sections between high velocity ions and free atoms, even

if the energies considered in these calculations are not so high as those here contemplated.

By using a lens system similar to the Institute's large high voltage tube for nuclear research (1) it will be possible to extend such investigations to comprise experiments with ions of greater energies than those considered in the present paper. In the case of heavy ions the magnetic field of the mass-spectrograph, however, will soon become too weak. In that event it will be possible to accelerate the ions after their passage through the mass-spectrograph and for this purpose either of two principles may be applied. One alternative is to use a constant acceleration potential which, however, entails the drawback that the apparatus for the investigation of the effects of the ions will attain a high, negative potential. The second alternative is the application of alternating electric fields as used by LAWRENCE and SLOAN (13) in the construction of their linear accelerator. By applying this principle we obtain the result that the ions which leave the earthed analyzing chamber with an energy corresponding to the acceleration potential will be further accelerated by the alternating fields and then will impinge on the likewise earthed target.

Summary.

The question of mass-spectrographic separation of isotopes has been discussed by several authors from many different points of view. A critical survey of previous investigations in connection with a series of experiments made in recent years at the Institute of Theoretical Physics has shown that hitherto the possibilities of separating isotopes by mass-spectrographic methods have not been fully exploited (9).

This paper describes a mass-spectrograph constructed on the basis of the experiments mentioned above and having a resolving power of more than $\Delta A/A = 1/238$ at an ion current of 10 μa and an acceleration potential of 50 kv. Experiments on the separation of isotopes may thus be extended even to the heaviest elements. The ion source used was a low voltage arc of the Lamar, Samson, and Compton type, as by means of this apparatus it is possible to produce beams of atomic ions of

probably all elements added to the arc in the gaseous state or in the form of vapours of chemical compounds.

For the focussing of the ion beam a simple tubular lens (retardation lens) was used. The dispersion of the beam was made by means of a homogeneous magnetic field, the mean radius of the path of the deflected ions being 80 cm. The maximum field force of the magnet for continuous operation is about 8000 Ørsted, which is enough to deflect uranium ions of an energy of 80 kev.

In a separate chapter the mass-dispersion of the mass-spectrograph and the breadth of the lines of the mass-spectrum at the exit from the magnetic field are calculated. An especially high resolving power was found experimentally at a distance of 80 cm. from the ends of the pole pieces. An attempt was made at estimating the disturbing influence of electrical space charges. In a later chapter a detailed technical description of the mass-spectrograph is given. To maintain a sufficient vacuum oil diffusion pumps were used capable of pumping all substances so far used in the experiments.

Photographs of the ion beam, which might be observed as a slightly luminous stripe in the evacuated space, show the focussing properties of the electrostatic lens. As examples of the resolving power of the mass-spectrograph, mass-spectra of boron, neon, bromium, krypton, and xenon are shown by photographs of the light from a glass screen coated with a fluorescent substance. The measured values of the mass-dispersion are somewhat smaller than the calculated values as the magnetic field diminishes towards the ends of the pole pieces.

From the breadth of the lines at the exit from the magnetic field it is in the first place possible to determine the maximum angle of the ions to the axis of the beam at the entrance to the magnetic field, which angle appears to be about 0.1°. Next, the mean initial energy of the ions when emitted from the ion source may be calculated at less than 0.2 ev, that is to say that the ions are emitted from the arc with energies nearly corresponding to the ion temperature in its plasma.

The mass-spectrograph described is in the first instance to be used for experiments on the separation of isotopes already commenced. Attention is, however, called to the fact that this

device seems well suited for a number of other experiments, such as e. g. investigations on the interaction between high velocity ions and other atomic particles.

Acknowledgements.

These experiments have been carried out at the Institute of Theoretical Physics of Copenhagen. We wish to thank the director of the Institute, Professor N. BOHR, Ph. D., for the great interest he has taken in these investigations. Further, our thanks are extended to the THOMAS B. THRIGE FOUNDATION, which has donated the magnet to the Institute, and especially to Mr. V. MEYER, C. E., who has designed it. We are also very grateful to MESSRS. BURMEISTER & WAIN, who have donated the semi-manufactured iron bars for the construction of the magnet, and to MESSRS. PHILIPS who have placed tungsten wire at our disposal for the experiments. Finally, we wish to thank Mr. H. W. OLSEN for having constructed several parts of the apparatus in the workshop of the Institute, and Mr. AUG. JENSEN for having made the wooden constructions.

Institute of Theoretical Physics,
University of Copenhagen.

References.

1) T. Bjerge, K. J. Brostrøm, J. Koch, and T. Lauritsen. D. Kgl. Danske Vidensk. Selskab, Mat.-fys. Medd. **18** (1940.)
2) E. T. Booth, J. R. Dunning, A. V. Grosse, and A. O. Nier. Phys. Rev. **58**, 475 (1940).
3) W. W. Buechner and E. S. Lamar. Phys. Rev. **57**, 1070 (1940).
4) W. W. Buechner, E. S. Lamar, and R. J. van de Graaff. Journ. of App. Phys. **12**, 141 (1941).
5) A. Hemmendinger and W. R. Smythe. Phys. Rev. **51**, 1052 (1937).
6) K. H. Kingdon and H. C. Pollock. Phys. Rev. **57**, 1072 (1940).
7) K. H. Kingdon, H. C. Pollock, E. T. Booth, and J. R. Dunning. Phys. Rev. **57**, 749 (1940).
8) J. Koch. Zs. f. Phys. **100**, 669 (1936).
9) J. Koch. Doctor's thesis; University of Copenhagen. Publishers: Thaning og Appel (1942). In Danish with a detailed summary in English and German.
10) J. Koch and W. Walcher. Zs. f. Phys. **97**, 131 (1935).
11) C. H. Kunsmann. Phys. Rev. **25**, 892 (1925).
12) E. S. Lamar, E. W. Samson, and K. T. Compton. Phys. Rev. **48**, 886 (1935).
13) E. O. Lawrence and D. H. Sloan. Proc. Nat. Acad. Sci. Wash. **17**, 64 (1931).
14) J. M. Lyshede. D. Kgl. Danske Vidensk. Selskab, Mat.-fys. Medd. **18** (1941).
15) A. O. Nier, E. T. Booth, J. R. Dunning, and A. V. Grosse. Phys. Rev. **57**, 546 (1940).
16) A. O. Nier, E. T. Booth, J. R. Dunning, and A. V. Grosse. Phys. Rev. **57**, 748 (1940).
17) M. L. E. Oliphant, E. S. Shire, and B. M. Crowther. Proc. Roy. Soc. of London, **146**, 922 (1934).
18) L. H. Rumbaugh. Phys.-Rev. **49**, 882 (1936).
19) W. R. Smythe and A. Hemmendinger. Phys. Rev. **51**, 146 (1937).
20) W. R. Smythe and A. Hemmendinger. Phys. Rev. **51**, 178 (1937).
21) W. R. Smythe, L. H. Rumbaugh and S. S. West. Phys. Rev. **45**, 724 (1934).
22) W. Walcher, Zs. f. techn. Phys. **18**, 535 (1937).
23) W. Walcher. Zs. f. Phys. **108**, 376 (1938).
24) W. Walcher. Zs. f. Phys. **121**, 604 (1943).
25) W. Walcher. Zs. f. Phys. **121**, 719 (1943).
26) E. E. Watson. Phil. Mag. **3**, 849 (1927).
27) E. L. Yates. Proc. Roy. Soc. London, **168**, 148 (1938).

Indleveret til Selskabet den 4. November 1943.
Færdig fra Trykkeriet den 3. November 1944.

DET KGL. DANSKE VIDENSKABERNES SELSKAB
MATEMATISK-FYSISKE MEDDELELSER, BIND XXI, Nr. 9

SOME INVESTIGATIONS OF THE SET OF VALUES OF MEASURES IN ABSTRACT SPACE

BY

KAI RANDER BUCH

KØBENHAVN
I KOMMISSION HOS EJNAR MUNKSGAARD
1945

Table of Contents.

Printed in Denmark
Bianco Lunos Bogtrykkeri A/S

PREFACE

As the nucleus of the theory of abstract measures and integrals is a generalization of the Lebesgue results, this theory must naturally be of rather new date, and actually the whole development has taken place in the present century. Fundamental works by RADON and FRÉCHET[1] had shown the possibility of transferring the Lebesgue integral to the abstract space, and had shown the fact that this new notion thereby acquired the greater part of the properties of the Lebesgue integral; although it was, of course, impossible to prove for this new notion the properties intimately connected with the metrical structure of the Euclidean space. After these works the theory developed rapidly, and out of the great number of papers whose results have been of the greatest importance for the rounding off of and the high stage reached by the theory to-day, we shall mention only those of BOCHNER, DANIELL, NIKODYM, and SAKS. In 1933 appeared a monography by STANISLAW SAKS about the theory of integrals in the Euclidean space, as well as in the abstract space[2]. Later on B. JESSEN has given a concentrated description of the theory in a series of articles in "Matematisk Tidsskrift"[3].

It is the purpose of the present paper to investigate some problems of existence in the abstract space or—to say it more precisely—to study more closely the set of values of certain functions of a set whose defining region is a collection of subsets of the abstract space.

The paper is divided into four parts. Owing to the fact that the theory of measure and integral in an abstract space is of

1) RADON [1]; FRÉCHET [1].
2) SAKS [1], [2].
3) JESSEN [1]—[5].

relatively recent date, and further because the terminology used is not quite fixed, we have considered it natural as well as necessary to give a rather detailed account of those parts of the theory underlying the further description. This account constitutes the first part of the paper. The special types of classes of sets, which will be treated in the following, will be introduced, and the special functions of a set, contents and measures as well as the most important theorems on these, will be mentioned. In the same section we shall, furthermore, briefly treat the important theorem on extension, stating how a content must be constituted in order to be extensible to a measure. After this will follow a description of the definite integral of non-negative functions. The two notions, an absolutely continuous and a singular function of a set, will then be introduced, and the important theorem on the unique decomposition of a function of a set in an absolutely continuous and a singular part (the Lebesgue decomposition) will be proved for a special case. As a help in the proof we shall make use of the theorem on representation of a function of a set as a difference between two measures (the Jordan decomposition). Finally we introduce in the last section of that part the indefinite integral; and the theorem of Radon-Nikodym on the necessary and sufficient condition of the possibility of writing a function of a set as an indefinite integral, is quoted; whereas the proof is given only for a special case essential for the following problems.

The first section of the second part contains an account of already well-known results regarding monotone functions[1]. The notions, the variation $V_f(x_1, x_2)$ and the total discontinuity $D_f(x_1, x_2)$ of a monotone function $f(x)$ in an interval (x_1, x_2) are introduced; and the proof is given for the theorem on decomposition of a monotone function $f(x)$ into two addends $g(x)$ and $h(x)$, one of which is continuous, whereas the other has in any interval a variation equal to its total discontinuity (which again is equal to the total discontinuity of the original function on the interval considered). In the next section we shall deal with theorems on functions of a set defined in the Borel class on the axis of the real numbers. It is well-known that the Borel class is the smallest totally additive ring, containing

[1] A detailed treatment is given in CARATHÉODORY [1].

all half open intervals of the form $[a \leqq x < b]$. It will be discussed on what conditions the function of an interval can be extended to a measure defined in the Borel class. Finally we shall conclude the second part by giving in its last section some considerations of the region of value of certain special types of functions of a set, whose defining region is the Borel class of the interval (0,1).

In the third part we first prove an auxiliary theorem on convergent series with positive terms. It is proved that the set of numbers, whose elements are all finite or enumerable partial sums of such a series, is a closed set. By application of this theorem, we can in the next section of the third part prove the set of numbers, whose elements are the values taken by a bounded measure, defined in the Borel class of the interval (0,1), to be a closed set. In the third section of this part one of the main results of this paper will be obtained. It is here shown that a bounded measure, having as defining region a class of sets consisting of subsets of the abstract space, and having the space itself as element, has the same property as the bounded measure of the Borel class, i. e. that the set of values is a closed set. As our chief means to prove this we make a representation from the class of sets in question in the abstract space on the Borel class of the interval. This representation can to some extent be regarded as a generalization of a well-known construction by PEANO[1]. The fact that we work in this paper especially with the Cantor set is of no consequence except its being the most fitted for our purpose. Many other methods of representation might have been used without essentially complicating the proof.

In the fourth part we shall regard pairs of bounded measures $(\varphi(A), \psi(A))$ instead of one bounded measure, thus extending the theorem proved in the preceding part. Suppose both measures to take on the value 1 on the abstract space E, i.e. $\varphi(E) = \psi(E) = 1$, and the point $(\varphi(A), \psi(A))$ will for every A belong to the unity square. It is proved that if the measures have the same defining region $\mathfrak{F}$, then the set of points defined by $(\varphi(A), \psi(A))$ will be a closed set. The proof takes place in several stages. The theorem

[1] Cf. HILBERT [1]; JESSEN [6]; LEBESGUE [1]; F. RIESZ [1]; DE LA VALLÉE-POUSSIN [1].

will first be proved for φ and ψ as bounded measures defined in the Borel class of the interval (0,1). By application of the theorem on decomposition of monotone functions this case can be retraced to two simple fundamental cases, which will then be dealt with separately. The first, which—rather unprecisely expressed—corresponds to the purely discontinuous elements of the monotone functions, is dealt with quite simply by application of the theorem on the convergent series of positive terms. The other, corresponding to the continuous elements of the monotone functions, is somewhat more complicate and requires a certain chain of constructions. After having proved the theorem for measures defined in the Borel class, we can then in the last section very easily transfer it to the abstract space by means of the same method of coupling which we used in the third part.

The paper is concluded with some remarks on the questions of the axiomatic theory of probabilities and the applications thereof, which have suggested the problems of this paper to the author.

Concluding this paper, I wish to express my warmest thanks to Professor Børge Jessen, and to Professor Richard Petersen, who have both taken interest in my work. I also thank Miss B. Ehlern-Møller, M. A., for the translation into English, and Niels Arley, Ph. D., for reading the proofs.

PART I.

On measure and integral in abstract space.

1. Classes of sets.

Given a set E, containing at least one element. We shall to denote the elements of E use the letters $x, y, z, \cdots$, and to denote subsets of E the letters $A, B, C, \cdots$. As subset of E we shall especially consider the empty set, which in the following will be denoted by 0. $x \in A$ will denote that the point x belongs to the set A. $A \subset B$ denotes A to be a (not necessarily proper) subset of B. Given a sequence of sets, be it finite $A_1, A_2, \cdots, A_k$ or infinite $A_1, A_2, \cdots, A_k, \cdots$, then $A_1 \dot{+} \cdots \dot{+} A_k$, respectively, $A_1 \dot{+} A_2 \dot{+} \cdots \dot{+} A_k \dot{+} \cdots$ or $\mathfrak{S}_n A_n$ will denote the set of elements belonging to at least one of the sets A_n and will be called the sum of the sets $A_1, \cdots, A_k$, respectively, $A_1, A_2, \cdots, A_k \cdots$. When we especially write $\sum_n A_n$ or $A_1 + A_2 + \cdots + A_k$, respectively, $A_1 + A_2 + \cdots + A_k + \cdots$, it is to be understood from the symbol that no two sets A_n have a common elements. $\mathfrak{D}_n A_n$ $\left(\text{or } \prod_n A_n\right)$ or $A_1 \cdots A_k$, respectively, $A_1 A_2 \cdots A_k \cdots$ will denote the set of elements belonging to all sets A_n, and will be termed the product (the common part) of the sets $A_1, \cdots, A_k$ respectively $A_1, A_2, \cdots, A_k, \cdots$. The symbol $A - B$ is only to mean anything when $B \subset A$, and is then to denote the set of elements belonging to A, but not to B. We shall call $E - A$ the complement of A.

In the remaining part of this section we shall deal with classes of sets. A class of sets is a set whose elements are subsets of E. To denote classes of sets we shall use German

capital letters $\mathfrak{F}$, $\mathfrak{G}$, $\cdots$. $A \varepsilon \mathfrak{F}$ will denote that the set A belongs to the class of sets $\mathfrak{F}$. A class of sets $\mathfrak{F}$ is called additive, respectively multiplicative, if $A_1 + A_2$, respectively $A_1 A_2$, belongs to $\mathfrak{F}$, whenever A_1 and A_2 both belong to $\mathfrak{F}$. It is called subtractive, if $A_1 - A_2$ belongs to $\mathfrak{F}$, whenever A_1 and A_2 both belong to $\mathfrak{F}$. It is termed totally additive, respectively multiplicative, if $\mathop{\mathfrak{S}}_n A_n$, respectively $\mathop{\mathfrak{D}}_n A_n$, belongs to $\mathfrak{F}$, any A_n belonging to $\mathfrak{F}$.

After these preliminary remarks it is now possible to set up the two following important definitions:

A class of sets $\mathfrak{F}$ is called a ring, if it contains at least one set and is additive and subtractive.

A class of sets $\mathfrak{F}$ is called a Borel ring, if it contains at least one set and is totally additive and subtractive.

It is immediately evident that any Borel ring is a ring. Suppose $A = \mathop{\mathfrak{S}}_n A_n$, and it will be clear from the relation

$$\mathop{\mathfrak{D}}_n A_n = A - \mathop{\mathfrak{S}}_n (A - A_n), \tag{1,1}$$

which is valid whether the number of the sets is finite or enumerable, that any ring is multiplicative, and that any Borel ring is totally multiplicative. Finally we shall mention that the smallest possible extension of a given set $\mathfrak{F}$ into a Borel ring is obtained as the product of all Borel rings, containing $\mathfrak{F}$. For this product is easily seen to be a Borel ring itself.

2. Functions of a set.

A function whose defining region is a class of sets $\mathfrak{F}$, and whose values are real numbers ($-\infty$ and $+\infty$ incl.), will be called a function of a set. To denote the latter we shall in the following use Greek small letters. A function of a set μ defined in $\mathfrak{F}$ will be termed additive, if $\mu(A_1 + \cdots + A_k) = \mu(A_1) + \cdots + \mu(A_k)$, when $A_n \varepsilon \mathfrak{F}$ for $n = 1, 2, \cdots, k$ and $A_1 + \cdots + A_k \varepsilon \mathfrak{F}$. In analogy μ will be called totally additive, if $\mu(\mathop{\Sigma}_n A_n) = \mathop{\Sigma}_n \mu(A_n)$, when all $A_n \varepsilon \mathfrak{F}$ and $\mathop{\Sigma}_n A_n \varepsilon \mathfrak{F}$.

On functions of a set we now give the two following definitions:

A function of a set μ, defined in $\mathfrak{F}$ will be called a content, if

1) $\mathfrak{F}$ *is a ring.*
2) $0 \leqq \mu(A) \leqq \infty$ *for every* $A \in \mathfrak{F}$.
3) μ *is additive.*
4) *to any* $A \in \mathfrak{F}$ *there corresponds a set* $\mathfrak{S}_n A_n$, *where all* $A_n \in \mathfrak{F}$ *and* $\mu(A_n) < \infty$ *for all* n, *such that* $A \subset \mathfrak{S}_n A_n$.

A function of a set μ, *defined in* $\mathfrak{F}$ *is called a measure, if*

1) $\mathfrak{F}$ *is a Borel ring.*
2) $0 \leqq \mu(A) \leqq \infty$ *for every* $A \in \mathfrak{F}$.
3) μ *is totally additive.*
4) *to any* $A \in \mathfrak{F}$ *there corresponds a set* $\mathfrak{S}_n A_n$, *where all* $A_n \in \mathfrak{F}$ *and* $\mu(A_n) < \infty$ *for all* n, *such that* $A \subset \mathfrak{S}_n A_n$.

For a content μ defined in $\mathfrak{F}$ the following theorems hold true

I) $\mu(0) = 0$.
II) $\mu(A) \leqq \mu(B)$, when $A \subset B$ and $A \in \mathfrak{F}$, $B \in \mathfrak{F}$.
III) $\mu(B - A) = \mu(B) - \mu(A)$ when $A \in \mathfrak{F}$, $B \in \mathfrak{F}$ and $\mu(A) < \infty$.
IV) $\mu(A_1 + A_2 + \cdots + A_n) \leqq \mu(A_1) + \mu(A_2) + \cdots + \mu(A_n)$ when $A_i \in \mathfrak{F}$ for $i = 1, 2, \cdots, n$.
V) $\mu\left(\sum_n A_n\right) \geqq \sum_n \mu(A_n)$ when all $A_n \in \mathfrak{F}$ and $\sum_n A_n \in \mathfrak{F}$.

A measure being a content as well, the same theorems, I—V, hold true if μ is a measure; further we have in that case the following theorems

VI) $\mu\left(\mathfrak{S}_n A_n\right) \leqq \sum_n \mu(A_n)$ when all $A_n \in \mathfrak{F}$.
VII) $\mu\left(\mathfrak{S}_n A_n\right) = \lim_n \mu(A_n)$ when $A_1 \subset A_2 \subset \cdots$ and all $A_n \in \mathfrak{F}$.
VIII) $\mu\left(\mathfrak{D}_n A_n\right) = \lim_n \mu(A_n)$ when $A_1 \supset A_2 \supset \cdots$, $\mu(A_1) < \infty$ and all $A_n \in \mathfrak{F}$.

As the proofs of these theorems I—VI must be considered evident, we shall in this account confine ourselves to prove the theorems VII and VIII. From $A_1 \subset A_2 \subset \cdots$ it follows that

$$\mathfrak{S}_n A_n = A_1 + (A_2 - A_1) + (A_3 - A_2) + \cdots + (A_n - A_{n-1}) + \cdots,$$

and hence

$$\mu\left(\mathop{\mathfrak{S}}_{n} A_n\right) = \mu(A_1) + \mu(A_2 - A_1) + \cdots + \mu(A_n - A_{n-1}) + \cdots =$$
$$\lim_n \left(\mu(A_1) + \mu(A_2 - A_1) + \cdots + \mu(A_n - A_{n-1})\right) =$$
$$\lim_n \mu(A_n),$$

and the proof of VII is completed.

From $A_1 \supset A_2 \supset A_3 \supset \cdots$ follows $A_1 - A_2 \subset A_1 - A_3 \subset \cdots$. Since $\mu(A_1) < \infty$ we get

$$\mu\left(A_1 - \mathop{\mathfrak{D}}_{n} A_n\right) = \mu(A_1) - \mu\left(\mathop{\mathfrak{D}}_{n} A_n\right),$$

and, furthermore, since $\mathop{\mathfrak{S}}_{n}(A_1 - A_n) = A_1 - \mathop{\mathfrak{D}}_{n} A_n$, it follows from VII that

$$\mu\left(A_1 - \mathop{\mathfrak{D}}_{n} A_n\right) = \lim_n \mu(A_1 - A_n) = \mu(A_1) - \lim_n \mu(A_n).$$

Taking these equations together, we obtain

$$\mu\left(\mathop{\mathfrak{D}}_{n} A_n\right) = \lim_n \mu(A_n),$$

and the proof of VIII is completed.

As conclusion of this section we shall mention an important theorem of extension, which tells how a content must be constituted in order to be extensible to a measure. We must, however, first specify the latter notion. Let μ be a content defined in $\mathfrak{F}$, and μ^* a measure defined in $\mathfrak{F}^*$. We then call μ^* an extension of μ, if every A, belonging to $\mathfrak{F}$, also belongs to $\mathfrak{F}^*$, and $\mu(A) = \mu^*(A)$ for any $A \in \mathfrak{F}$. It is obvious that μ must satisfy the condition of being totally additive, if it shall be possible to extend μ into a measure. This condition is, however, also sufficient, the theorem being as follows:

Let μ be a content defined in $\mathfrak{F}$. This content can be extended to a measure μ^* defined in $\mathfrak{F}$, when and only when μ is totally additive. One of the possible extensions is the most restricted one, i. e. any other extension is an extension of this.

Without entering into the proofs, we shall indicate how the most restricted extension, mentioned in the theorem, arises. Let $\mathfrak{F}^*$ be the smallest Borel ring containing $\mathfrak{F}$. For every $A \in \mathfrak{F}^*$ we put

$$\mu^*(A) = \text{lower bound } \mathop{\Sigma}_{n} \mu(A_n), \qquad (2,1)$$

where the lower bound is to be taken over all $\sum_n \mu(A_n)$, $A_n \in \mathfrak{F}$ for all n and $A \subset \mathfrak{S}_n A_n$. This function of a set defined in $\mathfrak{F}^*$ will then be a measure.

For certain applications it is of interest to note that a content μ defined in $\mathfrak{F}$, where $\mu(A) < \infty$ for any $A \in \mathfrak{F}$, is totally additive, when and only when it is valid for any sequence of sets $A_1 \supset A_2 \supset \cdots$, where all $A_n \in \mathfrak{F}$ and $\mathfrak{D}_n A_n = 0$ that $\lim_n \mu(A_n) = 0$.

3. The definite integral of non-negative functions.

In the following we shall deal with functions in E, whose value region consists of real numbers, $-\infty$ and $+\infty$ included. By $[f]$ we shall denote the defining region of f, i. e. the set of $x \in E$ for which f is defined. The set of those $x \in [f]$, for which $f > a$ will be termed $[f > a]$. It is now evident what is to be understood by the symbols $[f \geqq a]$, $[f < a]$, $[f \leqq a]$, $[f = a]$ etc.

Now suppose a Borel ring $\mathfrak{F}$ to be given. The function f is said to be a function on $\mathfrak{F}$, if the sets $[f]$, $[f \geqq a]$, $[f > a]$, $[f \leqq a]$, and $[f < a]$ belong to $\mathfrak{F}$ for any a. These conditions can be considerably reduced. Thus for instance f will be a function on $\mathfrak{F}$, if the sets $[f]$ and $[f \geqq r]$ belong to $\mathfrak{F}$ for any rational r.

If f is a function on $\mathfrak{F}$, we see that $[f = a] \in \mathfrak{F}$, since $[f = a] = [f \leqq a]\,[f \geqq a]$.

We shall further note that simple calculations with functions on $\mathfrak{F}$ will again lead to functions on $\mathfrak{F}$.

By f_A we shall denote the contraction of f to A, i. e. the function defined in A, for which $f_A(x) = f(x)$ for any $x \in A$. If f is a function on the Borel ring $\mathfrak{F}$ and $A \in \mathfrak{F}$, then also f_A will be a function on $\mathfrak{F}$, as we have e. g.

$$[f_A \geqq a] = A\,[f \geqq a].$$

After these preliminary observations we may now go over to discuss the definite integral of non-negative functions.

Let μ be a measure defined in $\mathfrak{F}$, and let f be a function on $\mathfrak{F}$, which is non-negative, and takes on a finite or at most an enumerable number of values. v_n denoting the values taken by f, the set $[f = v_n]$ will belong to $\mathfrak{F}$ for any n. We now

put $i_n = v_n \mu([f = v_n])$, when this product exists, and $i_n = 0$, if either $v_n = 0$ and $\mu([f = v_n]) = \infty$ or $v_n = \infty$ and $\mu([f = v_n]) = 0$.

The definite integral of the function f with respect to the measure μ, $I(f)$, will then be defined by

$$I(f) = \sum_n i_n .$$

Next let f be a function on $\mathfrak{F}$, which is non-negative. Together with f we shall consider all functions g on $\mathfrak{F}$ where $[g] = [f]$, which are non-negative, and which take on a finite or at most enumerable number of values, and for which $g \leq f$ for every $x \varepsilon [f]$. The function $g = 0$ is an example of such a function. We then put

$$\underline{I}(f) = \text{upper bound } I(g).$$

Similarly we introduce

$$\bar{I}(f) = \text{lower bound } I(h),$$

where h runs through all functions on $\mathfrak{F}$ where $[h] = [f]$, which are non-negative, and which take a finite or at most an enumerable number of values, and for which $h \geq f$ for every $x \varepsilon [f]$. The function $h = \infty$ is an example of such a function. It is now easily seen that we have

$$\underline{I}(f) = \bar{I}(f).$$

For if we choose a number a, $1 < a < \infty$, and put

$$f_a(x) = \begin{cases} 0 \text{ for } x \varepsilon [f = 0] \\ a^n \text{ for } x \varepsilon [a^n \leq f < a^{n+1}], \; n = 0, \pm 1, \pm 2, \cdots \\ \infty \text{ for } x \varepsilon [f = \infty], \end{cases}$$

then the function $f_a(x)$ is a g-function in the above sense, and the function $a f_a(x)$ is an h-function. Thus we have

$$I(f_a) \leq \underline{I}(f)$$

and furthermore (cf. theorem II page 13)

$$I(a f_a) = a I(f_a) \geq \bar{I}(f).$$

From these inequalities it follows that

$$\bar{I}(f) \leqq a \underline{I}(f)$$

giving for $a \to 1$

$$\bar{I}(f) \leqq \underline{I}(f)$$

which in connection with the trivial relation

$$\underline{I}(f) \leqq \bar{I}(f)$$

gives the result wanted.

Thus we have been led to the following definition:

The definite integral of the function f with respect to the measure μ, $I(f)$, *is defined by the common value of* $\underline{I}(f)$ *and* $\bar{I}(f)$

$$I(f) = \underline{I}(f) = \bar{I}(f).$$

If $I(f) < \infty$ we shall call the function f μ-integrable[1]. If f is such a function, and A is a subset of $[f]$, belonging to $\mathfrak{F}$, we write

$$I(f_A) = \int_A f(x)\mu(dE),$$

and call this quantity the integral over the set A of the function f with respect to the measure μ.

For the definite integral introduced above a number of theorems are valid, of which we shall mention the following ones:

I) $I(f) \geqq 0$, and the sign of equality holds true when and only when $\mu[f > 0] = 0$.

II) $I(cf) = cI(f)$ for every $c > 0$.

III) If $[f] = \sum_n A_n$, where all $A_n \varepsilon \mathfrak{F}$, we have $I(f) = \sum_n I(f_{A_n})$.

IV) If $[f] = [g]$ then $I(f+g) = I(f) + I(g)$.

V) If $[f] = [g]$ and $f \leqq g$ then $I(f) \leqq I(g)$, and the sign of equality holds true when and only when we have either $I(f) = \infty$ or $I(f) < \infty$ and $\mu([f < g]) = 0$.

[1] If a function f is μ-integrable, we have $\mu[f = \infty] = 0$; thus the function is finite, at most with the exception of a zero-set.

VI) If $[f_1] = [f_2] = \cdots$ and $f_1 \leqq f_2 \leqq \cdots$ then $I(\lim_n f_n) = \lim_n I(f_n)$.

VII) If $[f_1] = [f_2] = \cdots$ then $I(\lim_n \inf f_n) \leqq \lim_n \inf I(f_n)$.

4. Absolutely continuous and singular functions of a set.

Let $\mathfrak{F}$ be a Borel ring for which $E \varepsilon \mathfrak{F}$, and let μ be a measure defined in $\mathfrak{F}$. We shall then introduce the following definitions:

A bounded totally additive function of a set φ defined in $\mathfrak{F}$ is called μ-continuous, if $\varphi(M) = 0$ for every set $M \varepsilon \mathfrak{F}$, for which $\mu(M) = 0$.

A bounded totally additive function of a set φ defined in $\mathfrak{F}$ is called μ-singular, if there exists a set $N \varepsilon \mathfrak{F}$ with $\mu(N) = 0$, such that $\varphi(A) = 0$ for every set $A \varepsilon \mathfrak{F}$, which is a subset of $E - N$.

If a function of a set φ is both μ-continuous and μ-singular it must vanish identically. This is seen as follows. For every $A \varepsilon \mathfrak{F}$ we have

$$\varphi(A) = \varphi(AN + (A - AN)) = \varphi(AN) + \varphi(A - AN).$$

From $\mu(N) = 0$ it follows that $\mu(AN) = 0$ and hence further that $\varphi(AN) = 0$. Since $A - AN \subset E - N$ it next follows that $\varphi(A - AN) = 0$. We thus have $\varphi(A) = 0$ for every $A \varepsilon \mathfrak{F}$.

Further it is evident that if φ is absolutely continuous (respectively singular), then also $c\varphi$ (c constant) will be absolutely continuous (respectively singular), and if φ_1 and φ_2 are absolutely continuous (respectively singular), then also $\varphi_1 + \varphi_2$ will be absolutely continuous (respectively singular).

The following important theorem on decomposition is true for functions of a set:

A bounded totally additive function of a set φ defined in $\mathfrak{F}$ can in one, and only one, way be written in the form

$$\varphi = \varphi_k + \varphi_s,$$

where φ_k and φ_s are bounded totally additive functions of sets defined in $\mathfrak{F}$, and φ_k is μ-continuous, and φ_s is μ-singular.

This theorem being of particular interest for our later applications of the theory we shall give the proof of it in the

special case, which we are to apply later on, namely, where μ is bounded, and φ is non-negative.

The fact that the decomposition can at most be carried out in one way is seen as follows. Suppose

$$\varphi = \varphi'_k + \varphi'_s = \varphi''_k + \varphi''_s,$$

where φ'_k and φ''_k are absolutely continuous, and φ'_s and φ''_s are singular. We then have for every $A \in \mathfrak{F}$

$$\varphi'_k - \varphi''_k = \varphi''_s - \varphi'_s = \varphi^*.$$

According to previous remarks φ^* is itself absolutely continuous, being a difference between two absolutely continuous functions of a set, and analogously it is obvious that φ^* is singular. Hence φ^* is identically zero, which was to be proved.

We shall now first observe that if the decomposition is possible, the set N corresponding to φ_s will have the following property: From $A \in \mathfrak{F}$, $A \subset E - N$, and $\mu(A) = 0$ it follows that $\varphi(A) = 0$, because $\mu(A) = 0$ implies $\varphi_k(A) = 0$, and from $A \subset E - N$ it follows that $\varphi_s(A) = 0$. Conversely, if it is possible to find a set $N \in \mathfrak{F}$ with $\mu(N) = 0$, such that $A \in \mathfrak{F}$, $A \subset E - N$, and $\mu(A) = 0$ implies that $\varphi(A) = 0$, then decomposition will be possible. This is seen as follows: For every $A \in \mathfrak{F}$ we have

$$\varphi(A) = \varphi(A - AN) + \varphi(AN)$$

We can prove the function of a set $\varphi_1(A) = \varphi(A - AN)$ to be μ-continuous. Suppose $A \in \mathfrak{F}$ and $\mu(A) = 0$. Hence $A - AN \subset E - N$ and $\mu(A - AN) = 0$. Thus we get $\varphi_1(A) = 0$. Next we can prove $\varphi_2(A) = \varphi(AN)$ to be μ-singular with N as corresponding set. From $A \in \mathfrak{F}$ and $A \subset E - N$ follows that $AN = 0$ and hence $\varphi_2(A) = \varphi(0) = 0$. Now the theorem will have been proved, if we can show the existence of a set N having the properties mentioned[1].

It will be natural in the course of the proof to form two auxiliary theorems.

1. $\mathfrak{F}$ being a class of sets, and φ being a bounded function of

[1] Hence we further see that $\varphi(A) \geqq 0$ implies that $\varphi_k(A) \geqq 0$ and $\varphi_s(A) \geqq 0$ for every $A \in \mathfrak{F}$.

a set defined in $\mathfrak{F}$, we introduce the functions of a set $\overline{\varphi}$ and $\underline{\varphi}$ by the definitions

$$\overline{\varphi}(A) = \text{upper bound } \varphi(B)$$
$$\underline{\varphi}(A) = \text{lower bound } \varphi(B),$$

where B runs through all subsets of A. We then have the following lemma:

A totally additive bounded function of a set φ, whose defining region $\mathfrak{F}$ is a Borel ring, may be written in the form

$$\varphi = \overline{\varphi} + \underline{\varphi}$$

where $\overline{\varphi}$ and $-\underline{\varphi}$ are measures[1].

We shall not in this place give the proof of this theorem, as it does not imply much new, but let it suffice to remark that with the conditions stated in the theorem it will be true for every $A \varepsilon \mathfrak{F}$, since $\varphi(0) = 0$, that

$$\underline{\varphi}(A) \leqq 0 \leqq \overline{\varphi}(A).$$

2. The other lemma is as follows:

Let $\mathfrak{F}$ be a Borel ring, containing E, and let φ be a bounded totally additive function of a set defined in $\mathfrak{F}$. E may then be decomposed into the form

$$E = E^+ + E^-,$$

where E^+ and E^- both belong to $\mathfrak{F}$, and such that

$$\underline{\varphi}(E^+) = 0 \text{ and } \overline{\varphi}(E^-) = 0,$$

i. e. $\varphi(A) \geqq 0$ for every $A \varepsilon \mathfrak{F}$, which is a subset of E^+ and $\varphi(A) \leqq 0$ for every $A \varepsilon \mathfrak{F}$, which is a subset of E^-.[2]

As a consequence of the meaning of $\underline{\varphi}(E)$ we may for every n ($n = 1, 2, 3, \cdots$) choose a set $A_n^- \varepsilon \mathfrak{F}$, such that

$$\varphi(A_n^-) < \underline{\varphi}(E) + \frac{1}{2^n}. \tag{4,1}$$

[1] $\overline{\varphi}$ and $\underline{\varphi}$ are both bounded.

[2] This decomposition is usually not unique.

Let $A_n^+ = E - A_n^-$, and we have

$$\varphi(A_n^+) + \varphi(A_n^-) = \varphi(E) = \overline{\varphi}(E) + \underline{\varphi}(E) > \overline{\varphi}(E) + \varphi(A_n^-) - \frac{1}{2^n},$$

and hence

$$\varphi(A_n^+) > \overline{\varphi}(E) - \frac{1}{2^n}.$$

$-\underline{\varphi}$ being a measure, we next have

$$\underline{\varphi}(A_n^+) = \varphi(E) - \varphi(A_n^-),$$

which together with (4,1) gives

$$\underline{\varphi}(A_n^+) > -\frac{1}{2^n}.$$

In analogy we get

$$\overline{\varphi}(A_n^-) < \frac{1}{2^n}.$$

Next we put

$$B_n^+ = \prod_{p=1}^{\infty} A_{n+p}^+ \text{ and } B_n^- = E - B_n^+ = \bigcup_p A_{n+p}^-.$$

Thus we have for any p

$$-\underline{\varphi}(B_n^+) \leq -\underline{\varphi}(A_{n+p}^+) < \frac{1}{2^{n+p}}$$

since

$$B_n^+ \subset A_{n+p}^+,$$

i. e.

$$-\underline{\varphi}(B_n^+) = 0.$$

By means of theorem VI, page 9, it is derived that

$$\overline{\varphi}(B_n^-) \leq \sum_{p=1}^{\infty} \overline{\varphi}(A_{n+p}^-) < \sum_{p=1}^{\infty} \frac{1}{2^{n+p}} = \frac{1}{2^n}. \qquad (4,2)$$

If we now introduce

$$E^+ = \bigcup_n B_n^+ \text{ and } E^- = E - E^+ = \bigcap_n B_n^-$$

we get

$$E = E^+ + E^-,$$

a decomposition of E having the properties mentioned in the theorem. For we have, again by means of theorem VI page 9,

$$-\underline{\varphi}(E^+) \leqq \sum_n -\underline{\varphi}(B_n^+) = 0$$

and consequently

$$\underline{\varphi}(E^+) = 0.$$

Since $E^- \subset B_n^-$ and applying (4,2) we see that

$$\overline{\varphi}(E^-) \leqq \overline{\varphi}(B_n^-) < \frac{1}{2^n}$$

is true for any n, and consequently

$$\overline{\varphi}(E^-) = 0.$$

After these preparations we can easily establish the proof of our main theorem. For every n $(n = 1, 2, 3, \cdots)$

$$\psi_n = \varphi - n\mu$$

is a bounded totally additive function of a set defined in $\mathfrak{F}$. According to our second lemma E may be written in the form

$$E = E_n^+ + E_n^-$$

where E_n^+ and E_n^- both belong to $\mathfrak{F}$, and such that

$$\underline{\psi}_n(E_n^+) = \overline{\psi}_n(E_n^-) = 0.$$

For every $A \in \mathfrak{F}$, where $A \subset E_n^+$, we now have

$$\psi_n(A) \geqq 0 \quad \text{i. e.} \quad \varphi(A) \geqq n\mu(A), \tag{4,3}$$

and for every $A \in \mathfrak{F}$, where $A \subset E_n^-$,

$$\psi_n(A) \leqq 0 \quad \text{i. e.} \quad \varphi(A) \leqq n\mu(A). \tag{4,4}$$

Applying (4,3) on E_n^+ we get, due to $E_n^+ \subset E$,

$$\varphi(E) \geqq \varphi(E_n^+) \geqq n\mu(E_n^+).$$

Since $\varphi(E) < \infty$ we get

$$\lim_n \mu(E_n^+) = 0. \tag{4,5}$$

If now

$$N = \mathfrak{D}_n E_n^+, \quad E - N = E - \mathfrak{D}_n E_n^+ = \mathfrak{S}_n E_n^-, \tag{4,6}$$

$N \subset E_n^+$ holds true for any n, from which it follows that

$$0 \leqq \mu(N) \leqq \mu(E_n^+),$$

which relation together with (4,5) gives

$$\mu(N) = 0. \tag{4,7}$$

Now let $A \varepsilon \mathfrak{F}$ be a set having the properties $A \subset E - N$ (i. e. according to (4,6) $A \subset \mathfrak{S}_n A E_n^-$) and $\mu(A) = 0$. Consequently we can show that $\varphi(A) = 0$, because due to theorem VI, page 9,

$$\varphi(A) = \varphi\left(\mathfrak{S}_n A E_n^-\right) \leqq \sum_n \varphi(A E_n^-),$$

and since $A E_n^- \subset E_n^-$ (4,4) gives

$$\varphi(A) \leqq \sum_n n \mu(A E_n^-);$$

since $\mu(A) = 0$ we know, however, that $\mu(A E_n^-) = 0$ for any n, i.e.

$$\varphi(A) = 0,$$

q. e. d.

5. Indefinite integral.

$\mathfrak{F}$ being a Borel ring, containing E, μ being a measure defined in $\mathfrak{F}$ and f being a function μ-integrable on $\mathfrak{F}$ with $[f] = E$, we now introduce the indefinite integral by the following definition:

The function of a set

$$\varphi(A) = I(f_A) = \int_A f(x)\, \mu(dE)$$

is called the indefinite integral of the function f with respect to the measure μ.

In the special case $f \geqq 0$, we get for any $A \varepsilon \mathfrak{F}$

$$0 \leqq \varphi(A) \leqq \varphi(E),$$

since $\varphi(E) = I(f) < \infty$, and by means of the theorems I and III, page 13. The theorem III, page 13, further shows that φ is totally additive. From $\mu(A) = 0$ it follows that $\mu[f_A > 0] = 0$, and hence, further, that $\varphi(A) = 0$. Consequently we see that the function φ is μ-continuous.

On the exact connection between functions of a set and indefinite integrals we have the following theorem:

A function of a set φ, whose defining region $\mathfrak{F}$ is a Borel ring, is the indefinite integral with respect to the measure μ of a function f with $[f] = E$, which is μ-integrable on $\mathfrak{F}$ when and only when it is bounded, totally additive and μ-continuous.

We have seen above that $f \geqq 0$ implies that φ is bounded, totally additive and μ-continuous. As we shall in the following chiefly consider non-negative functions of a set, we shall in this account confine ourselves to mention how the function f may be defined in the following special case:

For a function of a set φ, which is non-negative, bounded, totally additive and μ-continuous, and whose defining region $\mathfrak{F}$ is a Borel ring, and a bounded measure μ, may be defined a function f on $\mathfrak{F}$, which is non-negative and μ-integrable, and where $[f] = E$, such that for every $A \varepsilon \mathfrak{F}$

$$\varphi(A) = \int_A f(x)\,\mu(dE).$$

For any a, $0 \leqq a < \infty$, we can determine a decomposition of E

$$E = E_a^+ + E_a^-,$$

where E_a^+ and E_a^- both belong to $\mathfrak{F}$, such that the function $\psi_a = \varphi - a\mu$ has the properties

$$\underline{\psi}_a(E_a^+) = 0 \quad \text{and} \quad \overline{\psi}_a(E_a^-) = 0$$

i. e.

$$\left.\begin{aligned} &\varphi(A) \geqq a\mu(A) \text{ for } A \varepsilon \mathfrak{F} \text{ and } A \subset E_a^+ \\ &\varphi(A) \leqq a\mu(A) \text{ for } A \varepsilon \mathfrak{F} \text{ and } A \subset E_a^- \end{aligned}\right\} \quad (5,1)$$

(cf. the lemma page 16), and this decomposition may be carried out in such a way that the following conditions are also satisfied:

1) $E_0^+ = E$

2) $E_a^+ \supset E_b^+$ for $b > a$

3) $E_a^+ = \mathop{\mathfrak{D}}_n E_{a_n}^+$ for $a =$ upper bound $\{a_1, a_2, \cdots\}$

4) $\mathop{\mathfrak{D}}_n E_n^+ = 0$.

(As to proof, see JESSEN [3].)

For every $x \varepsilon E$ we shall now find the values of a for which x belongs to E_a^+. These values will constitute a bounded closed interval. The fact that it is an interval is a consequence of 2), the fact that it is bounded is a consequence of 4), and the fact that it is closed is a consequence of 1) and 3). The function $f(x)$ is now introduced by the following definition

$$f(x) = \max_a \{a;\ x \varepsilon E_a^+\},$$

or expressed in another way

$$x \varepsilon E_a^+ \text{ for } 0 \leqq a \leqq f(x).$$

The function f for which $[f] = E$ is finite and non-negative; we further see that $[f \geqq a] = E_a^+$, from which follows that f is a function defined in $\mathfrak{F}$. Thus, for any $A \varepsilon \mathfrak{F}$ $I(f_A)$ exists. Finally we shall show that

$$\varphi(A) = I(f_A).$$

For this purpose it will suffice to show that the inequalities

$$I(g) \leqq \varphi(A) \leqq I(h) \tag{5,2}$$

hold true, when g and h are functions on $\mathfrak{F}$, where $[g] = [h] = A$, which takes on only a finite or enumerable number of values, and for which $g \leqq f_A$ and $h \geqq f_A$ for any $x \varepsilon A$.

φ being totally additive, it will suffice to show the inequalities (5,2) in the case of the functions g and h being constant. Thus let $g(x) = c_1$ and $h(x) = c_2$ for every $x \varepsilon A$. From $g(x) = c_1 \leqq f_A$ for every $x \varepsilon A$ it follows that $A \subset [f \geqq c_1] = E_{c_1}^+$, and hence further by means of (5,1) that

$$\varphi(A) \geqq c_1 \mu(A) = I(g).$$

From $h(x) = c_2 \geqq f_A$ for every $x \varepsilon A$ it follows that $A \subset [f < c] = E_c^-$ for any $c < c_2$, and hence by means of (5,1) that

$$\varphi(A) \leq c\,\mu(A).$$

This inequality being valid for any $c > c_2$ we get

$$\varphi(A) \leq c_2\,\mu(A) = I(h)$$

and the proof is completed.

PART II.

On monotone functions. Functions of a set on Borel classes.

6. A theorem on decomposition.

The purpose of this section is to give an account of a theorem valid for monotone functions, a theorem which we shall apply in the following[1]. We shall confine ourselves to nondecreasing functions, but this is of no significance, as analogous theorems are immediately seen to be valid also for non-increasing functions. The non-decreasing functions are fixed by the following definition:

A function $f(x)$ *defined in* $a < x < b$ *is called non-decreasing, if* $f(x_2) \geqq f(x_1)$ *for* $x_2 > x_1$.

Together with the function $f(x)$ we shall consider two other functions, $\underline{f}(x)$ and $\overline{f}(x)$, determined by the following definitions:

$$\underline{f}(x) = \operatorname*{upper\ bound}_{a<\xi<x} f(\xi) \tag{6,1}$$

$$\overline{f}(x) = \operatorname*{lower\ bound}_{x<\xi<b} f(\xi). \tag{6,2}$$

Hence the following inequalities are immediately seen to be true

$$\underline{f}(x) \leqq f(x) \leqq \overline{f}(x) \tag{6,3}$$

$$f(x_1) \leqq \underline{f}(x_2) \text{ for } x_1 < x_2 \tag{6,4}$$

$$\overline{f}(x_1) \leqq f(x_2) \text{ for } x_1 < x_2. \tag{6,5}$$

1) Cf. CARATHÉODORY [1].

From (6,3), (6,4) and (6,5) the two functions $\underline{f}(x)$ and $\bar{f}(x)$ are seen to be non-decreasing.

We shall now show that $f(x)$ has in every point x a limit value from the left, $f(x-0)$, as well as a limit value from the right, $f(x+0)$, and that

$$f(x-0) = \underline{f}(x) \tag{6,6}$$

$$f(x+0) = \bar{f}(x). \tag{6,7}$$

In order to prove the first of these relations we must, consequently, prove that we can to an arbitrary $\varepsilon > 0$ determine a $\delta > 0$ such that

$$\underline{f}(x) - \varepsilon < f(\xi) < \underline{f}(x) + \varepsilon \tag{6,8}$$

for

$$x - \delta < \xi < x.$$

From (6,4) it is obvious that the right side of (6,8) will be true for every $\xi < x$. From (6,1) it follows that we can find a point ξ_1, $a < \xi_1 < x$, such that

$$f(\xi_1) > \underline{f}(x) - \varepsilon.$$

If $\delta = x - \xi_1$, the left hand side of (6,8) will, because of the monotony of $f(x)$, be true for every ξ of the interval $x - \delta < \xi < x$. In exactly the same way (6,7) is proved.

For every x we shall introduce the quantity $S(x)$ by the definition

$$S(x) = f(x+0) - f(x-0) = \bar{f}(x) - \underline{f}(x), \tag{6,9}$$

and call it *the saltus of the function in the point* x.

$f(x)$ is continuous in the point x (cf. (6,3)) if $S(x) = 0$ for this value of x, whereas the function is discontinuous in the point x if $S(x) > 0$.

In the remaining part of this section we shall assume the function $f(x)$ to be bounded in the interval $a < x < b$, i. e.

$$f(a+0) > -\infty \quad \text{and} \quad f(b-0) < \infty. \tag{6,10}$$

We shall denote by A_n the set of the points x, $a < x < b$, in which $S(x) > \frac{1}{n}$ (n positive, integer). Of this set of points is

true that it is either empty or consists of a finite number of points. Thus let $x_1, x_2, \cdots, x_p$ be p points of the interval $a < x_1 < x_2 < \cdots < x_p < b$, in which $S(x) > \frac{1}{n}$. We then have

$$f(b-0) - f(a+0) \geq (f(b-0) - f(x_p+0)) + \sum_{i=1}^{p} (f(x_i+0) - f(x_i-0)) + (f(x_1-0) - f(a+0)) > p \cdot \frac{1}{n}, \tag{6,11}$$

and hence

$$p < n\{f(b-0) - f(a+0)\}.$$

This being so, it is easily seen that *the set, A, of points of discontinuity of the function $f(x)$ of the interval $a < x < b$ is at most enumerable,* because

$$A = A_1 + A_2 + \cdots + A_n + \cdots.$$

For any choice of the two points x_1 and x_2 of the interval $a < x < b$, $x_1 < x_2$, we introduce the quantity $V_f(x_1, x_2)$ by the definition

$$V_f(x_1, x_2) = f(x_2) - f(x_1), \tag{6,12}$$

and call it the *variation of* $f(x)$ in the interval considered[1]. Furthermore we introduce the quantity $D_f(x_1, x_2)$ by the definition

$$D_f(x_1, x_2) = (f(x_1+0) - f(x_1)) + \sum_{i} S(\xi_i) + (f(x_2) - f(x_2-0)), \tag{6,13}$$

where the summation is extended over the (at most enumerably many) points of discontinuity of $f(x)$ contained in the interval $x_1 < x < x_2$. This latter quantity, $D_f(x_1\, x_2)$, will be called *the total discontinuity of* $f(x)$ in the interval considered[2].

By a transcription analogous to (6,11) it is clear that the following inequality holds true for every p concerned

$$\sum_{i=1}^{p} S(\xi_i) \leq f(x_2-0) - f(x_1+0),$$

[1] It is immediately evident that $V_f(x_1, x_2) \geq 0$.

[2] For any choice of x_1 and x_2 $(x_1 < x_2)$ is valid that $D_f(x_1, x_2) \geq 0$.

and hence

$$\sum_i S(\xi_i) \leq f(x_2 - 0) - f(x_1 + 0). \tag{6,14}$$

Inserting (6,14) in (6,13) we obtain

$$D_f(x_1, x_2) \leq (f(x_1 + 0) - f(x_1)) + (f(x_2 - 0) - f(x_1 + 0)) + (f(x_2) - f(x_2 - 0))$$
$$= f(x_2) - f(x_1) = V_f(x_1, x_2). \tag{6,15}$$

Thus we see that the total discontinuity of an interval never exceeds the variation of the function.

From the definition (6,13) it is immediately obvious that

$$D_f(x_1, x_3) = D_f(x_1, x_2) + D_f(x_2, x_3) \tag{6,16}$$

for $x_1 < x_2 < x_3$.

After these preliminary remarks we can go over to the proof of the important theorem of decomposition:

Let $f(x)$ be a bounded non-decreasing function defined in $a < x < b$. This function may then be written as

$$f(x) = g(x) + h(x), \tag{6,17}$$

where both $g(x)$ and $h(x)$ are non-decreasing functions, and where, furthermore, $g(x)$ is continuous, whereas for $h(x)$

$$V_h(x_1, x_2) = D_h(x_1, x_2) = D_f(x_1, x_2) \tag{6,18}$$

for any choice of x_1 and x_2, $a < x_1 < x_2 < b$.

We choose a fixed point x_0 of the interval $a < x < b$ and introduce a function $h(x)$ by the definition

$$h(x) = \begin{cases} -D_f(x, x_0) & \text{for } a < x < x_0 \\ 0 & \text{for } x = x_0 \\ D_f(x_0, x) & \text{for } x_0 < x < b. \end{cases} \tag{6,19}$$

We shall now prove the function thus defined to have the properties expressed in the relations (6,18).

By means of (6,16) it is immediately seen that for two arbitrary numbers x_1 and x_2, $x_1 < x_2$, we have

$$V_h(x_1, x_2) = h(x_2) - h(x_1) = D_f(x_1, x_2), \tag{6,20}$$

from which it particularly follows that $h(x)$ is a non-decreasing function. (6,20) in connection with (6,13) gives

$$h(x_2) - h(x_1) \leq f(x_1 + 0) - f(x_1) \tag{6,21}$$

$$h(x_2) - h(x_1) \leq f(x_2) - f(x_2 - 0), \tag{6,22}$$

and (6,20) in connection with (6,15)

$$h(x_2) - h(x_1) \leq f(x_2) - f(x_1). \tag{6,23}$$

(6,21) being true for every $x_1 < x_2$, we can deduce the following inequality

$$h(x_1 + 0) - h(x_1) \geq f(x_1 + 0) - f(x_1).^{1)} \tag{6,24}$$

Similarly we deduce from (6,23) that

$$h(x_1 + 0) - h(x_1) \leq f(x_1 + 0) - f(x_1). \tag{6,25}$$

From (6,24) and (6,25) it follows for every x, $a < x < b$, that

$$h(x + 0) - h(x) = f(x + 0) - f(x). \tag{6,26}$$

After the analogy of (6,26) we can deduce

$$h(x) - h(x - 0) = f(x) - f(x - 0), \tag{6,27}$$

which in connection with (6,26) gives

$$h(x + 0) - h(x - 0) = f(x + 0) - f(x - 0). \tag{6,28}$$

By application of (6,20), (6,26), (6,27) and (6,28) the definition (6,13) gives

$$D_h(x_1, x_2) = D_f(x_1, x_2) = V_h(x_1, x_2).$$

Thus we see that the function $h(x)$ has the properties expressed in the relations (6,18).

The proof will be complete, if we can prove the function

1) The existence of $h(x_1 + 0)$ is a consequence of $h(x)$ being a non-decreasing function.

$$g(x) = f(x) - h(x) \tag{6,29}$$

to be non-decreasing and continuous. From (6,29) we obtain

$$g(x_2) - g(x_1) = (f(x_2) - f(x_1)) - (h(x_2) - h(x_1)),$$

which for $x_1 < x_2$ by application of (6,23) gives

$$g(x_2) \geq g(x_1).$$

Thus we get

$$g(x+0) - g(x-0) = (f(x+0) - f(x-0)) - (h(x+0) - h(x-0)),$$

which by application of (6,28) gives

$$g(x+0) = g(x-0).$$

Since we, furthermore, (cf. (6,3), (6,6) and (6,7)) have the inequalities

$$g(x-0) \leq g(x) \leq g(x+0)$$

the proof of the continuity of $g(x)$ is completed.

We shall conclude this section with some remarks on the connection between the various decompositions of $f(x)$. In case

$$f(x) = g(x) + h(x)$$

is a decomposition with the properties mentioned in the theorem, it will be true (for every c) that

$$f(x) = (g(x) + c) + (h(x) - c)$$

will also be so, and thus all decompositions will be comprised. Let for instance

$$f(x) = g_1(x) + h_1(x)$$

be a decomposition having the properties mentioned in the theorem. Then we can prove that $h_1(x) = h(x) - c$ (and hence $g_1(x) = g(x) + c$).

From (6,18) it follows that

$$V_h(x_1, x_2) = V_{h_1}(x_1, x_2) \; (= D_f(x_1, x_2))$$

for $x_1 < x_2$ which, if we substitute x for x_2, gives

$$h(x) - h(x_1) = h_1(x) - h_1(x_1) \text{ for } x > x_1$$

or, if we substitute x for x_1 and x_1 for x_2

$$h(x_1) - h(x) = h_1(x_1) - h_1(x) \text{ for } x < x_1.$$

Thus we have for every x, $a < x < b$,

$$h(x) = h_1(x) - \big(h_1(x_1) - h(x_1)\big) = h_1(x) - c,$$

which was to be proved.

7. Functions of a set having the Borel class as defining region.

The set of points lying on the axis of the real numbers constitutes a set of points, which in this section will be called E. When we in this section speak of a set, it will be understood to be a subset of E. By an *interval* I will in the following be understood a set of points having the form $[a \leqq x < b]$, where a and b are finite. All the intervals form a class of sets $\mathfrak{F}$. The smallest extension of $\mathfrak{F}$ to a ring we shall denote by $\mathfrak{G}$. It is clear that this ring consists of the empty set together with all finite sums of intervals. The smallest extension of $\mathfrak{F}$ to a Borel ring will be called $\mathfrak{B}$. This class of sets $\mathfrak{B}$ we shall call *the Borel class on the axis of the real numbers*, and every set $A \varepsilon \mathfrak{B}$ will be called a *Borel set*.

A function of a set φ defined in $\mathfrak{F}$ will be called a *function of an interval.* A function of an interval φ will be called *continuous from the inside*, if for every interval $I = [a \leqq x < b]$ and for every sequence of intervals $I_1, I_2, \cdots, I_n, \cdots$, where $I_n = [a \leqq x < b_n]$, $b_1 < b_2 < \cdots < b$ and $\lim_n b_n = b$, we have that $\varphi(I) = \lim_n \varphi(I_n)$.

On the connection between functions of an interval and measures the following theorem can be proved:

A finite, additive function of an interval φ can then and only then be extended to a measure φ^* defined in $\mathfrak{B}$, when it is non-negative and continuous from the inside.

We shall first prove the conditions to be necessary. From $\varphi^* \geqq 0$ for every $A \varepsilon \mathfrak{B}$ it follows that $\varphi \geqq 0$ for every $A \varepsilon \mathfrak{F}$, i.e. φ is non-negative. From $a < b_1 < b_2 < \cdots < b$ and $\lim_n b_n = b$ it follows that

$$\mathfrak{D}_n [b_n \leqq x < b] = 0, \tag{7,1}$$

and hence further (see theorem VIII, page 9)

$$\lim_n \varphi([b_n \leqq x < b]) = 0. \tag{7.2}$$

Since

$$\varphi([a \leqq x < b]) = \varphi([a \leqq x < b_n]) + \varphi([b_n \leqq x < b])$$

for every n, (7,2) implies that

$$\lim_n \varphi([a \leqq x < b_n]) = \varphi([a \leqq x < b]),$$

i. e. φ is continuous from the inside.

Next we shall prove the conditions to be sufficient. The extension can be performed in such a manner that we first extend φ to a content ψ defined in $\mathfrak{G}$, and then prove that this content can be extended to a measure (defined in $\mathfrak{B}$).

For every set $A \varepsilon \mathfrak{G}$ we put

$$\psi(A) = 0 \text{ when } A = 0$$

$$\psi(A) = \sum_{i=1}^{n} \varphi(I_i) \text{ when } A = I_1 + I_2 + \cdots + I_n.^{1)}$$

The function of a set ψ thus derived, is at once seen to be an extension of φ to a content. If ψ is totally additive, this content can be extended to a measure defined in $\mathfrak{B}$ (cf. the theorem on extension page 10).

So our problem is to show that if $A_1, A_2 \cdots, A_n, \cdots$ is a sequence of sets, all belonging to $\mathfrak{G}$, and for which $A_1 \supset A_2 \supset \cdots \supset A_n \supset \cdots$ and $\psi(A_n) \geqq k > 0$ for all n, then the set $\mathfrak{D}_n A_n$ is empty (see page 11).

Since $A_n \varepsilon \mathfrak{G}$ it can be written in the form

$$A_n = \sum_p{}^{*} [a_{np} \leqq x < b_{np}],$$

where $\sum^{*}$ is to denote that the number of the addends is finite. φ being continuous from the inside, we can for every n determine a set $B_n \subset A_n$

1) It can easily be proved that this definition determines the function $\psi(A)$ uniquely.

$$B_n = \sum_p{}^{*}[a_{np} \leqq x < c_{np}], \quad (a_{np} < c_{np} < b_{np})$$

such that

$$\psi(A_n - B_n) \leqq \frac{k}{2^n}. \tag{7,3}$$

If we put

$$C_n = B_1 B_2 \cdots B_n,$$

we have $C_n \subset B_n$ and $C_1 \supset C_2 \supset \cdots$. Further we get

$$A_n - C_n \subset (A_1 - B_1) \dotplus \cdots \dotplus (A_n - B_n),$$

and hence, by means of (7,3),

$$\psi(A_n - C_n) \leqq \frac{k}{2} + \cdots + \frac{k}{2^n} < k.$$

Since $\psi(A_n) \geqq k$, we see that C_n is non-empty for every value of n. In every C_n we may thus choose a point x_n, and by that get the sequence $x_1, x_2, \cdots, x_n, \cdots$. Since $C_n \subset A_n \subset A_1$ for every n, we see that this sequence is bounded. Thus it is possible to choose a convergent subsequence from it. Its limit point is called x. Due to $B_n \supset C_n \supset C_{n+1} \supset \cdots$ all the points $x_n, x_{n+1}, \cdots$ will belong to B_n, which will further imply that

$$x \varepsilon \sum_p{}^{*}[a_{np} \leqq x \leqq c_{np}] \subset A_n.$$

Thus we have

$$x \varepsilon \mathfrak{D}_n A_n,$$

i. e. the set $\mathfrak{D}_n A_n$ is non-empty, which was to be proved.

If the function of an interval in question for every interval $[a \leqq x < b]$ has the value $b - a$, we shall call the measure, obtained by the extension and having $\mathfrak{B}$ as defining region, *the Borel measure on the axis of the real numbers*, and therefore $\mathfrak{B}$ will also be called *the class of Borel measurable sets on the axis of the real numbers.*

If $f(x)$ is a finite function defined in E, it is possible from this to form a finite additive function of an interval by the following definition

$$\varphi([a \leqq x < b]) = f(b) - f(a). \tag{7,4}$$

Conversely it is possible to find to a finite, additive function of an interval φ a function $f(x)$ defined in E, so that (7,4) is satisfied for every interval, and it is clear that the difference between two such possible functions f is constant.

The function of an interval φ is then and only then non-negative, when it is valid for any pair of numbers (a, b) where $a < b$ that $f(a) \leq f(b)$, i. e. when $f(x)$ is *non-decreasing*. We see furthermore that φ is then and only then *continuous from the inside*, when $f(x)$ is *continuous from the left* for every x.

Applying the theorem page 29 we now have:

To a finite function $f(x)$ defined in E we have then and only then a corresponding measure φ defined in $\mathfrak{B}$, so that

$$\varphi([a \leq x < b]) = f(b) - f(a)$$

for every interval $[a \leq x < b]$, when $f(x)$ is non-decreasing and continuous from the left. This measure φ will be uniquely defined.

If $F(x)$ is a function in $\mathfrak{B}$ and $A \in \mathfrak{B}$, we denote the integral of $F(x)$ over A with respect to the measure φ by

$$\int_A F(x)\, d f(x)$$

or, if especially $A = [a \leq x < b]$,

$$\int_a^b F(x)\, d f(x).$$

This integral is called the *Lebesgue-Stieltjes-integral* with respect to $f(x)$.

8. Functions of a set having $\mathfrak{B}_1$ as defining region.

The set of points x, belonging to the interval $0 \leq x < 1$, forms a set of points, which we in this section shall denote by E_1, and speaking in this section of a set, we shall always mean a subset of E_1. The set of intervals $[a \leq x < b]$, $0 \leq a < b \leq 1$, forms a class of sets $\mathfrak{F}_1$. The smallest extension of $\mathfrak{F}_1$ to a ring we shall denote by $\mathfrak{G}_1$, and the smallest extension of $\mathfrak{F}_1$ to a Borel ring we shall call $\mathfrak{B}_1$. This class of sets $\mathfrak{B}_1$ we shall call *the Borel class of the interval* (0,1). It is evident that the theorems

formulated in the preceding section will still hold true, even if we confine ourselves to the interval (0,1).

Now suppose given a finite function $f(x)$ defined in $0 \leqq x \leqq 1$, which is non-decreasing and continuous from the left in every point. We may then (cf. the theorem page 32) uniquely determine a measure φ^* defined in $\mathfrak{B}_1$, such that

$$\varphi^*([a \leqq x < b]) = f(b) - f(a) \tag{8,1}$$

for every choice of a and b, $0 \leqq a < b \leqq 1$.

In the following we shall put $f(0) = 0$, which does not limit the generality of our investigation.

According to the theorem on decomposition (page 26) $f(x)$ may be written in the form

$$f(x) = g(x) + h(x), \tag{8,2}$$

where $g(x)$ and $h(x)$ are non-decreasing functions, $g(x)$ being furthermore continuous, whereas for $h(x)$

$$V_h(a, b) = D_h(a, b) = D_f(a, b) \tag{8,3}$$

for every choice of a and b, $0 \leqq a < b \leqq 1$. This decomposition can, furthermore, be performed in such a way that $g(0) = 0$ (and hence $h(0) = 0$), and is in that case uniquely defined. Since $f(x)$ was given to be continuous from the left and $g(x)$ is continuous, it follows that $h(x)$ is continuous from the left in any point.

We can now uniquely determine two measures φ_1^* and φ_2^* defined in $\mathfrak{B}_1$, such that

$$\varphi_1^*([a \leqq x < b]) = g(b) - g(a) \tag{8,4}$$

and

$$\varphi_2^*([a \leqq x < b]) = h(b) - h(a) \tag{8,5}$$

for every choice of a and b.

Regarding the connection between φ^*, φ_1^* and φ_2^* we can prove the relation

$$\varphi^* = \varphi_1^*(A) + \varphi_2^*(A) \tag{8,6}$$

for every set $A \varepsilon \mathfrak{B}_1$.

We only remark that the function of a set

$$\varphi_1^*(A) + \varphi_2^*(A)$$

is a measure defined in $\mathfrak{B}_1$, and that, if A is an interval $[a \leqq x < b]$, it will take on the value

$$\varphi_1^*([a \leqq x < b]) + \varphi_2^*([a \leqq x < b]) = g(b) - g(a) + h(b) - h(a),$$

which by application of (8,2) can be changed to

$$\varphi_1^*([a \leqq x < b]) + \varphi_2^*([a \leqq x < b]) = f(b) - f(a).$$

If we compare this result with (8,1), we shall see that the two measures $\varphi^*(A)$ and $\varphi_1^*(A) + \varphi_2^*(A)$ coincide in every interval. Consequently they are both an extension of the same function of an interval, and will naturally coincide for the whole of $\mathfrak{B}_1$.

We shall conclude this section with an investigation of what values the two functions of a set φ_1^* and φ_2^* can take on in $\mathfrak{B}_1$.

From $0 \subset A \subset E_1$ for every $A \in \mathfrak{B}_1$ it follows that

$$0 \leqq \varphi_1^*(A) \leqq \varphi_1^*(E_1) = g(1),$$

and since $g(x)$ is continuous, it will take on any value y_0 between 0 and $g(1)$ for at least one value of x, $x = x_0$. If we choose $A = [0 \leqq x < x_0]$ we get $\varphi_1^*(A) = y_0$. *Thus we see that the values of φ_1^* constitute a closed interval.*

The points of discontinuity of the function $h(x)$ (or, what is the same, of the function $f(x)$) form an at most enumerable set of points $N = \{\xi_n\}$ situated in the interval $0 \leqq x < 1$.[1] By the saltus at a point x we understood (cf. (6,9)) the quantity

$$S(x) = h(x+0) - h(x-0).$$

For the special case $x = 0$ we write

$$S(x) = h(x+0) - h(x).$$

[1] The fact that the eventual points of discontinuity are situated in this half-open interval is a consequence of $f(x)$ being continuous from the left.

We shall now prove that we have for every set $A \in \mathfrak{B}_1$

$$\varphi_2^*(A) = \sum_{\xi_i \in A} S(\xi_i), \tag{8,7}$$

where the summation is extended over the—at most enumerably many—points of discontinuity for $h(x)$, belonging to the set A.

We first note that the function of a set

$$\sum_{\xi_i \in A} S(\xi_i) \tag{8,8}$$

is a measure defined in $\mathfrak{B}_1$. If, especially, A is an interval $[a \leq x < b]$, we have

$$\sum_{\xi_i \in A} S(\xi_i) = h(b) - h(a). \tag{8,9}$$

Applying (6,12), (6,13), and (8,3) we get

$$h(b) - h(a) = h(a+0) - h(a) + \sum_i S(\xi_i) + h(b) - h(b-0),$$

where the summation is extended over the points of discontinuity situated in the interval $a < x < b$. Since $h(x)$ is continuous from the left ($h(a) = h(a-0)$ and $h(b) = h(b-0)$), this may be written

$$h(b) - h(a) = \sum_{\xi_i \in A} S(\xi_i),$$

and the proof of (8,9) is completed.

If we compare (8,9) with (8,5), we see that the two measures $\varphi_2^*(A)$ and $\sum_{\xi_i \in A} S(\xi_i)$ agree in every interval. Consequently they are both an extension of the same function of an interval, and thus they must coincide in the whole of $\mathfrak{B}_1$, and we have proved (8,7). The formula (8,7) may also be written

$$\varphi_2^*(A) = \sum_{\xi_i \in AN} S(\xi_i). \tag{8,10}$$

If the set A consists of only one point a, we get the special case

$$\varphi_2^*(A) = S(a). \tag{8,11}$$

Thus we have realized what values the function φ_2^* can take on. If the number of points of discontinuity of the function $f(x)$ is finite: $\xi_1, \xi_2, \cdots, \xi_n$, respectively enumerable $\xi_1, \xi_2, \cdots, \xi_n, \cdots$, *the values of* φ_2^* *will be all numbers of the form*

$$e_1 S(\xi_1) + e_2 S(\xi_2) + \cdots + e_n S(\xi_n), \tag{8,12}$$

respectively

$$e_1 S(\xi_1) + e_2 S(\xi_2) + \cdots + e_n S(\xi_n) + \cdots, \tag{8,13}$$

where the e's independently of each other take on the values 0 *or* 1.

PART III.

A theorem on bounded measures in abstract space.

9. A theorem on series of positive terms.

Given a convergent series of positive terms

$$a = \sum_{n=1}^{\infty} a_n = a_1 + a_2 + \cdots + a_n + \cdots \quad (a_n > 0). \tag{9,1}$$

Together with this series we shall consider all series having the form

$$\sum_{n=1}^{\infty} e_n a_n = e_1 a_1 + e_2 a_2 + \cdots + e_n a_n + \cdots, \tag{9,2}$$

where the e's independently of each other take on the values 0 or 1. Each of these series (9,2) is convergent, and its sum satisfies the relation

$$0 \leq \sum_{n=1}^{\infty} e_n a_n \leq a. \tag{9,3}$$

We shall now prove that the set of numbers, whose elements are the sums of the series (9,2), is *closed*. Let

$$\left.\begin{aligned} s_1 &= a_{11} + a_{12} + \cdots + a_{1n} + \cdots \\ s_2 &= a_{21} + a_{22} + \cdots + a_{2n} + \cdots \\ &\cdots\cdots\cdots\cdots\cdots\cdots \\ s_m &= a_{m1} + a_{m2} + \cdots + a_{mn} + \cdots \\ &\cdots\cdots\cdots\cdots\cdots\cdots \end{aligned}\right\} \tag{9,4}$$

be a sequence of series of the form (9,2), i. e. a_{mn} has for every m one of the values 0 or a_n, and let furthermore the sequence

$$s_1, s_2, \cdots, s_m, \cdots$$

be convergent to the limit value s. We shall now prove that among the series (9,2) at least one has the sum s. In the sequence of numbers

$$a_{11}, a_{21}, \cdots, a_{m1}, \cdots$$

at least one of the numbers 0 or a_1 will appear an infinite number of times. Let a_1^* denote one of these two numbers satisfying this condition. In the sequence of pairs of numbers

$$(a_{11}, a_{12}), (a_{21}, a_{22}), \cdots, (a_{m1}, a_{m2}), \cdots$$

there will, consequently, be an infinite number having a_1^* in the first place. Let a_2^* be a number which in the corresponding subsequence appears an infinite number of times in the second place. In the sequence of set of numbers

$$(a_{11}, a_{12}, a_{13}), (a_{21}, a_{22}, a_{23}), \cdots, (a_{m1}, a_{m2}, a_{m3}), \cdots$$

there will thus be an infinite number having (a_1^*, a_2^*) in the two first places. Let a_3^* be a number which in the corresponding subsequence appears an infinite number of times in the third place. By continuing this process the number a_n^* is defined for every n. The series

$$a_1^* + a_2^* + \cdots + a_n^* + \cdots \tag{9,5}$$

is, being a subseries of (9,1), convergent, and we shall now prove that it has the sum s. Suppose we for the present term the sum of it s^*. The convergence of (9,1) implies that to a given $\varepsilon > 0$ we may determine N, such that

$$\sum_{n=N+1}^{\infty} a_n < \frac{\varepsilon}{3}.$$

Moreover we may, among the series (9,1), determine one having $a_1^*, a_2^*, \cdots, a_N^*$ in the N first places

$$s_i = a_1^* + a_2^* + \cdots + a_N^* + a_{i,N+1} + a_{i,N+2} + \cdots, \qquad (9,6)$$

and such that $\left| s - s_i \right| < \frac{\varepsilon}{3}$.

Accordingly we have

$$\begin{aligned} |s^* - s| &= |(s^* - (a_1^* + \cdots + a_N^*)) - (s_i - (a_1^* + \cdots + a_N^*)) + (s_i - s)| \\ &\leqq |s^* - (a_1^* + \cdots + a_N^*)| + |s_i - (a_1^* + \cdots + a_N^*)| + |s_i - s| \\ &< \frac{\varepsilon}{3} + \frac{\varepsilon}{3} + \frac{\varepsilon}{3} = \varepsilon. \end{aligned}$$

Hence we obtain

$$s^* = s$$

and the proof is completed.

10. Bounded measures having $\mathfrak{B}_1$ as defining region.

In II, 3 we have already mentioned the class of sets $\mathfrak{B}_1$, the so-called Borel class, defined in the interval (0,1). The interval $[0 \leqq x < 1]$ was termed E_1. Now let φ be a bounded measure defined in $\mathfrak{B}_1$, i. e. $\varphi(E_1) < \infty$. On such a measure we shall in this section prove the following theorem:

The set of numbers whose elements are the values of a bounded measure φ defined in $\mathfrak{B}_1$ is closed.

Together with the measure φ we shall consider the function $f(x)$ defined in $0 \leqq x \leqq 1$ determined by

$$\varphi([0 \leqq x < a]) = f(a)$$

$$f(0) = 0. \qquad (10,1)$$

The non-decreasing function $f(x)$ may then be decomposed to the form

$$f(x) = g(x) + h(x)$$

(cf. (8,2)), and this decomposition givesr ise to a decomposition of φ to the form

$$\varphi(A) = \varphi_1(A) + \varphi_2(A) \qquad (10,2)$$

for every $A \varepsilon \mathfrak{B}_1$ (cf. (8,6)). The set of points of discontinuity of the function $f(x)$ is at most an enumerable set $N = \{\xi_n\}$. We have previously shown that the set of numbers M_1, whose

elements are the values of $\varphi_1(A)$, is closed. We have furthermore (cf. (8,10)) proved that

$$\varphi_2(A) = \sum_{\xi_i \in AN} S(\xi_i), \tag{10,3}$$

for every $A \in \mathfrak{B}_1$. The set of numbers M_2, whose elements are the values of $\varphi_2(A)$, has (cf. (8,12) and (8,13)) either the form

$$e_1 S(\xi_1) + e_2 S(\xi_2) + \cdots + e_n S(\xi_n) \tag{10,4}$$

or

$$e_1 S(\xi_1) + e_2 S(\xi_2) + \cdots + e_n S(\xi_n) + \cdots. \tag{10,5}$$

If the set of numbers is of the form (10,4), it is obvious that it is closed, as it is finite. If it is of the form (10,5), we may from the result obtained in the previous section conclude that it is closed.

The set of numbers M, whose elements are the values of $\varphi(A)$, is according to (10,2) produced by adding elements of M_2 to elements of M_1. If we can prove that the sum of an arbitrary element α of M_1 and an arbitrary element β of M_2 gives an element of M, our proof will be completed. Let, therefore, $\varphi_1(A) = \alpha$ and $\varphi_2(B) = \beta$, $A \in \mathfrak{B}_1$, $B \in \mathfrak{B}_1$. Our task is now to show the existence of a set $A^* \in \mathfrak{B}_1$, such that

$$\varphi(A^*) = \alpha + \beta. \tag{10,6}$$

If we put

$$A^* = (A - AN) + BN, \tag{10,7}$$

we have $A^* \in \mathfrak{B}_1$. It now follows, on account of (10,2), that

$$\left.\begin{aligned} \varphi(A^*) &= \varphi(A - AN) + \varphi(BN) = \\ &\varphi_1(A - AN) + \varphi_2(A - AN) + \varphi_1(BN) + \varphi_2(BN). \end{aligned}\right\} \tag{10,8}$$

AN being at most an enumerable set, it follows that

$$\varphi_1(AN) = 0. \tag{10,9}$$

From $A - AN \subset E_1 - N$ follows

$$0 \leqq \varphi_2(A - AN) \leqq \varphi_2(E_1 - N) = 0. \tag{10,10}$$

After the analogy of (10,9) we have

$$\varphi_1(BN) = 0. \tag{10,11}$$

Finally we derive

$$\varphi_2(BN) = \sum_{\xi_i \in BN}' S(\xi_i) = \varphi_2(B) = \beta. \tag{10,12}$$

Comprising (10,8)—(10,12) we get

$$\varphi(A^*) = \alpha + 0 + 0 + \beta = \alpha + \beta.$$

Hence the set A^* has the property expressed by (10,6), and the proof is completed.

11. Bounded measures in abstract space.

In this section will be shown that the theorem on measures defined in $\mathfrak{B}_1$, formulated and proved in III, 10, is valid in the abstract space too.

Let E be an arbitrary set, and let $\mathfrak{F}$ be a class of sets containing E. Further let ψ be a bounded measure defined in $\mathfrak{F}$, i. e. $\psi(E) < \infty$. Without loss of generality we may assume that $\psi(E) = 1$. On such a measure we shall in this section prove the following theorem:

The set of numbers whose elements are the values of a bounded measure ψ defined in $\mathfrak{F}$ is closed.

To prove the theorem we shall make use of a representation from the class of sets $\mathfrak{F}$ to the class of sets $\mathfrak{B}_1$, whereby the theorem is retraced to the theorem proved in the previous section.

Let

$$A_1, A_2, \cdots, A_n, \cdots \tag{11,1}$$

be a sequence of sets all belonging to $\mathfrak{F}$, and for which the corresponding sequence of numbers

$$\psi(A_1), \psi(A_2), \cdots, \psi(A_n), \cdots \tag{11,2}$$

is convergent to the limit value g. We now prove the existence of a set $A \in \mathfrak{F}$, for which

$$\psi(A) = g. \tag{11,3}$$

Without loss of generality we may assume that $A_2 = E - A_1$. The importance of this special choice of the set A_2 will be evident later on.

The coupling mentioned above will now be carried out by two stages:

I). To E is coupled the interval (0,1). To the sets $C_1 = A_1$, $C_0 = 0$ and $C_2 = E - A_1$, all belonging to $\mathfrak{F}$, are, in the order given, coupled the intervals $(0, \frac{1}{3})$, $(\frac{1}{3}, \frac{2}{3})$ and $(\frac{2}{3}, 1)$. The sets $C_{11} = A_1 A_2$, $C_{10} = 0$ and $C_{12} = A_1 (E - A_2)$, which are all subsets of C_1 and have the sum C_1, all belong to $\mathfrak{F}$. To these are coupled, in the order given, the intervals $(0, \frac{1}{9})$, $(\frac{1}{9}, \frac{2}{9})$ and $(\frac{2}{9}, \frac{1}{3})$. The sets $C_{21} = (E - A_1) A_2$, $C_{20} = 0$ and $C_{22} = (E - A_1)(E - A_2)$, which are all subsets of C_2 and have the sum C_2, likewise belong to $\mathfrak{F}$. To these are coupled the intervals $(\frac{2}{3}, \frac{7}{9})$, $(\frac{7}{9}, \frac{8}{9})$ and $(\frac{8}{9}, 1)$. The sets $C_{111} = A_1 A_2 A_3$, $C_{110} = 0$, $C_{112} = A_1 A_2 (E - A_3)$, $C_{121} = A_1 (E - A_2) A_3$, $C_{120} = 0$ and $C_{122} = A_1 (E - A_2)(E - A_3)$ all belong to $\mathfrak{F}$. To these are coupled the intervals $(0, \frac{1}{27})$, $(\frac{1}{27}, \frac{2}{27})$, $(\frac{2}{27}, \frac{1}{9})$, $(\frac{2}{9}, \frac{7}{27})$, $(\frac{7}{27}, \frac{8}{27})$ and $(\frac{8}{27}, \frac{1}{3})$. Thus we go on infinitely. Each of the produced C-sets will belong to $\mathfrak{F}$. It is a product of as many factors as the number of indices. A number 0 in the last place of the series of indices means that the set is empty. A number 1 in the n'th place of the series of indices means that A_n appears as a factor, whereas a number 2 in the n'th place means that $E - A_n$ appears as a factor. Thus we give as an example

$$C_{11211121} = A_1 A_2 (E - A_3) A_4 A_5 (E - A_6) A_7$$

$$C_{21211120} = 0 .$$

As an illustration we have in fig. 1 (cf. the end of the paper) given an outline of this decomposition and the corresponding intervals.

II). To each number of the form

$$\frac{k}{3^n} \quad (n \text{ positive integer}, \; k = 1, 2, \cdots, 3^n - 1)$$

is now coupled a set $C_{\frac{k}{3^n}}$. If the number $\frac{k}{3^n}$ is *in the interior* of an interval, to which we have above coupled the empty set,

$C_{\frac{k}{3^n}}$ is put equal to the empty set 0. Concerning an end point of one of the intervals shown in fig. 1 we shall, however, proceed as follows. We select all the sets in our outline of which one end point of the corresponding interval is the number $\frac{k}{3^n}$ and whose series of indices does not comprise the number 0, and $C_{\frac{k}{3^n}}$ equal to the product of these sets. $\mathfrak{F}$ being a Borel ring, and all the sets in fig. 1 belonging to $\mathfrak{F}$, the same will be true for any set $C_{\frac{k}{3^n}}$. By this method we get

$$\left.\begin{aligned} C_{\frac{1}{3}} &= C_1 C_{12} C_{122} \cdots \\ C_{\frac{2}{3}} &= C_2 C_{21} C_{211} \cdots \\ C_{\frac{1}{9}} &= C_{11} C_{112} C_{1122} \cdots \\ C_{\frac{2}{9}} &= C_{12} C_{121} C_{1211} \cdots \end{aligned}\right\} \qquad (11,4)$$

and so on.

The decomposition (fig. 1) carried out in I) is now modified as follows. To the set E is coupled the interval $0 \leqq x < 1$. To the sets $C_1 - C_{\frac{1}{3}}$, $C_{\frac{1}{3}}$, 0, $C_{\frac{2}{3}}$ and $C_2 - C_{\frac{2}{3}}$, in the order given, are coupled the interval $0 \leqq x < \frac{1}{3}$, the point $x = \frac{1}{3}$, the interval $\frac{1}{3} < x < \frac{2}{3}$, the point $x = \frac{2}{3}$ and the interval $\frac{2}{3} < x < 1$. To the sets $C_{11} - C_{\frac{1}{9}}$, $C_{\frac{1}{9}}$, 0, $C_{\frac{2}{9}}$, $C_{12} - C_{\frac{2}{9}} - C_{\frac{1}{3}}$ (which, as we know, have the sum $C_1 - C_{\frac{1}{3}}$) are coupled, in the order given, the interval $0 \leqq x < \frac{1}{9}$, the point $x = \frac{1}{9}$, the interval $\frac{1}{9} < x < \frac{2}{9}$, the point $x = \frac{2}{9}$ and the interval $\frac{2}{9} < x < \frac{1}{3}$, and so on. This new decomposition of E and the corresponding intervals are outlined in fig. 2.

It must be emphasized that *any* of the sets appearing in the outline fig. 2 belongs to $\mathfrak{F}$, as well as the fact that each of the sets appearing in the sequence (11,1) are obtained by summation from the sets in the figure. For instance we thus have

$$A_1 = (C_1 - C_{\frac{1}{3}}) + C_{\frac{1}{3}}$$

and

$$A_2 = (C_{11} - C_{\frac{1}{9}}) + C_{\frac{1}{9}} + (C_{21} - C_{\frac{2}{3}} - C_{\frac{7}{9}}) + C_{\frac{2}{3}} + C_{\frac{7}{9}}.$$

Now we shall introduce a function $f(x)$ defined in $0 \leqq x \leqq 1$, which is done by the following definitions:

1) $f(0) = 0$.

2) Let x^* be a number of the form $\frac{k}{3^n}$ (n positive, integer, $k = 1, 2, \cdots, 3^n$). We then put

$$f(x^*) = \psi(C^*), \tag{11,5}$$

where C^* is the set coupled to the interval $0 \leqq x < x^*$. As an example we thus get $f(1) = \psi(E) = 1$, $f(\frac{1}{3}) = \psi(C_1 - C_{\frac{1}{3}})$, $f(\frac{2}{3}) = \psi(C_1)$, $f(\frac{7}{9}) = \psi(C_1 + C_{21} - C_{\frac{7}{9}})$. Especially we observe that $f(x)$ has, for every $x^* > \frac{7}{9}$, the value 1, because the set C_{22} (on account of the special assumption that $A_2 = E - A_1$) is empty.

If x_1 and $x_2\,(> x_1)$ both are of the form $\frac{k}{3^n}$, we get

$$f(x_2) - f(x_1) = \psi(D) \geqq 0, \tag{11,6}$$

where D is the set coupled to the interval $x_1 \leqq x < x_2$.

By this definition of $f(x)$ the function acquires the following property: if $x^*\,(< 1)$ as well as $x_1, x_2, \cdots, x_n, \cdots$ are numbers of the form $\frac{k}{3^n}$, for which $x_1 < x_2 < \cdots < x_n < \cdots < x^*$ and $\lim_n x_n = x^*$, then the equation

$$\lim_n f(x_n) = f(x^*)$$

holds true.

This is understood in the following way. Denote by D_n the set corresponding to the interval $0 \leqq x < x_n$, for any n, and denote by C^* the set corresponding to the interval $0 \leqq x < x^*$. It now remains to be proved that

$$\lim_n \psi(D_n) = \psi(C^*).$$

For any n we have $D_n \subset C^*$. Consequently we obtain

$$\lim_n \left(\psi(C^*) - \psi(D_n)\right) = \lim_n \psi(C^* - D_n).$$

From $C^* - D_1 \supset C^* - D_2 \supset \cdots \supset C^* - D_n \supset \cdots$ we may next conclude (see VIII page 9) that

$$\lim_n \psi(C^* - D_n) = \psi\left(\prod_n (C^* - D_n)\right). \tag{11,7}$$

From our construction it is, however, easy to see that

$$\prod_n (C^* - D_n) = 0,$$

together with which (11,7) gives

$$\lim_n \psi(C^* - D_n) = \psi(0) = 0,$$

which was to be proved.

The function has the same property also for $x^* = 1$, because $f(x)$ has, as above remarked, the value 1, when x is of the form $\frac{k}{3^n}$ and greater than $\frac{7}{9}$.

3) Supposing further that x_0 is a number which is not of the form $\frac{k}{3^n}$. Corresponding to this we choose a sequence of numbers $x_1, x_2, \cdots, x_n, \cdots$ which all have the form $\frac{k}{3^n}$, and for which $x_1 < x_2 < \cdots < x_n < \cdots < x_0$ and $\lim_n x_n = x_0$. We shall again denote by D_n the set corresponding to the interval $0 \leq x < x_n$. The set $\mathfrak{S}_n D_n$ is at once seen to be independent of the sequence chosen and dependent only on x_0. We now let the set $\mathfrak{S}_n D_n$ correspond to the interval $0 \leq x < x_0$ and write

$$f(x_0) = \psi\left(\mathfrak{S}_n D_n\right), \tag{11,8}$$

by which the function $f(x)$ is defined for each x in the interval $0 \leq x \leq 1$. From $D_1 \subset D_2 \subset \cdots \subset D_n \subset \cdots$ follows (see VII page 9)

$$\psi\left(\mathfrak{S}_n D_n\right) = \lim_n \psi(D_n)$$

and hence

$$f(x_0) = \lim_n \psi(D_n). \tag{11,9}$$

About the function introduced by these definitions it now remains to be proved that it is non-decreasing and *continuous from the left* in any point.

We shall first prove that $f(x)$ is non-decreasing. Let $x_1 < x_2$. If x_1 and x_2 are both of the form $\frac{k}{3^n}$, the assertion is a con-

sequence of (11,6). We next assume x_2 to be of the form $\frac{k}{3^n}$, x_1, however, not having this property. For each x of the form $\frac{k}{3^n}$ and less than x_1 we have $f(x) \leqq f(x_2)$, according to which (11,9) gives $f(x_1) \leqq f(x_2)$. The remaining cases are now dealt with immediately by insertion of a number of the form $\frac{k}{3^n}$ between x_1 and x_2.

Hence it is obvious that $f(x)$ is continuous from the left in every point x, it being possible to find for any $\varepsilon < 0$ a number $x' < x$ of the form $\frac{k}{3^n}$, for which

$$f(x) - f(x') < \varepsilon .$$

$f(x)$ being non-decreasing and continuous from the left, we may, according to II, 8, to $f(x)$ determine a measure φ defined in $\mathfrak{B}_1$ such that

$$\varphi([a \leqq x < b]) = f(b) - f(a) \tag{11,10}$$

for any choice of a and b, $0 \leqq a < b \leqq 1$.

Together with this Borel ring $\mathfrak{B}_1$ we shall consider the smallest Borel ring in E, containing all the sets of the sequence (11,1) $A_1, A_2, \cdots, A_n, \cdots$. This we shall call $\mathfrak{F}_1$. The defining region of ψ being the Borel ring $\mathfrak{F}$, any set belonging to $\mathfrak{F}_1$, will belong to $\mathfrak{F}$ as well. We know that the set of values of the function of a set φ is closed (see preceding section). If we can now prove that any value assumed by ψ at $\mathfrak{F}_1$ is assumed also by φ at $\mathfrak{B}_1$, and conversely, the proof of our theorem will be completed.

It is obvious that $\mathfrak{F}_1$ must contain each of the sets shown in the decomposition, fig. 2, and as any A_n may be produced by summation from these sets, $\mathfrak{F}_1$ may also be defined as the smallest Borel ring containing all the sets appearing in fig. 2.

The class of sets consisting of all finite sums of the sets given in fig. 2 is a ring, and according to the preceding considerations the slightest extension of this ring to a Borel ring is just the class of sets $\mathfrak{F}_1$.

We now first observe that if C is a set in fig. 2, to which is coupled a point x_0,

$$\psi(C) = \varphi(x_0) \tag{11,11}$$

holds true.

As $\varphi(x_0) = f(x_0+0) - f(x_0)$, we have consequently to prove that

$$\psi(C) = f(x_0+0) - f(x_0). \tag{11,12}$$

We choose a sequence of numbers $x_1, x_2, \cdots, x_n, \cdots$, for which $x_1 > x_2 > \cdots > x_n > \cdots > x_0$ and $\lim_n x_n = x_0$, and for every n we denote by D_n the set coupled to the interval $x_0 \leqq x < x_n$. Hence we get $D_1 \supset D_2 \supset \cdots \supset D_n \supset \cdots$, and, owing to the special procedure of the decomposition, $\prod_n D_n = C$. Hence

$$\psi(C) = \psi\left(\prod_n D_n\right) = \lim_n \psi(D_n) = \lim_n (f(x_n) - f(x_0)) = f(x_0+0) - f(x_0),$$

which was to be proved.

If D is a set in fig. 2 to which is coupled an interval $x_0 < x < x_1$, we have analogously

$$\psi(D) = \varphi([x_0 < x < x_1]). \tag{11,13}$$

Since

$$\left.\begin{aligned} &\varphi([x_0 < x < x_1]) = \varphi([x_0 \leqq x < x_1]) - \varphi(x_0) = \\ &f(x_1) - f(x_0) - (f(x_0+0) - f(x_0)) = f(x_1) - f(x_0+0), \end{aligned}\right\} \tag{11,14}$$

we have consequently to prove that

$$\psi(D) = f(x_1) - f(x_0+0).$$

C denoting the set coupled to the point x_0, we get

$$\psi(D) = \psi(D+C) - \psi(C)$$

which, if we apply (11,12), will give

$$\psi(D) = (f(x_1) - f(x_0)) - (f(x_0+0) - f(x_0)) = f(x_1) - f(x_0+0),$$

which together with (11,14) gives (11,13).

Finally, suppose A to be an arbitrary set of the class of sets $\mathfrak{F}_1$. We can then to this set determine a sequence of sets $K_1, K_2, \cdots, K_n, \cdots$, in which each K_n is a finite or enumerable sum of the sets appearing in fig. 2, and such that

$$1)\ K_1 \supset K_2 \supset \cdots \supset K_n \supset \cdots,$$

$$2)\ A \subset K_n \text{ for every } n,$$

$$3)\ \psi(A) = \text{lower bound } \psi(K_n) = \lim_n \psi(K_n),$$

(see page 10). To each set K_n in $\mathfrak{F}_1$ we have a corresponding set I_n in $\mathfrak{B}_1$, and according to the remarks above on the special cases they satisfy

$$1)\ \varphi(I_n) = \psi(K_n)$$

and

$$2)\ I_1 \supset I_2 \supset \cdots \supset I_n \supset \cdots.$$

Since the set $\prod_n I_n$ belongs to $\mathfrak{B}_1$, and

$$\varphi\left(\prod_n I_n\right) = \lim_n \varphi(I_n) = \lim \psi(K_n) = \psi(A),$$

$\prod_n I_n$ is a set in $\mathfrak{B}_1$ having the property wanted. In nearly the same way the other half of the proof may be carried out.

Each of the numbers appearing in the sequence (11,2) are thus taken on by φ at $\mathfrak{B}_1$. Consequently also the value g is taken on by φ at $\mathfrak{B}_1$, but according to the preceding this value is then also taken on by ψ at $\mathfrak{F}_1$ and thus by ψ at $\mathfrak{F}$; and our proof is completed.

PART IV.

Bounded measures in abstract space.

12. A theorem on two bounded measures having $\mathfrak{B}_1$ as defining region.

In this section we shall establish a theorem on bounded measures defined in $\mathfrak{B}_1$, comprising as special case the theorem proved in III, 10. $\mathfrak{B}_1$ will as usual denote the Borel class on the interval (0,1), where the interval $[0 \leqq x < 1]$ is denoted by E_1. Now let φ and ψ be two bounded measures defined in $\mathfrak{B}_1$. Without reducing the generality of our research, we may assume that $\varphi(E_1) = \psi(E_1) = 1$. Now let A be an arbitrarily chosen set belonging to $\mathfrak{B}_1$. The point $(\varphi(A), \psi(A))$ will then belong to the unity-square $0 \leqq x \leqq 1, 0 \leqq y \leqq 1$. About the set of points of the unity-square, obtained when A runs throughout $\mathfrak{B}_1$, we shall prove the following theorem:

The set of points which is determined by $(\varphi(A), \psi(A))$, *where* φ *and* ψ *are bounded measures defined on* $\mathfrak{B}_1$, *is a closed set.*

Together with the measures φ and ψ we shall consider the functions $f_1(x)$ and $f_2(x)$ defined on $0 \leqq x \leqq 1$ and determined by

$$f_1(a) = \begin{cases} 0 \text{ for } a = 0 \\ \varphi([0 \leqq x < a]) \text{ for } a > 0, \end{cases}$$

and

$$f_2(a) = \begin{cases} 0 \text{ for } a = 0 \\ \psi([0 \leqq x < a]) \text{ for } a > 0. \end{cases}$$

The non-decreasing functions $f_1(x)$ and $f_2(x)$ may be written in the form

$$f_1(x) = g_1(x) + h_1(x)$$

and

$$f_2(x) = g_2(x) + h_2(x)$$

(cf. page 26), and correspondingly will arise a decomposition of φ and ψ

$$\left.\begin{aligned} \varphi(A) &= \varphi_1(A) + \varphi_2(A) \\ \text{and} \\ \psi(A) &= \psi_1(A) + \psi_2(A) \end{aligned}\right\} \quad (12,1)$$

for any $A \varepsilon \mathfrak{B}_1$.

From (12,1) follows

$$(\varphi(A), \psi(A)) = (\varphi_1(A), \psi_1(A)) + (\varphi_2(A), \psi_2(A)).$$

We shall first show that if M_1 and M_2 are sets, both belonging to $\mathfrak{B}_1$, and for which

$$(\varphi_1(M_1), \psi_1(M_1)) = (\alpha, \beta)$$

and

$$(\varphi_2(M_2), \psi_2(M_2)) = (\gamma, \delta),$$

then we may determine a set $M \varepsilon \mathfrak{B}_1$, for which

$$(\varphi(M), \psi(M)) = (\alpha + \gamma, \beta + \delta).$$

Let the set of points of discontinuity of the function $f_1(x)$ be the, at most enumerable, set $N_1 = \{\xi_n\}$. Similarly let $N_2 = \{\eta_n\}$ denote the, at most enumerable, set of points of discontinuity of the function $f_2(x)$. The sum of N_1 and N_2 is termed N, i.e. $N = N_1 \dot{+} N_2$. As the set $M \varepsilon \mathfrak{B}_1$ we may now use the set

$$M = (M_1 - M_1 N) + M_2 N.$$

From (12,1) follows

$$\left.\begin{aligned} \varphi(M) &= \varphi(M_1 - M_1 N) + \varphi(M_2 N) = \\ \varphi_1(M_1 - M_1 N) &+ \varphi_2(M_1 - M_1 N) + \varphi_1(M_2 N) + \varphi_2(M_2 N). \end{aligned}\right\} \quad (12,2)$$

$M_1 N$ and $M_2 N$ both being at most enumerable sets, we have

$$\varphi_1(M_1 N) = \varphi_1(M_2 N) = 0. \quad (12,3)$$

From $M_1 - M_1 N \subset E_1 - N_1$ follows

$$\varphi_2(M_1 - M_1 N) = 0. \quad (12,4)$$

Finally we derive

$$\varphi_2(M_2 N) = \sum_{\xi_i \in M_2 N}' S_{f_1}(\xi_i) = \sum_{\xi_i \in M_2 N_1}' S_{f_1}(\xi_i) = \varphi_2(M_2) = \gamma. \qquad (12,5)$$

Thus it follows from (12,2)—(12,5) that

$$\varphi(M) = \alpha + 0 + 0 + \gamma.$$

In analogy it is seen that

$$\psi(M) = \beta + \delta,$$

and we have proved our assertion.

Hence we can, as in section III,10, conclude that if the sets of points

$$(\varphi_1(A), \psi_1(A))$$

and

$$(\varphi_2(A), \psi_2(A))$$

are both closed, the set of points

$$(\varphi(A), \psi(A))$$

is also a closed set.

In the two following sections we shall deal with these special cases.

13. First special case.

Let φ and ψ be bounded measures defined in $\mathfrak{B}_1$, and let the two non-decreasing functions $f_1(x)$ and $f_2(x)$ be defined by

$$f_1(a) = \begin{cases} 0 \text{ for } a = 0 \\ \varphi([0 \leq x < a]) \text{ for } a > 0 \end{cases}$$

and

$$f_2(a) = \begin{cases} 0 \text{ for } a = 0 \\ \psi([0 \leq x < a]) \text{ for } a > 0 \end{cases}$$

and satisfy

$$D_{f_1}(x_1, x_2) = V_{f_1}(x_1, x_2)$$

and

$$D_{f_2}(x_1, x_2) = V_{f_2}(x_1, x_2)$$

for any choice of x_1 and x_2, $0 \leq x_1 < x_2 \leq 1$.

The set of points of discontinuity of $f_1(x)$ is the, at most enumerable, set $N_1 = \{\xi_n\}$, and the set of points of discontinuity of $f_2(x)$ is the, at most enumerable, set $N_2 = \{\eta_n\}$. The sum of N_1 and N_2 then again is at most an enumerable set, termed $N = \{\zeta_n\}$. For any $A \in \mathfrak{B}_1$ we now have

$$\left.\begin{aligned} \varphi(A) &= \sum_{\zeta_i \in A} S_{f_1}(\zeta_i) \\ \text{and} \\ \psi(A) &= \sum_{\zeta_i \in A} S_{f_2}(\zeta_i) \end{aligned}\right\} \qquad (13,1)$$

(cf. page 35). In the following the set N is assumed to be enumerable, and we put

$$\left.\begin{aligned} S_{f_1}(\zeta_n) &= a_n \ (\geq 0) \\ \text{and} \\ S_{f_2}(\zeta_n) &= b_n \ (> 0). \end{aligned}\right\} \qquad (13,2)$$

Hence we obtain

$$(\varphi(A), \psi(A)) = \left(\sum_{n=1}^{\infty} e_n a_n, \sum_{n=1}^{\infty} e_n b_n\right), \qquad (13,3)$$

where e_n has the value 1, if ζ_n belongs to A, and otherwise the value 0.

We shall now show that the set $(\varphi(A), \psi(A))$ is closed. Suppose $A_1, A_2, \cdots, A_n, \cdots$ to be a sequence of sets, all belonging to $\mathfrak{B}_1$, and for which the sequence of points $(\varphi(A_n), \psi(A_n))$ is convergent to the limit point (s, t). We shall now prove the existence of a set $A \in \mathfrak{B}_1$, for which

$$(\varphi(A), \psi(A)) = (s, t).$$

In section III, 9, where a method how to determine A^* (respectively A^{**}) as a subset of N has been given, we have already proved the existence of a set A^*, for which $\varphi(A^*) = s$, and a set A^{**}, for which $\psi(A^{**}) = t$. A closer analysis of the process of choice will immediately show the possibility of determining a subset of N, for which both $\varphi(A) = s$ and $\psi(A) = t$. More precisely, if only A is determined in the way shown, such that $\varphi(A) = s$, it will be an immediate consequence that $\psi(A) = t$.

14. Second special case.

Let φ and ψ be bounded measures defined on $\mathfrak{B}_1$. We shall in this section assume that the non-decreasing functions $f_1(x)$ and $f_2(x)$, corresponding to φ and ψ, given by the definitions

$$f_1(a) = \begin{cases} 0 \text{ for } a = 0 \\ \varphi([0 \leq x < a]) \text{ for } a > 0 \end{cases}$$

and

$$f_2(a) = \begin{cases} 0 \text{ for } a = 0 \\ \psi([0 \leq x < a]) \text{ for } a > 0 \end{cases}$$

are both continuous in the interval $0 \leq x \leq 1$, and we shall show that the set of points

$$(\varphi(A), \psi(A)), \; A \in \mathfrak{B}_1 \tag{14,1}$$

is closed. Without loss of generality, we may assume that

$$\varphi(E_1) = \psi(E_1) = 1.$$

In order to simplify the writing, we shall further in this section use the letter E instead of E_1 to denote the interval $0 \leq x < 1$.

According to the theorem on decomposition, page 14, φ may be written in the form

$$\varphi = \varphi_k + \varphi_s, \tag{14,2}$$

where φ_k is ψ-continuous, and φ_s is ψ-singular. Thus $\varphi_k(A)$ will have the value 0 for each $A \in \mathfrak{B}_1$, for which $\psi(A) = 0$, and there exists a set $N \in \mathfrak{B}_1$ where $\psi(N) = 0$, such that $\varphi_s(A) = 0$ for each $A \in \mathfrak{B}_1$ which is a subset of $E - N$.

φ_k being ψ-continuous, there will exist a function $f \geq 0$ defined in E, such that

$$\varphi_k(A) = \int_A f \psi(dE) \tag{14,3}$$

for each $A \in \mathfrak{B}_1$ (see page 20).

It follows from $A - AN \subset E - N$ that

$$\varphi_s(A) = \varphi_s(AN), \tag{14,4}$$

and from $\psi(AN) = 0$ that

$$\varphi_k(AN) = 0, \tag{14,5}$$

according to which (14,2)—(14,5) give

$$\varphi(A) = \varphi(AN) + \int_A f\psi(dE) \tag{14,6}$$

for each $A \in \mathfrak{B}_1$.

Our first problem is to find out what values φ can take on, when ψ is fixed. Suppose γ to be a fixed number of the interval $0 \leqq x \leqq 1$. We shall now consider all sets $A \in \mathfrak{B}_1$, for which $\psi(A) = \gamma$. The existence of such sets is evident on account of the continuity of the function $f_2(x)$. Let A_1 and A_2 be two such sets. We thus have

$$\psi(A_1) = \psi(A_2) = \gamma. \tag{14,7}$$

Suppose, furthermore, the numbers α and β to be defined by

$$\varphi(A_1N) = \alpha \quad \text{and} \quad \int_{A_2} f\psi(dE) = \beta. \tag{14,8}$$

We can then prove the existence of a set $A \in \mathfrak{B}_1$, where $\psi(A) = \gamma$, for which

$$\varphi(A) = \alpha + \beta.$$

As a set A we may use

$$A = A_1N + (A_2 - A_2N),$$

for from $\psi(N) = 0$ follows

$$\psi(A) = \psi(A_2) = \gamma,$$

and by means of (14,6) we get

$$\varphi(A) = \varphi(A_1N) + \varphi(A_2 - A_2N) = \alpha + \varphi((A_2 - A_2N)N) + \int_{A_2 - A_2N} f\psi(dE)$$
$$= \alpha + \beta$$

since $(A_2 - A_2N)N = 0$ and $\int_{A_2N} f\psi(dE) = 0$.

From the above follows that if, only, we can prove that each of the addends in (14,6) runs throughout a closed set, when A runs throughout the sets belonging to $\mathfrak{B}_1$, for which $\psi(A) = \gamma$, we have also proved that the set of values of $\varphi(A)$ is closed.

The set of values of $\varphi(AN)$ we shall prove to be *a closed interval*, which is moreover *independent* of γ.

Let A be a set belonging to $\mathfrak{B}_1$, and for which $\psi(A) = \gamma$. Thus we immediately derive

$$0 \leq \varphi(AN) \leq \varphi(N). \tag{14,9}$$

Since $\psi(N) = 0$ we have for the set $A^* = A - AN$ that

$$\psi(A^*) = \psi(A) = \gamma$$

and that

$$\varphi(A^*N) = \varphi((A - AN)N) = 0.$$

For the set $A^{**} = A \dot{+} N = A + (N - AN)$ we have

$$\psi(A^{**}) = \psi(A) = \gamma$$

and

$$\varphi(A^{**}N) = \varphi((A \dot{+} N)N) = \varphi(N).$$

Consequently we have sets for which the signs of equality in (14,9) hold true. We have now to prove for each number between 0 and $\varphi(N)$, the existence of a set with φ having this value. Let A_t denote the set $[0 \leq x < t]$, and let B_t denote the set NA_t belonging to $\mathfrak{B}_1$ for any t. We now put

$$B = A^* + B_t$$

and have for every t

$$\psi(B) = \psi(A^*) + \psi(B_t) = \gamma$$

since $\psi(N) = 0$.

The function $g(t)$ is introduced by the definition

$$g(t) = \varphi(BN) = \varphi((A^* + B_t)N) = \varphi(B_t N) = \varphi(B_t).$$

It is obvious that $g(t)$ is non-decreasing. We shall further prove the fact that it is continuous. If h denotes a positive number, we see that

$$g(t+h)-g(t) = \varphi(B_{t+h})-\varphi(B_t) = \varphi(B_{t+h}-B_t) =$$

$$\varphi(N(A_{t+h}-A_t)) < \varphi(A_{t+h}-A_t) = f_1(t+h)-f_1(t)$$

holds true.

$f_1(x)$ being assumed continuous, we see that $g(t)$ is continuous from the right. Similarly we see that $g(t)$ is continuous from the left. Thus the function $g(t)$ takes on any value between $g(0) = 0$ and $g(1) = \varphi(N)$, and the proof that the values of $\varphi(AN)$ make out a closed set is completed. Now remains an investigation of the set of values of

$$\int_A f\psi(dE),$$

$A \varepsilon \mathfrak{B}_1$ running throughout the sets for which $\psi(A) = \gamma$. We shall again show that the values make out *a closed interval*.

In our proof we shall apply the following lemma:

For any number ξ *of the interval* $0 < \xi < 1$ *we can determine a set* $A_\xi \varepsilon \mathfrak{B}_1$ *for which* $\psi(A_\xi) = \xi$, *and a corresponding number* a_ξ *such that*

$$[f < a_\xi] \subset A_\xi \subset [f \leqq a_\xi], \tag{14,10}$$

and this determination may be carried out in such a way that

$$A_{\xi_1} \subset A_{\xi_2} \quad \text{for } \xi_1 < \xi_2. \tag{14,11}$$

To prove this we shall define two functions

$$F(a) = \psi([f < a]) \tag{14,12}$$

and

$$G(a) = \psi([f \leqq a]) \tag{14,13}$$

having $a \geqq 0$ as defining region.

Since $[f < a] \subset [f \leqq a]$ we have

$$F(a) \leqq G(a), \tag{14,14}$$

and similarly we see that

$$\left.\begin{aligned} &F(a_1) \leqq F(a_2) \quad \text{for} \quad a_1 < a_2 \\ \text{and} \quad &G(a_1) \leqq G(a_2) \quad \text{for} \quad a_1 < a_2. \end{aligned}\right\} \tag{14,15}$$

Our next problem is to prove that the function $F(a)$ is continuous from the left, and that the function $G(a)$ is continuous from the right in every point. Let

$$a_1 < a_2 < \cdots < a_n < \cdots < a \quad \text{and} \quad \lim_n a_n = a,$$

it then follows that

$$F(a) - F(a_n) = \psi([f < a]) - \psi([f < a_n]) = \psi([a_n \leqq f < a]).$$

Since

$$\prod_n [a_n \leqq f < a] = 0$$

it next follows that

$$\lim_n (F(a) - F(a_n)) = \lim_n ([a_n \leqq f < a]) = 0,$$

i. e. $F(a)$ is continuous from the left. Now let

$$a_1 > a_2 > \cdots > a_n > \cdots > a \quad \text{and} \quad \lim_n a_n = a,$$

we then analogously obtain

$$G(a_n) - G(a) = \psi([f \leqq a_n]) - \psi([f \leqq a]) = \psi([a < f \leqq a_n]).$$

On account of

$$\prod_n [a < f \leqq a_n] = 0$$

we obtain

$$\lim_n (G(a_n) - G(a)) = \lim_n \psi([a < f < a_n]) = 0,$$

i. e. $G(a)$ is continuous from the right.

For a fixed value of ξ in the interval $0 < \xi < 1$ we now have to determine the upper bound of the values of a for which $F(a) \leqq \xi$. We shall term the latter a_ξ, and we have $a_\xi < \infty$.[1) 2)] $F(a)$ being continuous from the left, we get $F(a_\xi) \leqq \xi$, and $G(a)$ being continuous from the right, (14,14) implies the fact that $G(a_\xi) \leqq \xi$. Hence we obtain

$$\psi([f < a_\xi]) \leqq \xi \leqq \psi([f \leqq a_\xi]). \tag{14,16}$$

1) It is easy to see that $\xi_1 < \xi_2$ implies $a_{\xi_1} \leqq a_{\xi_2}$.

2) It follows namely from $F(a) = \psi([f < a]) \leqq \xi$ for every a that $\psi([f \geqq a]) \geqq 1 - \xi > 0$ for every a, and hence further that $\psi([f = \infty]) > 0$, in nonconformity to φ being finite.

Concluding after the analogy of the proof page 55 it is obvious that in the set $[f = a_\xi]$ there is a subset $\varepsilon \mathfrak{B}_1$ having any ψ-measure between 0 and $\psi([f = a_\xi])$.

Accordingly we can determine a set $A_\xi \varepsilon \mathfrak{B}_1$ where $\psi(A_\xi) = \xi$, such that

$$[f < a_\xi] \subset A_\xi \subset [f \leqq a_\xi].$$

Furthermore it is immediately obvious that this process of determination may be carried out in such a way that

$$A_{\xi_1} \subset A_{\xi_2} \quad \text{for} \quad \xi_1 < \xi_2,$$

and the proof of our lemma is completed.

We shall now again consider

$$\varphi_k(A) = \int_A f \psi(dE)$$

for the sets $A \varepsilon \mathfrak{B}_1$, for which $\psi(A) = \gamma$. As to the special values of γ, $\gamma = 0$ and $\gamma = 1$, the case is evident. Thus if $A \varepsilon \mathfrak{B}_1$ is a set for which $\psi(A) = 0$, we obviously have $\varphi_k(A) = 0$, and if $A \varepsilon \mathfrak{B}_1$ is a set for which $\psi(A) = 1$, we have $\varphi_k(A) = \varphi_k(E) - \varphi_k(E - A) = \varphi_k(E)$, since $\psi(E - A) = 0$. Suppose next γ to be a number of the interval $0 < \gamma < 1$, and let A_γ be the set determined by our lemma. We can then prove the inequality

$$\int_A f \psi(dE) \geqq \int_{A_\gamma} f \psi(dE) \tag{14,17}$$

for any $A \varepsilon \mathfrak{B}_1$ for which $\psi(A) = \gamma$.

First we notice that

$$\left.\begin{aligned} \int_A f \psi(dE) &= \int_{A - AA_\gamma} f \psi(dE) + \int_{AA_\gamma} f \psi(dE) \\ \text{and} \\ \int_{A_\gamma} f \psi(dE) &= \int_{A_\gamma - AA_\gamma} f \psi(dE) + \int_{AA_\gamma} f \psi(dE) \end{aligned}\right\} \tag{14,18}$$

where

$$\psi(A - AA_\gamma) = \psi(A_\gamma - AA_\gamma).$$

By means of (14,10) we next see that $f \geq a_\gamma$ for the set $A - AA_\gamma$, and that $f \leq a_\gamma$ for the set $A_\gamma - AA_\gamma$. Hence we obtain

$$\int_{A-AA_\gamma} f\psi(dE) \geq \int_{A_\gamma - AA_\gamma} f\psi(dE)$$

according to which (14,18) will give

$$\int_A f\psi(dE) \geq \int_{A_\gamma} f\psi(dE),$$

which was to be proved.

Analogous to (14,17) we can show that for each $A \in \mathfrak{B}_1$, for which $\psi(A) = \gamma$, the following inequality holds true

$$\int_A f\psi(dE) < \int_{E-A_{1-\gamma}} f\psi(dE) \tag{14,19}$$

where $A_{1-\gamma}$ is the set determined by our lemma. The set $E - A_{1-\gamma}$ we shall denote A^*, and we then have

$$\psi(A^*) = \psi(E) - \psi(A_{1-\gamma}) = 1 - (1-\gamma) = \gamma.$$

Similar to (14,18) we have

$$\left.\begin{aligned} \int_A f\psi(dE) &= \int_{A-AA^*} f\psi(dE) + \int_{AA^*} f\psi(dE) \\ \text{and} \\ \int_{A^*} f\psi(dE) &= \int_{A^*-AA^*} f\psi(dE) + \int_{AA^*} f\psi(dE) \end{aligned}\right\} \tag{14,20}$$

where

$$\psi(A - AA^*) = \psi(A^* - AA^*).$$

From (14,10) follows

$$[f < a_{1-\gamma}] \subset A_{1-\gamma},$$

from which it is obvious that $f \geq a_{1-\gamma}$ for the set $A^* - AA^*$. Similarly we derive from (14,10) that $f \leq a_{1-\gamma}$ for the set $A - AA^*$. This being so, we obtain

$$\int_{A-AA^*} f\psi(dE) \leqq \int_{A^*-AA^*} f\psi(dE)$$

according to which (14,20) will give

$$\int_{A} f\psi(dE) \leqq \int_{E-A_{1-\gamma}} f\psi(dE),$$

which was to be proved.

If we comprise (14,17) and (14,19) we get for each $A \varepsilon \mathfrak{B}_1$, having $\psi(A) = \gamma$,

$$\int_{A_\gamma} f\psi(dE) \leqq \int_{A} f\psi(dE) \leqq \int_{E-A_{1-\gamma}} f\psi(dE), \tag{14,21}$$

and we shall now show that $\int_A f\psi(dE)$ takes on *any value in the closed interval* from $\int_{A_\gamma} f\psi(dE)$ to $\int_{E-A_{1-\gamma}} f\psi(dE)$.

For that purpose we form the function

$$H(\xi) = \int_{A_{\xi+\gamma}-A_\xi} f\psi(dE), \qquad 0 \leqq \xi \leqq 1-\gamma \tag{14,22}$$

where A_ξ and $A_{\xi+\gamma}$ are the sets we have determined by means of our lemma, yet especially fixing $A_0 = 0$ and $A_1 = E$. For any ξ we then have

$$\psi(A_{\xi+\gamma} - A_\xi) = \psi(A_{\xi+\gamma}) - \psi(A_\xi) = (\xi+\gamma) - \xi = \gamma. \tag{14,23}$$

Further we derive

$$\left.\begin{aligned} H(0) &= \int_{A_\gamma - A_0} f\psi(dE) = \int_{A_\gamma} f\psi(dE) \\ \text{and} \\ H(1-\gamma) &= \int_{A_1 - A_{1-\gamma}} f\psi(dE) = \int_{E-A_{1-\gamma}} f\psi(dE). \end{aligned}\right\} \tag{14,24}$$

It now only remains to be proved that the function $H(\xi)$ is a *continuous function* in the interval $0 \leqq \xi \leqq 1-\gamma$.

We shall first show that the function $H(\xi)$ is *non-decreasing* in the interval $0 \leqq \xi \leqq 1-\gamma$. For that purpose we shall, for $\xi_1 < \xi_2$, consider

$$H(\xi_2) - H(\xi_1) = \int_{A_{\xi_2+\gamma}-A_{\xi_2}} f\psi(dE) - \int_{A_{\xi_1+\gamma}-A_{\xi_1}} f\psi(dE).$$

For brevity we put

$$A_{\xi_2+\gamma} - A_{\xi_2} = C \quad \text{and} \quad A_{\xi_1+\gamma} - A_{\xi_1} = D,$$

and we thus have

$$H(\xi_2) - H(\xi_1) = \int_C f\psi(dE) - \int_D f\psi(dE) = \int_{C-CD} f\psi(dE) - \int_{D-CD} f\psi(dE) \qquad (14{,}25)$$

where

$$\psi(C-CD) = \psi(D-CD).$$

From (14,10) we derive

$$f(x) \geqq \max\{a_{\xi_2}, a_{\xi_1+\gamma}\} \quad \text{for} \quad x \varepsilon C - CD$$

and

$$f(x) \leqq \min\{a_{\xi_2}, a_{\xi_1+\gamma}\} \quad \text{for} \quad x \varepsilon D - CD,$$

which inserted into (14,25) gives

$$H(\xi_2) - H(\xi_1) \geqq \psi(C-CD) \cdot [\max\{a_{\xi_2}, a_{\xi_1+\gamma}\} - \min\{a_{\xi_2}, a_{\xi_1+\gamma}\}] \geqq 0,$$

which was to be proved.

In order to show that $H(\xi)$ is continuous from the right in any point of the interval $0 \leqq \xi < 1-\gamma$ we shall now for h positive and sufficiently small consider

$$H(\xi+h) - H(\xi) = \int_{A_{\xi+h+\gamma}-A_{\xi+h}} f\psi(dE) - \int_{A_{\xi+\gamma}-A_{\xi}} f\psi(dE) = \int_{F-FG} f\psi(dE) - \int_{G-FG} f\psi(dE), \quad (14{,}26)$$

in which we have put

$$A_{\xi+h+\gamma} - A_{\xi+h} = F \quad \text{and} \quad A_{\xi+\gamma} - A_{\xi} = G.$$

For $h < \gamma$ we have

$$F - FG = A_{\xi+h+\gamma} - A_{\xi+\gamma},$$

and thus we derive by means of (14,10)

$$\int_{F-FG} f\psi(dE) = \int_{A_{\xi+h+\gamma}-A_{\xi+h}} f\psi(dE) \leqq h \cdot a_{\xi+h+\gamma},$$

since $\psi(A_{\xi+h+\gamma} - A_{\xi+\gamma}) = h$. Hence we get

$$\int_{F-FG} f\psi(dE) \to 0 \quad \text{for} \quad h \to 0. \tag{14,27}$$

In analogy we find

$$\int_{G-FG} f\psi(dE) = \int_{A_{\xi+h}-A_{\xi}} f\psi(dE) \leqq h \cdot a_{\xi+h},$$

hence

$$\int_{G-FG} f\psi(dE) \to 0 \quad \text{for} \quad h \to 0. \tag{14,28}$$

From (14,26), (14,27) and (14,28) it thus follows that $H(\xi)$ is continuous from the right. To show next that $H(\xi)$ is continuous from the left in any point of the interval $0 < \xi \leqq 1 - \gamma$, we consider for h positive and sufficiently small

$$H(\xi) - H(\xi - h) = \int_{A_{\xi+\gamma}-A_{\xi}} f\psi(dE) - \int_{A_{\xi-h+\gamma}-A_{\xi-h}} f\psi(dE) = \int_{K-KL} f\psi(dE) - \int_{L-KL} f\psi(dE), \tag{14,29}$$

in which we have put

$$A_{\xi+\gamma} - A_{\xi} = K \quad \text{and} \quad A_{\xi-h+\gamma} - A_{\xi-h} = L.$$

For $h < \gamma$ we have

$$K - KL = A_{\xi+\gamma} - A_{\xi-h+\gamma},$$

and hence we get by means of (14,10)

$$\int_{K-KL} f\psi(dE) = \int_{A_{\xi+\gamma}-A_{\xi-h+\gamma}} f\psi(dE) \leqq h \cdot a_{\xi+\gamma},$$

since $\psi(A_{\xi+\gamma'} - A_{\xi-h+\gamma'}) = h$. Hence we obtain

$$\int_{K-KL} f\psi(dE) \to 0 \quad \text{for} \quad h \to 0.^{1)} \tag{14,30}$$

In analogy we obtain

$$\int_{L-KL} f\psi(dE) = \int_{A_\xi - A_{\xi-h}} f\psi(dE) \leqq h \cdot a_\xi$$

since $\psi(A_\xi - A_{\xi-h}) = h$. Hence we get

$$\int_{L-KL} f\psi(dE) \to 0 \quad \text{for} \quad h \to 0. \tag{14,31}$$

According to (14,29), (14,30) and (14,31) we see that $H(\xi)$ is continuous from the left. And now we have proved that the values of

1) The number $a_{\xi+\gamma'}$ being not introduced for $\xi = 1-\gamma'$, a special investigation of the conditions for $\xi = 1-\gamma'$ is required. In this case we have

$$\int_{K-KL} f\psi(dE) = \int_{E-A_{1-h}} f\psi(dE) = \varphi_k(E - A_{1-h}).$$

If $h_1 > h_2 > \cdots > h_n > \cdots > 0$ and $\lim_n h_n = 0$, we get

$$E - A_{1-h_1} \supset E - A_{1-h_2} \supset \cdots \supset E - A_{1-h_n} \supset \cdots.$$

According to (14,10)

$$E - A_{1-h_n} \subset [f \geqq a_{1-h_n}]$$

for every n.

We shall now perform the proof indirectly, assuming

$$\varphi_k(E - A_{1-h_n}) \geqq t > 0 \text{ for all values of } n.$$

If the set of numbers $\{a_\xi\}$, determined by our lemma, is not upward bounded, we accordingly get

$$\varphi_k([f = \infty]) \geqq t$$

in nonconformity to $\psi([f = \infty]) = 0$. Is on the contrary the set of numbers $\{a_\xi\}$ upward bounded, there will exist a number a^* such that $\psi([f \geqq a^*]) = 0$. Hence we have

$$\int_{E-A_{1-h_n}} f\psi(dE) = \int_{(E-A_{1-h_n})\cdot[f<a^*]} f\psi(dE) \leqq h_n \cdot a^* < \varepsilon \quad \text{for} \quad n > N$$

which was to be proved.

$$\varphi_k(A) = \int_A f\psi(dE) \qquad (\psi(A) = \gamma)$$

makes out a closed interval.

Comprising (14,9) and (14,21) we next find that the region of values of $\varphi(A)$, $A \in \mathfrak{B}_1$ running throughout the sets for which $\psi(A) = \gamma$, $0 \leqq \gamma < 1$, is determined by

$$\int_{A_\gamma} f\psi(dE) \leqq \varphi(A) \leqq \int_{E-A_{1-\gamma}} f\psi(dE) + \varphi(N), \tag{14,32}$$

and that any value in this closed interval appears as a value of the function $\varphi(A)$.

Thus our proof that the set of points $(\varphi(A), \psi(A))$ is a closed set is completed if we can prove that the end points of the closed interval (14,32) vary continuously with respect to γ.

For this purpose we shall first consider

$$\int_{A_\gamma} f\psi(dE).$$

If $0 \leqq \gamma < 1$ and $h\,(< h_0)$ is positive and sufficiently small, we have

$$\int_{A_{\gamma+h}} f\psi(dE) - \int_{A_\gamma} f\psi(dE) = \int_{A_{\gamma+h}-A_\gamma} f\psi(dE) < h \cdot a_{\gamma+h_0}, \tag{14,33}$$

since $\psi(A_{\gamma+h} - A_\gamma) = h$ and $A_{\gamma+h} \subset [f \leqq a_{\gamma+h_0}]$.

If $0 < \gamma \leqq 1$ and h is positive and sufficiently small, we similarly get

$$\int_{A_\gamma} f\psi(dE) - \int_{A_{\gamma-h}} f\psi(dE) = \int_{A_\gamma - A_{\gamma-h}} f\psi(dE) \leqq h \cdot a_\gamma, \tag{14,34}$$

since $\psi(A_\gamma - A_{\gamma-h}) = h$ and $A_\gamma \subset [f \leqq a_\gamma]$ (as to the case $\gamma = 1$ cf. the footnote page 63). From (14,33) and (14,34) it is evident that the left end point of the interval varies continuously with respect to γ. By a quite similar consideration we clearly see

that the right end point of the interval, which with the exception of a constant is equal to

$$\int_{E=A_{1-\gamma}} f\psi(dE),$$

varies continuously with respect to γ.

15. A theorem on two bounded measures in abstract space.

In this section we shall see that the theorem proved and formulated in the preceding section of this part, on two bounded measures having $\mathfrak{B}_1$ as defining region, holds true in the abstract space too.

Let E be an arbitrary set, and let $\mathfrak{F}$ be a class of sets, which is a Borel ring and contains E. Let further φ and ψ be two bounded measures defined in $\mathfrak{F}$.

The following theorem will then hold true:

The set of points defined by

$$(\varphi(A), \psi(A)),$$

where φ and ψ are bounded measures defined in $\mathfrak{F}$, is a closed set.

Accordingly our problem is to prove that if

$$A_1, A_2, \cdots, A_n, \cdots$$

is a sequence of sets, all belonging to $\mathfrak{F}$, and for which the corresponding sequence of points

$$(\varphi(A_1), \psi(A_1)), (\varphi(A_2), \psi(A_2)), \cdots, (\varphi(A_n), \psi(A_n)), \cdots$$

is convergent to the limit point (t, s), then there will exist a set $A \varepsilon \mathfrak{F}$, for which

$$(\varphi(A), \psi(A)) = (t, s).$$

In proving this we apply exactly the same representation from the smallest Borel ring $\mathfrak{F}_1$, containing all the sets A_n, to the Borel class $\mathfrak{B}_1$, as applied in III, 11. Corresponding to φ and ψ there will exist bounded measures φ_1 and ψ_1 defined in $\mathfrak{B}_1$, and it is easily seen that to each set in $\mathfrak{F}_1$ there will be a corresponding set in $\mathfrak{B}_1$, such that

$$(\varphi, \psi) = (\varphi_1, \psi_1)$$

for these sets, and conversely.

The theorem being valid for (φ_1, ψ_1) we see that there is a set $A \varepsilon \mathfrak{F}_1$ (or weaker $A \varepsilon \mathfrak{F}$) having the property wanted. Thus the assertion of the theorem is proved.

Putting $\varphi = \psi$ it will be seen that the above theorem contains the theorem of III, 11 as a special case.

16. Final remarks.

The appearance in 1933 of KOLMOGOROFF's book "Grundbegriffe der Wahrscheinlichkeitsrechnung"[1] made it at once clear to many mathematicians that with this book the theory of probability had won its natural place among the theories of mathematics. It is KOLMOGOROFF's merit to have shown how simply the theory can be axiomatized, and how it is possible from the axioms to prove the theorems of the theory of probability. The number of the possible axiomatizations was immense, but the system used by KOLMOGOROFF seems natural and for the applications most simple. Here the space of single occurrences is abstract, moreover a class of sets consisting of subsets of this abstract space is supposed to be given. This class is assumed to be a ring and to contain as an element the space itself. In this ring is supposed defined a non-negative, additive function of a set, such that its value for the abstract space is 1. The value of the function of a set for a set of the ring will then be the probability of the realization of one of the single occurrences contained in this set. It is proved that it is possible to confine oneself to regarding Borel fields of probability, (in a Borel field of probability the defining region of the function of a set is a Borel ring), introducing an axiom of continuity equivalent with the claim of complete additivity of the function of a set in its defining region.

The book mentioned above roused the author's interest in the theory of probability and its applications. This interest was strengthened by several visits to the Stockholm University Institute of Insurance Mathematics and Mathematical Stati-

[1] KOLMOGOROFF [1].

stics[1]. Here was also roused the author's interest in the theory of testing statistical hypotheses[2], formed by NEYMAN and PEARSON. It was clear to everybody that the theory in the form it had obtained by then suffered from certain shortcomings, and as it was rather evident what amendments might be wanted, and what results were likely to be obtained, the problem must be to change the foundation in such a direction that this was made possible.

Unfortunately my investigations into this problem were on the whole without any result, as I did not succeed in giving them a form which satisfied me in the sense of being mathematically unimpeachable, and at the same time having the connection with experience and practice which must reasonably be claimed. By my study of various questions in this connection I was led on to certain problems of existence, which must necessarily be treated first. Here too I met with difficulties, now of this and now of that kind. Thus it was natural first to try to answer these problems in the abstract space, i. e. when the theory was unimpeded by everything superfluous.

These investigations gave birth to this paper.

Fundamental for the present formulation and treatment of the problem of the testing of statistical hypotheses is the above mentioned paper by NEYMAN and PEARSON, 1933. In this work is given a detailed account of the nature of the problem, and a mathematical treatment in the main features of the problems raised. The problem is by these two authors formulated as follows: Let a stochastic variable be given. An assumption of the structure of the distribution of this variable is called a statistical hypothesis. A set of observations of the stochastic variable is called a sample, and as a test of this statistical hypothesis a function of the result of the sample is now computed. If this sample has certain properties further stated, it will be discarded; whereas it will be maintained, if the function has not got these properties. This test is of course not absolute in the sense of giving us information whether the hypothesis laid down is correct or false, but we endeavour to arrange it in such a way

[1] The author wants to express his gratitude to the institute and its director, Professor HARALD CRAMÉR, Ph. D., for hospitality and interest.

[2] See for instance NEYMAN-PEARSON [1].

that it may in the long run give good results. To be more precise, we arrange it in such a manner that the probability of discarding the hypothesis when it is true, does not exceed a certain limit fixed beforehand, and correspondingly that the probability of maintaining the hypothesis, even if it is false, is kept under a reasonable limit. A number of calculated examples prove the method to be available in many cases arising in practice. Yet several authors have objected to certain special items of the theory. Thus FELLER has in an excellent paper from 1938 shown the shortcomimg of the proposed procedure in a whole series of cases, which may easily crop up in practice[1].

It was natural at the beginning of this research to leave the categorical claim of dividing into two parts the sphere of samples, such that the hypothesis was maintained if the point of the sample fell inside one of these parts, whereas it was discarded if the point of the sample fell inside the other. It was natural to eliminate the sharp limit that must arise between these two parts by introducing a third set, a transition set in which the question whether the hypothesis is correct or false is left open.

In its simplest form this leads up to the following problems in the abstract space. Suppose given two measures φ and ψ, both defined in a Borel ring $\mathfrak{F}$, and about which it is further supposed that $\varphi(E) = \psi(E) = 1$. Now the problem is to prove the existence of two sets having no elements in common, A and F in E, such that

1) $\varphi(F) \leqq \varepsilon_1$

2) $\psi(A) \leqq \varepsilon_2$

3) $\varphi(A) + \psi(F)$ as great as possible.

The investigation of this question apparently requires knowledge of a certain class of functions of a set in the abstract space, which has not yet been dealt with. This is seen in the following way. Let F be an arbitrary set of the space E, thus not necessarily subject to condition 1). Among the subsets of $E - F$ there must then, according to our earlier investigation, exist a set A_F, such that $\psi(A_F) \leqq \varepsilon_2$, while at the same time $\varphi(A_F)$

[1] FELLER [1].

is as great as possible. Our task is now to prove that the function of a set

$$\eta(F) = \psi(F) + \varphi(A_F) \tag{16,1}$$

has a greatest value, when F runs through the sets for which $\varphi(F) \leqq \varepsilon_1$.

The function of a set $\eta(F)$ is seen at once to satisfy the relation

$$\eta(F_1 + F_2) \leqq \eta(F_1) + \eta(F_2). \tag{16,2}$$

It is obvious that a thorough knowledge of the functions of a set satisfying (16,2) would be of significance. As far as known to the author, there exists only one investigation of this type of functions of a set, undertaken by BANACH[1], but with BANACH another condition is required satisfied at the same time. We can with certainty say that this condition in our problems is not accomplished.

1) BANACH [1].

List of papers quoted.

BANACH, S. (1). Sur une classe de fonctions d'ensemble. Fundamenta Mathematicae 6 (1924). Pag. 170—188.

CARATHÉODORY, C. (1). Vorlesungen über reelle Funktionen, 2. Auflage. Leipzig-Berlin 1927.

FELLER, W. (1). Note on Regions Similar to the Sample Space. Statistical Research Memoirs II (1938). Pag. 117—125.

FRÉCHET, M. (1). Sur l'intégrale d'une fonctionelle étendue à un ensemble abstrait. Bull. Soc. Math. France 43 (1915). Pag. 249—267.

HILBERT, D. (1). Über die stetige Abbildung einer Linie auf ein Flächenstück. Mathematische Annalen 38 (1891). Pag. 459—460.

JESSEN, B. (1). Abstrakt Maal- og Integralteori. 1. Matematisk Tidsskrift B, 1934. Pag. 73—84.

— (2). Abstrakt Maal- og Integralteori. 2. Matematisk Tidsskrift B, 1935. Pag. 60—74.

— (3). Abstrakt Maal- og Integralteori. 3. Matematisk Tidsskrift B, 1938. Pag. 13—26.

— (4). Abstrakt Maal- og Integralteori. 4. Matematisk Tidsskrift B, 1939. Pag. 7—21.

— (5). Abstrakt Maal- og Integralteori. 5. Matematisk Tidsskrift B, 1942. Pag. 43—53.

— (6). Bidrag til Integralteorien for Funktioner af uendelig mange Variable. København 1930.

KOLMOGOROFF, A. (1). Grundbegriffe der Wahrscheinlichkeitsrechnung. Ergebnisse der Mathematik II_3. Berlin 1933.

LEBESGUE, H. (1). Sur l'intégration des fonctions discontinues. Ann. École norm. 27 (1910). Pag. 361—450.

NEYMAN, J. and PEARSON, E. S. (1). On the Problem of the most Efficient Tests of Statistical Hypotheses. Phil. Trans. Roy. Soc. London A, 231 (1933). Pag. 289—337.

RADON, J. (1). Theorie und Anwendungen der absolut additiven Mengenfunktionen. S.-B. Akad. Wiss. Wien 122 (1913) Pag. 1295—1438.

RIESZ, F. (1). Über Systeme integrierbarer Funktionen. Math. Ann. 69 (1910). Pag. 449—497.

SAKS, S. (1). Theorie de l'Intégrale. Monografje Matematyczne, Warszawa 1933.

— (2). Theory of the Integral. Monografje Matematyczne, Warszawa-Lwow 1937.

DE LA VALLÉE-POUSSIN, C. (1). Sur la transformation d'une intégrale multiple en une intégrale simple. Ann. Soc. Sci. Bruxelles 35 (1911), Pag. 189—190.

Indleveret til Selskabet den 29. Juni 1944.
Færdig fra Trykkeriet den 26. Marts 1945.

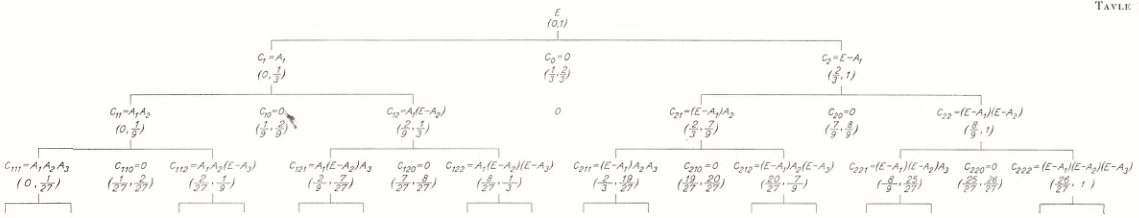
E
(0,1)
$C_1=A_1$
$(0,\frac{1}{3})$
$C_0=0$
$(\frac{1}{3},\frac{2}{3})$
$C_2=E-A_1$
$(\frac{2}{3},1)$
$C_{11}=A_1A_2$
$(0,\frac{1}{9})$
$C_{10}=0$
$(\frac{1}{9},\frac{2}{9})$
$C_{12}=A_1(E-A_2)$
$(\frac{2}{9},\frac{1}{3})$
0
$C_{21}=(E-A_1)A_2$
$(\frac{2}{3},\frac{7}{9})$
$C_{20}=0$
$(\frac{7}{9},\frac{8}{9})$
$C_{22}=(E-A_1)(E-A_2)$
$(\frac{8}{9},1)$
$C_{111}=A_1A_2A_3$
$(0,\frac{1}{27})$
$C_{110}=0$
$(\frac{1}{27},\frac{2}{27})$
$C_{112}=A_1A_2(E-A_3)$
$(\frac{2}{27},\frac{1}{9})$
$C_{121}=A_1(E-A_2)A_3$
$(\frac{2}{9},\frac{7}{27})$
$C_{120}=0$
$(\frac{7}{27},\frac{8}{27})$
$C_{122}=A_1(E-A_2)(E-A_3)$
$(\frac{8}{27},\frac{1}{3})$
$C_{211}=(E-A_1)A_2A_3$
$(\frac{2}{3},\frac{19}{27})$
$C_{210}=0$
$(\frac{19}{27},\frac{20}{27})$
$C_{212}=(E-A_1)A_2(E-A_3)$
$(\frac{20}{27},\frac{7}{9})$
$C_{221}=(E-A_1)(E-A_2)A_3$
$(\frac{8}{9},\frac{25}{27})$
$C_{220}=0$
$(\frac{25}{27},\frac{26}{27})$
$C_{222}=(E-A_1)(E-A_2)(E-A_3)$
$(\frac{26}{27},1)$

Fig. 1.

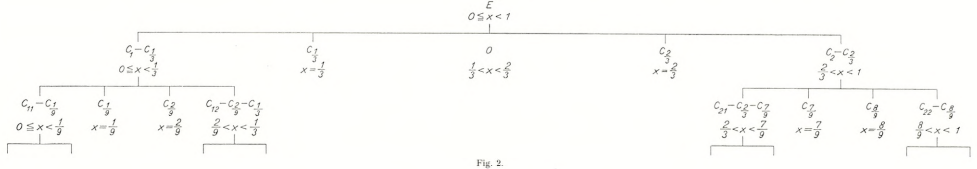
E
$0\le x<1$
$C_1-C_{\frac{1}{3}}$
$0\le x<\frac{1}{3}$
$C_{\frac{1}{3}}$
$x=\frac{1}{3}$
0
$\frac{1}{3}<x<\frac{2}{3}$
$C_{\frac{2}{3}}$
$x=\frac{2}{3}$
$C_2-C_{\frac{2}{3}}$
$\frac{2}{3}<x<1$
$C_{11}-C_{\frac{1}{9}}$
$0\le x<\frac{1}{9}$
$C_{\frac{1}{9}}$
$x=\frac{1}{9}$
$C_{\frac{2}{9}}$
$x=\frac{2}{9}$
$C_{12}-C_{\frac{2}{9}}-C_{\frac{1}{3}}$
$\frac{2}{9}<x<\frac{1}{3}$
$C_{21}-C_{\frac{2}{3}}-C_{\frac{7}{9}}$
$\frac{2}{3}<x<\frac{7}{9}$
$C_{\frac{7}{9}}$
$x=\frac{7}{9}$
$C_{\frac{8}{9}}$
$x=\frac{8}{9}$
$C_{22}-C_{\frac{8}{9}}$
$\frac{8}{9}<x<1$

Fig. 2.

DET KGL. DANSKE VIDENSKABERNES SELSKAB
MATEMATISK-FYSISKE MEDDELELSER, BIND XXI, NR. 10

A DETERMINATION OF THE ABUNDANCES OF SODIUM AND MAGNESIUM IN THE SOLAR ATMOSPHERE FROM LINES NEAR THE SERIES LIMITS

BY

MOGENS RUDKJØBING

KØBENHAVN
I KOMMISSION HOS EJNAR MUNKSGAARD
1945

Printed in Denmark.
Bianco Lunos Bogtrykkeri A/S

1. A theoretical investigation of the discontinuities at the edges of metal absorption continua in the solar spectrum has been carried out by UNSÖLD,[1] who demonstrated how the magnitude of a discontinuity could be determined from equivalent widths of the higher members of the corresponding series of absorption lines by an extrapolation process.

UNSÖLD in this way showed that the discontinuities of the absorption edges of the metals must be very small, indeed. This result, deduced from the observed strength of absorption lines, was in sharp contrast to the results obtained from the theoretical calculations of the coefficient of continuous absorption and its variation with wave-length, the latter leading to a discontinuity that was many times greater.

It is now known that the discrepancy was due to the fact that the effect of continuous absorption of the negative hydrogen ion had not been included in the theoretical calculations of the absorption coefficient. It is, in fact, assumed now that the greater part of the continuous absorption in the solar atmosphere is due to the negative hydrogen ion.[2, 3, 4, 5, 6, 7]

The aim of the present paper is to determine metal abundances from absorption edge discontinuities determined according to UNSÖLD's method. The ratio of the absorption coefficient of the metal at the edge in question to that of the negative hydrogen ion can be found from the magnitude of the discontinuity. The atomic continuous absorption coefficient of the metal and of the negative hydrogen ion being known from quantum-mechanical calculations, the abundance ratio of the metal in question and of hydrogen can be found.

The present investigation deals with two of the series considered by UNSÖLD, *viz.* the "sharp" series of neutral sodium

and the "Bergman" triplet series of neutral magnesium. The reasons for using these series were partly theoretical, because the absorption coefficients at the series limits were known, and partly practical, both of the series having lines, the total strength of which could be measured with reasonable certainty from the curves given in the Photometric Atlas of the Solar Spectrum.[8]

The atlas is very useful, because it makes it easy to find out if a line is disturbed to such a degree that it has to be omitted from the investigation. As we shall see later, few lines only could, in fact, be used.

2. The basic assumption in UNSÖLD's method is that we may treat the line absorption in the series as if it were continuous, that is, we may use the formulae for the intensity in the continuous spectrum when the absorption—expressed as an equivalent width—of each line is evenly distributed over the interval of wave-length "belonging to" that line in the series. This "continuous absorption" is a direct continuation of the true continuous absorption on the short wave-length side of the series limit, and its "coefficient of continuous absorption" may—in not too great a distance from the limit—be found by extrapolation from the known continuous absorption coefficient. The process is therefore equivalent to a displacement of the limit to the place in the spectrum of the line in question. When the correction of the line intensities to the case of absorption in an "optically thin layer" is small, *i.e.* when the intensity measured at the centre of the line is great, this method yields reliable results.

The atlas of the solar spectrum gives the spectral distribution of the radiation of the centre of the solar disc. We must then use the following formula giving the intensity for light of frequency ν in the direction perpendicular to the atmosphere:[9]

$$I_\nu(0,\theta) = B_\nu(T_e)\left[1 - \frac{1}{8}u_e\frac{1}{1-e^{-u_e}} + \frac{1}{n_\nu}\cdot\frac{3}{16}\cdot u_e\cdot\frac{1}{1-e^{-u_e}}\cos\theta\right], \quad (1)$$

where $\theta = 0$.

Here $B_\nu(T_e)$ is the black-body intensity at the effective temperature T_e, $u_e = \dfrac{h\nu}{kT_e}$ and n_ν is the ratio of the coefficient

of continuous absorption at the frequency ν to the opacity (the Rosseland-mean); h and k have their usual meanings.

This formula holds only if n_ν is constant through the atmosphere. We shall see later to what degree this assumption is justified in the cases in question.

On the short and the long wave-length side of the "limit" the intensity has the values $I_{\nu 1}$ and $I_{\nu 2}$, respectively, and the constant n_ν the values $n_{\nu 1}$ and $n_{\nu 2}$, respectively.

$$\text{Then } \Delta I_\nu = I_{\nu 2} - I_{\nu 1} = B_\nu(T_e) \cdot \left[\frac{1}{n_{\nu 2}} - \frac{1}{n_{\nu 1}}\right] \cdot \frac{3}{16} \cdot \frac{u_e}{1 - e^{-u_e}} \qquad (2)$$

and

$$\frac{\Delta I_\nu}{I_{\nu 2}} = \frac{\left[\frac{1}{n_{\nu 2}} - \frac{1}{n_{\nu 1}}\right] \cdot \frac{3}{16} \cdot \frac{u_e}{1 - e^{-u_e}}}{1 - \frac{1}{8} \frac{u_e}{1 - e^{-u_e}} + \frac{1}{n_{\nu 2}} \cdot \frac{3}{16} \cdot \frac{u_e}{1 - e^{-u_e}}} = \frac{\frac{1}{n_{\nu 2}} - \frac{1}{n_{\nu 1}}}{\frac{16}{3} \cdot \frac{1 - e^{-u_e}}{u_e} - \frac{2}{3} + \frac{1}{n_{\nu 2}}}. \qquad (3)$$

When small quantities are neglected, we get:

$$\frac{\Delta I_\nu}{I_\nu} = \frac{-\frac{\Delta n_\nu}{n_\nu^2}}{\frac{16}{3} \cdot \frac{1 - e^{-u_e}}{u_e} - \frac{2}{3} + \frac{1}{n_\nu}}, \qquad (4)$$

where $I_\nu \backsim I_{\nu 1} \backsim I_{\nu 2}$, $n_\nu \backsim n_{\nu 1} \backsim n_{\nu 2}$ and $\Delta n_\nu = n_{\nu 2} - n_{\nu 1}$.

As to the solar atmosphere, the continuous spectrum is very nearly that of "grey" matter, n_ν being for all frequencies equal to 1.

When we put n_ν equal to 1 in the above equation, we get:

$$-\Delta n_\nu = \frac{\Delta I_\nu}{I_\nu} \cdot \frac{1}{3} \cdot \left[16 \cdot \frac{1 - e^{-u_e}}{u_e} + 1\right]. \qquad (5)$$

The negative sign in front of Δn_ν means that I_ν takes its greatest value when n_ν takes the smallest and *vice versa*.

The negative hydrogen ions are believed to produce practically the whole of the total absorption on the long wave-length side of the Balmer limit, where its coefficient of absorption is near its maximum value.[10]

The constant value of the continuous absorption coefficient is therefore put equal to this maximum value ($2.6 \cdot 10^{-17}$ cm^2).

Δn_ν is the ratio of the metal absorption to the total absorption at the frequency ν. When a part x of the total absorption is due to negative hydrogen ions, the ratio of metal absorption to negative hydrogen ion absorption is $\frac{\Delta n_\nu}{x}$.

When the coefficient of continuous absorption per metal atom in the state in question is $\varkappa_{\nu m}$ and per negative hydrogen ion $\varkappa_{\nu H^-}$, the ratio of the number of metal atoms in this state to the number of negative hydrogen ions is

$$\frac{n_m}{n_{H^-}} = \frac{\Delta n_\nu}{x} \cdot \frac{\varkappa_{\nu H^-}}{\varkappa_{\nu m}}; \tag{6}$$

$\varkappa_{\nu H^-}$ is equal to x times its maximum value; $\varkappa_\nu$ is proportional to the oscillator strength per interval of energy $\frac{df}{dE}$;

$$\varkappa_\nu = 8.06 \cdot 10^{-18} \cdot \frac{df}{dE} \tag{7}$$

when E is measured in Rydberg units.[11]

When $\left(\frac{df}{dE}\right)_m$ denotes this quantity for the metal, we get:

$$\frac{n_m}{n_{H^-}} = \Delta n_\nu \cdot \frac{3.2}{\left(\frac{df}{dE}\right)_m}, \tag{8}$$

where x has disappeared.

As we shall see later, the ratio $\frac{n_m}{n_{H^-}}$ varies little for neutral sodium and magnesium. The situation will be similar for other neutral metals.

The assumption of constant n_ν (and Δn_ν) through the atmosphere is therefore justified when x is near unity. The influence of the possible variation of the rest of the continuous absorption is of course smaller, the smaller $1 - x$, and is wholly neglected in our calculations.

3. The coefficient of continuous absorption of the "sharp" and the "diffuse" series of neutral sodium is known from quan-

tum-mechanical calculation.[12] $\frac{df}{dE}$ for the two series is 0.13 and 0.82, respectively, at the (common) series limit and 0.08 and 0.31 at a distance of 0.05 Rydberg units on the short wave-length side of the limit.

The extrapolation of the $\frac{df}{dE}$-function on the long wave-length side of the limit could not be carried out with any certainty for the "diffuse" series, but was thought to be possible in the case of the "sharp" series, at least in not too great distance from the limit.

The first doublet of this series is placed in the infrared. The second (wave-lengths 6161 and 6154 Å) was considered to be placed too far from the limit. Of the lines visible in the solar spectrum only the lines of the third and fourth doublet remained. The wave-lengths of these lines are:[1]

third doublet: { 5153.42 Å
5148.85 -

fourth doublet: { 4751.83 -
4747.98 -

The line at 5153 Å could not be measured because it is strongly blended with other lines. The line at 5149 Å is placed close to another line of nearly the same intensity and shape. The curve in the atlas here has the form of a nearly symmetrical double figure. Because we are here nearly dealing with "absorption in an optically thin layer," the absorption may be taken to be equal to the sum of the absorptions from each of the lines. We may therefore take as the intensity of the sodium line its part of the "double" measured from the base of the figure, which is not necessarily thought to be placed at the top of the true continuous spectrum. Its equivalent width is found to be 0.009 Å.

In the fourth doublet the line at 4752 Å is placed in the wing of a stronger line and is therefore measured in a similar way. Its equivalent width was found to be 0.009 Å.

The second (weak) component of this doublet (at 4748 Å) is seen only as an irregularity of a stronger neighbouring line and its intensity therefore is not measurable.

The equivalent widths of the two measured lines are about one seventh of the (double) Doppler widths of the lines. Hence, the correction to absorption in "optically thin" layer is about 10 per cent. and the corrected intensities are taken to be 0.010 Å for both of the lines.

The line at 5149 Å is the weaker component of the doublet, and hence the sum of the corrected intensities of the doublet components should be 0.030 Å. The line at 4752 Å is the stronger doublet-component, and hence the total corrected intensity of this doublet is put equal to 0.015 Å.

The "interval per line" is found in the following way:

The wave number $\tilde{\nu}$ of a line in a series is given by $\tilde{\nu} = -\frac{R}{n_e^2} + \tilde{\nu}_0$, where R is the Rydberg wave number, n_e the "effective" quantum number of the upper state, and $\tilde{\nu}_0$ the wave number of the lower state common to the lines in the series.

Hence
$$\frac{d\tilde{\nu}}{dn_e} = \frac{2R}{n_e^3}; \tag{9}$$

$$\frac{d\lambda}{dn_e} = \frac{d\lambda}{d\tilde{\nu}} \cdot \frac{d\tilde{\nu}}{dn_e} = -\frac{1}{\tilde{\nu}^2} \cdot \frac{2R}{n_e^3} = -2R \cdot \frac{\lambda^2}{n_e^3}. \tag{10}$$

The difference between n_e and the term number is nearly constant for the lines in a series; therefore dn_e is put equal to one and $2R \cdot \frac{\lambda^2}{n_e^3}$ used as a measure of the "interval of wavelength" per line. For the two doublets considered, n_e takes the values 4.65 and 5.65 and hence the two intervals are 582 and 275 Å, respectively, and $\frac{\Delta I}{I}$ for the two lines is 0.000052 and 0.000055.

Inserting the numerical values of the constants, we find

$$u_e = \frac{h\nu}{kT_e} = \frac{h}{k} \cdot \frac{c}{\lambda} \cdot \frac{1}{T_e} = \frac{1.439}{\lambda \cdot T_e}. \tag{11}$$

With $T_e = 5740°$ and $\lambda = 5151$ and 4750 Å we get $u_e = 4.87$ and 5.28. Hence, $1 - e^{-u_e}$ is practically equal to 1.

For Δn_ν numerically we find in the two cases 0.000074 and 0.000074. The $\frac{df}{dE}$-function is linearly extrapolated. As its numerical value is known in two points only, we have no indication for the extrapolation in any other way than this, the simplest one.

The E-values corresponding to the two wave-lengths above are 0.177 and 0.192, respectively. The limit is placed at $E = 0.223$. We then extrapolate the $\frac{df}{dE}$-values (p. 7) and find for the places of the two lines $\frac{df}{dE} = 0.17_5$ and 0.16.

We find from formula (8) $\frac{n_{Na\,3^2P}}{n_{H^-}} = 0.0013_5$ and 0.0014_8, where $n_{Na\,3^2P}$ is the number of sodium atoms in the $3\,p$-state (the upper state of the resonance lines of sodium). As a mean value we shall adopt 0.0014.

From SAHA's equation we get:[13]

$$\left.\begin{aligned} \log\left(\frac{n_H}{n_{H^-}}\right) &= -0.70\cdot\theta+\frac{5}{2}\log T-0.48+\log\left(\frac{2\cdot 2}{1}\right)-\log P_e \\ \text{and } \log\left(\frac{n_{Na^+}}{n_{Na\,3^2P}}\right) &= -3.02\cdot\theta+\frac{5}{2}\log T-0.48+\log\left(\frac{2\cdot 1}{6}\right)-\log P_e, \end{aligned}\right\} \quad (12)$$

the ionization potential of the $3\,p$-state of neutral sodium being 3.02 volt and its statistical weight 6. θ is equal to $\frac{5040^\circ}{T}$.

From these equations we get:

$$\log\left(\frac{n_H}{n_{Na^+}}\cdot\frac{n_{Na\,3^2P}}{n_{H^-}}\right) = 2.32\cdot\theta+\log 12.$$

In the solar atmosphere practically all the hydrogen atoms are neutral and in the ground state and practically all the sodium atoms in the ground state of the Na^+ ion.

We see that the electron pressure has disappeared from the equation and that the variation of $\frac{n_{Na\,3^2P}}{n_{H^-}}$ with the temperature is small. For θ we use as a representative value $\theta_e = \frac{5040^\circ}{T_e} = 0.878$. Hence we get:

$$\log\left(\frac{n_H}{n_{Na^+}}\cdot\frac{n_{Na\,3^2P}}{n_{H^-}}\right) = 3.12.$$

When inserting

$$\log\left(\frac{n_{Na\,3^2P}}{n_{H^-}}\right) = 0.15 - 3,$$

we get:

$$\log\left(\frac{n_H}{n_{Na^+}}\right) = 6.0.$$

This is in good agreement with the value (6.1) found by B. Strömgren.[14]

4. The magnesium series dealt with—the "Bergman" triplet series—has single lines, the multiplet structure being wholly negligible in comparison with the width of the lines in the solar spectrum. The lines of the corresponding singlet series are weaker and are more disturbed by other lines, because its series limit is placed at a shorter wave-length (6547 Å) than the limit of the triplet series (7289 Å).

The lines—especially the higher members of the series—are very much broadened by damping. Unless the lines are placed in regions practically free from disturbing influences of other lines, the wings cannot be traced to so great distances from the centres of the lines that the total intensity can be found with reasonable certainty. This is probably the reason for the seemingly irregular run of the intensities (cf. Unsöld[1]).

Of the lines given by Unsöld the following six are found in the atlas:

λ(Å) = 8736.04, 8346.13, 8098.75, 7930.82, 7811.16, 7722.64.[15] Of these, the lines at 8346, 8099, 7931 Å are disturbed. The line at 7811 Å is blended with a sharper line placed at one of its wings. The other half of the line is free and hence the total intensity of the line may be found by doubling the equivalent width of this part. The line at 7723 Å is very broad and difficult to measure.

The equivalent widths of the lines at 8736 Å and 7811 Å are found to be 0.266 Å and 0.059 Å, respectively.

When reducing the values to the case of absorption in an "optically thin" layer, we use our knowledge of the intensity at the centres of the lines, which in this case—comparatively broad lines—may be taken from the profiles in the atlas. Hence, we need not know the value of the damping constants for the

lines, provided their profiles are determined by damping alone. This probably applies to the weaker of the two lines here considered. For the stronger, we calculate for comparison the reduction factor for the other ideal case, that of pure Doppler-broadening. The constants differ so little that we may use a mean value of the two factors.

In the calculation of these factors we have—for the sake of convenience—used the formula for the line profile in the integrated spectrum and put the value of $x_e = u_e\,(1-e^{-u_e})^{-1}$ equal to 4. The errors introduced in this way are not serious in our, on the whole, comparatively rough calculations.

The formula used for r (the intensity in units of the intensity in the neighbouring continuous spectrum) hence is[16]

$$r = \frac{\lambda + \frac{2}{3}\sqrt{3\lambda}}{1+\frac{2}{3}\sqrt{3\lambda}}, \tag{13}$$

where $\lambda = \frac{1}{1+\eta}$, and $\eta = \frac{l_\nu}{k_\nu}$, where l_ν and k_ν denote the coefficient of scattering in the line and the coefficient of continuous absorption at the place of the line, respectively. (We here neglect the absorption part of the line "absorption" coefficient.)

The central intensities of the two lines are 0.60 and 0.91, respectively. The corresponding values of λ are 0.33 and 0.817 and the values of η are 2.0 and 0.224, respectively.

In the damping and the Doppler case η is equal to

$$\frac{\eta_0}{1+\left(\frac{\omega-\omega_0}{\delta}\right)^2} \quad \text{and} \quad \eta_0 \cdot e^{-ln\,2\left(\frac{\omega-\omega_0}{\delta}\right)^2}, \tag{14}$$

respectively, when η_0 is the value of η at the centre of the line.[17] $\frac{\omega-\omega_0}{\delta}$ is the distance from the centre of the line in units of δ, the distance for which η takes the value $\frac{\eta_0}{2}$.

With the aid of the formula (13) for r, we calculate the integral of $1-r$ over the line and compare it with the value we should get, if η were vanishingly small.

We have

$$1-r=\frac{1-\lambda}{1+\frac{2}{3}\sqrt{3\lambda}}=\frac{\frac{\eta}{1+\eta}}{1+\frac{2}{3}\sqrt{3\lambda}}; \tag{15}$$

when $\eta \to 0$, $\lambda \to 1$, and we get:

$$1-r=\frac{\eta}{1+\frac{2}{3}\sqrt{3}}. \tag{16}$$

Hence, the integral of η divided by $1+\frac{2}{3}\sqrt{3}$ is the total intensity in the case of an "optically thin" layer, and this integral divided by the integral of the true $1-r$ (both taken with the correct η_0) gives the required correction factor.

For the line at 8736 Å the correction factor in the case of pure damping broadening is 1.5 and for pure Doppler broadening 1.9. As a mean value we shall use 1.7.

For the line at 7811 Å the factor in the damping case is 1.2, which is the value adopted.

The corrected intensities then are 0.45 Å and 0.070 Å.

The effective quantum numbers of the upper terms of the two transitions are 7 and 11, respectively, and the corresponding wave-length intervals 488 Å and 101 Å.

Using the formula (5) we find for Δn_ν 0.00192 and 0.00135. $\frac{df}{dE}$ at the series limit is calculated from the corresponding hydrogen-value. For sodium it is known that a difference of nearly one between the true and the effective quantum number of the ground term of a series makes a difference of only 15 per cent. from the approximate correction factor

$$\left(\frac{\nu_H}{\nu}\right)^3 \cdot \left(\frac{n}{n_e}\right)^3, \tag{17}$$

where ν_H and ν are the frequencies of the hydrogen and the metal limits.[18] In our case $n-n_e$ is only 0.2, so that we simply use the correction factor given above.

$\frac{df}{dE}$ for the corresponding hydrogen limit is 2.2, being one half of the value of $f \cdot n^3$ for the high members of the series given by BETHE[19] (cf. our formula (9)). Hence, $\frac{df}{dE}$ for the magnesium limit is 1.84. We extrapolate to greater wave-lengths, using the approximate law found for hydrogen, *i. e.* $\frac{df}{dE}$ is proportional to λ^3. For the two lines we find $\frac{df}{dE}$ equal to 3.16 and 2.26 and $\frac{n_{Mg\,3^3D}}{n_H}$ equal to 0.00194 and 0.00191, respectively. (The good agreement between these two values is of course only accidental.) We use the value 0.0019 in our further calculations.

The equation corresponding to the sodium equation (12) is:

$$\log\left(\frac{n_{Mg^+}}{n_{Mg\,3^3D}}\right) = -1.69 \cdot \theta + \frac{5}{2}\log T - 0.48 + \log\left(\frac{2 \cdot 2}{15}\right) - \log P_e, \quad (18)$$

and we get:

$$\log\left(\frac{n_H}{n_{Mg^+}} \cdot \frac{n_{Mg\,3^3D}}{n_H}\right) = 0.99 \cdot \theta + \log 15.$$

As before, we put θ equal to $\theta_e = 0.878$, and we get:

$$\left(\log \frac{n_H}{n_{Mg^+}} \cdot \frac{n_{Mg\,3^3D}}{n_H}\right) = 2.05.$$

$$\text{We thus find } \log\left(\frac{n_H}{n_{Mg^+}}\right) = 4.77.$$

Magnesium is not so completely ionized in the solar atmosphere as is sodium. In the model atmosphere with $\log A = 3.8$[20] three per cent. of the magnesium atoms are neutral at $\theta = \theta_e$. Hence we get 4.7_5 for $\log\left(\frac{n_H}{n_{Mg}}\right)$.

5. If we trust this hydrogen-magnesium ratio, we find that the relative proportions of the metals magnesium, calcium, sodium, and potassium are nearly equal to those found by GOLDSCHMIDT for these metals in meteorites.[21]

Normalizing GOLDSCHMIDT's relative proportions so that the sum of the abundances of the metals is equal to one, we get the values in the first column of the table below.

Fe	0.30	—	—
Si	0.33	—	—
Mg	0.30	0.000018	0.00006
Ca	0.020	0.0000016	0.00008
Na	0.015	0.0000009	0.00006
K	0.0023	0.00000020	0.00009

In the next column we write the abundances relative to hydrogen. For *Ca* and *K* we use the values found by B. STRÖMGREN, for *Mg* the value found above, and for *Na* the mean value of B. STRÖMGREN's and our values. (The *Mg* abundance found by B. STRÖMGREN was determined by comparison of a *Mg* and a *Ca* line and is probably less accurate than the other abundances).

The third column gives the ratio of the abundances in the two first. The mean of the different values of this ratio is found to be $0{,}00007_2$. The logarithm of A—the number of hydrogen atoms per metal atom—hence being 4.1_5.

The value of $\log A$ (3.9) found by B. STRÖMGREN in his investigations is a parameter of the model atmosphere which measures the number of free electrons per hydrogen atom. In view of the various sources of errors no great weight should be attached to this discrepancy. Nevertheless the following consideration may be of some interest. That part of the electrons—nearly 50 per cent.—which, if we trust the numbers given above, is delivered by elements other than the metals, may be due to the ionization of carbon. This element has an ionization potential intermediate between the potentials of hydrogen and the metals, and its abundance is possibly so high that its contribution to the electron pressure may be of the required order.

A method for the correction of the model atmosphere tables for different values of the carbon abundance is given by B. STRÖMGREN.[22]

References.

1) A. Unsöld: Zs. f. Aph. **17**, 1, 1939.
2) R. Wildt: Ap. J. **89**, 295, 1939; **90**, 611, 1939.
3) E. Hylleraas: Zs. f. Phys. **60**, 624, 1930.
4) H. S. W. Massey and R. A. Smith: Proc. Roy. Soc. A **155**, 472, 1936.
5) C. K. Jen: Phys. Rev. **43**, 540, 1933.
6) H. S. W. Massey and D. R. Bates: Ap. J. **91**. 202, 1940.
7) B. Strömgren: Festschrift für Elis Strömgren, 218, 1940.
8) M. Minnaert, G. F. W. Mulders, J. Houtgast: Photometric Atlas of the Solar Spectrum, Amsterdam 1940.
9) B. Strömgren: Handb. d. Astroph. Bd. VII, 211 (68), Berlin 1936.
10) B. Strömgren: Festschrift für Elis Strömgren, 232, 1940.
11) A. Unsöld: Physik d. Sternatmosphären (35,1), Berlin 1938.
12) M. Rudkjøbing: Publ. og m. Medd. fra Kbhvns. Obs., **124**, 10, 1940.
13) A. Unsöld: Physik d. Sternatmosphären (22,5), Berlin 1938.
14) B. Strömgren: Festschrift für Elis Strömgren, 254, 1940.
15) Erroneously given as 7822.64 by Unsöld.
16) B. Strömgren: Handb. d. Astroph. Bd. VII, 231 (142), Berlin 1936.
17) V. Weisskopf: Phys. Z. **34**, 1, 1933.
18) M. Rudkjøbing: Publ. og m. Medd. fra Kbhvns. Obs. **124**, 12, 1940.
19) H. Bethe: Hand. d. Physik XXIV/1, 443, Berlin 1933.
20) B. Strömgren: Festschrift für Elis Strömgren, 236, 1940.
21) B. Strömgren: Festschrift für Elis Strömgren, 256, 1940.
22) B. Strömgren: Tables of Model Stellar Atmospheres. Publ. og m. Medd. fra Kbhvns. Obs. **138**, 1944.

Indleveret til Selskabet den 31. Marts 1944.
Færdig fra Trykkeriet den 12. Marts 1945.

DET KGL. DANSKE VIDENSKABERNES SELSKAB
MATEMATISK-FYSISKE MEDDELELSER, BIND XXI, NR. 11.

ON THE STRUCTURE OF GENERALIZED ALMOST PERIODIC FUNCTIONS

BY

ERLING FØLNER

KØBENHAVN
I KOMMISSION HOS EJNAR MUNKSGAARD
1945

Printed in Denmark.
Bianco Lunos Bogtrykkeri A/S

§ 1. Introduction.

Throughout the paper we operate with complex Lebesgue measurable functions of a real variable defined on the whole axis. For every $p \geq 1$ we consider the well-known norms[1] (which may be ∞)

$$\| f(x) \|_O = \underset{-\infty < x < \infty}{u.\,b.} | f(x) |,$$

$$\| f(x) \|_{S_L^p} = \underset{-\infty < x < \infty}{u.\,b.} \sqrt[p]{\frac{1}{L} \int_x^{x+L} | f(\xi) |^p \, d\xi} \quad (L > 0),$$

$$\| f(x) \|_{W^p} = \lim_{L \to \infty} \| f(x) \|_{S_L^p}$$

(the limit always exists),

$$\| f(x) \|_{B^p} = \overline{\lim_{T \to \infty}} \sqrt[p]{\frac{1}{2T} \int_{-T}^{T} | f(x) |^p dx}$$

as well as the corresponding limit notions, O-convergence (uniform convergence on the whole axis), S^p-convergence (the norms $\| f \|_{S_L^p}$ correspond for different values of L to the same limit notion), W^p-convergence, and B^p-convergence. Understanding by a trigonometric polynomial a finite sum of the form

$$\sum_{n=1}^{N} a_n e^{i \lambda_n x}$$

[1] See e.g. Besicovitch and Bohr [I] or Besicovitch [II]. The norms $\| f \|_{S_L^p}$, $\| f \|_{W^p}$, and $\| f \|_{B^p}$ are named after Stepanoff [I], Weyl [I], and Besicovitch [I] respectively.

where the coefficients a_n are complex numbers and the "exponens" λ_n are real numbers, the different types of almost periodic functions may be defined in the following manner:

The ordinary almost periodic functions (the O-a. p. functions) may be defined as the functions which can be O-approximated by trigonometric polynomials.

The S^p-a. p. functions may be defined as the functions which can be S^p-approximated by trigonometric polynomials.

The W^p-a. p. functions may be defined as the functions which can be W^p-approximated by trigonometric polynomials.

The B^p-a. p. functions may be defined as the functions which can be B^p-approximated by trigonometric polynomials.

The proper main theorem in the theory of O-a. p. functions is the following generalization of Weierstrass's theorem concerning continuous periodic functions:

An O-a. p. function $f(x)$ may be characterized as a continuous function possessing to every $\varepsilon > 0$ a relatively dense set of O-translation numbers τ. By a relatively dense set of numbers we understand a set to which can be found a length L such that every interval $\alpha < x < \alpha + L$ of this length contains a number of the set. By an O-translation number τ of $f(x)$ belonging to ε we understand a number satisfying

$$\| f(x+\tau) - f(x) \|_O \leqq \varepsilon, \text{ i. e. } | f(x+\tau) - f(x) | \leqq \varepsilon$$

for every x.

Quite an analogous main theorem holds good of the S^p-a. p. functions:

An S^p-a. p. function $f(x)$ may be characterized as a p-integrable[1] *function possessing for fixed $L > 0$ to every $\varepsilon > 0$ a relatively dense set of S_L^p-translation numbers τ.* By an S_L^p-translation number τ belonging to ε we understand, of course, a number satisfying the inequality

$$\| f(x+\tau) - f(x) \|_{S_L^p} \leqq \varepsilon .$$

For the W^p-a. p. and the B^p-a. p. functions the analogous

[1] A function $f(x)$ is called p-integrable if $\int_a^b | f(x) |^p dx < \infty$ for every finite interval (a, b).

theorems are wrong. This may be seen from considering the example

$$F(x) = \begin{cases} 1 \text{ for } x \geqq 0 \\ -1 \text{ for } x < 0. \end{cases}$$

The limits

$$\lim_{T \to \infty} \frac{1}{T} \int_0^T F(x)\, dx \qquad \text{and} \qquad \lim_{T \to \infty} \frac{1}{T} \int_{-T}^0 F(x) dx$$

being different the function $F(x)$ is neither W^p-a. p. nor B^p-a. p.. On the other hand for an arbitrary real number τ we have

$$| F(x+\tau) - F(x) | = \begin{cases} 2 \text{ for } x \text{ lying between } 0 \text{ and } -\tau \text{ (inclusive the smaller, exclusive the larger number)} \\ 0 \text{ elsewhere} \end{cases}$$

so that

$$\| F(x+\tau) - F(x) \|_{W^p} = \| F(x+\tau) - F(x) \|_{B^p} = 0$$

for every τ.

Still the W^p-a. p. functions may be characterized in a simple way by structural properties which are very similar to those in the O-a. p. and the S^p-a. p. cases. In fact the following main theorem is valid:

A W^p-a.p. function may be characterized as a p-integrable function possessing to every $\varepsilon > 0$ for L sufficiently large, i.e. for $L \geqq L_0(\varepsilon)$ a relatively dense set of S_L^p-translation numbers.

It is of course obvious that a W^p-translation number belonging to ε is an S_L^p-translation number belonging to—say—2ε for L sufficiently large, $L \geqq L_0'(\tau)$, but the difference between the last theorem and the (wrong) theorem analogous to the above mentioned main theorems is that in the first case the same L_0 must be applicable to all translation numbers belonging to the given ε. It is also immediately seen that the function $F(x)$ from the example above does not possess this property; the larger the modulus of τ, the larger $L_0'(\tau)$ is to be used.

In the case of B^p-a.p. functions the characterization by means of structural properties known is not nearly as simple as in the O-a. p., S^p-a. p., and W^p-a. p. cases. We quote it after Be-

SICOVITCH and BOHR [I] or BESICOVITCH [II] where proofs of the main theorems in the S^p-a. p. and W^p-a. p. cases are also to be found.

A set of real numbers is called satisfactorily uniform if there exists a positive number L such that the ratio of the maximum number of numbers from the set included in an interval of length L to the minimum number is less than 2. A B^p-a. p. function can then be characterized as a p-integrable function for which to every $\varepsilon > 0$ can be found a satisfactorily uniform set of B^p-translation numbers $\{\tau_n\}$, $n = 0, \pm 1, \pm 2, \cdots$, i. e. numbers with

$$\| f(x+\tau_n) - f(x) \|_{B^p} \leq \varepsilon,$$

and such that further for every $c > 0$

$$\overline{\lim_{T\to\infty}} \frac{1}{2T} \int_{-T}^{T} \left(\overline{\lim_{n\to\infty}} \frac{1}{2n+1} \sum_{\nu=-n}^{n} \frac{1}{c} \int_{x}^{x+c} | f(\xi+\tau_\nu) - f(\xi) |^p d\xi \right) dx \leq \varepsilon^p.$$

§ 2. Summary of the Paper.

Our counter example from § 1 shows that by a structural characterization of the B^p-a. p. functions a stronger uniformity property must be imposed upon the translation numbers belonging to a given ε than that of being merely B^p-translation numbers belonging to the same ε. The structural characterization of Besicovitch and Bohr shows one way of choosing this uniformity property. By the W^p-a. p. functions the situation was a similar one. In my efforts to find a simpler structural characterization than that of Besicovitch-Bohr I was therefore led to consider a special class of functions which will be called K-a. p. functions.

A function $f(x)$ is called K-a. p. if it is finite outside a K-zero set Z, i. e. a set[1] with

$$\overline{m}_B Z = \overline{\lim_{T\to\infty}} \frac{1}{2T} m(Z; -T, T) = 0,^{2)}$$

[1] We operate only with measurable sets.

[2] By $(Z; a, b)$ we denote the part of the set Z which is included in the interval $[a, b]$.

and to every $\varepsilon > 0$ there exists a relatively dense set of numbers $\tau = \tau(\varepsilon)$ and a set $E = E(\varepsilon) \supseteq Z$ with

$$\overline{m}_B E = \overline{\lim_{T \to \infty}} \frac{1}{2T} m(E; -T, T) \leqq \varepsilon$$

such that

$$|f(x+\tau) - f(x)| \leqq \varepsilon$$

when both $x \in CE$ and $x + \tau \in CE$ (where CE denotes the complement of E).

My hope was that this class of functions should be identical with the class of functions $f(x)$ which can be K-approximated by trigonometric polynomials, i. e. for which to every $\varepsilon > 0$ there exists a trigonometric polynomial $s(x)$ and a set E with $\overline{m}_B E \leqq \varepsilon$ such that

$$|f(x) - s(x)| \leqq \varepsilon$$

when $x \in CE$, and as we shall see in § 3 this is really the case. The latter class of functions has first been considered by A. S. Kovanko who gave a structural characterization for the functions of the class analogous to that of Besicovitch-Bohr, upon which his proof was also based (Kovanko [I]).

Starting from the approximation properties of the K-a. p. functions it is easy to show that a B^p-a. p. function means the same thing as a K-a. p. function for which $\|f(x) - (f(x))_N\|_{B^p} \to 0$ for $N \to \infty$. Here $(f(x))_N$ denotes the function $f(x)$ "cut off" at the number N, i.e. the function

$$(f(x))_N = \begin{cases} f(x) & \text{for } |f(x)| \leqq N \\ N \operatorname{sign} f(x) & \text{for } |f(x)| \geqq N. \end{cases}$$

Instead of the additional condition mentioned one may also—as Kovanko has done it—use the additional condition $\|f_E(x)\|_{B^p} \to 0$ for $\overline{m}_B E \to 0$ where $f_E(x)$ denotes the function which is equal to $f(x)$ for x lying in (the arbitrary set) E and equal to 0 elsewhere.

In § 4 instead of the additional condition $\|f(x) - (f(x))_N\|_{B^p} \to 0$ for $N \to \infty$ we consider the simpler condition $\|f(x)\|_{B^p} < \infty$, i. e. we investigate the B^p-bounded K-a. p. functions. It is shown that such a function means the same thing as a function which can be written in the form

$$f(x) = g(x) + j(x)$$

where $g(x)$ is B^p-a. p. and $j(x)$ is a B^p-bounded K-zero function, i. e. a function with $\|j(x)\|_{B^p} < \infty$ and $\overline{m}_B [|j(x)| > \varepsilon] = 0$ for every $\varepsilon > 0$. Denoting a set of functions which differ from one and the same B^p-bounded K-a. p. function by B^p-bounded K-zero functions as a B^p-bounded K-a. p. point, we can therefore say that in every B^p-bounded K-a. p. point there is lying a B^p-a. p. point, and it is easy further to show that there can only lie one B^p-a. p. point.

If $p > 1$ a B^p-bounded K-a. p. function is $B^{p'}$-a. p. for $1 \leq p' < p$.

A B^p-bounded K-a. p. function need not have a mean value in the Besicovitch sense if $p = 1$, but the mean value notion can be generalized as to comprehend these functions by putting

$$M^* \{f(x)\} = \lim_{N \to \infty} M \{(f(x))_N\}.$$

After that one can in the usual way associate to every B^p-bounded K-a. p. function a Fourier series which will be the same for all functions in the surrounding B^p-bounded K-a. p. point and therefore identical with the Fourier series of the B^p-a. p. point in that point. Hence the Bochner-Fejér polynomials will B^p-converge to a function which only differs from $f(x)$ by a B^p-bounded K-zero function.

We can say that we almost have a structural characterization of a B^p-a. p. function in that of being a B^p-bounded K-a. p. function, viz. in the sense that *the set of B^p-bounded K-a. p. functions gives rise to just the same Fourier series as the set of B^p-a. p. functions.*

§ 3. The Main Theorem for the K-a. p. Functions. The Additional Condition $\|f(x) - (f(x))_N\|_{B^p} \to 0$.

We repeat the definition of a K-a. p. function given in § 2.

Definition. *A (measurable) function $f(x)$ is called K-a. p. if it is finite outside a K-zero set Z, i. e. a set with*

$$\overline{m}_B Z = \overline{\lim_{T \to \infty}} \frac{1}{2T} m(Z; -T, T) = 0,$$ [1]

[1] By $(Z; a, b)$ we denote the part of the set Z which is included in the interval $[a, b]$.

and to every $\varepsilon > 0$ *there exists a relatively dense set of numbers* $\tau = \tau(\varepsilon)$ *and a set* $E = E(\varepsilon) \supseteq Z$ *with*

$$\overline{m}_B E = \overline{\lim_{T \to \infty}} \frac{1}{2T} m(E; -T, T) \leqq \varepsilon$$

such that

$$|f(x+\tau) - f(x)| \leqq \varepsilon$$

when both $x \in CE$ *and* $x + \tau \in CE$. The numbers τ and the set E are called (joined) translation numbers and exception set of the function $f(x)$ belonging to ε.

We are to show the following

Theorem 1. Main Theorem. *A K-a.p. function may be characterized as a (measurable) function which can be K-approximated by trigonometric polynomials, i.e. for which to every* $\varepsilon > 0$ *there exists a trigonometric polynomial* $s(x)$ *and a set* E *with* $\overline{m}_B E \leqq \varepsilon$ *such that*

$$|f(x) - s(x)| \leqq \varepsilon$$

for $x \in CE$. The trigonometric polynomial $s(x)$ and the set E are called (joined) approximating polynomial and exception set of the function $f(x)$ belonging to ε.[1)]

We first show the simple part of the theorem, viz. that a function $f(x)$ which can be K-approximated by trigonometric polynomials is K-a.p.. It is obvious that $Z = [|f(x)| = \infty]$ is a K-zero set, for a trigonometric polynomial being finite this set must be contained in the exception set $E(\varepsilon)$ belonging to an arbitrarily small $\varepsilon > 0$, and $E(\varepsilon)$ has $\overline{m}_B E(\varepsilon) \leqq \varepsilon$. Next we prove the translation properties. Let $\varepsilon > 0$ be arbitrarily given. Belonging to ε we choose a trigonometric polynomial $s(x)$ and an exception set E ($\supseteq Z$). Then

[1)] Incidentally the K-approximation can be defined by help of the K_N-norm

$$\|f(x)\|_{K_N} = \|(f(x))_N\|_{B^p}$$

where $(f(x))_N$ denotes the function $f(x)$ cut off at the number N (see p. 7) and $N > 0$ is an arbitrarily chosen fixed number. As easily seen the K_N-norm fulfills the triangel inequality

$$\|f(x) + g(x)\|_{K_N} \leqq \|f(x)\|_{K_N} + \|g(x)\|_{K_N}.$$

$$|f(x)-s(x)|\leq\varepsilon$$

for $x\varepsilon CE$, and $\overline{m}_B E\leq\varepsilon$. The trigonometric polynomial $s(x)$ being an ordinary almost periodic function it has a relatively dense set of O-translation numbers τ belonging to ε, so that

$$|s(x+\tau)-s(x)|\leq\varepsilon$$

for all x. Hence

$$|f(x+\tau)-f(x)|\leq|f(x+\tau)-s(x+\tau)|+|s(x+\tau)-s(x)|+|s(x)-f(x)|\leq 3\varepsilon$$

when both $x\varepsilon CE$ and $x+\tau\varepsilon CE$. This proves the first part of the main theorem.

In order to prove the second part of the main theorem we set up four lemmas.

Lemma 1. *Let $f(x)$ be a K-a. p. function. To every $\varepsilon>0$ it is then possible to choose a number $\Gamma=\Gamma(\varepsilon)$ and a set $E^*=E^*(\varepsilon)$ with $\overline{m}_B E^*\leq\varepsilon$ such that*

$$|f(x)|\leq\Gamma$$

for $x\varepsilon CE^*$.

Proof. Let Z denote the set $[|f(x)|=\infty]$. Then $\overline{m}_B Z=0$. Belonging to $\frac{1}{12}\varepsilon$ we choose a relatively dense set $\{\tau\}$ of translation numbers and an exception set E of $f(x)$. The set $\{\tau\}$ being relatively dense we can choose a length L so large that every interval of this length contains a translation number τ. Next we choose a length $L_0\left(\geq\frac{1}{2}L\right)$ so large that $\frac{L}{2L_0}\leq\frac{1}{3}\varepsilon$, $\frac{1}{2L_0}m(Z;-L_0,L_0)\leq\frac{1}{12}\varepsilon$, and $\frac{1}{2L_0}m(E;-L_0,L_0)\leq\frac{1}{6}\varepsilon$. As is well-known in every bounded set a finite function is bounded outside a set of arbitrarily small measure. In the interval $\left[-L_0+\frac{1}{2}L,\ L_0-\frac{1}{2}L\right]$ the function $f(x)$ is finite outside the set $E_1=\left(Z;-L_0+\frac{1}{2}L,\ L_0-\frac{1}{2}L\right)$ with $\frac{1}{2L_0}mE_1\leq\frac{1}{12}\varepsilon$, and in the interval mentioned $f(x)$ is therefore bounded, $|f(x)|\leq K$, outside a set E_2 with $\frac{1}{2L_0}mE_2\leq\frac{1}{6}\varepsilon$. In the interval $2nL_0-\frac{1}{2}L<x<2nL_0+\frac{1}{2}L$ $(n=\pm1,\pm2,\cdots)$ we choose a translation number τ_n from

$\{\tau\}$. We form the set E_3 obtained by performing the translations $\tau_0 = 0, \tau_1, \tau_{-1}, \tau_2, \tau_{-2}, \cdots$ on the set $E_2 \dot{+} \left(E; -L_0 + \frac{1}{2}L, L_0 - \frac{1}{2}L\right)$ and next forming the sum of all the translated sets. The set obtained by the translation τ_n lying entirely in the interval $(2n-1)L_0 < x < (2n+1)L_0$ we have

$$\overline{m}_B E_3 = m_B E_3 \leqq \frac{1}{2L_0} mE_2 + \frac{1}{2L_0} m\left(E; -L_0 + \frac{1}{2}L, L_0 - \frac{1}{2}L\right) \leqq$$

$$\frac{1}{2L_0} mE_2 + \frac{1}{2L_0} m(E; -L_0, L_0) \leqq \frac{1}{6}\varepsilon + \frac{1}{6}\varepsilon = \frac{1}{3}\varepsilon.$$

Let E_4 denote the complement of the set obtained from performing the translations $\tau_0 = 0, \tau_1, \tau_{-1}, \tau_2, \tau_{-2}, \cdots$ on the interval $\left[-L_0 + \frac{1}{2}L, L_0 - \frac{1}{2}L\right]$ and next forming the sum of all the translated intervals. The interval obtained by the translation τ_n lying entirely in the interval $(2n-1)L_0 < x < (2n+1)L_0$, we have

$$\overline{m}_B E_4 = m_B E_4 = \frac{L}{2L_0} \leqq \frac{1}{3}\varepsilon.$$

Putting

$$E^* = E \dot{+} E_3 \dot{+} E_4$$

obviously

$$\overline{m}_B E_3 \leqq \overline{m}_B E + \overline{m}_B E_3 + \overline{m}_B E_4 \leqq \frac{1}{12}\varepsilon + \frac{1}{3}\varepsilon + \frac{1}{3}\varepsilon < \varepsilon.$$

Further for every $x \varepsilon CE^*$ we have

$$|f(x)| \leqq K + \frac{1}{12}\varepsilon,$$

for as $x \varepsilon CE_4$ for some n the argument x will lie in the interval obtained from the interval $\left[-L_0 + \frac{1}{2}L, L_0 - \frac{1}{2}L\right]$ by means of the translation τ_n, and as $x \varepsilon CE_3$ the number $x - \tau_n$ will lie in CE_2 and in CE, so that

$$|f(x)| \leqq |f(x-\tau_n)| + |f(x) - f(x-\tau_n)| \leqq K + \frac{1}{12}\varepsilon.$$

This accomplishes the proof of lemma 1.

The lemma 1 may also be expressed by saying that for every K-a. p. function $f(x)$

$$\overline{m}_B[|f(x)-(f(x))_N|>0]\to 0 \quad \text{when} \quad N\to\infty,$$

where $(f(x))_N$ as usual denotes the cut-off function (see p. 7). Hence the cut-off function $(f(x))_N$ will K-converge towards $f(x)$ for $N\to\infty$. A simple geometric consideration shows that for every τ we have

$$|(f(x+\tau))_N-(f(x))_N|\leq|f(x+\tau)-f(x)|,$$

and from this it is seen that *if $f(x)$ is K-a. p. so is $(f(x))_N$*, viz. with the same translation numbers and the same exception sets. These two properties of $(f(x))_N$ show that it is sufficient to prove the second part of our main theorem in the case of bounded K-a. p. functions.

Lemma 2. *Let $f(x)$ be a bounded K-a. p. function. Then the "smoothed" function*

$$\varphi_\delta(x)=\frac{1}{\delta}\int_x^{x+\delta} f(\xi)\,d\xi \qquad \delta>0$$

will K-converge towards $f(x)$ for $\delta\to 0$.

Proof. Belonging to ε^2 we choose a relatively dense set $\{\tau\}$ of translation numbers and an exception set E of $f(x)$. The set $\{\tau\}$ being relatively dense we can choose a length L so large that every interval of this length contains a translation number τ. Next we choose an $L_0\left(\geq\frac{1}{2}(L+2)\right)$ so large that $\frac{L+2}{2L_0}\leq\varepsilon$ and $\frac{1}{2L_0}m(E;-L_0,L_0)\leq 2\varepsilon^2$. In the interval $[-L_0,L_0]$ the smoothed function $\varphi_\delta(x)$ will converge towards $f(x)$ almost everywhere, and we can therefore determine a δ_0, $0<\delta_0<1$, such that for every δ, $0<\delta<\delta_0$, there exists a set $E_1=E_1(\delta)$ inside $[-L_0,L_0]$ with $\frac{1}{2L_0}mE_1\leq\varepsilon$ such that

$$|f(x)-\varphi_\delta(x)|\leq\varepsilon$$

when $x\in(CE_1;-L_0,L_0)$. For an arbitrarily fixed δ, $0<\delta<\delta_0\,(<1)$,

the interval $\left[-L_0+\frac{1}{2}L, L_0-\frac{1}{2}L\right]$ is divided beginning at the left in as many subintervals of the length δ as possible. Let these subintervals fill out the interval $\left[-L_0+\frac{1}{2}L, L_1\right]$. The number δ being <1 the interval $\left[-L_0+\frac{1}{2}L, L_1\right]$ has a length which is $\geqq 2L_0-L-1$. In the interval $2nL_0-\frac{1}{2}L<x<2nL_0+\frac{1}{2}L$ $(n=\pm 1, \pm 2, \cdots)$ we choose a translation number τ_n from $\{\tau\}$. We then consider the set E_2 obtained by performing the translations $\tau_0=0, \tau_1, \tau_{-1}\tau_2, \tau_{-2}, \cdots$ on the set $\left(E; -L_0+\frac{1}{2}L, L_1\right)$ and next forming the sum of all the translated sets. The set obtained by the translation τ_n lying entirely in the interval $(2n-1)L_0<x<(2n+1)L_0$ we have

$$\overline{m}_B E_2 = m_B E_2 = \frac{1}{2L_0} m\left[E; -L_0+\frac{1}{2}L, L_1\right] \leqq \frac{1}{2L_0} m(E; -L_0, L_0) \leqq 2\varepsilon^2.$$

Putting

$$E_3 = E \dot{+} E_2$$

we obviously have

$$\overline{m}_B E_3 \leqq \overline{m}_B E + \overline{m}_B E_2 \leqq \varepsilon^2 + 2\varepsilon^2 = 3\varepsilon^2.$$

Corresponding to the division of $\left[-L_0+\frac{1}{2}L, L_1\right]$ in subintervals of length δ we consider the division in subintervals of length δ of all the intervals translated by $\tau_0=0, \tau_1, \tau_{-1}, \tau_2, \tau_{-2}, \cdots$. Let E_4 denote the set consisting of all the subintervals whose intersection with E_3 have relative measures $>\varepsilon$. Then $\overline{m}_B E_4 \leqq 3\varepsilon$. Let further E_5 denote the complement of the set obtained by performing the translations $\tau_0=0, \tau_1, \tau_{-1}, \tau_2, \tau_{-2}, \cdots$ on the interval $\left[-L_0+\frac{1}{2}L, L_1\right]$ and next forming the sum of all the translated intervals. The interval obtained by the translation τ_n lying entirely in the interval $(2n-1)L_0<x<(2n+1)L_0$ we have

$$\overline{m}_B E_5 = m_B E_5 \leqq \frac{L+1}{2L_0}.$$

Let E_4' denote the set E_4 after being expanded δ to the left, i.e. the set of points whose distances in right-hand direction to

E_4 are $\leqq \delta$. Analogously let E_5' denote the set E_5 after being expanded δ to the left. Then

$$\overline{m}_B E_4' \leqq 6\varepsilon \quad \text{and} \quad \overline{m}_B E_5' \leqq \frac{L+2}{2L_0} \leqq \varepsilon .$$

For $x \in C(E_4' \dot{+} E_5')$ the interval $[x, x+\delta]$ is lying entirely in $C(E_4 \dot{+} E_5)$ and hence entirely in the sum of two successive subintervals of the length δ whose intersection with E_3 have a relative measure $< \varepsilon$. The intersection $P(x)$ of $[x, x+\delta]$ with E_3 therefore has a relative measure $\leqq 2\varepsilon$. For a suitable value of n the interval $[x, x+\delta]$ by the translation $-\tau_n$ will be brought over in an interval $[x-\tau_n, x-\tau_n+\delta]$ included in the interval $\left[-L_0+\frac{1}{2}L, L_1\right]$, and if ξ is lying in $[x, x+\delta]$ outside $P(x)$ the number $\xi-\tau_n$ in $[x-\tau_n, x-\tau_n+\delta]$ will lie outside E. Hence

$$|\varphi_\delta(x)-\varphi_\delta(x-\tau_n)| = \left|\frac{1}{\delta}\int_x^{x+\delta} f(\xi)\,d\xi - \frac{1}{\delta}\int_{x-\tau_n}^{x-\tau_n+\delta} f(\xi)\,d\xi\right| \leqq \frac{1}{\delta}\int_x^{x+\delta} |f(\xi)-f(\xi-\tau_n)|\,d\xi$$

$$\leqq \frac{1}{\delta}\int_{P(x)} |f(\xi)-f(\xi-\tau_n)|\,d\xi + \frac{1}{\delta}\int_{(CP(x);\,x,\,x+\delta)} |f(\xi)-f(\xi-\tau_n)|\,d\xi \leqq 2\Gamma\cdot 2\varepsilon + \varepsilon^2 = 4\Gamma\varepsilon + \varepsilon^2$$

where Γ denotes the upper bound of $|f(x)|$. Let E_6 denote the set obtained by performing the translations $\tau_0 = 0$, τ_1, τ_{-1}, τ_2, τ_{-2}, $\cdots$ on the set $\left(E_1; -L_0+\frac{1}{2}L, L_1\right)$ and next forming the sum of all the translated sets. Then

$$\overline{m}_B E_6 = m_B E_6 = \frac{1}{2L_0}\, m\left(E_1; -L_0+\frac{1}{2}L, L_1\right) \leqq \frac{1}{2L_0}\, m E_1 \leqq \varepsilon .$$

Finally let

$$E_7 = E_7(\delta) = E_3 \dot{+} E_4' \dot{+} E_5' \dot{+} E_6 .$$

Then in the first place

$$\overline{m}_B E_7 \leqq \overline{m}_B E_3 + \overline{m}_B E_4' + \overline{m}_B E_5' + \overline{m}_B E_6 \leqq 3\varepsilon^2 + 6\varepsilon + \varepsilon + \varepsilon = 8\varepsilon + 3\varepsilon^2 .$$

And secondly for $x \in C E_7(\delta)$ where $0 < \delta < \delta_0$—determining τ_n as above—we have

$$|\varphi_\delta(x)-f(x)|\leq|\varphi_\delta(x)-\varphi_\delta(x-\tau_n)|+|\varphi_\delta(x-\tau_n)-f(x-\tau_n)|+$$
$$+|f(x-\tau_n)-f(x)|\leq(4\Gamma\varepsilon+\varepsilon^2)+\varepsilon+\varepsilon^2=4\Gamma\varepsilon+\varepsilon+2\varepsilon^2.$$

Letting $\varepsilon\to 0$ both $8\varepsilon+3\varepsilon^2$ and $4\Gamma\varepsilon+\varepsilon+2\varepsilon^2$ will converge towards 0. This accomplishes the proof of lemma 2.

Lemma 3. *Let $f(x)$ be a bounded K-a.p. function and let us consider the smoothed function*

$$\varphi_\delta(x)=\frac{1}{\delta}\int_x^{x+\delta}f(\xi)\,d\xi$$

for a fixed value af $\delta>0$. Then to every $\varepsilon>0$ there exists a relatively dense set $I=I(\varepsilon)$ of intervals with the same length $2\zeta_0=2\zeta_0(\varepsilon)$ the one of which has its central point in 0 as well as a set $E^*=E^*(\varepsilon)$ with $\overline{m}_B E^*\leq\varepsilon$ such that for every τ from the intervals mentioned

$$|\varphi_\delta(x+\tau)-\varphi_\delta(x)|\leq\varepsilon$$

when both $x\varepsilon CE^*$ and $x+\tau\varepsilon CE^*$.

Proof. The function $f(x)$ being bounded, $|f(x)|\leq\Gamma$, the smoothed function $\varphi_\delta(x)$ is obviously a uniformly continuous function, for

$$|\varphi_\delta(x+\zeta)-\varphi_\delta(x)|=\left|\frac{1}{\delta}\int_{x+\zeta}^{x+\zeta+\delta}f(\xi)\,d\xi-\frac{1}{\delta}\int_x^{x+\delta}f(\xi)\,d\xi\right|=$$
$$\left|\frac{1}{\delta}\int_{x+\delta}^{x+\zeta+\delta}f(\xi)\,d\xi-\frac{1}{\delta}\int_x^{x+\zeta}f(\xi)\,d\xi\right|\leq\frac{2|\zeta|\Gamma}{\delta}$$

which $\to 0$ for $\zeta\to 0$. Belonging to ε^2 we choose a relatively dense set $\{\tau\}$ of translation numbers and an exception set E of $f(x)$. We divide the axis in subintervals of the length δ. Let E_1 denote the set consisting of all the subintervals whose intersections with E have relative measures $>\varepsilon$. Then $\overline{m}_B E_1\leq\varepsilon$. Let E_2 denote the set E_1 after being expanded 2δ to the left and δ to the right (see p. 13). Then $\overline{m}_B E_2\leq 4\varepsilon$. The function $\varphi_\delta(x)$ being uniformly continuous we can choose an ζ_0, $0<\zeta_0<\delta$, such that

$$|\varphi_\delta(x+\zeta)-\varphi_\delta(x)|\leqq\varepsilon$$

for $|\zeta|\leqq\zeta_0$. Now let τ be a number from $\{\tau\}$, let $|\zeta|\leqq\zeta_0$, and let both x and $x+\tau+\zeta$ lie in CE_2. Then the intervals $[x, x+\delta]$ and $[x+\tau,\ x+\tau+\delta]$ will lie entirely in CE_1 and their intersections $P(x)$ and $P(x+\tau)$ with E will therefore have relative measures $\leqq 2\varepsilon$. Hence, denoting by $P(x+\tau)_{-\tau}$ the set $P(x+\tau)$ translated $-\tau$, we have

$$|\varphi_\delta(x+\tau+\zeta)-\varphi_\delta(x)|\leqq|\varphi_\delta(x+\tau+\zeta)-\varphi_\delta(x+\tau)|+|\varphi_\delta(x+\tau)-\varphi_\delta(x)|\leqq$$

$$\varepsilon+\left|\frac{1}{\delta}\int_{x+\tau}^{x+\tau+\delta}f(\xi)\,d\xi-\frac{1}{\delta}\int_{x}^{x+\delta}f(\xi)\,d\xi\right|\leqq\varepsilon+\frac{1}{\delta}\int_{x}^{x+\delta}|f(\xi+\tau)-f(\xi)|\,d\xi\leqq$$

$$\varepsilon+\frac{1}{\delta}\int_{P(x)\,+\,P(x+\tau)_{-\tau}}|f(\xi+\tau)-f(\xi)|\,d\xi+\frac{1}{\delta}\int_{(C(P(x)\,+\,P(x+\tau)_{-\tau});\,x,\,x+\delta)}|f(\xi+\tau)-f(\xi)|\,d\xi\leqq\varepsilon+8I\varepsilon+\varepsilon^2.$$

All numbers in the ζ_0-neighbourhoods of our translation numbers τ are therefore "fine" translation numbers of $\varphi_\delta(x)$ with a "small" exception set E_2. Further all numbers from the ζ_0-neighbourhood of 0 are fine translation numbers (even O-translation numbers) of $\varphi_\delta(x)$. This accomplishes the proof of lemma 3.

Lemma 4. *Let $f(x)$ be a K-a.p. function. Then to every $\varepsilon>0$ there exists a relatively dense set $I=I(\varepsilon)$ of intervals with the same length $2\zeta_0=2\zeta_0(\varepsilon)>0$ the one of which has its central point in 0 as well as a set $E^*=E^*(\varepsilon)\subseteq[|f(x)|=\infty]$ with $\overline{m}_B E^*\leqq\varepsilon$ such that for every τ from the intervals mentioned*

$$|f(x+\tau)-f(x)|\leqq\varepsilon$$

when both $x\varepsilon CE^*$ and $x+\tau\varepsilon CE^*$.

Proof. Corresponding to $\frac{1}{3}\varepsilon$ we may on account of lemma 1 choose a number $N>0$ and a set $E_1\supseteq[|f(x)|=\infty]$ with $\overline{m}_B E_1\leqq\frac{1}{3}\varepsilon$ such that

$$f(x)=(f(x))_N$$

for $x\varepsilon CE_1$. For $(f(x))_N$ we form the smoothed function

$$\varphi_\delta(x) = \frac{1}{\delta}\int_x^{x+\delta} (f(\xi))_N \, d\xi$$

and may on account of lemma 2 choose $\delta > 0$ and a set E_2 with $\overline{m}_B E_2 \leqq \frac{1}{3}\varepsilon$ such that

$$|(f(x))_N - \varphi_\delta(x)| \leqq \frac{1}{3}\varepsilon$$

for $x \varepsilon CE_2$. Finally on account of lemma 3 there exists a relatively dense set I of intervals with the same length $2\zeta_0 > 0$ the one of which has its central point in 0 as well as a set E_3 with $\overline{m}_B E_3 \leqq \frac{1}{3}\varepsilon$ such that for every τ from the intervals mentioned

$$|\varphi_\delta(x+\tau) - \varphi_\delta(x)| \leqq \frac{1}{3}\varepsilon$$

when both $x \varepsilon CE_3$ and $x+\tau \varepsilon CE_3$. Putting

$$E^* = E_1 \dot{+} E_2 \dot{+} E_3$$

we have

$$\overline{m}_B E^* \leqq \overline{m}_B E_1 + \overline{m}_B E_2 + \overline{m}_B E_3 \leqq \frac{1}{3}\varepsilon + \frac{1}{3}\varepsilon + \frac{1}{3}\varepsilon = \varepsilon.$$

Further for every τ from I we have

$$|f(x+\tau) - f(x)| = |(f(x+\tau))_N - (f(x))_N| \leqq$$

$$|f(x+\tau)_N - \varphi_\delta(x+\tau)| + |\varphi_\delta(x+\tau) - \varphi_\delta(x)| + |\varphi_\delta(x) - (f(x))_N| \leqq$$

$$\frac{1}{3}\varepsilon + \frac{1}{3}\varepsilon + \frac{1}{3}\varepsilon = \varepsilon$$

when both $x \varepsilon CE^*$ and $x+\tau \varepsilon CE^*$. This accomplishes the proof of lemma 4.

We now pass to the proper proof of the second part of the main theorem. As mentioned before (p. 12) we need only consider bounded K-a. p. functions. Let then $f(x)$ be a bounded K-a. p. function, $|f(x)| \leqq \Gamma$, for all x. In the following we may assume $\Gamma \leqq 1$, otherwise we only consider the function $\frac{1}{\Gamma} f(x)$. We are

to show that $f(x)$ can be K-approximated by trigonometric polynomials or—what on account of the main theorem in the theory of the O-a. p. functions amounts to the same thing—by ordinary almost periodic functions. Let $\varepsilon > 0$ be arbitrarily given. We are to indicate an ordinary almost periodic function $\varphi(x)$ and a set E^* with $\overline{m}_B E^* \leqq \eta_1(\varepsilon)$ such that

$$|f(x) - s(x)| \leqq \eta_2(\varepsilon)$$

for $x \varepsilon C E^*$ where $\eta_1(\varepsilon) \to 0$ and $\eta_2(\varepsilon) \to 0$ for $\varepsilon \to 0$. For the function $f(x)$ and belonging to ε^2 we may on account of lemma 4 choose a relative dense set I' of intervals consisting of translation numbers and with the same length δ as well as an exception set E. The length L is chosen so large that every interval of this length contains an interval of length δ from I'. Next L_0 $(\geqq L + \delta)$ is chosen so large that $\frac{L+\delta}{L_0} \leqq \varepsilon$. In every one of the intervals $nL_0 < x < nL_0 + L$ $(n = 0, \pm 1, \pm 2, \cdots)$ we choose an interval of translation numbers from I' with the length δ. We consider the total set I of these translation numbers. Let $m_B I = \eta$. Next we define a function $K(t)$ by

$$K(t) = \begin{cases} 1 \text{ for } t \varepsilon I \\ \eta \\ 0 \text{ for } t \varepsilon CI. \end{cases}$$

Then

$$M\{K(t)\} = 1.$$

We consider the expression

$$\frac{1}{2T} \int_{-T}^{T} f(x+t) K(t)\, dt.$$

The modulus of this expression is $\leqq \frac{1}{\eta}$. Denoting by $x_1, x_2, \cdots$ an enumerable everywhere dense set on the whole axis and by $0 < T_1 < T_2 < \cdots \to \infty$ an arbitrary sequence, by the diagonal procedure we can extract a subsequence—again denoted T_n—such that for the new sequence T_n

$$\frac{1}{2T_n} \int_{-T_n}^{T_n} f(x+t) K(t)\, dt$$

is convergent for x equal to $x_1, x_2, \cdots$. We first show that the expression then converges for all x. Let $\varepsilon_0 > 0$ be arbitrarily given. We choose a set E^* with $\overline{m}_B E^* \leqq \varepsilon_0 \eta$ and a positive ζ_0 such that

$$|f(x+\zeta) - f(x)| \leqq \varepsilon_0 \eta$$

for $|\zeta| \leqq \zeta_0$ when both $x \varepsilon CE^*$ and $x + \zeta \varepsilon CE^*$ (lemma 4). Next we choose an x_m from our enumerable set above such that $|x - x_m| \leqq \zeta_0$. Letting E^*_{-x} denote the set E^* after being translated $-x$ we have

$$\frac{1}{2T_n}\int_{-T_n}^{T_n} |f(x+t) - f(x_m+t)|\,dt = \frac{1}{2T_n}\int_{(E^*_{-x} \dotplus E^*_{-x_m};\, -T_n,\, T_n)} |f(x+t) - f(x_m+t)|\,dt +$$

$$\frac{1}{2T_n}\int_{(C(E^*_{-x} \dotplus E^*_{-x_m});\, -T_n,\, T_n)} |f(x+t) - f(x_m+t)|\,dt \leqq \frac{1}{2T_n}\, 2m\left(E^*_{-x} \dotplus E^*_{-x_m}; -T_n, T_n\right) + \varepsilon_0\eta \leqq$$

$$2\,\frac{1}{2T_n}\, m\left(E^*_{-x}; -T_n, T_n\right) + 2\,\frac{1}{2T_n}\, m\left(E^*_{-x_m}; -T_n, T_n\right) + \varepsilon_0\eta$$

which for n sufficiently large, $n \geqq n_0$, is

$$\leqq 4\varepsilon_0\eta + 4\varepsilon_0\eta + \varepsilon_0\eta = 9\varepsilon_0\eta.$$

Hence for $n \geqq n_0$

$$\left|\frac{1}{2T_n}\int_{-T_n}^{T_n} f(x+t)\,K(t)\,dt - \frac{1}{2T_n}\int_{-T_n}^{T_n} f(x_m+t)\,K(t)\,dt\right| \leqq$$

$$\frac{1}{2T_n}\int_{-T_n}^{T_n} |f(x+t) - f(x_m+t)|\,K(t)\,dt \leqq \frac{1}{\eta}\,\frac{1}{2T_n}\int_{-T_n}^{T_n} |f(x+t) - f(x_m+t)|\,dt \leqq 9\varepsilon_0.$$

This together with the fact that the expression

$$\frac{1}{2T_n}\int_{-T_n}^{T_n} f(x_m+t)\,K(t)\,dt$$

has a limit for $n \to \infty$ shows that for n_1 and n_2 sufficiently large

$$\left|\frac{1}{2T_{n_1}}\int_{-T_{n_1}}^{T_{n_1}} f(x+t)\,K(t)\,dt - \frac{1}{2T_{n_2}}\int_{-T_{n_2}}^{T_{n_2}} f(x+t)\,K(t)\,dt\right| \leqq 19\varepsilon_0,$$

and hence the limit

$$\lim_{n\to\infty}\frac{1}{2T_n}\int_{-T_n}^{T_n} f(x+t)\,K(t)\,dt$$

exists for our arbitrarily chosen x. We then consider the function

$$\varphi(x)=\lim_{n\to\infty}\frac{1}{2T_n}\int_{-T_n}^{T_n} f(x+t)\,K(t)\,dt$$

which—as we shall see—will have the properties desired.

We first show that $\varphi(x)$ is an ordinary almost periodic function. Let $\varepsilon_0>0$ be arbitrarily given. Belonging to $\varepsilon_0\eta$ we choose a relatively dense set $\{\tau\}$ of translation numbers which contains an interval with central point 0, as well as an exception set E^* of $f(x)$ (lemma 4). For each such τ

$$|\varphi(x+\tau)-\varphi(x)|\leq\overline{\lim_{n\to\infty}}\frac{1}{2T_n}\int_{-T_n}^{T_n}|f(x+t+\tau)-f(x+t)|\,K(t)\,dt\leq$$

$$\overline{\lim_{n\to\infty}}\frac{1}{2T_n}\int_{(E^*_{-x}+E^*_{-x-\tau};\,-T_n,\,T_n)}|f(x+t+\tau)-f(x+t)|\,K(t)\,dt+$$

$$\overline{\lim_{n\to\infty}}\frac{1}{2T_n}\int_{(C(E^*_{-x}+E^*_{-x-\tau});\,-T_n,\,T_n)}|f(x+t+\tau)-f(x+t)|\,K(t)\,dt\leq$$

$$\frac{2}{\eta}\overline{m}_B(E^*_{-x}+E^*_{-x-\tau})+\frac{1}{\eta}\varepsilon_0\eta\leq\frac{2}{\eta}\overline{m}_B E^*_{-x}+\frac{2}{\eta}\overline{m}_B E^*_{-x-\tau}+\varepsilon_0\leq$$

$$2\varepsilon_0+2\varepsilon_0+\varepsilon_0=5\varepsilon_0.$$

All our numbers τ thus being 0-translation numbers of $\varphi(x)$ belonging to $5\varepsilon_0$ we conclude that $\varphi(x)$ is an ordinary almost periodic function.

We now come to the salient point of the proof, viz. the demonstration that $\varphi(x)$ only differs "a little" from $f(x)$ outside an exception set with "small" $\overline{m}_B$. As $M\{K(t)\}=1$ we have

$$f(x) = \lim_{n\to\infty} \frac{1}{2T_n} \int_{-T_n}^{T_n} f(x)\, K(t)\, dt,$$

and hence

$$\varphi(x) - f(x) = \lim_{n\to\infty} \frac{1}{2T_n} \int_{-T_n}^{T_n} (f(x+t) - f(x))\, K(t)\, dt.$$

Letting T_n for abbreviation also denote an arbitrary subsequence of the above sequence T_n we get the estimation

$$|\varphi(x) - f(x)| \leq \overline{\lim_{n\to\infty}} \frac{1}{2T_n} \int_{-T_n}^{T_n} |f(x+t) - f(x)|\, K(t)\, dt =$$

$$\overline{\lim_{n\to\infty}} \frac{1}{2T_n} \int_{(I;\,-T_n,\,T_n)} |f(x+t) - f(x)|\, K(t)\, dt,$$

and for $x \varepsilon CE$ this is

$$\leq \overline{\lim_{n\to\infty}} \frac{1}{2T_n} \int_{(IE_{-x};\,-T_n,\,T_n)} |f(x+t) - f(x)|\, K(t)\, dt + \overline{\lim_{n\to\infty}} \frac{1}{2T_n} \int_{(ICE_{-x};\,-T_n,\,T_n)} |f(x+t) - f(x)|\, K(t)\, dt \leq$$

$$\frac{2}{\eta}\, \overline{m}_B(IE_{-x}) + \varepsilon^2$$

where $\overline{m}_B$ is formed through the subsequence T_n. Now $m_B\, I = \eta$ and the problem thus is only to prove that the intersection IE_{-x} of I and E_{-x} for a suitable subsequence T_n will have an $\overline{m}_B$ (formed through the subsequence T_n) which is essentially smaller than the m_B of I for all x outside a set with small $\overline{m}_B$. Instead of IE_{-x} we may as well consider the set $I_x E$ obtained by the translation x, because $\overline{m}_B(IE_{-x}) = \overline{m}_B(I_x E)$. We investigate $I_x E$ when x runs through one of the intervals $[nL_0, (n+1)L_0]$ and we are to show that for a suitable subsequence T_n (the same for all intervals $[nL_0, (n+1)L_0]$) the measure $\overline{m}_B(I_x E)$ (formed through this subsequence T_n) will be essentially smaller than η for x in the interval mentioned outside a set with small

relative measure. All intervals being treated analogously we may content ourselves with considering detailed only the interval $[0, L_0]$. When x runs through the interval $[0, L_0 - L]$ every one of the small intervals in I_x will decribe an interval lying entirely in one of the intervals $[mL_0, (m+1)L_0]$. The interval $[0, L_0 - L]$ is divided beginning at the left in as many subintervals of length δ as possible. Let $N\delta$ denote the last point of division. Then $L_0 - L - N\delta < \delta$. Corresponding to the points of division $0, \delta, 2\delta, \cdots, N\delta$ we consider the sets $I, I_\delta, I_{2\delta}, \cdots, I_{N\delta}$. Any two of these sets are non-intersecting (with exception of endpoints of intervals) and all sets together fill out the set being decribed of I_x when x runs through the interval $[0, N\delta]$. We now choose our subsequence T_n such that

$$\lim_{n \to \infty} \frac{1}{2T_n} m(I_{q\delta} E; -T_n, T_n)$$

exists for $q = 1, 2, \cdots, N$ and such that the analogous limits exist for all the remaining intervals $[nL_0, (n+1)L_0]$. For this subsequence T_n we will use the above estimation of $|\varphi(x) - f(x)|$. We first ask: How many of the sets $I_{q\delta}$ have an intersection with E with relative measure (formed through the subsequence T_n) which is $> \varepsilon\eta$. As the sets are non-intersecting and $\overline{m}_B E \leqq \varepsilon^2$ the number A in question must satisfy the relation

$$A\,\varepsilon\eta \leqq \varepsilon^2,$$

i. e. $A \leqq \frac{\varepsilon}{\eta}$. For x lying in $[0, N\delta]$ the set I_x has only points in common with $I_{q\delta}$ for $|x - q\delta| \leqq \delta$. Letting x in $[0, N\delta]$ avoid the intervals $|x - q\delta| \leqq \delta$ corresponding to the A sets $I_{q\delta}$ above with $m_B(I_{q\delta} E) > \varepsilon\eta$ (m_B formed through the subsequence T_n) the sets I_x must be contained in the sum of two neighbour-$I_{q\delta}$'s with $m_B(I_{q\delta} E) \leqq \varepsilon\eta$. Together the intervals which x must avoid have a relative measure $\leqq A \frac{2\delta}{L_0} \leqq \frac{\varepsilon}{\eta} \frac{2\delta}{L_0} = \frac{\varepsilon}{\eta} 2\eta = 2\varepsilon$. Then $\overline{m}_B(I_x E) \leqq 2\varepsilon\eta$ ($\overline{m}_B$ formed through T_n) and this quantity is essentially smaller than η. Considering the whole interval $[0, L_0]$ the argument x must further avoid the interval $[N\delta, L_0]$ of a length $\leqq L + \delta$. Hence the relative measure of the intervals which x must avoid in $[0, L_0]$ is $\leqq \frac{L + \delta}{L_0} + 2\varepsilon \leqq \varepsilon + 2\varepsilon = 3\varepsilon$. Analogous results are

obtained for the remaining intervals $[nL_0, (n+1)L_0]$. Letting E_1 denote the sum of exception sets from all the intervals $[nL_0, (n+1)L_0]$ we get

$$\overline{m}_B(I_x E) \leqq 2\varepsilon\eta \qquad (\overline{m}_B \text{ formed through } T_n)$$

for $x \varepsilon C E_1$, where $\overline{m}_B E_1 \leqq 3\varepsilon$. Inserting in the estimation on page 21 we get for $x \varepsilon C(E \dot{+} E_1)$

$$|g(x) - f(x)| \leqq \frac{2}{\eta} 2\varepsilon\eta + \varepsilon^2 = 4\varepsilon + \varepsilon^2$$

and further

$$\overline{m}_B(E \dot{+} E_1) \leqq \overline{m}_B E + \overline{m}_B E_1 \leqq \varepsilon^2 + 3\varepsilon.$$

Letting $\varepsilon \to 0$ both $4\varepsilon + \varepsilon^2$ and $3\varepsilon + \varepsilon^2$ will converge towards 0. This accomplishes the proof of the main theorem.

Remark. The main theorem is still valid if instead of the "B-measure" $\overline{m}_B$ we use an S-measure or a W-measure. This is easily seen from the fact that the cut-off function still in the corresponding sense will converge to the function considered, in connection with the fact that the K-a. p. properties of the cut-off function (with S or W instead of B) immediately involve that it possesses the S^p-a. p. respectively W^p-a. p. properties mentioned in the introduction. For the cut-off function can then be S-, respectively W-approximated by trigonometric polynomials and this involves that the cut-off function and with it the original function itself can be K-approximated by trigonometric polynomials. In the S-case we obviously need not claim the exception set to be the same for all τ belonging to the same ε, cp. W. STEPANOFF [I], especially definition I and lemma II.

The connection between the K-a. p. and the B^p-a. p. functions appears from the following simple

Theorem 2. *A B^p-a. p. function means the same as a K-a. p. function $f(x)$ for which $\|f(x) - (f(x))_N\|_{B^p} \to 0$ for $N \to \infty$.*

This theorem has the corollary

Theorem 3. *A bounded K-a.p. function is B^p-a.p. for all p.*

If $f(x)$ is K-a.p. so is $(f(x))_N$ (see p. 12). The corollary thus gives:

Theorem 4. *If $f(x)$ is K-a.p. the cut-off function $(f(x))_N$ is B^p-a.p. for all p.*

We now turn to the proof of theorem 2.

1°. If $f(x)$ is B^p-a.p. then as is well-known we shall have $\|f(x)-(f(x))_N\|_{B^p} \to 0$ for $N \to \infty$. Further a sequence $s_n(x)$ of trigonometric polynomials can be found such that $\|f(x)-s_n(x)\|_{B^p} \to 0$, and from this follows that

$$\overline{m}_B[|f(x)-s_n(x)|>\varepsilon] \to 0$$

for every fixed $\varepsilon > 0$; hence $s_n(x)$ K-converges towards $f(x)$ which is therefore K-a.p.

2°. Let $f(x)$ be K-a.p. and let $\|f(x)-(f(x))_N\|_{B^p} \to 0$ for $N \to \infty$. From the first assumption follows that we can find a sequence of ordinary almost periodic functions $\varphi_n(x)$ which K-converges towards $f(x)$. As

$$|(f(x))_N-(\varphi_n(x))_N| \leqq |f(x)-\varphi_n(x)|$$

the sequence $(\varphi_n(x))_N$ (N fixed) of almost periodic functions K-converges towards $(f(x))_N$. The functions $(f(x))_N$ and $(\varphi_n(x))_N$ being uniformly bounded $(\varphi_n(x))_N$ (N fixed) will also B^p-converge towards $(f(x))_N$; for to every $\varepsilon > 0$ we can choose a number n_0 such that

$$|(f(x))_N-(\varphi_n(x))_N| < \varepsilon \quad \text{for} \quad x \varepsilon C E_n \quad \text{and} \quad n \geqq n_0$$

where $\overline{m}_B E_n < \varepsilon$ and from this follows that

$$\|(f(x))_N-(\varphi_n(x))_N\|_{B^p}^p \leqq \varepsilon^p + (2N)^p \varepsilon \quad \text{for} \quad n \geqq n_0.$$

Hence $(f(x))_N$ is B^p-a.p. The second assumption $\|f(x)-(f(x))_N\|_{B^p} \to 0$ then involves that $f(x)$ is B^p-a.p., too.

Instead of the additional condition $\|f(x)-(f(x))_N\|_{B^p} \to 0$ for $N \to \infty$ one may also—as Kovanko has done it—use the additional condition $\|f_E(x)\|_{B^p} \to 0$ for $\overline{m}_B E \to 0$ where $f_E(x)$ denotes the function which is equal to $f(x)$ in (the arbitrary set)

E and equal to 0 outside E. This is easily seen by means of lemma 1.

Remark. If we substitute for $\overline{m}_B$ either $\overline{m}_S$ or $\overline{m}_W$ and at the same time for the B^p-norm respectively the S_L^p-norm or the W^p-norm the theorems 2—4 are obviously still valid.

§ 4. The Connection between the B^p-bounded K-a. p. Functions and the B^p-a. p. Functions.

Instead of the additional condition $\|f(x)-(f(x))_N\|_{B^p} \to 0$ for $N \to \infty$ we shall in this section consider the simpler additional condition $\|f(x)\|_{B^p} < \infty$, i. e. we shall investigate the B^p-bounded K-a. p. functions. In the proofs given or referred to in this section one always uses the characterization by approximation of the K-a. p. functions. The connection between B^p-bounded K-a. p. functions and the B^p-a. p. functions is expressed in the following

Theorem 5. *A B^p-bounded K-a. p. function $f(x)$ can be written in the form*

$$f(x) = g(x) + j(x)$$

where $g(x)$ is B^p-a. p. and $j(x)$ is a B^p-bounded K-zero function, i. e. a function for which $\|j(x)\|_{B^p} < \infty$ and $\overline{m}_B[|j(x)| > \varepsilon] = 0$ for every $\varepsilon > 0$. Conversely every function of this form is a B^p-bounded K-a. p. function.

Proof. 1°. The last part of the theorem is obvious.

2°. For the proof of the first part of the theorem we refer to the proof of an analogous theorem in Bohr and Følner [I], p. 99, viz. the theorem that a B^1-a. p. point which contains a B^p-bounded function also contains a B^p-a. p. function. This theorem relies on a theorem of Jessen [I] stating that every real B^1-a. p. function has an asymptotic distribution function. Further Jessen and Wintner [I] have shown that every real K-a. p. function has an asymptotic distribution function. By means of this theorem it is possible—just as in Bohr and Følner [I]—to show that for a B^p-bounded K-a. p. function $f(x)$ the cut-off functions $(f(x))_N$ $(N = 1, 2, \cdots)$ will form a B^p-fundamental sequence which on account of theorem 4 and the completeness of the B^p-a. p. spaces will B^p-converge towards a B^p-a. p.

function $g(x)$. The sequence $(f(x))_N$ K-converging both towards $f(x)$ and $g(x)$ the function $j(x) = f(x) - g(x)$ is a K-zero function and $f(x)$ and $g(x)$ being both B^p-bounded so is $j(x)$.

Remark. This theorem is not valid if $\overline{m}_B$ is replaced by $\overline{m}_S$ and the B^p-norm by the S^p-norm (in which case functions of the type $j(x)$ is 0 almost everywhere). For $p > 1$ we have a counter example in BOHR and FØLNER [I], main example 2, p. 70, and for $p = 1$ an analogous example may easily be constructed. The theorem is valid no more if $\overline{m}_B$ is replaced by $\overline{m}_W$ and the B^p-norm by the W^p-norm. For $p > 1$ we have a counter example in BOHR and FØLNER [I], main example 3, p. 83 and for $p = 1$ an analogous example may easily be constructed.

By a B^p-bounded K-point we shall understand the set of functions which only differ from one and the same B^p-bounded function by B^p-bounded K-zero functions. If function one in the points is a (B^p-bounded) K-a. p. function so are all functions in the point and the point is called a B^p-bounded K-a. p. point. The non obvious part of our theorem may then be expressed: In every B^p-bounded K-a. p. point there is lying a B^p-a. p. point. On the other hand only one B^p-a. p. point can be lying in a B^p-bounded K-a. p. point, for if $j(x)$ is a K-zero function and B^p-a. p. then $(j(x))_N$ is a $B^{p'}$-zero function for all p', specially a B^p-zero function, and $\|j(x) - (j(x))_N\|_{B^p} \to 0$ for $N \to \infty$, so that $j(x)$ is also a B^p-zero function.

Theorem 6. *For $p > 1$ a B^p-bounded K-zero function $j(x)$ is a $B^{p'}$-zero function for $1 < p' < p$.*

Proof. We have

$$\|j(x)\|_{B^{p'}} = \overline{\lim_{T \to \infty}} \sqrt[p']{\frac{1}{2T}\int_{-T}^{T} |j(x)|^{p'} dx} \leq \overline{\lim_{T \to \infty}} \sqrt[p']{\frac{1}{2T}\int_{(\{|j(x)| \leq \varepsilon\}; -T, T)} |j(x)|^{p'} dx} +$$

$$\overline{\lim_{T \to \infty}} \sqrt[p']{\frac{1}{2T}\int_{(\{|j(x)| > \varepsilon\}; -T, T)} |j(x)|^{p'} dx} = I_1 + I_2.$$

Here $I_1 \leq \varepsilon$. For I_2 we have

$$I_2 = \| j(x)\, e(x) \|_{B^{p'}}$$

where $e(x) = 1$ in $[|j(x)| > \varepsilon]$ and $e(x) = 0$ outside $[|j(x)| > \varepsilon]$. By means of Hölder's inequality we get

$$I_2^{p'} = \overline{\lim_{T\to\infty}} \frac{1}{2T} \int_{-T}^{T} |j(x)|^{p'} e(x)^{p'} dx <$$

$$\left(\overline{\lim_{T\to\infty}} \frac{1}{2T} \int_{-T}^{T} |j(x)|^{p} dx \right)^{\frac{p'}{p}} \left(\overline{\lim_{T\to\infty}} \frac{1}{2T} \int_{-T}^{T} e(x)^{\frac{1}{p'-\frac{1}{p}}} dx \right)^{1-\frac{p'}{p}} =$$

$$\| j(x) \|_{B^p}^{p'} \left(\overline{m}_B [|j(x)| > \varepsilon] \right)^{1-\frac{p'}{p}} = 0$$

so that $I_2 = 0$. Hence $\| j(x) \|_{B^{p'}} \leq \varepsilon$ for every $\varepsilon > 0$, i. e. $\| j(x) \|_{B^{p'}} = 0$.

Moreover the following theorem is valid:

Theorem 7. *For $p > 1$ a B^p-bounded K-a. p. function $f(x)$ is a $B^{p'}$-a. p. function for $1 \leq p' < p$.*

Proof. This is a consequence of theorem 5 and theorem 6. The theorem, however, may also be proved directly by means of Hölder's inequality which shows that $\| f(x) - (f(x))_N \|_{B^{p'}} \to 0$ for $N \to \infty$.

As is easily seen a B^1-bounded K-zero function (which a fortiori is a K-a. p. function) need not possess a mean value in the Besicovitch sense. We are to prove, however, that the mean value notion can be generalized such that every B^1-bounded K-a. p. function gets a mean value and a B^1-bounded K-zero function especially the mean value 0. For a B^1-bounded K-a. p. function $f(x)$ we simply define the generalized mean value $M^*\{f(x)\}$ by

$$M^*\{f(x)\} = \lim_{N\to\infty} M\{(f(x)_N\}.$$

The mean value $M\{(f(x)_N\}$ exists since $(f(x))_N$ — on account of theorem 4 — is a B^1-a. p. function. And as mentioned in the proof of theorem 5 the sequence $(f(x))_N$ $(N = 1, 2, \cdots)$ is a B^1-fundamental sequence from which follows that $M\{(f(x))_N\}$ is a fundamental sequence since

$$|M\{(f(x))_{N_1}\} - M\{(f(x))_{N_2}\}| \leq M\{|(f(x))_{N_1} - (f(x))_{N_2}|\} =$$
$$\|(f(x))_{N_1} - (f(x))_{N_2}\|_{B^1}$$

and hence $\lim_{N\to\infty} M\{(f(x))_N\}$ exists. If $f(x)$ is a B^1-a. p. function then $\|f(x) - (f(x))_N\|_{B^1} \to 0$ and an estimation analogous to the above one gives

$$M^*\{f(x)\} = M\{f(x)\}.$$

Let $f(x)$ be a B^p-bounded (and a fortiori B^1-bounded) K-a. p. function. From theorem 5 follows that

$$f(x) = g(x) + j(x)$$

where $g(x)$ is B^p-a. p. and $j(x)$ is a B^p-bounded K-zero function. We will show that

$$M^*\{f(x)\} = M\{g(x)\}.$$

Proof. For $x \varepsilon [|j(x)| \leq \varepsilon]$ we have

$$|(g(x) + j(x))_N - (g(x))_N| \leq |j(x)| \leq \varepsilon$$

and as $\overline{m}_B[|j(x)| > \varepsilon] = 0$ we get

$$|M\{(g(x) + j(x))_N\} - M\{(g(x))_N\}| \leq \varepsilon$$

so that

$$M\{(g(x) + j(x))_N\} = M\{(g(x))_N\}.$$

Letting $N \to \infty$ we get

$$M^*\{f(x)\} = M^*\{g(x) + j(x)\} = M\{g(x)\}, \text{ q. e. d.}$$

Now let

$$g(x) \sim \sum A_n e^{i\lambda_n x}.$$

Together with $f(x)$ the function $f(x)e^{-i\lambda x}$ is also a B^p-bounded K-a. p. function, and together with $j(x)$ the function $j(x)e^{-i\lambda x}$ is also a B^p-bounded K-zero function. We then get

$$M^*\{f(x)e^{-i\lambda x}\} = M^*\{g(x)e^{-i\lambda x} + j(x)e^{-i\lambda x}\} = M\{g(x)e^{-i\lambda x}\}.$$

By means of the new mean value notion we can in the usual manner ascribe to $f(x)$ a Fourier series which will be identical with the Fourier series of $g(x)$:

$$f(x) \sim \sum A_n e^{i\lambda_n x}.$$

The Bochner-Fejér polynomials of the series will B^p-converge towards a B^p-a. p. function (viz. $g(x)$) which only differs from $f(x)$ by a B^p-bounded K-zero function.

References.

A. S. Besicovitch: [I] On generalized almost periodic functions, Proc. London Math. Soc. (2), 25, p. 495—512 (1926). [II] Almost periodic functions, Cambridge University Press, 1932.

A. S. Besicovitch and H. Bohr: [I] Almost periodicity and general trigonometric series, Acta math. 57, p. 200—292 (1934).

H. Bohr and E. Følner: [I] On some types of functional spaces, Acta math. 76, p. 31—155 (1944).

B. Jessen: [I] A note on distribution functions, J. London Math..Soc. 8, p. 247—250 (1933).

B. Jessen and A. Wintner: [I] Distribution functions and the Riemann zeta function, Trans. Amer. Math. Soc. 38, p. 48—88 (1935).

A. S. Kovanko: [I] Sur la structure des fonctions presque périodiques généralisées, C. R. Acad. Sci. Paris 198, p. 792—794 (1934).

W. Stepanoff: [I] Über einige Verallgemeinerungen der fastperiodischen Funktionen, Math. Ann. 95, p. 473—498 (1926).

H. Weyl: [I] Integralgleichungen und fastperiodischen Funktionen, Math. Ann. 97, p. 338—356 (1926).

Indleveret til Selskabet den 29. September 1944.
Færdig fra Trykkeriet den 13. Marts 1945.